Evaluating zooplankton community responses to aquaculture wastewater using eDNA metabarcoding and morphological identification

by

Leah Dickenson

A Thesis submitted to the Faculty of Graduate Studies of

The University of Manitoba

in partial fulfilment of the requirements of the degree of

MASTER OF SCIENCE

Department of Environment and Geography

University of Manitoba

Winnipeg, Manitoba

Abstract

Inland aquaculture wastewater (AWW) is nutrient-rich due to the high stocking densities of cultivated organisms and intensive feeding inputs. Finding sustainable wastewater management strategies is critical as aquaculture is the fastest-growing food production system globally. Using aquaculture wastewater as a fertilizer for wild rice cultivation presents a potential solution since wild rice requires high nitrogen and phosphorus for sufficient growth. However, this raises concerns about possible impacts on aquatic ecosystems within the wild rice system or on receiving environments of the flooded paddy drainage. For instance, the high nutrient concentration of AWW can contribute to eutrophication and deterioration of water quality, and ammonia and metals within the AWW can result in significant toxicological effects. This research assessed the ecological effects of AWW on ecosystem health, using zooplankton communities as biological indicators within mesocosms planted with wild rice. Three experiments were conducted in different simulated Northern wild rice (*Zizania palustris)* ecosystems: established wild rice wetlands (UM-EW), natural wild rice stands (UM-WR), and commercial paddies (R&L). AWW was applied to treatment mesocosms across a gradient of loadings. Environmental DNA (eDNA) metabarcoding was used to analyze the zooplankton communities and was compared to standard morphological identifications to determine the efficacy of this emerging method. At environmentally relevant AWW loadings, the effects on zooplankton communities were minimal. However, calanoid copepods in the R&L study exhibited a significant sensitivity to AWW exposure. In high AWW loading treatments, increased eutrophication and declining water quality led to shifts in zooplankton community dynamics. Ammonia and metal toxicity were not identified as primary drivers of these changes. Using eDNA metabarcoding proved highly effective in achieving significant taxonomic depth of the

zooplankton taxa present. While community composition results did vary between methods, similar trends and responses were observed. Additionally, using designed targeted primer sets rather than a universal primer provided a more comprehensive assessment of the zooplankton community. This research advances our understanding of AWW impacts on aquatic ecosystems and demonstrates the potential of eDNA metabarcoding for biodiversity monitoring. These findings will help inform future wild rice-AWW systems of acceptable nutrient loadings to minimize ecosystem impacts.

Acknowledgements

From the start to the end of my master's, there have been so many amazing experiences and opportunities, including making many friendships, visiting or living in new cities, and so much learning and growth as a student and person. I would first like to thank my supervisors, Dr. Vince Palace and Dr. Mark Hanson. Vince, thank you for bringing me onto a project that has provided me with so much experience, knowledge, and enjoyment, and for continuously providing ample advice, support, and encouragement throughout this process. Mark, thank you again for entrusting me to be one of your students and for the constant guidance on this journey. The largest thank you ever goes to my co-master's students, Krista Robertson and Nic Blandford; this research could not have been possible without the kindness, intelligence, and support from you both. I view our friendship as the most valuable takeaway from this whole process, and I will cherish the many memories we made together. I miss seeing you two daily, but I will catch you rats in the swamp soon.

I would also like to thank the many other people who provided assistance and guidance along the way, either big or small, you are appreciated. This includes all the amazing people of the ELA Tox Crew including Lauren Timlick, Dr. Madeline Stanley, Carolyn Currie, Kailey Carriere, Heather Jovanovic, Dr. Lisa Peters, Hakeem Omilowo, and Dr. José Luis Rodríguez-Gil. Everyone in the Docker Lab, particularly Jessie Ogden, thank you for training and educating me. Then, with the most emphasis, a big thank you to Braedon Humeniuk for training me in zooplankton identification and for always going out of your way to give a helping hand. Also, thank you to R&L Acres for providing space and resources to conduct our research. And thank you to Kenton McCorquodale-Bauer for your help with DNA bioinformatics.

Shelby Mackie of the University of Windsor was a pillar in the success of my research. She graciously provided me with training, guidance, and assistance for the eDNA lab work I completed at the University of Windsor. Working closely together while I was in Windsor, we quickly became friends, and I am so thankful to have had this cheerful person in my life while I was away from home. I would also like to thank Daniel Heath for welcoming me into his lab at GLIER, providing me with lab space, supplies, and mentorship.

The funding that made this project possible was provided by the Myera Group and the IISD Experimental Lakes Area. I am also grateful to have been awarded funding from the University of Manitoba Faculty of Graduate Studies, NSERC (Canada Graduate Scholarship – Master's & Indigenous Scholars Supplement Award), IISD – Experimental Lakes Area (Graduate Fellowship), and the University of Manitoba (Master's Award for Indigenous Students).

Finally, I would like to thank the amazing support system in my personal life, including my parents, my sister Sarah, my grandparents, Rick and Char Cardinal, and my lovely friends. Thank you for supporting me throughout the last few years; despite what I do basically being a big question mark, you all provided so much help and encouragement and for that, I could not be more thankful. The final person that I can't thank enough for getting me through the worst days and for always believing in me is my partner, Mack. Thank you for always being there with motivation, laughter, and love.

Table of Contents

List of Tables

List of Figures

Chapter 1: Introduction

1.1 Thesis Overview

Aquaculture wastewater (AWW) is high in nitrogen and phosphorus, making it a highly beneficial and sustainable fertilizer source for wild rice cultivation (Cripps & Bergheim, 2000; Dauda et al., 2019; Piedrahita, 2003). Inland aquaculture systems in Canada have been found to increase phosphorus, total nitrogen, and ammonia concentrations in receiving waters by 8, 2.5, and 12 times, respectively, compared to upstream concentrations due to AWW discharge (Lalonde et al., 2015). Wild rice requires significant inputs of conventional fertilizers to achieve successful growth; thus, pairing wild rice with AWW is a sustainable method of capitalizing on the nutrient rich aquaculture wastewater that would have otherwise gone unused (Blandford, 2024; Sims et al., 2012; Porter, 2019). Wild rice exists in the natural environment or as a commercial strain within flooded paddy fields. The use of AWW as a fertilizer poses concerns for the aquatic environment, both within the wild rice systems and to downstream environments that receive drainage from the flooded paddies. The concerns to the aquatic ecosystem include eutrophication, ammonia toxicity, metal toxicity, and other negative impacts often associated with nutrient loading.

This thesis focuses on the effects of AWW loading on ecosystem health, using zooplankton community response as a bioindicator. This study was conducted in Winnipeg and Sperling, Manitoba, using experimental mesocosms to simulate AWW loading within established wetlands, natural wild rice stands, and commercial flooded paddy systems. This thesis is presented in a traditional format since each of the three studies had similar and overlapping components. The outcomes of this research will help to identify the maximum AWW loading that

can be applied to wild rice systems that optimize growth without compromising the health of freshwater ecosystems.

1.2 Aquaculture Wastewater

As the global population continues to rise, the Earth's food production systems are attempting to meet this demand (Boyd & McNevin, 2015). An industry that is drastically increasing production to meet these needs is aquaculture. Aquaculture is the fastest growing food production system in the past 50 years growing 7.5% per year globally since 1970 (FAO, 2020). In addition, the global consumption of fish has increased; fish accounts for 17% of the global population's total animal protein intake (FAO, 2020). In 2022, the Canada aquaculture industry produced 166,265 tonnes of product, this is triple the aquaculture production that occurred 30 years ago in the country (Statistics Canada, 2023). Marine-based aquaculture is the dominant sector in Canadian finfish aquaculture, with farming predominantly focused on Atlantic salmon (*Salmo salar*), followed by inland aquaculture that farms species like rainbow trout (*Oncorhynchus mykiss)*, tilapia, and Arctic char (*Salvelinus alpinus*) (Podemski and Blanchfield, 2015). Aquaculture is defined as the cultivation of aquatic animals and plants in either freshwater or marine systems and can be quite diverse depending on if the site is an inland or coastal system (Boyd & McNevin, 2015). This thesis will focus on the effect of AWW generated from inland finfish aquaculture systems on ecosystem health, as these systems are the most abundant globally and the most relevant to the broader research objectives of the study (FAO, 2020).

Constructed ponds, flow-through systems, cages, and land-based recirculating systems are the various types of inland systems used for aquaculture (Boyd & McNevin, 2015; Dauda et al., 2019). Each system manages aquaculture differently regarding, fish species, rearing conditions, fish feed, and waste management (Cripps & Bergheim, 2000; Dauda et al., 2019).

Thus, the type of cultivation system can greatly influence the properties and abundance of the waste produced (Dauda et al., 2019; Piedrahita, 2003). As the aquaculture industry intensifies, there needs to be consideration of the possible environmental impacts of the waste generated from these facilities. In addition, Podemski and Blanchfield (2015) indicated that we have a lack of research on the environmental effects of land-based freshwater aquaculture systems and cited the need for research on the effects of AWW to the species composition, biomass, and productivity of zooplankton and other aquatic biota.

The quantity, composition, and toxicity of the AWW depends on several different production factors (Dauda et al., 2019; Piedrahita, 2003). For example, various chemicals can be used in aquaculture including antibiotics, disinfectants, and antifoulants (Boyd & Massaut, 1999; Boyd & McNevin, 2015; Dauda et al., 2019). The release of these contaminants of concern in AWW vary from facility to facility, because their use is on a case-by-case basis (Dauda et al., 2019). However, the antifoulants used can contain metals including zinc and copper that can have potential toxic effects to aquatic life, which will be discussed later in this chapter. The primary component of AWW is typically waste products derived from the feed supplied to the fish (Cripps & Bergheim, 2000; Dauda et al., 2019; Piedrahita, 2003). This includes uneaten feed and/or the corresponding excretion products. The phosphorus and nitrogen within these products are of the greatest environmental concern and their effect are the focus of this thesis.

The release of AWW to the aquatic environment can result in increased turbidity, nutrients, and organic matter, all of which can degrade water quality (Cripps & Bergheim, 2000). Phosphorus and nitrogen for example can exist in either the suspended solid or dissolved form within AWW. Suspended solids are generated from uneaten food and feces. Fish fecal matter can contain anywhere between 3.6-35% of the nitrogen and 15-70% of the phosphorus from the

nutrients present in the feed consumed, largely because fish typically retain less than 50% of the nutrients they consume (Dauda et al., 2019; Piedrahita, 2003). A study on 14 inland aquaculture facilities in Atlantic Canada, farming either Atlantic salmon, speckled trout, rainbow trout, or Arctic char, found at the locations of effluent discharge mean concentrations of total phosphorus, total nitrogen, and ammonia of 0.101 mg/L, 0.83 mg/L, and 0.35 mg/L, respectively (Lalonde et al., 2015). When compared to the upstream location of these facilities, the concentrations of total phosphorus, total nitrogen, and ammonia, were 8, 2.5, and 12 times greater at the effluent discharge site, respectively (Lalonde et al., 2015). In addition, measurements 100 metres downstream of the effluent discharge location were collected, elevated concentrations of these nutrients were still seen but to a lesser extent, with concentrations increased to a magnitude of 2-7 times greater than the upstream location (Lalonde et al., 2015). This indicates that discharged AWW, can result in changes to the nutrient dynamics of the ecosystem in the direct area surrounding the site of discharge, as well as at locations further downstream.

Dissolved nutrients in AWW are either a product of excretion or microbial decomposition of suspended solids. Dissolved nitrogenous compounds within AWW can be in the form of ammonia, which is typically a product of excretion, or as a further decomposed nitrite and nitrate (Dauda et al., 2019). The un-ionized (NH_3) and ionized (NH_4^+) forms of ammonia exist in equilibrium within water and speciation is dependent on water temperature and pH (Emerson et al., 1975). The summation of both forms of ammonia is described as total ammonia nitrogen (TAN). The concentration of TAN in AWW is highly variable due to the range released from excretion. Piedrahita (2003) calculated estimated concentrations of total nitrogen in effluent based on water use, aquaculture system type, and cold-water fish nutrient retention from feed, resulting in a range of 0.2-18 mg/L, with fully recirculating systems on the maximum end of this

range. In addition, it has been recommended that aquaculture effluents contain less than 5 mg/L of TAN (Dauda et al., 2019). The release of ammonia into the receiving environment, especially when conditions allow for a high concentration of un-ionized (NH_3), is concerning because it is highly toxic to aquatic organisms, the toxicity of ammonia to invertebrates will be discussed further below (Environment Canada, 1999). Dissolved phosphorus in AWW is typically found as phosphate. When released into the aquatic environment in high concentrations, phosphorus will drive primary productivity, as phosphorus is often limiting, resulting in eutrophication of the receiving waters (Schindler, 2008). Highly eutrophic environments are typically described as systems of poor water quality (Wetzel, 2001). Changes to aquatic ecosystems because of aquaculture effluent have been reported, for example, downstream of several inland salmon hatcheries, discharged effluent resulted in increased concentrations of phosphate with the greatest concentrations reaching 80-115 μg/L (Munro et al., 1985). They also reported elevated downstream chlorophyll-*a* concentrations as a response of the nutrient loading from effluent (Munro et al., 1985). The subsequent effects of degraded water quality on zooplankton communities will be explored later within this chapter.

Metals can be found in AWW as they are typically used as antifouling agents or as additives to fish feed for nutritional purposes (Ahmad et al., 2021; Burridge et al., 2010). The two most used metals for antifouling are copper and zinc as they have been described as having less environmental impact, since they are highly insoluble in water and will likely bind to sediment (Boyd & McNevin, 2015; Chen et al., 2021). However, several studies have found copper and zinc accumulating near aquaculture discharge locations, with concentrations in sediment often exceeding water quality guidelines (Burridge et al., 2010). Other studies have found the mean concentrations of copper and zinc at aquaculture effluent discharge locations to

be 2.4 and 3.9 μg/L (Lalonde et al., 2015). Settled solid fish manure from rainbow trout farms in Ontario were tested for copper and zinc, the concentrations found were a range of 17-99 mg/kg and 274-916 mg/kg, respectively (Naylor et al., 1999). These concentrations of copper and zinc, when directly loaded into an aquatic environment, would pose significant threats to aquatic organisms, as guideline concentrations (see Section 1.3.4) could likely be exceeded. Nonetheless, the use of antifoulants and feed containing metals is variable and highly unknown, some studies have even reported that minimal or undetected concentrations of metals were found within proximity of aquaculture facility discharges sites (Boyd & McNevin, 2015). The potential ecological toxicity and guidance limits of copper and zinc will be discussed later in this chapter (Section 1.3.4).

1.3 Zooplankton

1.3.1 Zooplankton as an indication of water quality

Zooplankton are important organisms within aquatic environments due to their intermediate position within the trophic food web (Gagneten & Paggi, 2009). Thus, zooplankton play a critical role in energy transport and nutrient cycling between primary producers and higher trophic levels (Carpenter et al., 1985). Zooplankton are also highly responsive to biotic and abiotic factors (Rusak et al., 2002). For example, biotically zooplankton are influenced by the abundance of both higher and lower trophic levels, resulting in top-down or bottom-up ecosystem dynamics, respectively (Carpenter et al., 1985). In addition, abiotic factors such as pH, temperature, turbidity, and water chemistry, can all contribute to a variety of zooplankton community responses, resulting in shifts in patterns of abundance, distribution, and diversity (Shurin et al., 2010). Zooplankton can also be found across a diverse range of aquatic habitats due to their rapid adaptability to most physicochemical factors (Gannon & Stemberger, 1978).

Additionally, using zooplankton to understand an ecosystem can be much more cost effective than using a fish monitoring program to gather similar insight (Jeppesen et al., 2011). Therefore, because of these many desirable attributes, zooplankton can successfully be used as effective indicators of the functioning and quality of the aquatic environment (Jeppesen et al., 2000).

Zooplankton are commonly utilized as indicators of water quality in aquatic ecosystems (Gannon & Stemberger, 1978). Many different parameters of zooplankton can be measured and analyzed including diversity, richness, abundance, biomass, zooplankton taxa ratios, and the presence or absence of particular species. The response of these zooplankton parameters can then be used to formulate an assessment of water quality. For instance, research on the effect of rainbow trout cage aquaculture established in a lake in northwestern Ontario found double the concentration of phytoplankton from background levels (Paterson et al., 2010). However, total zooplankton communities and densities did not change, indicating water quality conditions remained optimal for zooplankton (Paterson et al., 2010). In this case, measuring the zooplankton metrics allowed for researchers to better understand the effects of the aquaculture operation that would not have been observed by solely measuring the nutrients or primary producers. Apart from the above study, the use of zooplankton as indicators of water quality when exposed to AWW is limited, but zooplankton have proven valuable as indicators within other contaminated or nutrient enriched environments. For example, Gagneten and Paggi (2009) analyzed zooplankton community response in rivers impacted by varying levels of metal contamination. They found that zooplankton diversity and richness corresponded to the level of observed contamination, thus, these parameters were reliable and effective indicators (Gagneten & Paggi, 2009). A different study, conducted by Stamou et al. (2020), used zooplankton to assess the ecological water quality in Mediterranean lakes. While they examined zooplankton

abundance and biomass, they also used a zooplankton ratio (abundance of Calanoida/abundance of Cladocera + Cyclopoida) for the water quality assessment since a higher abundance of calanoid copepods can reflect an oligotrophic system, while cladocerans and cyclopoid copepods are usually more abundant in eutrophic systems (Gannon & Stemberger, 1978; Kane et al., 2009; Stamou et al., 2020). Each of these metrics used were significantly correlated to eutrophication status of the lakes and ecological water quality, indicating the effectiveness of using zooplankton as indicators of ecosystem health (Stamou et al., 2020). The presence of specific zooplankton species can also be indicators of water quality. For example, the species from the rotifer genera, *Trichocerca*, *Pompholyx*, *Filinia*, are often associated with eutrophication (Gannon & Stemberger, 1978).

1.3.2 Zooplankton community response to eutrophication

The potential effects of eutrophication can include increased biomass of algal communities, the increased presence of toxic algal species, decreases in hypolimnetic dissolved oxygen and subsequent fish kills, increased turbidity, and reduced species diversity (Smith & Schindler, 2009). Some of the consequences of eutrophication can have secondary impacts on zooplankton; thus, there are multiple stressors to consider when assessing the effect of eutrophication. For instance, an increase in algal biomass has been found to positively influence zooplankton abundance due to increased food availability, demonstrating a bottom-up response (Patalas & Salki 1973; Blomqvist et al., 1993). However, at a certain threshold of abundance of algae, this relationship can shift, leading to reduced zooplankton taxonomic diversity and richness (Jeppesen et al., 2000). Cremona et al. (2021) determined total nitrogen and phosphorus concentrations of 700 μg/L and 70 μg/L, respectively, to be the threshold concentration at which a decrease in zooplankton abundance or biomass occured.

Zooplankton species that are more tolerable to undesirable water quality conditions will tend to dominate over time (Sternberger & Lazorchak, 1994). Generally, under eutrophic conditions an increased relative abundance of rotifer species is common, thus reducing overall diversity (Sternberger & Lazorchak, 1994). Gutierrez et al. (2020) examined zooplankton community composition in streams of varying trophic status. They found that in eutrophic streams, rotifers represented 96% of all zooplankton taxa measured, compared to only 42% in mesotrophic streams. Rotifers and other small-bodied taxa tend to dominate under stressed conditions due to their rapid turnover and growth rates, as well as general tolerance (Gannon & Stemberger, 1978; Shurin et al., 2010). In addition, cladoceran (e.g., *Daphnia* spp.) are known to be a more competitively advantageous zooplankton taxa; however, they are more sensitive to changes in environmental conditions (Gagneten & Paggi, 2009). Therefore, as the cladoceran taxa abundance decreases as a response to eutrophication, the community structure will change, and, as a result, the more tolerant species will typically increase in abundance. Similar findings of declines in species diversity and richness as a result of increased trophic status have been observed in other studies (Declerck et al., 2011; Gannon & Stemberger, 1978; Jeppesen et al., 2000; Shurin et al., 2010; Stemberger & Lazorchak, 1994). This relationship is typically shown as a significant negative association between various zooplankton community metrics and total phosphorus and/or chlorophyll-*a*.

Another direct effect of eutrophication is the depletion of dissolved oxygen which generates hypoxic (dissolved oxygen <2 mg/L) or anoxic (dissolved oxygen <0.5 mg/L) environments and secondary effects on zooplankton (Jenny et al., 2016). General hypoxia will occur at night when the production of oxygen through photosynthesis is limited and respiration dominates (Karpowicz et al., 2020). Hypolimnetic oxygen depletion occurs when the algal

blooms produced during eutrophic conditions sink and undergo decomposition, resulting in an increased biological oxygen demand (Diaz, 2001; Doubek et al., 2018). Reduced dissolved oxygen concentrations have been documented downstream of aquaculture facilities due to increased biological oxygen demand, resulting in dissolved oxygen reductions of 0.7 to 2.4 mg/L (Podemski & Blanchfield, 2015). These oxygen deficient conditions can then significantly impair the functioning of zooplankton communities, as oxygen is a required component of their respiration (Devol, 1981). As a result of oxygen stress, communities will generally shift to the dominance of smaller-bodied taxa which are prone to be more tolerant to low-oxygen conditions (Doubek et al., 2018; Karpowicz et al., 2020). Rotifers have specifically demonstrated excellent tolerance of low-oxygen conditions, and as such have been found to have the greatest biomass during anoxic conditions of all zooplankton taxa (Esparcia et al., 1989; Karpowicz et al., 2020). In addition, zooplankton often vertically migrate daily to the hypolimnion to avoid predation and cellular damage from UV radiation that would occur within the epilimnion during the day (Doubek et al., 2018; Karpowicz et al., 2020). If hypoxic conditions are present within the hypolimnion, zooplankton can experience increased mortality conditions in the epilimnion, or significant metabolic stress within the hypolimnion (Doubek et al., 2018). However, the effect of hypoxia varies among zooplankton species; some species are more tolerant to reductions in dissolved oxygen compared to their predators, as such these zones can then be utilized as a place of refugia (Vanderploeg et al., 2009; Nolan et al., 2019). For instance, *Daphnia* spp. have been found residing in extremely hypoxic waters (dissolved oxygen <0.09 mg/L), which can be attributed to their ability to produce and utilize hemoglobin as a strategy to withstand low oxygen stress (Nolan et al., 2019; Wieder & Lampert, 1985).

Another stressor as a result of eutrophication to consider is the effect of cyanobacteria, which are typically the most dominant phytoplankton group within algal blooms (Spencer & King, 1987). Zooplankton communities that co-exist with cyanobacteria tend to demonstrate decreased abundance and growth rates, and an increased dominance of small-bodied zooplankton (Hansson et al., 2007; Jiang et al., 2017). This effect has been hypothesized to be caused by hepatotoxins, which are secondary metabolites produced by many cyanobacteria species (Carmichael, 1994; Ger et al., 2016). Microcystin, a common cyanobacteria toxin, induces a toxic effect through the inhibition of protein phosphatases, which results in oxidative stress and intracellular problems (Zong et al., 2018). For instance, Hansson et al. (2007) observed a negative relationship between zooplankton biomass and microcystin concentration, within six eutrophic Swedish lakes. Another contributing factor is the poor food quality of cyanobacteria for zooplankton, due to their filamentous morphology and low nutrient content (Ger et al., 2016, Wilson et al., 2006).

Food quantity versus food quality also plays an major role in the community composition of zooplankton. Eutrophication can lead to changes in algal abundance as previously discussed, but alterations to food resource quality may simultaneously occur, including changes to the species composition and nutritional content of phytoplankton (Taipale et al., 2019). For instance, in a mesocosm experiment, nutrient loading has been shown to shift the composition of primary producers to predominately filamentous algae (Butzler & Chase, 2009). Other responses have been seen including an increase in phytoplankton species with lower nutritional content, as reflected by a lower measured concentration of essential biomolecules (Taipale et al., 2019). As a result, when an ecosystem is eutrophic, resource availability is not always the sole factor influencing zooplankton abundance. Resource quality and digestibility have been shown to better

drive zooplankton production in these instances (Kelly et al., 2024). A study was conducted on eutrophic lakes at Fort Whyte in Winnipeg, Manitoba and found that an increase in the percentage of filamentous algae resulted in a negative effect to Daphnia abundance (Dupuis and Hann, 2009). Filamentous algae tend to have this effect on larger-sized zooplankton, like Daphnia, because these longer strands have been shown to impact the filtering rates and feeding abilities (Dupuis & Hann, 2009). The effect eutrophication can have on phytoplankton composition can cause indirect effects to zooplankton, as phytoplankton have different fatty acids, amino acids, and sterols that zooplankton must obtain from their diet for optimal performance (Taipale et al., 2019). Research by Zhu et al. (2023) found that zooplankton increased their grazing rates to compensate for the lack of essential nutritional components obtained from phytoplankton within a nutrient-rich ecosystem. Additionally shifts to zooplankton species that are more adapted to changes in nutritional quality will more likely persist under extreme eutrophication conditions (Moody & Wilkinson, 2019).

1.3.3 Ammonia toxicity to zooplankton

Ammonia is a known toxicant to zooplankton and other aquatic life, which has been tested through laboratory toxicity tests and whole-ecosystem settings (ECCC, 1999; EPA, 2013; Thurston et al., 1981). The Canadian water quality guideline for un-ionized ammonia (NH_3) in the aquatic environment to ensure the protection of all organisms is 0.019 mg/L (CCME, 2010). The guideline sets limits for the un-ionized species because it is the principal toxic form of ammonia (Environment Canada, 1999). The guideline for TAN takes into consideration temperature and pH because these factors will considerably influence the equilibrium between un-ionized and ionized ammonia (Emerson et al., 1975; Thurston et al., 1981). For reference, the concentration of un-ionized ammonia in freshwater can increase ten-fold with one unit increase

in pH (Environment Canada, 1999). It is especially important to be cognizant of this equilibrium when considering the effect of ammonia during algal blooms. Prolific algal blooms can deplete carbon dioxide within the water, due to the mass carbon fixation occurring as part of photosynthesis, which in turn can cause an increase in pH (Verspagen et al., 2014). Thus, blooms can shift the equilibrium to a larger proportion of the un-ionized ammonia fraction present. Moreover, as previously indicated, hypoxic conditions are common due to respiration and decay of algal blooms; however, un-ionized ammonia is increasingly toxic as dissolved oxygen decreases (Thurston et al., 1981; Ip et al., 2003).

Standardized laboratory toxicity tests have demonstrated that un-ionized ammonia is toxic to zooplankton. Environment Canada (1999) reported that the zooplankton species *Daphnia pulicaria* and *Simocephalus vetulus* mean acute (48-96 hr) LC_{50} values from exposure to un-ionized ammonia are 1.160 mg/L and 1.185 mg/L, respectively. The most recent EPA (2013) ammonia report used standardized values of TAN (adjusted to pH of 7 and temperature of 20°C), to indicate the mean acute toxicity results of all applicable studies. The most sensitive zooplankton were *Daphnia* spp., with a reported genus mean acute value (48-hr LC_{50}) of 125.0 mg/L TAN, followed closely by *Simocephalus vetulus*, *Ceriodaphnia* spp., and *Chydorus sphaericus* with values of 142.9, 143.9, and 162.6 mg/L TAN, respectively (EPA, 2013). The mechanism of ammonia toxicity on zooplankton has not been extensively studied throughout the literature, as much of the focus is on fish. However, it has been demonstrated that ammonia exposure to zooplankton exhibits a negative effect on enzymatic activities of glutathione (GSH), which is a critical extracellular tripeptide that prevents oxidative stress in organisms (Liang et al., 2020; Park et al., 2017). Thus, if GSH is deficient, there is an increased potential for oxidative stress, which is likely the cause of ammonia toxicity in zooplankton (Liang et al. 2019). Select

fish and crustacean species are relatively more sensitive to ammonia than zooplankton; regardless, it is still important to consider the effect on zooplankton due to the important functional components they provide to an ecosystem. In addition, within the present study fathead minnows (*Pimephales promelas*) are the only test fish species included, and this species is comparatively less acutely sensitive than all the previously indicated test zooplankton species (EPA, 2013). The genus mean acute value (4-day LC_{50}) for fathead minnows is 159.2 mg/L TAN. However, when considering chronic exposure to un-ionized ammonia, fathead minnows are comparatively more sensitive (mean 28-day EC_{20} of 0.173 mg/L NH_3) than the most sensitive zooplankton species (*Ceriodaphnia dubia*) with a measured mean 7-day EC_{20} of 0.520 mg/L NH_3 (ECCC, 1999; EPA, 2013).

The ecological and toxicological effects of ammonia to zooplankton within the environment are not as intensively studied as the effects within a laboratory setting (Camargo & Alonso, 2006). The effect within the environment is important to consider because high concentrations of nitrogenous species are released into aquatic environments from anthropogenic sources globally, resulting in inorganic nitrogen pollution (Camargo & Alonso, 2006). In addition, evaluating the effect within the environment considers multiple stressors and will provide a site-specific community response that cannot be easily represented within laboratory tests (Calow & Forbes, 2003; Yang et al., 2017). For instance, a study on the effect of ammonia on zooplankton communities was conducted in Tai Lake, China; a system with deteriorated water quality due to intensive nutrient loading. Yang et al. (2017) found ammonia to significantly influence zooplankton community structure more than any other environmental factor assessed. Observed trends included, decreased relative abundance of copepods and cladocerans with increasing TAN concentration, and rotifers were less sensitive to increases in TAN compared to

other zooplankton taxa (Yang et al., 2017). Similar trends have also been observed within other zooplankton community studies (Arauzo, 2003; Cremona et al., 2021; Zhao et al., 2021). Yang et al. (2017), also calculated an HC_5 value, based on the species sensitivity distribution of the study, to be 1.4 mg/L TAN, this value indicates the threshold of TAN in the natural environment that could minimize the effect to zooplankton communities (Yang et al., 2017).

1.3.4 Metal toxicity to zooplankton

Metals used in aquaculture, particularly copper and zinc, when released into the environment through AWW could harm zooplankton as these metals have been found to be toxic (De Schamphelaere & Janssen, 2009; Hoang et al., 2018; Martins et al., 2018). The aquatic ecosystem composition can influence the toxicity of copper and zinc, as they can alter the speciation and bioavailability of these metals (Burridge et al., 2010). For instance, when aquatic environments are high in dissolved organic carbon the metals will bind to the organic matter resulting in decreased bioavailability and subsequently, reduced toxicity (Guardiola et al., 2012). If these metals are available for uptake into biota, they have the potential to persist and bioaccumulate which can exacerbate their toxicological effects (Ahmad et al., 2021; Garcia-Bueno & Marin, 2021). The copper guideline for the protection of aquatic life is between 2-4 µg/L, depending on water hardness as it alters the toxicity of copper (CCME, 1987). More specifically for zooplankton, the chronic toxicity of copper has been tested on *Daphnia magna*, which found a 21-d EC_{50} ranging from 41.5 µg/L to 316 µg/L (Schamphelaere & Janssen, 2009). This range in toxicity is due to the significant negative effect that was found to copper toxicity by increased pH and dissolved organic carbon. The acute and chronic exposure guideline for the protection of aquatic life are 37 µg/L and 7 µg/L of zinc, respectively (CCME, 2018). These values can be calculated more precisely using equations when pH and hardness data are known,

as these parameters can alter zinc toxicity (CCME, 2018). A microcosm study found a 98-d EC_{50} of 24.23 µg/L of zinc to total abundance of zooplankton (Hoang et al., 2021). They also observed changes to the zooplankton community composition that differed from the controls, with cladoceran shifting from the most abundant prior to exposure, to complete disappearance of this group by the end of the study (Hoang et al., 2021). To further illustrate the toxicity of copper and zinc within an aquaculture setting, a review examined the ecotoxicity of specific aquaculture antifoulants, including the common copper- and zinc-based types, using calculated predicted no effect concentrations (PNEC) derived from available laboratory toxicity datasets (Martins et al., 2018). The zinc and copper based antifoulants had calculated PNECs of 0.071 µg/L and 0.019 µg/L, respectively (Martins et al., 2018). They also found zooplankton to be among the most sensitive species to these antifoulants (Martins et al., 2018).

1.4 Environmental DNA Metabarcoding

The efficient and reliable use of environmental DNA (eDNA) metabarcoding to assess biodiversity within the aquatic environment has increased substantially in the past decade (Taberlet et al., 2012a; Valentini et al., 2016). All organisms shed DNA via metabolic waste, cellular, or extracellular tissue (Fitzgerald et al., 2021; Taberlet et al., 2012b). This genetic material or the DNA from the whole organism in its entirety (e.g., microorganisms or micro-invertebrates), both referred to as eDNA, can be extracted from water that was sampled from the aquatic environment (Fitzgerald et al., 2021; Taberlet et al., 2012b; Wu et al., 2022). The methods of analysing eDNA to detect various species, from microorganism to macro-vertebrates, have expanded and revolutionized immensely (Sato et al., 2017; Seymour et al., 2021; Wu et al., 2022). The two most common methods of eDNA analyses for species detection currently include quantitative polymerase chain reaction (qPCR) and metabarcoding. The qPCR method is a

species-specific technique that uses polymerase chain reaction (PCR) primers to target and amplify specific DNA fragments allowing for the detection of the particular species of interest (Creer et al., 2016; Ficetola et al., 2008; Wu et al., 2022). This method is commonly used to detect the presence of invasive or at-risk species (Creer et al., 2016; Ficetola et al., 2008; Taberlet et al., 2012b). The focus of this thesis is on the use of metabarcoding, which can be used to detect the entire taxonomy of a sample using next-generation sequencing (NGS), generating valuable information for biodiversity and community assessments (Kelly et al., 2014; Valentini et al., 2016; Wu et al., 2022).

Metabarcoding stems from barcoding, which uses PCR primers that are gene-specific to amplify a 'DNA barcode'; the most used gene for animal-based detections is the mitochondrial cytochrome c oxidase subunit I gene (COI) (Hebert et al., 2003; Ji et al., 2013; Taberlet et al., 2012b). As a result, extensive reference libraries exist that contain the barcode of any species that has been identified and sequenced (Marquina and Andersson, 2019). The entirety of the COI gene region is too large for current NGS technology; thus, shorter amplicon fragments (up to ~450 base pairs [bp]) from a portion of the gene region are used to identify thousands of species within a bulk sample, thus metabarcoding (Govender et al., 2022; Marquina & Andersson 2019). Several zooplankton metabarcoding studies have employed other gene regions in addition to COI, including the nuclear 18S or mitochondrial 16S small subunit ribosomal RNA genes (rRNA) (Casas et al., 2017; Lindeque et al., 2013; Meredith et al., 2021; Zhang et al., 2018). The use of smaller fragments is beneficial because of the improvement in the amplification of degraded or fragmented DNA that is typical of environmental samples, while still maintaining accurate taxonomic resolution (Govender et al. 2022; Taberlet et al., 2012a). One or more primers pairs can be used to amplify these smaller DNA fragments; a commonly used primer set

for zooplankton amplification was developed by Leray et al. (2013) to target a 313 bp long COI fragment. This primer pair was first used by Leray et al. (2013) where they designed a forward primer “mICOIintF” and used a reverse primer “jgHCO2198” that was redesigned by Geller et al. (2013). They used this primer to amplify DNA of the stomach contents of coral reef fish; however, the use of this primer has since expanded and research on its effectiveness for amplifying various freshwater organisms including zooplankton has been conducted (Leray et al., 2013; Zhang et al., 2018). To improve species detection, other studies have used multiple primers, targeted multiple different gene regions, designed new primers specific to their study, or a combination of each of these strategies (Clarke et al., 2017; Meredith et al, 2021; Zhang et al, 2018). These methods have been shown to better capture the taxonomic diversity of the sample and avoid underrepresentation of a species that would not have been found with just using one primer set (Clarke et al., 2017; Zhang et al., 2018). For example, Clarke et al. (2017) found that if they had only used a 18S primer set, they would have failed to identify cladocerans in their samples; however, when using COI primers they could capture the significant contribution to diversity that cladocerans had. Designing a new primer can be useful when a commonly used primer has been shown to poorly amplify specific species you may be trying to target, otherwise described as primer bias (Elbrecht and Leese, 2017; Pinol et al., 2014). Also, many of the commonly used primers were likely not originally designed to target the same research question your study may be trying to address; thus, designed primers can be more specific to the taxon and ecosystem of interest (Elbrecht and Leese, 2017).

After amplification of the DNA, high-throughput NGS is used to sequence the DNA, the sequences are then grouped into operational taxonomic units (OTUs) or amplicon sequence variants (ASVs), depending on the approach used to process the sequences (Creer et al., 2016; Ji

et al., 2013). Then the OTUs/ASVs can be assigned to specific taxonomic identification using various databases (e.g., GenBank) (Ji et al., 2013; Wu et al., 2022). The metabarcoding method is particularly beneficial because it can effectively identify a wide range of species. Although, incomplete taxonomic representation of all species in reference libraries is a common limitation of metabarcoding (Chen et al., 2023; Jo & Sasaki, 2024). Achieving this response using conventional enumeration methods would be quite challenging, costly, and time consuming (Kelly et al., 2014; Taberlet et al., 2012b; Valentini et al., 2016). In addition, existing biodiversity assessments can be destructive, invasive, or require a skilled taxonomist (Fitzgerald et al., 2021; Valentini et al., 2016).

From an ecotoxicology perspective, metabarcoding can be a useful tool for assessing community response to various contaminants (Ankley et al., 2021; Zhang, 2019). Typical ecotoxicology studies use laboratory tests of select representative species or indicator species as a means of identifying the effects of toxicants (Calow & Forbes, 2003). However, monitoring of community responses can help to better understand the impact on the entire ecosystem, especially in situations involving multiple stressors or regional specificities (Calow & Forbes, 2003; Yang et al., 2017; Zhang, 2019). It has been recommended that the use of metabarcoding in ecotoxicology studies be paired with conventional methods, as there are still limitations associated with eDNA metabarcoding (Zhang, 2019). For example, the developmental stage or sex of an organism cannot be defined from metabarcoding and this is a concern for chronic ecotoxicology tests that often use these parameters as endpoints in assessing contaminant response (Valentini et al., 2016). Other commonly cited concerns with metabarcoding across a range of taxonomy includes, primer bias associated with the use of a universal primer, and

underrepresentation of biodiversity due to missed detection of species (Pinol et al., 2019; Seymour et al., 2021; Wu et al., 2022).

Metabarcoding methods have been used to identify zooplankton communities within lakes and ecotoxicology related mesocosm studies. For instance, Mychek-Londer et al. (2020), used metabarcoding with COI primers to identify the aquatic invertebrates within eDNA samples of the Sydenham River and Grand River, two major tributaries of the Great Lakes in southwestern Ontario. Their analyses identified the following zooplankton: 160 rotifer species, 372 calanoid species, 19 bosminid species, 35 chydorid species, and 76 daphnid species. This study improved the understanding of the biodiversity of zooplankton and other invertebrate taxa at these locations, including the identification of known invasive and at-risk species (Mychek-Londer et al., 2020). Ankley et al. (2021) assessed the ecotoxicological effect of two oil-spill remediation methods on zooplankton communities within a shoreline enclosure study at the IISD Experimental Lakes Area, using conventional (i.e., morphologically identified taxonomy) and metabarcoding identification techniques. Metabarcoding and conventional identification rendered similar results at the family and genus level; however, more dissimilarities were evident at the species level. Additionally, both methods observed a negative impact to zooplankton community richness over the duration of the study when exposed to one of the examined remediation techniques (Ankley et al., 2021). A biodiversity focused study examined how the density of an exotic brook trout (*Salvelinus fontinalis*) species impacted crustacean zooplankton communities, using eDNA metabarcoding to monitor the response (Trepanier-Leroux et al., 2023). Using metabarcoding allowed for valuable information about the zooplankton communities to be gathered, including finding a presence of larger zooplankton where the brook

trout was not located and a shift to predation resistant small-bodied species where the brook trout was introduced (Trepanier-Leroux et al., 2023).

An issue previous metabarcoding studies have in common was the lack of complete reference libraries to pair the OTUs with a taxonomic identification. In the Ankley et al. (2021) study, eight zooplankton species that were identified taxonomically were not represented in the GenBank database at the time of analysis. Another issue surrounding metabarcoding was raised in Trepanier-Leroux et al. (2023), who commented that although *Daphnia middendorfiana* was abundant in taxonomically identified samples and COI reference sequences for this species exist in the databases, this species was not detected in their eDNA metabarcoding dataset (Trepanier-Leroux et al., 2023). This suggests that this species was misidentified when the sequence was added to the reference database and the incorrect sequence was paired with this species. Thus, to improve the effectiveness of metabarcoding to capture whole ecosystem diversity, reference sequences of the less commonly studied organisms and species specific to geographic regions need to be added accurately and with greater frequency to better capture the genetic diversity of a species and increase the probability of detection (Trepanier-Leroux et al., 2023).

Another area that lacks understanding related to eDNA is whether metabarcoding can be used to reliably track abundance and community composition over time (Bourque et al., 2023). This is due to the knowledge that environmental conditions, such as water temperature, can influence DNA quality and quantity (Stewart, 2019). Biotic factors can also influence DNA quantity, such as the movement of organisms within the water effecting the spatial and temporal detection of species (Jo et al., 2024). The organisms physiology can also effect DNA results, for example some zooplankton species will molt and release their exoskeleton, resulting in genetic material that could skew results using DNA reads as an estimate of abundance (Jo et al., 2024).

Additionally, eDNA reflects all genetic material in the collected sample and cannot be used to distinguish whether the source of the DNA at the time of collection came from a dead or alive organism (Dunker et al., 2017). Meanwhile, taxonomic identification typically just measures whole, living organisms which can be clearly observed by the analyst. Thus, there exists the potential for an over estimation of actual abundance when using eDNA methods (Dunker et al., 2017). A study conducted by Bourque et al. (2023) monitored *Daphnia magna* abundance over time in mesocosms and found that the eDNA results closely followed abundance counts, suggesting that eDNA can be used as a predictor of abundance. They hypothesized that dead organisms accumulating in their mesocosms did not contribute to an accumulation of DNA over time, and that when spikes of abundance occurred the surplus of living *D. magna* DNA was more likely reflected in the results than the DNA of dead ones (Bourque et al., 2023). These caveats of metabarcoding emphasize that conventional methods may still be required alongside metabarcoding to validate the results when assessing zooplankton community response, especially when the aim of the study requires an analysis of the species-level response.

1.5 Northern Wild Rice

Northern wild rice (*Zizania palustris*) is highly valued ecologically, culturally, and economically within its endemic regions. Wild rice is an emergent macrophyte that typically grows in littoral zones of lakes and in wetlands located in the northwestern United States and the Boreal Forest region of Canada (Porter 2019). Wild rice provides many ecosystem services including habitat for various birds, fish, invertebrates, epiphytes, and mammals (David, 2019). For Indigenous people, wild rice, or known as manoomin by the Anishinaabe, is an incredibly significant resource for sustenance, culture, and livelihood (David, 2019; MNDMR, 2008). The grains from wild rice stands have been harvested by Indigenous communities for thousands of

years for consumption, medicinal use, and for spiritual and sacred properties for use in ceremonies, feasts, and celebrations (David, 2019; MNDMR, 2008). In addition, wild rice grains can be harvested commercially from cultivated flooded paddy systems, resulting in an economically valuable product that meets the increased demand for this product (Ahmad et al., 2018; Porter et al., 2019). The consumer demand for wild rice can be attributed to its many nutritional benefits, as it has been found that wild rice is elevated in amounts of minerals, vitamins, proteins, fibre, and antioxidants (Surendiran et al., 2014). Also, the use of wild rice as a test species for ecotoxicity testing has been argued due to the aforementioned points, in addition to its sensitivity to contaminants and the ability for the plant to withstand routine monitoring in acute and chronic tests (Kornberger et al., 2023).

Wild rice plants also have the potential to enhance water quality through bioremediation. For instance, the feasibility of wetland plants as a tool to remediate wastewater effluents and other contaminants has been extensively explored and shown to be effective (Blandford et al., 2024; Pilon-Smits, 2005; Stanley et al., 2022). The natural processes within plants and microbes associated with their root zones (i.e., rhizosphere) can assimilate or biodegrade compounds of concern (Pilon-Smits, 2005). Wild rice specifically, assimilates a significant amount of nutrients from the surrounding environment for growth and production (Carpenter & Lodge, 1986; Sims et al., 2012). The most essential nutrient for wild rice growth is nitrogen followed by phosphorus (Pastor et al., 2017; Sims et al., 2012). In addition, root plaques, composed of ferric hydroxide precipitate via iron oxidation processes, absorb or are incorporated along with phosphates by plant roots, including wild rice (Jorgenson et al., 2013; Xu et al., 2009). Thus, via assimilation and nutrient sequestration, wild rice could effectively improve water quality by reducing the potential for algal blooms, decreasing the concentration of toxic nitrogenous and phosphorous

compounds, and improving physical and chemical parameters (e.g., dissolved oxygen, turbidity, etc.) in the water (Ahmed et al., 2021; Sims et al., 2012; Jorgenson et al., 2013).

Traditional monoculture crops are struggling to produce enough yield to meet the demands of the global population due to reductions in water supply, soil fertility, and consistent growing conditions (Rosenzweig et al., 2013). Wild rice has a high potential as a commercial crop to supplement current production (Porter, 2019). Ahmad et al. (2018) argue that wild rice as a crop in Canada is not reaching its fullest potential. The production of underutilized crops, like wild rice, generates an alternate food supply to the global food demand, thus, aiding in global food scarcity issues (Ahmad et al., 2018). Furthermore, a sustainable approach to wild rice cultivation may be achieved through the use of AWW as a nutrient rich fertilizer (Ahmed et al., 2020; Blandford, 2024). Commercial wild rice is often grown in flooded paddies, but this type of production requires a substantial amount of additional nutrients, often applied in the form of conventional fertilizer with the primary objective of augmenting nitrogen (Oelke et al., 1982; Porter, 2019; Sims et al., 2012). When aquaculture is paired with wild rice cultivation in flooded paddies, this could provide a practical and beneficial use for AWW, which would have otherwise been released into receiving waters, while still ensuring the successful growth of wild rice. In addition, since the wild rice will assimilate the nutrients from the surrounding waters it will act as a nutrient sink during periods of peak growth (Carpenter & Lodge, 1986; Sims et al., 2012). Thus, wild rice has the potential to bioremediate the surrounding nutrient-rich water, resulting in the reduction of the concentration of nutrients downstream of wild rice cultivation when the fields are drained for harvest. The acceptable amount of AWW that should be applied to wild rice paddies without causing significant deleterious impacts to the aquatic environment is currently

unknown. In addition, the use of AWW as a fertilizer source has several serious implications for the receiving aquatic ecosystem that must be considered, as discussed previously in this chapter.

1.6 The Use of Mesocosms in Ecotoxicology

Mesocosms are used in ecotoxicological studies to simulate a natural ecosystem, typically existing within an artificial stream, experimental pond, or enclosure system (Caquet, 2002). Using mesocosms allows for a thorough investigation of the potential effects of a contaminant within a contained, moderately controlled, and scaled-down system (Caquet et al., 2000). These systems can provide valuable information about an ecosystems response to a contaminant that could not be generated from laboratory studies, where their ability to extrapolate effects to the natural environment are often questioned (Graney, 1993). For instance, mesocosms studies can capture, effects to trophic cascades, species interactions, indirect effects, and effects to non-target organisms (Caquet, 2002; Fleeger, 2022). Moreover, attempting to assess ecosystem responses within the natural environment can be complex and only capture the current state of the system, whereas mesocosms can allow for replication and testing of a range of contaminant exposures to determine cause and effect, while still maintaining environmental realism (Caquet, 2002; Semlitsch & Boone, 2009). As a result, mesocosms provide a suitable middle ground between field and laboratory studies when needing to understand the effect of a stressor.

1.7 Objectives and Hypotheses

The focus of this research was to better understand how the pairing of AWW with wild rice systems could affect the ecosystem health within the wild rice aquatic environment and the receiving downstream environment. This was tested within experimental mesocosms, using the zooplankton community response as an indicator of ecosystem effects. During commercial wild rice cultivation, flooded rice paddies are typically drained into receiving waterways. As a result, the flooded paddy ecosystem prior to drainage represented the most extreme AWW loading scenario for zooplankton community exposure; thus, mesocosms were used to simulate these conditions. The objectives of this thesis were to:

1) Assess the response of zooplankton communities in mesocosms planted with wild rice and fertilized with a range of AWW

2) Determine the efficacy of eDNA to identify the zooplankton community biodiversity using metabarcoding techniques

The following hypotheses will be tested:

1) Zooplankton abundance and community composition will be affected by loading-dependent AWW additions

2) eDNA metabarcoding will be equally as effective as conventional taxonomic methods for identifying the diversity and abundance of the zooplankton communities.

To expand on the first hypothesis, several different predictions can be made about how the zooplankton community will respond. The AWW composition, and its fate in the ecosystem over time, will dictate how these predictions manifest. The generalized visualization of the

hypothesized direct and indirect effects of AWW can be seen in the conceptual model (Figure 1.1).

1) AWW will be high in nutrients like phosphorus and nitrogen which will increase algal abundance, thus, indirectly increasing zooplankton abundance.
2) AWW high in ammonia nitrogen will directly decrease zooplankton abundance.
3) AWW may contain metals that will directly decrease zooplankton abundance.
4) Should eutrophication persist with additional AWW additions, conditions will become deleterious indirectly resulting in a decrease in zooplankton abundance and shifts in the zooplankton community composition to species that are more tolerant to poor ecosystem conditions.

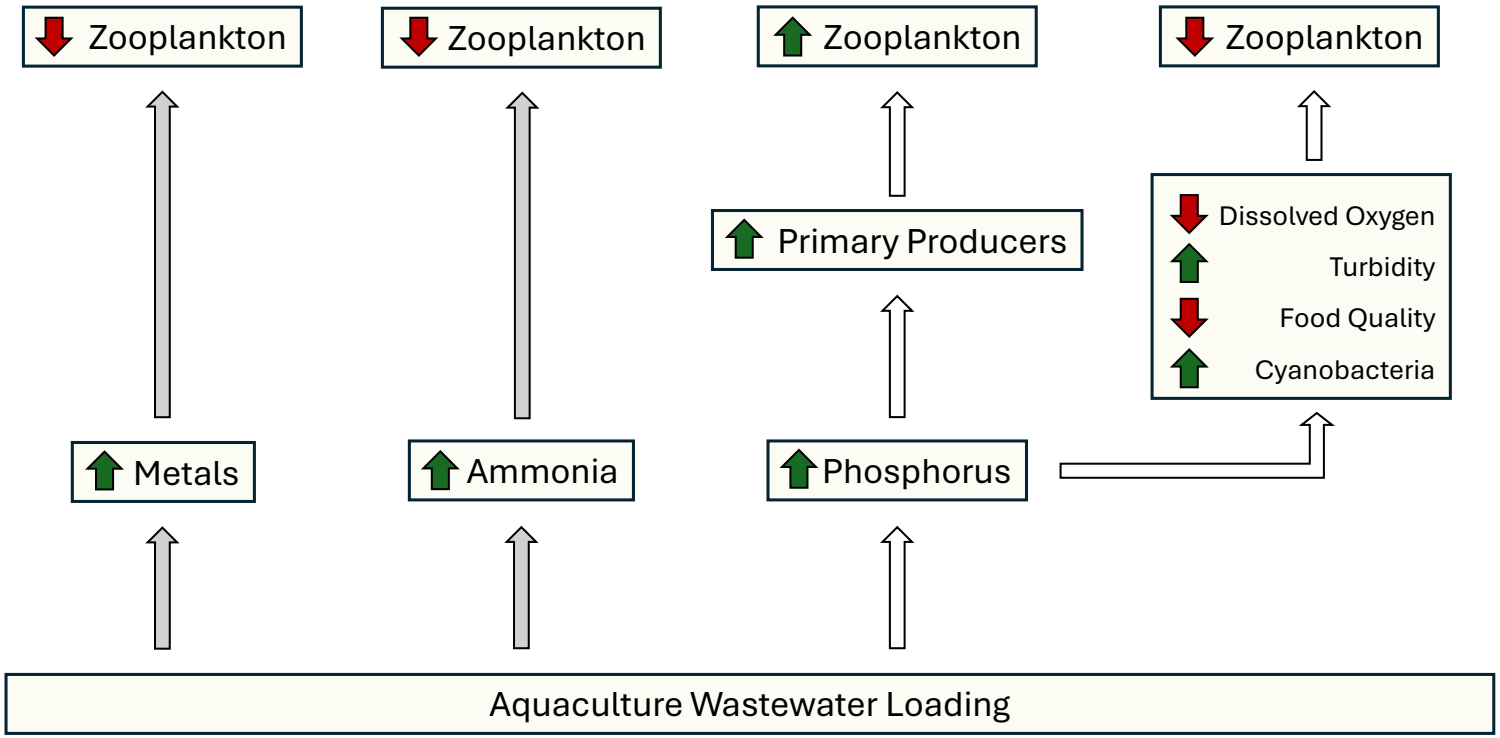

Figure 1.1: A conceptual model of the hypothesized effects to zooplankton due to aquaculture wastewater loading. The grey arrows between boxes represent direct effects on zooplankton and the white arrows represent indirect effects on zooplankton. The arrows beside each variable represent the hypothesized effect, red equals an expected decrease and green equals an expected increase.

Chapter 2: Methodology

2.1 Experiment Overview

To address the effect of AWW as a fertilizer for wild rice cultivation on zooplankton communities, two mesocosm studies were performed at different sites from May to September 2022. The first study occurred at R&L Acres, north of Sperling, Manitoba, Canada where 15 mesocosms were planted with a commercial strain of wild rice and were designed to simulate a commercial flooded wild rice paddy system. The second study occurred simultaneously at the Prairie Wetland Research Facility at the University of Manitoba, Winnipeg, Manitoba, Canada where 17 mesocosms were planted with a natural strain of wild rice. Of these 17 systems, seven of the mesocosms simulated a wetland system containing natural wild rice and other wetland vegetation, while the remaining ten mesocosms simulated a flooded natural wild rice paddy system with wild rice as the sole type of vegetation planted in the system. In addition to wild rice, all mesocosms at both sites were amended with soil, water, zooplankton, and fish to understand how AWW affects other ecosystem components (Figure 2.1). Other components of this study including nutrient dynamics, wild rice plant growth, bioremediation, and the ecotoxicological effect of AWW on resident fish are described elsewhere (Blandford, 2024; Robertson, 2024). The present study used two approaches to understand and identify the zooplankton communities, morphological identification and eDNA metabarcoding. These methods are detailed below along with the experimental design of both sites, water quality methodology, and statistical analyses.

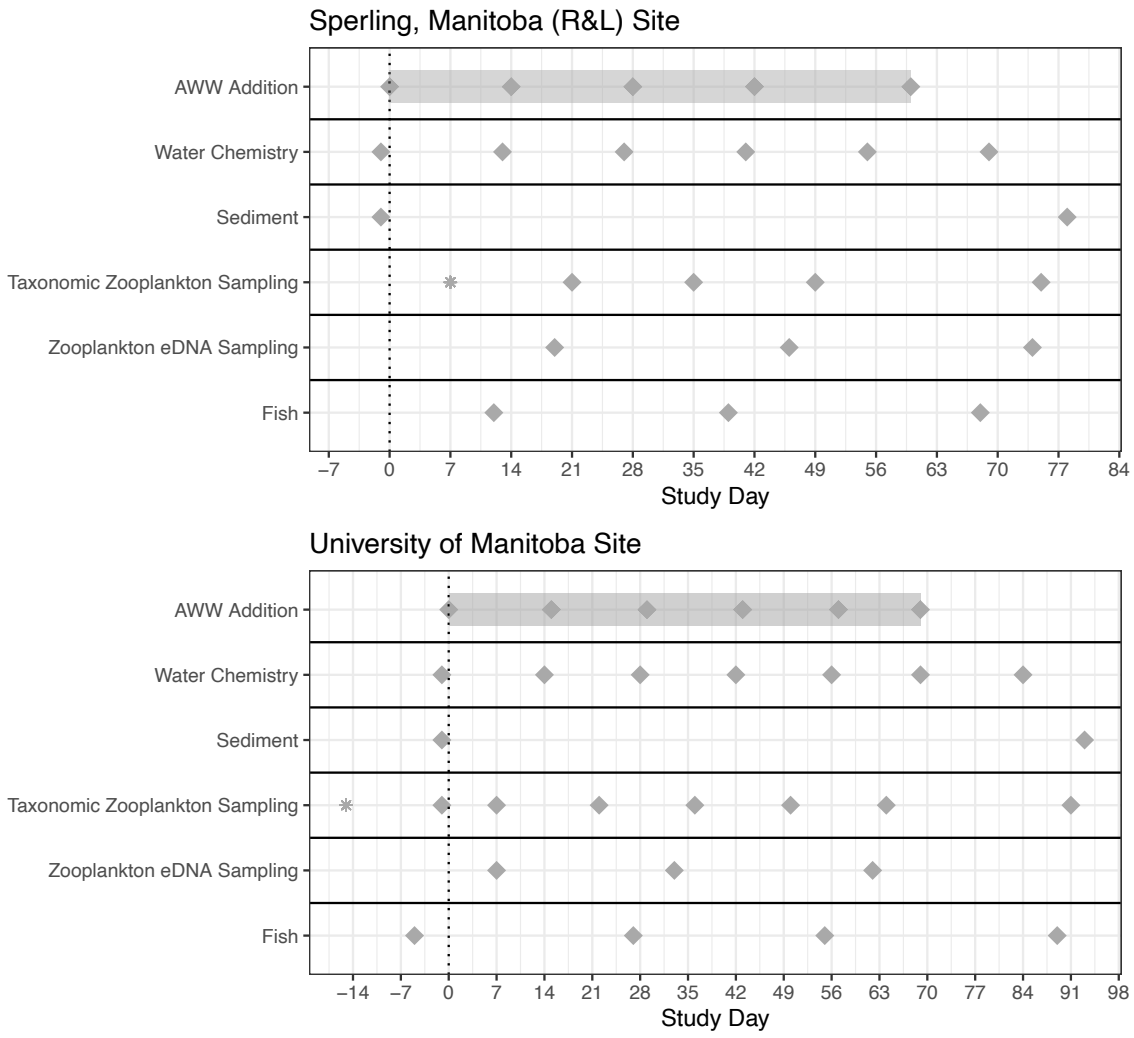

Figure 2.1: A timeline of sampling events at both experimental sites. The asterisk indicates the day zooplankton were added to the mesocosms. The dashed line represents the first waste addition (i.e., study day 0). The shaded grey band represents the aquaculture wastewater (AWW) application period.

2.2 Experiment Design

2.2.1 Site One – R&L

Site one (referred to herein as R&L), was located at R&L Acres, Sperling, MB and consisted of 15 mesocosms (3000 L [n = 2, 2.7 m in diameter x 0.72 m in height] or 1500 L [n = 13, 2.56 m in diameter x 0.57 m in height] capacities) (Figure 2.2). Each mesocosm was an above ground, circular, flat-bottomed, low-density polyethylene tub, with no inflows or outflows. The mesocosms were filled with approximately 20 cm of topsoil sourced locally to act as a sediment layer and 30 cm of water from a nearby pond. The water was routinely topped up with Carmen, Manitoba tap water to this depth throughout the study to ensure a consistent water depth within all the mesocosms. Each mesocosm was seeded on June 11, 2022, with 300 grams (80 g/m^2) of a commercial strain (Franklin) of northern wild rice (*Zizania palustris*) obtained from the North Central Research and Outreach Center at the University of Minnesota. These mesocosms simulated a commercial wild rice flooded paddy system. The seed had been stored over winter submerged in water below 4°C to simulate the natural dormancy pattern of wild rice seed. Germination successfully first occurred on June 16th, 2022, determined by visual inspection. In addition to the 15 mesocosms, another 3000 L mesocosm, with the same water and soil conditions, was left unseeded to serve as a reference for atmospheric nutrient inputs. Initial zooplankton communities were established in each of the seeded mesocosms from the pond water that was used to fill the mesocosms. To ensure an abundant community was established, invertebrates were collected from the source water pond at R&L Acres using a tow net (35-µm mesh) on July 7, 2022 (Day 7) (Figure 2.1). The invertebrates were pooled and immediately distributed to the mesocosms by adding equal aliquots of the pooled sample to each mesocosm. Invertebrates were only added after the first AWW additions at the R&L site because of concern

that they might impair the growth of wild rice during the critical floating leaf stage. All mesocosms were left uncovered to allow for possible aerial colonization by insects. Each mesocosm received twelve adult fathead minnows (*Pimephales promelas*) (n = 12) that were originally collected from Fort Whyte Alive (Winnipeg, MB). The minnows were sampled monthly for various endpoints, these details are described elsewhere (Figure 2.1) (Robertson, 2024). Fish were collected and handled according to the animal use protocols administered by the Animal Care Committee at the University of Manitoba, a Scientific Collection Permit number 41189175 (SCP-05-2022), and a Live Fish Handling Permit number 41191149 (LFH-ITP 06-2022), administered by the Province of Manitoba.

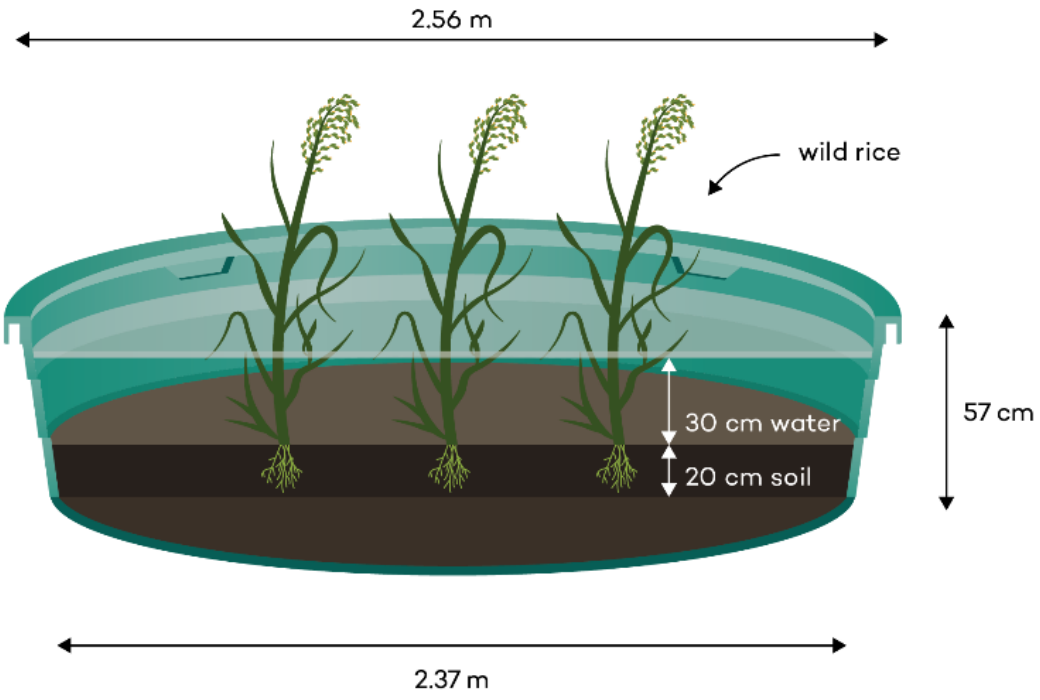

Figure 2.2: Schematic of the mesocosms used for the study, the dimensions displayed are of the 1500 L sized mesocosms.

The AWW used for the study was collected from an inland Arctic char (*Salvelinus alpinus)* aquaculture facility (Ridgeland Aquafarms, Anola, MB, Canada). The AWW was acquired from a wastewater solids settling tank using a two-inch diameter pump, thus allowing for the collection of liquids and suspended solids. Aquaculture wastewater was collected twice during the study and was stored in a 1000 L Intermediate Bulk Container (IBC). The mesocosms were randomly assigned treatments of AWW based on a logarithmic regression design. The AWW was applied bi-weekly over nine weeks (5 additions) to nine treatment mesocosms resulting in a range of 7 L to 105 L of total AWW by the end of the study, with the midpoint of the regression targeting realistic and relevant commercial wild rice nutrient loadings (Table 2.1) (Blandford, 2024; Kaiser and Piotrowski, 2023). Prior to each addition the AWW was mixed to ensure even distribution and retrieved from a drain at the bottom of the IBC container. The corresponding AWW volume was then measured using a graduated cylinder and the AWW was poured evenly onto the surface of the mesocosm water. Six mesocosms (one being the unseeded mesocosm) were left unexposed to AWW (volume = 0 L) to serve as reference treatments. A gradient of AWW volumes was used as opposed to nutrient concentrations because the concentration of the AWW was unknown at the time of application. The first addition day (day 0) was June 30, 2022 (Figure 2.1). The subsequent additions occurred on July 14 (day 14), July 28 (day 28), August 11 (day 42), August 29 (day 60). The AWW was sub-sampled prior to each waste addition. The first addition sub-sample was measured spectrophotometrically with HACH kits (London, Ontario, Canada) for TKN, NH_4-N, and TP (APHA, 2012). The subsequent additions sub-samples were analyzed by Farmers Edge Laboratories (https://farmersedge.ca/calab/, basic +S manure analysis) for total Kjeldahl nitrogen (TKN), total ammonium nitrogen (TAN), total phosphorus (TP), total potassium (TK), and total sulfur (TS).

Sub-samples of AWW from three timepoints (June 22, July 28, August 29, 2022) were selected for metal analysis (ALS Laboratory Group, Winnipeg, MB).

Prior to the last two AWW additions (day 42 and 60), additional AWW was collected from the same source and using the same technique as the initial AWW collection. Additions of AWW were doubled for these last two additions to ensure we captured the remediation potential of the wild rice plants that were at a high density.

Total nutrient loading to the treatments was reported as a mass per unit area loading rate (mg/m^2) to facilitate comparisons to fertilizer application rates in literature. To determine the loading rate the total mass of the nutrients in the AWW applied to the treatments was divided by the surface area of the mesocosm.

Table 2.1: Volume of aquaculture wastewater added to each RL mesocosm per addition and the total amount of aquaculture wastewater added to each mesocosm by the end of the study. Additions were added bi-weekly, resulting in a total of five additions. The volume added for the last two additions was doubled.

Treatment ID	Volume added per addition (L)	Cumulative total added (L)
REF-A	0	0
REF-B	0	0
REF-C	0	0
REF-D	0	0
REF-E	0	0
7L	1	7
9.8L	1.4	9.8
12.6L	1.8	12.6
17.5L	2.5	17.5
23.1L	3.3	23.1
31.5L	4.5	31.5
42.7L	6.1	42.7
57.4L	8.2	57.4
77.7L	11.1	77.7
105L	15	105

2.2.2 Site Two – University of Manitoba

Site two (referred to herein as UM) was located at the Prairie Wetland Research Facility at the University of Manitoba, Manitoba, Canada and consisted of 17 mesocosms of the same type used at the R&L site. There were four 3000 L (2.7 m in diameter x 0.72 m in height) and thirteen 1500 L (2.56 m in diameter x 0.57 m in height) mesocosms (Figure 2.2). The mesocosms were filled with approximately 20 cm of topsoil to act as a sediment layer (Reimer Soils, Winnipeg, MB) and 30 cm of tap water from the City of Winnipeg. The water was routinely topped up to this depth throughout the study to ensure a consistent water depth within all the mesocosms. Each mesocosm was seeded in October 2021 with a natural strain of northern wild rice received from growers at Floating Leaf™ (Winnipeg, MB) at a seeding rate of 10 g/m^2. Germination successfully occurred after overwintering, determined by visual inspection. First observed wild rice emergence was May 26th, 2022. In addition to the 17 mesocosms, another 700 L mesocosm with the same water and soil conditions, was left unseeded to serve as a reference for atmospheric nutrient inputs. Zooplankton communities used to establish communities in each of the mesocosms were sourced from Oak Hammock Marsh, Manitoba, Canada using tow nets and kick nets (35-µm and 73-µm mesh) on June 7, 2022 (Day -15) (Figure 2.1). The invertebrates were transported in water to the University of Manitoba site, where they were evenly distributed among the mesocosms. All mesocosms were left uncovered to permit potential aerial colonization. Each mesocosm received an addition of adult fathead minnows (n = 12) as described for the R&L site.

Eight mesocosms at the site were used the year prior (June-August, 2021) to assess the phytoremediation potential of cattail (*Typha* spp.) in AWW exposed waters (Blandford et al., 2024). The cattail and all other wetland plants were harvested by cutting at their base at the end

of the 2021 study, however soil, water, and residual plant components remained. The wild rice was then seeded into these mesocosms. In addition to wild rice, these mesocosms, due to their use in the previous study, grew a more diverse and abundant submerged vegetation population and had different physiochemical properties, when compared to the other ten mesocosms not used for the previous study (Blandford, 2024). This subset of mesocosms will be described as the 'established wetland mesocosms (UM-EW)' as they simulate a wetland ecosystem containing wild rice among other wetland plants. The other ten mesocosms grew the seeded natural wild rice strain and served to simulate a flooded natural wild rice paddy ecosystem, as such they will be described as the 'wild rice mesocosms (UM-WR)'.

The AWW used for the study was as described for the R&L site. However, only the first collection was used for the UM site. The established wetland and wild rice mesocosms were randomly assigned to be treated with additions of a given volume of AWW, based on a logarithmic regression design. To capture realistic and relevant nutrient loading values within the regression, nutrient loading values commonly used in commercial wild rice cultivation were targeted by the midpoint of the regression (Blandford, 2024; Kaiser and Piotrowski, 2023). The AWW was applied bi-weekly over 12 weeks (6 additions) to twelve treatment mesocosms (n = 7 wild rice & n = 5 established) resulting in a range of 6 L to 90 L of total AWW volumes by the end of the study (Table 2.2, Table 2.3). Prior to each addition the AWW was mixed to ensure even distribution and retrieved from a drain at the bottom of the IBC container. The AWW volume was then measured using a graduated cylinder and the AWW was poured evenly onto the surface of the mesocosm water. Three wild rice mesocosms and three established wetland mesocosms (one being the unseeded mesocosm) were left unexposed to AWW (volume = 0 L) to serve as reference treatments. A gradient of AWW volumes was used as opposed to nutrient

concentrations because the concentration of the AWW was unknown at the time of application. The first AWW addition date (day 0) was June 22, 2022 (Figure 2.1). Then subsequent additions occurred on July 7 (day 15), July 21 (day 29), August 4 (day 43), August 18 (day 57), and August 30 (day 69). The AWW was sub-sampled prior to each waste addition. The first and fifth additions sub-samples were measured spectrophotometrically with HACH kits (London, Ontario, Canada) for TKN, TAN, and TP (APHA, 2012). The second, third, fourth and sixth additions sub-samples were analyzed by Farmers Edge Laboratories (https://farmersedge.ca/calab/, basic +S manure analysis) for total Kjeldahl nitrogen (TKN), total ammonium nitrogen (TAN), total phosphorus (TP), total potassium (TK), and total sulfur (TS). Sub-samples of AWW from three timepoints (June 22, August 17, August 30, 2022) were selected for metal analysis (ALS Laboratory Group, Winnipeg, MB).

Total nutrient loading to the treatments was reported as a mass per unit area loading rate (mg/m^2) to facilitate comparisons to fertilizer application rates in literature. To determine the loading rate the total mass of the nutrients in the AWW applied to the treatments was divided by the surface area of the mesocosm.

Table 2.2: Volume of aquaculture wastewater added to each UM established wetland mesocosm per addition and the total amount of aquaculture wastewater added by the end of the study. Additions were added bi-weekly, resulting in a total of six additions.

Treatment ID	Volume added per addition (L)	Cumulative total added (L)
REF-A	0	0
REF-B	0	0
15L	2.5	15
23.4L	3.9	23.4
36.6L	6.1	36.6
57.6L	9.6	57.6
90L	15	90

Table 2.3: Volume of aquaculture wastewater added to each UM wild rice mesocosm per addition and the total amount of aquaculture wastewater added by the end of the study. Additions were added bi-weekly, resulting in a total of six additions.

Treatment ID	Volume added per addition (L)	Cumulative total added (L)
REF-A	0	0
REF-B	0	0
REF-C	0	0
6L	1	6
9.6L	1.6	9.6
15L	2.5	15
23.4L	3.9	23.4
36.6L	6.1	36.6
57.6L	9.6	57.6
90L	15	90

2.3 Water Quality Monitoring

A handheld YSI ProQuatro Multiparameter meter was used twice a week at an exact reference point in each mesocosm and time, for the duration of the study, to measure general water quality parameters including, dissolved oxygen, pH, temperature, and conductivity. Wireless loggers, placed 0.5 cm above the top of the sediment, were used to record light intensity data every 30 minutes (Onset HOBO MX2202 Pendant). At R&L the loggers were only placed in one reference and the 9.8L and 105L treatments. At UM the loggers were placed in established wetland mesocosms of a reference, 36.6L, and 57.6L treatments, then in wild rice mesocosms of 15L, 23.4L, 36.6L, and 57.6L treatments. Water was sampled (500 mL grab sample from a random location in each mesocosm ~10 cm below the surface) bi-weekly prior to each wastewater addition to measure nutrient and chlorophyll *a* concentrations within each mesocosm (UM: days -1, 14, 28, 42, 56, 69, and 84; R&L: days -1, 13, 27, 41, 55, and 69) (Figure 2.1). The samples were stored in a cooler and immediately brought to the laboratory for processing. The water depth was recorded prior to retrieving the water sample from a reference location in each

mesocosm, to allow for volume calculations to be made. First, the water was measured spectrophotometrically with HACH kits (London, Ontario, Canada). The chemical constituents measured from this method include, total phosphorus (TP), total dissolved phosphorus (TDP), total nitrogen (TN), total dissolved nitrogen (TDN), and alkalinity. Then, following the methods as described in Rice et al. (2012), the following components were measured using a flow injection analyzer, soluble reactive phosphorus (SRP), nitrate nitrogen (NO_3^--N), nitrite nitrogen (NO_2^--N), and total ammoniacal nitrogen (NH_4^+-N) (Lachat QuickChem 8500, HACH). The remaining parameters, dissolved organic carbon (DOC), soluble reactive silica (SRSi), particulate phosphorus (Part-P), and chlorophyll *a*, were all analysed at the IISD-Experimental Lakes Area (IISD-ELA) chemical analysis laboratory using methods described in Stainton et al. (1977). Any analysis that measured dissolved nutrients used water filtered through a Whatman GF/C glass microfiber filter (1.2 µm effective pore size; Cytiva; Marlborough, MA, USA). Un-ionized ammonia was calculated from total ammonia nitrogen, and the measure at the time of nutrient sampling of pH and water temperature, using the calculation in Armstrong et al. (2012) and Delos and Erickson (1999). For more detailed water quality methodology refer to Blandford, 2024.

2.4 Meteorological Data

Meteorological data documented for the R&L was measured at the nearest Environment Canada and Climate Change weather station in Carmen, Manitoba (~20 km away from the R&L site). The UM Meteorological data was measured at the nearest Environment Canada weather station in Winnipeg, Manitoba (~10 km from the UM site). Light intensity was recorded every 30 minutes using light loggers placed at each site (Onset HOBO MX2202 Pendant). Light intensity below the water was also recorded within the RL site with the same loggers in one reference and

the 9.8L and 105L treatments. The loggers recorded light intensity under the surface in the following UM-EW mesocosms, one reference and the 36.6L and 57.6L treatments, and in the following UM-WR mesocosms, 15L, 23.4L, 36.6L, and 57.6L.

2.5 Soil Sampling

Mesocosm soil was sampled from all the mesocosms once prior to any AWW additions and again at the end of the study, several weeks after the AWW additions ended. UM was sampled on days -1 and 92, and R&L was as sampled on days -1 and 78 (Figure 2.1). The sediment was grab sampled in triplicate from each mesocosm, stored in 7 oz. whirl-pack bags, and freeze-dried. The dried samples were analyzed by Farmers Edge Laboratories (https://farmersedge.ca/calab/, complete soil analysis package) for the following constituents, organic matter, pH, boron, calcium, chlorine, copper, iron, potassium, magnesium, manganese, sodium, nitrate, phosphate, sulfur, and zinc.

2.6 Zooplankton Sampling

2.6.1 Morphological Identification

Passive traps were selected as the best method to sample the zooplankton communities without causing a disturbance to the mesocosm environment. The trap consisted of a 1 L glass mason jar with a 243 mL Nalgene polypropylene funnel fastened into the opening of the jar and secured with an elastic band and two s-hooks (adapted from Murkin et al., 1983; Sibley et al., 2001) and deployed successfully previously in these types of mesocosms (Lobson et al., 2018; Vanderpont et al., 2022) (Figure 2.3). Clear nylon string was sewn through the smaller opening of the funnel to prevent fathead minnows from entering the traps. Three traps were deployed at the bottom of each mesocosm for a total of 24 hours. The unseeded mesocosms were not

sampled for zooplankton. After 24 hours, the traps were removed from the mesocosms, filtered through 53 µm mesh to collect the organisms from all the traps, and the isolated zooplankton were stored in 120 mL jars with 5% sugar formalin and distilled water to preserve the sample until identification and enumeration following standard methods (USEPA, 2016). The sampling events at the UM site occurred on days -1, 8, 22, 36, 50, 64, and 91 (Figure 2.1). The R&L sampling events took place on days 21, 35, 49, and 75 (Figure 2.1).

Figure 2.3: A picture of one of three passive samplers, that were placed within each mesocosm for 24 hours, used to sample the zooplankton.

All samples collected from the passive samplers were enumerated and taxonomically identified to determine the abundance and diversity of the zooplankton in the samples. The samples had unique IDs and were analysed upon completion of the field study in a random order

to avoid possible bias. Prior to enumeration, zooplankton samples were concentrated to a volume of 50 mL. The samples were inverted to ensure even distribution of the organisms. Then using a pipette, with a modified tip to allow for passage of the larger zooplankton species, a 5 mL subsample was transferred into a Borgorov zooplankton counting chamber. Enumeration and identification required viewing the subsample at 40-50 times magnification using a dissecting microscope. A minimum of one subsample was counted if the sample was valid. For a subsample to be valid the following must have been found: 1) at least 40 individuals across 4 taxa, 2) no more than 4 taxa cannot have less than 40 individuals each (adapted from USEPA, 2016). If the sample was not valid, another 5 mL subsample was analyzed, however, only taxa that were below the criteria were counted. For the first and second subsample taxa that were reassessed, the counts were averaged. The keys of Balcer et al. (1984), and Eddy and Hobson (1950) were used for morphological zooplankton identification. Zooplankton taxa were identified to the lowest level possible while still maintaining strong certainty; thus, cladocerans were identified to family or genus, copepods to order, ostracods to class, and rotifers to phylum.

2.6.2 Zooplankton eDNA Sampling

Zooplankton communities were also assessed using eDNA, however only from the R&L site mesocosms. For this analysis, water samples (0.5 L) were collected in triplicate from each of the mesocosms monthly (R&L: days 19/20, 46, 74) (Figure 2.1). The first sampling event at the R&L site could not be completed in one day, thus half of the mesocosms were sampled on day 19 and the remaining on day 20. The samples were filtered following the GEN-FISH eDNA sampling protocol (University of Windsor, 2022). The water samples were immediately filtered on-site using a “DIY” peristaltic pump system (Figure 2.4). The samples collected from R&L on day 19 were filtered off-site at the University of Manitoba due to weather. These samples were

retained on ice while in transport. The water was filtered through 1.5 µm binder-free glass microfiber filters (grade 934-AH, 47 mm circles). The filter apparatus was rinsed in-between each mesocosm and a negative control of distilled water was filtered prior to each sample to track potential contamination. The filters were preserved in sterile 15 mL tubes filled with molecular grade 100% ethanol. All sampling equipment went through a strict cleaning protocol of ethanol, ELIMINase™ decontaminant (Decon™), and UV light exposure to ensure the equipment was DNA/RNA free. Field protocols were also established and followed to ensure contamination did not occur between mesocosms (e.g., changing gloves, clean equipment bags kept separate from used equipment, sterile forceps). All the filters were then stored in a freezer (-20°C) until later extraction.

Figure 2.4: The "DIY" peristaltic pump filtering system used to sample eDNA within water samples from the mesocosms.

2.6.3 eDNA Extraction

From each sampling event, select samples from the R&L mesocosms were processed for extraction and metabarcoding due to time and cost constraints of NGS (i.e. REF-A, REF-B, REF-E, 7L, 17.5L, 31.5L, 57.4L, 77.7L, 105L). For DNA extraction, each sample was extracted separately within a UV workstation. The station was decontaminated using ELIMINase™ (Decon™) and UV between each sample extraction. A negative extraction control, using a sterile filter, was included in each extraction. DNA extractions were completed with the DNeasy Blood and Tissue DNA Extraction Kit (Qiagen Inc.). This procedure follows a series of steps that result in a final product of purified DNA, free from any contaminants and enzyme inhibitors. The extraction followed the protocols outlined by the manufacturer and the Docker Lab at the University of Manitoba, which are described as follows. All centrifuging was conducted using the Fisher Scientific accuSpin Micro 17. The filters were first removed from the ethanol solution and allowed to dry for 30 minutes to remove ethanol from the filters. Next, to lyse any cells and tissue within the samples, each of the filters were cut into 8 pieces and suspended in 50 µL of proteinase K and 450 µL of buffer ATL. Samples were incubated on a thermomixer for 18-24 hours on 56°C. Once complete, 6 µL of RNase A was added to the samples to digest any RNA present, since the goal was to isolate genomic DNA. Samples were centrifuged at 16,278 g for 10 seconds, incubated for 5 minutes, and centrifuged again. To homogenize the lysate, the filter and any remaining liquid were moved to QIAshredder (Qiagen Inc.) tubes, designed to homogenize cell and tissue lysates as they pass through the spin column, and centrifuged at 11,655 g for two minutes. Then, the solution was collected and transferred to 400 µL of buffer AL and 400 µL of 100% ethanol, which was used to purify the DNA, vortexed, and centrifuged at 16,278 g for 10 seconds. This solution was transferred to a DNeasy Mini Spin Column and centrifuged at 6164 g

for 1 minute causing the DNA to bind to the filter as the solution passed through. Next, the DNA was washed first with 500 µL of Buffer AW1 and centrifuged at 6164 g for 1 minute, then washed with 500 µL of Buffer AW2 and centrifuged at 18,879 g for 3 minutes. Lastly, to elute the DNA from the filter, 100 µL of Buffer AE, that was heated at 70°C for 30 minutes, was added directly to the filter, then centrifuged at 6164 g for 1 minute. The flow through solution containing the purified DNA was collected and frozen at -20°C until PCR analysis. Two replicates were disposed of during extraction due to extraction errors (17.5L treatment Replicate 3 from day 20, 17.5L treatment Replicate 2 from day 74).

2.6.4 Primer Design

Several primers were designed with the goal that each would be successful at amplifying zooplankton species that were present in the R&L samples. Zooplankton target species were determined from results of the morphological identifications, described previously. Since we did not identify zooplankton to species level, these results only allowed us to narrow down to, class Copepoda, class Ostracoda, and phylum Rotifera. Taxonomic identification results also helped to further identify the zooplankton present within the order Cladocera; for instance, the samples contained the following cladoceran taxa; family Chydoridae, and genera *Daphnia*, *Ceriodaphnia*, *Scapholeberis*, and *Diaphanosoma*. Although the morphological identification methodology did not include further specification of the copepods beyond order, for more precise copepod classification for designing the primers we identified the copepods present in randomly collected samples to possible genera. The next strategy used to determine which species to target for cladocerans and copepods, and which genera for rotifers, was a combination of freshwater zooplankton keys and literature of the zooplankton found in Manitoba (Balcer et al., 1984;

Dupuis & Hann, 2009; Grothe & Grothe, 1977; Haney et al., 2013; Hann & Salki, 2017; Loadman, 1980; Pettigrew et al., 1997).

We targeted the 658 bp portion of the mitochondrial COI gene region for primer design. The National Center for Biotechnology Information (NCBI) nucleotide database was used to extract sequences from the COI gene region when available for each zooplankton of interest. When searching for cladoceran and copepod species the search input was as such: "Species name COI AND (Canada OR USA)". When searching for rotifers the search input was: "Genus name COI AND (Canada OR USA)". Only the genus was used, as this was the furthest taxonomic level we were able to identify using the previously described criteria, as rotifers are very challenging to identify to the species level and there is limited information on which species are present in Manitoba. Since ostracods were not very abundant in the R&L samples, we did not do a more in-depth search beyond class Ostracoda. Thus, the search for ostracods was: "Ostracoda COI AND (Canada OR USA)". For each search the top 5-10 sequences were downloaded when available. Alignment of the sequences was conducted in Geneious Prime 2023.2.1 with default settings. The most successful alignments occurred when grouping according to taxonomic groups such as, order Cladocera, subclass Copepoda, phylum Rotifera, genus *Daphnia* or *Diaphanosoma*, and class Ostracoda. Primer pairs were then designed from these alignments by manually selecting conserved regions of nucleotides of at least 18 bps long and forward and reverse locations that would result in a short fragment length between 200-350 bp long (Table 2.4). When all the rotifer sequences were aligned, a primer pair could not be created due to the dissimilarity of all the sequences. Thus, the rotifer sequences were separated into two alignments based off similarity thus, two rotifer primers pairs were created. A total of 15 primers pairs were designed from multiple different alignments of zooplankton species, with the goal of at least four

to be successful at amplifying the zooplankton DNA in the samples. However, only seven primer pairs were tested in the primer optimization trials, described in the next section, so only these primers are outlined in Table 2.5. As a result, 60 species were targeted from these seven primers (Table A1). Lastly, all the primers were constructed with NGS adapters to the 5' tails, Uni-A for the forward primers (5'-ACCTGCCTGCCG-3') and Uni-B for the reverse primers (5'-ACGCCACCGAGC-3'). The primer pairs will be referred to as their name listed in Table 2.4 and primer refers to the forward and reverse pairing from herein.

Table 2.4: The primers designed for this study and tested in primer optimization trials for the amplification of target zooplankton species. The first four primer pairs were the final primers used for first round PCR of all the samples. Associated average melting temperature (T_M). The D (A, G, or T), H (A, C, or T), M (A or C), R (A or G), V (A, C, or G), W (A or T), Y (C or T) symbols in the sequences represent ambiguity codes for nucleotide degeneracy, with the possible bases they can substitute for in brackets.

Primer Name	Direction	Sequence (5'-end → 3'-end)	Fragment Length (bp)	T_M (°C)
Daphnia	F	TTCCCTCGMYTWAATAAT	237	45
	R	ATCGTATATTRATRRTAGTWGTA		45
Copepod	F	GTDATRCCWATTYTDATYG	289	44
	R	CTAATRAARTTWACHGCHC		45
Rotifer 1	F	ACHGGDTGRACDRTDTAYC	259	51
	R	ARYATWGTRATRGCWCCWG		49
Rotifer 2	F	GHACHGGDTGRACHRTDTA	288	51
	R	GMDGTRTTMADRTTDCGRTC		50
Cladoceran	F	TTYCCHCGHYTDAAYAAY	217	50
	R	DCGYATRTTVATDRYVGTDG		50
Diaphanosoma	F	CTTATTGGTGATGACCARAT	248	49
	R	GTARACAGTYCAACCYGT		50
Ostracod	F	AAYGAYCARATYTATAAYACWATYGT	249	51
	R	ADARVGGRGGRTADACWGT		52

2.6.5 Primer Optimization

Primer optimization, PCR #1, PCR #2, NGS library preparation, and NGS of the samples were conducted in collaboration with the Heath laboratory at the University of Windsor, in February 2024. To determine the success of designed primers at amplifying zooplankton DNA, seven of the primer pairs went through various trials of PCR reactions. In addition, two primer pairs that had previously been used in zooplankton metabarcoding studies were tested (Gibson et al., 2015; Leray et al., 2013; Meredith et al., 2021) (Table 2.5). These primer pairs also had the same NGS adapters constructed to the 5'-end of the forward and reverse primers. PCR conditions for each optimization round varied in terms of the volume of each of the reagents to use, the annealing temperature, and the thermal cycling conditions. To test the amplification success of these primer pairs, a sample was created that combined a small volume of all the DNA extract samples into one concentrated sample, namely the combined batch. PCR conditions for each primer pair and each round of optimalizations can be seen in Table A2 and Table A3 of Appendix A. The total volume of each PCR was 25 µL consisting of: 2 µL of the combined batch DNA, 0.5 µL of 10 mM forward primer (Integrated DNA Technologies [IDT]), 0.5 µL of 10 mM reverse primer (IDT), 0.5 µL of 10 mM dNTPs (Bio Basic), and the remaining 21.5 µL varied depending on the primer pair optimization round (Table A2). Thermal cycling conditions also depended on the primer pair and optimization round (Table A3). To determine amplification success after each primer pair optimization round, 4 µL of PCR product and 2 µL of 1x loading dye were combined and loaded onto a 2% TBE agarose gel stained with 5 µL of Gel Red to conduct gel electrophoresis. The gels were imaged using UV light. The band strength was used to determine the amplification success. After seven rounds of primer pair optimization, four designed primer pairs (Daphnia, Copepod, Rotifer 1 and Rotifer 2) and one primer pair from

literature were selected (Leray). Thus, the designed primers used cover 47 of the 60 targeted zooplankton species.

Table 2.5: Primers pairs from literature tested during the primer optimization trials. The D (A, G, or T), H (A, C, or T), I (A, C, G, or T), M (A or C), R (A or G), V (A, C, or G), W (A or T), Y (C or T) symbols in the sequences represent ambiguity codes for nucleotide degeneracy, with the possible bases they can substitute for in brackets.

Primer Name	Direction	Sequence (5'-end → 3'-end)	Fragment Length (bp)	Reference
Leray (m1COIintF/ jgHCO2198)	F	GGWACWGGWTGAACWGTWTAYCCYCC	313	Leray et al., 2013; Geller et al., 2013
	R	TAIACYTCIGGRTGICCRAARAAYCA		
B/R5	F	CCIGAYATRGCITTYCCICG	314	Gibson et al., 2015
	R	GTRATIGCICCIGCIARIAC		

2.6.6 First Round PCR

Separate PCRs of the eDNA samples were conducted for each primer set, resulting in five different sets of PCR conditions (Table 2.6). All samples, including field blanks were processed. In addition, only three extraction blanks were included (REF-A on July 19, 77.7L on August 15, and 17.5L on September 12). The first extraction blank (REF-A, July 19) was selected because this was the first extraction completed; thus due to inexperience this would be the most likely time for contamination to occur. The other two extraction blanks were selected because they were completed on different days when multiple extractions occurred and they were the last extraction of the day, thus also having a higher probability of showing contamination had it occurred. We determined it was unnecessary to process additional extraction blanks for NGS,

since the 3 extraction blanks showed no sign of contamination in the UV images. The laboratory protocol of conducting each extraction separately within a UV workstation also increased our confidence that no contamination had occurred among the extraction blanks. Each round of PCRs included a blank, these blanks contained the same reagents as the other reactions and 2 µg/L of ultrapure water instead of DNA. However, these blanks were not prepped for NGS as they showed no contamination. The volume in a single PCR was 25 µg/L consisting of: 10x Taq buffer (Bio Basic), 25 mM $MgCl_2$ (Bio Basic), 20 mg/mL bovine serum albumin (BSA) (Bio Basic), 10 mM dNTPs (Bio Basic), 10 mM forward primer (IDT), 10 mM reverse primer (IDT), Taq Polymerase at 5 u/µL (Bio Basic), and extracted eDNA sample. The volume of each component varied depending on the primer set, this can be seen in Table 2.6. Thermal cycling conditions of the PCRs were identical for all primers, besides the initial single round of denaturation of 95°C for the designed primers and 94°C for the Leray primer set, both occurred for 5 minutes. Then for all primers 30 cycles of the following: denaturation at 94°C for 30 seconds, annealing at variable temperatures depending on the primer set (see Table 2.6) for 1 minute, and extension at 72°C for 1 minute. Lastly, a single final extension at 72°C for 5 minutes, and a hold at 4°C until removal. All PCRs were assessed by gel electrophoresis and UV light imaging, as described previously, to ensure successful amplification and to ensure no contamination occurred in the PCR blanks.

Table 2.6: The first round PCR conditions for each primer set, including the volume used of each reagent (in µL) and the annealing temperature used. All reactions were 25 µL in total volume.

Primer	ddH_20	10x buffer	$MgCl_2$	BSA	dNTPs	F Primer	R Primer	Taq	DNA	Annealing Temp. (°C)
Copepod	15.15	2.5	2.5	1.25	0.5	0.5	0.5	0.1	2	44
Daphnia	15.15	2.5	2.5	1.25	0.5	0.5	0.5	0.1	2	44
Rotifer 1	15.15	2.5	2.5	1.25	0.5	0.5	0.5	0.1	2	50
Rotifer 2	14	2.5	3.4	1.5	0.5	0.5	0.5	0.1	2	42
Leray	14.65	2.5	3	1.25	0.5	0.5	0.5	0.1	2	48

2.6.7 Bead Cleaning

PCR product was cleaned using Sera-Mag SpeedBeads (Cytiva) which aid in the removal of DNA amplicons fewer than 100 bp in length and primer dimer. The procedure first required 15 µL of bead solution (10 g of PEG-8000 powder, 25 mL of 5M NaCl, 24 mL of ultrapure water, and 1 mL of washed Sera-Mag SpeedBeads) to be mixed with 10 µL of first round PCR product and allowed to rest for 5 minutes to ensure binding. A magnetic plate then suspended the beads and any solution not bound was removed, then the beads went through two washes of 200 µL of 70% ethanol while the sample plate remained on the magnetic plate. Once all the ethanol was removed, 40 µL of TE buffer was mixed with the beads to elute the DNA from the beads, followed by a 5 minute incubation at room temperature. Then the magnetic plate was used to remove the beads from the cleaned solution and this solution was transferred to a new plate for the second round PCR.

2.6.8 Second Round PCR

A short cycle PCR of each primer was conducted to attach unique barcodes and sequencing adaptors to the PCR fragments as a NGS library preparation step. The PCRs were 25 µL in volume and consisted of: 10 µL of cleaned PCR product, 2.5 µL 10x Taq buffer (Bio Basic), 2.5 µL 25 mM $MgCl_2$ (Bio Basic), 0.5 µL 10 mM dNTPs (Bio Basic), 0.1 µL Taq Polymerase at 5 u/µL (Bio Basic), 8.4 µL ultrapure water, 0.5 µL reverse primer (P1+Uni-B: 5'-CCACTACGCCTCCGCTTTCCTCTCTATGGGCAGTCGGTGATacgccaccgagc-3') (IDT), and 0.5 µL of 10 mM forward primer composed of a unique barcode for each well, the unique barcode for each corresponding sample was recorded. PCR cycling conditions were first a single denaturation of 95°C for 2 minutes, followed by 8 cycles of, denaturation at 95°C for 30 seconds, annealing at 55°C for 30 seconds, and extension at 72°C for 30 seconds. Then a final single extension at 72°C for 5 minutes occurred. All PCRs were assessed by gel electrophoresis and UV light imaging, using the same method as previously described, to ensure improved band strength concentration because of the bead cleaning procedure.

2.6.9 Sample Pooling and Gel Extraction

PCR products were pooled into one sample to create a library for each primer. A differential volume was pooled for each sample; this depended on band intensity observed in the gel electrophoresis images completed after the second round PCR. This technique allowed for both successful sequencing of DNA that was less present and prevention of oversaturation of DNA that was more present (Anand et al. 2016). The images were assessed and where no bands were observed 10 µL of sample was added, while for bands of light-medium and medium-dark intensity, 5 µL and 2 µL of sample were added, respectively. To prepare for gel extraction, 10 µL of the pooled library for one of the primers was mixed with 7 µL of 1x loading dye, this was

repeated for each primer library in duplicate, these were then added to separate lanes in a 2% TAE buffer gel where gel electrophoresis occurred for 4 hours at 96 V. The gel band was then removed at the target fragment length for each primer and gel extracted using the GenCatch™ Gel Extraction Kit (Epoch Life Sciences Inc.).

2.6.10 Next-Generation Sequencing

Samples were analyzed using an Agilent 2100 Bioanalyzer with a High Sensitivity DNA chip (Agilent, Santa Clara, CA, USA) to determine the final DNA concentration. Each library was diluted to 60 pmol/L, then all the libraries were pooled together and 50 µL was sequenced on the Life Technologies Ion GeneStudio S5 system utilizing the ExT Chef sequencing kit and a 530 chip.

2.6.11 Bioinformatic Processing

QIIME2 2024.2 software was used for the bioinformatic processing of the demultiplexed raw sequence data (Bolyen et al., 2019). The adapters were trimmed from the sequences using the 'cutadapt' plugin and denoised with the 'DADA2' plugin to remove primers, barcodes, low-quality sequences and to generate amplicon sequence variants (ASVs) (Callahan et al. 2016; Martin, 2011). The sequences from the Copepod, Daphnia, Rotifer 1, Rotifer 2, and Leray primers were truncated to 250, 200, 200, 200, and 275 bp, respectively; any fragments smaller than these values were discarded. The ASV's were then compared against the NCBI nucleotide database using BLASTn to match the best unique hits. The BLASTn search parameters used returned the top 15 hits with 97% or greater identity. From the output file, only zooplankton taxa were retained for analysis. Singletons were also removed from subsequent analyses. When genus level and species level were identified to the same ASV, the species level was inferred as the

correct identification. When there were differing taxonomic identifications for the same ASV, the lowest shared taxonomic level was used. The replicate samples reads were pooled for analysis.

The field blank and extraction control reads were normalized based on the quantity of PCR product added during library preparation prior to controlling for contamination. Any ASV reads present in the field blanks were removed from the dataset prior to statistical analyses following a two-step approach. First, if contamination was greater in the field blanks than the pooled sample, we assumed all contamination came from the previous mesocosm and the reads in the sample were not true reads for that mesocosm; thus, the ASV reads were removed from the sample. If contamination in the field blank was less than contamination in the pooled sample, the proportion of ASV reads in the field blank out of the total sample reads was subtracted from the ASV sample reads. This assumes that a proportion of reads can be attributed to contamination from the previous site and the remaining after removal were true reads for that site. The Rotifer 1 and Rotifer 2 samples did not have contamination removed due to contamination of the field and extractions blanks; thus, a reliable removal method could not be conducted; the limitations of this will be discussed further in Chapter 4. Minor contamination also occurred in the extraction blanks; however, the read count in the field blanks was minimal compared to the total read count (<0.002-0.03% of total reads); thus, the reads observed in the field blanks can be attributed to general noise and were not removed. The field blank and extraction control reads are reported in Appendix A (Table A4). The zooplankton sample reads used were not rarified due to the low sequencing depth of some samples (<1000 reads). When rarified to the lowest sequencing depth, this resulted in species loss (McMurdie & Holmes, 2014, Cameron et al., 2021). Therefore, richness was not included as a diversity index for the zooplankton reads because, without normalization, the within and between sample comparisons are not reliable. In addition, there

were no significant relationships between total zooplankton reads and richness; thus, sequencing depth had minimal effect on the diversity results and rarifying was not required (Beaulieu et al., 2024) (Figures A1-A3). However out of precaution, the relative zooplankton read abundance was used for visualizations, and for statistical analyses the data was transformed as described to facilitate comparisons. A Venn diagram was used to demonstrate the species detected and shared from each primer using the *ggVennDiagram* package in R (Gao & Dusa, 2024).

2.7 Statistical Analysis

All statistical analysis were conducted in R version 4.3.1 and RStudio version 2023.06.2 using *tidyverse* approaches (R Core Team, 2023; Rstudio Team, 2023, Wickham et al., 2019). Data visualizations were prepared using the *ggplot2* package version 3.5.1 (Wickham, 2016). Multivariate assessments and zooplankton diversity metrics were conducted using the *vegan* package version 2.6-4 (Oksanen et al., 2022). Correlation analyses were conducted using the *stats* package version 4.3.1 (Rstudio Team, 2023).

2.7.1 Univariate Statistics

Linear regression analysis was used to assess the relationship between AWW treatments and several dependant morphological variables including, total zooplankton abundance, cladoceran abundance, copepod abundance, cyclopoid copepod abundance, calanoid copepod abundance, rotifer abundance, and zooplankton diversity, as well as eDNA variables including zooplankton diversity. Individual linear regressions were conducted for each respective study day associated with each dependent variable, due to the repeated sampling within each treatment resulting in the violation of independence required for linear models. Additionally, assessing each time point separately allows for the natural variability within the population over time to be

eliminated from the response. The effect of time was visualized from abundance figures and via multivariate analysis, as described below. The AWW treatment exposure had the potential to accumulate throughout the experiment due to the repeated AWW additions. Thus, to ensure the maximum and worse possible exposure conditions was considered, for each study day analysed, the cumulative AWW exposure up to and including the respective study day that was used in the linear regressions. To determine the cumulative concentration of the exposure conditions, the mass of nutrients applied up to and including the respective study day were summed and then divided by the most recently measured mesocosm volume. The cumulative total phosphorus concentration was used as a representative measure of the AWW exposure, given each AWW nutrient parameter measured (i.e., TP, TKN, and NH_4) were all found to be correlated. The cumulative TP concentrations were $\log_{10}$ transformed to ensure linearity of the logarithmically designed AWW treatments. A constant value of 1 was added to all the cumulative TP concentrations prior to the transformation, to account for the zero value of the reference treatments. The mean of the reference treatments was used within the linear models. Diagnostics of each model were analyzed and when assumptions of linear regression were violated (e.g., normality, homoscedasticity), the dependent variable was $\log_{10}$ transformed to improve model fit. A constant of 1 was added to all values when zero values were among the variable assessed.

Overall, AWW treatment effects were assessed on each individual study day, using the log-transformed cumulative total phosphorus concentration [log10(x + 1)] linearly regressed against each dependant variable previously mentioned. Statistical significance was determined from an alpha of 0.05.

For the R&L site, the cladoceran abundance on study day 49 and 75, and calanoid copepod abundance on study day 75 violated the assumptions of simple linear regression due to

frequent zero values in the data. For these instances, zero-inflated or negative binomial generalized linear models (GLM) were used alongside simple linear regression to assess the effect of AWW treatment, as they are better suited in dealing with zero-inflated or over dispersed data. The ideal model candidate was determined by evaluating model diagnostics including overdispersion and zero inflation, as well as model fit using Akaike Information Criterion. The best model fit for cladoceran abundance on study day 49 was a negative binomial GLM, and for both cladoceran and calanoid abundance on study day 75 was a zero-inflated negative binomial GLM. However, due to small sample sizes, the GLM model may not provide reliable results. Thus, the simple linear regression and GLM results will be evaluated together to ensure an accurate and comprehensive assessment of the treatment effects.

Simple linear regression was used to determine the effect of fish on zooplankton abundance. The first fish related variable considered was the number of fathead minnows retrieved (from the 12 initially added to the mesocosms) during the final fish sampling point (study day 79). Since we only know the number of fish at this point, only the effect to the final zooplankton study day could be assessed (study day 75). The other fish related variable considered was the occurrence of larval fish within the zooplankton passive samplers. Unintentionally the fathead minnows were able to spawn, due to both sexes having been added to the mesocosms. As a result, larval fathead minnows hatched and used the passive samplers as a place of refuge. At the R&L site and the UM established wetland site, the occurrence of larval fish found in the jars was infrequent, thus a binomial model was used for this variable. For the UM wild rice site, larval fish were caught in the samplers frequently, thus, the abundance of larval fish was used as the independent variable. Zooplankton abundance was $\log_{10}$ transformed to satisfy the assumptions of linear regression modelling.

2.7.2 Multivariate Statistics

2.7.2.1 Principal Response Curve

Principal response curve (PRC) analysis was used to assess the effect of AWW loading on the zooplankton community composition over time relative to the reference treatments (Van den Brink et al., 1999). PRC is a multivariate method of constrained ordination that was developed from redundancy analysis statistics but designed to isolate factors more relevant to ecotoxicology based mesocosm studies, by using treatment, time, and their interaction as predictors (Van den Brink et al., 1999; Szocs et al., 2015). The components of PRC include: coefficient of community response (C_{dt}) which demonstrates the effect of the treatment group on the community at a given point in time; species score (b_k) which is used to interpret the species level response; and the overall species response to the treatment at a given point of time (t_{dtk}) (Van den Brink et al., 1999). The responses generated by the PRC are assessed relative to the reference treatments, which are set to zero. Morphological zooplankton abundance data was $\log_{10}$ transformed to meet the assumption of linearity when conducting a PRC analysis.

The PRC model outputs the explained variance of the treatments and time on community composition. The first axis captures the largest amount of the variance and was used to interpret the zooplankton community response (Lawrence et al., 2018). The coefficients and curves generated from the PRC analysis are also used to interpret the community response. This data, when paired with the species scores, allows for an interpretation of the response of a species to the treatments on a specific day and over time. When the product of the coefficient and species score is highly positive, this indicates a positive response of that taxon, whereas a highly negative product indicates a negative response (Lawrence et al., 2018). When the species score is

near zero, this indicates that species did not respond strongly to treatment effect (Lawrence et al., 2018).

Significance of the overall PRC model, the PRC axes, and each PRC term were tested using the non-parametric approach of permutation testing (n = 999). The significance of each study day was also tested using permutations. When significance of a study day was found, post-hoc analysis was conducted to determine which specific treatments significantly differed from the references. Pairwise permutation tests (n = 999) were performed to compare the difference between the treatment PRC scores and the mean PRC scores of the references. The proportion of permuted differences greater than or equal to the observed differences was used to determine the p-values of each treatment. A non-parametric approach was used, as opposed to a Dunnett's Test, due to this study design not having replication within the AWW applied treatment groups.

2.7.2.2 Redundancy Analysis

The effect of the environmental variables on morphological zooplankton community composition was tested using a partial redundancy analysis (RDA). A partial RDA is a multivariate method of constrained ordination that allows for the influence of time to total variance to be controlled out of the model, by including study day as a conditional variable in the analysis (Legendre and Legendre, 2012). Thus, the relationship of the environmental variables to the treatment groups and the zooplankton community composition is the primary focus of the RDA. The species data was Hellinger transformed to normalize the data. The environmental variables were standardized to allow for comparisons across the different measurements used and then evaluated for multicollinearity. Any variable with a correlation coefficient greater than 0.7 was removed. To further assess for multicollinearity, the Variance Inflation Factor (VIF) was calculated for each environmental variable. Variables with VIF values greater than 10 were

typically removed, unless environmentally relevant. The initial variables included for consideration into the RDA were, water temperature, dissolved oxygen, pH, TP, TN, TDP, TDN, TAN, SRP, nitrite, nitrate, particulate phosphorus, chlorophyll-*a*, DOC, and un-ionized ammonia. All RDA visualization and results are presented using a scaling of 2, which focuses on the relationship and correlations between species and environmental variables.

Significance of the overall RDA model, the RDA axes, and the environmental variables, in explaining the variance in the zooplankton community composition was tested using permutations (n = 999). The relationships were also assessed by visual interpretation of the RDA biplot figure, with the length and direction of the environmental variable vectors and the location of the species and treatments in relation to these vectors, indicting the strength of the relationships.

2.7.2.3 Principal Coordinate Analysis

To visualize the variation in zooplankton community composition across AWW treatments and study days a Principal Coordinate Analysis (PCoA) was conducted for the results generated from each primer. The morphological zooplankton abundance was also assessed with a PCoA; however, this was performed for comparison purposes to eDNA results, as the morphological results were assessed using additional methods addressed above. PCoA is an unconstrained ordination method that uses a dissimilarity matrix to quantify the differences in community composition between samples, it is considered a flexible analysis that does not require linearity, as the zooplankton read data was not linear this method was selected (Legendre & Legendre, 2012). The following samples were removed from the analysis for the Daphnia primer due to zero amplification: REF-C (study day 46 & 74), 17.5L (study day 46), and due to low amplification, REF-B (study day 46). The following samples were removed from the Rotifer

1 primer data also due to low amplification: 57.4L (study day 20), 17.5L (study day 46), 105L (study day 46). The 17.5L sample on study day 46 was removed from the Rotifer 2 primer due to low amplification. Minimal differences occurred when these samples were included or removed from the analysis as determined from a sensitivity analysis, however, these samples were kept out of the analysis. All species data were Hellinger transformed to standardize the data and reduce any variability in sequencing depth. The PCoA was conducted based on a Bray-Curtis dissimilarity matrix and the first two principal coordinate axes were plotted for visualization. Study day was distinguished using different shapes to allow for any differences related to study day to be assessed. Prior to statistical testing, the assumption of homogeneity of multivariate dispersion was tested and confirmed.

Statistical differences in community composition across treatments and study days was performed using a Permutational Multivariate Analysis of Variance (PERMANOVA) with significance assessed from permutations (n = 999). Pairwise comparisons were performed when significance was found in the PERMANOVA, using the *pairwiseAdonis* package version 0.4.1 (Martinez Arbizu, 2020). The p-value from pairwise comparisons was adjusted using a Benjamini-Hochberg correction due to the multiple comparisons conducted that can potentially lead to a false positive significance detection.

2.7.3 Zooplankton Methodology Correlation Analysis

To assess the relationship between morphologically obtained zooplankton abundance and eDNA metabarcoding obtained zooplankton reads across each primer Spearman rank correlation was conducted. The following relationships were assessed: total abundance vs. total reads, cladoceran abundance vs. cladoceran reads, rotifer abundance vs. rotifer reads, copepod abundance vs. copepod reads. The absolute and relative abundances were both tested. All

variables were log10 (x + 1) transformed prior to improve distribution and comparability. The correlation coefficient, or rho, was used to interpret the strength and direction of the relationship and the significance of the relationship was also included. To visualize the relationships, scatterplots of raw values were generated with a line of best fit and correlation results were displayed within each figure. Samples with zooplankton read counts below 500 were removed from the correlation analyses.

Chapter 3: Results

3.1 Site One – R&L

3.1.1 Aquaculture Wastewater Characterization

The nutrient composition of each AWW addition is listed in Table B1 and the corresponding total nutrient loading to each treatment from the AWW are in Table 3.1. The first three additions were from the first AWW collection source with a mean TP, TAN, and TKN concentration of 43.0, 229.2, 296.2 mg/L respectively. The second collection source had higher TP and TKN concentrations than the first collection with mean concentrations of 346 and 623.1 mg/L, respectively, while TAN was similar with a mean concentration of 263.6 mg/L. When considering the water volume of the mesocosms, the average nutrient concentration loaded in the water following each AWW application ranged from 0.30 – 4.65 mg/L TP, 0.65 – 10.05 mg/L TKN, and 0.35 – 5.45 mg/L TAN (Table B5). The cumulative nutrient concentration as a result of each AWW addition, which was used for the linear model analyses, are in Tables B2-B4. The metal content in the first AWW additions contained an average of 0.073 mg of copper and 0.448 mg of zinc. The fourth and fifth additions contained an average of 0.054 mg of copper and 0.380 mg of zinc. Then when considering the mesocosm volumes, the mean and cumulative copper and zinc concentrations within the mesocosm water as a result of AWW loading are in Table B6.

Table 3.1: The total loading of AWW with the corresponding total phosphorus (TP), total ammonia nitrogen (TAN), and total Kjeldahl nitrogen (TKN) loadings. The loadings are adjusted to the mesocosm surface area. Table modified from Blandford (2024).

Total AWW added (L)	TP (mg/m^2)	TAN (mg/m^2)	TKN (mg/m^2)
7.0	399.7	461.2	867.8
9.8	559.6	645.6	1214.9
12.6	719.5	830.1	1562.0
17.5	792.0	913.8	1719.4
23.1	1319.0	1521.9	2863.7
31.5	1798.6	2075.3	3905.0
42.7	2438.2	2813.2	5293.4
57.4	3277.5	3781.7	7115.8
77.7	4436.7	5119.1	9632.3
105.0	5995.5	6917.7	13016.7

3.1.2 Mesocosm Water Quality

The mesocosm water quality results and statistical analysis were reported and conducted in depth by Blandford (2024). Summaries of the relevant water quality results are reported here for reference however, for further interpretations and results see Blandford (2024). The mean concentrations of each water quality variable are reported in Tables B7-B8.

Water temperature, dissolved oxygen, pH, and specific conductivity did not vary considerably between AWW treatments or following any AWW additions (Figure B1-B4). Dissolved oxygen decreased across the study duration in all treatments, including references, indicating the reduction in DO was not related to the effect of AWW loading (Figure B2). After

study day 42, dissolved oxygen levels reached concentrations that can be limiting for zooplankton (<2 mg/L) (Karpowicz et al., 2020; Vanderploeg et al., 2009).

Light intensity loggers within three mesocosms measured mean light intensity of 1140 lux, 1658 lux, and 2025 lux, respectively (Figure B5). The light intensity was greatest in June and July, at the start of the study period. By August and September, the light intensity drastically decreased in all measured treatments.

TP, TDP, and SRP were initially high in concentration prior to AWW addition in all treatments, indicating the source water and soil quantities in the mesocosms contributed to the high nutrient concentrations initially (Figures B6-B8). The concentration of these phosphorus species decreased following the start of AWW, up until study day 41. Following the AWW addition on study day 42, the concentration of the phosphorus species increased in concentration (Figures B6-B9). The concentration of TP in the two highest treatments (77.7L and 105L) are notably higher than the other treatments reaching TP concentrations of 1.3 and 1.23 mg/L, respectively. Dissolved phosphorus comprised a majority of the total phosphorus measured in the mesocosms, following by SRP, then Part-P (Figure 3.1).

The concentration of TN, TDN, TAN, un-ionized ammonia, nitrite and nitrate also did not vary between treatments on most study days (Figures B10-B15). A spike in TDN on study day 69 was observed in the 77.7L mesocosm, following the final AWW addition. A spike in TAN and un-ionized ammonia to 0.64 and 0.02 mg/L appeared in the 42.7 L mesocosm on study day 13 following the first AWW addition, the concentrations then stabilized for the remainder of the study duration. Nitrate was significantly lower in all treatments over the duration of the study, with the concentration highest prior to the first AWW addition (~1.25 mg/L). TDN made up the largest proportion of the total nitrogen measured in the mesocosms, followed by nitrate, then

nitrite and TAN in similar proportions (Figure 3.2). Although, prior to the first AWW addition nitrate composed as significant of a contribution to nitrogen as TDN in the mesocosms.

Alkalinity, DOC, and SRSi concentrations over time within each treatment are presented in Figures B16-B18. Minimal treatment related differences occurred as the concentrations of these parameters generally remained consistent throughout the study duration.

Variations in chlorophyll *a* concentrations occurred between treatments and throughout the study duration, with the greatest difference following the fourth AWW addition (Figure 3.3). An increase in chlorophyll *a* was seen in several treatments following the second, fourth, and fifth AWW additions, including an elevation in chlorophyll *a* concentration in the 31.5L, 42.7L, 77.7L, 105L treatments to between 10-25 µg/L.

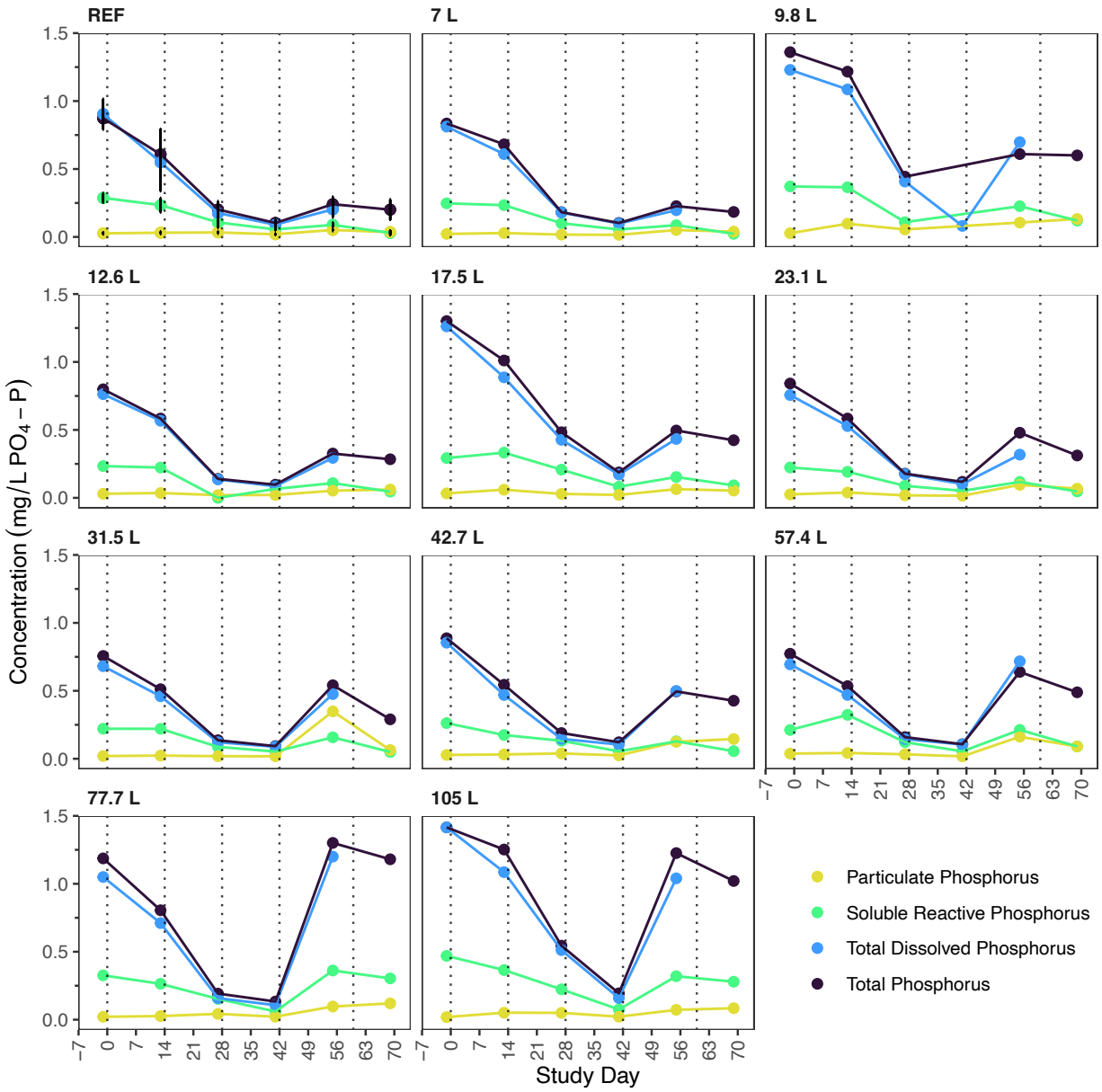

Figure 3.1: Concentration of total phosphorus, soluble reactive phosphorus, total dissolved phosphorus, and particulate phosphorus over the study duration with each plot separated by treatment. The REF plot displays the mean value of the references (n = 5) with error bars representing the ± standard deviation. The vertical dotted lines represent AWW addition days. Figure modified from Blandford (2024).

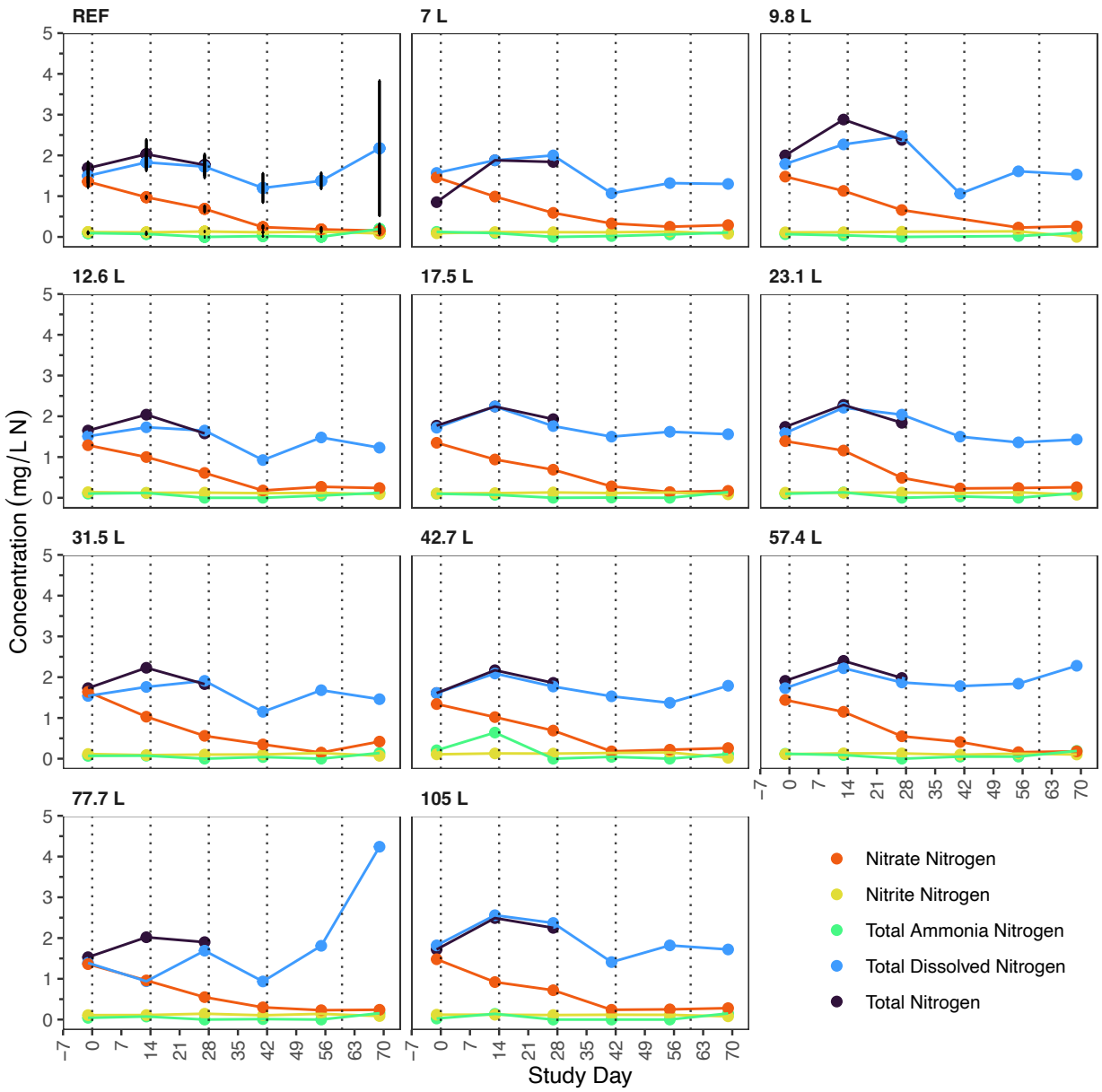

Figure 3.2: Concentration of total nitrogen (mg/L N), total dissolved nitrogen (mg/L N), total ammonia nitrogen (mg/L NH4-N), nitrate (mg/L NO3-N), and nitrite (NO2-N) over the study duration with each plot separated by treatment. The REF plot displays the mean value of the references (n = 5) with error bars representing the ± standard deviation. The vertical dotted lines represent AWW addition days. Figure modified from Blandford (2024).

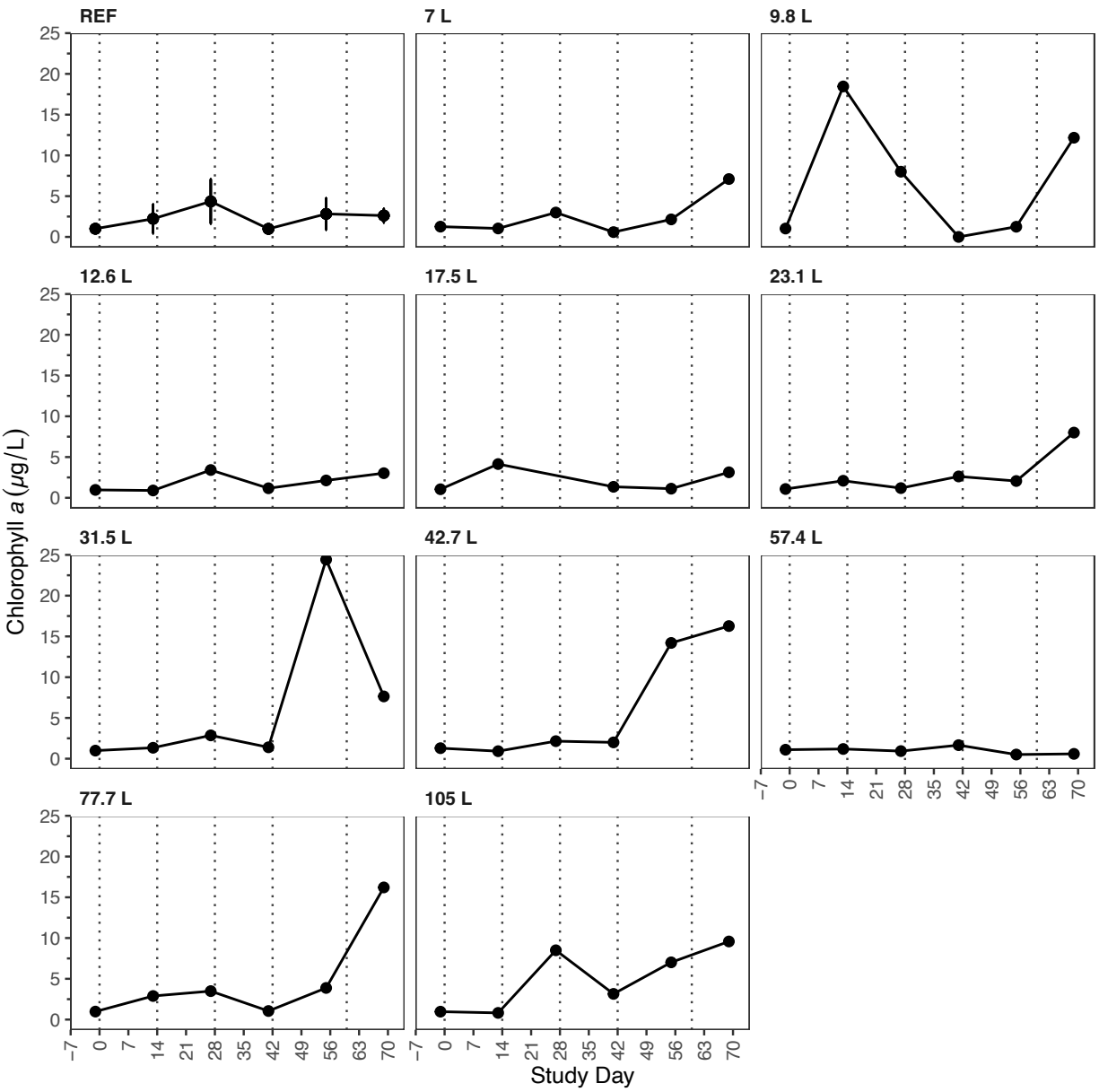

Figure 3.3: Concentration of chlorophyll *a* over the study duration with each plot separated by treatment. The REF plot displays the mean value of the references (n = 5) with error bars representing the ± standard deviation. The vertical dotted lines represent AWW addition days. Figure modified from Blandford (2024).

3.1.3 Meteorological

The mean monthly values for the air temperature, relative humidity, wind speed, precipitation, and light intensity for the study duration are presented in a summary table in Table B9. The air temperature and light intensity over the study duration are in Figures B19 and B20.

3.1.4 Soil

All soil properties and soil nutrient content are in figures for both sampling days (Figures B21-B23). The soil pH and organic matter did not undergo significant changes over the study duration. Boron, chlorine, copper, iron, manganese, sodium, nitrate, and sulfur all generally increased in concentration in all treatments from the initial sample to the final sample. Calcium, potassium, phosphate, and zinc all generally decreased in concentration in all treatments over time. Statistical interpretations of the soil properties are found in Blandford (2024).

3.1.5 Zooplankton – Morphological Identification

3.1.5.1 Total Zooplankton Abundance

A total of 10 zooplankton taxa were identified within the samples across the study period (when including copepod nauplii). The dominant taxa in each treatment varied, with the most predominant taxa being copepod nauplii, rotifers, and cyclopoid copepods, which made up 41%, 25%, and 21% of the total zooplankton abundance among all samples, respectively (Tables B12-B15). The next most abundant taxa was *Daphnia* sp., which comprised only 7% of the total abundance. The relative proportion of each major zooplankton group within the treatment is in Figure 3.6.

The abundance of zooplankton varied throughout the exposure period and following each AWW addition (Figure 3.4 and 3.5). By study day 21, two AWW additions had occurred, and

total zooplankton abundance ranged from 2400 – 10330 zooplankton per sample. At study day 35, total abundance remained consistent to the previous sampling day with abundance ranging from 2160-12240 zooplankton per sample. By study day 49 and 75, an overall reduction in total zooplankton abundance occurred in most treatments, except for the 31.5L and 77.7L treatments where an increase in total abundance over time occurred. On study days 21, 35, 49, and 75 the relationship between total abundance and AWW load was not statistically significant (Figure 3.7 and Table B10). However, on study day 49 and 75, a positive trend was observed between total abundance and AWW load, with marginal significance on study day 49 ($R^2 = 0.31$, $p = 0.073$).

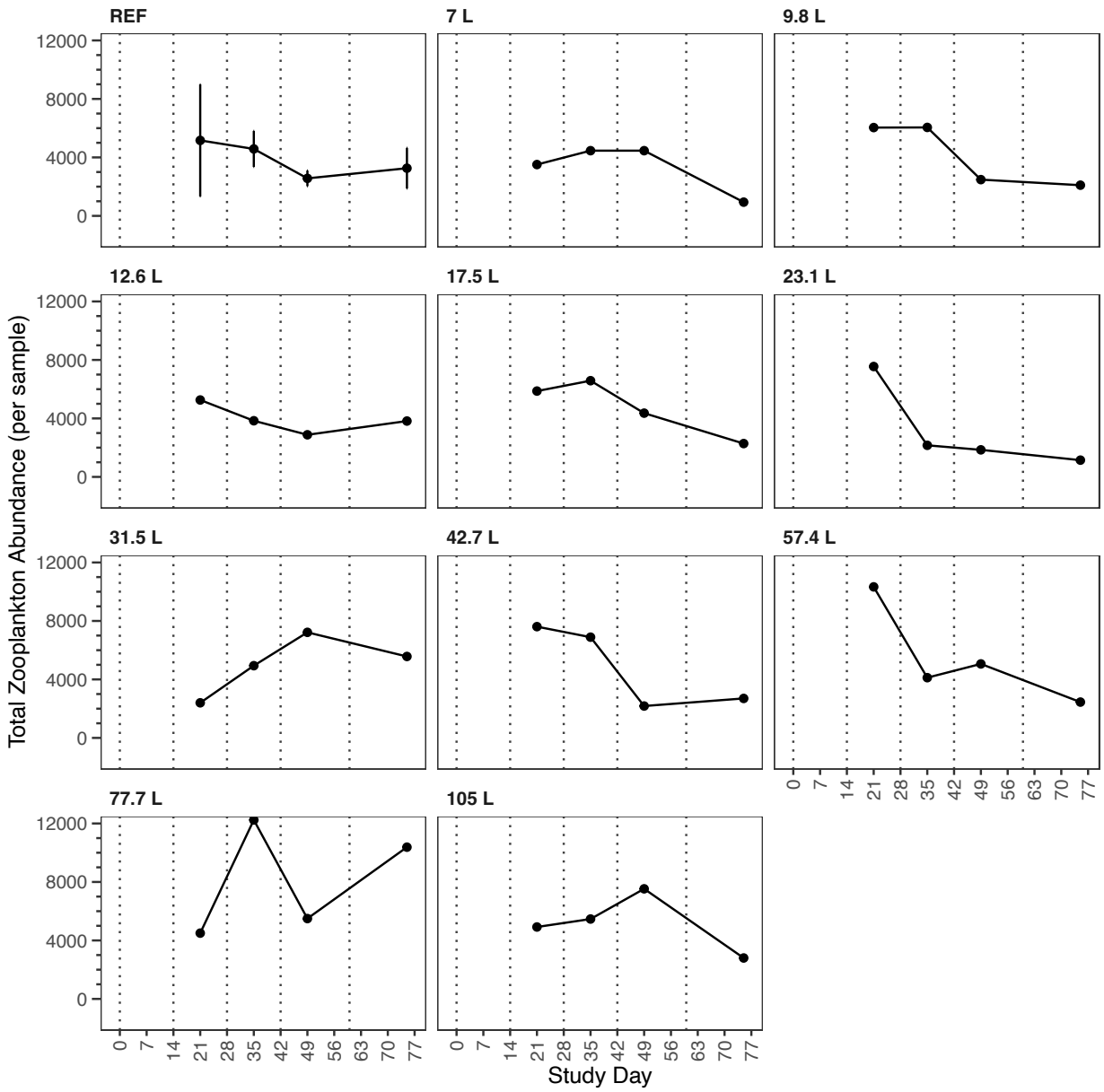

Figure 3.4: Total zooplankton abundance over the duration. The plots are separated by AWW treatment. The REF plot displays the mean value of the references (n = 5) with error bars representing the ± standard deviation. The dotted vertical lines represent the study days AWW was added to the treatments.

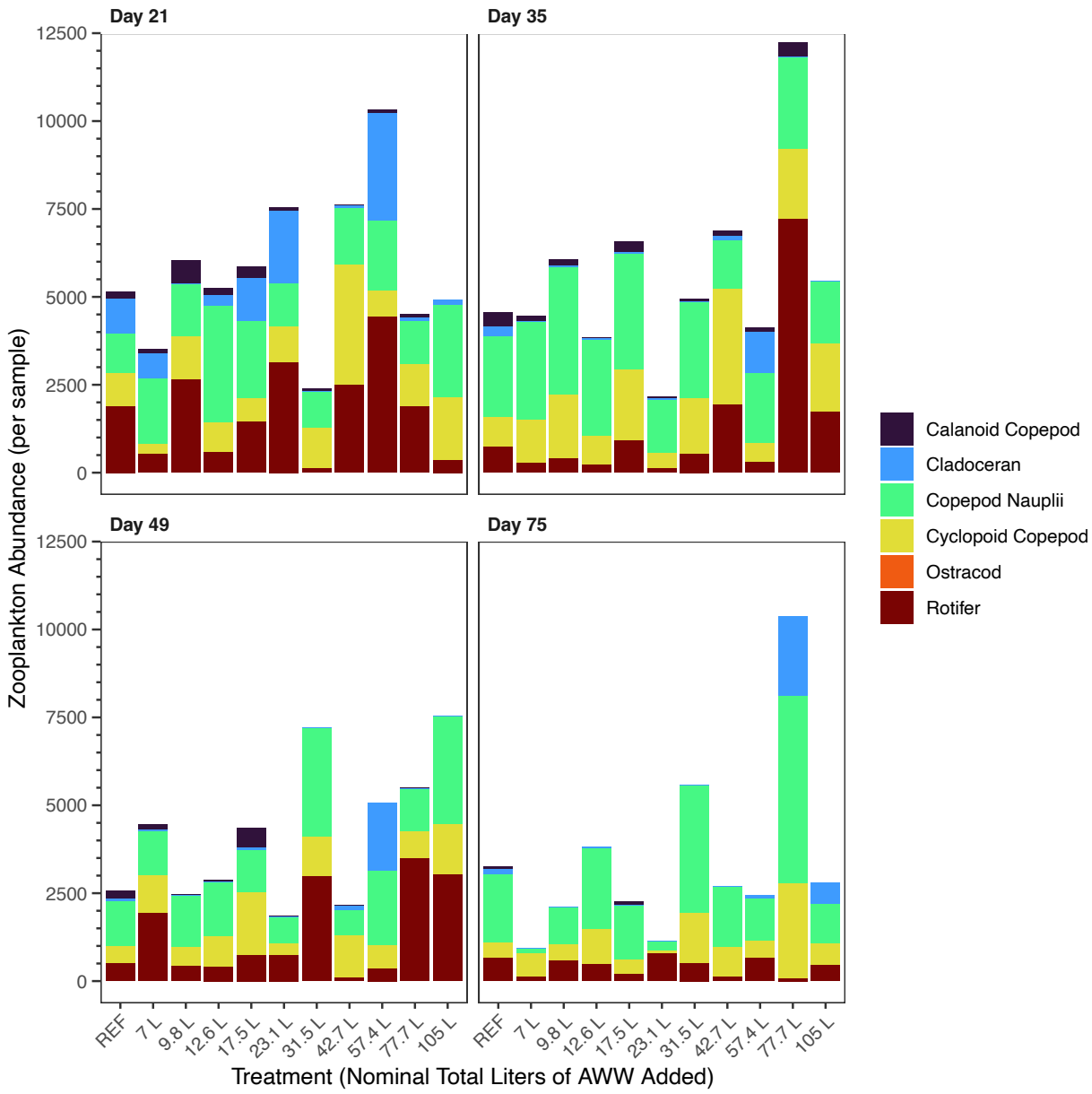

Figure 3.5: Total zooplankton abundance for each AWW treatment with each plot displaying the results for each study day on which zooplankton were sampled. REF presents the mean for the references (n = 5).

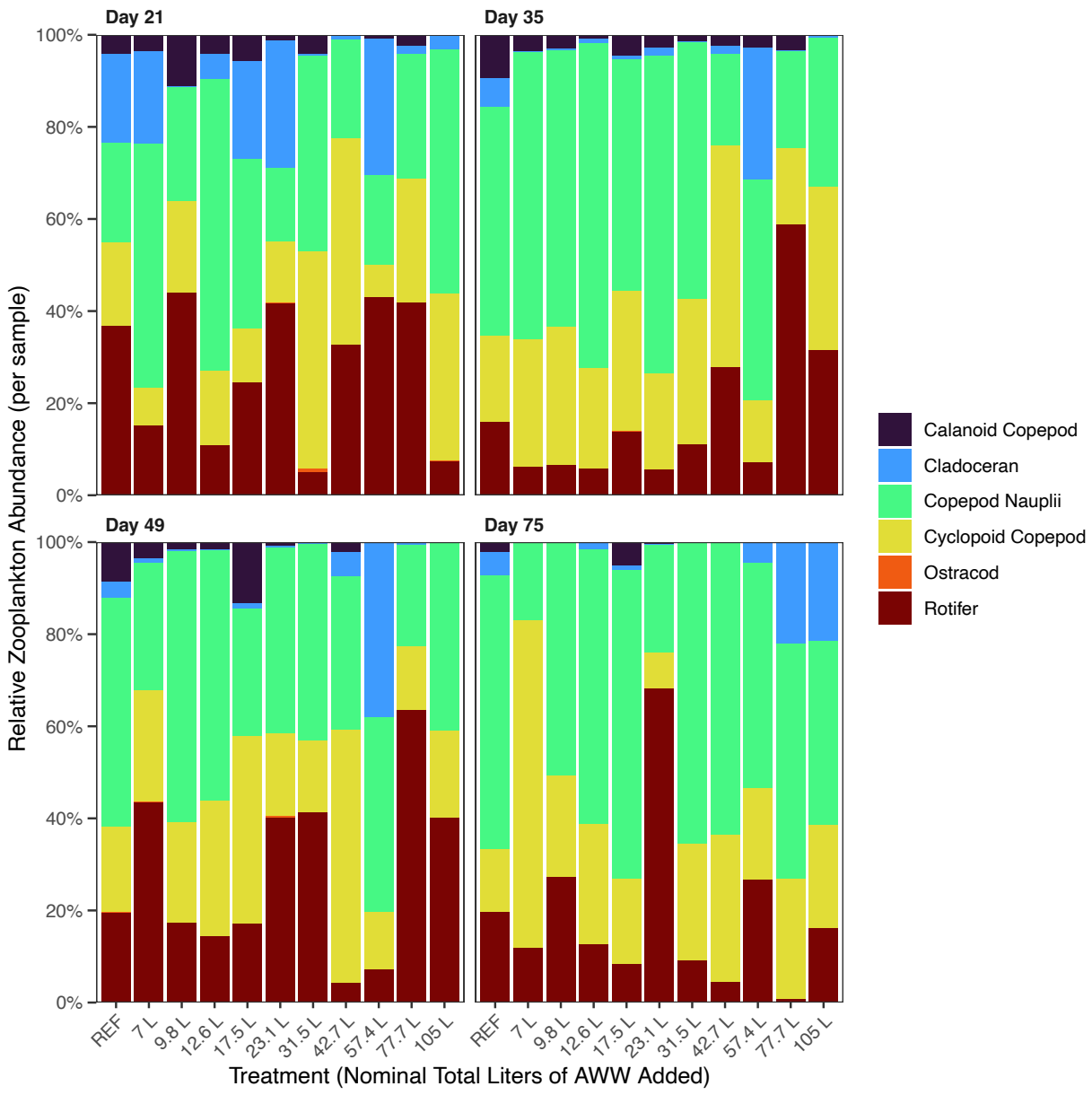

Figure 3.6: Relative abundance (%) of each major zooplankton group for each AWW treatment with the separate plots displaying the results for each study day on which the zooplankton were sampled. REF presents the mean for the references (n = 5).

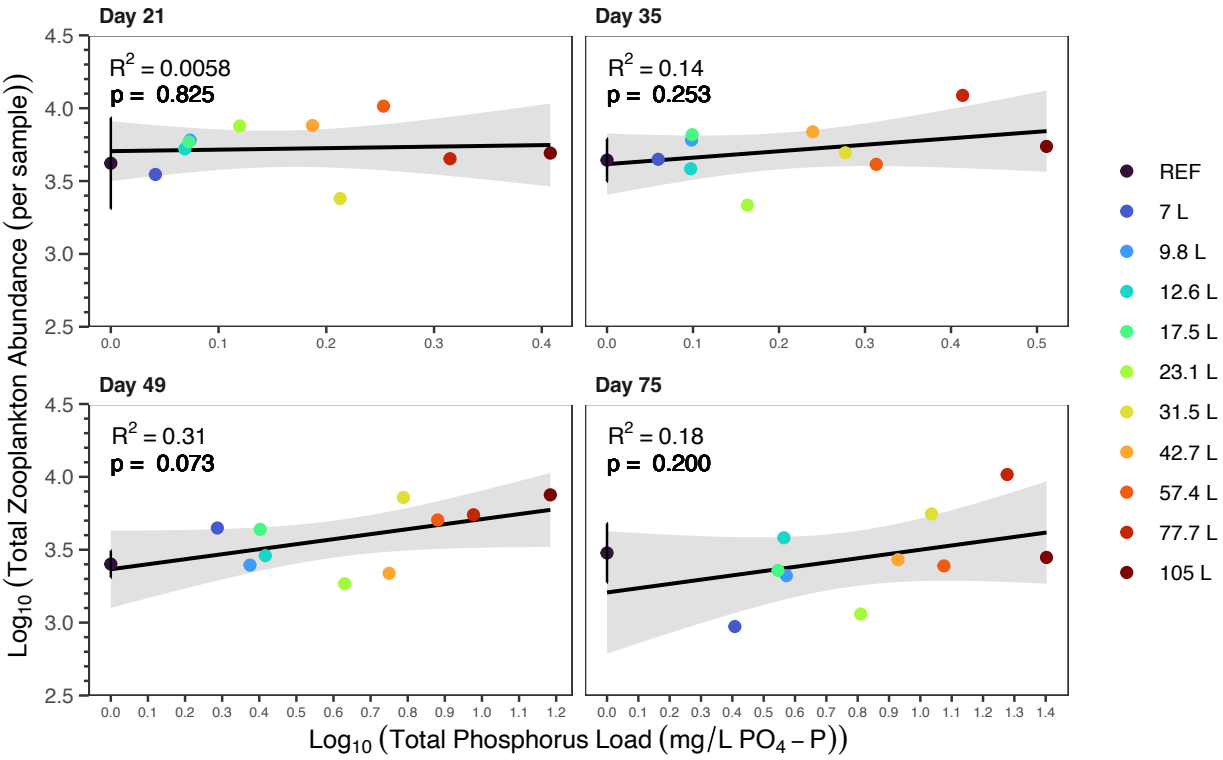

Figure 3.7: Linear regression model results of the relationship between log10(x + 1) of cumulative AWW load concentration (TP used as the representative variable) and total zooplankton abundance. REF displays the mean of the references (n = 5) with the error bars representing ± standard deviation. Each plot represents the model results for each study day.

The PRC analysis of the zooplankton community composition identified that treatment (i.e. AWW) explained 56% of the variance observed in zooplankton abundance (Figure 3.8). Then 16% of the variation in zooplankton abundance was explained by time, and the remaining 27% went unexplained. The first PRC axis explained 41% of the variation in abundance due to the AWW treatments, however, permutation testing found this response was not significant ($p = 0.83$). The significance of each PRC term (i.e. time and treatment) and each study day individually was assessed, and permutation testing revealed no significant results. The community response over time generated by the PRC analysis is variable between treatments compared to the references, as observed by the coefficient of community response (C_{dt}). Besides the responses in the 57.4L and 77.7L treatments, which were consistent for the first three sampling points, the response was generally negative. In the treatments with a negative C_{dt} recovery was observed by study day 75; however, the 77.7L treatment response remained unchanged and negative, but these responses were small (±0.3), resulting in marginal variance from the references, leading to the aforementioned non-significant result. As indicated by the species scores generated from the PRC analysis, *Daphnia* sp. had the highest positive species score ($b_k = 2.56$) (Table B17). Based off the PRC community response and the *Daphnia* sp. species score, most treatments initially had a high abundance of *Daphnia* sp. then over the rest of the study duration reduced in abundance relative to the references. The other taxa had species scores near zero, indicating little to no significant response to treatment effect.

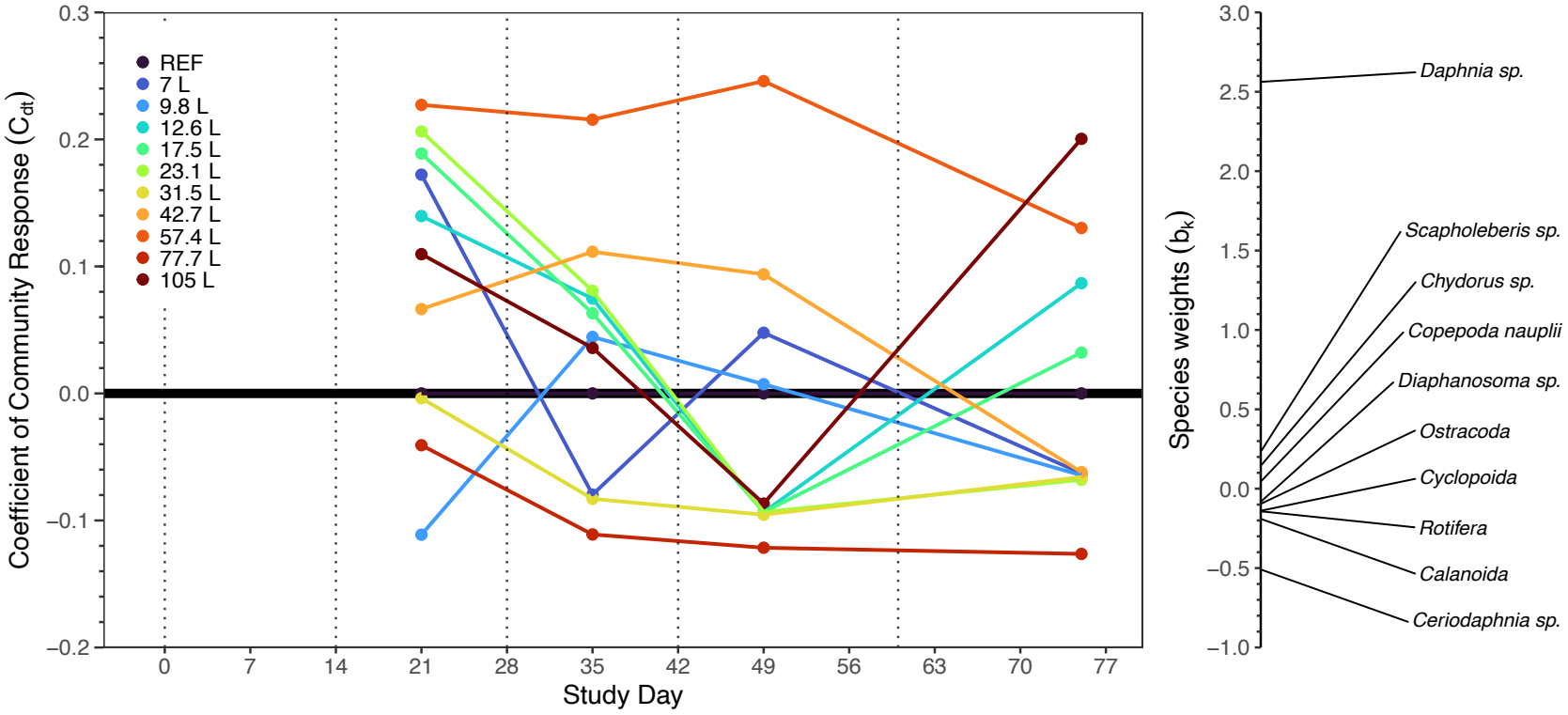

Figure 3.8: Principal response curve (PRC) generated for the RL zooplankton abundance and community composition. Zooplankton abundance was $\log_{10}$ transformed prior to analysis. Species weights are displayed on the right. The thick black line (x = 0) represents the references. The dotted vertical lines represent the days AWW was added to the treatments.

3.1.5.2 Cladoceran Abundance

The cladoceran abundance was comprised of the following genera: *Ceriodaphnia*, *Chydorus*, *Daphnia*, *Diaphanosoma*, *Scapholeberis*. This zooplankton group had the smallest relative abundance compared to rotifers and copepods (Figure 3.6). On study day 21, cladocerans were observed in most of the treatments. Over time, the abundance of cladocerans relative to the other groups decreased and they were absent in most treatments (Figure 3.9). By study day 75, greater than 200 cladocerans per sample was only observed in the two highest treatments, with 2280 and 600 zooplankton per sample, respectively.

From linear regression of study day 21, 35, 49, and 75, there was no significant effect of AWW on cladoceran abundance (Figure 3.10 and Table B10). A negative binomial GLM analysis was also conducted on day 49 and no significant relationship between cladoceran abundance and AWW load was observed (Table B11). Zero-inflated negative binomial GLM analyses on study day 75 found a significant positive relationship between cladoceran abundance and AWW load ($p = 0.016$), demonstrating the possible stimulatory effect of AWW loading on cladoceran abundance (Table B10).

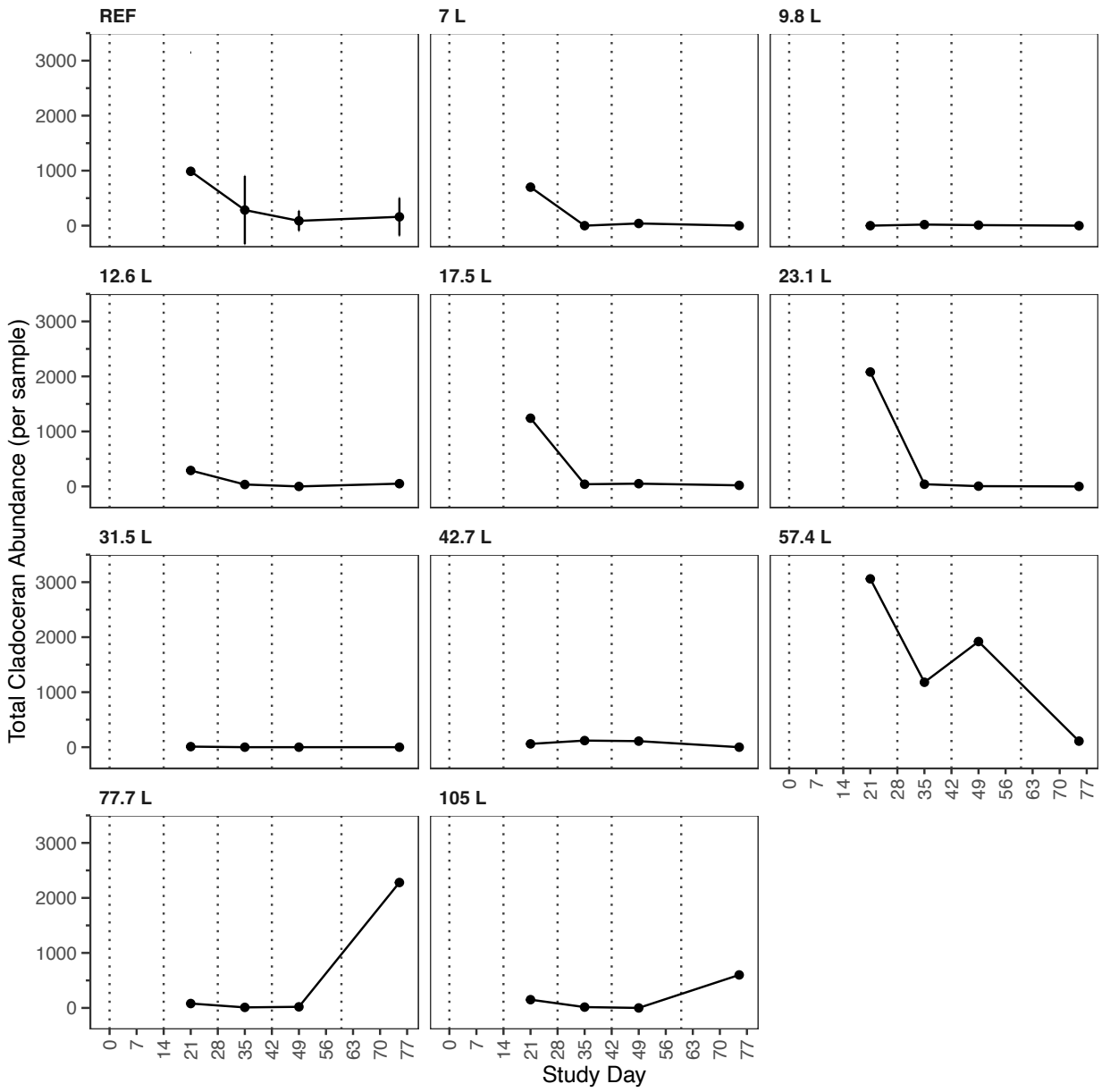

Figure 3.9: Total cladoceran abundance over the duration of the RL study within each treatment. The REF plot displays the mean value of the references (n = 5) with error bars representing the ± standard deviation. The dotted vertical lines represent the days AWW was added to the treatment mesocosms.

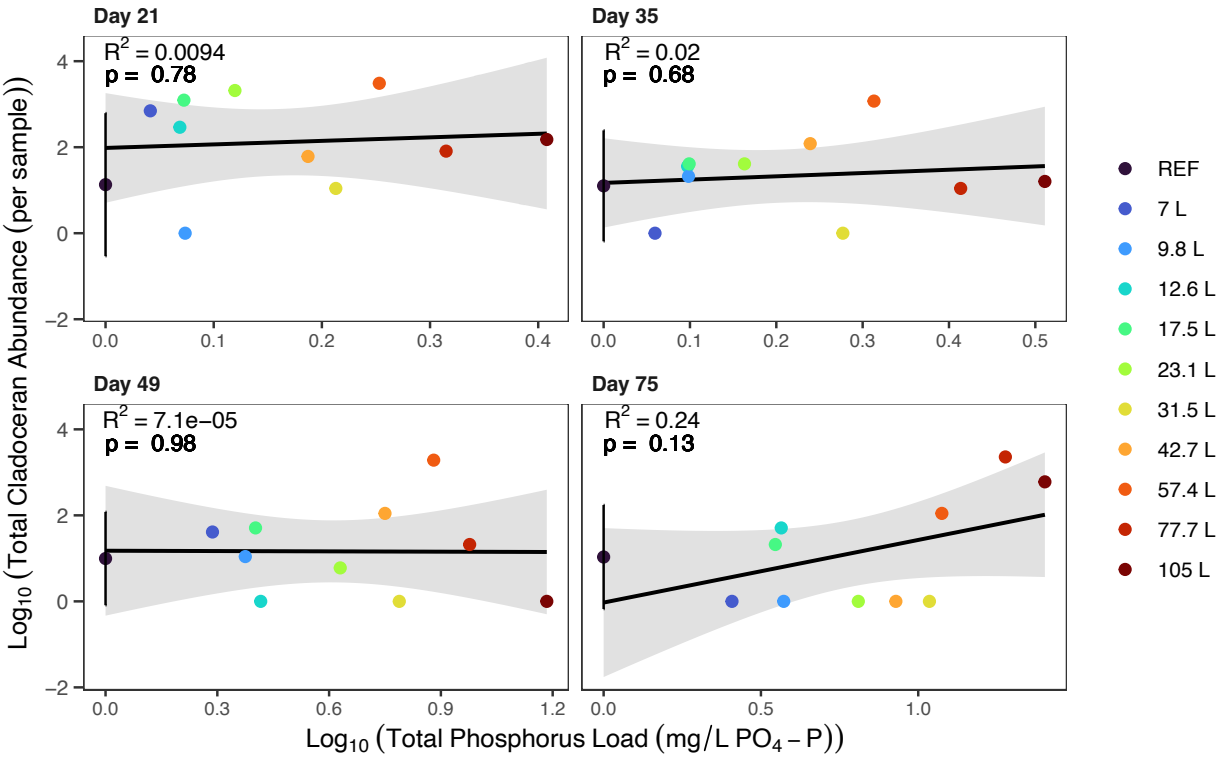

Figure 3.10: Linear regression model results of the relationship between log10(x + 1) of cumulative AWW load concentration (TP used as the representative variable) and cladoceran abundance. REF displays the mean of the references (n = 5) with the error bars representing ± standard deviation. Each plot displays the model results on according to study day.

3.1.5.3 Copepod Abundance

The copepod group was comprised of the order Calanoida and Cyclopodia, referred to as calanoids and cyclopoids. Copepod nauplii were also included in this group. Cyclopoids and copepod nauplii were consistently abundant in all samples, often encompassing over 50% of the sample (Figure 3.6). Calanoids were observed consistently within each sample but at a much lower abundance, only accounting for 4% of total abundance. Copepod abundance peaked in several of the mid-range treatments (7L, 9.8L, 17.5L, 23.1L, 42.7L) around study day 35 (Figure 3.11). Then copepod abundance decreased in most treatments by study day 49 and 75, with the exception of the 31.5L and 77.7L treatments. A large spike in cyclopoid and nauplii abundance occurred in the 77.L treatment by study day 75. Calanoids were observed in all treatments (besides one reference mesocosm) on study day 21 and 35 (Figure 3.12). By study day 49 the abundance of calanoids had decreased or was absent from several treatments, particularly the higher treatments. By study day 75, calanoids were only present in four of the references, 12.6L, 17.5 L, and 23.1L treatments.

Linear regression analysis revealed no significant relationship between AWW load and either total copepod abundance, cyclopoid abundance, or copepod nauplii abundance on any study day (Table B10 and Figures B24-B26). On study day 21 and 49 there was a significant negative relationship between calanoid abundance and AWW load (21: $p = 0.011$, $R^2 = 0.53$; 49: $p = 0.003$, $R^2 = 0.64$) (Figure 3.13). This relationship was not significant on study day 35 and marginally significant on study 75 ($p = 0.053$, $R^2 = 0.35$) (Figure 3.13). Study day 75 was also analysed using a zero inflated negative binomial GLM, which found a marginally significant negative relationship between calanoid abundance and AWW load ($p = 0.0582$) (Table B11). The data for study day 75 violates the linear regression assumptions of normality, thus resulting in the

inclusion of the ZINB-GLM. Due to only 4 treatments (references averaged) containing calanoids and the small sample size, the results from the GLM and the LM should be interpreted carefully. However, the abundance data and statistical analyses indicate AWW load resulted in the reduction of calanoid copepods.

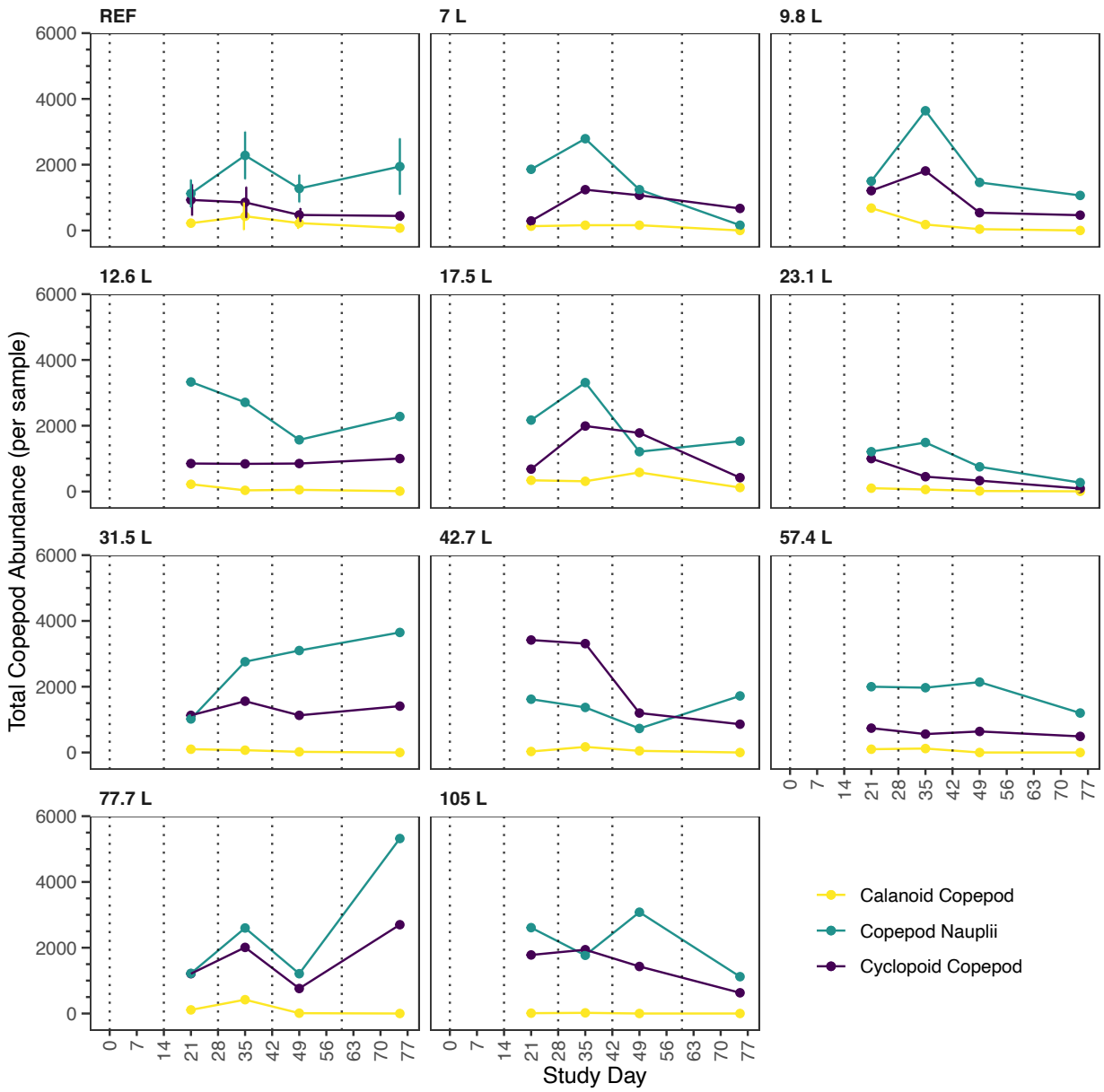

Figure 3.11: Total copepod abundance over the duration of the RL study within each treatment. The REF plot displays the mean value of the references (n = 5) with error bars representing the ± standard deviation. The dotted vertical lines represent the days AWW was added to the treatments.

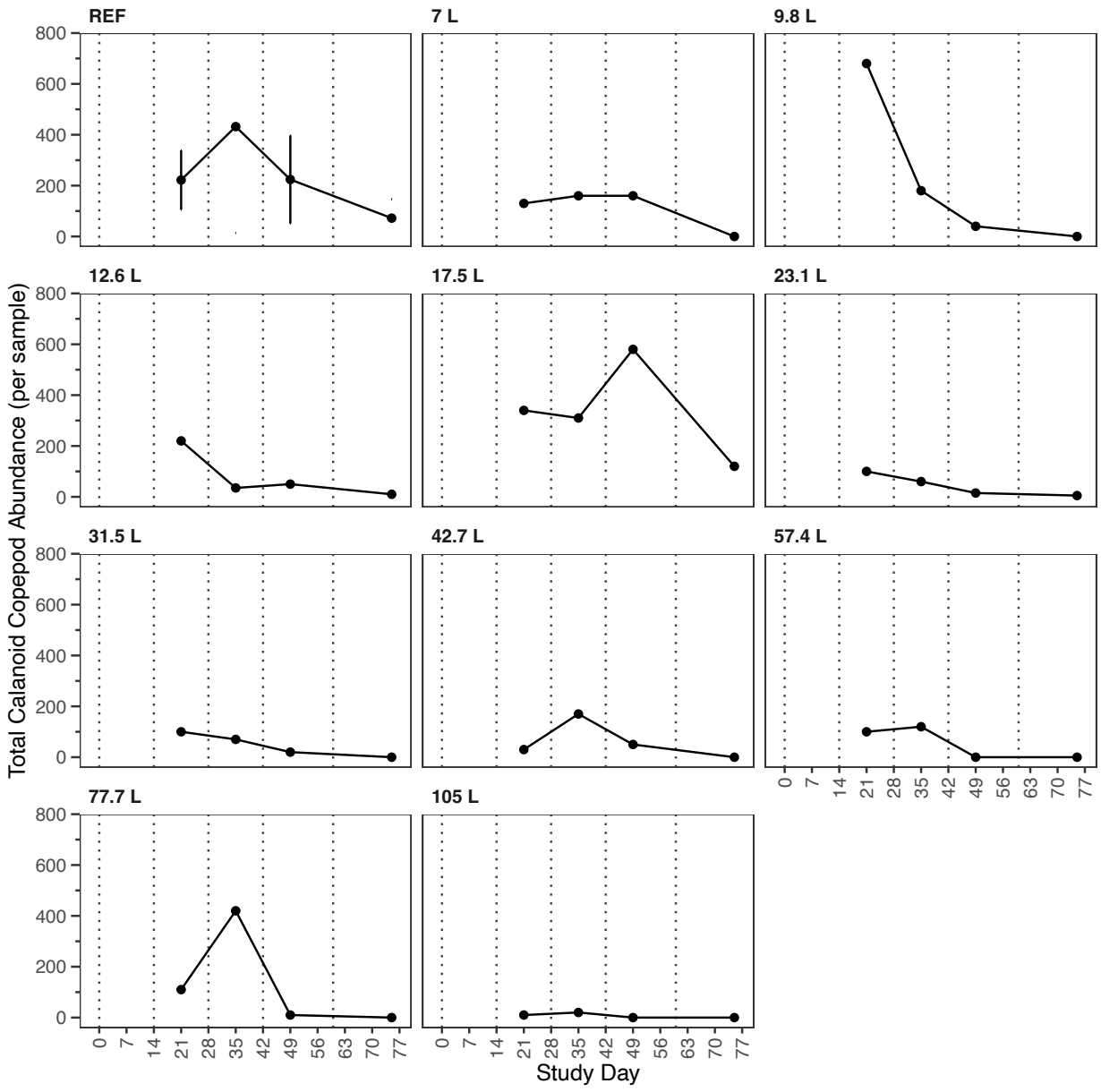

Figure 3.12: Total calanoid copepod abundance over the duration of the RL study within each treatment. The REF plot displays the mean value of the references (n = 5) with error bars representing the ± standard deviation. The dotted vertical lines represent the days AWW was added to the treatments.

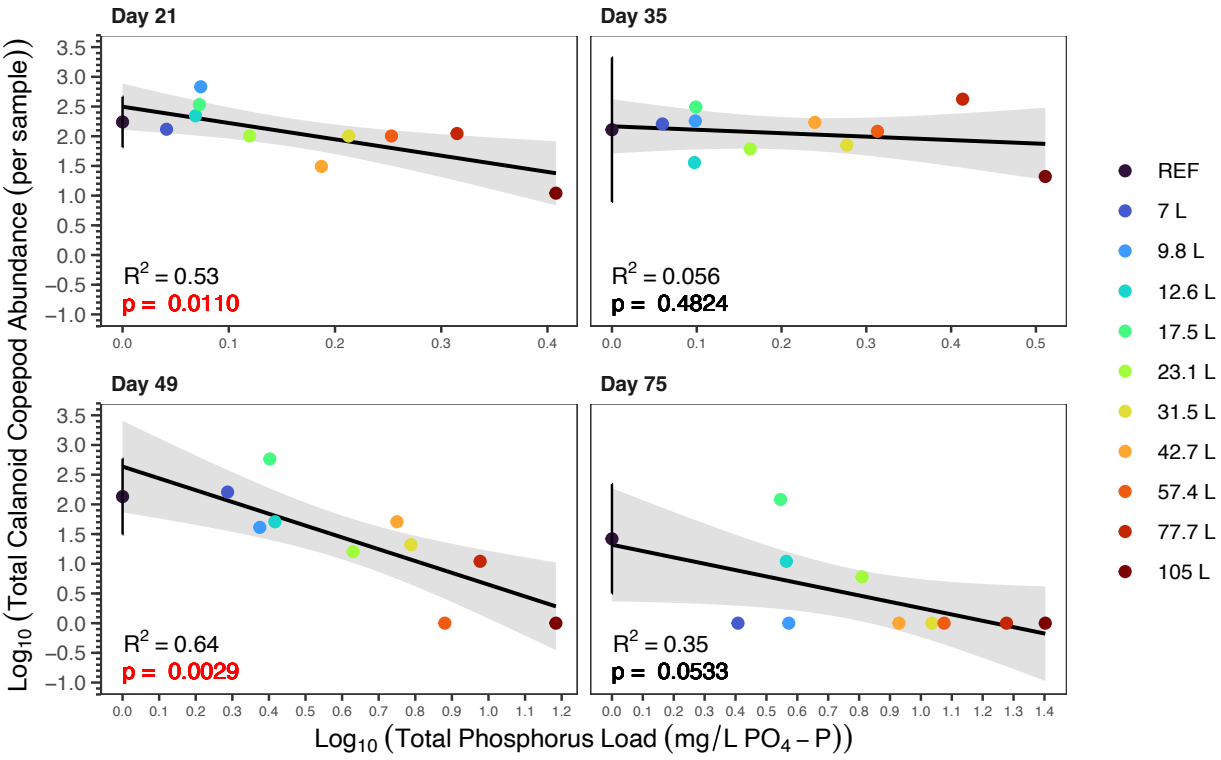

Figure 3.13: Linear regression model results of the relationship between log10(x + 1) of cumulative AWW load concentration (TP used as the representative variable) and calanoid copepod abundance. REF displays the mean of the references (n = 5) with the error bars representing ± standard deviation. Each plot displays the model results according to study day.

3.1.5.4 Rotifer Abundance

The rotifer group included all rotifers identified in the samples. Rotifers were among the most abundant groups across all treatments (Figure 3.6 and Tables B12-B15). The abundance of rotifers varied across treatments and over time (Figure 3.14). From study day 21, which varied in rotifer abundance across treatments, to study day 35, where the overall rotifer abundance generally decreased. However, on study day 35 in the 77.7L treatment the rotifer abundance dramatically increased compared to the rest of the treatments, comprising 59% of total abundance in that treatment. By study day 49, the rotifer abundance in most of the treatments remained unchanged, besides a noticeably higher abundance observed in treatments 31.1L, 77.7L, and 105L. A decline in rotifer abundance was observed across all treatments by study day 75. Linear regression analyses found no significant relationship between rotifer abundance and AWW load on any study day (Figure 3.15 and Table B10). On study day 35, a positive marginally significant relationship can be observed ($p = 0.073$, $R^2 = 0.31$).

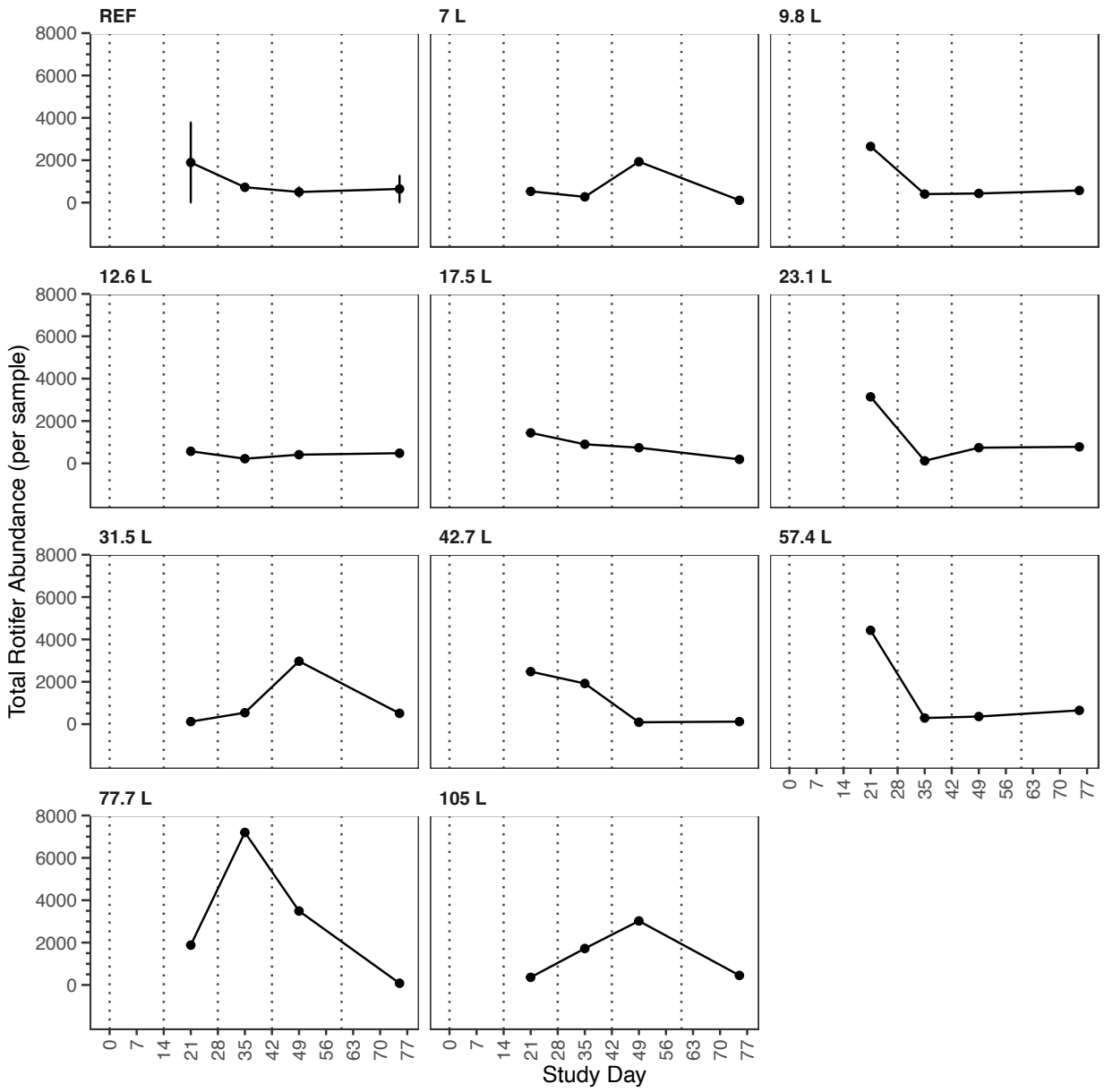

Figure 3.14: Total rotifer abundance over the duration of the RL study within each treatment. The REF plot displays the mean value of the references (n = 5) with error bars representing the ± standard deviation. The dotted vertical lines represent the days AWW was added to the treatments.

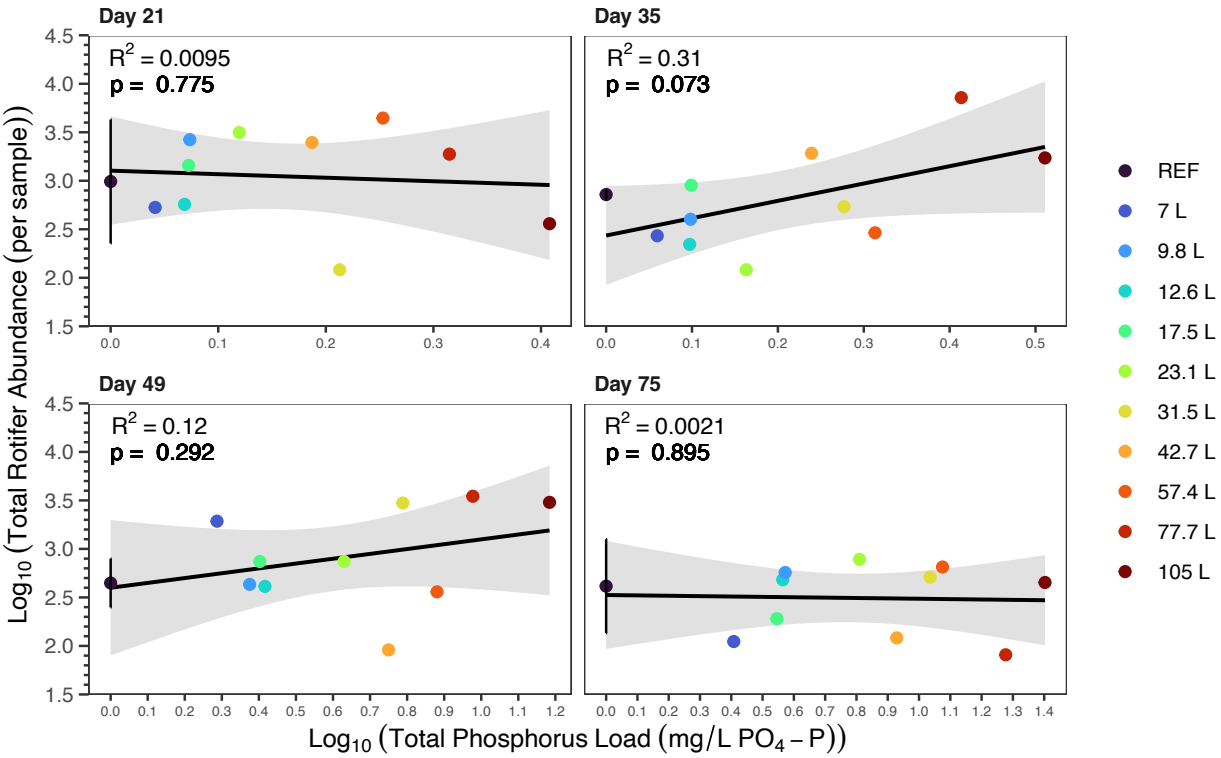

Figure 3.15: Linear regression model results of the relationship between log10(x + 1) of cumulative AWW load concentration (TP used as the representative variable) and rotifer abundance. REF displays the mean of the references (n = 5) with the error bars representing ± standard deviation. Each plot displays the model results according to study day.

3.1.5.5 Zooplankton Diversity

Zooplankton diversity, richness, and evenness values for each study day are presented in Tables B12 – B15. Zooplankton diversity, measured by the Inverse Simpson Index ranged from 2.26 – 3.87, with the lowest diversity measured in the 105L and 17.5L treatment (Figure B27). Over the study duration diversity changed in each treatment yet remained mostly within the same range across treatments. The species evenness generally ranged from 0.35 – 0.66, indicating no strong species dominance (Figure B28). By study day 75, species evenness peaked in the 9.8L and 105L treatments. Species richness varied from 3 – 6 and generally decreased over the study duration (Figure B29).

There was no significant relationship determined by linear regressions between each diversity index and AWW load at each study day (Table B10 & Figures B30 – B33). A marginally significant positive relationship was observed on study day 75 between AWW load and both Inverse Simpson Index ($p = 0.1$, $R^2 = 0.27$) and species evenness ($p = 0.11$, $R^2 = 0.26$).

3.1.5.6 Influence of Fish on Zooplankton

A range of 5 – 12 fish were retrieved from the mesocosms by the final sampling date of September 17 (Table B19). Since we only had information on fish abundance for the end of the study, the effect of fish abundance to total zooplankton abundance could only be evaluated on study day 75. Linear regression revealed no significant relationship between fish abundance and total zooplankton abundance (Table B16).

On study day 75, fish larvae were found within multiple zooplankton sampling jars in one reference sample and in the 23.1 L treatment. There was no significant relationship between total

zooplankton abundance and fish presence in the sampling jars as a binomial term based on linear regression analysis on study day 75 (Table B16).

3.1.5.7 Influence of Environmental Variables on Zooplankton

The RDA model only explained 8.6% of the zooplankton community variation indicating that there were no strong relationships between the environmental variables and zooplankton community composition. Permutation testing of the overall RDA model ($p = 0.073$) and the axes did not significantly explain the zooplankton variance. The environmental variables explained 22.9% of the variance in zooplankton composition, while 66.3% of the variation went unexplained. The variance due to study day was 10.7%, which was controlled out of the RDA model, via the conditional term.

The environmental variables included in the analysis are within Figure 3.17. Variables excluded were Part-P due to correlation with chlorophyll-*a*; NH_3 due to its correlation with TAN, dissolved oxygen, and water temperature; PO_4 due to correlation with TP; NO_3 due to correlation with pH; and water temperature due to correlation with TAN, dissolved oxygen, NH_3, and NO_3. These removed variables can be interpreted in the same manner as their correlated counterparts. Dissolved oxygen and TAN exceeded VIF criteria; however, due to the ecological relevance of these variables they were retained within the RDA.

The environmental variables that had the strongest influence on the RDA, as indicated by the length of the arrows in Figure 3.16, were TDN, pH, and chlorophyll-*a*, with TDN having a significant effect on the zooplankton community, determined from permutation testing ($p = 0.04995$). TP and dissolved oxygen also correlate with these variables, as indicated by the arrows pointing in the same direction demonstrating that an increase in nutrients was related to an increase in chlorophyll-*a* and dissolved oxygen. Most AWW treatments were also correlated with

these variables, indicting this was a response that occurred across these treatments. The reference treatments were negatively correlated to these variables, indicating this response likely was not as prominent. *Daphnia* and calanoid copepods are located nearest to the reference treatments and opposite the nutrient driven response, indicating these taxa responded negatively to AWW loading. There is no clear pattern related to study day, indicating that seasonal variance did not strongly drive the variation in the zooplankton community.

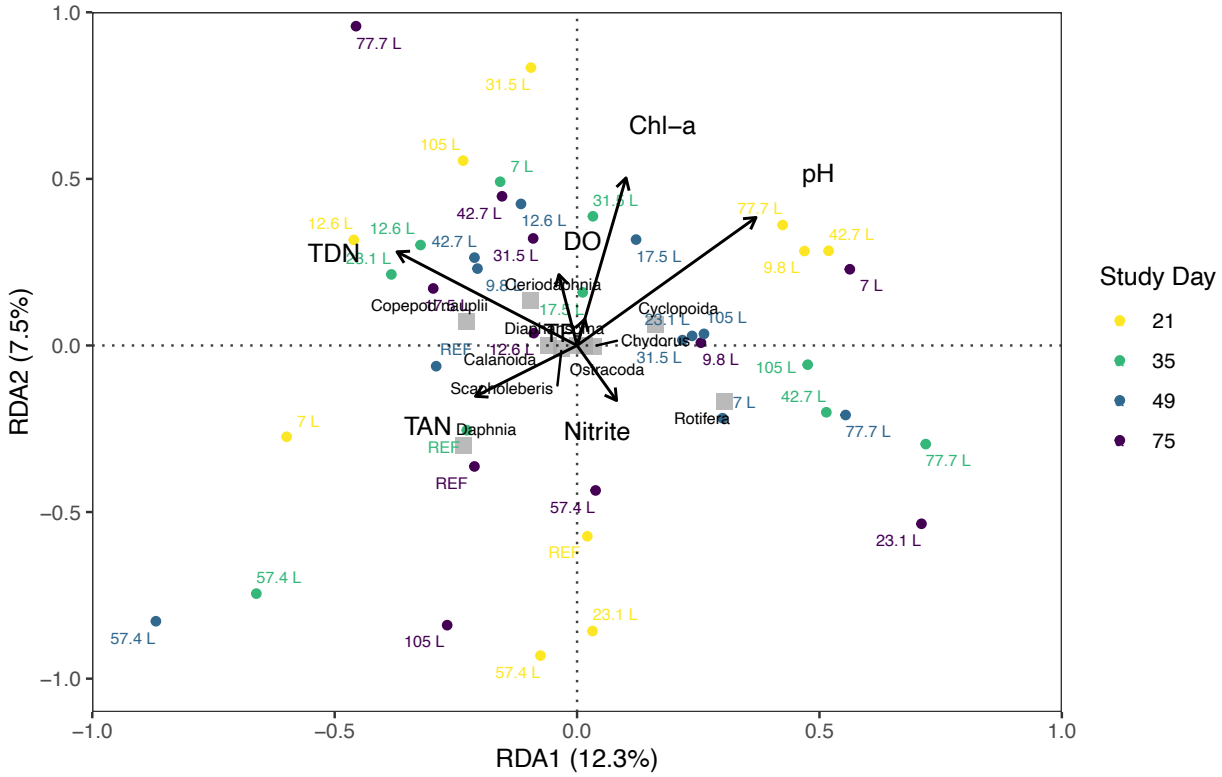

Figure 3.16: Redundancy Analysis (RDA) plot demonstrating the relationship between environmental variables (arrows), zooplankton species (squares), and AWW treatments and references on each study day (points). The references are represented by the mean value (n = 5). The axis explained 12.3% (Axis 1) and 7.5% (Axis 2) of the total variance. The 9.8 L treatment on day 35 and the 17.5 L treatment on study day 21 were removed due to missing measurements. Environmental variables with correlation greater then 0.7 were removed.

3.1.6 Zooplankton – eDNA Metabarcoding Identification

3.1.6.1 Overview

The total reads obtained after sequencing, quality filtering and denoising, and filtering for zooplankton taxa are all presented in Table 3.2. The Leray primer generated the highest read count following sequencing, followed closely by the Copepod primer. Each of the Daphnia, Rotifer 1, and Rotifer 2 primers provided approximately 3 million fewer reads. Quality filtering from the Leray, Copepod, Daphnia, Rotifer 1, and Rotifer 2 primers resulted in the retention of 47%, 44%, 62%, 57%, and 59% of the reads, respectively. Approximately 50% of the filtered reads belonged to zooplankton taxa reads for the Leray, Copepod, and Daphnia primers. However, only 11% and 27% of the filtered reads corresponded to zooplankton taxa reads for the Rotifer 1 and Rotifer 2 primers, respectively. Also, when evaluating only the samples collected at the R&L site (i.e., not including field blanks, extraction blanks, and the 2 UM samples), there were significantly fewer zooplankton associated reads in the Rotifer 1 and Rotifer 2 primers when compared to the other taxa, which when combined produced greater than one million zooplankton reads. The low zooplankton read count for the Rotifer 1 and Rotifer 2 primers can likely be attributed to the contamination observed in the blanks, resulting in inflated results for the total sequenced reads. Contamination likely did not occur in the field as the field blank ASVs read counts do not correspond to ASVs recorded within the samples. The contamination also did not occur during extractions as minimal contamination was typically observed within extraction blanks of the other primers. The PCR reactions were run separately for the controls and the samples; thus, a majority of the contamination must have occurred in the lab for the Rotifer 1 and Rotifer 2 controls reactions. Since contamination of the blanks occurred, there was no way to determine if contamination contributed to the Rotifer 1 and Rotifer 2 reads; thus no

contamination was removed from the samples and the results from these primers must be interpreted carefully.

Table 3.2: The sequenced read count, quality filtered read count, zooplankton read count, and zooplankton read count in the R&L samples. The total number of zooplankton taxa identified are also presented.

Primer	Total Sequenced Reads	Total Quality Filtered Reads	Total Zooplankton Reads (samples and controls)	Total Zooplankton reads (RL samples)	Total Zooplankton Taxa
Leray	8,701,400	4,081,461	1,926,955	1,824,066	25
Copepod	8,437,365	3,698,823	1,946,788	1,735,143	23
Daphnia	5,655,385	3,505,244	1,705,159	1,395,260	21
Rotifer 1	5,543,980	3,165,549	345,818	116,000	25
Rotifer 2	6,726,314	3,995,006	1,073,309	185,727	22

A similar number of zooplankton taxa were detected for all of the primers, with 16 common taxa observed across all primers (Figure 3.17). The Daphnia and Rotifer 1 primers both had four unique taxa, and the Leray and Rotifer 2 primers produced two. The Copepod primer did not generate any unique zooplankton taxa. However, several taxa were uniquely shared between the Copepod, Leray, and Rotifer 2 primers. The specific zooplankton taxa identified using each primer are presented in SI Table 24. Although the designed primers were developed to target the specific zooplankton groups indicated by their name, this was not necessarily observed. The designed primers identified zooplankton groups beyond the scope of their targeted design, resulting in overlap of species identifications across the primers. However, the proportion of reads for each taxon varied depending on the primer and often reflected the targeted zooplankton group. Generally, the Leray and Copepod primers were dominated by cyclopoid copepods, while the Daphnia primer predominately amplified cladoceran species and more specifically *Daphnia* species. The Rotifer 1 and Rotifer 2 primers were more variable in which taxa dominated;

however, the rotifer group was highly represented in relative abundance using those primers. Overall, there was a significant taxonomic overlap among the primers; yet the proportion of each taxon varied considerably across primers. The results from the specific primers are described separately and in more detail in the following sections.

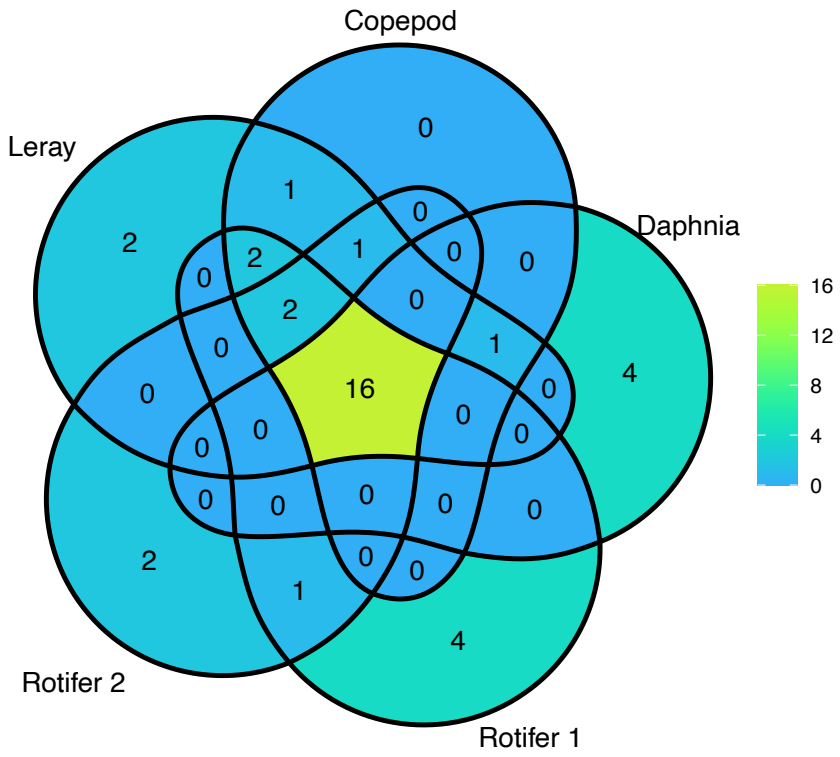

Figure 3.17: The number of zooplankton taxa identified from each primer set. Overlapping sections indicate a shared taxa between primers.

3.1.6.2 Leray Primer

The Leray primer identified 15 taxa to species level, four taxa to genus, two to family, three to order, and one to class (Figure B34). Cyclopoid copepods detected belonged to the genera *Acanthocyclops*, *Eucyclops*, *Macrocyclops*, and *Mesocyclops*, as well as more generally, Cyclopoida and Cyclopidae. Calanoid copepods were identified to either the order Calanoida or within genus *Leptodiaptomus*. The cladocerans identified belonged to the genera *Daphnia*, *Moina*, *Ceriodaphnia*, and *Scapholeberis*. Rotifers included the class Monogononta and genera *Brachionus*, *Euchlanis, Platyias, Polyarthra, Proales,* and *Rotaria*. The cyclopoid group consistently comprised over 80% of the reads (relative abundance) from the samples (Figure 3.18). Rotifers were identified in the highest proportion on study day 20, then decreased in relative abundance in all treatments over time. The relative abundance of calanoid copepods increased in the reference and lower treatments on study day 46 and 74. A slight increase in cladocerans was observed in the 57.4L, 77.7L, and 105L treatments by study day 74. *Acanthocyclops vernalis* dominated from the cyclopoid copepod group across all treatments over the study duration (Figure 3.19). However, by study day 74 a shift in the cyclopoid community can be observed with *Macrocyclops albidus* and *Mesocyclops edax* comprising 10 – 20% more of relative cyclopoid copepod abundance.

Zooplankton diversity metrics are presented in Table B21. Shannon Diversity Index and Inverse Simpson Diversity Index did not vary among treatments on study day 20. By study day 46, diversity increased 1.5 to 2-fold in the 7L and 17.5L treatments and then diversity stabilized in the low treatments (7L, 17.5L, and 31.5L) to between an Inverse Simpson Index of 1.2 to 1.34 by study day 74, whereas diversity slightly increased in the higher treatments (57.4L, 77.7L,

105L) by around 1.5 to 2-fold. Linear regression analyses revealed no significant relationships between each diversity index and AWW load at each study day (Table B22, Figures B35 – B36).

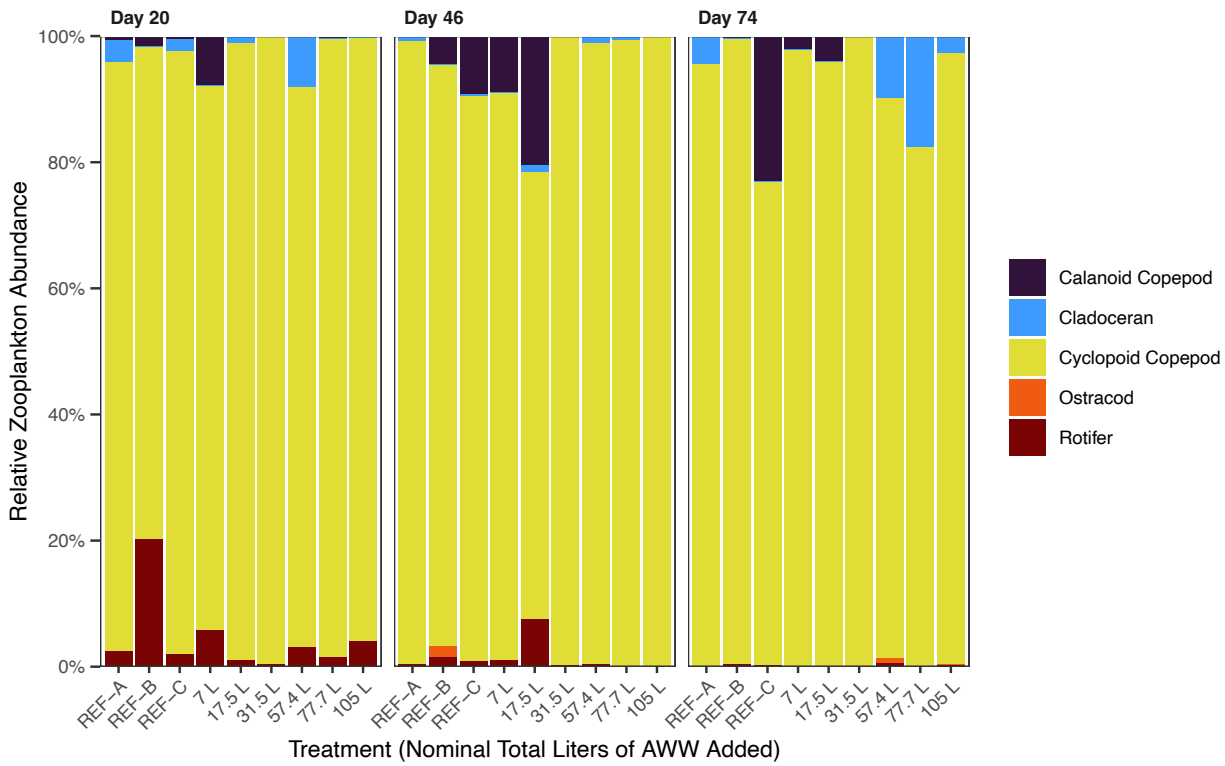

Figure 3.18: RL relative zooplankton abundance (%) of each major zooplankton group for each treatment with the separate plots displaying the results for each study day the eDNA was sampled. These results reflect the use of the Leray primer.

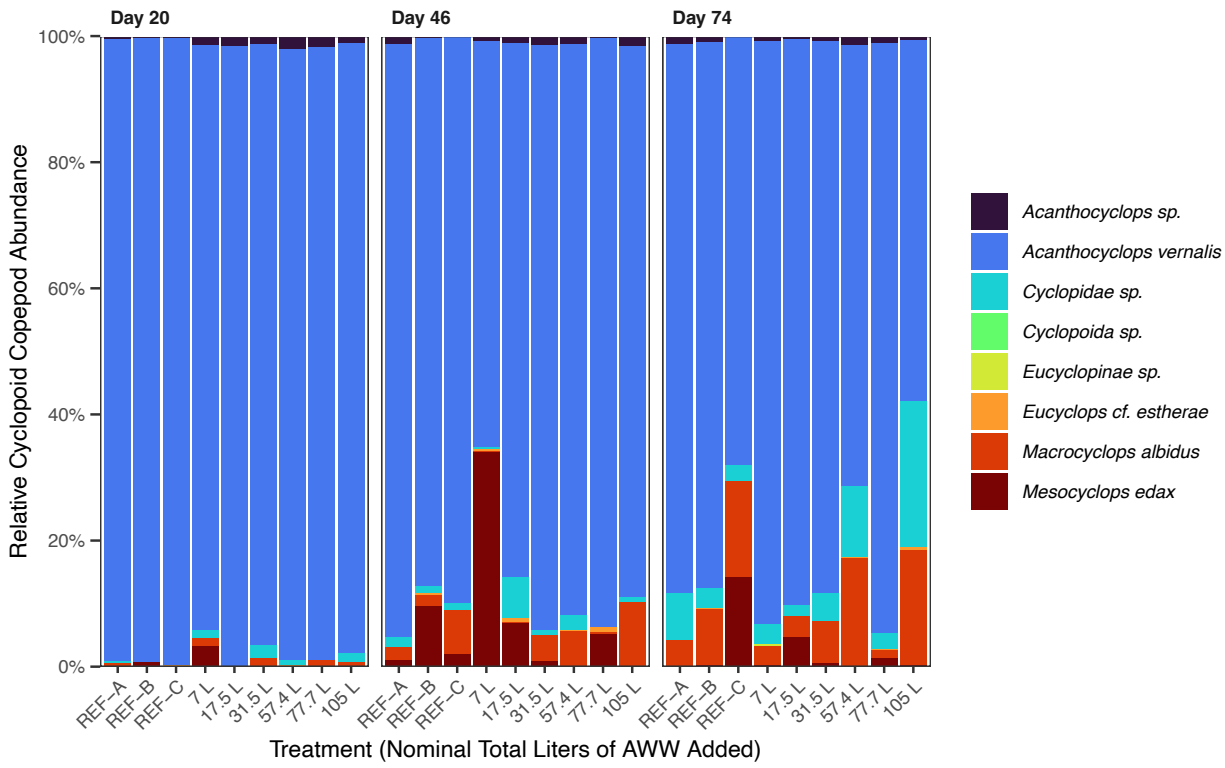

Figure 3.19: RL relative cyclopoid copepod abundance (%) of each major zooplankton group for each treatment with the separate plots displaying the results for each study day the eDNA was sampled. These results reflect the use of the Leray primer.

Principal Coordinates Analysis (PCoA) was performed to visualize differences in community composition across AWW treatments and study days for the Leray primer results. The first axis, PCoA1, explained 35.1% of the variation in community composition, while the second axis, PCoA2, explained 28.1% (Figure 3.20). PERMANOVA analyses found a statistically significant effect of study day ($R^2 = 0.21$, $p = 0.001$) and treatment ($R^2 = 0.3$, $p = 0.012$) on zooplankton community composition (Table B23). Pairwise comparisons of study days found significant differences between study days 20 and 46 ($R^2 = 0.19$, $p_{adj} = 0.015$), in addition to study days 20 and 74 ($R^2 = 0.32$, $p_{adj} = 0.003$) (Table B24). The PCoA figure supports a distinct grouping of the study day 46 and 74 treatments, while study day 20 treatments are dispersed separately across the positive side of the PCoA2 axis. Additional pairwise comparisons of treatments found no significant individual pairing, indicating that the variation between specific treatments was not strong and that treatment effect was instead present across the entire treatment gradient (Table B25). In the PCoA figure a clustering of the higher treatments (31.5L, 57.4L, 77.7L, and 105L) on the positive end of PCoA1 occurred; however, this cluster also included overlap of reference treatments and the 17.5L treatment, which dampens the detection of a treatment effect and likely contributed to the insignificant pairwise results we observed.

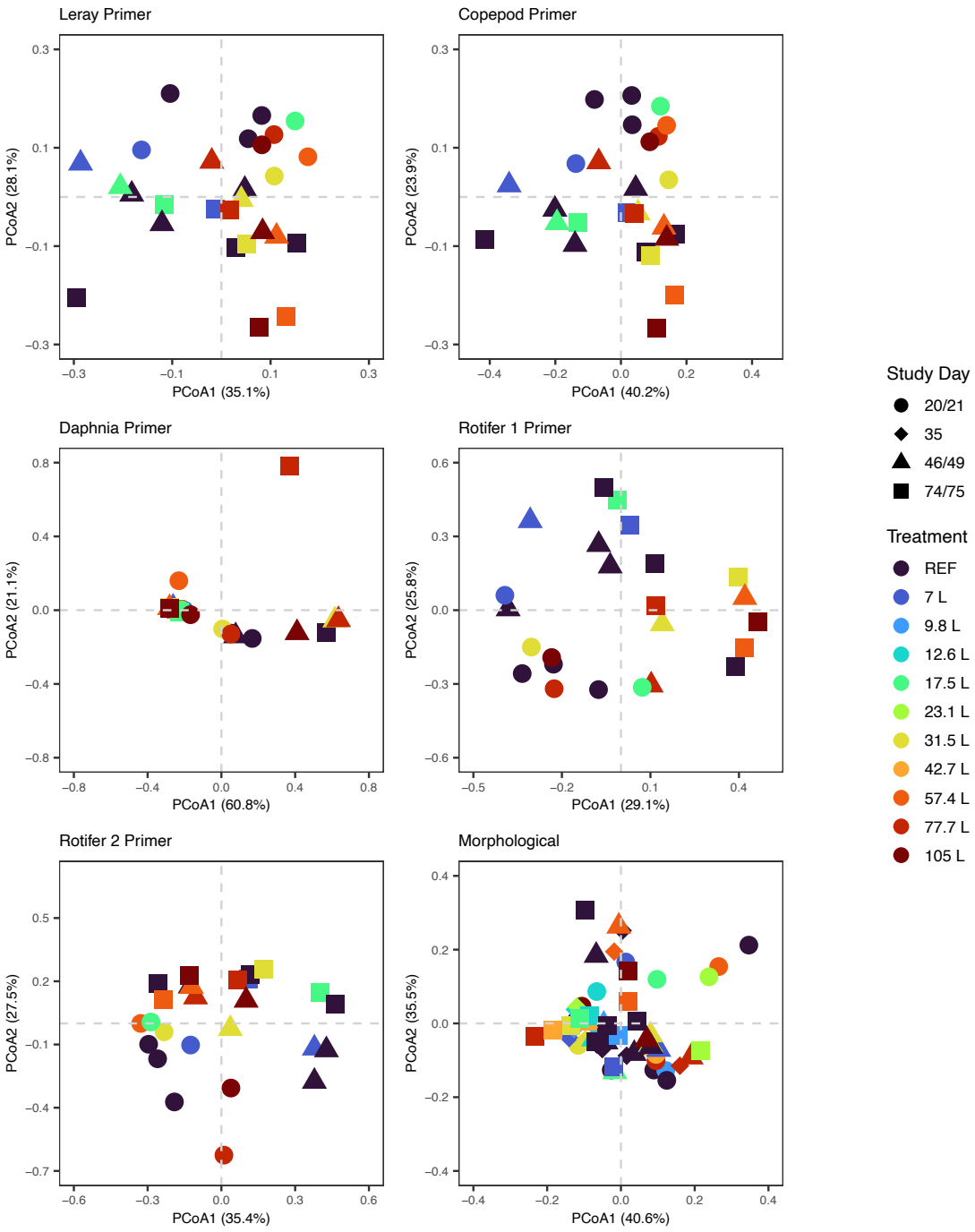

Figure 3.20: Principal Coordinates Analysis (PCoA) of zooplankton community composition among treatments and across study days based on Bray-Curtis dissimilarity distance matrix. The plots are based on morphological and eDNA identification methods (separated according to primer). The eDNA samples were always collected prior to morphological identifications to prevent contamination; for each study day point indicated in the legend the first study day represents eDNA and the second represents morphological. Note only morphological data was collected on study day 35.

3.1.6.3 Copepod Primer

The copepod primer identified 14 taxa to species level, four taxa to genus, two to family, two to order, and one to class (Figure B37). Cyclopoid copepods identified within the samples belonged to four genera, *Acanthocyclops*, *Eucyclops*, *Macrocyclops*, and *Mesocyclops*, as well as more generally, Cyclopidae. Calanoid copepods were identified to either the order Calanoida or within the genus *Leptodiaptomus*. The cladocerans identified belonged to the genera *Daphnia*, *Moina*, *Ceriodaphnia*, and *Scapholeberis*. Rotifers included the class Monogononta and genera *Brachionus*, *Euchlanis, Polyarthra, Proales,* and *Rotaria*. The copepod primer generally had the same relative abundance results as the Leray primer, with cyclopoid copepods dominating relative abundance (Figure 3.21).

Zooplankton diversity, assessed using Shannon Diversity Index and Inverse Simpson Diversity Index as metrics, did not vary between treatments on study day 20. By study day 46, diversity increased 1.5 to 2.5-fold in the 7L and 17.5L treatments, and then diversity stabilized in the low treatments (7L, 17.5L, and 31.5L) to between an Inverse Simpson Index of 1.3 to 1.58 by study day 74, whereas diversity slightly increased in the 57.4L and 105L treatments by approximately 2-fold. Linear regression analyses found there were no significant relationships between each diversity index and AWW load at each study day (Table B22, Figures B38 – B39).

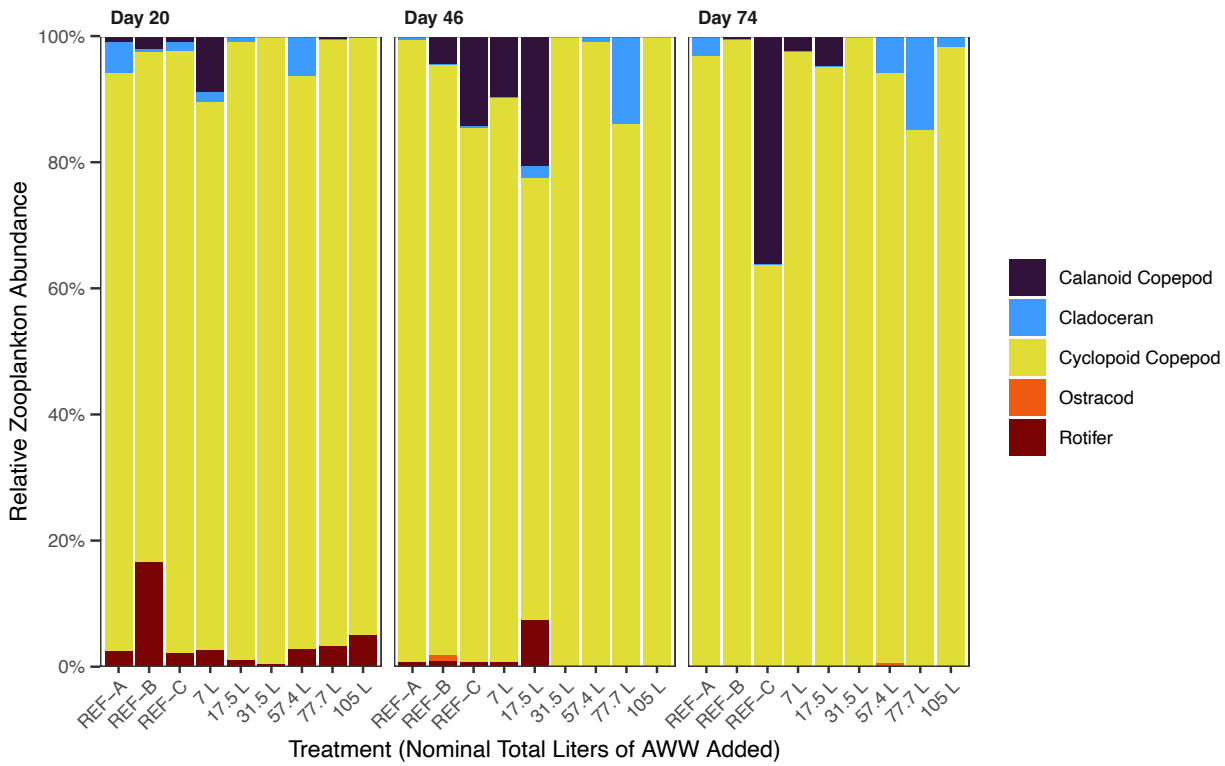

Figure 3.21: RL relative zooplankton abundance (%) of each major zooplankton group for each treatment with the separate plots displaying the results for each study day the eDNA was sampled. These results reflect the use of the Copepod primer.

Principal Coordinates Analysis (PCoA) was performed to visualize differences in community composition across AWW treatments and study days for the Copepod primer results. The first axis, PCoA1, explained 40.2% of the variation in community composition, while the second axis, PCoA2, explained 23.9% (Figure 3.20). PERMANOVA analyses showed a statistically significant effect of study day ($R^2 = 0.18$, $p = 0.001$) on zooplankton community composition, while treatment was only marginally significant ($p = 0.058$) (Table B23). Pairwise comparisons of study days found significant differences between study days 20 and 46 ($R^2 = 0.21$, $p_{adj} = 0.008$), in addition to study days 20 and 74 ($R^2 = 0.28$, $p_{adj} = 0.003$) (Table B24). The PCoA figure supports this as there is distinct grouping of the study day 46 and 74 treatments, while study day 20 treatments are dispersed across the positive side of the PCoA2 axis. In the PCoA figure a clustering of the higher treatments (31.5L, 57.4L, 77.7L, and 105L) on the positive end of PCoA1 occurred.

3.1.6.4 Daphnia Primer

The Daphnia primer identified 12 taxa to species level, three taxa to genus, three to family, two to order, and one to class (Figure B40). Cyclopoid copepods identified within the samples belonged to five genera, *Acanthocyclops*, *Eucyclops*, *Macrocyclops*, *Dicyclops*, and *Mesocyclops*, as well as the more generally, Cyclopidae. Calanoid copepods were identified to either the order Calanoida or within the genus *Leptodiaptomus*. The cladocerans identified belonged to the genera *Daphnia*, *Ceriodaphnia*, and *Scapholeberis*, as well as the family Bosminidae. Rotifers included the class Monogononta, family Flosculariaceae, and genera *Euchlanis, Polyarthra,* and *Synchaeta*. In most of the treatments the cladoceran group comprised 60 – 100% of the relative abundance (Figure 3.22). By day 46, the relative abundance of cladocerans was not as high in most treatments and the relative abundance of cyclopoid

copepods increased in the 31.5 L, 77.7 L, and 105 L. Then by day 74 only one reference treatment had multiple zooplankton groups in abundance, and the other treatments predominately amplified only cladocerans. Within the cladoceran group the *Daphnia* sp. drove the dominance in relative abundance (Figure B40). However, on study day 74 in the 77.7 L treatment *Ceriodaphnia* sp. represented most of the relative abundance (Figure B40).

Zooplankton diversity, assessed using Shannon Diversity Index and Inverse Simpson Diversity Index as metrics, did not vary among treatments on study day 20 and the highest diversity calculated was in the references (Table B27). Diversity then decreased in all treatments over time with a maximum 2-fold reduction by study day 74. However, the 105L treatment had a large peak in diversity on study day 46 reaching a 3-fold increase. This then declined to a value consistent with the other treatments by study day 74. Diversity changes were not driven by AWW treatment as linear regression analyses found there were no significant relationships between each diversity index and AWW load at each study day (Table B22, Figures B41 – B42).

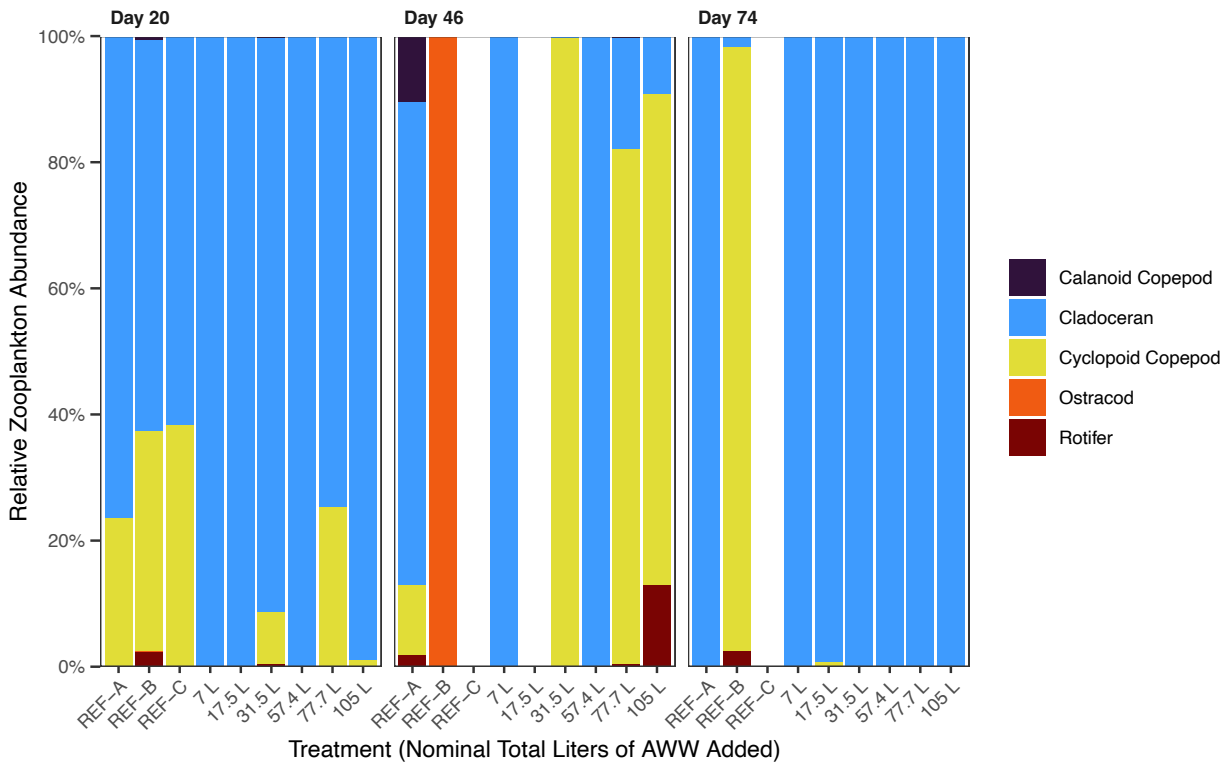

Figure 3.22: RL relative zooplankton abundance (%) of each major zooplankton group for each treatment with the separate plots displaying the results for each study day the eDNA was sampled. These results reflect the use of the Daphnia primer. Treatments without any data indicate where no zooplankton reads were detected.

Principal Coordinates Analysis (PCoA) was performed to visualize differences in community composition across AWW treatments and study days for the Daphnia primer results. The first axis, PCoA1, explained 60.8% of the variation in community composition, while the second axis, PCoA2, explained 21.1% (Figure 3.20). Neither treatment nor study day had a statistically significant effect on zooplankton community composition when tested using PERMANOVA analyses (Table B23). The PCoA figure also supports these findings as there was considerable overlap between treatments and study days. Thus, the observed variation in community composition was unrelated to treatment and time. The 77.7L treatment from study day 74 did vary considerably from the main cluster which is likely a result of the dominance of *Ceriodaphnia* sp. within this treatment and time, as indicated previously.

3.1.6.5 Rotifer 1 Primer

The Rotifer 1 primer identified 16 taxa to species level, three taxa to genus, three to family, two to order, and one to class. Cyclopoid copepods identified within the samples belonged to three genera: *Acanthocyclops*, *Eucyclops*, and *Mesocyclops*, as well as more generally, Cyclopidae (Figure B43). Calanoid copepods were identified to either the order Calanoida or within the genus *Leptodiaptomus*. The cladocerans identified belonged to the genera *Daphnia*, *Ceriodaphnia*, *Moina*, and *Scapholeberis,* as well as the family Daphniidae. Taxa belonging to the rotifer group included class Monogononta and genera *Euchlanis, Rotaria, Proales, Asplanchna, Lecane, Polyarthra,* and *Synchaeta*. The dominant zooplankton group varied across study days, with rotifers comprising most of relative abundance on study day 20 (Figure 3.23). By study day 46 and continuing to day 74, the rotifer relative abundance decreased within the treatments. The relative abundance of calanoid copepods was below 10% in most of the treatments on study day 20; however, in the references and 7 L and 17.5 L treatments, shifts

in relative abundance ranged from 20-80%. A temporal shift specifically occurred in the rotifer community (Figure 3.24). The species *Polyarthra vulgaris* and class Monogononta were initially the dominant rotifer taxa then an increase in *Euchlanis dilatata* and *Proales fallaciosa* occurred over time.

Zooplankton diversity, assessed using Shannon Diversity Index and Inverse Simpson Diversity Index as metrics, did not show any specific treatment related effects (Table B28). The reference treatment consistently had the highest measures of diversity; however, this difference was marginal and diversity among the other treatments exhibited no pattern relative to the references. The 77.7L treatment did steadily decline over the study duration from an Inverse Simpson Diversity Index of 3.41 to 1.02 between study days 20 to 74. The minimal effect of AWW treatment on diversity was also reflected in the linear regression analyses which found no significant relationship between each diversity index and AWW load at any study day (Table B22, Figures B44 – B45).

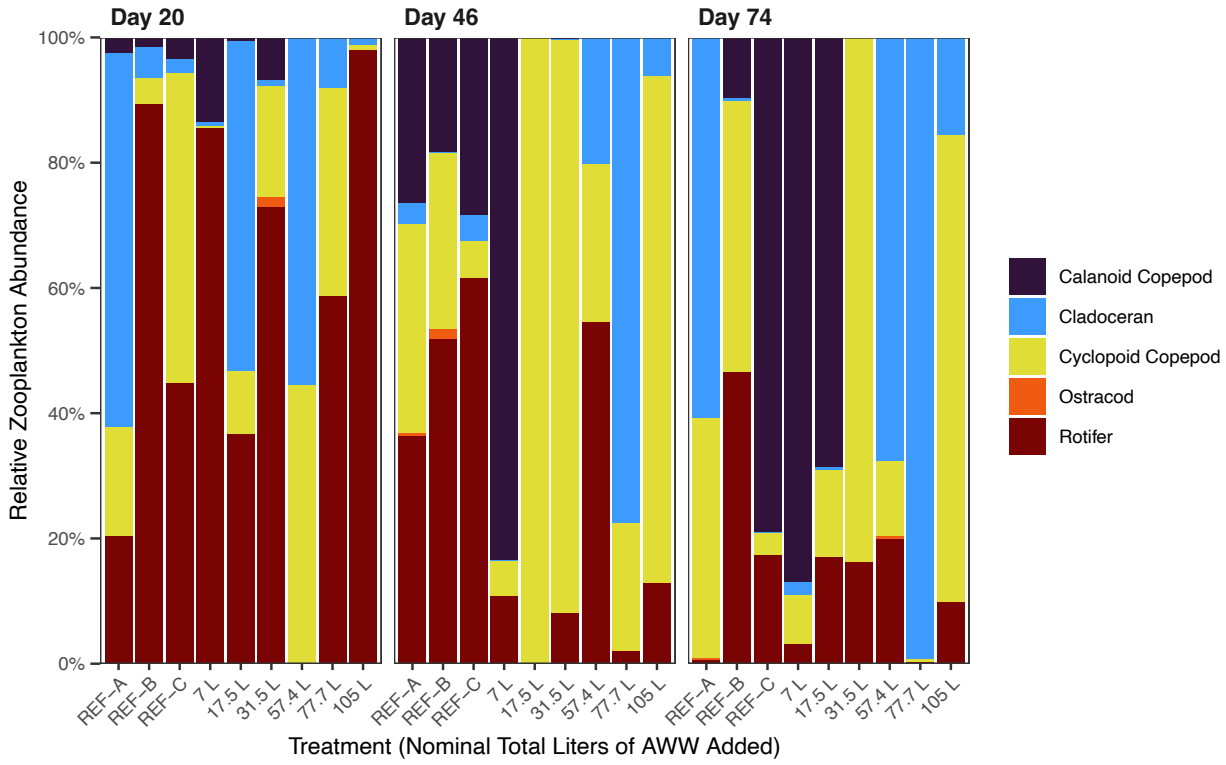

Figure 3.23: RL relative zooplankton abundance (%) of each major zooplankton group for each treatment with the separate plots displaying the results for each study day the eDNA was sampled. These results reflect the use of the Rotifer 1 primer.

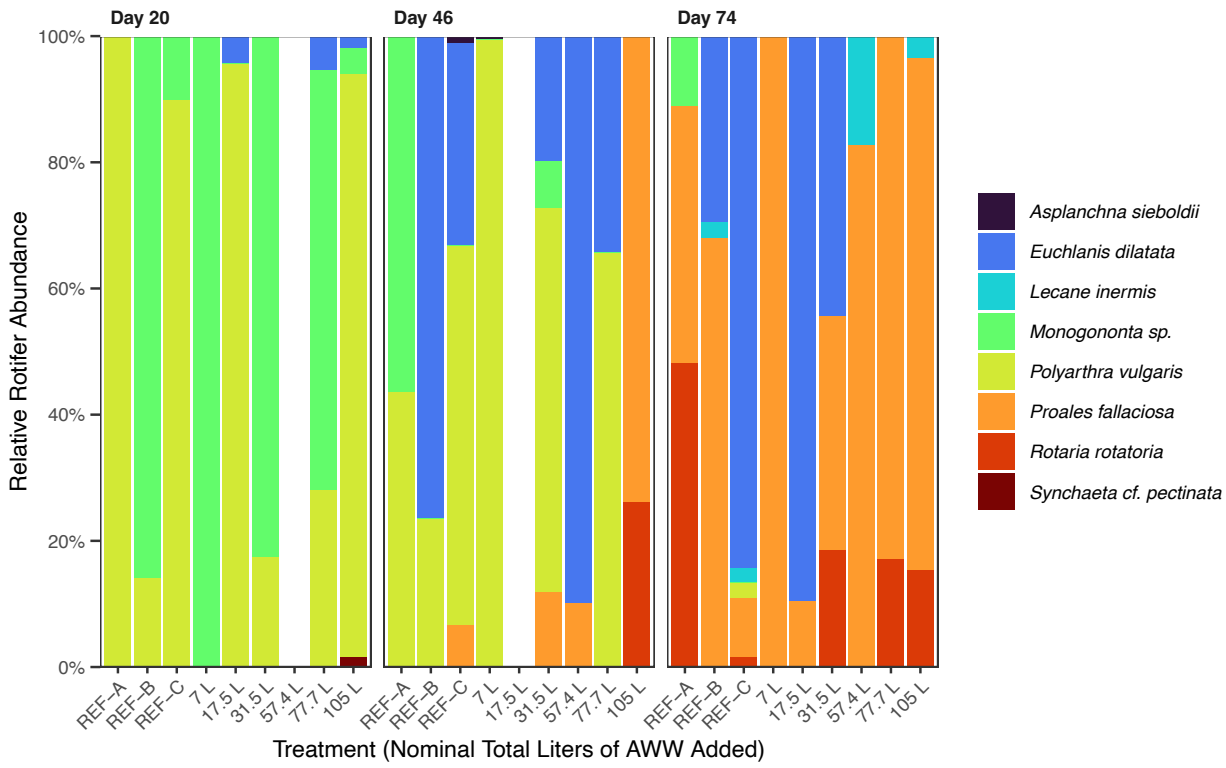

Figure 3.24: RL relative rotifer abundance (%) of each major zooplankton group for each treatment with the separate plots displaying the results for each study day the eDNA was sampled. These results reflect the use of the Rotifer 1 primer. Treatments without any data indicate where no zooplankton reads were detected.

Principal Coordinates Analysis (PCoA) was performed to visualize differences in community composition across AWW treatments and study days for the Rotifer 1 primer results. The first axis, PCoA1, explained 29.1% of the variation in community composition, while the second axis, PCoA2, explained 25.8% (Figure 3.20). PERMANOVA analyses showed a statistically significant effect of study day ($R^2 = 0.21$, $p = 0.001$) and treatment ($R^2 = 0.33$, $p = 0.005$) on zooplankton community composition (Table B23). Pairwise comparisons of study days found significant differences between study days 20 and 46 ($R^2 = 0.17$, $p_{adj} = 0.02$), in addition to study days 20 and 74 ($R^2 = 0.3$, $p_{adj} = 0.003$) (Table B24). The PCoA figure supports a distinct separation of study day 20 treatments on the negative PCoA1 side, while study days 46 and 74 are more dispersed and vary from study day 20. Additional pairwise comparisons of treatments found no significant individual pairing according to adjusted p-values (Table B29). This indicates similar findings to the Leray primer, that is, the variation between specific treatment is not strong and treatment effect is instead present as a gradient across the entire treatments. However, within the PCoA figure the 57.4L treatments are clustered on the far positive side of PCoA1, while the references clustered more to the negative side.

3.1.6.6 Rotifer 2 Primer

The Rotifer 2 primer identified 12 taxa to species level, five taxa to genus, three to family, two to order, and one to class (Figure B46). Cyclopoid copepods identified within the samples belonged to three genera, *Acanthocyclops*, *Eucyclops*, and *Mesocyclops*, as well as more generally, Cyclopidae. Calanoid copepods were identified to either the order Calanoida or within the genus *Leptodiaptomus*. The cladocerans identified belonged to the genera *Daphnia*, *Ceriodaphnia*, *Diaphanosoma*, and *Scapholeberis*. Taxa belonging to the rotifer group included class Monogononta and genera *Euchlanis, Brachionus, Rotaria, Lecane,* and *Polyarthra*. The

zooplankton groups relative abundance varied over time (Figure 3.25). On study day 20 the rotifer group made up over 50% of the relative abundance in most of the treatments. In the highest treatments (77.7L and 105L) rotifers comprised over 75% of relative abundance on study day 20. The rotifer relative abundance then decreased over time while cyclopoid copepods increased. No particular species dominated in the rotifer group (Figure B46). Within the cyclopoid copepod group a shift occurred from predominately *Acanthocyclops* to a more diverse community of cyclopoid copepods from the genera *Ancathocyclops*, *Eucyclops*, and *Mesocyclops*. The cladoceran group was often only comprised of taxa from the *Daphnia* genus with only the 77.7L and 105L treatment also including *Ceriodaphnia* species.

Zooplankton diversity, assessed using Shannon Diversity Index and Inverse Simpson Diversity Index as metrics, had minimal variation among treatments or over the study duration (Table B30). Inverse Simpson Diversity Index primarily ranged from 1.0 – 3.8 with treatments changing only 1 – 2 units over time. However, on study day 46 the 105L treatment increased in diversity 3.5-fold, indicating a strong variation from reference diversity. This treatment then declined in diversity by study day 74 to a level consistent with other treatments. There was a significant relationship determined by linear regressions between Shannon Diversity Index and AWW load on study day 20 ($R^2 = 0.67$, $p = 0.02$) and a marginally significant relationship between Simpson Diversity Index and AWW load on study day 20 ($R^2 = 0.54$, $p = 0.06$) (Table B22 and Figure 3.26). All diversity metrics were not significant when tested by linear regressions for other study days (Table B22, Figure 3.26, Figure B47).

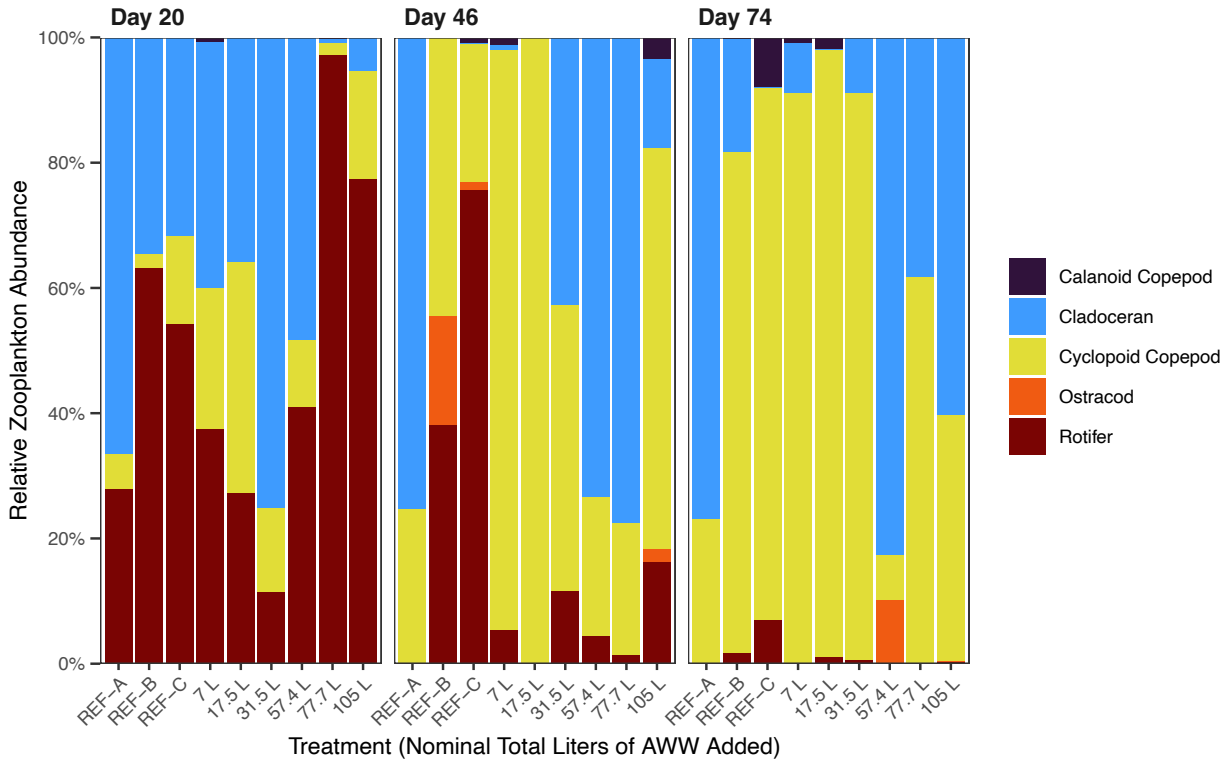

Figure 3.25: RL relative zooplankton abundance (%) of each major zooplankton group for each treatment with the separate plots displaying the results for each study day the eDNA was sampled. These results reflect the use of the Rotifer 2 primer.

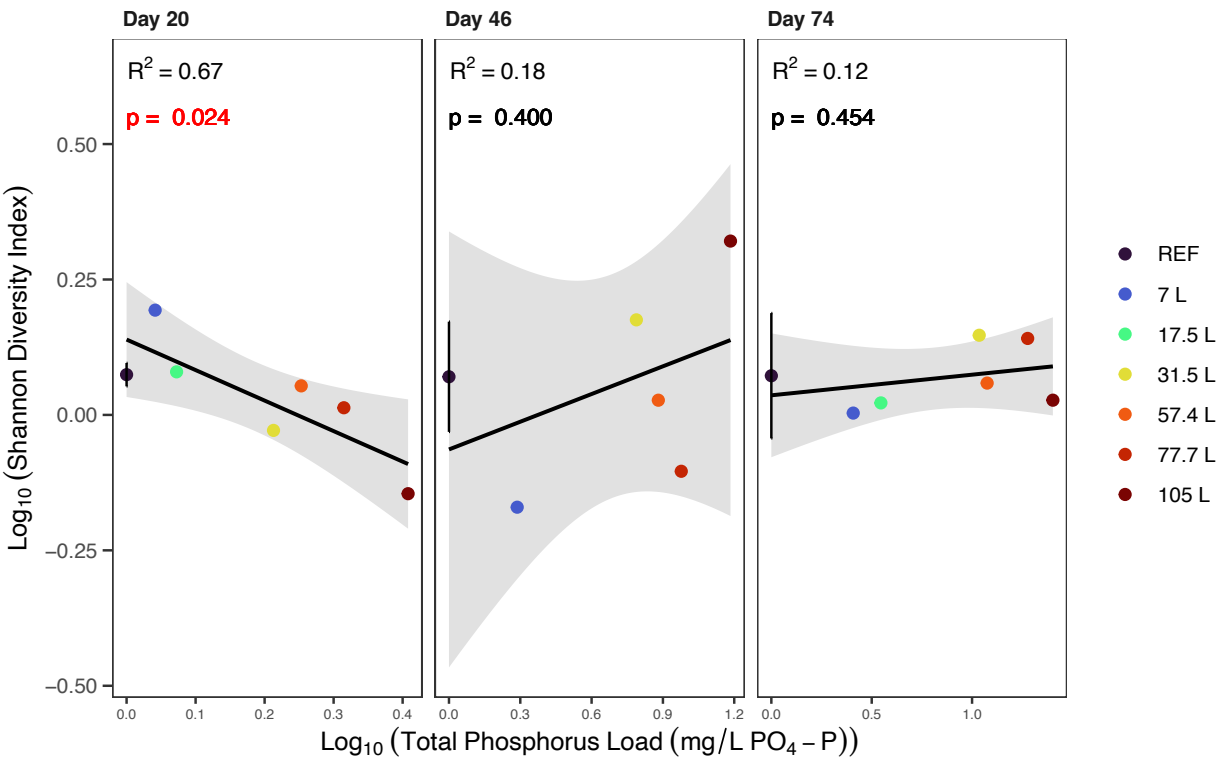

Figure 3.26: Linear regression model results of the relationship between log10(x + 1) of cumulative AWW load concentration (TP used as the representative variable) and Shannon Diversity Index. REF displays the mean of the references (n = 3) with the error bars representing ± standard deviation. Each plot displays the model results according to study day. Diversity calculated from zooplankton eDNA reads acquired using from the Rotifer 2 primer.

Principal Coordinates Analysis (PCoA) was performed to visualize differences in community composition across AWW treatments and study days for the Rotifer 2 primer results. The first axis, PCoA1, explained 35.4% of the variation in community composition, while the second axis, PCoA2, explained 27.5% (Figure 3.20). PERMANOVA analyses showed a statistically significant effect of study day ($R^2 = 0.22$, $p = 0.001$) on zooplankton community composition, while treatment was not significant (Table B23). Pairwise comparisons of study days showed significant differences between study days 20 and 46 ($R^2 = 0.25$, $p_{adj} = 0.003$), in addition to study days 20 and 74 ($R^2 = 0.33$, $p_{adj} = 0.003$) (Table B24). The PCoA figure supports the apparent separation of study day 20 as these treatments are distinctly clustered together on the negative side of the PCoA1 axis, while study days 46 and 74 are clustered separately from study day 20 and contain significant overlap indicating minimal variation from each other. The treatments do not display any noticeable patterns within the PCoA figure, thus supporting the insignificant effect of AWW load on zooplankton community composition.

3.1.7 Zooplankton – Method Comparison

A series of correlational analyses were applied to the results from each eDNA primer versus the morphological data. Among all the primers, there was no significant correlation between total abundance and total reads, copepod abundance and copepod reads, relative abundance of rotifers and relative reads of rotifers, or relative abundance of copepods and relative reads of copepods (Table B31, Figures B48 – B51). For every primer, there was high correlation between cladoceran abundance and cladoceran reads ($r = 0.564 - 0.764$, $p < 0.005$, Table B31) (Figure 3.27). This was also the case in all primers, but to a lesser extent in the Daphnia primer, for the correlation between the relative abundance of cladocerans and the relative reads of cladocerans ($r = 0.476 – 0.764$, $p < 0.05$; Table B31, Figure B52). For the

Copepod primer and Rotifer 2 primer, there was a weaker yet significant correlation between rotifer abundance and rotifer reads ($r = 0.552$ & 0.403, $p < 0.05$), while for Leray, Rotifer 1, and Daphnia primers there was no relationship between these variables (Table B31, Figure B53).

Principal Coordinates Analysis (PCoA) and PERMANOVA testing was conducted to assess differences in community composition across AWW treatments and study days using the eDNA data from each primer and the morphological method data (Figure 3.20). The eDNA data from each primer, besides the Daphnia primer, showed a significant temporal effect with study day 20 varying from the other study days, as described previously. The morphological method also determined that study day had a significant effect on community composition from PERMANOVA testing ($R^2 = 0.08$, 0.001) (Table B23). The only significant temporal pairwise combination was between study day 21 and study day 75 ($R^2 = 0.16$m $p_{adj} = 0.012$), resulting in a similar conclusion to eDNA methods (Table B24). When focusing on the treatment effect, the results vary depending on the primer and methodology. For eDNA, only the Leray and Rotifer 1 primer results found a significant treatment effect, while for the morphological data PERMANOVA testing determined a significant effect of treatment on community composition ($R^2 = 0.26$, $p = 0.01$) (Table B23). However, between each of these significant datasets, no treatment pairwise comparison of community composition was significant when accounting for an adjusted p-value (Table B32). The PCoA figures display similar clustering of the 57.4 L treatment on the positive side of the PCoA1 axis for Rotifer 1 and on the positive side of the PCoA2 axis for morphological.

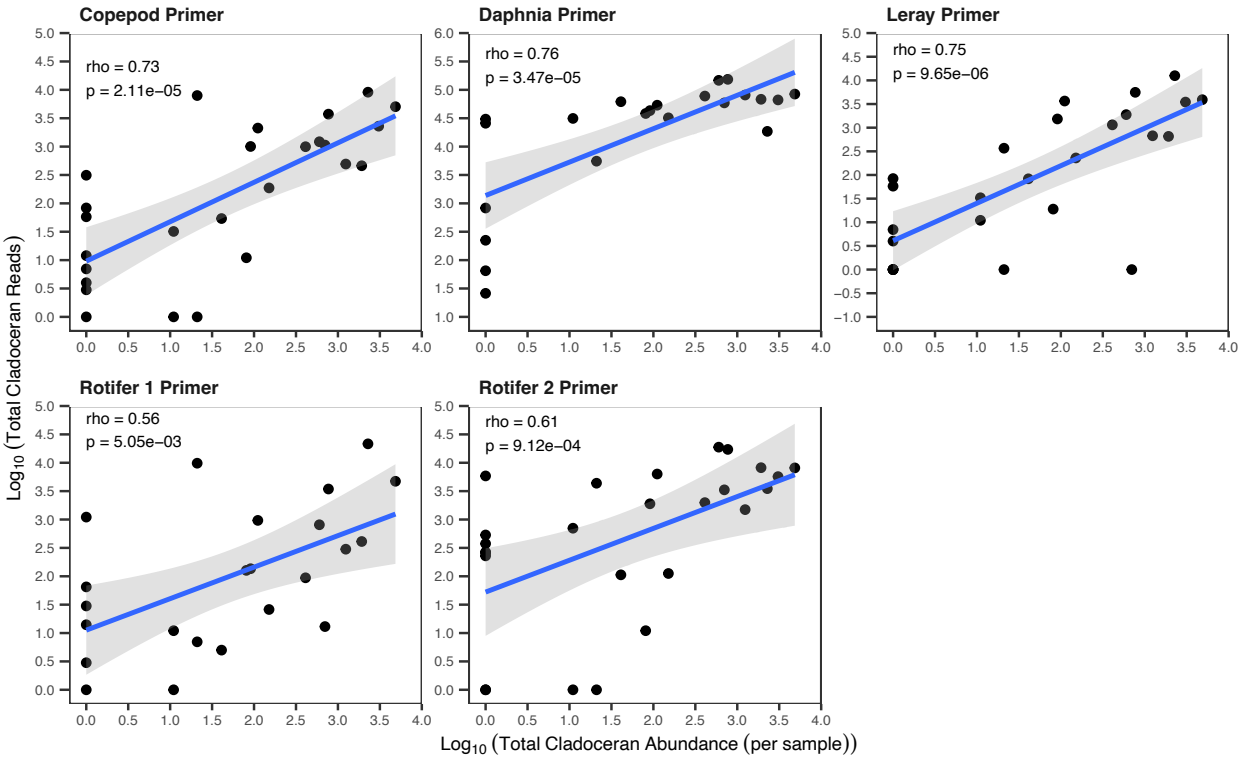

Figure 3.27: Correlation between log10(x + 1) transformed cladoceran abundance derived from morphological methods and log10(x + 1) transformed cladoceran reads from eDNA metabarcoding methods. Each plot represents the results from a different primer while the morphological data remains the same for each plot. The figure includes correlation coefficients (rho) and p-values for each correlation determined though Spearman's rank correlations. The linear line-of-best fit is included for visualization purposes.

3.2 Site Two – UM Established Wetlands

3.2.1 Aquaculture Wastewater

The nutrient composition of each AWW addition is listed in Table C1 and the corresponding total nutrient loading to each treatment from the AWW are in Table 3.3. The AWW average TP, TAN, and TKN concentrations were 43.0, 229.2, 296.2 mg/L respectively. When considering the water volume of the mesocosms, the average nutrient concentration in the water following each AWW application ranged from 0.10 – 0.58 mg/L TP, 0.87 – 4.38 mg/L TKN, and 0.57 – 3.17 mg/L TAN (Table C5). The cumulative nutrient concentration resulting from each AWW addition, was used for the linear model analyses, and are presented in Tables C2 – C4. The fate of the nutrients from the AWW additions are explored further in Blandford (2024). The metal content in all the AWW additions contained a mean total mass of 0.42 mg of copper and 3.29 mg of zinc. Then when considering the mesocosm volumes, after all AWW additions the total and average loading concentration of copper and zinc are shown in Table C6.

Table 3.3: The total loading of AWW with the corresponding total phosphorus (TP), total ammonia nitrogen (TAN), and total Kjeldahl nitrogen (TKN) loadings. The loadings are adjusted to the mesocosm surface area. Table modified from Blandford (2024).

Total AWW added (L)	TP (mg/m^2)	TAN (mg/m^2)	TKN (mg/m^2)
15	165.4	945.1	1383.5
23.4	205.5	1123.2	1521.1
36.6	321.5	1756.7	2379.2
57.6	638.4	3488.4	4724.3
90	997.5	5450.6	7381.8

3.2.2 Mesocosm Water Quality

The mesocosm water quality results and statistical analyses were reported and conducted in depth by Blandford (2024). Brief summaries of the relevant water quality results are reported here for reference; however, for further interpretations and results see Blandford (2024). The mean concentrations of each water quality variable are reported in Table C7 – C8.

Water temperature, pH, and conductivity did not vary considerably between AWW treatments (Figures C1, C1, C4). Dissolved oxygen decreased with duration in all mesocosms, including references, indicating the reduction in dissolved oxygen was not related to the effect of AWW load (Figure C3). On study day 77, dissolved oxygen levels reached concentrations that can be limiting for zooplankton (<2 mg/L) (Karpowicz et al., 2020; Vanderploeg et al., 2009).

Light intensity loggers placed along the bottom of one of the reference mesocosms, 36.6L and 57.6L treatments, measured mean light intensity of 7444.5 lux, 2892.8 lux, and 4370.5 lux, respectively (Figure C5). The light intensity was greatest in June and July, at the start of the study period. By mid-July the light intensity decreased in the 36.6L and 57.6L treatment for the remainder of the study period. In the reference mesocosm the light intensity did not decrease until mid-August.

Prior to AWW additions, TDP and TP concentrations among all treatments ranged from 0.02 – 0.41 mg/L and SRP concentrations ranged from 0 – 0.11 mg/L (Figures C6-C8). The concentrations remained consistent between treatments following the first AWW addition. After the second AWW addition, the TP, TDP, and SRP concentrations increased in the 36.6L and 57.6L treatments. For the remainder of the study period the TP, TDP, and SRP concentrations in these treatments remained consistently higher at mean TP concentrations of 0.29 and 0.32 mg/L,

while the other treatments decreased in concentration (Table C7). Peaks in Part-P occurred in the 15L, 36.6L, 57.6L, and 90L treatments near the end of the study (Figure C9). Dissolved phosphorus made up the majority of the total phosphorus measured in the treatments, followed by SRP, then Part-P (Figure 3.28).

Total nitrogen (TN), nitrate, nitrite, and TAN did not vary considerably between treatments (Figures C10, C12, C14, C15). TDN had small differences between treatments, with the 57.6 L treatment maintaining the highest concentration at most study days and had the highest mean concentration of 2.20 mg/L N (Figure C11). The concentration of un-ionized ammonia in the treatments only varied on study day 28 and 70, with a large difference observed in the 36.6L mesocosm, reaching a peak of 0.2 mg/L NH_3 on study day 69 compared the other treatments that were all below 0.01 mg/L (Figure C13). TDN made up a majority of the nitrogen measured in the mesocosms, followed by nitrate and TAN. However, following the first two AWW additions, nitrate represented a significant contribution to the total nitrogen in all treatments (Figure 3.29).

Alkalinity, DOC, and SRSi concentrations within each treatment are in Figures C16-C18. Minor treatment related differences occurred for chlorophyll-*a* (Figure 3.30). The concentration of chlorophyll-*a* in the 90 L treatment on study day 69 peaked at 24.6 µg/L compared to the other treatments with concentrations around 5 µg/L. Another difference occurred in the 15L and 90L treatments on study day 84 where the chlorophyll *a* concentration was greater than 20 µg/L. By the final sampling day, the concentration of chlorophyll-*a* did not vary across treatments.

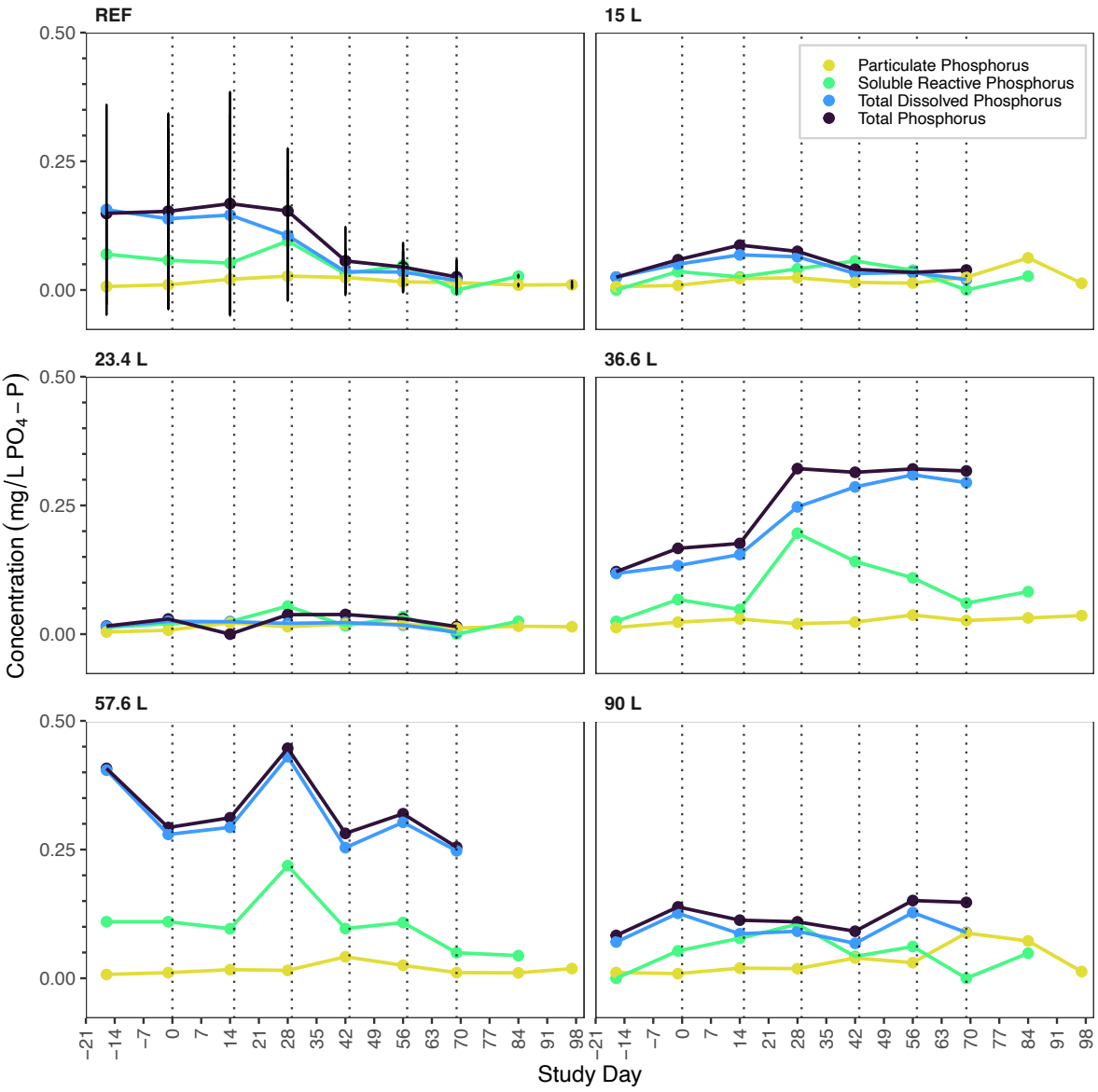

Figure 3.28: Concentration of total phosphorus, soluble reactive phosphorus, total dissolved phosphorus, and particulate phosphorus over the study duration with each plot separated by treatment. The REF plot displays the mean value of the references (n = 2) with error bars representing the ± standard deviation. The vertical dotted lines represent AWW addition days. Figure modified from Blandford (2024).

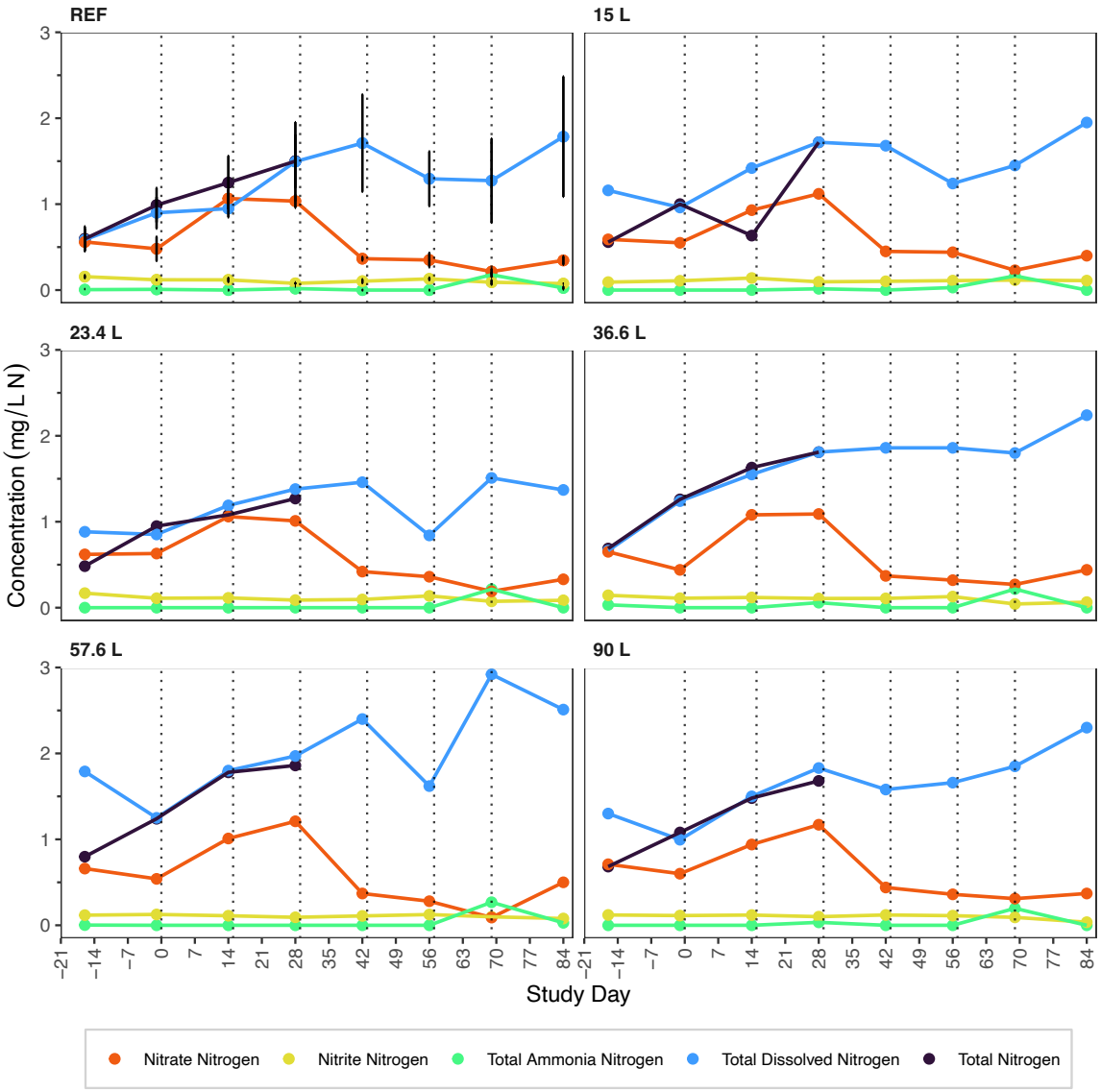

Figure 3.29: Concentration of total nitrogen (mg/L N), total dissolved nitrogen (mg/L N), total ammonia nitrogen (mg/L NH_4-N), nitrate (mg/L NO_3-N), and nitrite (NO_2-N) over the study duration with each plot separated by treatment. The REF plot displays the mean value of the references (n = 2) with error bars representing the ± standard deviation. The vertical dotted lines represent AWW addition days. Figure modified from Blandford (2024).

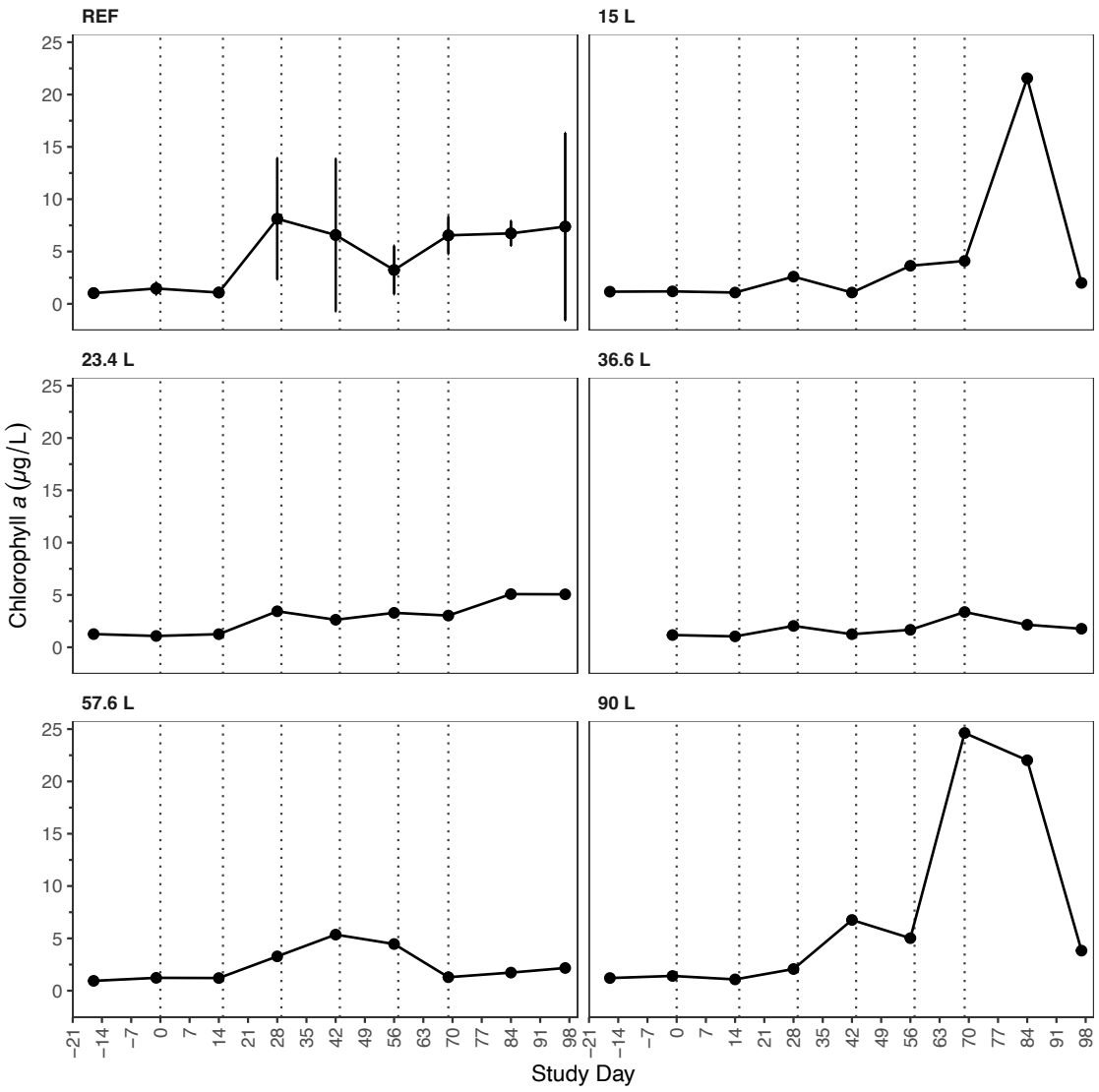

Figure 3.30: Concentration of chlorophyll-*a* over the study duration with each plot separated by treatment. The REF plot displays the mean value of the references (n = 2) with error bars representing the ± standard deviation. The vertical dotted lines represent AWW addition days. Figure modified from Blandford (2024).

3.2.3 Meteorological

The mean monthly values for the air temperature, relative humidity, wind speed, precipitation, and light intensity for the study duration are presented in Table C9. The air temperature and light intensity over the study duration are in Figures C19 and C20.

3.2.4 Soil

All soil properties and soil nutrient content are in Figures C21 – C23. The soil pH and organic matter did not vary between treatments over the study duration. Boron, chlorine, copper, iron, nitrate nitrogen, sulfur, and zinc all generally increased in concentration in all treatments from the initial sample to the final sample. Calcium, potassium and phosphate all generally decreased in concentration in all treatments over time. Magnesium, manganese, and sodium all went generally unchanged over the study duration in all mesocosm. Statistical interpretations of the soil properties are found in Blandford (2024).

3.2.5 Zooplankton – Morphological Identification

3.2.5.1 Total Zooplankton Abundance

A total of 14 zooplankton taxa were identified within the samples across the study period. Prior to the first AWW addition, the total zooplankton abundance was similar between all treatments, with total abundance ranging from 447 – 1970 zooplankton per sample (Figure 3.31). The most dominant taxa varied across treatments and only made up between 34 – 43% of the total abundance depending on the treatment (Figure 3.32). After the first AWW addition the total abundance increased in the 23.4L treatment due to the increase in rotifers which made up 49% of the total abundance (Figure 3.32). The total abundance in this treatment peaked at 4730 zooplankton per sample, resulting in more than double the number of zooplankton relative to the

background sample (Figure 3.33). By study day 22, total abundance increased in the 36.6L, 57.6L, and 90L treatments. After the third AWW addition, total abundance continued to increase in these treatments and the 15L treatment. Abundance continued to increase, albeit by a lesser amount by study day 64 and then a significant decline occurred in total abundance in all treatments by study day 91. The most predominant taxa in all samples were rotifers, copepod nauplii, and cyclopoid copepods which made up 28%, 24%, and 16% of the total zooplankton.

There were no significant relationships identified from the linear models between total zooplankton abundance and AWW load (Table C10 & Figure 3.34). However, on study day 91 a marginally significant positive relationship was observed between total abundance and AWW load ($R^2 = 0.61$, $p = 0.065$).

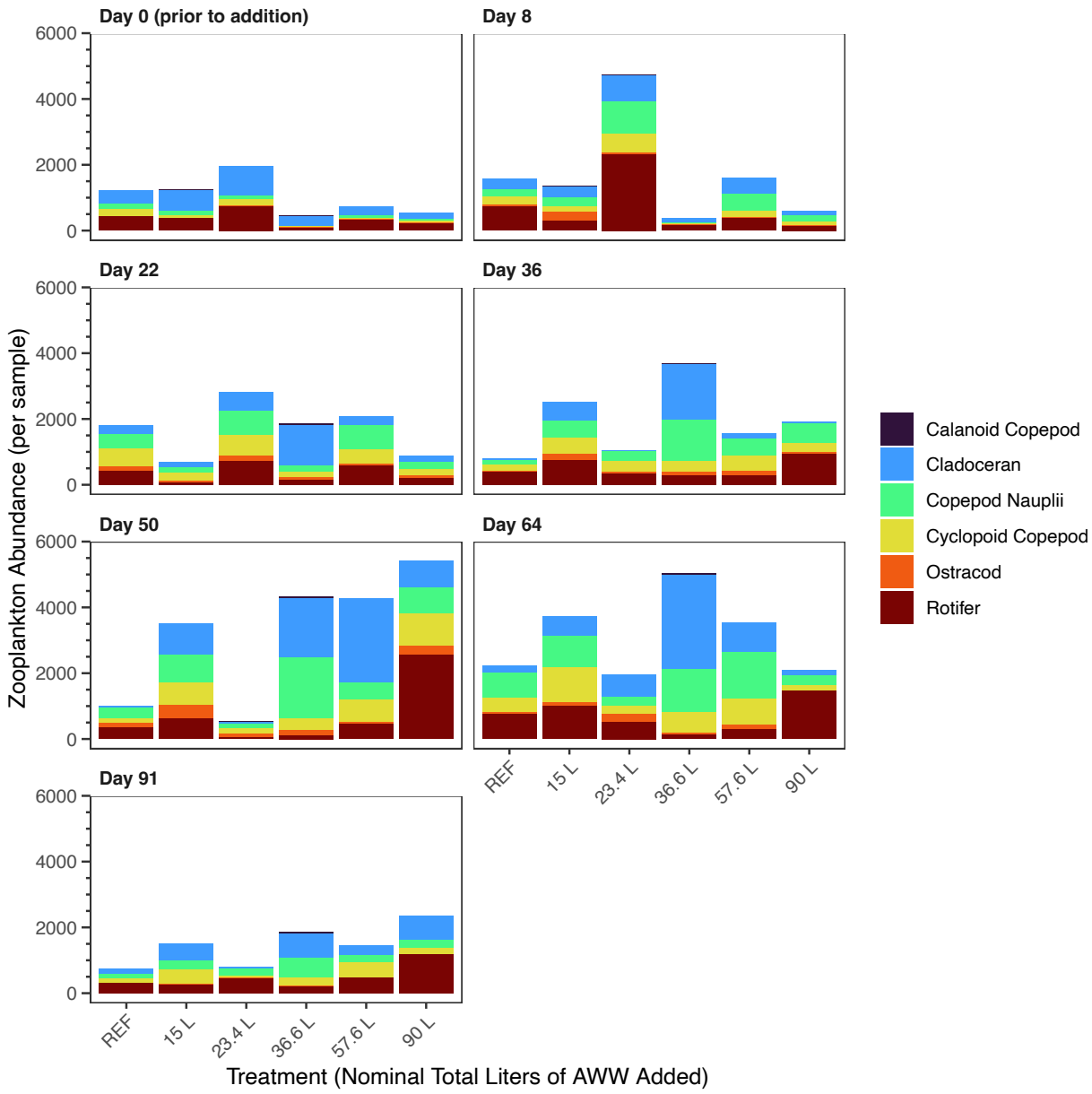

Figure 3.31: UM-EW zooplankton abundance for each treatment on the study day the zooplankton were sampled. REF represents the mean of the references (n = 2).

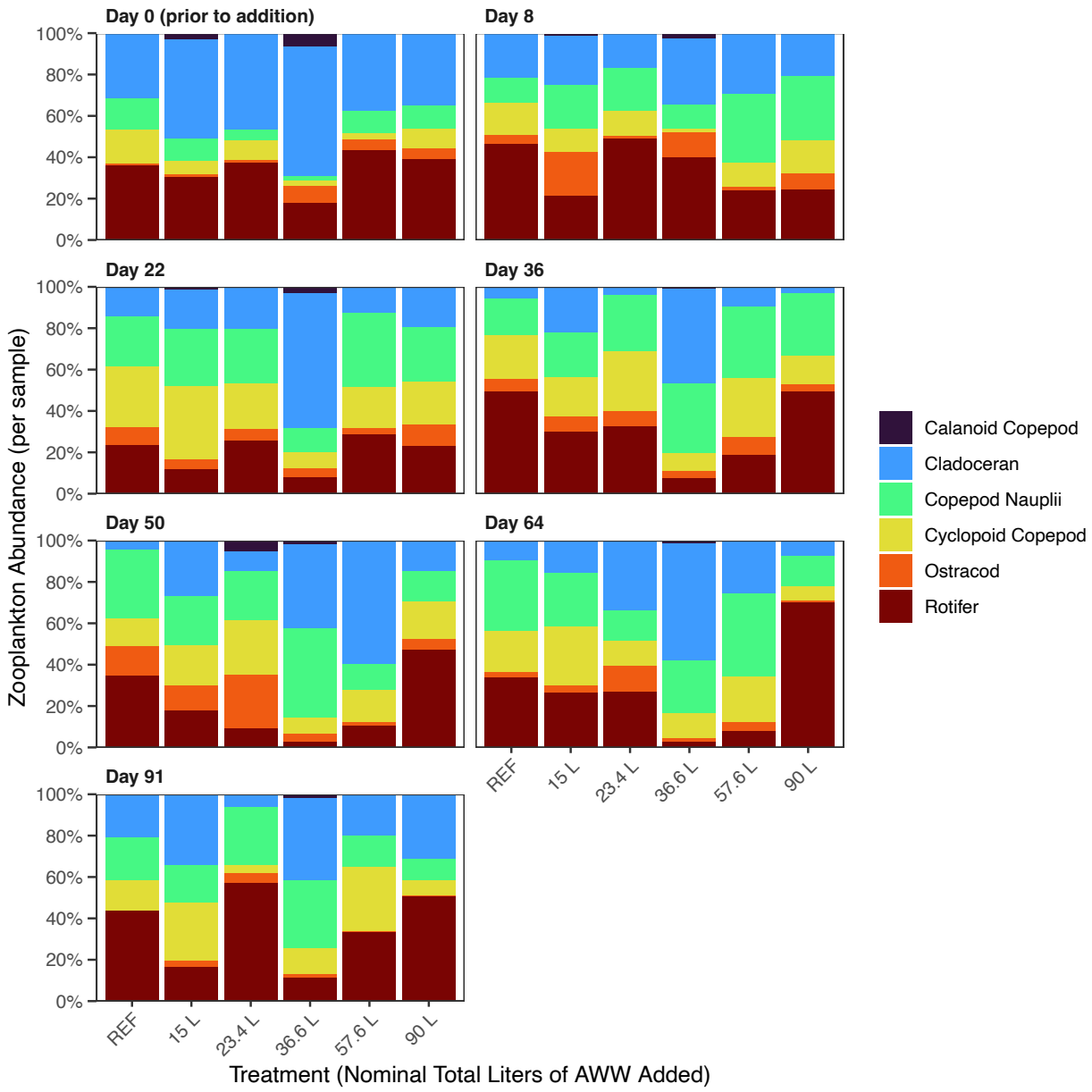

Figure 3.32: UM-EW zooplankton relative abundance (%) for each treatment on the study day the zooplankton were sampled. REF represents the mean of the references (n = 2).

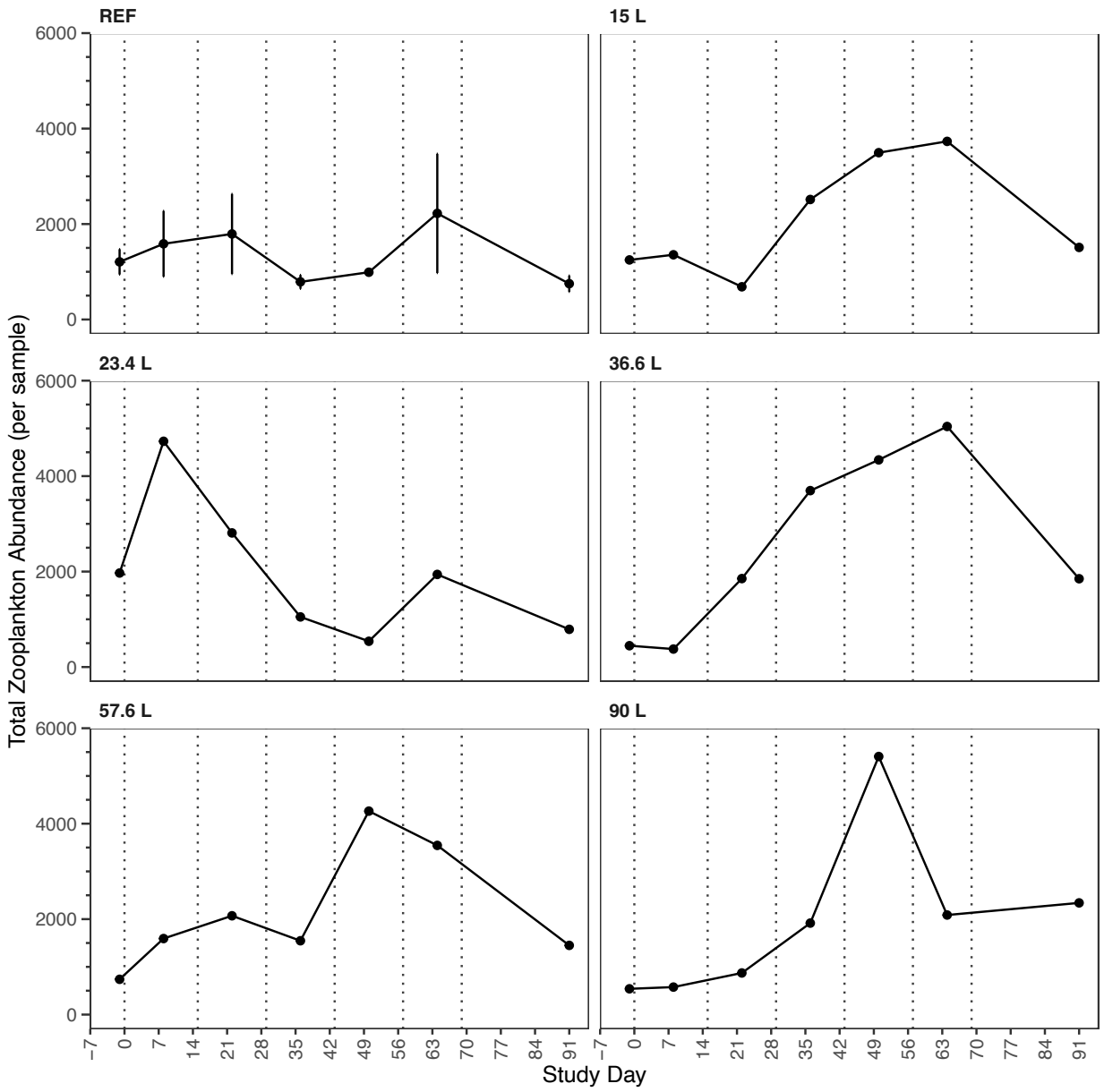

Figure 3.33: Total zooplankton abundance over the duration of the UM established wetland study within each treatment. The REF plot displays the mean value of the references (n = 2) with error bars representing the ± standard deviation. The dotted vertical lines represent the days AWW was added to the treatments.

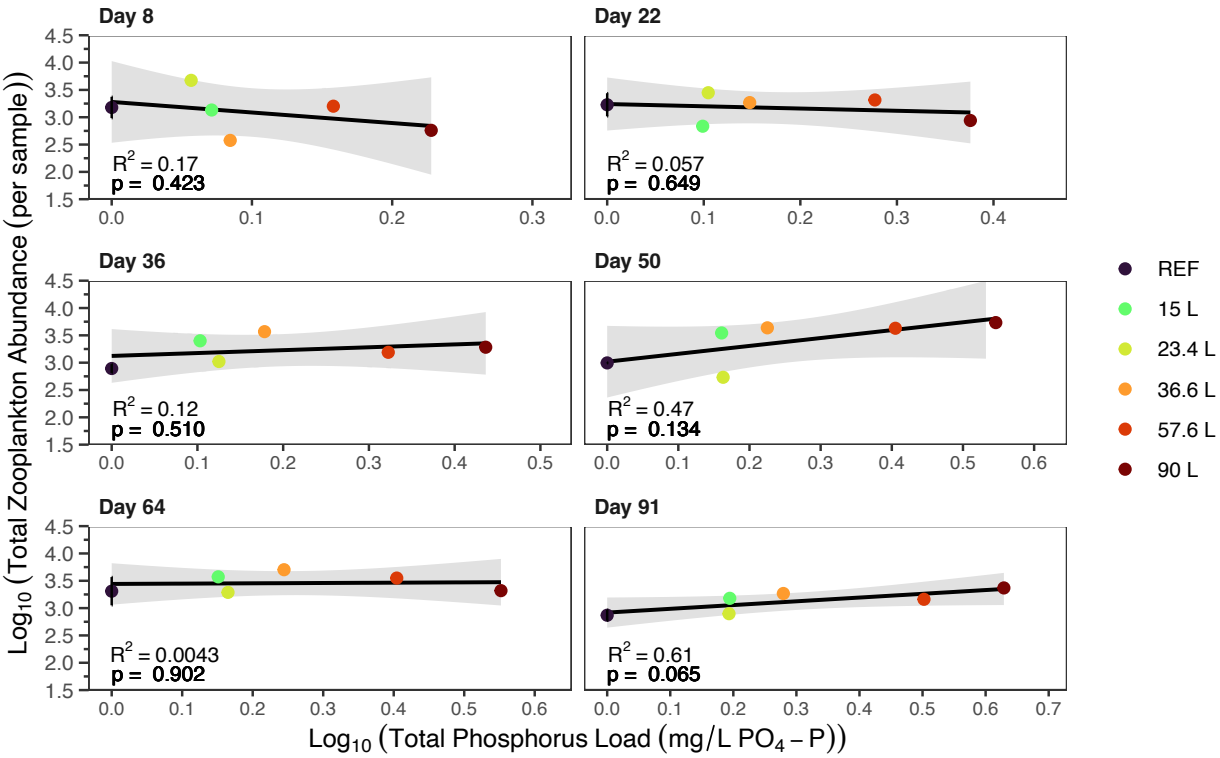

Figure 3.34: Linear regression model results of the relationship between log10(x + 1) of cumulative AWW load concentration (TP used as the representative variable) and total zooplankton abundance. REF displays the mean of the references (n = 2) with the error bars representing ± standard deviation. Each plot displays the model results according to study day.

The PRC analysis of the zooplankton community composition identified that treatment (AWW load) explained 71% of the variance observed in zooplankton abundance. Then 24% of the variation in zooplankton abundance was explained by time, with the remaining 6% unexplained. The first PRC axis explained 45% of the variation in abundance due to the AWW treatments. Permutation testing found the first axis was marginally significant ($p = 0.051$). The significance of the PRC terms, time ($p = 0.039$) and the interaction between time and treatment ($p = 0.039$), were both significant from permutation testing. The PRC analysis also revealed that AWW load had a significant effect on zooplankton community composition on study days -1 ($p = 0.049$), 50 ($p = 0.044$), and 91 ($p = 0.046$), with marginal significance on study day 64 ($p = 0.051$). Pairwise permutation testing was conducted for these significant days to find which treatments were significantly different from the reference. On study day -1, no treatments were significantly different from the references. On study days 50 and 91, the zooplankton composition in the 36.6L treatment varied significantly from the references ($p = 0.025$ and $p = 0.007$, respectively). Although study day 64 was not significant, the zooplankton composition in the 36.6L treatment significantly varied from the references ($p = 0.026$). Other trends in community composition were observed, including a general increase in community response over time in all treatments compared to the references (Figure 3.35).

As indicated by the species scores generated from the PRC analysis, *Ceriodaphnia* sp. had the highest positive species score ($b_k = 2.12$) (Table C19). This high positive score when the community response is positive indicates that *Ceriodaphnia* sp. abundance was greater when compared to the controls, which is the case for most of the community response. *Diaphanosoma* sp. and calanoid copepods had the next highest positive species scores, 1.75 and 0.92,

respectively. The remaining taxa have scores near zero, indicating little to no significant response to treatment (Table C19).

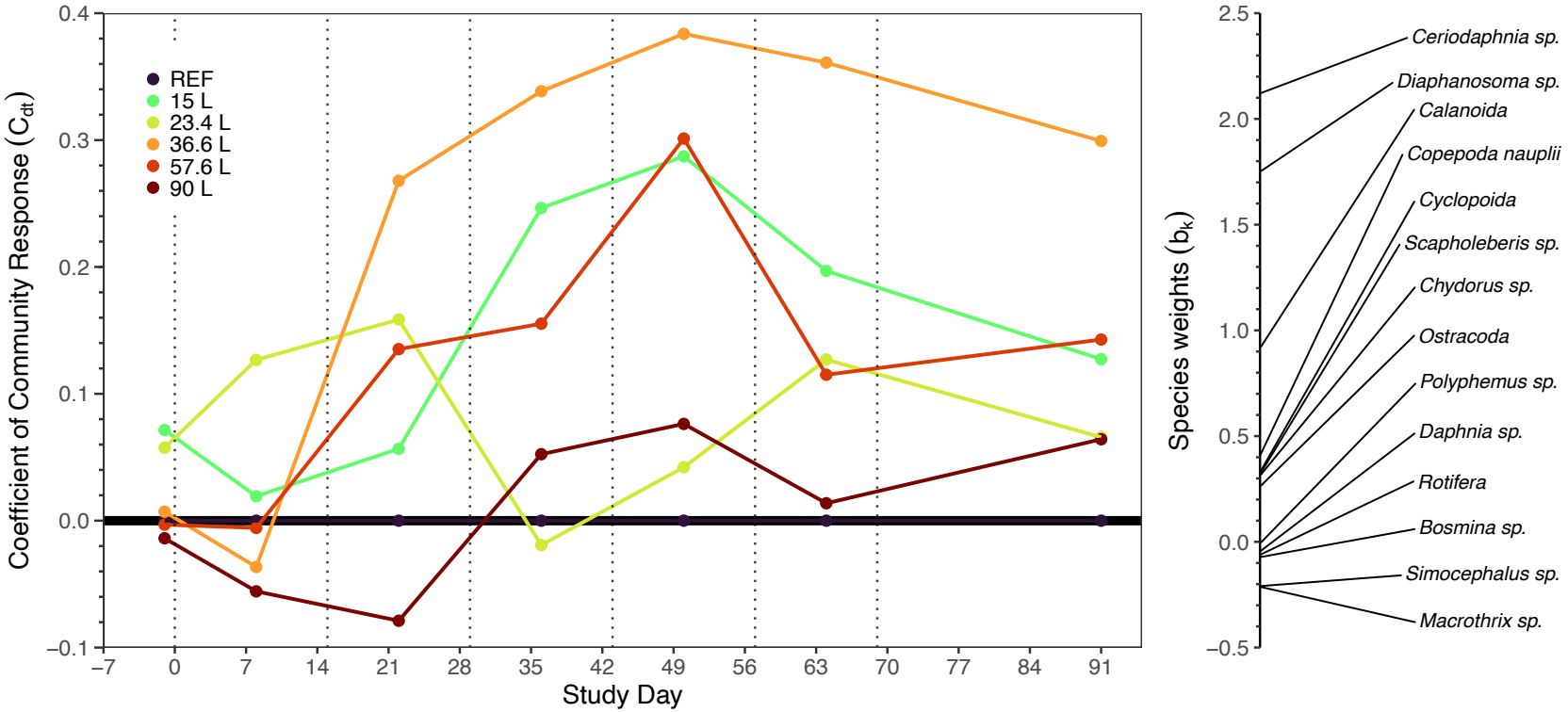

Figure 3.35: Principal response curve (PRC) generated for the RL zooplankton abundance and community composition. Zooplankton abundance was $\log_{10}$ transformed prior to analysis. Species weights are displayed on the right. The thick black line (x = 0) represents the references. The dotted vertical lines represent the days AWW was added to the treatments.

3.2.5.2 Cladoceran Abundance

The cladoceran abundance was comprised of the following genera within the Cladocera order; *Ceriodaphnia*, *Chydorus*, *Daphnia*, *Diaphanosoma*, *Scapholeberis, Macrothrix, Simocephalus, Bosmina, and Polyphemus*. The cladoceran group often made up a considerable proportion of the sample abundance, resulting in a 27% proportion across all samples (Figure 3.32). *Ceriodaphnia* and *Chydorus* zooplankton contributed the most with total proportions of 8% and 14% of total abundance in all samples. The cladoceran abundance was consistent among all mesocosms prior to AWW additions and after the first AWW addition (Figure 3.36). An increase in cladoceran abundance occurred on study day 22 in the 36.6L treatments. *Ceriodaphnia* drove this increase and made up 48% of the proportion of abundance in this treatment on this day. The cladoceran abundance continued to increase in the 36.6L treatment to study day 64, where cladoceran abundance peaked at 2,860 per sample. Another peak in cladoceran abundance on study day 50 following the fourth AWW addition in the 57.6L treatment occurred. By study day 91, the cladoceran abundance across all treatments declined. From linear regression, there was no significant effect of AWW load in cladoceran abundance on any study day (Table C10, Figure 3.37). On study day 50, a weak positive trend between cladoceran abundance and AWW load was observed (Figure 3.37).

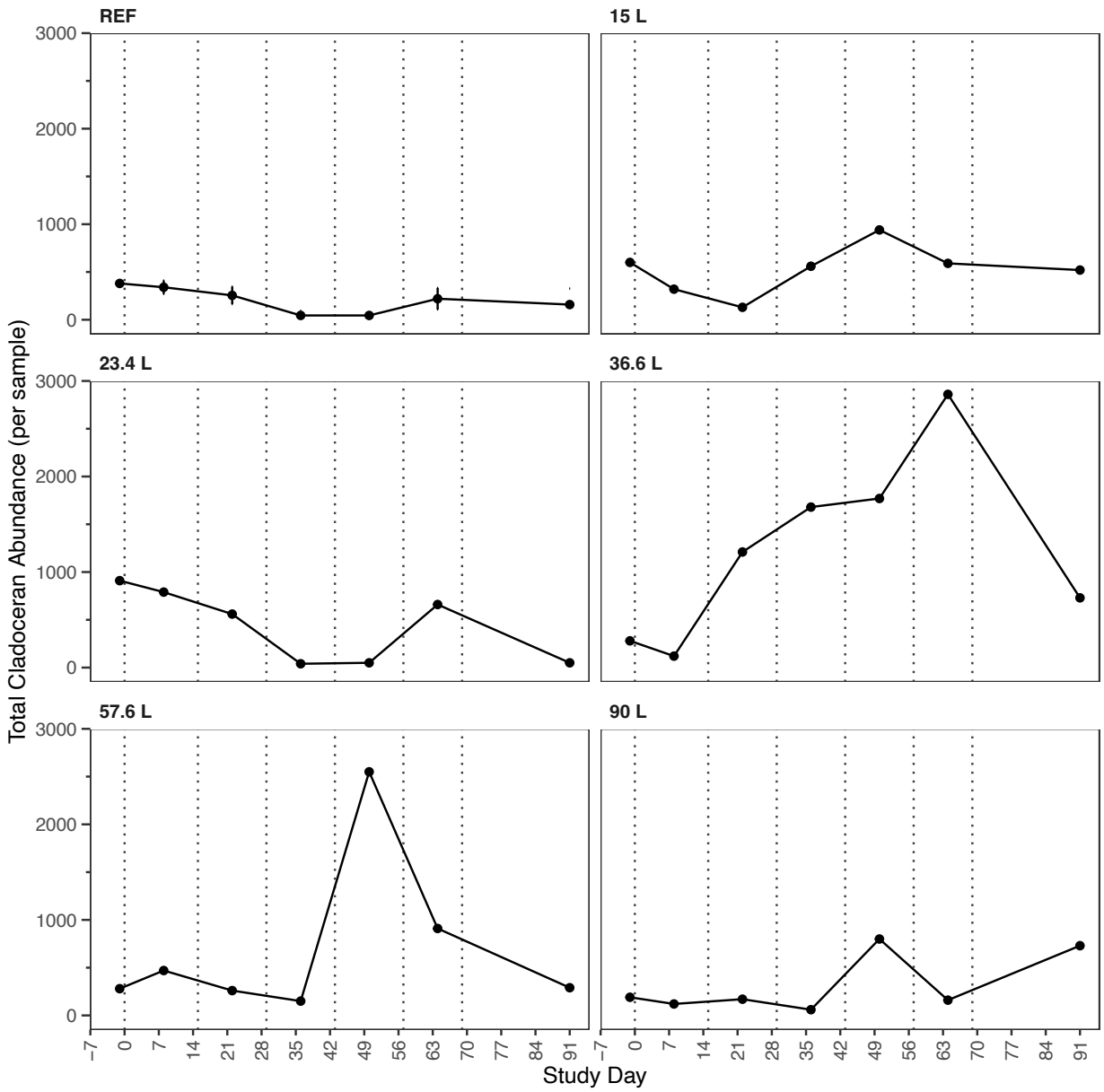

Figure 3.36: Total cladoceran abundance over the duration of the UM established wetland study within each treatment. The REF plot displays the mean value of the references (n = 2) with error bars representing the ± standard deviation. The dotted vertical lines represent the days AWW was added to the treatments.

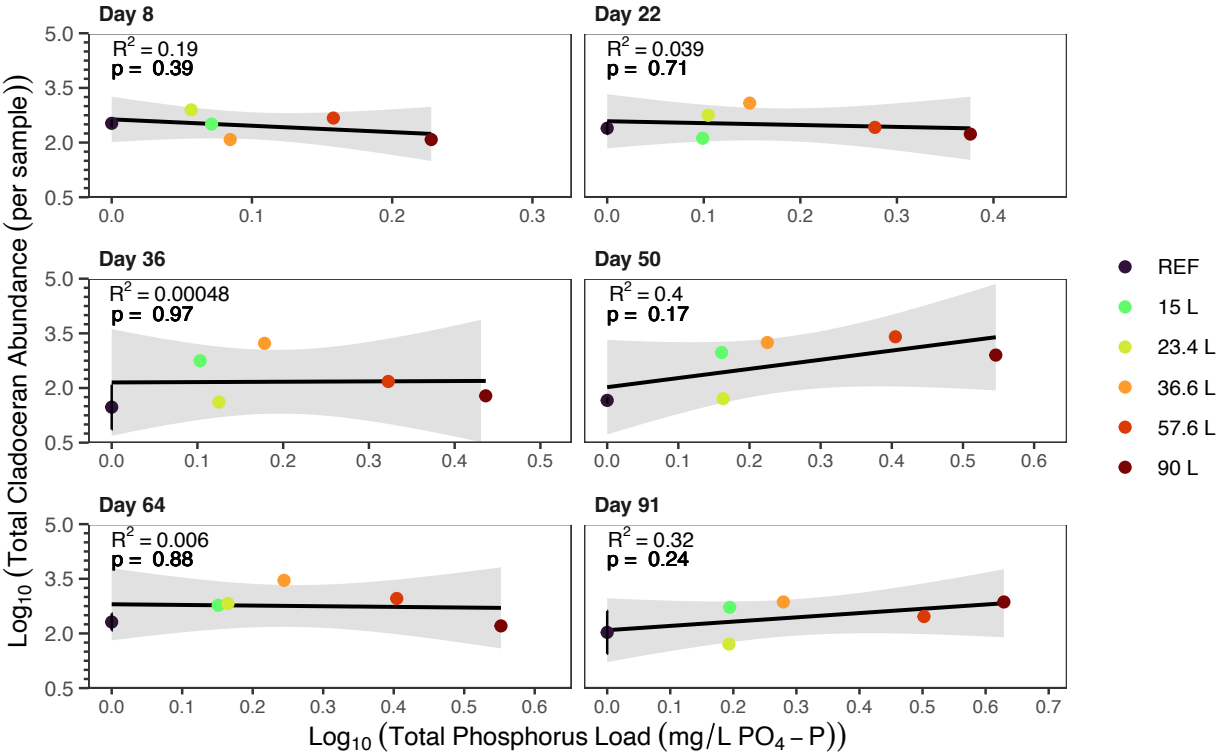

Figure 3.37: Linear regression model results of the relationship between log10(x + 1) of cumulative AWW load concentration (TP used as the representative variable) and total cladoceran abundance. Each plot displays the model results according to study day.

3.2.5.3 Copepod Abundance

Copepod abundance was comprised of the orders Calanoida and Cyclopodia, referred to as calanoids and cyclopoids. Copepod nauplii were also included in this group. Cyclopoids and copepod nauplii were consistently abundant in all samples, often encompassing over 50% of the proportion of zooplankton in the samples (Figure 3.32). Calanoids were only identified in the 15L, 23.4L, and 36.6L treatments over the study duration and in small abundances ranging from 10 – 80 per sample. The cyclopoid and copepod nauplii abundance peaked in the 23.4L treatment following the first AWW addition, then decreased in abundance following the third addition (Figure 3.38). All other treatments, including the references to a lesser degree, followed a similar trend of cyclopoid and copepod nauplii gradually increasing in abundance following the first AWW addition, then hitting a peak abundance at either study day 50 or 64 (Figure 3.38). The highest abundance was on study day 50 in the 36.6L treatment, where copepod nauplii had a maximum abundance of 1870 per sample. All copepod abundances declined and did not vary across treatments by study day 91.

From linear regression analysis, there was no significant relationship between AWW load and either total copepod abundance, cyclopoid abundance, or copepod nauplii abundance on any study day (Table C10, Figure 3.39, Figures C24 – C25). There was a marginally significant positive relationship on study day 50 between cyclopoid abundance and AWW load ($R^2 = 0.65$, $p = 0.053$) (Figure 3.39). Due to the small sample size and inconsistent occurrence of calanoid copepods in the treatments, statistical analyses were not conducted on this taxon.

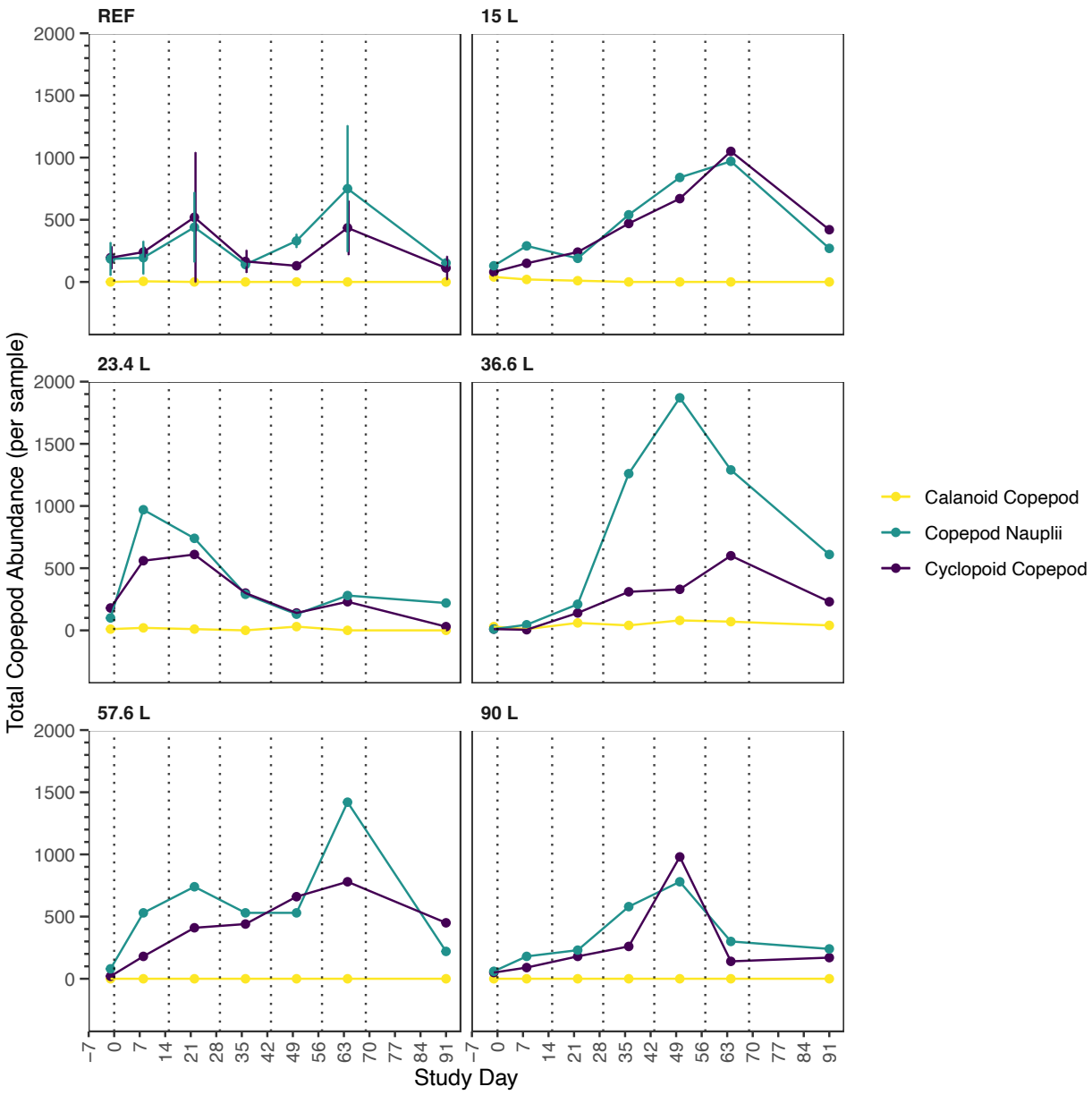

Figure 3.38: Total calanoid copepod, cyclopoid copepod, and copepod nauplii abundance over the duration of the UM established wetland study within each treatment. The REF plot displays the mean value of the references (n = 2) with error bars representing the ± standard deviation. The dotted vertical lines represent the days AWW was added to the treatments.

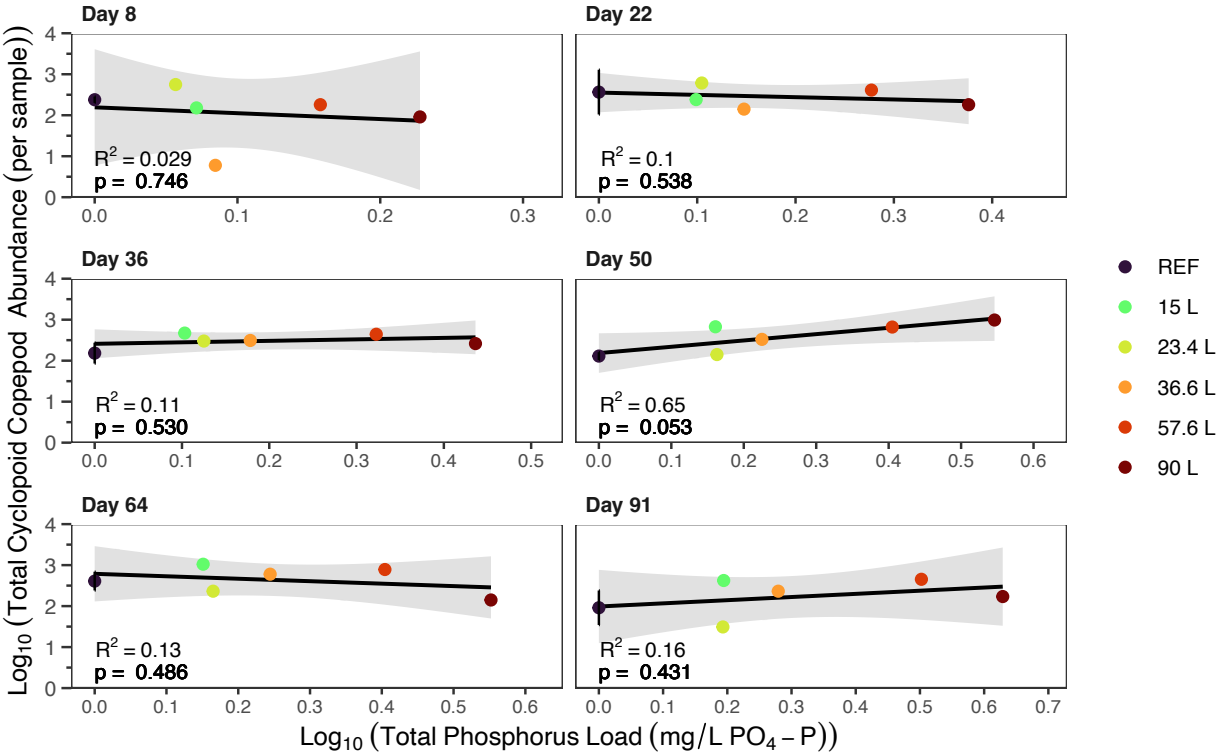

Figure 3.39: Linear regression model results of the relationship between log10(x + 1) of cumulative AWW load concentration (TP used as the representative variable) and total cyclopoid copepod abundance. REF displays the mean of the references (n = 2) with the error bars representing ± standard deviation. Each plot displays the model results according to study day.

3.2.5.4 Rotifer Abundance

The rotifer group is comprised of all rotifers identified in the samples as more specific taxonomic identifications were not made. Rotifers were among the most dominant groups in all samples (Figure 3.32). The rotifer abundance was similar among all mesocosms prior to any AWW additions, ranging from 80 – 740 per sample. After the first AWW addition, the rotifer abundance increased in the references and the 23.4L treatment (Figure 3.40). Abundance in the 90L treatment increased following the third AWW addition then peaked on study day 50 with a total of 2560 rotifers per sample. A decline in rotifer abundance was observed in all samples by study day 91. Linear regression analyses found no significant relationship between rotifer abundance and AWW load on any study day (Table C10, Figure 3.41). On study day 50 and 91, a weak positive trend occurred (Figure 3.41).

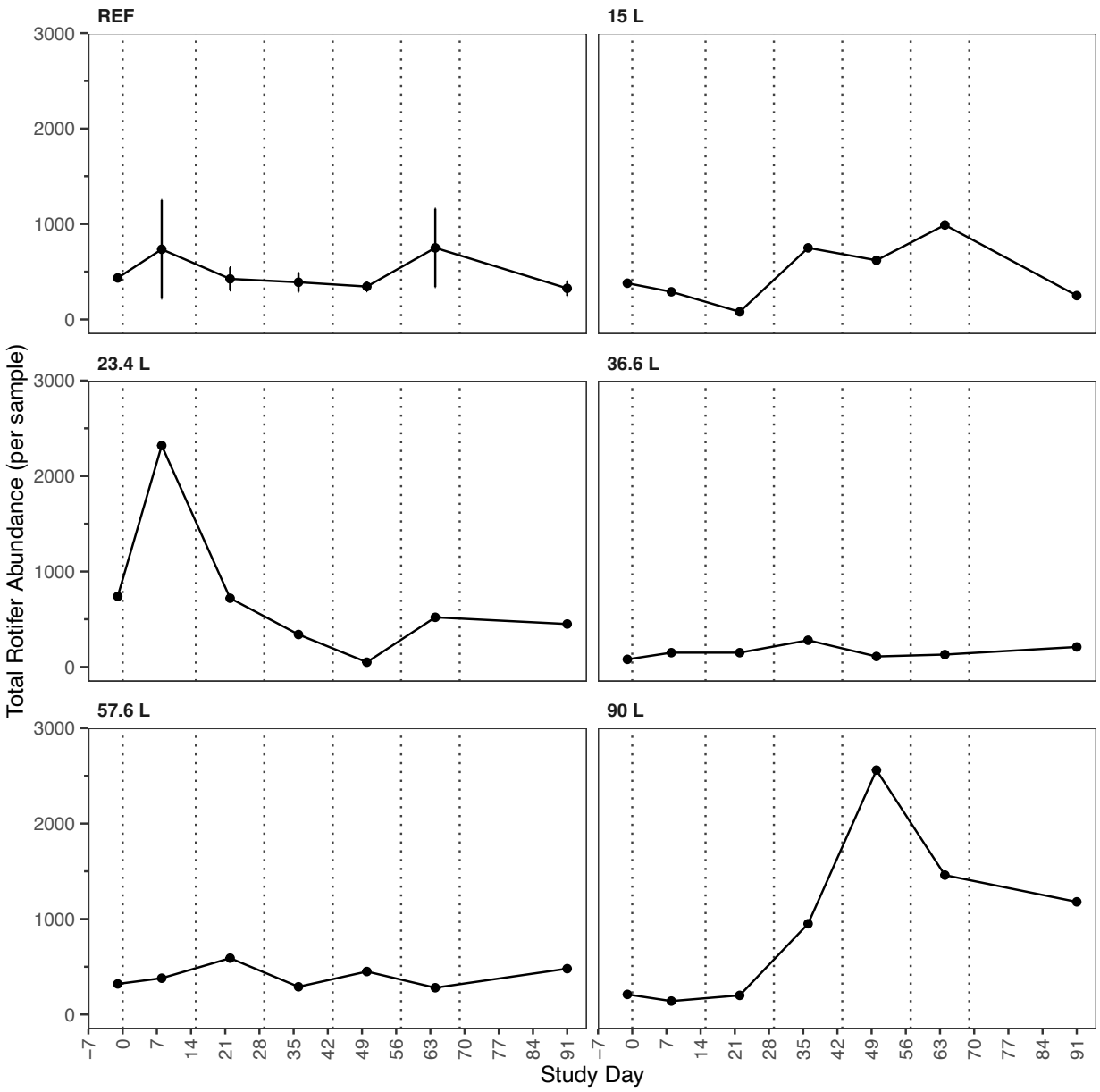

Figure 3.40: Total rotifer abundance over the duration of the UM established wetland study within each treatment. The REF plot displays the mean value of the references (n = 2) with error bars representing the ± standard deviation. The dotted vertical lines represent the days AWW was added to the treatments.

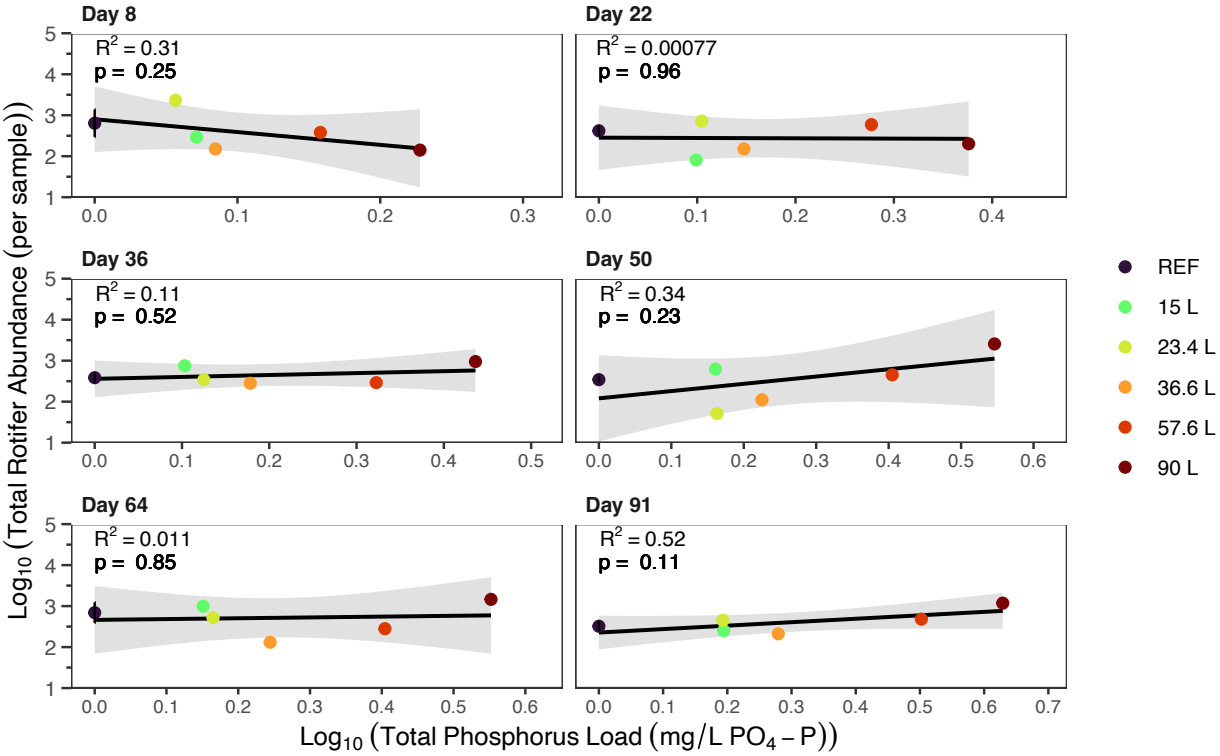

Figure 3.41: Linear regression model results of the relationship between log10(x + 1) of cumulative AWW load concentration (TP used as the representative variable) and total rotifer abundance. REF displays the mean of the references (n = 2) with the error bars representing ± standard deviation. Each plot displays the model results according to study day.

3.2.5.5 Zooplankton Diversity

Zooplankton diversity, richness, and evenness values for each study day and treatment are presented in SI Tables C11 – C17. Zooplankton diversity, measured by the Inverse Simpson Index ranged from 1.98 – 5.84 over the study duration, with the lowest diversity measured in the 90L treatment (Figure C26). Diversity of the 36.6L and 57.6L treatments remained consistent throughout the study duration and did not vary from the references. The 15L, 23.4L, and 90L treatments all were higher in diversity following the second AWW addition compared to the references. The 15L and 23.4L treatments remained consistently higher for most of the study duration, whereas the 90L treatment decreased in diversity below the references. The species evenness ranged from 0.28 – 0.78 but generally remained consistently between 0.4 – 0.7 (Figure C27). Species richness varied from 4 – 10 and declined in the references over the study duration and stayed consistent in the treatments between 7 – 9 (Figure C28). From linear regressions, a significant negative relationship was found between evenness and AWW load on study day 64 ($R^2 = 0.71$, $p = 0.035$), this significance was not found on the other study days (Table C10, Figure 3.42). There was no significant relationship determined by linear regressions between species diversity or species richness and AWW load at each study day (Table C10, Figures C29-C30).

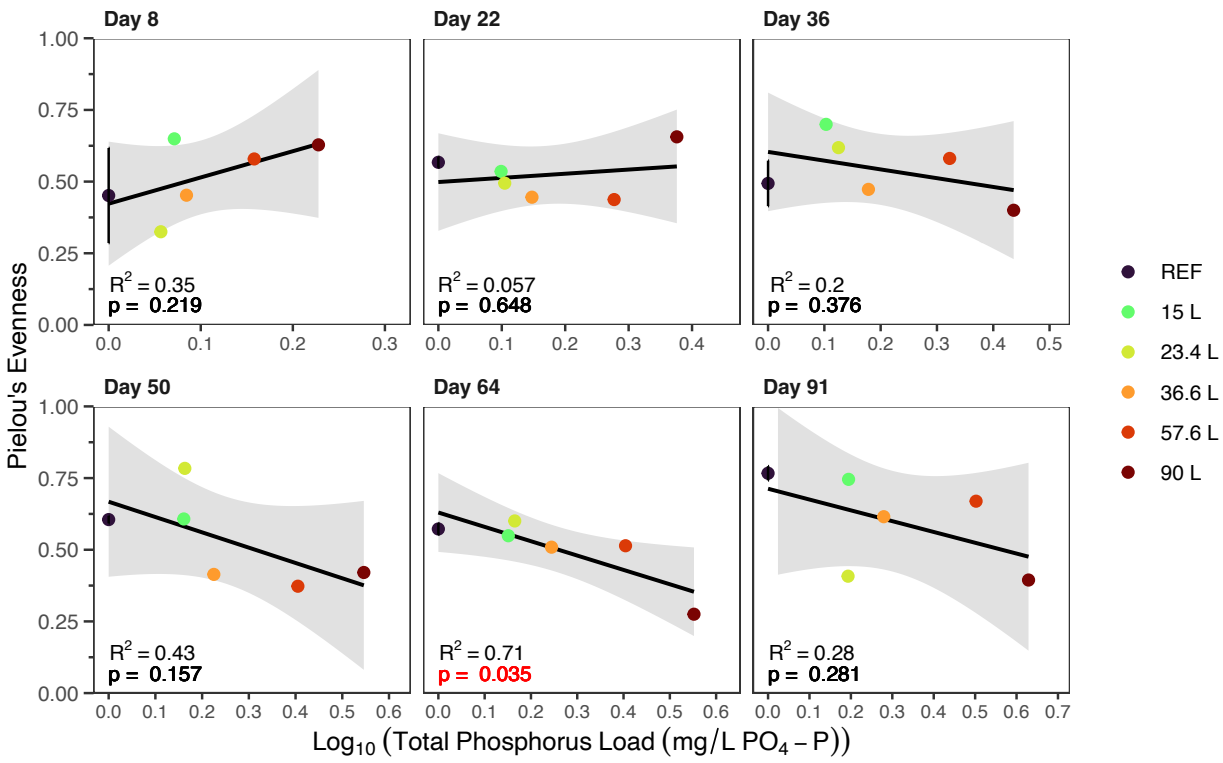

Figure 3.42: Linear regression model results of the relationship between log10(x + 1) of cumulative AWW load concentration (TP used as the representative variable) and Pielou's evenness. REF displays the mean of the references (n = 2) with the error bars representing ± standard deviation. Each plot displays the model results on according to study day.

3.2.5.6 Influence of Fish on Zooplankton

A range of 1 - 9 fish were retrieved from the mesocosms by the final sampling date of September 30, 2022 (Table C21). Linear regression analysis did not reveal a significant relationship between fish abundance and total zooplankton abundance on study day 91 (Table C18).

On study days 22, 36, 50, 64, and 91, fish larvae were captured within multiple zooplankton sampling jars. Linear regression analysis on study day 91 found a significant negative relationship between total zooplankton abundance and the presence of larval fish in the sampling jars ($R^2 = 0.86$, $p = 0.0027$) (Table C18). The treatments that had a presence of fish on study day 91 were both references (n = 13, n = 1) and the 23.4L treatment (n = 2).

3.2.5.7 Influence of Environmental Variables on Zooplankton

The RDA demonstrated trends and relationships between the included environmental variables and the zooplankton community with the overall model significantly explaining 22% of the variation in zooplankton community composition (Figure 3.43, $p = 0.001$). The first RDA axis explained a dominant proportion of this variance compared to the other axis, with a 31% proportion which was significant in explaining zooplankton variation ($p = 0.001$). The environmental variables explained 30% of the variance in zooplankton community composition, while 43% of the variation went unexplained. The variance due to study day was 27%, which was controlled out of the RDA model, via the conditional term.

The environmental variables included in the analysis are within Figure 3.43. Variables excluded were Part-P due to its correlation with chlorophyll-*a,* and pH due to its correlation with dissolved oxygen. These removed variables would exhibit similar responses to their included

correlated variables with the RDA. Other variables excluded from the RDA were water temperature, TAN, and NO_3 due to elevated VIFs.

The environmental variables that had the strongest influence on the RDA, were SRP, dissolved oxygen, and un-ionized ammonia (Table C20). From permutation tests of the environmental variables, dissolved oxygen and TDN were determined to have a significant effect on the zooplankton community composition ($p = 0.001$ & $p = 0.02$). Dissolved oxygen, TDN, un-ionized ammonia, and SRP were all positively correlated. The 36.6L treatment was strongly associated with these variables and demonstrated a different grouping then a majority of the other treatments. *Ceriodaphnia* and *Diaphanosoma* zooplankton taxa were also strongly correlated with these variables and the 36.6L treatment, indicting a strong dominance of these species within this treatment. The 90L treatments from the last four study days, were grouped together near the chlorophyll-*a* variable and located further from other treatments, indicating stronger differences in this treatment. Rotifers also strongly varied from the other species and were correlated with the 90L treatment and the chlorophyll-*a* variable.

There was a trend demonstrated from the study days, with the earlier study days -1 and 8, clustered together in the center indicating little variance between treatments prior to and at the onset of the study. However, the later study days 36, 50, 64, and 91, tend to be located further apart, and vary in location depending on treatment. This suggests that over time the environmental variables changed in the mesocosms and had a stronger influence on zooplankton community over time.

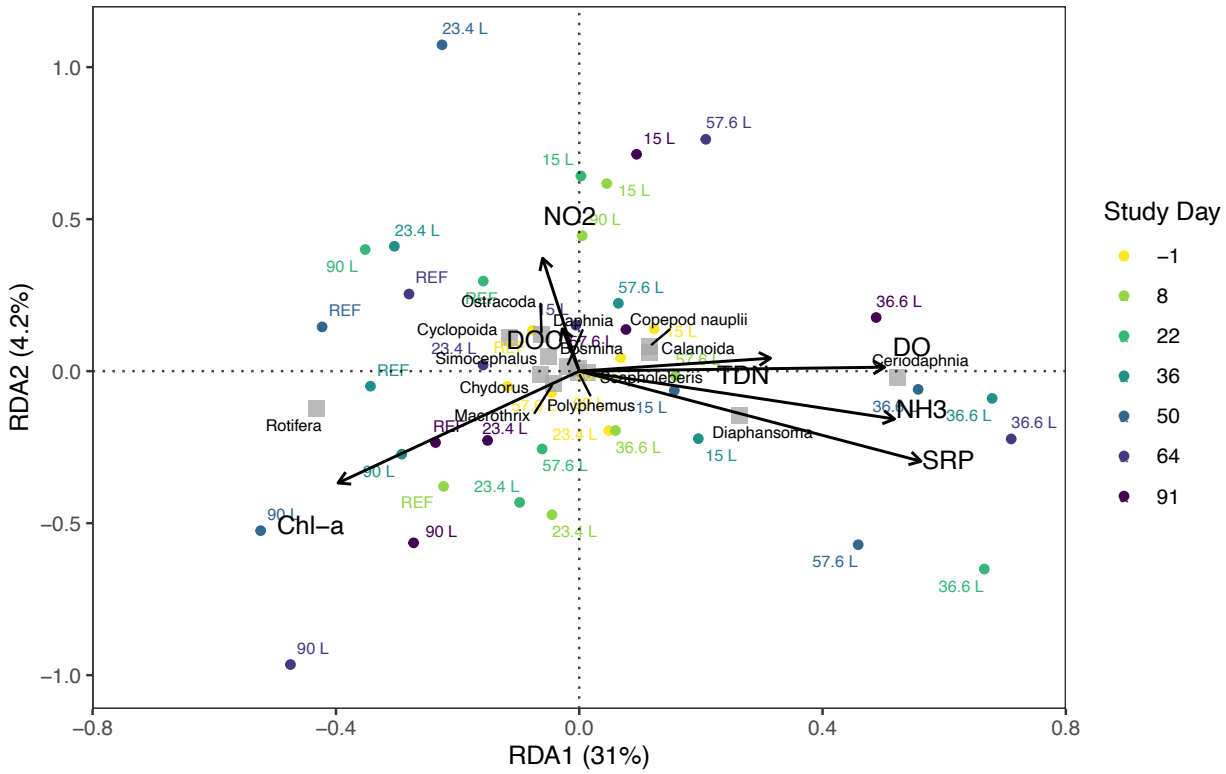

Figure 3.43: Redundancy Analysis (RDA) plot demonstrating the relationship between environmental variables (arrows), zooplankton species (squares), and AWW treatments and references on each study day (points). The references are represented by the mean value (n = 2). The axes explained 31% (Axis 1) and 4.2% (Axis 2) of the total variance. Environmental variables with correlation greater then 0.7 were removed.

3.3 Site Two – UM Wild Rice

3.3.1 Aquaculture Wastewater

The nutrient composition of each AWW addition is listed in Table C1 and the corresponding total nutrient loading to each treatment from the AWW are in Table 3.4. The AWW average TP, TAN, and TKN concentrations were 43.0, 229.2, and 296.2 mg/L respectively. When considering the water volume of the mesocosms, the average nutrient concentration in the water following each AWW application ranged from 0.03 – 0.51 mg/L TP, 0.18 – 2.8 mg/L TAN, and 0.24 – 3.8 mg/L TKN (Table D4). The cumulative nutrient concentrations from each AWW addition, which was used for the linear model analyses, are in Tables D1-D3. The fate of the nutrients from the AWW additions are assessed further in Blandford (2024). The AWW additions contained a mean total mass of 0.42 mg of copper and 3.29 mg of zinc. Then when considering the mesocosm volumes, after all AWW additions the total and average loading concentration of copper and zinc are in Table D5.

Table 3.4: The total loading of AWW with the corresponding total phosphorus (TP), total ammonia nitrogen (TAN), and total Kjeldahl nitrogen (TKN) loadings. The loadings are adjusted to the mesocosm surface area. Table modified from Blandford (2024).

Total AWW added (L)	TP (mg/m^2)	TAN (mg/m^2)	TKN (mg/m^2)
6.0	66.5	363.4	492.1
9.6	106.4	581.4	787.4
15	166.3	908.4	1230.3
23.4	259.4	1417.1	1919.3
36.6	405.7	2216.6	3001.9
57.6	638.4	3488.4	4724.3
90	997.5	5450.6	7381.8

3.3.2 Water Quality

Summaries of the relevant water quality results are reported here for reference, however, further interpretations, details, and results are found in Blandford (2024). The mean concentrations of each water quality variable are reported in Tables D6 – D7.

Water temperature, dissolved oxygen, pH, and specific conductivity did not vary considerably between treatments (Figures D1 – D4). An increase in pH occurred after the first AWW addition in all treatments and then remained consistently in the range of around 9 – 10.5 for the study duration. Light intensity loggers placed along the bottom of the 15L, 23.4L, 36.6L, and 57.6 L treatments measured mean light intensity of 10,828.0 lux, 1325.6 lux, 3748.5 lux, and 1737.4 lux, respectively (Figure D5).

Major elevations in phosphorus species following AWW additions were only observed in the 6L, 23.4L, and 57.6L treatments (Figures D6-D9) while the other treatments maintained consistent concentrations of phosphorus species or decreased in concentration after AWW additions (Figures D6-D9). When TP was elevated, TDP generally comprised a majority of the total phosphorus measured in the treatments (Figure 3.44).

TN, TDN, nitrite, nitrate, and TAN generally did not vary between treatments over the study duration (Figures D10 – D15). Un-ionized ammonia increased in a majority of treatments following the second and fifth AWW additions to maximum concentrations of approximately 0.05 mg/L and 0.3 mg/L, respectively. TDN and nitrate made up a majority of the total nitrogen concentration in the treatments for the first 28 study days, then nitrate decreased in concentration and TDN made up the majority for the remainder of the study duration (Figure 3.45).

Alkalinity, DOC, and SRSi concentrations are in Figures D16-D18. The chlorophyll-*a* concentrations varied following the second AWW addition through the remainder of the study duration and higher concentrations were evident in the 6L, 23.4L, and 57.6L treatments (Figure 3.46). The 57.6L treatment reached a peak chlorophyll-*a* concentration of 36.1 µg/L.

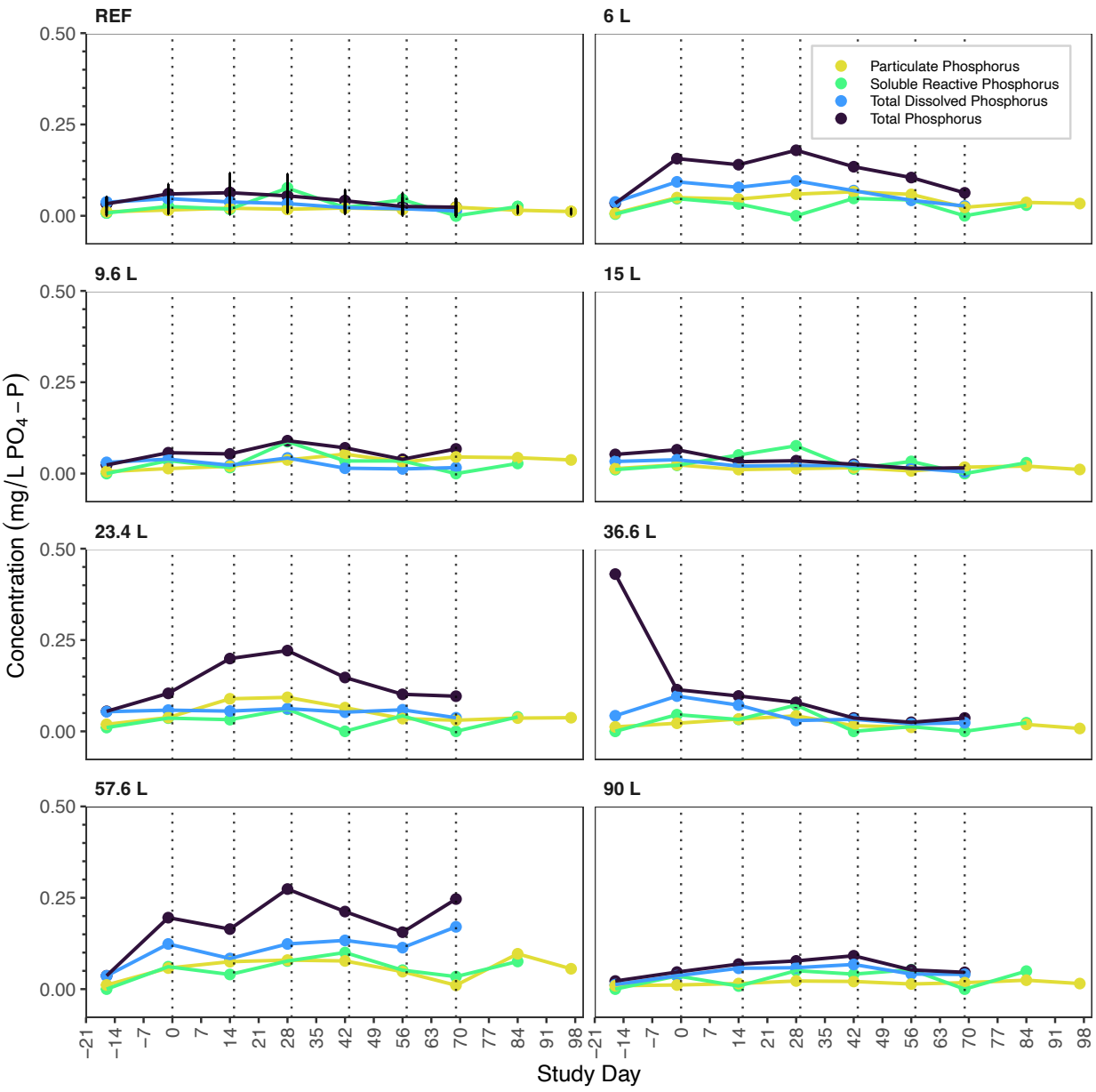

Figure 3.44: Concentration of total phosphorus, soluble reactive phosphorus, total dissolved phosphorus, and particulate phosphorus over the study duration with each plot separated by treatment. The REF plot displays the mean value of the references (n = 3) with error bars representing the ± standard deviation. The vertical dotted lines represent AWW addition days. Figure modified from Blandford (2024)

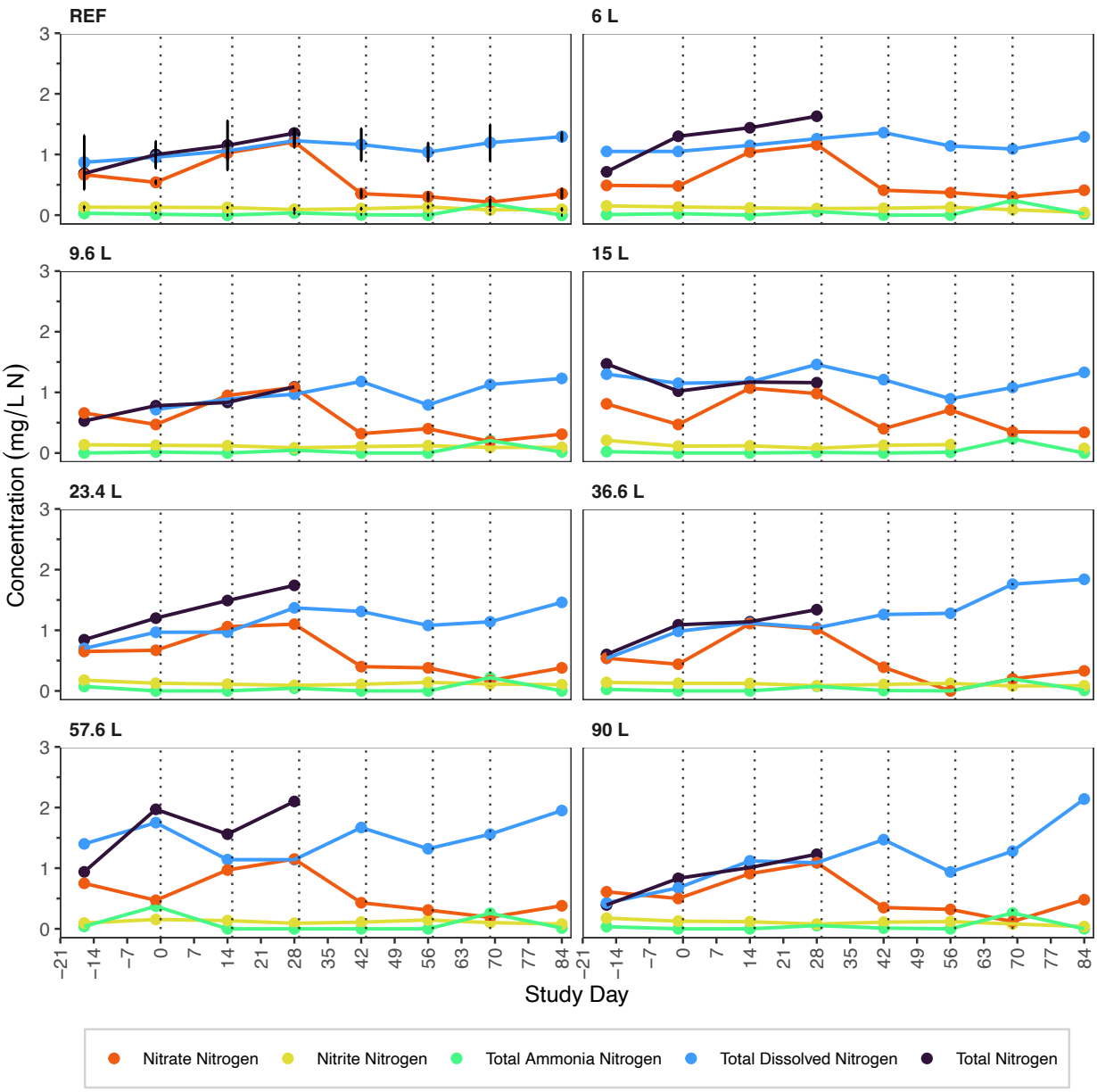

Figure 3.45: Concentration of total nitrogen (mg/L N), total dissolved nitrogen (mg/L N), total ammonia nitrogen (mg/L NH_4-N), nitrate (mg/L NO_3-N), and nitrite (NO_2-N) over the study duration with each plot separated by treatment. The REF plot displays the mean value of the references (n = 3) with error bars representing the ± standard deviation. The vertical dotted lines represent AWW addition days. Figure modified from Blandford (2024).

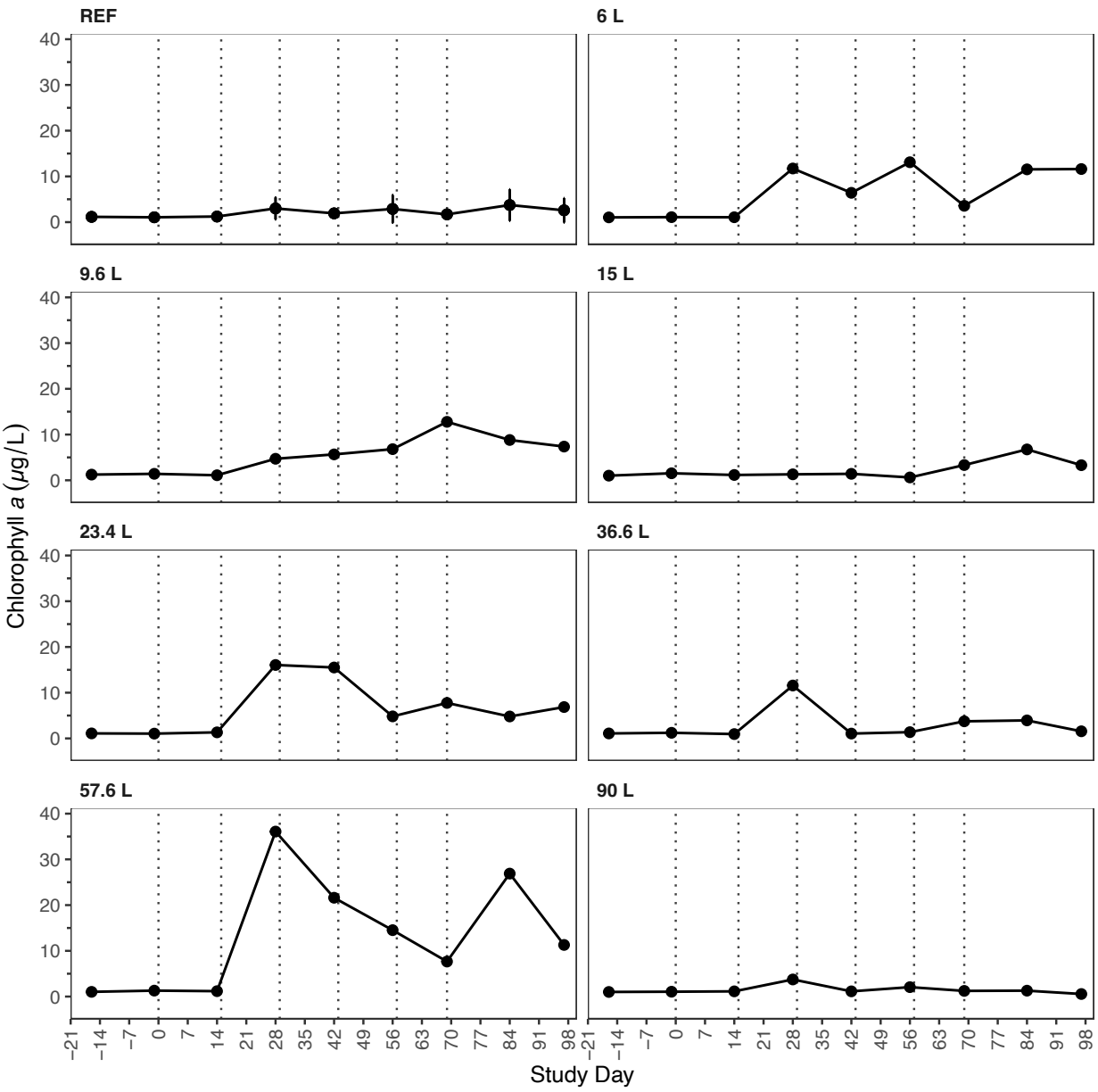

Figure 3.46: Concentration of chlorophyll-*a* over the study duration with each plot separated by treatment. The REF plot displays the mean value of the references (n = 3) with error bars representing the ± standard deviation. The vertical dotted lines represent AWW addition days. Figure modified from Blandford (2024).

3.3.3 Meteorological

The mean monthly values for the air temperature, relative humidity, wind speed, precipitation, and light intensity for the study duration are presented in Table C9. The air temperature and light intensity over the study duration are in Figures C19 and C20.

3.3.4 Soil

All soil properties and soil nutrient content are in Figures D19 – D21. The soil pH and organic matter did not vary between treatments over the study duration. Boron, chlorine, copper, iron, manganese, and nitrate all generally increased in concentration in all mesocosms from the initial sample to the final sample. Calcium, potassium and magnesium all generally decreased in concentration in all treatments over time. Sodium, phosphate, sulfur, and zinc all went generally unchanged over the study duration in all treatments. Statistical interpretations of the soil properties are found in Blandford (2024).

3.3.5 Zooplankton – Morphological Identification

3.3.5.1 Total Zooplankton Abundance

A total of 13 zooplankton taxa were identified within the samples across the study period. Prior to AWW additions, most treatments *Ceriodaphnia* sp. was the most dominant taxa, however, in the 36.6L treatment *Daphnia* sp. had a considerable dominance over the other species comprising 82% of proportion of abundance (Table D9). The dominant taxa shifted to copepod nauplii within most of the treatments following AWW additions, and their dominance increased over the study duration (Figures 3.47 – 3.48). This was also reflected in the most dominant zooplankton groups across all samples, with copepods, cladocerans and rotifers comprising 52%, 21%, and 21%, respectively.

The abundance of zooplankton varied throughout the study duration and between treatments (Figures 3.47 – 3.49). Prior to the first AWW addition the total zooplankton abundance varied among mesocosms, with total abundance ranging from 770 – 3950 zooplankton per sample, with the 15L and 90L treatments having had the highest background abundance (Figure 3.47). After the first addition total abundance increased in a majority of the treatments and the 6L, 15L, 23.4L, and 57.6L treatments hit their peak in abundance reaching between 4846 – 10119 zooplankton per sample. Following the second AWW addition, abundance decreased or plateaued for the remainder of the study duration in these treatments and did not vary from the reference treatments (Figure 3.49). The 90L treatment continued to increase in abundance following the second AWW addition, reaching a maximum of 11640 zooplankton per sample. Abundance then slightly decreased but maintained a large variation from the other treatments (Figure 3.49). There were no significant relationships identified from the linear models between total zooplankton abundance and AWW load (Table D8, Figure 3.50). On study day 91 a weak positive trend was observed between total abundance and AWW load (Figure 3.50).

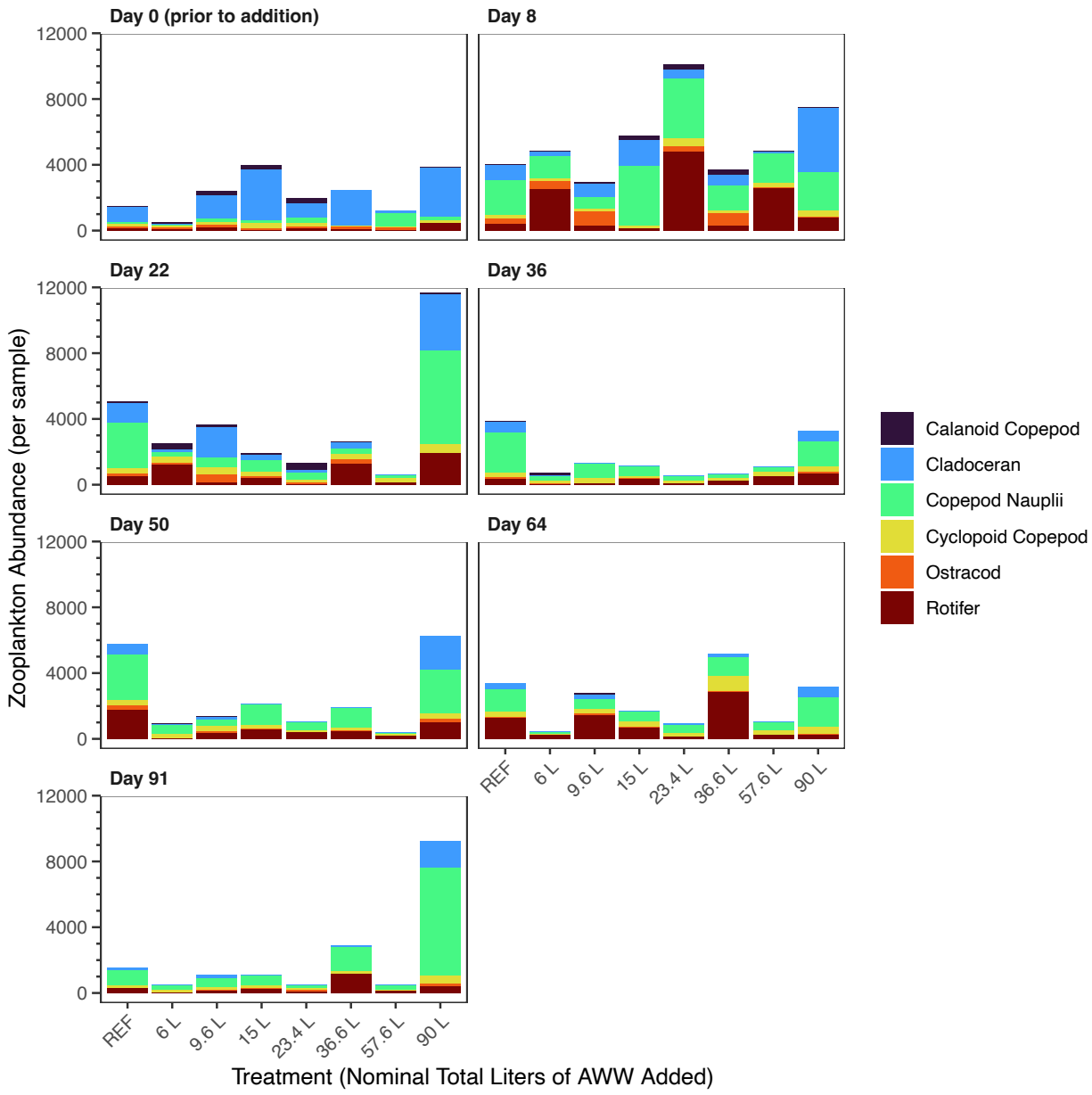

Figure 3.47: UM-WR zooplankton abundance for each treatment on the study day the zooplankton were sampled. REF represents the mean of the references (n = 3).

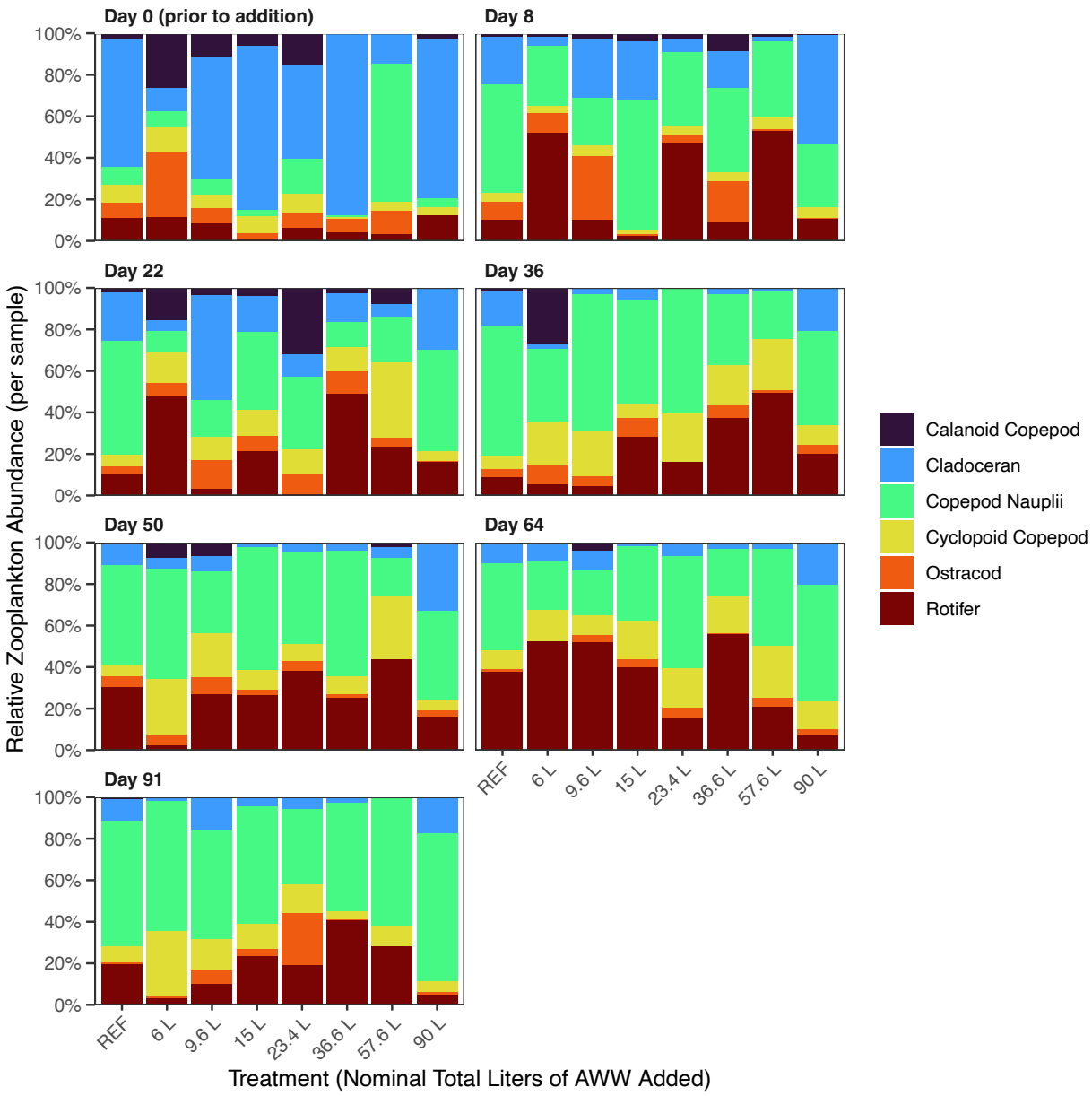

Figure 3.48: UM-WR zooplankton relative abundance (%) for each treatment on the study day the zooplankton were sampled. REF represents the mean of the references (n = 3).

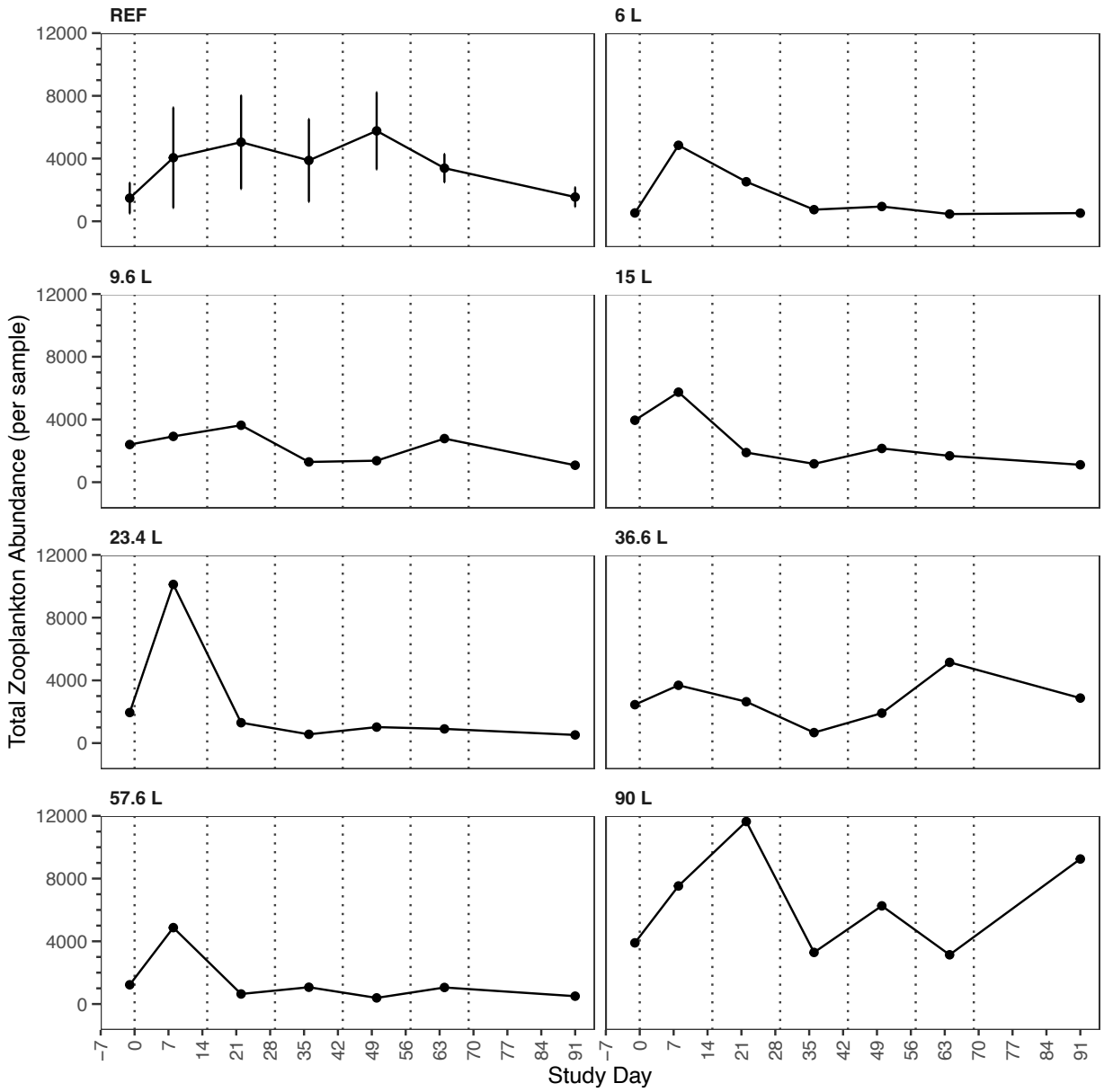

Figure 3.49: Total zooplankton abundance over the duration of the UM wild rice study within each treatment. The REF plot displays the mean value of the references (n = 3) with error bars representing the ± standard deviation. The dotted vertical lines represent the days AWW was added to the treatments.

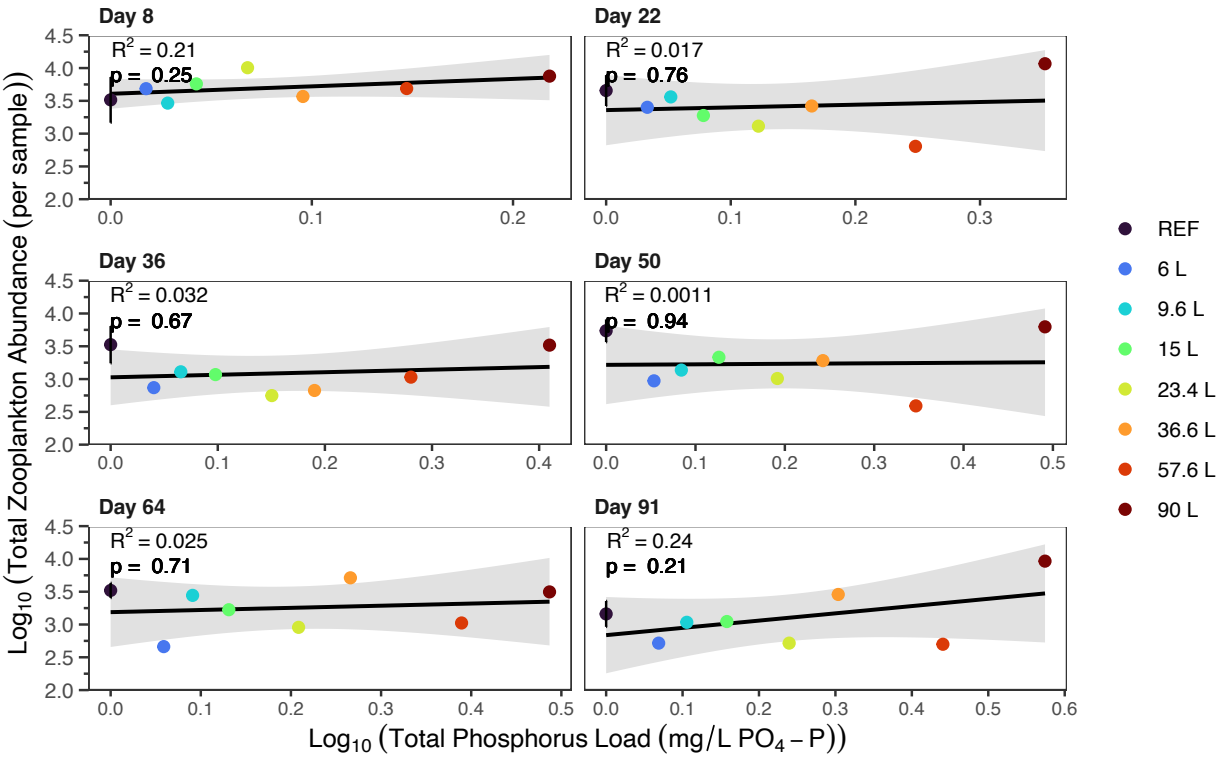

Figure 3.50: Linear regression model results of the relationship between log10(x + 1) of cumulative AWW load concentration (TP used as the representative variable) and total zooplankton abundance. REF displays the mean of the references (n = 3) with the error bars representing ± standard deviation. Each plot displays the model results according to study day.

The PRC analysis of the zooplankton community composition identified that treatment (AWW load) explained 57% of the variance observed in zooplankton abundance. Then 31% of the variation in zooplankton abundance was explained by time, with the remaining 11% unexplained. The first PRC axis explained 48% of the variation in abundance due to the AWW treatments. Both the PRC terms for time ($p = 0.12$) and the interaction between time and treatment ($p = 0.18$) were not significant upon permutation testing. The overall significance of the PRC analysis was found to be significant from permutation testing ($p = 0.04$). The PRC analysis also revealed that AWW load had a significant effect on zooplankton community composition on study day 64 ($p = 0.038$). On study day 64, pairwise permutation testing found that no treatments were significantly different from the references, indicating that no treatment had a strong enough deviance from the references.

Trends in the community response of the PRC output were observed, including an increase in response when compared to the references following either the second or third AWW addition, depending on the treatment (Figure 3.51). A negative community response was observed in the 90L treatment relative to the other treatments and references. *Ceriodaphnia* sp. had the greatest response to AWW treatment reflected by a species score of -1.98, followed by *Diaphanosoma* sp. and *Chydorus* sp. with scores of -1.71 and -1.35. These negative scores, when analyzed with the positive community response of most treatments, indicates a reduced abundance of these taxon occurred. In the 90L treatment a negative community response and negative species score indicate increased abundance of these taxon. The remaining taxa have species scores near zero, indicating little to no significant response to treatment effect (Table D17).

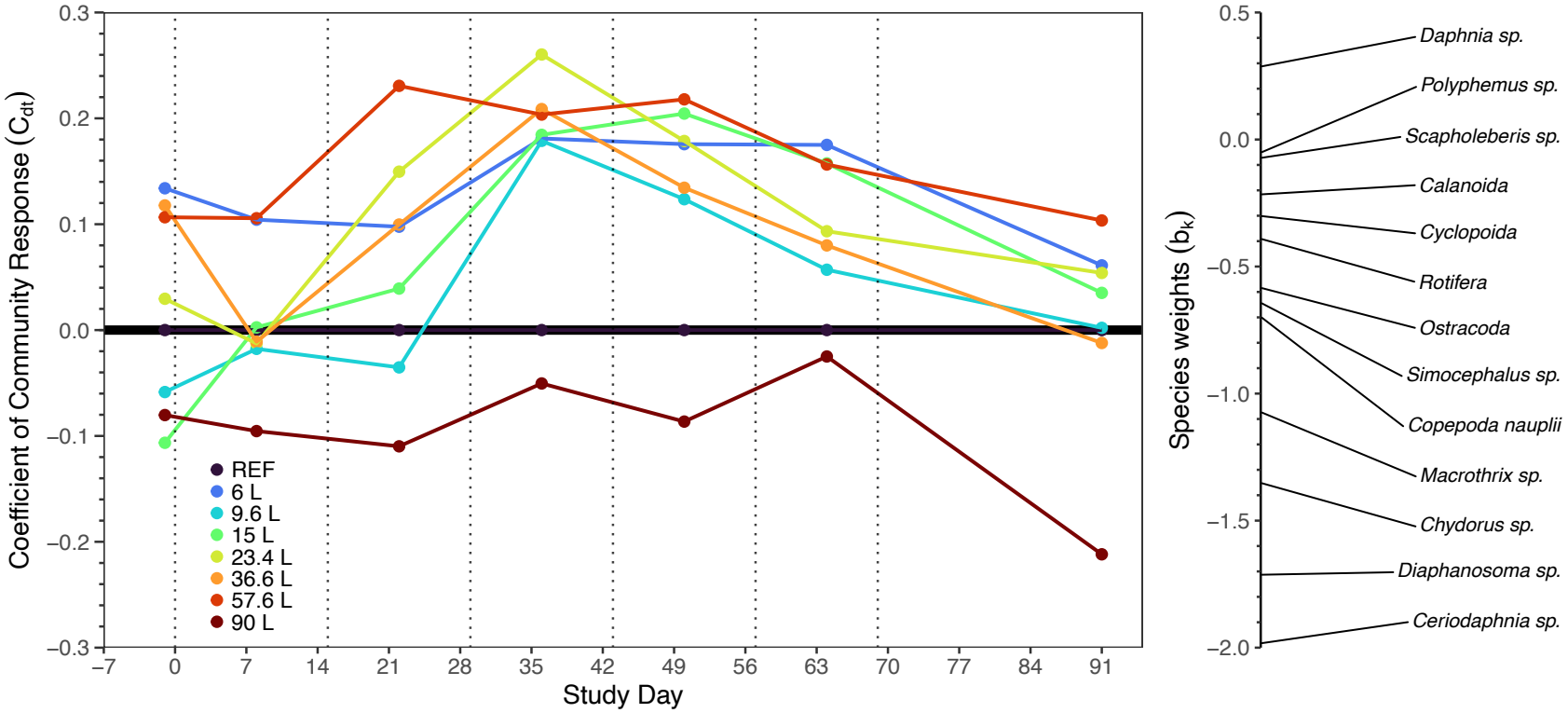

Figure 3.51: Principal response curve (PRC) generated for the RL zooplankton abundance and community composition. Zooplankton abundance was $\log_{10}$ transformed prior to analysis. Species weights are displayed on the right. The thick black line (x = 0) represents the references. The dotted vertical lines represent the days AWW was added to the treatments.

3.3.5.2 Cladoceran Abundance

The cladoceran abundance was comprised of the following genera within the Cladocera order; *Ceriodaphnia*, *Chydorus*, *Daphnia*, *Diaphanosoma*, *Scapholeberis, Macrothrix, Simocephalus,* and *Polyphemus*. The cladoceran group often made up a considerable proportion of the sample abundance, representing a 22% proportion of the total abundance across all samples (Figure 3.48). *Ceriodaphnia* contributed the most to total abundance with total proportions of 9% of total abundance in all samples, followed by *Chydorus* and *Diaphanosoma* each comprising 4% of the total abundance across all samples. The cladoceran abundance varied prior to AWW additions, with the lowest abundance of 60 per sample in the 6L treatment and the highest abundance of 3130 per sample in the 15L treatment (Figure 3.52). Following the first AWW addition, only the 90L treatment experienced an increase in cladoceran abundance and reached a maximum abundance of 3910 cladoceran per sample, driven by an increase in *Ceriodaphnia* abundance. The other treatments declined or remained consistent in cladoceran abundance for the duration of the study. The 90L treatment continued to vary from the other treatments over the study duration, with abundance remaining consistently greater than the other treatments. From linear regression, there was no significant effect of AWW load in cladoceran abundance on any study day (Figure D22, Table D8).

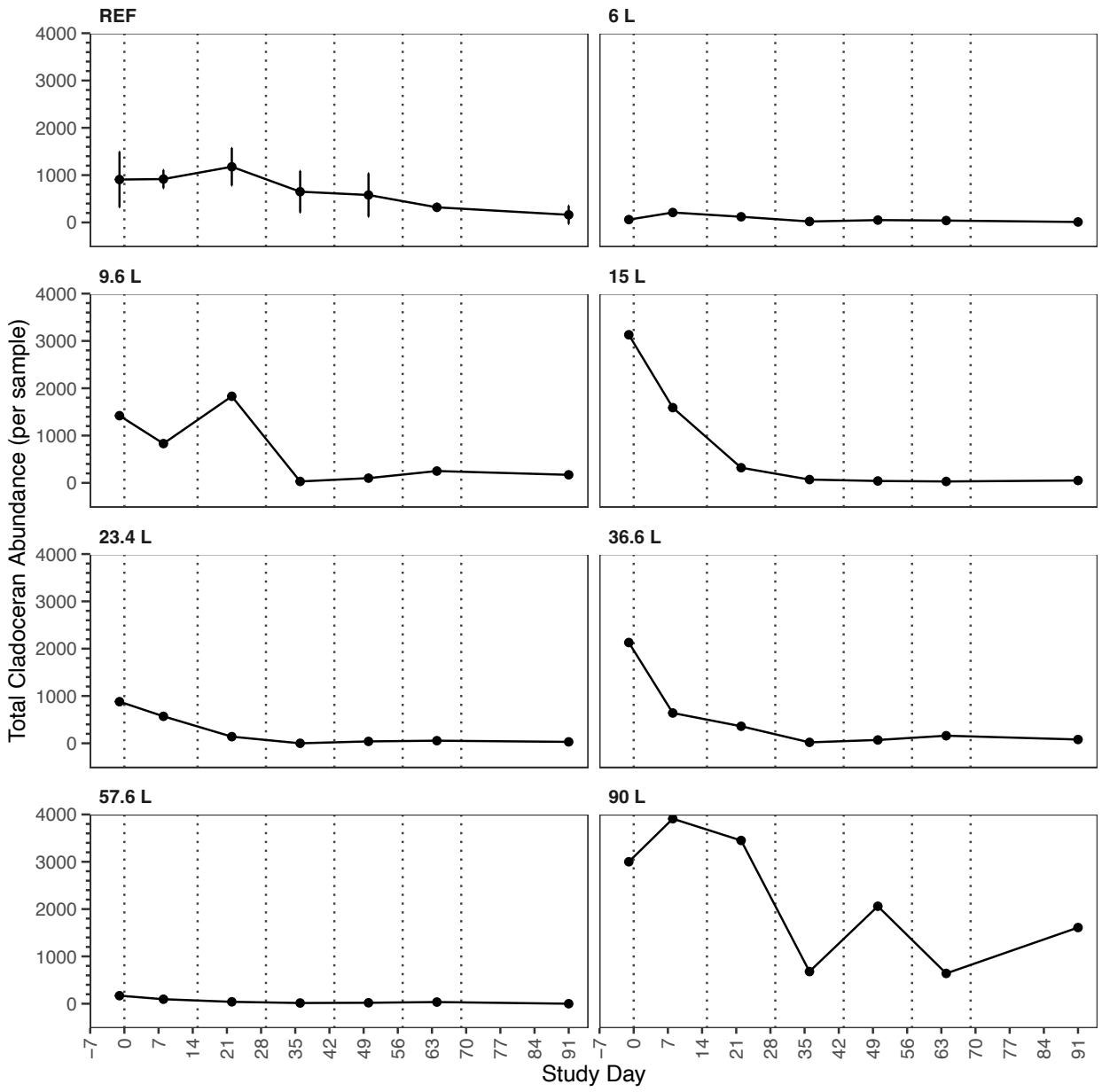

Figure 3.52: Total cladoceran abundance over the duration of the UM wild rice study within each treatment. The REF plot displays the mean value of the references (n = 3) with error bars representing the ± standard deviation. The dotted vertical lines represent the days AWW was added to the treatments.

3.3.5.3 Copepod Abundance

The copepod group abundance was comprised of the orders Calanoida and Cyclopodia, referred to as calanoids and cyclopoids. Copepod nauplii were also included in this group. Prior to AWW additions, the copepod abundance was low in the treatments relative to cladoceran abundance (Figure 3.48). The 57.6L treatment, however, was dominated by copepod nauplii. Following the first AWW addition, copepod nauplii increased and were consistently abundant in all samples, often encompassing over 50% of the proportion of zooplankton in the samples (Figure 3.48). Following the second AWW addition, copepod nauplii abundance decreased in most treatments below reference levels, then plateaued in abundance for the remainder of the study duration (Figure 3.53). The 90L treatment copepod nauplii abundance varied compared to the other treatments, with increased abundance following the second AWW addition, and consistently greater abundance for the remainder of the study (Figure 3.53). Cyclopoids did not vary considerably between treatments, with an average abundance of 222.2 (±150) cyclopoids per sample, across all samples. Calanoids were identified in much smaller abundances compared to the other copepod groups, ranging from 0 – 420 per sample. Following the first or second AWW addition an increase in calanoid abundance occurred in the 6L, 23.4L, 36.6L, and 57.6L treatments. For the remainder of the study duration the calanoid abundance decreased in all treatments and did not vary from the reference abundance.

From linear regression analysis, there was no significant relationship between AWW load and either total copepod abundance, cyclopoid abundance, calanoid abundance, or copepod nauplii abundance on any study day (Table D8, Figures D23 – D26). There was a marginally significant positive relationship between cyclopoid abundance and AWW load on study day 8 (R^2

= 0.48, p = 0.057). A negative trend was observed between calanoid abundance and AWW load, across study days 22, 36, 50, 64.

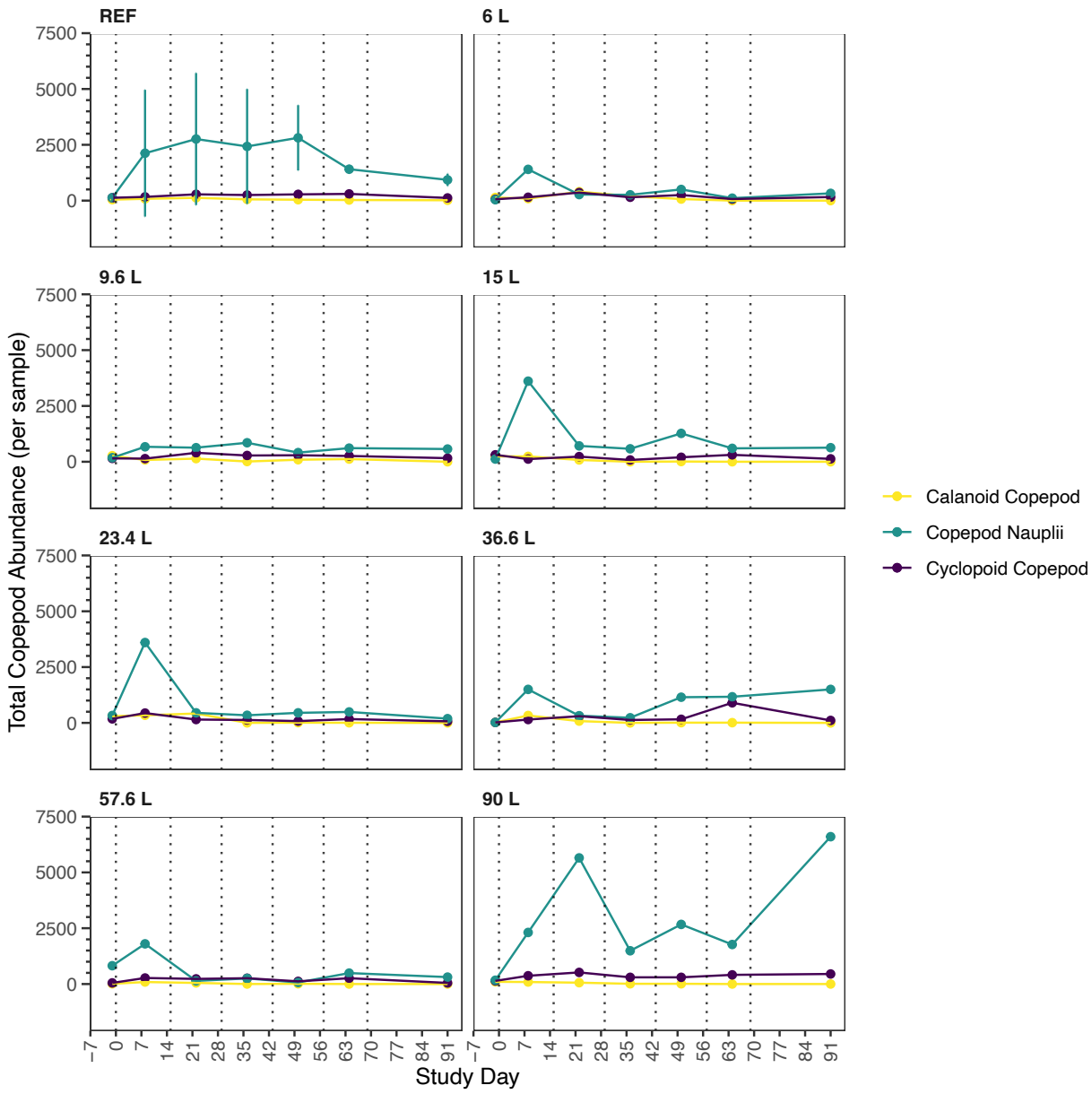

Figure 3.53: Total calanoid copepod, cyclopoid copepod, and copepod nauplii abundance over the duration of the UM wild rice study within each treatment. The REF plot displays the mean value of the references (n = 3) with error bars representing the ± standard deviation. The dotted vertical lines represent the days AWW was added to the treatments.

3.3.5.4 Rotifer Abundance

The rotifer group was comprised of all rotifers identified in the samples. Rotifers were among the most abundant groups in all samples (Figure 3.48). The abundance of rotifers varied across samples and over time (Figure 3.54). The rotifer abundance was similar prior to any AWW additions and did not dominate in any treatments, ranging from 0 - 480 per sample. After the first AWW addition the rotifer abundance increased in all treatments. In the 6L, 23.4L, and 57.6L treatments large peaks of rotifer abundance occurred at 2530, 4790, and 2570, respectively. Then in most treatments rotifers declined in abundance over the remainder of the study duration. An increase in rotifer abundance occurred in the 36.6L treatment on study day 64. A decline in rotifer abundance was observed in all samples by study day 91. Linear regression analyses found a significant relationship between rotifer abundance and AWW load on study day 36 ($R^2 = 0.54$, $p = 0.038$) (Figure 3.55). On all other study days, no relationship between rotifer abundance and AWW load was observed (Table D8, Figure 3.55).

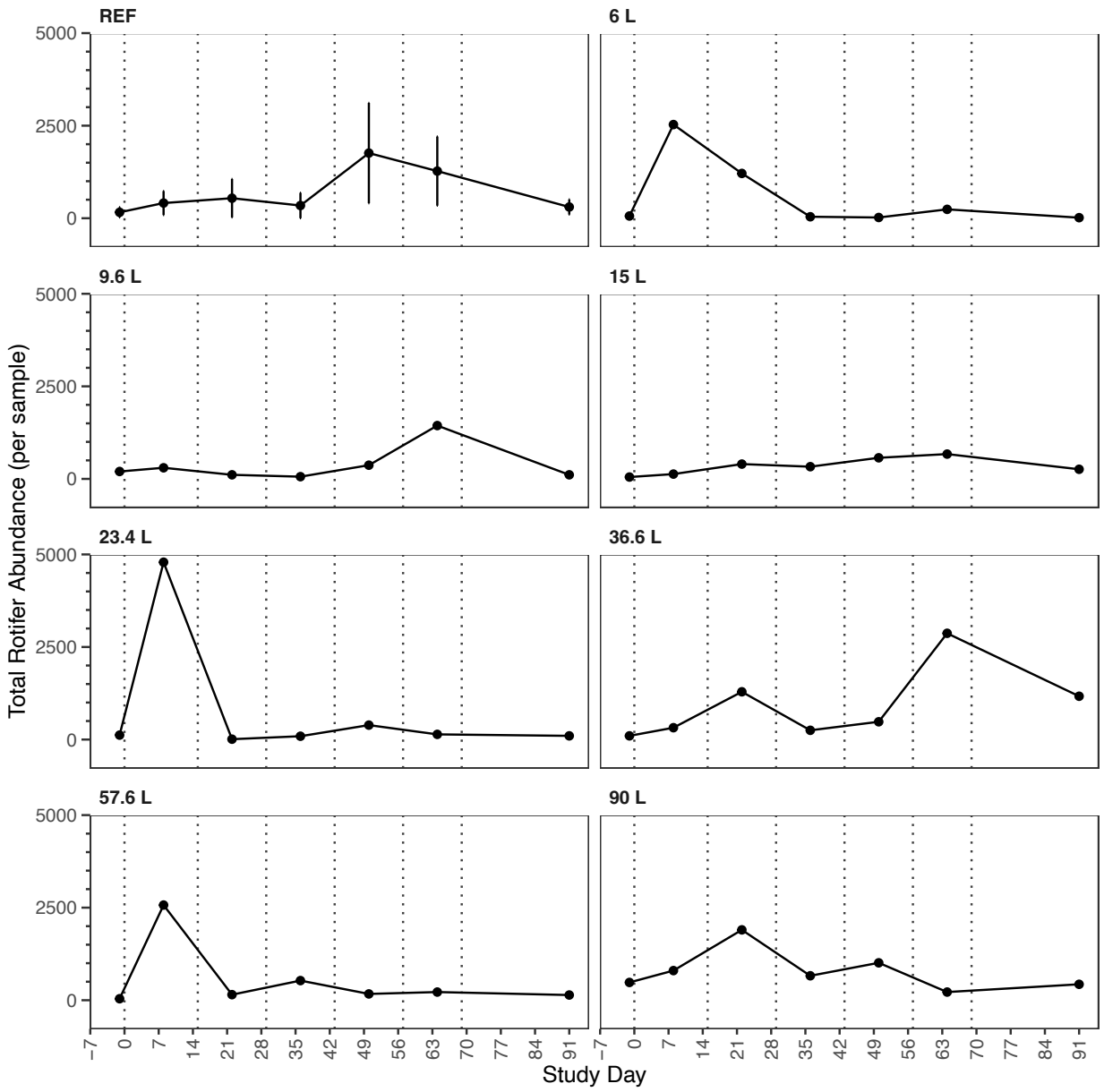

Figure 3.54: Total rotifer abundance over the duration of the UM wild rice study within each treatment. The REF plot displays the mean value of the references (n = 3) with error bars representing the ± standard deviation. The dotted vertical lines represent the days AWW was added to the treatments.

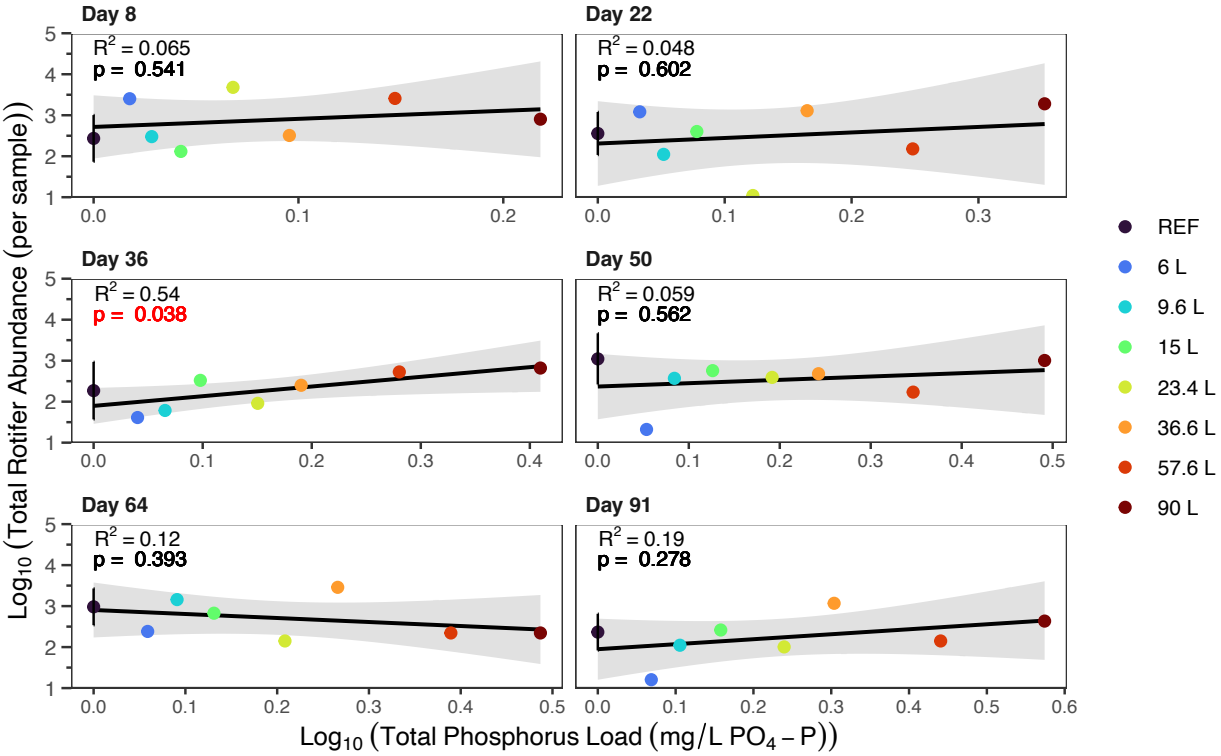

Figure 3.55: Linear regression model results of the relationship between log10(x + 1) of cumulative AWW load concentration (TP used as the representative variable) and total rotifer abundance. REF displays the mean of the references (n = 3) with the error bars representing ± standard deviation. Each plot displays the model results according to study day.

3.3.5.5 Zooplankton Diversity

Zooplankton diversity, richness, and evenness values for each study day are presented in Tables D9-D15. Zooplankton diversity, measured by the Inverse Simpson Index ranged from 1.47 – 5.74 over the study duration, with the lowest diversity measured in the 36.6L treatment (Figure D28). The treatments followed a similar declining trend in diversity over the study duration and did not vary considerably from the references. The evenness of the zooplankton community was generally between 0.3 – 0.6 for the study duration in all treatments (Figure D29). Species richness ranged between 3 – 11 species over the study duration (Figure D30). A general decrease in richness occurred that was below the reference treatment richness. By study day 91, species richness declined in all treatments, as all treatments were primarily composed of copepod nauplii, rotifers, and cyclopoid copepods. There were no statistically significant relationships determined by linear regressions between any of the diversity indexes and AWW load at each study day (Table D8, Figures D31 – D33).

3.3.5.6 Influence of Fish on Zooplankton

A range of 2 – 6 fish were retrieved from the mesocosms by the final sampling date of September 30, 2022 (Table D19). Linear regression analysis did not reveal a significant relationship between fish abundance and total zooplankton abundance on study day 91 (Table D16).

On study days 22, 36, 50, 64, and 91, fish larvae were captured within multiple zooplankton sampling jars. No statically significant relationship was observed between the number of larval fish in the jars and the total zooplankton abundance on any of the study days (Table D16).

3.3.5.7 Influence of Environmental Variables on Zooplankton

The RDA illustrated minor trends and relationships between the included environmental variables and the zooplankton community with the overall model significantly explaining 13% of variation in zooplankton community composition ($p = 0.001$). The first RDA axis significantly explained 15.5% of the total variation in zooplankton composition, with the second axis explaining 6.4% (RDA1: $p = 0.001$). The environmental variables explained 22% of the variance in zooplankton community composition, while 45% of the variation went unexplained. The variance due to study day was 33%, which was controlled out of the RDA model, via the conditional term.

The environmental variables included in the analysis are in Figure 3.56. Un-ionized ammonia was excluded from the variables due to its correlation with TAN. This removed variable would exhibit similar responses to the included correlated variable within the RDA. Other variables excluded from the RDA were water temperature and NO_3 due to elevated VIFs.

The environmental variables that had the strongest influence on the variance in the first RDA axis were particulate P, chlorophyll-*a*, pH and dissolved oxygen (Table D17). The second RDA axis were most influenced by TAN and TDN (Table D17). From permutation tests of the environmental variables, dissolved oxygen, nitrite, and particulate P were determined to have had a significant effect on the zooplankton community composition ($p = 0.001$, $p = 0.005$, $p = 0.006$, respectively). The majority of environmental variables were positively correlated including, chlorophyll-*a,* particulate P, nitrite, SRP, TDN, and TAN. The 6L, 23.4L, 36.6L, and 57.6L treatments differed from the other treatments along RDA1 and were positively correlated with these variables. Rotifer taxa also followed a similar trend, indicting a dominance of this zooplankton taxa within these treatments. However, many cladoceran taxa including

Ceriodaphnia, *Diaphanosoma*, *Chydorus*, and *Macrothix*, were all negatively correlated with these variables. The references and the 90L treatments were grouped together separately from the other treatments, suggesting the zooplankton community responded differently in these treatments (Figure 3.56).

There was a trend that study days 36, 50, 64 and 91, clustered together in the center indicating little variance between treatments later in the study duration (Figure 3.56). This agrees with the abundance figures, as most of the zooplankton communities collapsed following AWW additions and showed minimal variance (Figure 3.47). More variance in the zooplankton communities was evident in the earlier study days -1, 8, and 22, suggesting that the effects of the environmental variables are more pronounced earlier in the study.

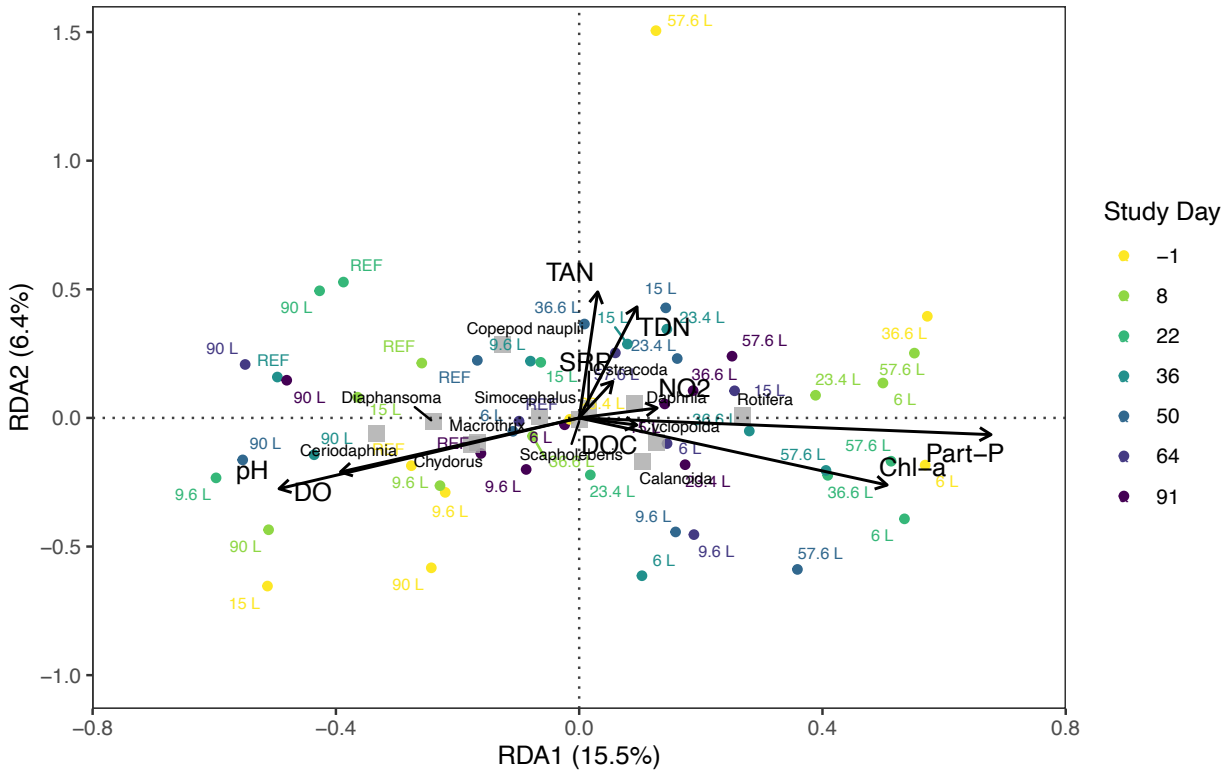

Figure 3.56: Redundancy Analysis (RDA) plot demonstrating the relationship between environmental variables (arrows), zooplankton species (squares), and AWW treatments and references on each study day (points). The references are represented by the mean value (n = 3). The axes explained 15.5% (Axis 1) and 6.4% (Axis 2) of the total variance. The 23.4L and 36.6L treatments on day 64 were removed due to missing measurements. Environmental variables with correlation greater then 0.7 were removed.

Chapter 4: Discussion

4.1 Overview

The first objective of this thesis was to assess the response of zooplankton communities exposed to AWW fertilized water from flooded wild rice environments (i.e., commercial wild rice paddy systems, natural wild rice stands, and established wetlands) to understand the optimal AWW loading that would not result in disruptions to ecosystem health. Overall, in the R&L and UM-EW studies, the zooplankton response was primarily controlled by the water quality conditions directly driven by AWW loading and the fate and availability of phosphorus within the mesocosm water. Meanwhile, the water quality in the UM-WR study was unrelated to AWW loading, and any effects on the zooplankton community from AWW loading could not be interpreted effectively. These details are elaborated below, along with other potential zooplankton effects related to AWW loading, including ammonia and metal toxicity. At commercially applied phosphorus and nitrogen fertilization rates, the effect to the zooplankton communities would be minimal. However, future wild rice applications should take caution to reduce the likelihood of water quality deteriorations that could lead to a potential reduction in ecosystem health as seen within the higher AWW loading treatments.

The second objective of this study was to determine the efficacy of eDNA metabarcoding for identifying and monitoring the zooplankton communities to understand if this method can be used reliably for future zooplankton monitoring research. Overall, this research demonstrated that eDNA metabarcoding could provide more taxonomic coverage than morphological identifications and could decipher accurate trends in the zooplankton communities in response to AWW loading. Regardless, eDNA metabarcoding should still be paired with morphological

identification methods for a more comprehensive and precise community assessment due to the limitations associated with eDNA metabarcoding.

4.2 Zooplankton Response – Morphological Identification

4.2.1 Commercial Wild Rice Paddies (R&L)

We predicted that zooplankton abundance and community composition would be indirectly altered due to elevated phosphorus and associated increases in algal biomass from the loading of nutrient-rich AWW. Phytoplankton abundance was estimated using chlorophyll-*a* in the mesocosm water as a proxy. Pronounced changes in chlorophyll-*a* were not seen until study day 55 because initially, as described in Blanford (2024), wild rice and soil sorption were significant sinks of phosphorus resulting in limited available phosphorus for phytoplankton growth. Additionally, wild rice would have assimilated the most nutrients earlier in the study as this is when wild rice plants require significant nutrients for growth (Carpenter & Lodge, 1986; Sims et al., 2012). The increase in chlorophyll-*a* by study day 55 also coincides with using the second collection of AWW, which contained a concentration of phosphorus approximately eight times greater than the first collection. As a result of the increase in chlorophyll-*a*, typically when concentrations were greater than 10 µg/L, an increase in zooplankton abundance was seen. Chlorophyll-*a* is a useful predictor of zooplankton abundance and often accounts for a large portion of variation seen within a community; a similar result was found here in the RDA that discovered chlorophyll-*a* concentration to be one of the main predictors driving community dynamics within the higher treatments (Sternberger & Lazorchak, 1994).

The increase of chlorophyll-*a* was not always AWW loading dependent for each treatment. As a result, the increase in zooplankton abundance could not be significantly detected

from the AWW loading-based models. When treatments are analyzed separately, the effect can be seen more clearly; for instance, on study day 75, the chlorophyll-*a* concentration was greatest in the 31.5L, 42.7L, 77.7L, and 105L treatments, and a similar increased trend was seen in zooplankton abundance in these treatments. This was a typical display of a bottom-up response that is often seen within aquatic ecosystems when exposed to an elevated nutrient concentration (Carpenter et al., 1985; Jeppesen et al., 2000; Šorf et al., 2015; Sternberger & Lazorchak, 1994). A wetland nutrient enrichment experiment that involved the loading of waterfowl waste at a TP load of 1.6 g/m^2 falling between the TP loading achieved in the 23.1L and 31.5L treatments, experienced similar response patterns to the present study (Pettigrew et al., 1997). For instance, the nutrients applied via waterfowl waste initially resulted in minimal changes to the N and P concentrations as it was predicted that the nutrients either underwent rapid assimilation by macrophytes, sorption to sediments, or denitrification (Pettigrew et al., 1997). Then, following a second addition, high concentrations of nutrients and chlorophyll-*a* were observed, leading to an observed increase in zooplankton abundance and biomass (Pettigrew et al., 1997). Our study, however, required much higher levels of loading for similar changes in ecosystem dynamics to be seen. This could be attributed to either the high initial background nutrient concentration within the water that may have required a larger nutrient addition to result in ecosystem changes (i.e., the secondary AWW collection source nutrient concentrations) or greater nutrient uptake and remediation from the large biomass of wild rice resulting in minimal available phosphorus for phytoplankton (Blandford et al., 2024).

The zooplankton groups that drove the observed increases in abundance were consistently cyclopoid copepods and copepod nauplii. Cyclopoids were likely driven by increased algal abundance, and due to their omnivore feeding strategy, they also potentially

benefitted from an increased rotifer abundance, which would have also increased due to the bottom-up dynamics (Sternberger & Lazorchak, 1994; Lampert & Sommer, 2007). However, the rotifer population demonstrated minimal treatment related variation on study days 21 and 75 but did increase in dominance on study days 35 and 49 within the 77.7L and 105L treatments. Minimal change in the rotifer population disagrees with the common prediction that rotifers will often be the most abundant in eutrophic conditions due to their rapid turnover rates and opportunistic nature within lower water quality conditions (Gannon & Stemberger, 1978). Nevertheless, Yoshida et al. (2003) concluded from an assessment of several boreal lakes that temporal variations in rotifer abundance within a lake result from top-down forces from predation by larger zooplankton. As with our study, a possible increase in rotifer abundance may have occurred indirectly due to AWW loading since this was observed to some degree in the 77.7L and 105L treatments but was then dampened by predation by larger dominant cyclopoids, thus further increasing cyclopoid abundance (Pace et al., 1998).

Cladocerans and calanoid copepods displayed evidence of a sensitivity to nutrient loading that was most pronounced initially in the study, as the relative abundance of these groups was much higher and then decreased after study day 21. The calanoid copepods also had a significant negative relationship with AWW loading. The decline in cladocerans and calanoids could have been due to stress from the new mesocosm environment or reduced food supply due to the initial low food availability as discussed previously. Environmental changes, exposure to toxicants, and poor water quality have also been shown as sensitivities to calanoid copepods (Gannon & Stemberger, 1978; Gutierrez et al., 2020; Jeppesen et al., 2000). The calanoid copepods did not return to reference levels and were absent in the 31.5L to 105L treatments by study day 75. By study days 49 and 75, eutrophication was the highest, hence further driving the decline in

calanoid copepods within treatments 31.5L or greater, which corresponds to a cumulative TP loading of 1798.6 mg/m^2. Conversely, the cladoceran population did increase again in the 77.7L and 105L treatments by study day 75, likely in response to the increased chlorophyll-*a* concentration. Cladocerans are prolific grazers and, in response to the increased algal biomass, were likely able to shift the community composition in their favour within these high nutrient treatments, indicating this zooplankton group was very responsive to both inhibitory and stimulatory food resource availability (Jeppesen et al., 2000, Lampert & Sommer, 2007). Additionally, in the 77.7L treatment, *Ceriodaphnia* sp. dominated during this increase in cladocerans. A characteristic of this genus is that they tend to increase in eutrophic conditions and are often used as indicators of poor water quality and disturbance, thus their increase further indicates the eutrophied state of this treatment (Gutierrez et al., 2020; Sternberger & Lazorchak, 1994).

The various changes that occurred within and between treatments for each zooplankton group may be why no major effects on zooplankton diversity metrics were detected. Typically, species richness and diversity will respond negatively to nutrient loading as the community will become dominated by select species (Declerck et al., 2011; Jeppesen et al., 2000). However, some studies have found minimal effects on the zooplankton dynamics following nutrient loadings despite increased phytoplankton biomass and total phosphorus (Forrest & Arnott, 2006; Paterson et al., 2010). The dynamic changes occurring within the treatments likely resulted in consistent diversity among zooplankton. Although calanoids decreased and other groups shifted, there was never a change that was large enough to completely alter the community. Also, since these systems are closed to external sources, neither colonization of new species that are more tolerable to particular conditions nor relocation of sensitive species would be possible, like in

lake or river ecosystems. In addition, the taxonomic resolution of zooplankton was general, especially for rotifers and copepods. As a result, information about species richness and diversity may have been lost, and different approaches could be implemented in future studies to better capture the composition of the zooplankton community.

Another prediction for this study was that TAN from AWW loading would directly affect the zooplankton abundance due to ammonia toxicity. We found no significant adverse effect related to TAN directly in the AWW or measured in the mesocosm water. A spike in TAN observed in the 42.7L treatment on study day 13 was recorded. Nevertheless, this was before any zooplankton sampling events occurred, so the effect could not be measured. However, on study day 21 in the 42.7L treatment, this first zooplankton measurement was generally consistent with the other treatments, indicating the spike likely did not chronically affect the zooplankton community. The mean TAN concentrations (Table B11) were well below documented acute toxicity values of 125 mg/L TAN for the most sensitive zooplankton species (EPA, 2013). When specifically evaluating un-ionized ammonia, the CCME guideline for the protection of aquatic life is 0.019 mg/L, and is significantly greater than any un-ionized ammonia concentration observed within this study (Table B11) (CCME, 2010). While the TAN concentrations measured directly within the AWW (Table B5) were greater than reported toxicity values, the TAN concentration would have been drastically reduced once added to the mesocosms due to dilution. In fact, we estimated that in the highest treatment (105L), the average TAN concentration in the water from each AWW addition would have been 5.45 mg/L. A toxicity test on *Daphnia carinata* exposed to ammonia within pig effluent had a survival rate of 100% at a TAN of 8 mg/L, indicating the diluted concentration of TAN within the AWW was likely non-toxic (Leung et al., 2010). Although an initial acute toxic effect may occur upon AWW addition due to the ammonia

in the raw wastewater, these effects were not seen in the zooplankton community by the time we measured the community days later. Additionally, the water from flooded paddy systems that zooplankton would be exposed to in a realistic setting where AWW was used to fertilize wild rice would undergo similar dilution prior to entering receiving waters, thus adding an element of protection.

We had also predicted that the water quality of the mesocosms would deteriorate from AWW loadings and cause indirect effects on the zooplankton community. One water quality change we did observe was a steady decline in dissolved oxygen to concentrations below 5 mg/L, with concentrations reaching below 1 mg/L in select treatments. Although low dissolved oxygen can negatively impact zooplankton, the decrease in dissolved oxygen was seen in all treatments, including references (Karpowicz et al., 2020; Vanderploeg et al., 2009). Thus, this effect cannot be attributed to AWW loading. The decline in dissolved oxygen was first documented in all treatments on study day 56 and continued to the last measurement on study day 76. The decline in zooplankton abundance in all treatments closely followed this timing. Zooplankton have been found to be generally tolerant to low dissolved oxygen, and it has been demonstrated that zooplankton will use hypoxic areas with dissolved oxygen as low as 1 mg/L as places of refuge from predators (Karpowicz et al., 2020; Vanderploeg et al., 2009). However, these findings are typically within stratified lakes where zooplankton will move to the hypolimnion to avoid predation and UV exposure; despite being under metabolic stress due to low dissolved oxygen, then at night, they return to the highly oxygenated surface waters (Vanderploeg et al., 2009; Lampert & Sommer, 2007). Since the entirely of the mesocosms were low in dissolved oxygen, the zooplankton would have nowhere oxygenated to go as a reprieve, potentially leading to metabolic stress and indirect effects like declines in feeding rates and

reproductive output overtime (Vanderploeg et al., 2009). At night, the dissolved oxygen was likely even lower than observed due to minimal oxygen producing photosynthetic activity, therefore further exacerbating the oxygen stress (Karpowicz et al., 2020). Zooplankton abundance also likely decreased by the end of the study duration due to the natural seasonal population decline observed in previous similar mesocosm studies (Lobson et al., 2018). The decline in dissolved oxygen combined with natural seasonal changes likely exacerbated the decreased abundance observed. Dissolved oxygen is important to consider for flooded paddy cultivation as introducing anoxic flooded water to a healthy receiving aquatic environment could induce adverse effects greater than or in combination with the potential nutrient related effects. This demonstrates the importance of understanding and measuring flooded paddy dissolved oxygen concentrations before field drainage to ensure the protection of ecosystem health.

Another potential indirect stressor due to AWW loading could have been an increased presence of cyanobacterial species. Although we did not specifically measure cyanobacteria, they are typically found in eutrophic systems that undergo excessive nutrient loading (Huisman et al., 2018). Additionally, based on the total phosphorus within the treatments (Table B11), approximately 55-65% of total phytoplankton biomass is estimated to correspond to cyanobacteria biomass (Downing et al., 2011). This indicates the likely presence of cyanobacteria within these treatments, with a greater dominance within treatments of high TP as cyanobacteria biomass percentage increases with elevated phosphorus concentration (Downing et al., 2011). The initial decline of cladocerans that was observed following study day 21 could potentially be attributed to a cyanobacterial bloom, as cladocerans tend to have a stronger sensitivity to cyanobacteria when compared to other zooplankton groups (Cremona et al., 2021). Cyanobacteria are problematic to grazer cladocerans, like *Daphnia*, as they do not selectively

feed thus consumed cyanobacteria can lead to reduced filtering rate and clogging of the digestive tract from the characteristically filamentous morphology (Cremona et al., 2021; Dupuis & Hann, 2009; Ger et al., 2016; Wilson et al., 2006). A cyanobacteria biomass threshold of greater than 2.25 mg/L has been found to result in declines in cladoceran biomass and abundance (Cremona et al., 2021). Other negative effects of cyanobacteria are that it is a low-quality food source and contains microcystin toxins, both of which can lead to reduced growth rates and reproduction (Cremona et al., 2021; Ger et al., 2016; Wilson et al., 2006). Therefore, it is possible that initially, the phytoplankton community contained predominately cyanobacteria, leading to the observed reductions in cladocerans then when chlorophyll-*a* drastically increased following the fourth AWW addition, this bloom may have been dominant in green algae communities that are more beneficial for cladoceran growth (Lampert & Sommer, 2007). Further, Hansson et al. (2007) found cyclopoid copepods, which are more selective in feeding, were not impacted by high microcystin concentrations, thus demonstrating why, in our study, the reductions in this group were not seen to the same extent as cladocerans. The validity of these predictions cannot be confirmed since neither phytoplankton speciation nor cyanobacterial pigments were measured. Regardless, cyanobacteria presence likely contributed to the zooplankton responses seen.

Another prediction was that metals, particularly zinc and copper, within the AWW, would result in direct effects on the zooplankton community. A large concentration of metals was measured within the AWW. This can likely be attributed to one or a combination of the following factors: the use of antifoulants, accumulation of metals from within the food supplied to the cultured fish, or metal from the holding tanks and septic system (Ahmad et al., 2021; Burridge et al., 2010). The average AWW metal concentrations (Section 3.1.1) are above the zinc CCME

short-term and long-term water quality guidelines for the protection of aquatic life of 334 µg/L and 155 µg/L, respectively (CCME, 2018). These values are based on the average hardness, pH, and DOC within the treatments. The average AWW copper concentrations (Section 3.1.1) are also above the CCME guideline of 4 µg/L, which is based on the average water hardness within the treatments (CCME, 1987). However, when the AWW was applied to the treatments, the metal concentrations would be diluted from the mesocosm water (Table B10). According to these concentrations, the amount of zinc still did not exceed the water quality guidelines. Regardless, copper exceedances of the guidelines may have occurred in the 77.7L and 105L treatments, as these total copper loading concentrations were greater than 4 µg/L.

When specifically focusing on zooplankton, the metals within the AWW could have potentially resulted in toxicological impacts. A microcosm study by Hoang et al. (2021) found a 98-day EC_{50} for zinc of 20.33 µg/L on total zooplankton abundance. They also found cladocerans to be the most sensitive zooplankton group to zinc, with a 98-day EC_{50} of 13.18 µg/L (Hoang et al., 2021). According to this concentration, the cladocerans within the 31.5 L to 105 L treatments would have been exposed to potentially toxic zinc concentrations. Moreover, copper toxicological effects on *Daphnia* include survival and reproductive effects from chronic pulse copper exposures of 20 µg/L, significant behavioural changes from acute copper exposure of 10 µg/L, and a predator-prey modelled population extinction at 16 µg/L (Ingersoll & Winner, 1982; Prosnier et al., 2015; Untersteiner et al., 2003). Although the metal concentrations within the water and AWW directly had the potential to cause toxic effects to zooplankton, there was no direct evidence of this. The decline in the populations by study day 75 occurred in all treatments, including references. Hence, AWW did not result in this effect, as described previously. The changes observed to calanoids could be attributed to metal loading, as this group showed a

significant decline in abundance with AWW loading. In addition, the AWW metal concentrations were highly variable, and the concentration of metals in the water were not measured. Therefore, the precise concentrations of metal exposures that occurred are unknown. Copper and zinc speciation and bioavailability are also indirectly influenced by environmental conditions; due to the high DOC concentration within the treatments, it is possible these metals formed complexes with the organic matter, resulting in reduced bioavailability and subsequent toxicity (Burridge et al., 2010; CCME, 2018; Meyer et al., 2007). Overall, the metals within the AWW had the potential to induce toxic effects, and further analysis of AWW and water concentrations would be required to determine specific and accurate impacts. Metals within the AWW should be monitored and limited within a practical wild rice cultivation setting, as metal toxicity is a large concern for aquatic life.

External factors unrelated to AWW loading could have also influenced the zooplankton communities. One of the largest determinants of zooplankton abundance is predation by planktivorous fish and macroinvertebrates. Although fish were present within the mesocosms, it was determined that the fathead minnows likely did not alter zooplankton abundance. Planktivorous fish have been found to drastically control the zooplankton population due to top-down forces (Carpenter et al., 1985). Yet, a mesocosm study conducted by Šorf et al. (2015) found that increased nutrient loading and fish biomass resulted in increased zooplankton biomass, indicating that despite fish predation, nutrients are a significant and primary determinant of zooplankton dynamics. They did, however, find a shift to smaller zooplankton body size with increased nutrient loading and fish predation, which points to a possible size selective grazing by the fish (Sorf et al., 2015). Further, macrophyte biomass has been shown to improve zooplankton richness and diversity typically because zooplankton will use macrophytes

as a place of refuge when in the presence of planktivorous fish (Declerk et al., 2011; Sternberger & Lazorchak, 1994). During our study, the wild rice grew abundantly within the mesocosms, thus providing ample protective habitat for the zooplankton communities (Blandford et al., 2024). Aquatic invertebrates are an important component of fathead minnow diets; however, a diet analysis study by Herwig and Zimmer (2007) found detritus was also a dominant food source for adult fathead minnows, with detritus making up 79% of their diet by mass. They also found adult fathead minnows to be more selective of macroinvertebrates over zooplankton (Herwig & Zimmer, 2007). In conclusion, the lack of effect of fathead minnows on zooplankton abundance can likely be attributed to a combination of nutrient loading effects outweighing the predation forces, fathead minnow dietary preference, and predator avoidance by zooplankton. Therefore, we can conclude that fish predation did not induce any external effects on the zooplankton community.

4.2.2 Established Wetlands (UM-EW)

We predicted that zooplankton abundance and community composition in the UM-EW treatments would be indirectly altered due to elevated phosphorus and associated increases in algal biomass from the loading of nutrient-rich AWW. Total phosphorus was elevated following AWW additions in the 36.6L and 57.6L treatments; however, phosphorus in the highest treatment (90L) did not see elevations to the same degree (Table C7). Despite elevations in phosphorus concentrations, the chlorophyll-*a* concentration, a proxy for phytoplankton biomass, in the 36.6L and 57.6L treatments did not increase throughout the study duration. The only major increase in chlorophyll-*a* was seen in the 90L treatment on study days 69 and 84 following the fifth and sixth AWW additions to 25 µg/L and 22 µg/L, respectively. Blandford (2024) concluded that the three highest treatments demonstrated eutrophication and decreased water quality, which was

reflected in the water data for the 36.6L and 57.6L treatments and the chlorophyll-*a* data in the 90L treatment. The elevated chlorophyll-*a* concentration in the 90L treatment indicated the assimilative capabilities of phytoplankton and other primary-producing biomass on phosphorus (e.g., wild rice, aquatic plants, algae mats) (Blandford, 2024). As a result of increased nutrient loading from AWW, zooplankton abundance trended positively over time across all treatments. The greatest shift in abundance was seen in the highest treatments (36.6L, 57.6L, 90L), which can be attributed to the changes observed in phosphorus and chlorophyll-*a* concentrations driven by AWW loading.

Despite chlorophyll-*a* concentrations not reflecting elevations in phosphorus within some treatments, zooplankton abundance did increase. Blandford (2024) attributed these absent elevations in chlorophyll-*a* concentrations to a variety of factors, including the competition for phosphorus from the wild rice, aquatic plants, and algal mats, in addition to the plants potentially limiting light availability for phytoplankton growth. This study demonstrates that zooplankton can also control phytoplankton abundance, otherwise referred to as a top-down response (Su et al., 2021). Using zooplankton to control phytoplankton biomass has been well studied, Carpenter et al. (2001) used piscivorous fish to suppress zooplankton predation, thus resulting in an increased zooplankton biomass that subsequently controlled phytoplankton production. Although our study did include planktivorous fish, they were found to have no significant effect on zooplankton abundance, therefore zooplankton abundance was not controlled by any top-down forces, ultimately contributing to the reduction of chlorophyll-*a* likely due to zooplankton grazing in the 36.6L and 57.6L treatments to some degree. Also, within the 36.6L and 57.6L treatments, cladocerans generally dominated abundance, particularly *Ceriodaphnia*. Typically, *Daphnia* is cited as more efficient grazers, however, in eutrophic conditions, *Ceriodaphnia* can

dominate over *Daphnia* due to their smaller size and ability to more effectively feed on lower quality food compared to *Daphnia* (Iwabuchi & Urabe, 2010; Gutierrez et al., 2020).

Higher AWW loading (90L treatment) led to the deterioration of water quality, resulting in shifts in the zooplankton community. In the 90L treatment, the phytoplankton population likely reached a point where the zooplankton could no longer control the abundance, resulting in the chlorophyll-*a* spike seen later in the study period. Increased nutrient loading has been shown to have a negative effect on zooplankton's top-down influence since the phytoplankton can reach too high of an abundance to control (Su et al., 2021). Further demonstrating the decline in water quality in the 90L treatment, the zooplankton community shifted to an increase in rotifers; this zooplankton group are known to dominate under eutrophic conditions due to their simpler life history, rapid reproduction, and opportunistic nature (Gannon & Stemberger, 1978). The change in zooplankton dominance with declines in water quality agrees with a study by Gutierrez et al. (2020) that found rotifers to dominate in eutrophic conditions, classified as chlorophyll-*a* concentration greater than 30 μg/L, and a shared distribution of rotifers and cladocerans in mesotrophic conditions, classified as chlorophyll-*a* between 10-30 μg/L. Although their eutrophic chlorophyll-*a* and SRP concentrations were greater than those observed in our study, this illustrates a trophic shift can occur within a zooplankton community in response to the environmental conditions. Additionally, a negative relationship between AWW loading and diversity was found that was likely driven by increased eutrophication in the high treatments; the decline in diversity with increased eutrophication is a common finding reported throughout zooplankton research (Declerck et al., 2011; Jeppesen et al., 2000). The PRC and RDA results also observed the differing zooplankton response within the 90L treatment. The 36.6L and 57.6L treatments had a strong positive community response in the PRC and were grouped together near

the nutrient related environmental variables in the RDA. Whereas the 90L treatment was grouped separately, with chlorophyll-*a* and rotifers indicating a strong differing response in the community. Overall, at a total phosphorus loading of 997 mg/m^2 (90L treatment), water quality conditions deteriorated, and the zooplankton community shifted in response to more tolerable species (i.e., rotifers) and decreased diversity.

We also predicted that TAN from AWW loading would directly affect the zooplankton abundance due to ammonia toxicity. TAN and other nitrogen species in the water did not vary considerably from the references, indicating AWW loading contributed minimally to the nitrogen response in the treatments (Blandford, 2024). Although PRC analysis found a significant effect of the interaction of time and AWW loading on zooplankton community response, this was likely driven more by both phosphorus, as described previously (Section 4.2.1), and nitrogen contributing to eutrophication and increased zooplankton abundance. TDN was also a significant environmental variable that contributed to the variation seen in the zooplankton community; however, this can likely be attributed to similar conclusions. Although phosphorus is typically highlighted as the most significant driver of eutrophication, nitrogen can also have significant contributions (Lewis & Wurtsbaugh, 2008; Schindler, 2006). Consequently, a significant negative effect of TAN was not captured within the zooplankton analyses. This was unsurprising as the average TAN concentrations in the treatment waters (Table C7) were well below documented acute toxicity values of 125 mg/L TAN for the most sensitive zooplankton species (EPA, 2013).

When specifically evaluating un-ionized ammonia, the principal toxic form of ammonia, minimal toxicological effects were observed. The CCME guideline for the protection of aquatic life for un-ionized ammonia is 0.019 mg/L; this was significantly greater than most

concentrations observed within this study (Table C7) (CCME, 2010). In the 36.6L treatment, un-ionized ammonia concentrations were below toxic concentrations on all measured study days except study days 28 and 69, as concentrations were 0.04 and 0.2 mg/L. The pH within this treatment was elevated to approximately 9.5-10, compared to the pH across the other treatments, consistently around 7.5-9. As a result, the TAN present within the 36.6L had a greater proportion of un-ionized ammonia due to the increased pH levels (Environment Canada, 1999; Emerson et al., 1975; Thurston et al., 1981). Despite these toxic elevations in un-ionized ammonia, the zooplankton community did not appear to be negatively affected as the diversity of this treatment did not vary considerably, and zooplankton abundance increased following day 28. The zooplankton abundance did decrease in this treatment following day 69. However, all treatments decreased in abundance by this point in the study, and the decrease was likely unrelated to un-ionized ammonia. The CCME guidelines are typically conservative values for the protection of all aquatic life, as zooplankton toxicity values are higher than these guidelines. For instance, a toxicity test on *Daphnia magna* to un-ionized ammonia reported a 48-h LC_{50} value of 2.94 mg/L (Gersich & Hopkins, 1985). These results conclude that the zooplankton likely were not suspectable to toxic effects at the un-ionized ammonia concentrations measured within this study.

The mean concentration of TAN within the AWW directly was greater than reported toxicity values; regardless, the TAN concentration would have been drastically reduced once added to the mesocosms due to dilution (Table C1). In fact, we estimated that in the highest treatment, 90 L, when factoring in the water volume of the mesocosm, the average TAN concentration of each AWW addition was 3.17 mg/L, thus indicating the diluted concentration of ammonia within the AWW was of minimal concern. As discussed previously (Section 4.2.1), although an initial acute toxic effect may occur upon AWW addition due to the ammonia in the

raw AWW, these effects were not seen in the zooplankton community by the time we measured the community days later. Additionally, the water from flooded paddy systems that zooplankton would be exposed to in a realistic setting would undergo similar dilution before entering receiving waters and add an element of protection.

We had also predicted that the water quality of the mesocosms would deteriorate due to AWW loadings, resulting in indirect effects to the zooplankton community. This was observed within the 90L treatment, as discussed previously (Section 4.2.2), due to eutrophication. Additional water quality changes can negatively affect the zooplankton community, such as dissolved oxygen declines. In this study we observed a steady decline in dissolved oxygen to concentrations below 5 mg/L, with concentrations reaching below 1 mg/L in select treatments. Although low dissolved oxygen can negatively impact zooplankton, the decrease in dissolved oxygen was seen in all treatments, including references (Karpowicz et al., 2020; Vanderploeg et al., 2009). Therefore, this effect cannot be attributed to AWW loading. Dissolved oxygen was found to be a significant environmental variable contributing to the variation in community composition. The only treatment that did not have dissolved oxygen concentrations below 5 mg/L was the 36.6L treatment. In the RDA, this treatment was grouped furthest from the other treatments on the RDA1 axis along with the dissolved oxygen variable. Hence, dissolved oxygen contributed positively to this treatment and negatively to the other treatments and was unrelated to AWW loading. Dissolved oxygen concentrations decreased in all other treatments to below 5 mg/L by study day 42 and continued the remainder of the study duration, with concentrations reaching below 1 mg/L on occasion. This also coincides with the decrease in zooplankton abundance within all treatments between study days 64 and 91. This follows a similar conclusion as discussed above (Section 4.2.1): natural seasonal decline paired with low dissolved oxygen

likely resulted in the decline in abundance observed within the treatments, as low oxygen can result in metabolic stress and indirect effects like declines in feeding rates and reproductive output overtime (Vanderploeg et al., 2009). In addition, since the 36.6L treatment did not undergo oxygen stress to the same degree, the effects were less pronounced as the zooplankton population within this treatment sustained higher abundance, diversity, and richness on study day 91 compared to the other treatments.

Another potential indirect stressor due to AWW loading could have been an increased presence of cyanobacterial species. Although we did not specifically measure cyanobacteria, they are typically found in eutrophic systems that undergo excessive nutrient loading (Huisman et al., 2018). Cyanobacteria was likely a potential driver in the variation seen in the 90L treatment compared to the other treatments, as a shift to rotifer dominance can occur when cyanobacteria blooms are present (Davis et al., 2012; Matsuzaki et al., 2018). In addition, cyanobacteria can become more prolific as nutrient loading increases due to the rapid growth rates and inherent characteristics of this group that provide an ability to outcompete and dominate other phytoplankton (Davis et al., 2012; Ger et al., 2016; Paerl & Otten, 2013). As discussed in greater detail above (Section 4.2.1), cladocerans are more sensitive to cyanobacteria due to several disadvantageous factors, including, low nutritional quality, toxins, and a filamentous nature that can clog feeding appendages (Cremona et al., 2021; Dupuis & Hann, 2009; Fulton & Paerl, 1987; Ger et al., 2016; Wilson et al., 2006). Whereas rotifers are typically more tolerable to cyanobacteria toxins compared to cladocerans, Fulton and Paerl (1987) found that despite the lower nutritional value of cyanobacteria, rotifer reproduction and growth were generally unaffected as rotifers can supplement their diet with cyanobacteria when more nutritional phytoplankton are limited. Phytoplankton speciation or phycocyanin concentrations would allow

for a more complete assessment of cyanobacteria impacts. Regardless, there is a high likelihood of cyanobacteria dominance in nutrient loaded systems and the consequences to zooplankton communities can be severe.

Another prediction was that metals, particularly zinc and copper, within the AWW would result in direct toxicological effects on the zooplankton community. The average metal concentrations measured directly in the AWW were 3290 µg/L of zinc and 422 µg/L of copper. This indicates a large concentration of metal was within the AWW that can likely be attributed to one or a combination of the following factors, the use of antifoulants, accumulation of metals from within the food supplied to the cultured fish, or metal from the holding tanks and septic system (Ahmad et al., 2021; Burridge et al., 2010). These values were above the zinc CCME short-term and long-term water quality guidelines for the protection of aquatic life of 334 µg/L and 155 µg/L, respectively (CCME, 2018). These values were based on the average hardness, pH, and DOC within the treatments. The copper concentrations were also above the CCME guideline of 4 µg/L, which were based on the average water hardness within the treatments (CCME, 1987). When the AWW was applied to the treatment mesocosms, the metal concentrations would be diluted from the mesocosm water. According to these concentrations (Table C6), zinc did not exceed the short-term water quality guidelines. However, exceedances of the long-term zinc guidelines still occurred in the 57.6L and 90L treatments. Also, copper exceedances of the guideline still occurred in all treatments despite dilution, as these total copper loading concentrations were greater than 4 µg/L.

When specifically focusing on zooplankton, the metals within the AWW could have potentially resulted in toxicological impacts. Comparative toxicity values were discussed previously (Section 4.2.1). Although metal was predicted to be at concentrations that were

concerning within the treatments, no apparent adverse effects on zooplankton were observed. The bioavailability and subsequent toxicity of the copper and zinc added to the treatments from AWW could also have been reduced due to the metals forming complexes with organic matter, which would have been possible considering the high concentrations of DOC (Burridge et al., 2010; CCME, 2018; Meyer et al., 2007). Also, the concentration of copper and zinc in the soil generally increased in all treatments, indicating that the metal within the AWW may have ended up in the soil. Yet no significant relationship between AWW and these metals were found, according to Blandford (2024), thus opposing this conclusion. Metals within the AWW should be monitored and limited within a practical wild rice cultivation setting, as metals can potentially induce toxic effects and are a large concern for aquatic life.

External factors unrelated to AWW loading could have also influenced the zooplankton communities. One of the largest determinants of zooplankton abundance is predation by planktivorous fish and macroinvertebrates. Although fish were present within the mesocosms, it was determined that the adult fathead minnows, added to the mesocosms, did not alter zooplankton abundance. As discussed in more detail above (Section 4.2.1), the minimal effect of the adult fathead minnows can be a result of nutrient loading effects outweighing the predation forces, fathead minnow dietary preference, and predator avoidance by zooplankton.

4.2.3 Natural Wild Rice (UM-WR)

We predicted that zooplankton abundance and community composition would be indirectly altered due to elevated phosphorus and associated increases in algal biomass driven by the loading of nutrient rich AWW. Within the phosphorus elevated treatments (6L, 23.4L, and 57.6L), chlorophyll-*a* concentrations were also elevated to greater than 10 µg/L compared to other treatments, with concentrations generally below 5 µg/L. Blandford (2024) attributed the

minimal elevations in phosphorus and chlorophyll-*a* within the other treatments to the large biomass of algal mats, or metaphyton, that developed and assimilated substantial available phosphorus, resulting in less availability for phytoplankton. In addition, the fresh soil used for the mesocosms had a high phosphorus binding capacity, resulting in more competition for phosphorus resources (Blandford, 2024). In the treatments with elevated chlorophyll-*a* concentrations, a corresponding elevation in zooplankton abundance did not occur, therefore pointing to minimal bottom-up effects.

Zooplankton abundance only increased following the first AWW addition, with abundance trending positively with increased AWW loading. This increase occurred prior to the measured elevations in chlorophyll-*a*. Before the first AWW addition, the zooplankton community was dominated by cladocerans. When the AWW was first added some top-down influence of zooplankton may have occurred, similar to previous discussions (Section 4.2.2). This effect, along with the phosphorus demand from other sources, could have contributed to the absent chlorophyll-*a* elevations seen within the first 3 weeks. By study day 21, the zooplankton abundance decreased in all treatments to below background levels, and little change was seen for the remainder of the study, besides the 90L and 36.6L treatments and the references to a lesser degree. Thus, the zooplankton community underwent a substantial die-off period in most treatments, which seems to be attributed to elevated pH and un-ionized ammonia, this will be discussed further below. As a result of the zooplankton decline, the chlorophyll-*a* concentrations increased in the 6L, 23.4L, and 57.6L treatments since zooplankton grazing would have been to a much lesser degree and metaphyton was not found within these treatments, contributing to phosphorus assimilation (Blandford, 2024).

The 36.6L and 90L treatments did not decrease in abundance to the same degree and maintained zooplankton abundance slightly above or around reference levels despite elevated pH and minimal chlorophyll-*a*. The reason for this response is not completely clear for at least two reasons. First, the zooplankton population did not suffer to the same extent as the other treatments despite elevated pH and un-ionized ammonia having occurred. Second, chlorophyll-*a* abundance was low, indicating minimal available food for zooplankton to proliferate. However, within the 90L treatment, a consistent proportion of cladocerans was sustained throughout the study duration. Therefore, potential top-down effects may have occurred (Section 4.2.2). The chlorophyll-*a* was not measured until approximately 2 weeks following each AWW addition, so algal blooms could have occurred during this period that were then regulated by the zooplankton resulting in low concentrations captured by the time of sampling. The zooplankton may have also compensated their diet by grazing on the abundant metaphyton within this treatment. The limited research on the relationship between zooplankton and metaphyton shows that it is not preferred in the zooplankton diet, likely due to the large filamentous nature of the mats (Barrow et al., 2019; Iacarella et al., 2018; Vinebrooke et al., 2001). Barrow et al. (2019) found that following nutrient additions to experimental ponds, prolific metaphyton growth occurred, resulting in resulted zooplankton abundance. They concluded this decline due to the disinterest of metaphyton as a food source for zooplankton. A more frequent sampling schedule of chlorophyll-*a* would have allowed for the zooplankton response to be better understood within the 90L treatment. However, since the metaphyton were found to be efficient sinks of phosphorus, they may have prevented a decline in water quality conditions that may have occurred in the other treatments. In summary, the zooplankton response was not strongly related to phosphorus loading as the abundance within these treatments did not vary significantly from the references.

We also predicted that TAN from AWW loading would result in direct toxicological effects on the zooplankton abundance due to ammonia toxicity. TAN and other nitrogen species were minimally altered by AWW loading (Blandford et al., 2024). The RDA found nitrite to be an environmental variable that had a significant effect on zooplankton community composition. Nonetheless, nitrite was not affected by AWW loading within the treatments and remained consistent over the study duration. The significance may be due to the 90L treatment driving the relationship since this treatment varied considerably from the other treatments. Additionally, the environmental variables only explained 22% of the variation in community composition. Hence, nitrite likely had minimal effect. Also, TAN did not influence zooplankton as the average concentrations measured within the treatments (Table D6) were well below documented acute toxicity values of 125 mg/L for the most sensitive zooplankton species (EPA, 2013).

When specifically evaluating un-ionized ammonia, the principal toxic form of ammonia, the concentrations of the mesocosm water were greater than CCME guidelines for the protection of aquatic life of 0.019 mg/L, indicating toxic concentrations of un-ionized ammonia were reached within all the treatments (CCME, 2010). Peaks in un-ionized ammonia to concentrations above 0.019 mg/L were observed on study days 28 and 69, with the largest elevation reaching greater than 0.1 mg/L. Although the AWW additions did not drive the elevations in ammonia, as the reference concentrations also increased, the zooplankton communities potentially suffered toxicological effects. Due to elevated pH, the TAN present within the treatments had a significant proportion of un-ionized ammonia (Environment Canada, 1999; Emerson et al., 1975; Thurston et al., 1981). Toxic concentrations of un-ionized ammonia within the treatments were likely a significant contributor to the die-off observed in all the treatments, besides the 90L treatment. However, the CCME guidelines are generally conservative estimate to ensure the protection of

all aquatic life, and zooplankton toxicity values are higher than these guidelines. For example, a toxicity test on *Daphnia magna* to un-ionized ammonia reported a 48-h LC_{50} value of 2.94 mg/L (Gersich & Hopkins, 1985). Leung et al. (2010) exposed *Daphnia carinata* to a gradient of ammonia in digested piggery effluent. They found a 24-hr LC_{50} for un-ionized ammonia of 2.2 mg/L and reproductive effects at concentrations of 1.5 mg/L. Yet, the sensitivity to un-ionized ammonia is highly variable and species-specific. Han et al. (2022) reported acute LC_{50} values of various zooplankton species ranging from 0.22 to 20.59 mg/L. In addition, chronic exposures can have effects on reproduction, life span, fecundity, and growth rates (Lyu et al., 2013). Lyu et al. (2013) found *Daphnia* reproduction per female reduced by 82% following exposure to un-ionized ammonia concentrations of 0.58 mg/L and an EC_{50} of 0.27 mg/L for total offspring per female. Although these concentrations are greater than the concentrations seen in our study, un-ionized ammonia likely contributed to the decline in zooplankton abundance in all treatments to some degree.

We had also predicted that the water quality of the mesocosms would deteriorate due to AWW loadings, resulting in indirect effects to the zooplankton community. We did not observe any significant changes in dissolved oxygen like in the R&L and UM-EW studies, as the mesocosms were highly oxygenated throughout the study. However, the pH did increase between study days -1 and 7 in all treatments, including the references, to between 9.5-10.5 and remained elevated for the whole study duration. The elevation in pH was unrelated to AWW loading as all treatments increased to a similar level, including references. Photosynthetic activity can increase pH in water due to the uptake of carbon dioxide by the primary producers, which may be a possible explanation due to the growth of aquatic plants, wild rice, biofilm, and phytoplankton to a lesser degree, seen within this study (O'Brien & de Noyelles, 1974; López-Archilla et al.,

2004). Alkaline conditions could have also resulted from the soil used in establishing the mesocosms. The slightly alkaline and high calcium concentration of the soil indicates that calcium carbonate was likely present within the soil (Bolan et al., 2023). Calcium carbonate can be released into the water, reacting with carbon dioxide and releasing bicarbonate. The bicarbonate will break down into carbonate and hydroxide, increasing pH (Moss, 1973). The soil in the UM-EW study had similar properties to the UM-WR soil, however, the UM-EW mesocosms were established a year prior as described in the methods. As a result, they likely had a higher buffering capacity as pH was high in these treatments but to a lesser degree. As discussed previously about ammonia, elevations in pH are a large concern because a greater fraction of toxic un-ionized ammonia would be present. Regardless, high pH has been shown to result in direct adverse effects on zooplankton (Jeppesen et al., 1990; Mitchell, 1992; O'Brian & de Noyelles, 1974). Jeppesen et al. (1990) reported that a pH greater than 10.5 led to a collapse in cladoceran abundance within a lake study. The high pH concentrations in combination with an increase in un-ionized ammonia contributed to the rapid decline in zooplankton by study day 21 and prevented any potential effects of AWW loading to be seen.

We also predicted that metals, particularly zinc and copper, within the AWW would result in direct toxicological effects to the zooplankton community. The AWW was the same for both UM studies (see Section 4.2.2). Although the zinc and copper concentrations could have potentially resulted in toxicological effects on the zooplankton community (Section 4.2.2), this was not evident. A decline in zooplankton abundance occurred, and the references were also affected, indicating that the AWW or any component of the AWW did not cause this result. In addition, the 90L treatment, which would have received the highest loading of metals, had an elevated and persistent zooplankton community for the entire study duration. Following previous

conclusions (Section 4.2.1 & Section 4.2.2), the metals within the AWW had the potential to induce toxic effects; however, the concentrations likely decreased due to the binding of metal with organic matter (Burridge et al., 2010; CCME, 2018; Meyer et al., 2007). Further analysis of metal concentrations in the water would have allowed for a more specific and accurate determination of the metal effects. Metals in AWW can pose a concern for aquatic health, and their use in aquaculture should be reduced or monitored if AWW is to be used as a fertilizer for wild rice where the drainage will reach receiving environments.

External factors unrelated to AWW loading could have also influenced the zooplankton communities. One of the largest determinants of zooplankton abundance is predation by planktivorous fish and macroinvertebrates. Similar to previous discussions (4.2.1 & 4.2.2), it was determined that the adult fathead minnows, added to the mesocosms, did not alter zooplankton abundance on study day 91. The minimal effect of the adult fathead minnows can be a result of nutrient loading effects outweighing the predation forces, fathead minnow dietary preference, and predator avoidance by zooplankton (See Section 4.2.1).

4.3 Zooplankton eDNA Metabarcoding

4.3.1 Taxonomic Identification and Coverage of eDNA

Metabarcoding of the zooplankton DNA was an effective method of identifying the zooplankton species present. A total of 36 taxa were identified across all primers, with nearly 60% identified to species level. Due to the less specific taxonomic identifications used in this study when morphologically identifying the zooplankton, we did not achieve the same level of detection detail compared to eDNA. The morphological method required approximately one hour per sample for sample collection and identification. Whereas eDNA metabarcoding per sample

took approximately two hours and 46 minutes total; 30 minutes for sampling, two hours and 15 minutes for DNA extraction, and one minute for PCR and barcoding. The time per sample with eDNA metabarcoding does not include the time required for designing the primers, primer optimization, or bioinformatics, as these steps are highly variable and would reduce in time required with experience. Based off these times, eDNA metabarcoding took longer than the morphological method per sample; however, to achieve the same specificity as eDNA methods, the morphological method would have required much more time and effort than used in this study. In contrast, eDNA did not require more beyond what was already conducted due to the efficient identification capabilities of metabarcoding technology (Rishan et al., 2023; Taberlet et al., 2012). A benefit of eDNA metabarcoding that is frequently cited is that it requires less time and effort compared to morphological identifications (Ruppert et al., 2019; Valentini et al., 2016). The findings of this study contrast that conclusion and indicate that morphological methods can be optimized by reducing the taxonomic specificity required.

Based on the methods we used, metabarcoding allowed for more taxonomic information about the zooplankton community to be obtained than morphological identification. More specific morphological identification (i.e., species level) would be required to confirm this with certainty. Nevertheless, similar conclusions have been reported in other metabarcoding studies that used more precise morphological identifications (Clarke et al., 2017; Song et al., 2023). A study by Song et al. (2023) found nearly double the number of zooplankton taxa identified using metabarcoding methods compared to morphological methods. In addition, the rotifer group can be challenging, costly, and time consuming to identify at the genus or species level. Yet, using eDNA metabarcoding, we acquired detailed information about this group as 12 rotifer taxa were identified across the primers (Chen et al., 2023). For example, with the Rotifer 1 primer, where a

large relative abundance of rotifers was found, allowed for a temporal shift to be seen from *Polyarthra vulgaris* and Monogononta species on study day 20 to *Proales fallaciosa* and *Euchlanis dilatata* species by study day 74. More detailed information on the community composition allows for a more substantial assessment and understanding of the aquatic ecosystem.

We also tested using five different COI primer pairs, one commonly used in zooplankton metabarcoding studies, and four designed primer sets designed to target specific zooplankton groups and found differences between each. The results between the commonly used Leray primer and the designed Copepod primer designed here generated the highest zooplankton read counts. They also had nearly identical results, except the Leray primer identified two more zooplankton taxa. Results using these primers were both dominated by cyclopoid copepods, whereas, cladocerans mostly dominated in the Daphnia primer results, and the Rotifer 1 and Rotifer 2 primers were variable in zooplankton group dominance across the study duration. However, the Rotifer 1 and Rotifer 2 primers had greater amplification of rotifers compared to the other primers. These differences highlight the amplification biases and inefficiencies that can occur across multiple primer pairs, therefore pointing at the need to include multiple primers within an analysis. The Leray and Copepod primers had greater amplification success of cyclopoid copepods compared to the other primers and lacked the complete detection of other major zooplankton groups. Beaulieu et al. (2024) also used the same Leray primer pair and found it failed to detect key cladoceran species that were known to be present based on microscopic identifications. Other studies have also cited the Leray primer to underrepresent the species present compared to microscopy; thus, primer amplification bias likely attributed to the poor

detectability of cladocerans from the use of the Leray primer in this study (Elbrecht & Leese, 2015; Jo & Sasaki, 2024; Trepanier-Leroux et al., 2023).

Rotifer abundance was also severely unrepresented with the Leray primer compared to morphological abundance. Rotifer relative abundance has been effectively identified using the Leray primer in other studies, yet biomass of an organism can greatly affect detection rates and sequence abundance (Evans et al., 2016; Jo & Sasaki, 2024; Matthews et al., 2021). In our study, cyclopoid relative abundance was high due to the high read count of this species within the Leray primer, indicating this species likely had a high biomass; this is unsurprising considering the large relative size of crustacean zooplankton (0.3-3.2 mm long) compared to rotifers (0.1-0.5 mm long) (Balcer et al., 1984; Orstan, 2021). However, since rotifers have a comparatively small biomass, the large-bodied cyclopoids may contain and generate more DNA and potentially mask the rotifer abundance in the eDNA samples (Evans et al., 2016). Determination of zooplankton biomass would have allowed for a more accurate conclusion to the reasoning for the disproportionate taxonomic coverage seen of the Leray primer.

The designed primers having more substantial amplification success of specific zooplankton groups is not a significant concern. These primers were designed to be used together due to the specific zooplankton groups each would target. However, the preferential amplification by the Leray primer is problematic as many zooplankton metabarcoding studies use only this primer, citing it as a “universal” primer for zooplankton amplification (Collins et al., 2019; Trepanier-Leroux et al., 2023). Depending solely on this primer could result in an inaccurate representation of the zooplankton communities. As a result, the versality and specificity of this primer has been questioned (Beaulieu et al., 2024; Chen et al., 2023; Jo & Sasaki, 2024). The designed primers had challenges and limitations, which will be addressed

later, but designing multiple primers to target specific taxonomic groups may render improved and more accurate results (Jo & Sasaki, 2024; Rishan et al., 2023; Valentini et al., 2016; Zhang et al., 2018). Zooplankton are also highly diverse, spanning a wide range of characteristics and genetic differences; therefore, using only one primer pair to capture such a wide taxonomic range is flawed (Zhang et al., 2018; Zhao et al., 2021). Other studies have used multiple different markers in an attempt to improve zooplankton detection, like mitochondrial COI, nuclear 18S rDNA, and mitochondrial 16S rDNA (Clarke et al., 2017; Song et al., 2023; Zhao et al., 2021). This study only focused on COI because we found the reference libraries for 18S and 16S to be limited for the species we aimed to target when designing our primers. Hence, this can also be a beneficial method to improve species detection and taxonomic resolution when combined with a COI primer (Clarke et al., 2017; Elbrecht et al., 2016; Zhang et al., 2018).

4.3.2 Zooplankton Response – eDNA Metabarcoding

The eDNA metabarcoding results showed minimal diversity and community composition changes in response to AWW loading, which agrees with the morphological results. Regardless, trends and changes occurred and varied across primers that reflect the AWW loading effects.

The results from the Leray and Copepod primers revealed an increase in diversity over time in the higher treatments by study day 74, with diversity approximately doubling. This was likely due to the decreased dominance of *Acanthocyclops vernalis*, allowing for cladocerans and other cyclopoid copepods (*Macrocyclops* sp.) to increase in abundance. The increase in cladocerans, specifically *Ceriodaphnia* sp., near the end of the study in the higher treatments is in alignment with morphological identifications and can likely be attributed to previously discussed factors like increased nutrient loading and chlorophyll-*a* concentration (See Section 4.2.1). Differences in calanoid copepod relative abundance were also observed between the

references and low treatments to high treatments, where calanoid copepods were not observed in almost all treatments 31.5L or greater. This indicates a probable sensitivity of high AWW loading to calanoids, which was also observed from the results of the morphological methods and was detailed previously (Section 4.2.1).

The Daphnia primer was most effective at targeting the treatment changes in the cladoceran taxa, as this was the zooplankton group most amplified by this primer. Treatment related changes to community composition are not clear from the relative abundance data since some treatments samples did to not amplify any DNA, indicating a probable deficiency of this primer. However, the general trend was a switch from a dominance of cladocerans to cyclopoid copepods from study day 20 to 48, then back to cladocerans by study day 74. This trend occurred across all treatments, and the references are highly variable, indicating this trend was likely not treatment related. On study day 74, *Ceriodaphnia* sp. represented a majority of relative read abundance within the 77.7L treatment. An increased abundance of this species was also observed from morphological methods on study day 75; this only occurred within this treatment and study day, indicating that the large spike in *Ceriodaphnia* abundance was effectively captured from both methods. This agrees with research conducted by Evans et al. (2016) that showed eDNA methods best capture a similar response to morphological methods when the relative abundance of a species is high, likely due to increased eDNA captured.

Compared to the other primer pairs, the rotifer and calanoid copepod groups were most effectively captured by the Rotifer 1 primer. Although there were no significant relationships between AWW loading and the diversity metrics, trends in the community response were observed. For instance, the rotifer species present shifted from *Polyarthra vulgaris* to *Euchlanis dilatata*, *Proales fallaciosa*, and *Rotaria rotatoria*, over the study duration, indicating a temporal

shift in the rotifer community, but this did not appear to relate to AWW loading. Additionally, calanoid copepods were only present on study day 20 in the references and treatments below 31.5L. Over time, they increased in dominance within the references and 7L and 17.5L treatments. Thus, a strong AWW loading response was observed, with a sensitivity of higher treatment levels on calanoid copepods. Although this primer may have overamplified calanoid copepods, this trend still agrees with previous calanoid copepod sensitivity conclusions of the morphological methods discussed previously (Section 4.2.1).

Only the Rotifer 2 primer displayed a significant negative relationship between diversity and AWW loading, and this only occurred on study day 20. This result was likely driven by the dominance of rotifers within the 77.7L and 105L treatments. This temporally varies from the morphological results, which did not display an increased dominance of rotifers in these treatments until study days 35 and 49. This demonstrates a possible lag in treatment effect detections between the different methods. Research using eDNA to track zooplankton abundance and biomass changes over time by Bourque et al. (2023) found eDNA concentration to increase following *Daphnia magna* abundance with a time lag of anywhere between 3.5 to 28 days. Therefore, the data obtained from both methods around the same study day may have reflected different information due to a temporal lag between eDNA and actual zooplankton abundance. Hence, the eDNA data on study day 20 was possibly representative of earlier community dynamics that were not measured from morphological methods. The rotifer species that drove the relative abundance of rotifers in the 77.7L and 105L treatments on study day 20 was *Polyarthra vulgaris*. Not only is a dominance of rotifers indicative of eutrophic conditions, as discussed previously (Section 4.2.2), *Polyarthra* sp. have been cited as indicators of eutrophication (Gannon & Stemberger, 1978). However, following study day 20, the dominance of cyclopoid

copepods increased in the references and lower treatments, and cladocerans dominated the higher treatments. This mirrors similar conclusions to morphological methods, which saw increased cyclopoid and cladoceran abundance due to nutrient loading following the second AWW source additions and predation of rotifers benefitting the omnivorous cyclopoid copepods (Section 4.2.1). The decrease in rotifer abundance could also be attributed to the aforementioned biomass differences between rotifers and cyclopoid copepods (Section 4.3.1), resulting in a pronounced disparity between these groups once cyclopoids dominate.

The loading of AWW was found to have a significant effect on zooplankton community composition from the Leray and Rotifer 1 primer results. The PCoA of these primers showed a distinct grouping of the higher treatment levels (31.5L, 57.4L, 77.7L, and 105L). Although not significant, there was a differing trend within treatments that received a greater loading of AWW. Several components directly and indirectly related to AWW loading could have resulted in these changes, including, as discussed previously, bottom-up responses, changes in food quality, increased metal concentration, and ammonia exposure (Section 4.2.1). Other zooplankton eDNA research has also reported changes in the zooplankton community in response to water quality and ecosystem conditions (Song et al., 2023; Yang & Zhang, 2020). A significant temporal difference in community composition also occurred between study day 20 and study days 46 and 74. Although this trend is unrelated to treatment, this demonstrates the ability of eDNA metabarcoding to also track temporal changes (Yang & Zhang, 2020; Zhao et al., 2021). The temporal changes seen were likely a result of factors that occurred over time within every treatment, outside the scope of AWW treatment, including, as highlighted previously (Section 4.2.1), natural zooplankton succession, competition for resources, decreased dissolved oxygen across all mesocosms, enclosure stress, or fish predation

Although eDNA relative abundance and taxonomic resolution varied across primers, we could still decipher consistent changes in community composition and diversity across each primer result. The observed changes were not directly proportional between methods or primers, and may have varied temporally in the representation of the communities, but eDNA was still an effective means to assess biodiversity and community dynamics within an ecotoxicological mesocosm experiment. An eDNA metabarcoding study by Song et al. (2023) reported a significant difference in community composition results between primers. Yet, they argue that the different taxonomic resolution resulted in a more comprehensive understanding of zooplankton diversity within their study. Thus, the information derived from each primer still provides valuable information to the community composition in response to AWW loading and strengthens the interpretation when viewed comprehensively.

4.3.3 Relationship Between eDNA Metabarcoding and Morphological Methods

The ability to use eDNA metabarcoding as an alternative zooplankton biodiversity monitoring tool could help improve the understanding of ecosystems in a time effective manner compared to standard taxonomic identification methods, which tend to be challenging and require expert taxonomists (Fitzgerald et al., 2021; Kelly et al., 2024; Valentini et al., 2016). The use of eDNA metabarcoding has often been critiqued based on whether eDNA can quantitatively represent the biological community present (Elbrecht & Leese, 2015; Piñol et al., 2019). Correlation analysis between zooplankton abundance from our morphological method results and zooplankton read counts only found a significant relationship when specifically parsing out the cladoceran group, indicating that the eDNA read counts did not reflect the relative or total abundance of rotifers or copepods within the samples. Song et al. (2023) reported a greater correlation between rotifer abundance and eDNA reads, highlighting that differences will likely

occur between eDNA studies due to primer selection and amplification biases. Also, the biomass of zooplankton plays an important role in interpreting eDNA results (Evans et al., 2016). Determining the biomass of the zooplankton through morphological methods may result in more quantitative similarities between both methods, as many studies have reported a relationship between biomass and eDNA abundance or concentration (Ankley et al., 2021; Clarke et al., 2017; Evans et al., 2016; Jo & Sasaki, 2024). Nonetheless, other studies have shown that eDNA methods disagree with morphological methods, further emphasizing the potential discrepancies and limitations in eDNA metabarcoding that have yet to be resolved (Chen et al., 2023; Elbrecht & Leese, 2015; Meredith et al., 2021).

The community composition analysis of morphological methods also generally agreed with the eDNA results. Several commonalities were discussed above (Section 4.3.2), including the sensitivity of calanoid copepods to high AWW loading and increased cladocerans following elevated chlorophyll-*a* concentrations. The relationship between diversity indices and AWW treatments was generally insignificant from linear regression analysis for both methods. Also, on study days 20/21 and 46/49, both methods demonstrated a general negative trend in diversity with AWW load. Additionally, PCoA found a significant effect of treatment on zooplankton community composition from the morphological results and the Leray and Rotifer 1 primers, in addition to the significant temporal change in community composition identified by eDNA and the morphological method. These results indicate that the different methods are capable of identifying the same variance and trends in community composition despite different relative abundance data. The consensus on this conclusion varies across studies; Song et al. (2023) found that eDNA metabarcoding was a more comprehensive method for identify zooplankton species and community changes. Conversely, Chen et al. (2023) cited that morphological methods were

more effective at detecting ecosystem stress induced changes in zooplankton community composition and relative abundance. This highlights the consistent variability in eDNA metabarcoding that occurs across studies, making comparisons challenging and potentially pointing at the need for a shift in the approaches and methods used (Rishan et al., 2023).

4.4 Conclusion

Both commercial wild rice paddy (R&L) and established natural wild rice systems (UM-EW), zooplankton communities were unaffected by AWW at standard fertilization loadings. Once water quality conditions deteriorated in response to high phosphorus loading of the AWW, as seen in the higher treatment levels, zooplankton abundance increased, and the communities shifted in zooplankton group dominance depending on the system. Other factors, including TAN, metals, cyanobacteria, and fish predation, did not appear to strongly affect total zooplankton abundance and diversity in these systems. Calanoid copepods, however, displayed significant sensitivities related to AWW loading in the R&L systems. The natural wild rice systems (UM-WR) underwent water quality changes unrelated to AWW that negatively affected the zooplankton abundance thus impairing the ability to interpret zooplankton changes clearly in response to AWW loading. The use of eDNA metabarcoding as a zooplankton monitoring tool was demonstrated, through improved taxonomic identifications and capturing of zooplankton responses to AWW loading. From using this method, several limitations and challenges were encountered, drawing the conclusion that eDNA metabarcoding should still be paired with morphological identifications to ensure an accurate representation of the zooplankton communities. Overall, the use of AWW for wild rice cultivation at standard loadings is unlikely to impact the ecosystem health of receiving environments; regardless, monitoring of the AWW and discharged waters is essential to ensure optimal conditions are maintained, as the

zooplankton effects were highly dependent on the remediation capabilities of the wild rice systems that drive water quality dynamics.

Chapter 5: Synthesis and Conclusion

This research aimed to understand the response of zooplankton communities when exposed to AWW applied to established wetlands, natural wild rice stands, and commercial wild rice paddy systems. This research demonstrated the strong relationship between water quality and zooplankton community response. AWW applications should be maintained at standard wild rice fertilization rates to ensure the protection of aquatic ecosystem health in receiving environments. Future research should focus on further development of eDNA metabarcoding to improve its use as an alternative zooplankton community assessment method and to better understand the ecosystem effects of other contaminants associated with AWW.

5.1 R&L and UM Comparison

The R&L and both UM studies aimed to achieve the same research objective of understanding zooplankton responses to AWW loading; however, major differences between the studies resulted in different observed responses. First, the wild rice growth was at a much greater density in the R&L study compared to the UM studies. As a result, the R&L study saw minimal zooplankton changes within the first 55 days as much of the nutrients applied to the treatments were seemingly assimilated by the plants or bound to soil (Blandford, 2024). As a result, the remediation capabilities of the plants directly affected the nutrient concentration in the water, thus indirectly affected the zooplankton community response that was largely driven by water quality. This was also seen to a different degree in the UM-EW study as biofilm, metaphyton, aquatic plants, and phytoplankton all contributed to the assimilation of nutrients resulting in increased zooplankton abundance that was not chlorophyll-*a* dependant. Then, in the UM-WR study, water quality conditions outside of AWW loading resulted in drastic changes to the zooplankton community. As such, across all studies the response of each zooplankton community

was strongly influenced by the dynamics within the mesocosms including nutrient fate, primary production, and water quality characteristics, hence pointing at the importance of maintaining suitable water quality conditions within wild rice systems to ensure a stable and consistent zooplankton community.

The R&L and UM zooplankton communities were also initially different as they were sourced from different locations, that can explain the variations in the responses observed. The UM studies were initially dominant in cladoceran and rotifers while the RL study was dominant in cyclopoids and copepod nauplii. The higher presence of cladocerans in the UM-EW study may have contributed in some capacity to initially controlling the phytoplankton biomass whereas top-down control was not evident in the R&L study as cladocerans were minimal in abundance. Also, an increase in rotifers within the 90L UM-EW treatment was indicative of eutrophication and poor water quality conditions. While in the R&L study when eutrophication increased in the latter half of the study duration, rotifers did not increase in response, and this was attributed to the omnivorous nature of the abundant cyclopoids within the zooplankton community. Therefore, the response seen across studies was often in part a function of the background zooplankton community present.

5.2 Future Research Recommendations

A limitation of these studies was the infrequent sampling of zooplankton and water quality parameters, specifically chlorophyll-*a* and TAN. To determine an accurate acute effect of TAN loading to the zooplankton would have required measuring TAN and zooplankton frequently upon AWW application or within a controlled laboratory exposure study. We predicted the concentrations of TAN following AWW additions as described previously, however the exact concentrations the zooplankton were exposed to are unknown as we did not directly measure

TAN and un-ionized ammonia in the water immediately following AWW additions. Additionally, to determine with more precision the trophic dynamics that occurred, it would have been useful to have more frequent chlorophyll-*a* measurements and phytoplankton speciation. Multiple chlorophyll-*a* measurements directly following AWW additions would have allowed for us to capture the phytoplankton response at a greater resolution. Within the approximate two weeks between AWW addition and chlorophyll-*a* measurements, the phytoplankton community could have drastically changed. This may explain why in the UM studies we saw an increase in zooplankton occur despite minimal change in chlorophyll-*a*. Also, having the knowledge of the phytoplankton species present would have helped address the zooplankton response seen, specifically if cyanobacteria were present as zooplankton can be sensitive to this algal taxon. We were limited in this information and only general predications as to what influenced the zooplankton could be made regarding cyanobacteria. Of course, additional measurements of water quality parameters can be costly and time consuming, thus we were limited in our study. Regardless, a greater understanding of the water quality would allow for a more thorough assessment of the zooplankton response. If AWW is to be used as a fertilizer for wild rice in the future, I recommend routine monitoring of both, the AWW and the drainage from the wild rice paddies to ensure protective concentrations of TAN and chlorophyll-*a* that will not result in changes to trophic dynamics.

I would also recommended additional parameters of AWW to be analyzed as several different chemicals and products are used in aquaculture that could have resulted in the zooplankton responses seen. A variety of contaminants of emerging concern (CEC) are used in aquaculture that could have been within the effluent including, antibiotics, antifoulants, disinfectants, and metals (Ahmad et al., 2021; Boyd & McNevin, 2015; Dauda et al., 2019;

Martins et al., 2018). The effect to the environment from many of these CEC are not well understood especially in combination with the nutrient loading dynamics illustrated within this study (Ahmad et al., 2021; Kashem et al., 2023). We were not provided with the contaminants potentially used at the aquaculture facility we sourced the AWW from and measuring all CEC in the AWW would have been a large undertaking that was greater than the scope of this research. Future studies should focus on the potential contaminants present in AWW and the associated effects to zooplankton and other aquatic organisms. Alternatively, if AWW is to be used as fertilizer for wild rice cultivation, awareness and reduction of the contaminants used in the source aquaculture facility should be a priority or measuring for CEC from the wild rice flooded paddy water prior to drainage into receiving environments should be conducted to minimize the exposure to zooplankton.

The use of eDNA metabarcoding for identifying and evaluating responses in zooplankton biodiversity can be a powerful method, however there are still several challenges and limitations with this approach. First, genetic marker region and specific primer sequence selection can have a drastic effect on eDNA metabarcoding results (Clarke et al., 2017; Song et al., 2013; Zhao et al., 2021). Within this study, the primers were designed to be specific to a particular zooplankton group (i.e., copepod, rotifer, *Daphnia*), yet this was not exactly the result as a large degree of species overlap occurred across primers. This indicates that these primers included too much degeneracy and could have been designed more effectively to target the zooplankton groups with more specificity (Leese et al., 2021; Collins et al., 2019). Also, the designed primers and the Leray primer, that is used extensively within zooplankton eDNA metabarcoding research, all varied in the taxonomic resolution of the zooplankton, indicating primer amplification bias had likely occurred, as discussed previously (Section 4.3.1) (Elbrecht & Leese, 2015; Evans et al.,

2016). However, the use of multiple designed primers within our study allowed for a better representation of the community dynamics when utilized together, thus minimizing the species-specific amplification concerns, compared to just the use of a universal primer. Future research should prioritize the development of zooplankton specific primers to ensure the accurate representation of this diverse group.

Other studies have cited the lack of zooplankton species in reference libraires as a limitation in eDNA metabarcoding, resulting in species that were known to be present from morphological identification found to not be identified by metabarcoding (Chen et al., 2023; Jo & Sasaki, 2024). Since we did not identify all taxa to species level it is unknown if this occurred within our study, however, this could be the reasoning for the low rotifer relative abundance across most of the primers, compared to morphological identifications. Chen et al. (2023) found eDNA metabarcoding failed to identify 22 species of rotifers that had been identified by morphological methods, and of these, 8 did not have reference barcodes in the NCBI library. These findings point at the need for future research to involve the improvement of reference libraries to maximize the effectiveness of eDNA metabarcoding.

As discussed previously (Section 4.3.1), the effectiveness of eDNA metabarcoding to quantitatively represent the zooplankton abundance and biomass present in an ecosystem is highly debated and varying conclusions have been presented (Clarke et al., 2017; Elbrecht & Leese, 2015; Evans et al., 2016; Jo & Sasaki, 2024; Piñol et al., 2019; Song et al., 2023). Also, the limited knowledge of zooplankton eDNA has been referenced as one of the reasons for the minimal understanding of using eDNA as a quantitative method (Jo & Sasaki al., 2024). Therefore, more research is needed on the following components: the source of the measured eDNA (i.e., DNA from the whole body or from shedding); the interaction of zooplankton eDNA

with environmental conditions; and decay rates of zooplankton eDNA (Bourque et al., 2023; Jo & Sasaki, 2024; Zhao et al., 2021). Since our mesocosms were closed systems, dead and alive zooplankton were likely measured from eDNA potentially resulting in the discrepancies in abundance seen between both methods (Bourque et al., 2023). From our morphological methods we were able to accurately identify copepod nauplii from adult copepods, this was not possible using eDNA metabarcoding. Thus, the inability for eDNA metabarcoding to detect life cycle or sex is often a cited limitation (Rishan et al., 2023; Valentini et al., 2016). Other studies will also use zooplankton egg abundance as an indicator of zooplankton reproduction and community response, which is also not possible to determine from eDNA metabarcoding (Brendonck & De Meester, 2002; Varpe et al., 2007). As a result, valuable information can be lost regarding the changes occurring within the zooplankton community when these components cannot be measured. Future research is needed in the field of eDNA metabarcoding to address these limitations.

A challenge we specifically faced with eDNA metabarcoding were contamination issues. The field blanks and extraction controls for the Rotifer 1 and Rotifer 2 primers were determined to have been contaminated during PCR amplification, as a result, any actual contamination that may have occurred during field sampling or DNA extractions could not be parsed out and removed from the sample reads since the controls were rendered inaccurate. Consequently, the read data of the samples from these primers may be skewed due to contamination. Contamination is of large concern in eDNA research, despite this metabarcoding studies often fail to include controls or the method they used for removing the contamination is often not addressed (Sepulveda et al., 2020; Rishan et al., 2023). Sepulveda et al. (2020) argue that low level contamination is often inevitable with metabarcoding studies. Therefore, standardized

protocols and guidelines and for how to monitor contamination and how to proceed if contamination occurs are needed for future research.

5.3 Research Implications

This research highlights the importance of water quality on zooplankton communities when exposed to AWW treated waters. Although numerous studies have been conducted on nutrient loading effects to zooplankton community dynamics, minimal research has explored the consequences of AWW on zooplankton, especially in the context of land-based aquaculture systems. Stojanovic et al. (2017) assessed the environmental effects of AWW discharged from a land-based trout farm and found a distinct shift in the zooplankton community from before the discharge point to after. They also saw an increase in cyclopoid copepods at the sampling location nearest the AWW discharge point, a dominance of cyclopoids was a similar finding in the R&L study (Stojanovic et al., 2017). However, they did not evaluate community changes in response to eutrophication and focused on the effect of increased ammonia and biological oxygen demand (Stojanovic et al., 2017). Another study specifically assessed rotifers exposed to AWW discharged from an in-land tank-based aquaculture system and found the dominance of *Brachionus* species most prevalent at the nearest effluent discharge point, they predicted this genus dominated due to the eutrophic conditions (Toth et al., 2020). They also cite that more information on other zooplankton groups could have added to the understanding of the zooplankton response, therefore, our study examining all zooplankton groups addresses this knowledge gap. Only one rice-fish coculture study was found that examined effects to zooplankton communities and they concluded that the AWW passed through a rice field was effectively remediated, thus, resulting in minimal effects to the zooplankton communities (Lie et al., 2024). Although this study was at a much larger scale compared to our research, we

expanded from this research by testing a gradient of AWW loadings that allow for us to better understand the maximum remediation capacity of wild rice and the subsequent effects that can occur when this point is exceeded. Overall, our research used a dynamic and multifaceted approach that adds to the limited research in this field. We were able to specifically demonstrate the strong influence of AWW on water quality and zooplankton community dynamics within a wild rice system, however, at commercially relevant AWW loadings the risk to zooplankton was minimal.

This research also contributed to the rapidly expanding field of eDNA metabarcoding as a biodiversity monitoring tool. This was one of few studies that practically applied eDNA metabarcoding approaches to assess zooplankton communities within a mesocosm based approach. We demonstrated similar conclusions to other zooplankton metabarcoding studies as discussed previously (Section 4.3) including, the benefits of using multiple primer pairs to enhance taxonomic resolution, that eDNA metabarcoding alone is not a well-developed enough tool to comprehensively understand zooplankton communities, and further research is needed to improve the limitations and challenges associated with eDNA metabarcoding. Nonetheless, we were able to show that designing primers pairs to amplify target zooplankton groups is a suitable approach for identifying zooplankton communities. Other zooplankton research has predominately used a "universal" primer pair, yet we demonstrated that the use of designed primers allowed for a comparatively better understanding of the zooplankton response and diversity. Overall, the use of eDNA metabarcoding for zooplankton monitoring has high potential and practicality; however, further development of zooplankton specific primers and solutions to the other limitations addressed previously are required before this method can stand alone.

The implications of this research also reach beyond the objectives of this study, the effect of nutrient loading on zooplankton communities, it provided insight into the environmental implications of using AWW as a fertilizer source for wild rice cultivation. In addition, the broader project research involves topics including Indigenous socio-economic development, the expansion of wild rice cultivation in Canada, and Indigenous food sovereignty and cultural significance. The conclusions reached in this study can be used to inform and navigate the direction of the broader project goals. Overall, wild rice paired with AWW may be a sustainable agriculture approach and as described in Blandford (2024) the use of this system can achieve a circular economy when also incorporating macrophytes for fish food. Yet, this research demonstrated that although nutrient assimilation by wild rice occurred, other primary producers can assimilate the applied nutrients and then contribute to water quality deteriorations. If this broader circular economy approach is accomplished in the future, the drainage of wild rice systems should be of suitable water quality to ensure the protection of receiving ecosystems. In addition, as suggested by Blandford (2024) an additional strategy could be included that removes metaphyton biomass for fish feed, which would have otherwise eventually resulted in deleterious water quality once decomposed. Overall, AWW paired with wild rice cultivation is a promising agricultural approach if loadings are maintained at concentrations that do not negatively affect downstream aquatic environments.

5.4 Conclusion

AWW was a nutrient rich fertilizer source within each wild rice system and the zooplankton communities responded strongly to the remediation capacity of the wild rice, nutrient assimilation of other primary producers, and soil sorption of nutrients. This study demonstrated that under standard wild rice fertilization rates negative effects to ecosystem health, as indicated by the zooplankton community response, will not occur. Regardless, the monitoring of water quality is essential as changes to the zooplankton communities were seen once water quality deteriorations and elevated eutrophication occurred. Future research should prioritize both the effects from other components of AWW that were not studied here and the continued refinement of eDNA metabarcoding to achieve confidence in this method as an alternative to standard monitoring approaches. Overall, wild rice paired with AWW is an effective and promising sustainable agricultural approach and nutrient loading to receiving environments will not negatively impact ecosystem health if deleterious conditions are not reached.

References

Ahmad, A., Kurniawan, S. B., Rozaimah, S., Abdullah, S., Othman, A. R., & Hasan, H. A. (2021). Contaminants of emerging concern (CECs) in aquaculture effluent: Insight into breeding and rearing activities, alarming impacts, regulations, performance of wastewater treatment unit and future approaches. *Chemosphere, 290,* 133319. https://doi.org/10.1016/j.chemosphere.2021.133319

Ahmad, F., Hameed, M., & Ahmad, M. S. A. (2018). Exploring potential of minor/ underutilized grasses for remote areas facing food scarcity. *Global Perspectives on Underutilized Crops*, 189–206. https://doi.org/10.1007/978-3-319-77776-4_7/COVER

Ahmed, N., Thompson, S., Hardy, B., & Turchini, G. M. (2020). An ecosystem approach to wild rice-fish cultivation. *Reviews in Fisheries Science and Aquaculture, 29*(4), 549–565. https://doi.org/10.1080/23308249.2020.1833833

Anand, S., Mangano, E., Barizzone, N., Bordoni, R., Sorosina, M., Clarelli, F., Corrado, L., Boneschi, F. M., D'Alfonso, S., & De Bellis, G. (2016). Next generation sequencing of pooled samples: Guideline for variants' filtering. *Scientific Reports, 6*, Article 33735. https://doi.org/10.1038/srep33735

Ankley, P. J., Xie, Y., Black, T. A., Debofsky, A., Perry, M., Paterson, M. J., Hanson, M., Higgins, S., Giesy, J. P., & Palace, V. (2021). Using zooplankton metabarcoding to assess the efficacy of different techniques to clean-up an oil-spill in a boreal lake. *Aquatic Toxicology, 236*, 105847. https://doi.org/10.1016/j.aquatox.2021.105847

APHA. (2012). *Standard Methods for the Examination of Water and Wastewater*. 22nd Edition, American Public Health Association, American Water Works Association, Water Environment Federation.

Arauzo, M. (2003). Harmful effects of un-ionised ammonia on the zooplankton community in a deep waste treatment pond. *Water Research, 37*, 1048–1054.

Armstrong B., Lazorchak, J., Murphy, C., Haring, H., Jensen K., & Smith, M. (2012). Determining the effects of ammonia on fathead minnow (*Pimephales promelas*) reproduction. *Science of the Total Environment, 420,* 127-133. https://doi.org/10.1016/j.scitotenv.2012.01.005

Balcer, M., Korda, N., & Dodson, S. (1984). *Zooplankton of the great lakes: A guide to the identification and ecology of the common crustacean species*. University of Wisconsin Press, Madison, Wisconsin, USA.

Barrow, J. L., Beisner, B. E., Giles, R., Giani, A., Domaizon, I., & Gregory-Eaves, I. (2019). Macrophytes moderate the taxonomic and functional composition of phytoplankton assemblages during a nutrient loading experiment. *Freshwater Biology, 64*(8), 1369–1381. https://doi.org/10.1111/FWB.13311

Beaulieu, J., Yates, M. C., Astorg, L., Trépanier-Leroux, D., Jeon, H., Rudko, S. P., Humphries, S., Fraser, D. J., Cristescu, M. E., & Derry, A. M. (2024). Environmental DNA for assessing impact and recovery of aquatic communities in an invaded mountain lake. *Lake and Reservoir Management, 40*(2), 111–131. https://doi.org/10.1080/10402381.2024.2309632

Blandford, N. C. (2024). *Remediation of aquaculture wastewater using wetland plants* [Master's Thesis, University of Manitoba]. MSpace. http://hdl.handle.net/1993/38695

Blandford, N. C., McCorquodale-Bauer, K., Grosshans, R., Hardy, B., Cicek, N., & Palace, V. (2024). Removal of nutrients from aquaculture wastewater using cattail (*Typha* spp.) constructed wetlands. *Journal of Environmental Quality*, *53*(5), 767-775. https://doi.org/10.1002/jeq2.20608

Blomqvist, P., Bell, R. T., Olofsson, H., Stensdotter, U., & Vrede, K. (1993). Pelagic ecosystem responses to nutrient additions in acidified and limed lakes in Sweden. *Ambio, 22*(5), 283–289.

Bolan, N., Srivastava, P., Srinivasa Rao, C., Satyanaraya, P. V., Anderson, G. C., Bolan, S., Abbott, L. K., Zhao, H., Mehra, P., Satyanarayana, S. V., Khan, N., Wang, H., Rinklebe, J., Siddique, K. H. M., & Kirkham, M. B. (2023). Distribution, characteristics and management of calcareous soils. In Sparks, D. L. (Eds.), *Advances in Agronomy* (182 ed., pp. 81-130). Academic Press.

Bolyen, E., Rideout, J. R., Dillon, M. R., Bokulich, N.A., Abnet, C. C., Al-Ghalith, G. A., Alexander, H., Alm, E. J., Arumugam, M., Asnicar, F., Bai, Y., Bisanz, J. E., Bittinger, K., Brejnrod, A., Brislawn, C. J., Brown, C. T., Callahan, B. J., Caraballo-Rodríguez, A. M., Chase, J., … Caporaso, J. G. (2019). Reproducible, interactive, scalable and extensible microbiome data science using QIIME 2. *Nature Biotechnology, 37*, 852–857. https://doi.org/10.1038/s41587-019-0209-9

Bourque, D. A., Wang, X. S., Fryxell, J. M., Betini, G. S., McCann, K. S., & Hanner, R. (2023). Environmental DNA tracks zooplankton population dynamics in experimental mesocosms. *Environmental DNA*, *5*(5), 880–893. https://doi.org/10.1002/EDN3.347

Boyd, C. E., & Massaut, L. (1999). Risks associated with the use of chemicals in pond aquaculture. *Aquacultural Engineering, 20*, 113–132.

Boyd, C. E., & McNevin, A. A. (2015). *Aquaculture, Resource Use, and the Environment*. John Wiley & Sons, Inc. https://doi.org/10.1002/9781118857915

Brendonck, L., & De Meester, L. (2003). Egg banks in freshwater zooplankton: Evolutionary and ecological archives in the sediment. *Hydrobiologia, 491*(1), 65–84. https://doi.org/10.1023/A:1024454905119/METRICS

Burridge, L., Weis, J. S., Cabello, F., Pizarro, J., & Bostick, K. (2010). Chemical use in salmon aquaculture: A review of current practices and possible environmental effects. *Aquaculture, 306*, 7-23. https://doi.org/10.1016/j.aquaculture.2010.05.020

Butzler, J. M., & Chase, J. M. (2009). The effects of variable nutrient additions on a pond mesocosm community. *Hydrobiologia*, *617*(1), 65–73. https://doi.org/10.1007/S10750-008-9443-8/TABLES/3

Callahan, B. J., McMurdie, P. J., Rosen, M. J., Han, A. W., Johnson, A. A., & Holmes, S. P. (2016). DADA2: High-resolution sample inference from Illumina amplicon data. *Nature Methods, 13*(7), 581-583. https://doi.org/10.1038/nmeth.3869

Calow, P., & Forbes, V. E. (2003). Peer reviewed: does ecotoxicology inform ecological risk assessment? *Environmental Science & Technology*, *37*(7), 146A-151A. https://doi.org/10.1021/ES0324003

Camargo, J. A., & Alonso, Á. (2006). Ecological and toxicological effects of inorganic nitrogen pollution in aquatic ecosystems: A global assessment. *Environmental International, 32,* 831-849. https://doi.org/10.1016/j.envint.2006.05.002

Cameron, E., Schmidt, P., Tremblay, B., Emelko, M., & Muller, K. (2021). Enhancing diversity analysis by repeatedly rarefying next generation sequencing data describing microbial communities. *Scientific Reports, 11*, 22302. https://doi.org/10.1038/s41598-021-01636-1

Canadian Council of Ministers of the Environment (CCME). (1987). *Canadian Water Quality Guidelines for the Protection of Aquatic Life: Copper.* https://ccme.ca/en/chemical/71

Canadian Council of Ministers of the Environment (CCME). (2010). *Canadian environmental quality guidelines for the protection of aquatic life: Ammonia*. https://ccme.ca/en/res/ammonia-en-canadian-water-quality-guidelines-for-the-protection-of-aquatic-life.pdf

Canadian Council of Ministers of the Environment (CCME). (2018). *Scientific criteria document for the development of the Canadian water quality guidelines for the protection of aquatic life: zinc.* Canadian Council of Ministers of the Environment, Winnipeg, MB. https://ccme.ca/en/res/2018-zinc-cwqg-scd-1580-en.pdf

Caquet, T. (2002). Use of aquatic mesocosms in ecotoxicology: State of the art and perspectives. *Radioprotection-Colloques, 37*(C1), C1-173-C1-177. https://doi.org/10.1051/radiopro/2002033

Carmichael, W. W. (1994). The toxins of cyanobacteria. *Scientific American, 270*, 64-72.

Carpenter, S. R., & Lodge, D. M. (1986). Effects of submersed macrophytes on ecosystem processes. *Aquatic Botany*, 341–370.

Carpenter, S. R., Caraco, N. F., Correll, D. L., Howarth, R. W., Sharpley, A. N., & Smith, V. H. (1998). Nonpoint pollution of surface waters with phosphorus and nitrogen. *Ecological Applications, 8*(3), 559–568. https://doi.org/10.1890/1051-0761

Carpenter, S. R., Cole, J. J., Hodgson, J. R., Kitchell, J. F., Pace, M. L., Bade, D., Cottingham, K. L., Essington, T. E., Houser, J. N., & Schindler, D. E. (2001). Trophic cascades, nutrients, and lake productivity: Whole-lake experiments. *Ecological Monographs, 71*(2), 163–186. https://www.jstor.org/stable/2657215

Carpenter, S. R., Kitchell, J. F., & Hodgson, J. R. (1985). Cascading trophic interactions and lake productivity. *BioScience, 35*(10), 634–639. https://www.jstor.org/stable/1309989

Casas, L., Pearman, J. K., & Irigoien, X. (2017). Metabarcoding reveals seasonal and temperature-dependant succession of zooplankton communities in the Red Sea. *Frontiers in Marine Science, 4*, 241. https://doi.org/10.3389/fmars.2017.00241

Chen, L., Duan, Y., Cui, M., Huang, R., Su, R., Qi, W., & He, Z. (2021). Biomimetic surface coatings for marine antifouling: natural antifoulants, synthetic polymers and surface

microtopography. *Science of the Total Environment, 766*, 144469. https://doi.org/10.1016/J.SCITOTENV.2020.144469

Chen, Y., Wang, H., Gong, Y., Zhang, P., Zhang, H., Wang, T., Xie, J., Xu, J., Wang, H., & Kong, X. (2023). Benefits of combined environmental DNA and microscopy for diversity monitoring in rotifer community: A mesocosm experiment. *Ecological Indicators, 155*, 110930. https://doi.org/10.1016/J.ECOLIND.2023.110930

Clarke, L. J., Beard, J. M., Swadling, K. M., & Deagle, B. E. (2017). Effect of marker choice and thermal cycling protocol on zooplankton DNA metabarcoding studies. *Ecology and Evolution*, *7*(3), 873–883. https://doi.org/10.1002/ECE3.2667

Collins, R. A., Bakker, J., Wangensteen, O. S., Soto, A. Z., Corrigan, L., Sims, D. W., Genner, M. J., & Mariani, S. (2019). Non-specific amplification compromises environmental DNA metabarcoding with COI. *Methods in Ecology and Evolution, 10*(11), 1985–2001. https://doi.org/10.1111/2041-210X.13276

Creer, S., Deiner, K., Frey, S., Porazinska, D., Taberlet, P., Thomas, W. K., Potter, C., & Bik, H. M. (2016). The ecologist's field guide to sequence-based identification of biodiversity. *Methods in Ecology and Evolution, 7*(9), 1008–1018. https://doi.org/10.1111/2041-210X.12574

Cremona, F., Blank, K., & Haberman, J. (2021). Effects of environmental stressors and their interactions on zooplankton biomass and abundance in a large eutrophic lake. *Hydrobiologia, 848*, 4401–4418. https://doi.org/10.1007/s10750-021-04653-3

Cripps, S. J., & Bergheim, A. (2000). Solids management and removal for intensive land-based aquaculture production systems. *Aquacultural Engineering, 22*, 33-56.

Dauda, A. B., Ajadi, A., Tola-Fabunmi, A. S., & Akinwole, A. O. (2019). Waste production in aquaculture: sources, components and managements in different culture systems. *Aquaculture and Fisheries, 4*(3), 81–88. https://doi.org/10.1016/J.AAF.2018.10.002

David, P. (2019). Manoomin, Version 1.0. *Great Lakes Indian Fish and Wildlife Commission*. https://www.1854treatyauthority.org/images/ManoominChapter.Appendices.2019.final.pdf

Davis, T. W., Koch, F., Marcoval, M. A., Wilhelm, S. W., & Gobler, C. J. (2012). Mesozooplankton and microzooplankton grazing during cyanobacterial blooms in the western basin of Lake Erie. *Harmful Algae, 15*, 26-35. https://doi.org/10.1016/j.hal.2011.11.002

De Schamphelaere, K. A. C., & Janssen, C. R. (2004). Effects of dissolved organic carbon concentration and source, pH, and water hardness on chronic toxicity of copper to Daphnia magna. *Environmental Toxicology and Chemistry*, *23*(5), 1115–1122. https://doi.org/10.1897/02-593

Declerck, S. A. J., Bakker, E. S., van Lith, B., Kersbergen, A., & van Donk, E. (2011). Effects of nutrient additions and macrophyte composition on invertebrate community assembly and diversity in experimental ponds. *Basic and Applied Ecology, 12*, 466–475. https://doi.org/10.1016/j.baae.2011.05.001

Delos, C., & Erickson, R. (1999). *Update of ambient water quality criteria for ammonia*. EPA/822/R-99/014. Final/Technical Report U.S. Environmental Protection Agency, Washington, DC.

Devol, A. H. (1981). Vertical distribution of zooplankton respiration in relation to the intense oxygen minimum zones in two British Columbia fjords. *Journal of Plankton Research, 3*, 593-602.

Diaz, R., & Rosenberg, R. (2008). Spreading dead zones and consequences for marine ecosystems. *Science, 321*, 926-929.

Doubek, J. P., Campbell, K. L., Doubek, K. M., Hamre, K. D., Lofton, M. E., McClure, R. P., Ward, N. K., & Carey, C. C. (2018). The effects of hypolimnetic anoxia on the diel vertical migration of freshwater crustacean zooplankton. *Ecosphere, 9*(7). https://doi.org/10.1002/ECS2.2332

Downing, J. A., Watson, S. B., & McCauley, E. (2011). Predicting Cyanobacteria dominance in lakes. *Canadian Journal of Fisheries and Aquatic Sciences, 58*(10), 1905–1908. https://doi.org/10.1139/F01-143

Dunker, K. J., Sepulveda, A. J., Massengill, R. L., Olsen, J. B., Russ, O. L., Wenburg, J. J. K., & Antonovich, A. (2017). Potential of environmental DNA to evaluate northern pike (*Esox lucius*) eradication efforts: An experimental test and case study. *PLoS One, 11*(9), 1-21. https://doi.org/10.5061/dryad.16m53

Dupuis, A. P., & Hann, B. J. (2009). Warm spring and summer water temperatures in small eutrophic lakes of the Canadian prairies: Potential implications for phytoplankton and

zooplankton. *Journal of Plankton Research*, *31*(5), 489–502. https://doi.org/10.1093/PLANKT/FBP001

Eddy, S., & Hobson, A. (1950). *Taxonomic keys to the common animals of the north central states*. Burgess Publishing Company, Minneapolis, Minnesota, USA.

Elbrecht, V., & Leese, F. (2015). Can DNA-based ecosystem assessments quantify species abundance? Testing primer bias and biomass-sequence relationships with an innovative metabarcoding protocol. *PLoS ONE, 10*(7), e0130324. https://doi.org/10.1371/journal.pone.0130324

Elbrecht, V., & Leese, F. (2017). Validation and development of COI metabarcoding primers for freshwater macroinvertebrate bioassessment. *Frontiers in Environmental Science*, *5*(APR), 237020. https://doi.org/10.3389/FENVS.2017.00011/BIBTEX

Elbrecht, V., Beermann, A. J., Goessler, G., Neumann, J., Tollrian, R., Wagner, R., Wlecklik, A., Piggott, J. J., Matthaei, C. D., & Leese, F. (2016). Multiple-stressor effects on stream invertebrates: a mesocosm experiment manipulating nutrients, fine sediment and flow velocity. *Freshwater Biology, 61*(4), 362–375. https://doi.org/10.1111/FWB.12713

Emerson, K., Russo, R. C., Lund, R. E., & Thurston, R. (1975). Aqueous ammonia equilibrium calculations: effect of pH and temperature. *Journal of the Fisheries Board of Canada, 32*, 2379–2383.

Environment Canada. (1999). *Priority substances list assessment report: Ammonia in the aquatic environment*. https://www.canada.ca/content/dam/hc-sc/migration/hc-sc/ewh-semt/alt_formats/hecs-sesc/pdf/pubs/contaminants/psl2-lsp2/ammonia/ammonia-eng.pdf

Environmental Protection Agency (EPA). (2013). *Aquatic life ambient water quality criteria for ammonia-freshwater*. https://www.epa.gov/sites/default/files/2015-08/documents/aquatic-life-ambient-water-quality-criteria-for-ammonia-freshwater-2013.pdf

Esparcia, A., Miracle, M. R., & Serra, M. (1989). *Brachionus plicatilis* tolerance to low oxygen concentrations. *Hydrobiologia*, *186*(1), 331–337. https://doi.org/10.1007/BF00048929

Evans, N. T., Olds, B. P., Renshaw, M. A., Turner, C. R., Li, Y., Jerde, C. L., Mahon, A. R., Pfrender, M. E., Lamberti, G. A., & Lodge, D. M. (2016). Quantification of mesocosm fish and amphibian species diversity via environmental DNA metabarcoding. *Molecular Ecology Resources, 16*(1), 29–41. https://doi.org/10.1111/1755-0998.12433

Ficetola, G. F., Miaud, C., Pompanon, F., & Taberlet, P. (2008). Species detection using environmental DNA from water samples. *Biology Letters, 4*(4), 423. https://doi.org/10.1098/RSBL.2008.0118

Fitzgerald, A., Halliday, J., Heath, D., Normando, S., & Biasetti, P. (2021). Environmental DNA as novel technology: lessons in agenda setting and framing in news media. *Animals, 11*(10), 2874. https://doi.org/10.3390/ANI11102874

Fleeger, J. W. (2020). How do indirect effects of contaminants inform ecotoxicology? A Review. *Processes, 8*(12), 1659. https://doi.org/10.3390/pr8121659

Food and Agriculture Organization of the United Nations (FAO). (2020). The state of world fisheries and aquaculture. https://www.fao.org/documents/card/en/c/ca9229en/

Forrest, J., & Arnott, S. E. (2006). Immigration and zooplankton community responses to nutrient enrichment: A mesocosm experiment. *Oecologia, 150*(1), 119–131. https://doi.org/10.1007/s00442-006-0490-4

Fulton, R. S., & Paerl, H. W. (1987). Toxic and inhibitory effects of the blue-green alga Microcystis aeruginosa on herbivorous zooplankton. *Journal of Plankton Research, 9*(5), 837–855. https://academic.oup.com/plankt/article/9/5/837/1492657

Gagneten, A. M., & Paggi, J. C. (2009). Effects of heavy metal contamination (Cr, Cu, Pb, Cd) and eutrophication on zooplankton in the lower basin of the Salado River (Argentina). *Water, Air, and Soil Pollution, 198*(1–4), 317–334. https://doi.org/10.1007/S11270-008-9848-Z/FIGURES/6

Gannon, J. E., & Stemberger, R. S. (1978). Zooplankton (especially crustaceans and rotifers) as indicators of water quality. *Transactions of the American Microscopical Society, 97*(1), 16–35.

Gao, C., & Dusa, A. (2024). *ggVennDiagram: A 'ggplot2' implement of Venn Diagram.* R package version 1.5.3, https://github.com/gaospecial/ggVennDiagram

García-Bueno, N., & Marín, A. (2021). Ecological management of biomass and metal bioaccumulation in fish-cage nettings: Influence of antifouling paint and fiber manufacture. *Aquaculture*, *544*, 737142. https://doi.org/10.1016/J.AQUACULTURE.2021.737142

Geller, J., Meyer, C., Parker, M., & Hawk H. (2013). Redesign of PCR primers for mitochondrial cytochrome c oxidase subunit I for marine invertebrates and application in all-taxa biotic

surveys. *Molecular Ecology Resources, 13*(5), 851-861. https://doi.org/10.1111/1755-0998.12138

Ger, K. A., Urrutia-Cordero, P., Frost, P. C., Hansson, L.-A., Sarnelle, O., Wilson, A. E., & Lü Rling, M. (2016). The interaction between cyanobacteria and zooplankton in a more eutrophic world. *Harmful Algae, 54*, 128-144. https://doi.org/10.1016/j.hal.2015.12.005

Gersich, F. M., & Hopkins, D. L. (1986). Site-specific acute and chronic toxicity of ammonia to Daphnia magna straus. *Environmental Toxicology and Chemistry, 5*(5), 443–447. https://doi.org/10.1002/ETC.5620050504

Gibson, J., Shokralla, S., Curry, C., Baird, D., Monk, W., King, I., & Hajibabaei, M. (2015). Large-scale biomonitoring of remote and threatened ecosystems via high-throughput Sequencing. *PLOS ONE, 10*(10), e0138432, 1-15. http://dx.doi.org/10.1371/journal.pone.0138432

Govender, A., Singh, S., Groeneveld, J., Pillay, S., & Willows-Munro, S. (2022). Experimental validation of taxon-specific mini-barcode primers for metabarcoding of zooplankton. *Ecological Applications*, *32*(1), e02469. https://doi.org/10.1002/EAP.2469

Graney, R. L. (1993). Introduction. In R. L. Graney (Eds.), *Aquatic Mesocosm Studies in Ecological Risk Assessment.* (pp. 1-4). CRC Press. https://doi.org/10.1201/9781003070016

Grothe, D. W., & Grothe, D. R. (1977). *An Illustrated Key to the Planktonic Rotifers of the Laurentian Great Lakes*. U.S. Environmental Protection Agency.

Guardiola, F. A., Cuesta, A., Meseguer, J., & Esteban, M. A. (2012). Risks of using antifouling biocides in aquaculture. *International Journal of Molecular Sciences, 13*(2), 1541–1560. https://doi.org/10.3390/IJMS13021541

Gutierrez, M. F., Simões, N. R., Frau, D., Saigo, M., & Licursi, M. (2020). Responses of stream zooplankton diversity metrics to eutrophication and temporal environmental variability in agricultural catchments. *Environmental Monitoring and Assessment, 192*(792), 1–17. https://doi.org/10.1007/s10661-020-08766-5

Han, C., Shimotsu, K., Kim, H.-J., Sakakura, Y., Lee, J.-S., Souissi, S., & Hagiwara, A. (2022). Comparison of ammonia thresholds for survival and reproduction between two copepods: The planktonic calanoid *Eurytemora affinis* and the benthic harpacticoid *Tigriopus japonicus*. *Aquaculture, 560*, 738534. https://doi.org/10.1016/j.aquaculture.2022.738534

Haney, J.F. (2013). "An-Image-based Key to the Zooplankton of North America" version 5.0. University of New Hampshire Center for Freshwater Biology. https://cfb.unh.edu/cfbkey/html/index.html

Hann, B., & Salki, A. (2017). Patterns in the crustacean zooplankton community in Lake Winnipeg, Manitoba: Response to long-term environmental change. *Journal of Great Lakes Research, 43*(1), 80-90. http://dx.doi.org/10.1016/j.jglr.2016.10.015

Hansson, L. A., Gustafsson, S., Rengefors, K., & Bomark, L. (2007). Cyanobacterial chemical warfare affects zooplankton community composition. *Freshwater Biology, 52*(7), 1290–1301. https://doi.org/10.1111/J.1365-2427.2007.01765.X

Hebert, P. D. N., Cywinska, A., Ball, S. L., & Dewaard, J. R. (2003). Biological identifications through DNA Barcodes. *Proceedings of the Royal Society, 270*(1512), 313–321. https://doi.org/10.1098/rspb.2002.2218

Herwig, B. R., & Zimmer, K. D. (2007). Population ecology and prey consumption by fathead minnows in prairie wetlands: importance of detritus and larval fish. *Ecology of Freshwater Fish, 16*(3), 282–294. https://doi.org/10.1111/J.1600-0633.2006.00220.X

Hoang, T. C., Brausch, J. M., Cichra, M. F., Phlips, E. J., Van Genderen, E., & Rand, G. M. (2021). Effects of zinc in an outdoor freshwater microcosm system. *Environmental Toxicology and Chemistry*, *40*(7), 2051–2070. https://doi.org/10.1002/ETC.5050

Huisman, J., Codd, G. A., Paerl, H. W., Ibelings, B. W., H Verspagen, J. M., & Visser, P. M. (2018). Cyanobacterial blooms. *Nature Reviews Microbiology, 16*, 471-483. https://doi.org/10.1038/s41579-018-0040-1

Humeniuk, B. W., Chaves-Barquero, L. G., Wong, C. S., & Hanson, M. L. (2019). Crushed glass as a constructed wetland Substrate: Invertebrate community responses to simulated wastewater inputs. *Proceeding of Manitoba's Undergraduate Science and Engineering Research, 5*(1), 14-27. https://doi.org/10.5203/pmuser.201951817

Iacarella, J. C., Barrow, J. L., Giani, A., Beisner, B. E., & Gregory-Eaves, I. (2018). Shifts in algal dominance in freshwater experimental ponds across differing levels of macrophytes and nutrients. *Ecosphere, 9*(1), e02086. https://doi.org/10.1002/ECS2.2086

Ingersoll, C. G., & Winner, R. W. (1982). Effect on *Daphnia pulex* (de geer) of daily pulse exposures to copper or cadmium. *Environmental Toxicology and Chemistry, 1*(4), 321–327. https://doi.org/10.1002/ETC.5620010407

Ip, Y. K., Chew, S. F., & Randall, D. J. (2003). Ammonia toxicity, tolerance, and excretion. *Fish Physiology, 20,* 109–148.

Iwabuchi, T., & Urabe, J. (2010). Phosphorus acquisition and competitive abilities of two herbivorous zooplankton, *Daphnia pulex* and *Ceriodaphnia quadrangula*. *Ecological Research, 25*(3), 619–627. https://doi.org/10.1007/S11284-010-0692-4/FIGURES/5

Jeppesen, E., Jensen, J. P., Sondergaard, M., Lauridsen, T., & Landkildehus, F. (2000). Trophic structure, species richness and biodiversity in Danish lakes: Changes along a phosphorus gradient. *Freshwater Biology, 45*(2), 201–218. https://doi.org/10.1046/J.1365-2427.2000.00675.X

Jeppesen, E., Søndergaard, M., Sortkjoær, O., Mortensen, E., & Kristensen, P. (1990). Interactions between phytoplankton, zooplankton and fish in a shallow, hypertrophic lake: a study of phytoplankton collapses in Lake Søbygård, Denmark. *Hydrobiologia, 191*(1), 149–164. https://doi.org/10.1007/BF00026049/METRICS

Ji, Y., Ashton, L., Pedley, S. M., Edwards, D. P., Tang, Y., Nakamura, A., Kitching, R., Dolman, P. M., Woodcock, P., Edwards, F. A., Larsen, T. H., Hsu, W. W., Benedick, S., Hamer, K. C., Wilcove, D. S., Bruce, C., Wang, X., Levi, T., Lott, M., … Yu, D. W. (2013). Reliable, verifiable and efficient monitoring of biodiversity via metabarcoding. *Ecology Letters, 16*(10), 1245–1257. https://doi.org/10.1111/ele.12162

Jiang, X., Xie, J., Xu, Y., Zhong, W., Zhu, X., & Zhu, C. (2017). Increasing dominance of small zooplankton with toxic cyanobacteria. *Freshwater Biology, 62*(2), 429–443. https://doi.org/10.1111/FWB.12877

Jo, T. S., & Sasaki, Y. (2024). Evaluating the quantitative performance of environmental DNA metabarcoding for freshwater zooplankton community: a case study in Lake Biwa, Japan. *Environmental Science and Pollution Research, 31*(47), 58069–58082. https://doi.org/10.1007/S11356-024-35025-8/TABLES/4

Jorgenson, K. D., Lee, P. F., & Kanavillil, N. (2013). Ecological relationships of wild rice, *Zizania* spp. 11. electron microscopy study of iron plaques on the roots of northern wild rice (*Zizania palustris*). *Botany, 91*(3), 189–201. https://doi.org/10.1139/CJB-2012-0198/ASSET/IMAGES/LARGE/CJB-2012-0198F9.JPEG

Kaiser, D., & Piotrowski, K. (2023). *Fertilizing wild rice in Minnesota*. University of Minnesota. https://extension.umn.edu/crop-specific-needs/wild-rice-fertilizer-guidelines

Kane, D. D., Gordon, S. I., Munawar, M., Charlton, M. N., & Culver, D. A. (2009). The Planktonic Index of Biotic Integrity (P-IBI): An approach for assessing lake ecosystem health. *Ecological Indicators, 9*, 1234-1247. https://doi.org/10.1016/j.ecolind.2009.03.014

Karpowicz, M., Ejsmont-Karabin, J., Kozłowska, J., Feniova, I., & Dzialowski, A. R. (2020). Zooplankton community responses to oxygen stress. *Water, 12*(3), 706. https://doi.org/10.3390/W12030706

Kelly, P. T., Taylor, J. M., Andersen, I. M., & Scott, J. T. (2024). Zooplankton densities reduced by increases in resource N:P in hypereutrophic mesocosms. *Hydrobiologia*, 1–13. https://doi.org/10.1007/S10750-024-05557-8/FIGURES/4

Kelly, R. P., Port, J. A., Yamahara, K. M., Martone, R. G., Lowell, N., Thomsen, P. F., Mach, M. E., Bennett, M., Prahler, E., Caldwell, M. R., & Crowder, L. B. (2014). Harnessing DNA to improve environmental management: Genetic monitoring can help public agencies implement environmental laws. *New Series, 344*(6191), 1455–1456. https://doi.org/10.1111/ele.l2162

Kornberger, S., Jovanovic, H. M. R., Hanson, M. L., & Humeniuk, B. W. (2023). Wild rice (*Zizania* spp.) as a model macrophyte toxicity test species for ecotoxicological risk assessment. In M. L. Menone, & C. M. Metcalfe (Eds.), *The Ecotoxicology of Aquatic Macrophytes*. Springer. https://doi.org/10.1007/978-3-031-27833-4_5

Lalonde, B. A., Ernst, W., & Garron, C. (2015). Chemical and physical characterisation of effluents from land-based fish farms in Atlantic Canada. *Aquaculture International*, *23*(2), 535–546. https://doi.org/10.1007/S10499-014-9834-Y/TABLES/3

Lampert, W., & Sommer, U. (2007). *Limnoecology: The Ecology of Lakes and Streams.* Oxford University Press.

Lawrence, A., Brown, K., Frampton, G., & van den Brink, P. (2018). Guidance for experimental design and statistical analysis of ecotoxicological community effect studies (field studies). *Report to UK Chemical Regulations Directorate*. 1-93.

Leese, F., Sander, M., Buchner, D., Elbrecht, V., Haase, P., & Zizka, V. M. A. (2021). Improved freshwater macroinvertebrate detection from environmental DNA through minimized nontarget amplification. *Environmental DNA, 3*(1), 261–276. https://doi.org/10.1002/EDN3.177

Legendre, P., & Legendre, L. (2012). Numerical Ecology. 3rd English edition. Elsevier.

Leray, M., Yang, J. Y., Meyer, C. P., Mills, S. C., Agudelo, N., Ranwez, V., Boehm, J. T., & Machida, R. J. (2013). A new versatile primer set targeting a short fragment of the mitochondrial COI region for metabarcoding metazoan diversity: application for characterizing coral reef fish gut contents. *Frontiers in Zoology*, *10*(34), 2-14. https://doi.org/10.1186/1742-9994-10-34

Leung, J., Kumar, M., Glatz, P., & Kind, K. (2010). Impacts of un-ionized ammonia in digested piggery effluent on reproductive performance and longevity of *Daphnia carinata* and *Moina australiensis*. *Aquaculture, 310*, 401-406. https://doi.org/10.1016/j.aquaculture.2010.11.015

Lewis, W. M., & Wurtsbaugh, W. A. (2008). Control of lacustrine phytoplankton by nutrients: Erosion of the phosphorus paradigm. *International Review of Hydrobiology, 93*, 446-465. https://doi.org/10.1002/iroh.200811065

Liang, Y., Shao, L., Jiang, Q., & Yang, J. (2020). Changes in the life-cycle parameters and glutathione-related antioxidant defense system of rotifer *Brachionus calyciflorus* under the combined stress of microcystin-LR and ammonia. *Aquatic Ecology, 54*(1), 243–256. https://doi.org/10.1007/S10452-019-09739-8/FIGURES/4

Lindeque, P. K., Parry, H. E., Harmer, R. A., Somerfield, P. J., & Atkinson, A. (2013). Next generation sequencing reveals the hidden diversity of zooplankton assemblages. *PLoS One, 8*(11), e81327. https://doi.org/10.1371/journal.pone.0081327

Liu, Q., Zhang, L., Yang, Y., Zou, J., Yang, Y., Ge, J., Yan, H., He., Yang, C., Tahir, R., Zhao, L., & Yang, S. (2024). Ecological performance of an integrated ex-situ rice-fish co-culture system. *Aquaculture, 582*, 740511. https://doi.org/10.1016/j.aquaculture.2023.740511

Loadman, N. L. (1980). *A comparison of the crustacean zooplankton populations of four man-made lakes in southern Manitoba [Master's thesis]*. University of Manitoba. https://mspace.lib.umanitoba.ca/items/de4510ce-e034-409f-984a-123514a814c7

Lobson C., Luong, K., Seburn, D., White, M., Hann, B., Prosser, R., Wong, C., & Hanson, M. (2018). Fate of thiamethoxam in the mesocosms and response of the zooplankton community. *Science of the Total Environment, 637*, 1150-1157. https://doi.org/10.1016/j.scitotenv.2018.05.087

López-Archilla, A. I., Moreira, D., López-García, P., & Guerrero, C. (2004). Phytoplankton diversity and cyanobacterial dominance in a hypereutrophic shallow lake with biologically produced alkaline pH. *Extremophiles, 8*(2), 109–115. https://doi.org/10.1007/S00792-003-0369-9/FIGURES/2

Lyu, K., Cao, H., Wang, Q., Chen, R., Minter, E. J. A., & Yang, Z. (2013). Differences in long-term impacts of un-ionized ammonia on life-history traits of three species of *Daphnia*. *International Review of Hydrobiology, 98*(5), 253–261. https://doi.org/10.1002/IROH.201301574

Marquina, D., Andersson, A. F., & Ronquist, F. (2019). New mitochondrial primers for metabarcoding of insects, designed and evaluated using in silico methods. *Molecular Ecology Resources, 19*(1), 90-104. https://doi.org/10.1111/1755-0998.12942

Martin, M. (2011). Cutadapt removes adapter sequences from high-throughput sequencing reads. *EMBnet.journal, 17*(1), 1-10. https://doi.org/10.14806/ej.17.1.200

Martinez Arbizu, P. (2020). *pairwiseAdonis: Pairwise multilevel comparison using adonis.* R package version 0.4, https://github.com/pmartinezarbizu/pairwiseAdonis

Martins, S. E., Fillmann, G., Lillicrap, A., & Thomas, K. V. (2018). Review: ecotoxicity of organic and organo-metallic antifouling co-biocides and implications for environmental hazard and risk assessments in aquatic ecosystems. *Biofouling*, *34*(1), 34–52. https://doi.org/10.1080/08927014.2017.1404036

Matsuzaki, S. ichiro S., Suzuki, K., Kadoya, T., Nakagawa, M., & Takamura, N. (2018). Bottom-up linkages between primary production, zooplankton, and fish in a shallow, hypereutrophic lake. *Ecology, 99*(9), 2025–2036. https://doi.org/10.1002/ECY.2414

Matthews, S. A., Goetze, E., Ohman, M. D., Matthews, S. A., Goetze, E., & Recommendations, O. (2021). Recommendations for interpreting zooplankton metabarcoding and integrating molecular methods with morphological analyses. *ICES Journal of Marine Science, 78*(9), 3387–3396. https://doi.org/10.1093/ICESJMS/FSAB107

McMurdie, P., & Holmes, S. (2014). Waste not, want not: why rarefying microbiome data is inadmissible. *PLoS Computational Biology, 10*(4), e1003531. https://doi.org/10.1371/JOURNAL.PCBI.1003531

Meredith, C., Hoffman, J., Trebitz, A., Pilgrim, E., Okum, S., Martinson, J., & Cameron, E. S. (2021). Evaluating the performance of DNA metabarcoding for assessment of zooplankton communities in Western Lake Superior using multiple markers. *Metabarcoding and Metagenomics, 5,* 83-97. https://doi.org/10.3897/MBMG.5.64735

Meyer, J. S., Clearwater, S. J., Doser, T. A., Rogaczewski, M. J., & Hansen, J. A. (2007). *Effects of water chemistry on bioavailability and toxicity of waterborne cadmium, copper, nickel, lead, and zinc to freshwater organisms*. Society of Environmental Toxicology and Chemistry (SETAC), Pensacola, FL.

Minnesota Department of Natural Resources (MNDNR). (2008). *Natural Wild Rice in Minnesota*. https://files.dnr.state.mn.us/fish_wildlife/wildlife/wildrice/natural-wild-rice-in-minnesota.pdf

Mitchell, S. A. (1992). The effect of pH on *Brachionus calyciflorus* Pallas (Rotifera). *Hydrobiologia, 245*(2), 87–93. https://doi.org/10.1007/BF00764768/METRICS

Moody, E. K., & Wilkinson, G. M. (2019). Functional shifts in lake zooplankton communities with hypereutrophication. *Freshwater Biology*, *64*(3), 608–616. https://doi.org/10.1111/FWB.13246

Moss, B. (1973). The influence of environmental factors on the distribution of freshwater algae: An experimental study: II. The role of pH and the carbon dioxide-bicarbonate system. *The Journal of Ecology, 61*(1), 157. https://doi.org/10.2307/2258925

Munro, K. A., Samis, S. C., & Nassichuk, M. D. (1985). The effects of hatchery effluents on water chemistry, periphyton and benthic invertebrates of selected British Columbia streams. *Canadian Manuscript Report of Fisheries and Aquatic Sciences, No. 1830*.

Murkin, H., Abbott, P., & Kadlec, J. (1983). A comparison of activity traps and sweep nets for sampling nektonic invertebrates in wetlands. *Freshwater Invertebrate Biology, 2*, 99–106. https://doi-org.uml.idm.oclc.org/10.2307/1467114

Mychek-Londer, J. G., Balasingham, K. D., & Heath, D. D. (2020). Using environmental DNA metabarcoding to map invasive and native invertebrates in two Great Lakes tributaries. *Environmental DNA, 2*(3), 283–297. https://doi.org/10.1002/EDN3.56

Naylor, S. J., Moccia, R. D., & Durant, G. M. (1999). The chemical composition of settleable solid fish waste (manure) from commercial rainbow trout farms in Ontario, Canada. *North American Journal of Aquaculture*, *61*, 21–26. https://doi.org/10.1577/1548-8454

Nolan, S., Bollens, S. M., & Rollwagen-Bollens, G. (2019). Diverse taxa of zooplankton inhabit hypoxic waters during both day and night in a temperate eutrophic lake. *Journal of Plankton Research, 4*, 431–447. https://doi.org/10.1093/plankt/fbz021

O'Brien, W. J., & de Noyelles, F. (1974). Relationship between nutrient concentration, phytoplankton density, and zooplankton density in nutrient enriched experimental ponds. *Hydrobiologia, 44*(1), 105–125. https://doi.org/10.1007/BF00036159/METRICS

Oelke, E. A., Grava, J., Noetzel, D., Barron, D., Percich, J., Schertz, C., Strait, J., & Stucker, R. (1982). *Wild rice production in Minnesota* [Extension Bulletin No. 464]. University of Minnesota. https://hdl.handle.net/11299/169068

Oksanen, J., Simpson, G., Blanchet, F., Kindt, R., Legendre, P., Minchin, P., O'Hara, R., Solymos, P., Stevens, M., Szoecs, E., Wagner, H., Barbour, M., Bedward, M., Bolker, B., Borcard, D., Carvalho, G., Chirico, M., De Caceres, M., Durand, S., …Weedon, J. (2022). vegan: Community Ecology Package. R package version 2.6-4, https://CRAN.R-project.org/package=vegan

Örstan, A. 2021. *An introduction to bdelloid rotifers and their study.* http://www.quekett.org/starting/microscopic-life/bdelloid-rotifers/

Pace, M. L., Cole, J. J., & Carpenter, S. R. (1998). Trophic cascades and compensation: Differential responses of microzooplankton in whole-lake experiments. *Ecology, 79*(1), 138–152. https://doi.org/10.1890/0012-9658(1998)079

Paerl, H. W., & Otten, T. G. (2013). Harmful cyanobacterial blooms: Causes, consequences, and controls. *Microbial Ecology, 65*(4), 995–1010. https://doi.org/10.1007/S00248-012-0159-Y/FIGURES/6

Park, J. C., Han, J., Lee, M. C., Seo, J. S., & Lee, J. S. (2017). Effects of triclosan (TCS) on fecundity, the antioxidant system, and oxidative stress-mediated gene expression in the copepod *Tigriopus japonicas*. *Aquatic Toxicology, 189*, 16–24.

Patalas, K., & Salki, A. (1973). Crustacean plankton and the eutrophication of lakes in the Okanagan valley, British Columbia. *Journal of the Fisheries Board of Canada, 30*, 519-542.

Paterson, M. J., Podemski, C. L., Findlay, W. J., Findlay, D. L., & Salki, A. G. (2010). The response of zooplankton in a whole-lake experiment on the effects of a cage aquaculture

operation for rainbow trout (*Oncorhynchus mykiss*). *Canadian Journal of Fisheries and Aquatic Sciences, 67*(11), 1852–1861. https://doi.org/10.1139/F10-106/SUPPL_FILE/F10-106SUPPL.PDF

Pettigrew, C., Hann, B., & Goldsborough, L. (1997). Water feces as a source of nutrients to a prairie wetland: Responses of microinvertebrates to experimental additions. *Hydrobiologia, 362*, 55-66. http://dx.doi.org/10.1023/A:1003167219199/METRICS

Piedrahita, R. H. (2003). Reducing the potential environmental impact of tank aquaculture effluents through intensification and recirculation. *Aquaculture, 226*, 35–44. https://doi.org/10.1016/S0044-8486(03)00465-4

Pilon-Smits, E. (2005). Phytoremediation. *Annual Review of Plant Biology, 56*, 15–39. https://doi.org/10.1146/ANNUREV.ARPLANT.56.032604.144214

Pinol, J., Mir, G., Gomez-Polo, P., & Agusti, N. (2014). Universal and blocking primer mismatches limit the use of high-throughput DNA sequencing for the quantitative metabarcoding of arthropods. *Molecular Ecology Resources, 15*, 1-12. https://doi.org/10.1111/1755-0998.12355

Piñol, J., Senar, M. A., & Symondson, W. O. C. (2019). The choice of universal primers and the characteristics of the species mixture determine when DNA metabarcoding can be quantitative. *Molecular Ecology, 28*(2), 407–419. https://doi.org/10.1111/MEC.14776

Podemski, C. L., & Blanchfield, P. J. (2006). Overview of the Environmental Impacts of Canadian Freshwater Aquaculture. *Fisheries and Oceans Canada, Canadian Technical*

Report of Fisheries and Aquatic Sciences 2450. https://waves-vagues.dfo-mpo.gc.ca/library-bibliotheque/326550.pdf

Porter, R. (2019). Wild rice (*Zizania L.*) in North America: Genetic resources, conservation, and use. In S.L. Green et al. (Eds.), *North American Crop Wild Relatives: Important Species, Volume 2*. (pp. 83–97). Springer Nature Switzerland. https://doi.org/10.1007/978-3-319-97121-6_3/FIGURES/6

Prosnier, L., Loreau, M., & Hulot, F. D. (2015). Modeling the direct and indirect effects of copper on phytoplankton-zooplankton interactions. *Aquatic Toxicology, 162*, 73–81. https://doi.org/10.1016/j.aquatox.2015.03.003

R Core Team (2023). *R: A language and environment for statistical computing*. R Foundation for Statistical Computing, Vienna, Austria. URL https://www.R-project.org/.

Rishan, S. T., Kline, R. J., & Rahman, M. S. (2023). Applications of environmental DNA (eDNA) to detect subterranean and aquatic invasive species: A critical review on the challenges and limitations of eDNA metabarcoding. *Environmental Advances, 12*, 100370. https://doi.org/10.1016/J.ENVADV.2023.100370

Robertson, K. (2024). *Assessing nutrient toxicity in fathead minnows using a multi-omics approach* [Master's Thesis, University of Manitoba]. MSpace. https://mspace.lib.umanitoba.ca/items/c12b25a7-a252-4276-a129-e9916f7f27e4

Rosenzweig, C., Elliott, J., Deryng, D., Ruane, A. C., Müller, C., Arneth, A., Boote, K. J., Folberth, C., Glotter, M., Khabarov, N., Neumann, K., Piontek, F., Pugh, T. A. M., Schmid, E., Stehfest, E., Yang, H., & Jones, J. W. (2014). Assessing agricultural risks of

climate change in the 21st century in a global gridded crop model intercomparison. *Proceedings of the National Academy of Sciences of the United States of America, 111*(9), 3268–3273. https://doi.org/10.1073/PNAS.1222463110/-/DCSUPPLEMENTAL

RStudio Team (2023). *RStudio: Integrated Development Environment for R*. RStudio, PBC, Boston, MA URL https://posit.co/.

Ruppert, K. M., Kline, R. J., Rahman, M. S. (2019). Past, present, and future perspectives of environmental DNA (eDNA) metabarcoding: A systematic review in methods, monitoring, and applications of global eDNA. *Global Ecology and Conservation, 17,* e00547. https://doi.org/10.1016/J.GECCO.2019.E00547

Rusak, J. A., Yan, N. D., Somers, K. M., Cottingham, K. L., Micheli, F., Carpenter, S. R., Frost, T. M., Paterson, M. J., & McQueen, D. J. (2002). Temporal, spatial, and taxonomic patterns of crustacean zooplankton variability in unmanipulated north-temperate lakes. *Limnology and Oceanography, 47*(3), 613–625. https://doi.org/10.4319/LO.2002.47.3.0613

Sato, H., Sogo, Y., Doi, H., & Yamanaka, H. (2017). Usefulness and limitations of sample pooling for environmental DNA metabarcoding of freshwater fish communities. *Scientific Reports, 7*(1), 1–12. https://doi.org/10.1038/s41598-017-14978-6

Schindler, D. W., Hecky, R. E., Findlay, D. L., Stainton, M. P., Parker, B. R., Paterson, M. J., Beaty, K. G., Lyng, M., & Kasian, S. E. M. (2008). Eutrophication of lakes cannot be controlled by reducing nitrogen input: Results of a 37-year whole-ecosystem experiment. *Proceedings of the National Academy of Sciences, 105*(32), 11254–11258. https://doi.org/10.1073/PNAS.0805108105

Semlitsch, R. D., & Boone, M. D. (2009). Aquatic Mesocosms. In Dodd, K. C. (Eds.), *Amphibian Ecology and Conservation*. (pp. 87-104). OUP Oxford.

Sepulveda, A., Hutchins, P. R., Forstchen, M., Mckeefry, M. N, & Swigris, A. M. (2020). The elephant in the lab (and field): Contamination in aquatic environmental DNA studies. *Frontiers in Ecology and Evolution, 8*, 609973. https://doi.org/10.3389/fevo.2020.609973

Seymour, M., Edwards, F. K., Cosby, B. J., Bista, I., Scarlett, P. M., Brailsford, F. L., Glanville, H. C., de Bruyn, M., Carvalho, G. R., & Creer, S. (2021). Environmental DNA provides higher resolution assessment of riverine biodiversity and ecosystem function via spatio-temporal nestedness and turnover partitioning. *Communications Biology, 4*(1), 1–12. https://doi.org/10.1038/s42003-021-02031-2

Shurin, J. B., Winder, M., Adrian, R., Keller, W. B., Matthews, B., Paterson, A. M., Paterson, M. J., Pinel-Alloul, B., Rusak, J. A., & Yan, N. D. (2010). Environmental stability and lake zooplankton diversity – contrasting effects of chemical and thermal variability. *Ecology Letters, 13*(4), 453–463. https://doi.org/10.1111/J.1461-0248.2009.01438.X

Sibley, P., Harris, M., Bestari, K., Steele, T., Robinson, R., Gensember, R., Day, K., & Solomon, K. (2001). Response of zooplankton communities to liquid creosote in freshwater microcosms. *Environmental Toxicology and Chemistry, 20*, 394–405. https://doi-org.uml.idm.oclc.org/10.1002/etc.5620200222

Sims, L., Pastor, J., Lee, T., & Dewey, B. (2012). Nitrogen, phosphorus and light effects on growth and allocation of biomass and nutrients in wild rice. *Oecologia, 170*(1), 65–76. https://doi.org/10.1007/S00442-012-2296-X/FIGURES/7

Smith, V. H., & Schindler, D. W. (2009). Eutrophication science: where do we go from here? *Trends in Ecology and Evolution, 24*(4), 201–207. https://doi.org/10.1016/j.tree.2008.11.009

Song, J., & Liang, D. (2023). Community structure of zooplankton and its response to aquatic environmental changes based on eDNA metabarcoding. *Journal of Hydrology, 622*, 129692. https://doi.org/10.1016/J.JHYDROL.2023.129692

Šorf, M., Davidson, T. A., Brucet, S., Menezes, R. F., Søndergaard, M., Lauridsen, T. L., Landkildehus, F., Liboriussen, L., & Jeppesen, E. (2015). Zooplankton response to climate warming: a mesocosm experiment at contrasting temperatures and nutrient levels. *Hydrobiologia, 742*(1), 185–203. https://doi.org/10.1007/S10750-014-1985-3/TABLES/2

Spencer, C. & King, D. (1987). Regulation of blue-green algal buoyancy and bloom formation by light, inorganic nitrogen, carbon dioxide and trophic level interactions. *Hydrobiologia, 144*, 183-192.

Stainton, M. P., Capel, M. J., Armstrong, F. A. (1977). The chemical analysis of fresh water. https://mspace.lib.umanitoba.ca/handle/1993/33786

Stamou, G., Katsiapi, M., Moustaka-Gouni, M., & Michaloudi, E. (2021). The neglected zooplankton communities as indicators of ecological water quality in Mediterranean Lakes. *Limnetica, 40*(2), 359-373. https://doi.org/10.23818/limn.40.24

Stanley, M., Palace, V., Grosshans, R., & Levin, D. B. (2022). Floating treatment wetlands for the bioremediation of oil spills: A review. *Journal of Environmental Management, 317*, 115416. https://doi.org/10.1016/J.JENVMAN.2022.115416

Statistics Canada (2023). Aquaculture, production and value. Table 32-10-0107-01. https://doi.org/10.25318/3210010701-eng

Sternberger, R. S., & Lazorchak, J. M. (1994). Zooplankton assemblage responses to disturbance gradients. *Canadian Journal of Fisheries and Aquatic Sciences, 51*(11), 2435–2447. https://doi.org/10.1139/F94-243

Sternberger, R. S., & Lazorchak, J. M. (1994). Zooplankton Assemblage Responses to Disturbance Gradients. *Canadian Journal of Fisheries and Aquatic Sciences, 51*(11), 2435–2447. https://doi.org/10.1139/F94-243

Stewart, K. A. (2019). Understanding the effects of biotic and abiotic factors on sources of aquatic environmental DNA. *Biodiversity and Conservation, 28*(5), 983-1001. https://doi.org/10.1007/s10531-019-01709-8

Stojanovic, K., Zivic, M., Dublic, Z., Markovic, Z., Krizmanic, J., Milosevic, D., Miljanovic, B., Jovanovic, J., Vidakovic, D., & Zivic, I. (2017). Comparative study of the effects of a small-scale trout farm on the macrozoobenthos, potamoplankton, and epilithic diatom communities. *Environmental Monitoring and Assessment, 189*, 403. https://doi.org/10.1007/S10661-017-6114-0

Su, H., Feng, Y., Chen, J., Chen, J., Ma, S., Fang, J., & Xie, P. (2021). Determinants of trophic cascade strength in freshwater ecosystems. *Ecology, 102*(7), 1–12. https://doi.org/10.2307/27070618

Surendiran, G., Alsaif, M., Kapourchali, F. R., & Moghadasian, M. H. (2014). Nutritional constituents and health benefits of wild rice (*Zizania* spp.). *Nutrition Reviews, 72*(4), 227–236. https://doi.org/10.1111/NURE.12101

Szocs, E., Van den Brink, P., Lagadic, L., Caquet, T., Roucaute, M., Auber, A., Bayona, Y., Liess, M., Ebke, P., Ippolito, A., ter Braak C., Brock, T., & Schafer, R. (2015). Analysing chemical-induced changes in macroinvertebrate communities in aquatic mesocosm experiments: a comparison of methods. *Ecotoxicology, 24*, 760-769. https://doi.org/10.1007/s10646-015-1421-0

Taberlet, P., Coissac, E., Hajibabaei, M., & Rieseberg, L. H. (2012b). Environmental DNA. *Molecular Ecology, 21*(8), 1789–1793. https://doi.org/10.1111/J.1365-294X.2012.05542.X

Taberlet, P., Coissac, E., Pompanon, F., Brochmann, C., & Willerslev, E. (2012a). Towards next-generation biodiversity assessment using DNA metabarcoding. *Molecular Ecology, 21*, 2045–2050. https://doi.org/10.1111/j.1365-294X.2012.05470.x

Taipale, S. J., Vuorio, K., Aalto, S. L., Peltomaa, E., & Tiirola, M. (2019). Eutrophication reduces the nutritional value of phytoplankton in boreal lakes. *Environmental Research*, *179*, 108836. https://doi.org/10.1016/J.ENVRES.2019.108836

Thurston, R. V., Russo, R. C., & Vinogradov, G. A. (1981). Ammonia toxicity to fishes. Effect of pH on the toxicity of the un-ionized ammonia species. *Environmental Science and Technology, 15*(7), 837–840. https://doi.org/10.1021/ES00089A012/ASSET/ES00089A012.FP.PNG_V03

Toth, F., Zsuga, K., Kerepeczki, E., Berzi-Nagy, L., Kormoczi, L., & Lovei, G. (2020). Seasonal differences in taxonomic diversity of rotifer communities in a Hungarian lowland oxbow lake exposed to aquaculture effluent. *Water, 12*, 1300. https://doi.org/10.3390/w12051300

Trépanier-Leroux, D., Yates, M. C., Astorg, L., Fraser, D. J., Humphries, S., Cristescu, M. E., & Derry, A. M. (2023). Density-dependent effects of exotic brook trout on aquatic communities in mountain lakes revealed by environmental DNA and morphological taxonomy. Hydrobiologia, 851, 1489-1512. https://doi.org/10.1007/s10750-023-05398-x

University of Windsor. (2022). *GEN-FISH eDNA sampling protocol – water sampling on-site using "DIY" peristaltic pump system*. https://gen-fish.ca/wp-content/uploads/2022/06/DIY-Peristaltic-Pump_Protocol-and-Checklist_30JUNE2022.pdf

Untersteiner, H., Kahapka, J., & Kaiser, H. (2003). Behavioural response of the cladoceran *Daphnia magna* straus to sublethal copper stress-validation by image analysis. *Aquatic Toxicology, 65*, 435–442. https://doi.org/10.1016/S0166-445X(03)00157-7

USEPA. (2016). *Standard operating procedure for zooplankton analysis*. https://www.epa.gov/sites/default/files/2017-01/documents/sop-for-zooplankton-analysis-201607-22pp.pdf

Valentini, A., Taberlet, P., Miaud, C., Civade, R., Herder, J., Thomsen, P. F., Bellemain, E., Besnard, A., Coissac, E., Boyer, F., Gaboriaud, C., Jean, P., Poulet, N., Roset, N., Copp, G. H., Geniez, P., Pont, D., Argillier, C., Baudoin, J. M., … Dejean, T. (2016). Next-generation monitoring of aquatic biodiversity using environmental DNA metabarcoding. *Molecular Ecology, 25*(4), 929–942. https://doi.org/10.1111/MEC.13428

van den Brink, P. J., & ter Braak, C. J. F. (1999). Principal response curves: analysis of time-dependent multivariate responses of biological community to stress. *Environmental Toxicology and Chemistry*, 18(2), 138–148. https://doi.org/10.1002/etc.5620180207

Vanderploeg, H. A., Ludsin, S. A., Cavaletto, J. F., Höök, T. O., Pothoven, S. A., Brandt, S. B., Liebig, J. R., & Lang, G. A. (2009). Hypoxic zones as habitat for zooplankton in Lake Erie: Refuges from predation or exclusion zones*? Journal of Experimental Marine Biology and Ecology, 381*, S108–S120. https://doi.org/10.1016/j.jembe.2009.07.015

Vanderpont, A., Lobson, C., Lu, Z., Luong, K., Arentsen, M., Vera, T., Moore, D., White, M. S., Prosser, R. S., Wong, C. S., & Hanson, M. L. (2022). Fate of thiamethoxam from treated seeds in mesocosms and response of aquatic invertebrates. *Ecotoxicology, 31*, 341-356. https://doi.org/10.1007/s10646-021-02500-8

Varpe, Ø., Jørgensen, C., Tarling, G. A., & Fiksen, Ø. (2007). Early is better: seasonal egg fitness and timing of reproduction in a zooplankton life-history model. *Oikos*, *116*(8), 1331–1342. https://doi.org/10.1111/J.0030-1299.2007.15893.X

Verspagen, J. M. H., van de Waal, D. B., Finke, J. F., Visser, P. M., & van Donk, E. (2014). Rising CO2 levels will intensify phytoplankton blooms in eutrophic and hypertrophic lakes. *PLoS ONE, 9*(8), 104325. https://doi.org/10.1371/journal.pone.0104325

Vinebrooke, R. D., Turner, M. A., Kidd, K. A., Hann, B. J., & Schindler, D. W. (2001). Truncated foodweb effects of omnivorous minnows in a recovering acidified lake. *Journal of the North American Benthological Society, 20*(4), 629–642. https://doi.org/10.2307/1468093/ASSET/IMAGES/LARGE/I0887-3593-20-4-629-F06.JPEG

Weider, L. J., & Lampert, W. (1985) Differential response of *Daphnia* genotypes to oxygen stress: respiration rates, hemoglobin content and low-oxygen tolerance. *Oecologia, 65*, 487–491.

Wetzel, R. G. (2001). *Limnology: lake and river ecosystems (3rd ed.).* San Diego Academic Press.

Wickham, H. (2016). *ggplot2: Elegant Graphics for Data Analysis.* R package version 3.5.1, https://ggplot2.tidyverse.org

Wickham, H., Averick, M., Bryan, J., Chang, W., McGowan, L. D., Francois, R., Grolemund, G., Hayes, A., Hester, J., Kuhn, M., Pedersen, T. L., Miller, E., Bache, S. M., Müller, K., Ooms, J., Robinson, D., Seidel, D. P., Spinu, V., Takahashi, K., …Yutani, H. (2019). Welcome to the tidyverse. *Journal of Open Source Software, 4*(43), 1686. https://doi.org/10.21105/joss.01686

Wilson, A. E., Sarnelle, O., Tillmanns, A. R., Brett, M., Carmichael, W., Fastner, J., Fulton, R., Gilbert, J., Gons, H., Krawietz, H., Nandini, S., Paerl, H., Repka, S., Vijverberg, K., Walz, N., Weithoff, G., Hall, S., Jumars, P., Parker, J., … Vanderploeg, H. (2006). Effects of cyanobacterial toxicity and morphology on the population growth of freshwater zooplankton: Meta-analyses of laboratory experiments. *Limnology and Oceanography, 51*(4), 1915–1924. https://doi.org/10.4319/LO.2006.51.4.1915

Wu, Y., Colborne, S. F., Charron, M. R., & Heath, D. D. (2022). Development and validation of targeted environmental DNA (eDNA) metabarcoding for early detection of 69 invasive fishes and aquatic invertebrates. *Environmental DNA*, 1-12. https://doi.org/10.1002/EDN3.359

Xu, D., Xu, J., He, Y., & Huang, P.M. (2009). Effect of iron plaque formation on phosphorus accumulation and availability in the rhizosphere of wetland plants. *Water, Air, & Soil Pollution, 200*(1–4), 79–87.

Yang, J., & Zhang, X. (2020). eDNA metabarcoding in zooplankton improves the ecological status assessment of aquatic ecosystems. *Environment International, 134*, 105230. https://doi.org/10.1016/J.ENVINT.2019.105230

Yang, J., Zhang, X., Xie, Y., Song, C., Sun, J., Zhang, Y., Giesy, J. P., & Yu, H. (2017). Ecogenomics of zooplankton community reveals ecological threshold of ammonia nitrogen. *Environmental Science & Technology, 51*, 3057-3064. https://doi.org/10.1021/acs.est.6b05606

Yoshida, T., Urabe, J., & Elser, J. J. (2003). Assessment of "top-down" and "bottom-up" forces as determinants of rotifer distribution among lakes in Ontario, Canada. *Ecological Research, 18*(6), 639–650. https://doi.org/10.1111/J.1440-1703.2003.00596.X/METRICS

Zhang, G. K., Chain, F. J. J., Abbott, C. L., & Cristescu, M. E. (2018). Metabarcoding using multiplexed markers increases species detection in complex zooplankton communities. *Evolutionary Applications*, *11*(10), 1901–1914. https://doi.org/10.1111/EVA.12694

Zhang, X. (2019). Environmental DNA shaping a new era of ecotoxicological research. *Environmental Science and Technology, 53*(10), 5605–5612. https://doi.org/10.1021/ACS.EST.8B06631/ASSET/IMAGES/LARGE/ES-2018-066318_0001.JPEG

Zhao, L., Zhang, X., Xu, M., Mao, Y., & Huang, Y. (2021). DNA metabarcoding of zooplankton communities: species diversity and seasonal variation revealed by 18S rRNA and COI. *PeerJ Computer Science, 9*, e11057–e11057. https://doi.org/10.7717/PEERJ.11057/

Zhu, K., Zhang, H., Zhang, P., Wang, P., Li, H., Feng, M., Wang, H., Wang, H., Zhang, M., & Xu, J. (2023). Interactive effects of warming and eutrophication on zooplankton could reverse the stoichiometric mismatch with phytoplankton. *Water Biology and Security*, *2*(4), 100205. https://doi.org/10.1016/J.WATBS.2023.100205

Zong, W., Wang, Q., Zhang, S., Teng, Y., & Du, Y. (2018), Regulation on the toxicity of microcystin-LR target to protein phosphatase 1 by biotransformation pathway: effectiveness and mechanism. *Environmental Science and Pollution Research, 25*, 26020–26029.

Appendix A: Methodology Supplemental Tables

Appendix Table A-1: Zooplankton species targeted from the designed primers. The COI region sequences were extracted from the NCBI database for each species. Only Rotifer 1, Rotifer 2, Daphnia, and Copepod primers were used for the sequencing of all samples.

Primer Name	Phylum	Class	Subclass	Order	Family	Genus	Species
Cladoceran	Arthropoda	Crustacea	Brachiopoda	Cladocera	Daphnidae	Ceriodaphnia	*Ceriodaphnia dubia*
							Ceriodaphnia pulchella
							Ceriodaphnia quadrangula
							Ceriodaphnia reticulata
						Scapholeberis	*Scapholeberis sp.*
						Daphnia	*Daphnia pulicaria*
							Daphnia pulex
							Daphnia magna
							Daphnia middendorffiana
							Daphnia schodleri
					Sididae	Diaphanosoma	*Diaphanosoma brachyurum*
							Diaphanosoma birgei
					Chydoridae	Chydorus	*Chydorus brevilabris*
							Chydorus sphaericus
						Leydigia	*Leydigia acanthocercoides*
						Pleuroxus	*Pleuroxus sp.*
Copepod	Arthropoda	Crustacea	Copepoda	Calanoida	Diaptomidae	Leptodiaptomus	*Leptodiaptomus ashlandi*
							Leptodiaptomus minutus
							Leptodiaptomus sicillis
						Skistodiaptomus	*Skistodiaptomus oregonesis*
							Skistodiaptomus pallidus
							Skistodiaptomus reighardi
				Cyclopodia	Cyclopidae	Macrocyclops	*Macrocyclops albidus*
							Macrocyclops fuscus
						Mesocyclops	*Mesocyclops edax*
						Acanthocyclops	*Acanthocyclops robustus*
							Acanthocyclops vernalis
						Eucyclops	*Eucyclops prionophorus*
						Tropocyclops	*Tropocyclops prasinus*
							Tropocycops prasinus mexicanus

						Microcyclops	*Microcyclops rubellus* *Microcyclops varicans*
Rotifer 1	Rotifera	Monogononta		Flosculariacea	Testudinellidae	Pompholyx	*Pompholyx sulcate*
				Collothecacecae	Collothecidae	Collotheca	*Collotheca sp.*
				Plolma	Gastropidae	Gastropus	*Gastropus stylifer*
					Brachionidae	Anuraeopsis	*Anuraeopsis sp.*
						Brachionus	*Brachionus calyciflorus*
						Euchlanis	*Euchlanis dilatata*
						Keratella	*Keratella hiemalis*
						Platyias	*Platyias quadricornis*
					Lecanidae	Lecane	*Lecane sp.*
					Synchaetidae	Synchaeta	*Synchaeta pectinate* *Synchaeta sp.*
Rotifer 2	Rotifera	Mongononta		Plolma	Gastropidae	Ascomorpha	*Ascomorpha ovalis*
					Brachionidae	Brachionus	*Brachionus sp.* *Brachionus plicatilis*
						Euchlanis	*Euchlanis dilatata*
						Keratella	*Keratella crassa* *Keratella cochlearis* *Keratella quadrata*
						Notholca	*Notholca acuminata*
					Lecanidae	Lecane	*Lecane sp.*
					Synchaetidae	Synchaeta	*Synchaeta sp.* *Synchaeta lakowitziana*
						Polyarthra	*Polyarthra sp.* *Polyarthra vulgaris*
					Asplanchnidae	Asplanchna	*Asplanchna priodonta*
					Trichocercidae	Trichocerca	*Trichocera multicrinis*
Daphnia	Arthropoda	Crustacea	Brachiopoda	Cladocera	Daphnidae	Daphnia	*Daphnia pulicaria* *Daphnia pulex* *Daphnia magna* *Daphnia middendorffiana* *Daphnia schodleri*
Diaphanosoma	Arthropoda	Crustacea	Brachiopoda	Cladocera	Sididae	Diaphanosoma	*Diaphanosoma brachyurum* *Diaphanosoma birgei*
Ostracod	Arthropoda	Ostracoda	NI	NI	NI	NI	*Ostracoda sp.*
			Podocopa	Podocopida	NI	NI	*Podocopida sp.*
			Podocopa	Podocopida	Cypridoidea	Cypria	*Cypria sp.*

Note: NI = Not identified

Appendix Table A-2: First round PCR conditions for each primer and primer optimization round. All volumes are in µg/L. Primer optimizations were conducted on the combined DNA sample.

Primer name	Primer optimization round	date of optimization	diH20	10x	MgCl2	BSA	dNTP	F	R	Taq	DNA	Total Volume
Copepod	1	01-23-2024	16.4	2.5	2.5	0	0.5	0.5	0.5	0.1	2	25
Cladoceran	1	01-23-2024	16.4	2.5	2.5	0	0.5	0.5	0.5	0.1	2	25
Cladoceran	1	01-23-2024	16.4	2.5	2.5	0	0.5	0.5	0.5	0.1	2	25
Cladoceran	1	01-23-2024	16.4	2.5	2.5	0	0.5	0.5	0.5	0.1	2	25
Rotifer 1	1	01-23-2024	16.4	2.5	2.5	0	0.5	0.5	0.5	0.1	2	25
Rotifer 1	1	01-23-2024	16.4	2.5	2.5	0	0.5	0.5	0.5	0.1	2	25
Rotifer 1	1	01-23-2024	16.4	2.5	2.5	0	0.5	0.5	0.5	0.1	2	25
Rotifer 2	1	01-23-2024	16.4	2.5	2.5	0	0.5	0.5	0.5	0.1	2	25
Rotifer 2	1	01-23-2024	16.4	2.5	2.5	0	0.5	0.5	0.5	0.1	2	25
Rotifer 2	1	01-23-2024	16.4	2.5	2.5	0	0.5	0.5	0.5	0.1	2	25
B/R5	1	01-23-2024	16.4	2.5	2.5	0	0.5	0.5	0.5	0.1	2	25
B/R5	1	01-23-2024	16.4	2.5	2.5	0	0.5	0.5	0.5	0.1	2	25
Leray	1	01-23-2024	16.4	2.5	2.5	0	0.5	0.5	0.5	0.1	2	25
Leray	1	01-23-2024	16.4	2.5	2.5	0	0.5	0.5	0.5	0.1	2	25
Cladoceran	2	01-24-2024	14.65	2.5	3	1.25	0.5	0.5	0.5	0.1	2	25
Cladoceran	2	01-24-2024	14.65	2.5	3	1.25	0.5	0.5	0.5	0.1	2	25
Rotifer 2	2	01-24-2024	14.65	2.5	3	1.25	0.5	0.5	0.5	0.1	2	25
Rotifer 2	2	01-24-2024	14.65	2.5	3	1.25	0.5	0.5	0.5	0.1	2	25
Rotifer 1	2	01-24-2024	15.9	2.5	3	0	0.5	0.5	0.5	0.1	2	25
B/R5	2	01-24-2024	15.4	2	2	2	0.5	0.5	0.5	0.1	2	25
Leray	2	01-24-2024	14.65	2.5	3	1.25	0.5	0.5	0.5	0.1	2	25
Cladoceran	3	01-24-2024	14	2.5	3.4	1.5	0.5	0.5	0.5	0.1	2	25
Cladoceran	3	01-24-2024	14	2.5	3.4	1.5	0.5	0.5	0.5	0.1	2	25
Rotifer 2	3	01-24-2024	14	2.5	3.4	1.5	0.5	0.5	0.5	0.1	2	25
Rotifer 2	3	01-24-2024	14	2.5	3.4	1.5	0.5	0.5	0.5	0.1	2	25
Rotifer 1	3	01-24-2024	16.4	2.5	2.5	0	0.5	0.5	0.5	0.1	2	25
B/R5	3	01-24-2024	16.5	2.5	2	0	0.5	0.5	0.5	0.5	2	25
Ostracod	4	01-25-2024	16.4	2.5	2.5	0	0.5	0.5	0.5	0.1	2	25
Ostracod	4	01-25-2024	16.4	2.5	2.5	0	0.5	0.5	0.5	0.1	2	25
Ostracod	4	01-25-2024	16.4	2.5	2.5	0	0.5	0.5	0.5	0.1	2	25
Ostracod	4	01-25-2024	16.4	2.5	2.5	0	0.5	0.5	0.5	0.1	2	25
Ostracod	4	01-25-2024	16.4	2.5	2.5	0	0.5	0.5	0.5	0.1	2	25

Ostracod	4	01-25-2024	16.4	2.5	2.5	0	0.5	0.5	0.5	0.1	2	25
Diaphanasoma	4	01-25-2024	16.4	2.5	2.5	0	0.5	0.5	0.5	0.1	2	25
Diaphanasoma	4	01-25-2024	16.4	2.5	2.5	0	0.5	0.5	0.5	0.1	2	25
Diaphanasoma	4	01-25-2024	16.4	2.5	2.5	0	0.5	0.5	0.5	0.1	2	25
Diaphanasoma	4	01-25-2024	16.4	2.5	2.5	0	0.5	0.5	0.5	0.1	2	25
Diaphanasoma	4	01-25-2024	16.4	2.5	2.5	0	0.5	0.5	0.5	0.1	2	25
Diaphanasoma	4	01-25-2024	16.4	2.5	2.5	0	0.5	0.5	0.5	0.1	2	25
Cladoceran	4	01-25-2024	13.6	2.5	3.4	1.5	0.5	0.5	0.5	0.5	2	25
Cladoceran	4	01-25-2024	13.6	2.5	3.4	1.5	0.5	0.5	0.5	0.5	2	25
Cladoceran	4	01-25-2024	13.6	2.5	3.4	1.5	0.5	0.5	0.5	0.5	2	25
Daphnia	4	01-25-2024	16.4	2.5	2.5	0	0.5	0.5	0.5	0.1	2	25
Daphnia	4	01-25-2024	16.4	2.5	2.5	0	0.5	0.5	0.5	0.1	2	25
Daphnia	4	01-25-2024	16.4	2.5	2.5	0	0.5	0.5	0.5	0.1	2	25
Ostracod	5	01-26-2024	15.15	2.5	205	1.25	0.5	0.5	0.5	0.1	2	25
Ostracod	5	01-26-2024	15.15	2.5	205	1.25	0.5	0.5	0.5	0.1	2	25
Ostracod	5	01-26-2024	15.15	2.5	205	1.25	0.5	0.5	0.5	0.1	2	25
Ostracod	5	01-26-2024	15.15	2.5	205	1.25	0.5	0.5	0.5	0.1	2	25
Cladoceran	5	01-26-2024	13.6	2.5	3.4	1.5	0.5	0.5	0.5	0.1	2	25
Cladoceran	5	01-26-2024	13.6	2.5	3.4	1.5	0.5	0.5	0.5	0.1	2	25
Cladoceran	5	01-26-2024	13.6	2.5	3.4	1.5	0.5	0.5	0.5	0.1	2	25
Daphnia	5	01-26-2024	15.15	2.5	2.5	1.25	0.5	0.5	0.5	0.1	2	25
Daphnia	5	01-26-2024	15.15	2.5	2.5	1.25	0.5	0.5	0.5	0.1	2	25
Daphnia	5	01-26-2024	15.15	2.5	2.5	1.25	0.5	0.5	0.5	0.1	2	25
Rotifer 2	6	01-29-2024	14.65	2.5	3	1.25	0.5	0.5	0.5	0.1	2	25
Rotifer 2	6	01-29-2024	14.65	2.5	3	1.25	0.5	0.5	0.5	0.1	2	25
Rotifer 2	6	01-29-2024	14	2.5	3.4	1.5	0.5	0.5	0.5	0.1	2	25
Rotifer 2	6	01-29-2024	14	2.5	3.4	1.5	0.5	0.5	0.5	0.1	2	25
Rotifer 1	7	02-05-2024	15.15	2.5	2.5	1.25	0.5	0.5	0.5	0.1	2	25
Rotifer 1	7	02-05-2024	15.15	2.5	2.5	1.25	0.5	0.5	0.5	0.1	2	25
Rotifer 1	7	02-05-2024	14.65	2.5	3	1.25	0.5	0.5	0.5	0.1	2	25
Rotifer 1	7	02-05-2024	14.65	2.5	3	1.25	0.5	0.5	0.5	0.1	2	25
Rotifer 1	7	02-05-2024	16.4	2.5	2.5	0	0.5	0.5	0.5	0.1	2	25
Rotifer 1	7	02-05-2024	16.4	2.5	2.5	0	0.5	0.5	0.5	0.1	2	25

Appendix Table A-3: The cycling conditions of each first round PCR of each primer optimization. All temperatures are in °C. All optimizations were conducted with the combined batch DNA sample.

Primer	Primer optimization round	Date of optimization	Initial denaturation temp	Initial denaturation duration	# of cycles	Denaturation temp	Denaturation duration	Annealing temp	Annealing duration	Extension temp	Extention duration	Final cycle extension temp	Final cycle extension duration	Band observed (Y/N)?	Band strength
Copepod	1	01-23-2024	95	5 mins	32	95	30s	44	30s	72	1min	72	1 min	Y	strong
Cladocera n	1	01-23-2024	95	5 mins	32	95	30s	48	30s	72	1min	72	1 min	N	not present
Cladocera n	1	01-23-2024	95	5 mins	32	95	30s	50	30s	72	1min	72	1 min	N	not present
Cladocera n	1	01-23-2024	95	5 mins	32	95	30s	52	30s	72	1min	72	1 min	N	not present
Rotifer 1	1	01-23-2024	95	5 mins	32	95	30s	48	30s	72	1min	72	1 min	N	not present
Rotifer 1	1	01-23-2024	95	5 mins	32	95	30s	50	30s	72	1min	72	1 min	Y	weak
Rotifer 1	1	01-23-2024	95	5 mins	32	95	30s	52	30s	72	1min	72	1 min	N	not present
Rotifer 2	1	01-23-2024	95	5 mins	32	95	30s	48	30s	72	1min	72	1 min	N	not present
Rotifer 2	1	01-23-2024	95	5 mins	32	95	30s	50	30s	72	1min	72	1 min	N	not present
Rotifer 2	1	01-23-2024	95	5 mins	32	95	30s	52	30s	72	1min	72	1 min	N	not present
B/R5	1	01-23-2024	95	5 mins	32	95	30s	57	30s	72	1min	72	1 min	N	not present
B/R5	1	01-23-2024	95	5 mins	32	95	30s	60	30s	72	1min	72	1 min	N	not present
Leray	1	01-23-2024	95	5 mins	32	95	30s	57	30s	72	1min	72	1 min	N	not present
Leray	1	01-23-2024	95	5 mins	32	95	30s	60	30s	72	1min	72	1 min	N	not present
Cladocera n	2	01-24-2024	95	5 mins	30	95	30s	44	30s	72	1min	72	1 min	N	not present
Cladocera n	2	01-24-2024	95	5 mins	30	95	30s	46	30s	72	1min	72	1 min	N	not present
Rotifer 2	2	01-24-2024	95	5 mins	30	95	30s	44	30s	72	1min	72	1 min	Y	very weak
Rotifer 2	2	01-24-2024	95	5 mins	30	95	30s	46	30s	72	1min	72	1 min	N	not present

Rotifer 1	2	01-24-2024	95	5 mins	30	95	30s	50	30s	72	1min	72	1 min	N	not present
B/R5	2	01-24-2024	94	2.5mins	30	94	30s	46	1min	72	1min	72	10min	N	not present
Leray	2	01-24-2024	94	2.5mins	30	94	30s	46	1min	72	1min	72	10min	Y	very strong
Cladocean	3	01-24-2024	95	5min	30	95	30s	42	30s	72	1min	72	5min	N	not present
Cladocean	3	01-24-2024	95	5min	30	95	30s	44	30s	72	1min	72	5min	N	not present
Rotifer 2	3	01-24-2024	95	5min	30	95	30s	42	30s	72	1min	72	5min	N	not present
Rotifer 2	3	01-24-2024	95	5min	30	95	30s	44	30s	72	1min	72	5min	N	not present
Rotifer 1	3	01-24-2024	95	5min	30	95	30s	50	30s	72	1min	72	5min	N	not present
B/R5	3	01-24-2024	95	5min	30	94	40s	46	1min	72	30s	72	5min	Y	fair
Ostracod	4	01-25-2024	95	5min	30	94	30s	42	1min	72	1min	72	5min	N	not present
Ostracod	4	01-25-2024	95	5min	30	94	30s	44	1min	72	1min	72	5min	N	not present
Ostracod	4	01-25-2024	95	5min	30	94	30s	46	1min	72	1min	72	5min	N	not present
Ostracod	4	01-25-2024	95	5min	30	94	30s	48	1min	72	1min	72	5min	N	not present
Ostracod	4	01-25-2024	95	5min	30	94	30s	50	1min	72	1min	72	5min	N	not present
Ostracod	4	01-25-2024	95	5min	30	94	30s	52	1min	72	1min	72	5min	N	not present
Diaphanasoma	4	01-25-2024	95	5min	30	94	30s	42	1min	72	1min	72	5min	N	not present
Diaphanasoma	4	01-25-2024	95	5min	30	94	30s	44	1min	72	1min	72	5min	N	not present
Diaphanasoma	4	01-25-2024	95	5min	30	94	30s	46	1min	72	1min	72	5min	N	not present
Diaphanasoma	4	01-25-2024	95	5min	30	94	30s	48	1min	72	1min	72	5min	N	not present
Diaphanasoma	4	01-25-2024	95	5min	30	94	30s	50	1min	72	1min	72	5min	N	not present
Diaphanasoma	4	01-25-2024	95	5min	30	94	30s	52	1min	72	1min	72	5min	N	not present

Cladoceran	4	01-25-2024	95	5min	30	94	30s	42	1min	72	1min	72	5min	N	not present
Cladoceran	4	01-25-2024	95	5min	30	94	30s	44	1min	72	1min	72	5min	N	not present
Cladoceran	4	01-25-2024	95	5min	30	94	30s	46	1min	72	1min	72	5min	N	not present
Daphnia	4	01-25-2024	95	5min	30	94	30s	42	1min	72	1min	72	5min	N	not present
Daphnia	4	01-25-2024	95	5min	30	94	30s	44	1min	72	1min	72	5min	N	not present
Daphnia	4	01-25-2024	95	5min	30	94	30s	46	1min	72	1min	72	5min	N	not present
Ostracod	5	01-26-2024	95	5min	30	94	30s	44	1min	72	1min	72	5min	N	not present
Ostracod	5	01-26-2024	95	5min	30	94	30s	46	1min	72	1min	72	5min	N	not present
Ostracod	5	01-26-2024	95	5min	30	94	30s	48	1min	72	1min	72	5min	N	not present
Ostracod	5	01-26-2024	95	5min	30	94	30s	50	1min	72	1min	72	5min	N	not present
Cladoceran	5	01-26-2024	95	5min	30	94	30s	46	1min	72	1min	72	5min	N	not present
Cladoceran	5	01-26-2024	95	5min	30	94	30s	48	1min	72	1min	72	5min	N	not present
Cladoceran	5	01-26-2024	95	5min	30	94	30s	50	1min	72	1min	72	5min	N	not present
Daphnia	5	01-26-2024	95	5min	30	94	30s	40	1min	72	1min	72	5min	Y	strong
Daphnia	5	01-26-2024	95	5min	30	94	30s	42	1min	72	1min	72	5min	Y	strong
Daphnia	5	01-26-2024	95	5min	30	94	30s	44	1min	72	1min	72	5min	Y	strong
Rotifer 2	6	01-29-2024	95	5min	30	94	30s	42	1min	72	1min	72	5min	Y	weak
Rotifer 2	6	01-29-2024	95	5min	30	94	30s	44	1min	72	1min	72	5min	N	not ptresent
Rotifer 2	6	01-29-2024	95	5min	30	94	30s	42	1min	72	1min	72	5min	Y	fair
Rotifer 2	6	01-29-2024	95	5min	30	94	30s	44	1min	72	1min	72	5min	Y	very weak
Rotifer 1	7	02-05-2024	95	5min	30	94	30s	50	1min	72	1min	72	5min	Y	good
Rotifer 1	7	02-05-2024	95	5min	30	94	30s	48	1min	72	1min	72	5min	Y	good
Rotifer 1	7	02-05-2024	95	5min	30	94	30s	50	1min	72	1min	72	5min	Y	good

Rotifer 1	7	02-05-2024	95	5min	30	94	30s	48	1min	72	1min	72	5min	Y	good
Rotifer 1	7	02-05-2024	95	5min	30	94	30s	50	1min	72	1min	72	5min	N	not ptresent
Rotifer 1	7	02-05-2024	95	5min	30	94	30s	48	1min	72	1min	72	5min	N	not present

Appendix Table A-4: Total field blank reads and extraction blank reads for each treatment and date sampled. The reads for each primer are included separately.

Treatment	Date	Blank Type	Primer	Number of Reads
Reference	2022-July-19	Field blank	Leray	23
Reference	2022-July-19	Field blank	Leray	1245.6
Reference	2022-July-20	Field blank	Leray	421.2
7L	2022-July-19	Field blank	Leray	11766
17.5L	2022-July-20	Field blank	Leray	0.4
31.5L	2022-July-19	Field blank	Leray	2232.8
57.4L	2022-July-20	Field blank	Leray	23.8
77.7L	2022-July-19	Field blank	Leray	4685
105L	2022-July-20	Field blank	Leray	1696.8
Reference	2022-Aug-15	Field blank	Leray	5.8
Reference	2022-Aug-15	Field blank	Leray	12.4
Reference	2022-Aug-15	Field blank	Leray	28.2
7L	2022-Aug-15	Field blank	Leray	590.2
17.5L	2022-Aug-15	Field blank	Leray	199.2
31.5L	2022-Aug-15	Field blank	Leray	25.2
57.4L	2022-Aug-15	Field blank	Leray	49.2
77.7L	2022-Aug-15	Field blank	Leray	2771.6
105L	2022-Aug-15	Field blank	Leray	44
Reference	2022-Sep-12	Field blank	Leray	4.2
Reference	2022-Sep-12	Field blank	Leray	117.2
Reference	2022-Sep-12	Field blank	Leray	896
7L	2022-Sep-12	Field blank	Leray	18.8
17.5L	2022-Sep-12	Field blank	Leray	6.2
31.5L	2022-Sep-12	Field blank	Leray	17
57.4L	2022-Sep-12	Field blank	Leray	204.6
77.7L	2022-Sep-12	Field blank	Leray	84
105L	2022-Sep-12	Field blank	Leray	288.4
Reference	2022-July-19	Field blank	Copepod	139
Reference	2022-July-19	Field blank	Copepod	1744.4
Reference	2022-July-20	Field blank	Copepod	636.8
7L	2022-July-19	Field blank	Copepod	5496
17.5L	2022-July-20	Field blank	Copepod	0
31.5L	2022-July-19	Field blank	Copepod	14728
57.4L	2022-July-20	Field blank	Copepod	1
77.7L	2022-July-19	Field blank	Copepod	13585
105L	2022-July-20	Field blank	Copepod	3576.4
Reference	2022-Aug-15	Field blank	Copepod	27.4
Reference	2022-Aug-15	Field blank	Copepod	120.6
Reference	2022-Aug-15	Field blank	Copepod	363
7L	2022-Aug-15	Field blank	Copepod	4212.8
17.5L	2022-Aug-15	Field blank	Copepod	1198.8
31.5L	2022-Aug-15	Field blank	Copepod	157.8
57.4L	2022-Aug-15	Field blank	Copepod	255.8

77.7L	2022-Aug-15	Field blank	Copepod	8824.2
105L	2022-Aug-15	Field blank	Copepod	100
Reference	2022-Sep-12	Field blank	Copepod	18.4
Reference	2022-Sep-12	Field blank	Copepod	409.4
Reference	2022-Sep-12	Field blank	Copepod	24254
7L	2022-Sep-12	Field blank	Copepod	86.6
17.5L	2022-Sep-12	Field blank	Copepod	18.6
31.5L	2022-Sep-12	Field blank	Copepod	56.2
57.4L	2022-Sep-12	Field blank	Copepod	957.4
77.7L	2022-Sep-12	Field blank	Copepod	384
105L	2022-Sep-12	Field blank	Copepod	4148.8
Reference	2022-July-19	Field blank	Daphnia	1306
Reference	2022-July-19	Field blank	Daphnia	33085
Reference	2022-July-20	Field blank	Daphnia	37965
7L	2022-July-19	Field blank	Daphnia	58265
17.5L	2022-July-20	Field blank	Daphnia	382
31.5L	2022-July-19	Field blank	Daphnia	6687.6
57.4L	2022-July-20	Field blank	Daphnia	37.8
77.7L	2022-July-19	Field blank	Daphnia	1444.4
105L	2022-July-20	Field blank	Daphnia	1279.4
Reference	2022-Aug-15	Field blank	Daphnia	514.4
Reference	2022-Aug-15	Field blank	Daphnia	208.4
Reference	2022-Aug-15	Field blank	Daphnia	268.4
7L	2022-Aug-15	Field blank	Daphnia	951
17.5L	2022-Aug-15	Field blank	Daphnia	504.8
31.5L	2022-Aug-15	Field blank	Daphnia	1403.2
57.4L	2022-Aug-15	Field blank	Daphnia	324.4
77.7L	2022-Aug-15	Field blank	Daphnia	50433
105L	2022-Aug-15	Field blank	Daphnia	15.8
Reference	2022-Sep-12	Field blank	Daphnia	2464
Reference	2022-Sep-12	Field blank	Daphnia	264.4
Reference	2022-Sep-12	Field blank	Daphnia	2201
7L	2022-Sep-12	Field blank	Daphnia	372.8
17.5L	2022-Sep-12	Field blank	Daphnia	21.6
31.5L	2022-Sep-12	Field blank	Daphnia	837.6
57.4L	2022-Sep-12	Field blank	Daphnia	439.6
77.7L	2022-Sep-12	Field blank	Daphnia	788
105L	2022-Sep-12	Field blank	Daphnia	133.6
Reference	2022-July-19	Extraction blank	Leray	0
77.7L	2022-Aug-15	Extraction blank	Leray	0
17.5L	2022-Sep-12	Extraction blank	Leray	0
Reference	2022-July-19	Extraction blank	Copepod	4.2
77.7L	2022-Aug-15	Extraction blank	Copepod	14
17.5L	2022-Sep-12	Extraction blank	Copepod	4.2
Reference	2022-July-19	Extraction blank	Daphnia	68.4
77.7L	2022-Aug-15	Extraction blank	Daphnia	421.6

17.5L	2022-Sep-12	Extraction blank	Daphnia	124

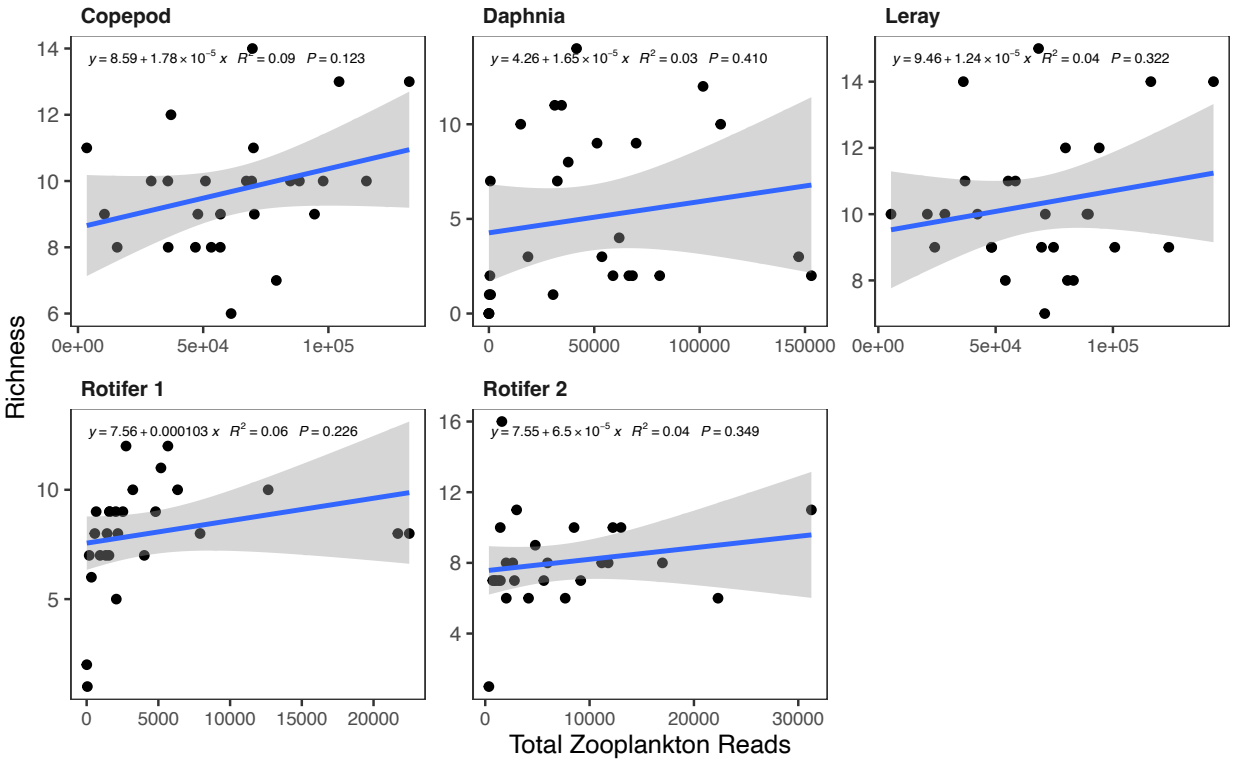

Appendix Figure A-1: The relationship between total zooplankton reads (read depth) and richness for each primer results. The linear equation, R squared, and p-value of the linear regression are included within each plot.

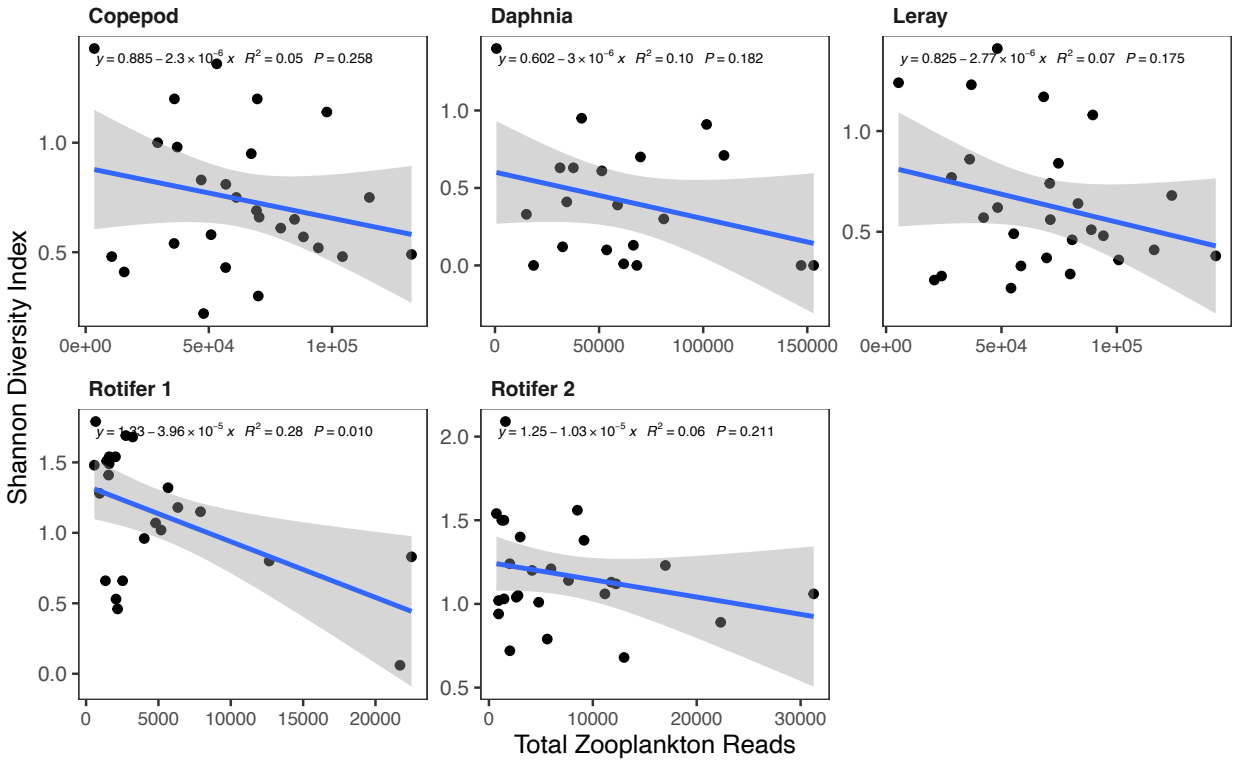

Appendix Figure A-2: The relationship between total zooplankton reads (read depth) and the Shannon Diversity Index for each primer results. The linear equation, R squared, and p-value of the linear regression are included within each plot.

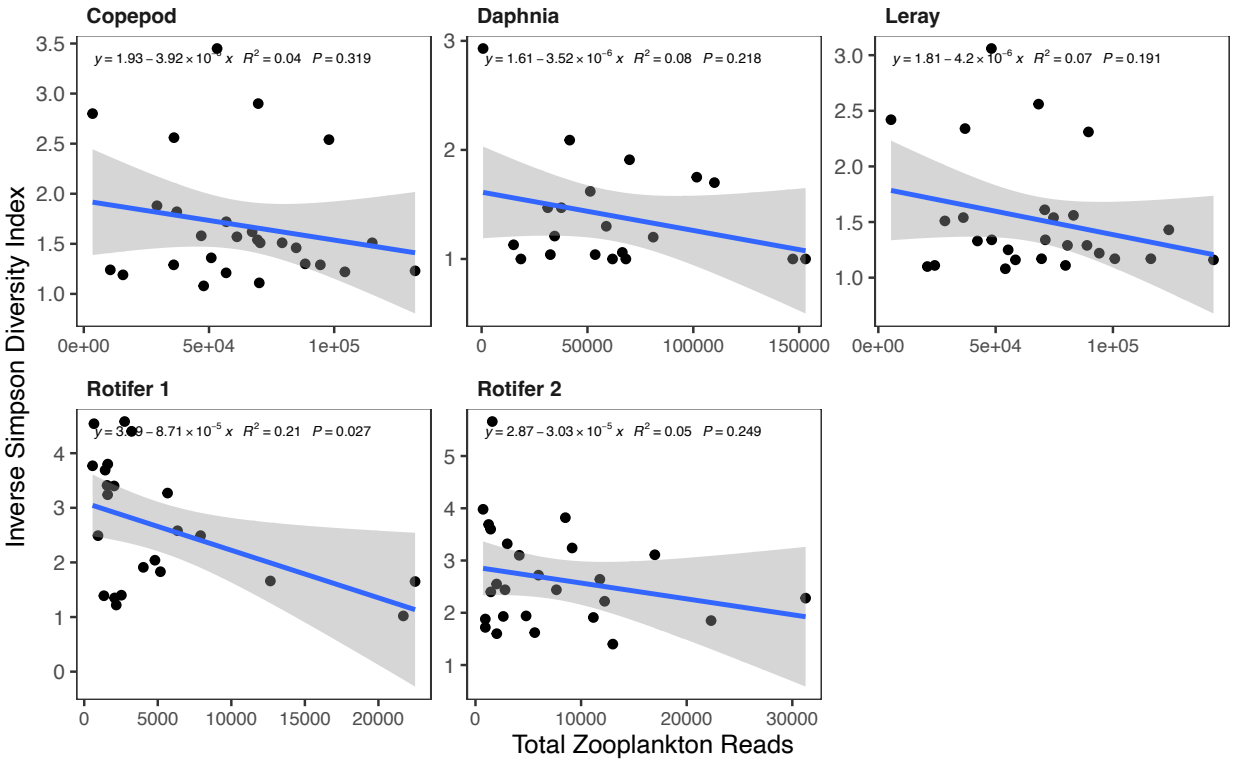

Appendix Figure A-3: The relationship between total zooplankton reads (read depth) and the Inverse Simpson Diversity Index for each primer results. The linear equation, R squared, and p-value of the linear regression are included within each plot.

Appendix B: R&L Supplemental Tables and Figures

Appendix Table B-1: The measured composition of the AWW prior to each addition.

Addition #	TP (mg/kg)	TAN (mg/kg)	TKN (mg/kg)	TK (mg/kg)	TS (mg/kg)	Dry Matter (%)	Moisture (%)	Density (g/mL)
1	48.8	285	296	NA	NA	NA	NA	0.998
2	48.0	185	246	5.05	165	0.189	99.8	0.998
3	39.8	223	267	5.78	92.4	0.157	99.8	0.998
4	417	236	955	7.02	721	1.52	98.5	0.985
5	275	291	291	22	156	0.439	99.6	0.996

Note: Mean value from collection source 1 used for TKN and density for Addition #1. NA represents data that was not obtained.

Appendix Table B-2: Cumulative nutrient concentration of TP (mg/L PO_4-P) within each treatment as a result of each AWW addition load. The cumulative concentration is a result of the sum of each mass of TP loaded, divided by the most recent volume.

Treatment	Addition #1	+Addition #2	+Addition #3	+Addition #4	+Addition #5
Reference	0	0	0	0	0
7 L	0.0452	0.0947	0.1375	0.9407	1.5077
9.8 L	0.0825	0.1741	0.2481	1.4246	2.4201
12.6 L	0.0805	0.1654	0.2385	1.6183	2.5895
17.5 L	0.0855	0.1755	0.2501	1.5594	2.4742
23.1 L	0.1542	0.3113	0.4442	3.2443	5.2274
31.5 L	0.2876	0.6011	0.8611	5.2717	8.8574
42.7 L	0.2542	0.5213	0.7353	4.7003	7.4256
57.4 L	0.3710	0.7631	1.0708	6.7297	10.6913
77.7 L	0.4996	1.0273	1.4909	8.7710	15.2929
105 L	0.7409	1.5132	2.1668	14.4182	23.2494

Appendix Table B-3: Cumulative nutrient concentration of TKN (mg/L) within each treatment as a result of each AWW addition load. The cumulative concentration is a result of the sum of each mass of TKN loaded, divided by the most recent volume.

Treatment	Addition #1	+Addition #2	+Addition #3	+Addition #4	+Addition #5
Reference	0	0	0	0	0
7 L	0.2740	0.5277	0.8149	2.6544	3.2547
9.8 L	0.5006	0.9691	1.4659	4.1603	5.2144
12.6 L	0.4880	0.9227	1.4137	4.5736	5.6020
17.5 L	0.5184	0.9789	1.4799	4.4786	5.4471
23.1 L	0.9351	1.7394	2.6311	9.0441	11.1438
31.5 L	1.7443	3.3489	5.0945	15.1955	18.9922
42.7 L	1.5420	2.9086	4.3456	13.4263	16.3119
57.4 L	2.2505	4.2567	6.3225	19.2826	23.4773
77.7 L	3.0305	5.7309	8.8430	25.5160	32.4216
105 L	4.4938	8.4460	12.8340	40.8923	50.2430

Appendix Table B-4: Cumulative nutrient concentration of NH_4 (mg/L NH_4-N) within each treatment as a result of each AWW addition load. The cumulative concentration is a result of the sum of each mass of NH_4 loaded, divided by the most recent volume.

Treatment	Addition #1	+Addition #2	+Addition #3	+Addition #4	+Addition #5
Reference	0	0	0	0	0
7 L	0.2641	0.4552	0.6950	1.1495	1.7498
9.8 L	0.4826	0.8353	1.2502	1.9160	2.9701
12.6 L	0.4704	0.7978	1.2078	1.9887	3.0171
17.5 L	0.4997	0.8465	1.2648	2.0058	2.9744
23.1 L	0.9013	1.5071	2.2516	3.8364	5.9361
31.5 L	1.6813	2.8898	4.3474	6.8435	10.6401
42.7 L	1.4863	2.5155	3.7155	5.9595	8.8450
57.4 L	2.1692	3.6801	5.4051	8.6077	12.8024
77.7 L	2.9210	4.9548	7.5534	11.6736	18.5792
105 L	4.3315	7.3080	10.9720	17.9056	27.2564

Appendix Table B-5: Average nutrient concentration within each treatment over the study duration (n = 5). Each concentration that contributed to the average is a result of the mass of the nutrient loaded divided by the known volume at the time of each addition.

Treatment	TP (mg/L PO_4-P)	NH_4 (mg/L NH_4-N)	TKN (mg/L)
Reference	0	0	0
7 L	0.3015	0.3500	0.6509
9.8 L	0.4840	0.5940	1.0429
12.6 L	0.5179	0.6034	1.1204
17.5 L	0.4948	0.5949	1.0894
23.1 L	1.0455	1.1872	2.2288
31.5 L	1.7715	2.1280	3.7984
42.7 L	1.4851	1.7690	3.2624
57.4 L	2.1383	2.5605	4.6955
77.7 L	3.0586	3.7158	6.4843
105 L	4.6499	5.4513	10.0486

Appendix Table B-6: The cumulative and mean concentration of copper and zinc within each treatment as a result of each AWW loading (n = 3).

Treatment	Cumulative Cu (mg/L)	Mean Cu (mg/L)	Cumulative Zn (mg/L)	Mean Zn (mg/L)
Reference	0	0	0	0
7 L	0.0004	0.0001	0.0030	0.0006
9.8 L	0.0008	0.0002	0.0052	0.0010
12.6 L	0.0008	0.0002	0.0051	0.0010
17.5 L	0.0006	0.0001	0.0048	0.0010
23.1 L	0.0016	0.0003	0.0104	0.0019
31.5 L	0.0028	0.0005	0.0187	0.0035
42.7 L	0.0022	0.0004	0.0142	0.0030
57.4 L	0.0031	0.0007	0.0207	0.0043
77.7 L	0.0052	0.0009	0.0340	0.0061
105 L	0.0070	0.0014	0.0461	0.0091

Appendix Table B-7: Mean (±SD) concentration of environmental variables after the first AWW treatment to the end of the study duration, within each treatment.

	TP (mg/L PO_4-P) (n = 5)	**TDP (mg/L PO_4-P)** (n = 4)	**SRP (mg/L PO_4-P)** (n = 5)	**Part-P (mg/L PO_4-P)** (n = 5)	**TN (mg/L N)** (n = 2)	**TDN (mg/L N)** (n = 5)	**TAN (mg/L NH_4-N)** (n = 5)	**NH_3 (mg/L NH_3)** (n = 5)	**NO_2 (mg/L NO_2-N)** (n = 5)	**NO_3 (mg/L NO_3-N)** (n = 5)	**Chl-*a* (µg/L)** (n = 5)
Reference	0.271 (0.200)	0.255 (0.210)	0.042 (0.042)	0.034 (0.013)	1.38 (0.29)	1.66 (0.79)	0.058 (0.091)	0.001 (0.002)	0.114 (0.022)	0.448 (0.337)	2.60 (1.95)
7L	0.275 (0.231)	0.271 (0.230)	0.031 (0.019)	0.030 (0.015)	1.18 (0.77)	1.51 (0.40)	0.057 (0.046)	0.001 (0.001)	0.112 (0.019)	0.490 (0.310)	2.77 (2.59)
9.8L	0.717 (0.341)	0.568 (0.427)	0.026 (0.018)	0.098 (0.032)	1.18 (0.13)	1.79 (0.58)	0.039 (0.042)	0.001 (0.001)	0.095 (0.064)	0.570 (0.422)	7.98 (7.69)
12.6L	0.286 (0.192)	0.271 (0.217)	0.106 (0.055)	0.038 (0.018)	1.72 (0.13)	1.40 (0.33)	0.059 (0.060)	0.001 (0.001)	0.115 (0.014)	0.460 (0.345)	2.13 (1.10)
17.5L	0.520 (0.301)	0.480 (0.298)	0.102 (0.063)	0.046 (0.019)	1.82 (0.06)	1.74 (0.30)	0.043 (0.062)	0.001 (0.001)	0.115 (0.019)	0.444 (0.354)	2.44 (1.45)
23.1L	0.334 (0.197)	0.281 (0.188)	0.056 (0.035)	0.047 (0.034)	1.58 (0.14)	1.71 (0.39)	0.055 (0.063)	0.001 (0.001)	0.116 (0.024)	0.476 (0.397)	3.19 (2.74)
31.5L	0.315 (0.207)	0.286 (0.210)	0.056 (0.035)	0.095 (0.143)	1.58 (0.14)	1.59 (0.30)	0.051 (0.059)	0.001 (0.002)	0.100 (0.025)	0.502 (0.330)	7.53 (9.79)
42.7L	0.356 (0.189)	0.305 (0.208)	0.056 (0.035)	0.073 (0.057)	1.58 (0.14)	1.71 (0.27)	0.160 (0.273)	0.004 (0.008)	0.114 (0.053)	0.474 (0.368)	7.11 (7.47)
57.4L	0.386 (0.238)	0.359 (0.289)	0.056 (0.035)	0.069 (0.059)	1.58 (0.14)	2.00 (0.23)	0.076 (0.072)	0.001 (0.001)	0.117 (0.015)	0.490 (0.403)	0.98 (0.47)
77.7L	0.723 (0.543)	0.544 (0.516)	0.056 (0.035)	0.062 (0.044)	1.58 (0.14)	1.92 (1.36)	0.049 (0.068)	0.001 (0.002)	0.117 (0.024)	0.456 (0.310)	5.50 (6.08)
105L	0.848 (0.463)	0.699 (0.444)	0.056 (0.035)	0.056 (0.024)	1.58 (0.14)	1.98 (0.48)	0.058 (0.079)	0.002 (0.003)	0.109 (0.016)	0.482 (0.317)	5.81 (3.70)

Appendix Table B-8: Mean (±SD) concentration of remaining environmental variables after the first AWW treatment to the end of the study duration (n = 5).

Treatment	Alkalinity (mg/L $CaCO_3$)	DOC (mg/L)	SRSi (mg/L)
Reference	334.4 (32.8)	55.6 (44.8)	6.31 (2.36)
7L	319.5 (13.4)	40.6 (38.3)	5.48 (1.87)
9.8L	436.5 (92.6)	64.8 (72.8)	8.54 (1.75)
12.6L	303.5 (2.1)	36.9 (34.7)	4.64 (1.39)
17.5L	337.0 (1.4)	61.4 (44.9)	6.45 (1.43)
23.1L	339.0 (21.2)	47.2 (47.8)	7.05 (1.76)
31.5L	391.5 (94.0)	63.8 (51.8)	5.02 (1.40)
42.7L	345.0 (1.4)	64.7 (46.7)	7.11 (1.87)
57.4L	331.5 (0.7)	32.4 (38.2)	5.92 (1.52)
77.7L	311.5 (51.6)	32.4 (40.6)	3.64 (1.15)
105L	388.5 (65.8)	52.3 (54.4)	4.75 (2.00)

Appendix Table B-9: Monthly mean (±SD) meteorological variables and total precipitation from May to September 2022. Light intensity was measured on site via loggers and all other data was retrieved from Environment Canada weather station in Carmen, Manitoba.

Month	Mean Air Temperature (°C)	Mean Relative Humidity (%)	Total Precipitation (mm)	Mean Wind Speed (km/h)	Mean Light Intensity (lux)
June	18.0 (5.9)	62.8 (20.1)	39.6	15.3 (9.1)	26414 (30357)
July	19.7 (4.8)	74.0 (15.9)	83	11.1 (5.7)	26892 (30106)
August	19.3 (5.0)	74.8 (16.4)	48.4	9.9 (6.6)	22308 (26759)
September	14.3 (6.3)	69.8 (21.1)	26.5	13.0 (7.4)	15022 (20290)

Appendix Table B-10: Linear regression model results of the relationship between log10(x + 1) of cumulative AWW load concentration (TP used as the dependant variable) and each zooplankton metric. The zooplankton metrics were log10 transformed when required to meet model assumptions. Significant when p-value <= 0.05.

Zooplankton metric	Transformation	Study Day	Intercept	Slope	R^2	p-value	Significant
Total zooplankton abundance	Log10	21	3.71	0.10	0.0058	0.825	No
	Log10	35	3.62	0.44	0.14	0.253	No
	Log10	49	3.36	0.34	0.31	0.073	No
	Log10	75	3.21	0.29	0.18	0.200	No
Copepod abundance	Log10	21	3.44	0.29	0.074	0.42	No
	Log10	35	3.60	-0.01	0.0002	0.96	No
	Log10	49	3.28	0.17	0.11	0.31	No
	Log10	75	3.11	0.24	0.074	0.42	No
Cyclopoid copepod abundance	Log10	21	2.84	1.05	0.25	0.12	No
	Log10	35	3.00	0.51	0.091	0.37	No
	Log10	49	2.79	0.20	0.095	0.36	No
	Log10	75	2.56	0.30	0.11	0.31	No
Calanoid copepod abundance	Log10	21	2.50	-2.75	0.53	0.011	Yes
	Log10	35	2.17	-0.58	0.056	0.482	No
	Log10	49	2.64	-1.99	0.64	0.003	Yes
	Log10	75	1.32	-1.07	0.35	0.053	No
Copepod Nauplii abundance	Log10	21	3.20	0.13	0.011	0.76	No
	Log10	35	3.43	-0.30	0.12	0.29	No
	Log10	49	3.01	0.24	0.16	0.22	No
	Log10	75	2.85	0.32	0.09	0.37	No
Cladoceran abundance	Log10	21	1.98	0.82	0.009	0.78	No
	Log10	35	1.17	0.77	0.02	0.68	No
	Log10	49	1.18	-0.02	$7.1x10^{-5}$	0.98	No
	Log10	75	-0.03	1.46	0.24	0.13	No
Rotifer abundance	Log10	21	3.10	-0.36	0.0095	0.775	No
	Log10	35	2.44	1.79	0.31	0.073	No
	Log10	49	2.60	0.50	0.12	0.292	No
	Log10	75	2.52	-0.04	0.0021	0.895	No
Inverse Simpson Diversity Index	NA	21	3.15	-1.15	0.093	0.36	No
	NA	35	2.27	1.04	0.14	0.26	No
	NA	49	2.93	-0.35	0.1	0.34	No
	NA	75	1.85	0.66	0.27	0.10	No
Pielou's Evenness	NA	21	0.66	-0.53	0.22	0.14	No
	NA	35	0.47	0.14	0.06	0.47	No
	NA	49	0.49	0.11	0.068	0.44	No
	NA	75	0.44	0.22	0.26	0.11	No
Species Richness	NA	21	4.96	2.55	0.23	0.13	No
	NA	35	4.86	0.48	0.027	0.68	No
	NA	49	5.67	-0.94	0.098	0.35	No

NA	75	4.60	-0.70	0.068	0.44	No

Appendix Table B-11: Generalized linear model regression results of the relationship between log10(x + 1) of cumulative AWW load concentration (TP used as the dependant variable) and each zooplankton metric. Significant when p-value <= 0.05.

Zooplankton metric	GLM Model	Study Day	Intercept	Slope	p-value	Significant
Cladoceran abundance	Negative Binomial	49	3.53	2.43	0.229	No
	Zero Inflated Negative Binomial	75	4.35	1.82	0.016	Yes
Calanoid Copepod	Zero Inflated Negative Binomial	75	8.13	-8.98	0.0582	No

Appendix Table B-12: Dominant zooplankton taxa, the proportion of the total sample abundance that the dominant taxa makes up, and species diversity metrics within each treatment on study day 21. Reference treatment represents the mean value (±SD) (n = 5).

Treatment	Dominant Taxa	Proportion of Abundance	Richness	Evenness	Shannon's Diversity	Inverse Simpson's Diversity
Reference	Rotifer	0.37	5 (1.22)	0.65 (0.21)	1.23 (0.08)	3.05 (0.42)
7 L	Copepod Nauplii	0.53	5	0.57	1.27	2.84
9.8 L	Rotifer	0.44	4	0.81	1.28	3.26
12.6 L	Copepod Nauplii	0.63	6	0.38	1.13	2.26
17.5 L	Copepod Nauplii	0.37	5	0.77	1.46	3.87
23.1 L	Rotifer	0.42	6	0.57	1.35	3.42
31.5 L	Cyclopoid Copepod	0.47	6	0.41	1.06	2.46
42.7 L	Cyclopoid Copepod	0.45	5	0.57	1.11	2.83
57.4 L	Rotifer	0.43	5	0.64	1.28	3.18
77.7 L	Rotifer	0.42	6	0.52	1.24	3.11
105 L	Copepod Nauplii	0.53	6	0.40	1.03	2.39

Appendix Table B-13: Dominant zooplankton taxa, the proportion of the total sample abundance that the dominant taxa makes up, and species diversity metrics within each treatment on study day 35. Reference treatment represents the mean value (±SD) (n = 5).

Treatment	Dominant Taxa	Proportion of Abundance	Richness	Evenness	Shannon's Diversity	Inverse Simpson's Diversity
Reference	Copepod Nauplii	0.50	4.6 (0.55)	0.64 (0.05)	1.22 (0.09)	2.95 (0.34)
7 L	Copepod Nauplii	0.63	4	0.53	0.94	2.11
9.8 L	Copepod Nauplii	0.60	5	0.44	0.97	2.19
12.6 L	Copepod Nauplii	0.71	5	0.36	0.83	1.82
17.5 L	Copepod Nauplii	0.50	6	0.46	1.18	2.74
23.1 L	Copepod Nauplii	0.69	5	0.38	0.92	1.91
31.5 L	Copepod Nauplii	0.56	5	0.47	1.00	2.36
42.7 L	Cyclopoid Copepod	0.48	5	0.57	1.19	2.87
57.4 L	Copepod Nauplii	0.48	5	0.60	1.27	2.99
77.7 L	Rotifer	0.59	5	0.48	1.06	2.39
105 L	Cyclopoid Copepod	0.35	5	0.61	1.13	3.03

Appendix Table B-14: Dominant zooplankton taxa, the proportion of the total sample abundance that the dominant taxa makes up, and species diversity metrics within each treatment on study day 49. Reference treatment represents the mean value (±SD) (n = 5).

Treatment	Dominant Taxa	Proportion of Abundance	Richness	Evenness	Shannon's Diversity	Inverse Simpson's Diversity
Reference	Copepod Nauplii	0.50	5 (0.71)	0.58 (0.13)	1.22 (0.06)	2.86 (0.41)
7 L	Rotifer	0.43	6	0.52	1.25	3.09
9.8 L	Copepod Nauplii	0.59	5	0.47	1.04	2.36
12.6 L	Copepod Nauplii	0.55	4	0.62	1.04	2.47
17.5 L	Cyclopoid Copepod	0.41	6	0.57	1.35	3.44
23.1 L	Copepod Nauplii	0.41	6	0.47	1.12	2.81
31.5 L	Copepod Nauplii	0.43	4	0.66	1.03	2.65
42.7 L	Cyclopoid Copepod	0.55	6	0.40	1.10	2.39
57.4 L	Copepod Nauplii	0.42	5	0.59	1.22	2.96
77.7 L	Rotifer	0.64	6	0.35	0.93	2.12
105 L	Copepod Nauplii	0.41	3	0.92	1.05	2.75

Appendix Table B-15: Dominant zooplankton taxa, the proportion of the total sample abundance that the dominant taxa makes up, and species diversity metrics within each treatment on study day 75. Reference treatment represents the mean value (±SD) (n = 5).

Treatment	Dominant Taxa	Proportion of Abundance	Richness	Evenness	Shannon's Diversity	Inverse Simpson's Diversity
Reference	Copepod Nauplii	0.60	4.6 (0.55)	0.52 (0.12)	1.02 (0.08)	2.33 (0.28)
7 L	Cyclopoid Copepod	0.71	3	0.61	0.79	1.82
9.8 L	Copepod Nauplii	0.51	3	0.88	1.03	2.63
12.6 L	Copepod Nauplii	0.60	6	0.38	1.00	2.27
17.5 L	Copepod Nauplii	0.67	6	0.34	0.99	2.02
23.1 L	Rotifer	0.68	4	0.48	0.83	1.90
31.5 L	Copepod Nauplii	0.66	3	0.66	0.84	1.99
42.7 L	Copepod Nauplii	0.64	3	0.65	0.79	1.96
57.4 L	Copepod Nauplii	0.49	4	0.71	1.16	2.84
77.7 L	Copepod Nauplii	0.51	4	0.66	1.06	2.64
105 L	Copepod Nauplii	0.40	4	0.89	1.33	3.54

Appendix Table B-16: Linear regression model results of the relationship between log10(x + 1) of zooplankton abundance and each fish metric. The fish in the sampling jars was treated as a binomial, with 0 being no fish in jar, and 1 being fish found in jar. Significant when p-value <= 0.05.

Fish Metric	Study Day	Intercept	Slope	R^2	p-value	Significant
Number of fish retrieved	75	2.86	0.064	0.14	0.253	No
Binomial larval fish in jar	75	3.50	-0.37	0.242	0.0625	No

Appendix Table B-17: Species scores (b_k) as generated from principal response curve analysis of the zooplankton taxa included in the analysis.

Zooplankton taxa	**b_k**
Daphnia sp.	2.562
Chydorus sp.	0.144
Scapholeberis sp.	0.233
Copepoda nauplii	0.044
Diaphanosoma sp.	-0.083
Ostracoda	-0.096
Cyclopoida	-0.139
Rotifera	-0.142
Calanoida	-0.190
Ceriodaphnia sp.	-0.509

Appendix Table B-18: Eigenvalues, explained variance, environmental variable canonical coefficients, and species scores, associated with the first and second RDA axis.

	RDA Axis 1	**RDA Axis 2**
Eigenvalue	0.01294	0.007878
Variance explained	0.12310	0.074911
Dissolved oxygen	-0.03750	0.21284
pH	0.36916	0.38425
Total phosphorus	0.01616	0.07945
Total dissolved nitrogen	-0.37143	0.28107
Total ammoniacal nitrogen	-0.20960	-0.15256
Nitrite	0.08150	-0.16527
Chlorophyll *a*	0.10094	0.50292
Daphnia sp.	-0.2345305	-0.3009673
Chydorus sp.	0.0341151	-0.0021459
Ceriodaphnia sp.	-0.0964340	0.1358844
Ostracoda	0.0149003	0.0001291
Calanoida	-0.0598887	0.0006501
Diaphanosoma sp.	0.0005805	0.0012345
Copepoda nauplii	-0.2282147	0.0723219
Cyclopoida	0.1614825	0.0638514
Rotifera	0.3049532	-0.1687960
Scapholeberis sp.	-0.0319546	-0.0092726

Appendix Table B-19: The number of adult fathead minnow (*Pimephales promelas*) fish retrieved from the mesocosms by the final fish sampling date on September 17, 2024. A total of 12 fish were originally introduced to the mesocosms.

Treatment	Fish abundance
Reference-A	7
Reference-B	8
Reference-C	11
Reference-D	11
Reference-E	5
7 L	7
9.8 L	11
12.6 L	12
17.5 L	7
23.1 L	9
31.5 L	11
42.7 L	9
57.4 L	9
77.7 L	9
105 L	7

Appendix Table B-20: The zooplankton taxa identified from each primer as indicated by the check symbol.

Taxa	**Leray**	**Copepod**	**Daphnia**	**Rotifer 1**	**Rotifer 2**
Acanthocyclops sp.	✓	✓	✓	✓	✓
Acanthocyclops vernalis	✓	✓	✓	✓	✓
Asplanchna sieboldii				✓	
Bosminidae sp.			✓		
Brachionus rubens	✓	✓			
Brachionus sp.		✓			✓
Calanoida sp.	✓	✓	✓	✓	✓
Ceriodaphnia cf. laticaudata	✓	✓	✓	✓	✓
Cyclopidae sp.	✓	✓	✓	✓	✓
Cyclopoida sp.	✓				
Daphnia carinata				✓	
Daphnia pulex	✓	✓	✓	✓	✓
Daphnia pulicaria	✓	✓	✓	✓	✓
Daphnia sp.	✓	✓	✓	✓	✓
Daphniidae sp.				✓	
Diacyclops thomasi			✓		
Diaphanosoma sp.					✓
Euchlanis dilatate	✓	✓	✓	✓	✓
Eucyclopinae sp.	✓	✓		✓	✓
Eucyclops cf. estherae	✓	✓	✓	✓	✓
Flosculariaceae sp.			✓		
Lecane bulla					✓
Lecane inermis				✓	✓
Leptodiaptomus siciloides	✓	✓	✓	✓	✓
Macrocyclops albidus	✓	✓	✓		
Mesocyclops edax	✓	✓	✓	✓	✓
Moina cf. affinis	✓	✓		✓	
Monogononta	✓	✓	✓	✓	✓
Platyias quadricornis	✓				
Podocopida sp.	✓	✓	✓	✓	✓
Polyarthra vulgaris	✓	✓	✓	✓	✓
Proales fallaciosa	✓	✓		✓	
Rotaria rotatoria	✓	✓		✓	✓
Scapholeberis sp.	✓	✓	✓	✓	✓
Synchaeta cf. pectinata				✓	
Synchaeta kitina			✓		

Appendix Table B-21: Species diversity metrics within each treatment and study day from the Leray primer eDNA zooplankton reads. Reference treatment represents the mean value (±SD) (n = 5).

Study Day	Treatment	Richness	Evenness	Shannon's Diversity	Inverse Simpson's Diversity
20	Reference	11.3 (3.1)	0.12 (0.1)	0.45 (0.2)	1.28 (0.2)
	7 L	9	0.17	0.84	1.54
	17.5 L	8	0.14	0.22	1.08
	31.5 L	9	0.12	0.28	1.11
	57.4 L	10	0.13	0.57	1.33
	77.7 L	10	0.11	0.26	1.10
	105 L	9	0.13	0.37	1.17
46	Reference	12.7 (2.3)	0.11 (0.03)	0.67 (0.2)	1.40 (0.2)
	7 L	10	0.23	1.08	2.31
	17.5 L	10	0.24	1.24	2.42
	31.5 L	9	0.13	0.36	1.17
	57.4 L	11	0.11	0.49	1.25
	77.7 L	11	0.11	0.33	1.16
	105 L	8	0.16	0.46	1.29
74	Reference	9.33 (0.6)	0.21 (0.1)	0.88 (0.5)	1.94 (1)
	7 L	12	0.10	0.48	1.22
	17.5 L	9	0.15	0.62	1.34
	31.5 L	10	0.13	0.51	1.29
	57.4 L	11	0.21	1.23	2.34
	77.7 L	7	0.23	0.74	1.61
	105 L	15	0.17	1.17	2.56

Appendix Table B-22: Linear regression model results of the relationship between log10(x + 1) of cumulative AWW load concentration (TP used as the dependant variable) and each zooplankton eDNA metric. The zooplankton metrics were log10 transformed when required to meet model assumptions. Significant when p-value <= 0.05.

Primer	Zooplankton metric	Transformation	Study Day	Intercept	Slope	R^2	p-value	Significant
Leray	Shannon Diversity Index	Log10	20	-0.36	-0.36	0.071	0.56	No
		Log10	46	-0.006	-0.35	0.45	0.099	No
		Log10	74	-0.23	0.13	0.16	0.37	No
	Inverse Simpson Diversity Index	Log10	20	0.11	-0.14	0.16	0.38	No
		Log10	46	0.30	-0.19	0.33	0.18	No
		Log10	74	0.14	0.11	0.19	0.33	No
Copepod	Shannon Diversity Index	Log10	20	-0.32	-0.08	0.0046	0.88	No
		Log10	46	0.04	-0.21	0.33	0.18	No
		Log10	74	-0.15	0.09	0.12	0.44	No
	Inverse Simpson Diversity Index	Log10	20	0.12	-0.10	0.081	0.54	No
		Log10	46	0.35	-0.16	0.25	0.25	No
		Log10	74	0.19	0.09	0.14	0.41	No
Daphnia	Shannon Diversity Index	Log10	20	-0.27	-1.19	0.33	0.18	No
		Log10	46	-1.19	0.26	0.006	0.89	No
		Log10	74	-1.62	-0.50	0.012	0.57	No
	Inverse Simpson Diversity Index	Log10	20	0.17	-0.30	0.23	0.28	No
		Log10	46	0.08	0.13	0.11	0.51	No
		Log10	74	0.02	-0.02	0.59	0.13	No
Rotifer 1	Shannon Diversity Index	Log10	20	1.10	-0.39	0.021	0.78	No
		Log10	46	1.32	-0.20	0.044	0.69	No
		Log10	74	1.31	-0.35	0.12	0.45	No
	Inverse Simpson Diversity Index	Log10	20	2.55	-0.77	0.015	0.82	No
		Log10	46	3.18	-0.72	0.075	0.60	No
		Log10	74	2.98	-0.77	0.15	0.40	No
Rotifer 2	Shannon Diversity Index	NA	20	0.14	-0.56	0.67	0.02	Yes
		NA	46	-0.06	0.17	0.18	0.40	No
		NA	74	0.04	0.04	0.12	0.45	No
	Inverse Simpson Diversity Index	NA	20	0.51	-0.65	0.54	0.06	No
		NA	46	0.24	0.22	0.19	0.39	No
		NA	74	0.36	0.06	0.13	0.43	No

Appendix Table B-23: The effect of treatment (AWW) and study day on zooplankton community composition based on Bray-Curtis dissimilarity tested using PERMANOVA. The results of both eDNA metabarcoding (each primer results analyzed separately) and morphological methodology are reported. Significant when p-value <= 0.05.

Method	Variable	R^2	F-statistic	p-value	Significant
eDNA – Leray Primer	Treatment	0.30	1.91	0.012	Yes
	Study Day	0.21	8.04	0.001	Yes
eDNA – Copepod Primer	Treatment	0.27	1.55	0.058	No
	Study Day	0.18	6.03	0.001	Yes
eDNA - Daphnia Primer	Treatment	0.40	1.54	0.132	No
	Study Day	0.02	0.51	0.514	No
eDNA - Rotifer 1 Primer	Treatment	0.33	1.92	0.005	Yes
	Study Day	0.21	7.12	0.001	Yes
eDNA - Rotifer 2 Primer	Treatment	0.18	0.88	0.652	No
	Study Day	0.22	6.58	0.001	Yes
Morphological	Treatment	0.26	1.94	0.01	Yes
	Study Day	0.08	5.98	0.001	Yes

Appendix Table B-24: The results of pairwise PERMANOVA testing the difference in zooplankton community composition between each study day combination based on Bray-Curtis dissimilarity. The results of both eDNA metabarcoding (each primer results analyzed separately) and morphological methodology are reported. Only significant PERMANOVA results were analyzed for pairwise comparisons. Significant when p-value <= 0.05.

Primer	Comparison	R^2	F-statistic	p-value	Adjusted p-value	Significance
Leray	20 vs. 46	0.19	3.78	0.006	0.015	Yes
	20 vs. 74	0.32	7.44	0.001	0.003	Yes
	46 vs. 74	0.11	1.88	0.097	0.109	No
Copepod	20 vs. 46	0.21	4.33	0.004	0.0075	Yes
	20 vs. 74	0.28	6.14	0.002	0.003	Yes
	46 vs. 74	0.07	1.25	0.241	0.274	No
Rotifer 1	20 vs. 46	0.17	2.78	0.014	0.0195	Yes
	20 vs. 74	0.30	6.54	0.001	0.003	Yes
	46 vs. 74	0.10	1.52	0.176	0.148	No
Rotifer 2	20 vs. 46	0.25	4.94	0.002	0.003	Yes
	20 vs. 74	0.33	8.02	0.001	0.003	Yes
	46 vs. 74	0.11	1.90	0.09	0.101	No
Morphological	21 vs. 35	0.10	3.26	0.06	0.12	No
	21 vs. 49	0.05	1.39	0.253	0.3048	No
	21 vs. 75	0.16	5.50	0.005	0.012	Yes
	35 vs. 49	0.04	1.10	0.339	0.341	No
	35 vs. 75	0.07	1.81	0.126	0.198	No
	49 vs. 75	0.07	2.10	0.066	0.172	No

Appendix Table B-25: The results of pairwise PERMANOVA testing the difference in zooplankton community composition between each treatment combination based on Bray-Curtis dissimilarity of the eDNA reads from the Leray primer. Significant when p-value <= 0.05.

Primer	Comparison	R^2	F-statistic	p-value	Adjusted p-value	Significance
Leray	REF_vs_7 L	0.08	0.83	0.54	0.74	No
	REF_vs_31.5 L	0.09	1.05	0.37	0.65	No
	REF_vs_77.7 L	0.14	1.64	0.13	0.45	No
	REF_vs_57.4 L	0.17	2.07	0.10	0.42	No
	REF_vs_17.5 L	0.06	0.60	0.69	0.77	No
	REF_vs_105 L	0.11	1.22	0.27	0.56	No
	7 L_vs_31.5 L	0.48	3.69	0.10	0.42	No
	7 L_vs_77.7 L	0.37	2.32	0.10	0.42	No
	7 L_vs_57.4 L	0.50	4.06	0.10	0.42	No
	7 L_vs_17.5 L	0.08	0.36	1.00	1.00	No
	7 L_vs_105 L	0.38	2.47	0.20	0.47	No
	31.5 L_vs_77.7 L	0.21	1.05	0.60	0.74	No
	31.5 L_vs_57.4 L	0.32	1.86	0.20	0.47	No
	31.5 L_vs_17.5 L	0.23	1.19	0.50	0.74	No
	31.5 L_vs_105 L	0.14	0.65	0.80	0.84	No
	77.7 L_vs_57.4 L	0.37	2.37	0.10	0.42	No
	77.7 L_vs_17.5 L	0.17	0.81	0.70	0.77	No
	77.7 L_vs_105 L	0.27	1.50	0.20	0.47	No
	57.4 L_vs_17.5 L	0.30	1.68	0.30	0.57	No
	57.4 L_vs_105 L	0.11	0.52	0.60	0.74	No
	17.5 L_vs_105 L	0.21	1.06	0.50	0.74	No

Appendix Table B-26: Species diversity metrics within each treatment and study day from the Copepod primer eDNA zooplankton reads. Reference treatment represents the mean value (SD) (n = 3).

Study Day	Treatment	Richness	Evenness	Shannon's Diversity	Inverse Simpson's Diversity
20	Reference	11.0 (2)	0.12 (0.04)	0.48 (0.2)	1.28 (0.2)
	7 L	10	0.16	0.95	1.62
	17.5 L	9	0.12	0.22	1.08
	31.5 L	8	0.15	0.41	1.19
	57.4 L	10	0.13	0.54	1.29
	77.7 L	9	0.14	0.48	1.24
	105 L	8	0.15	0.43	1.21
46	Reference	11.67 (1.5)	0.14 (0.1)	0.83 (0.3)	1.64 (0.4)
	7 L	10	0.25	1.14	2.54
	17.5 L	11	0.25	1.43	2.80
	31.5 L	9	0.14	0.52	1.29
	57.4 L	10	0.14	0.58	1.36
	77.7 L	9	0.19	0.81	1.72
	105 L	7	0.22	0.61	1.51
74	Reference	9.33 (1.2)	0.25 (0.2)	0.93 (0.4)	2.17 (1.1)
	7 L	10	0.13	0.57	1.30
	17.5 L	8	0.20	0.83	1.58
	31.5 L	10	0.15	0.65	1.46
	57.4 L	8	0.32	1.20	2.56
	77.7 L	6	0.26	0.75	1.57
	105 L	14	0.21	1.20	2.90

Appendix Table B-27: Species diversity metrics within each treatment and study day from the Daphnia primer eDNA zooplankton reads. Reference treatment represents the mean value (SD) (n = 3).

Study Day	Treatment	Richness	Evenness	Shannon's Diversity	Inverse Simpson's Diversity
20	Reference	11.0 (2.7)	0.18 (0.03)	0.79 (0.1)	1.90 (0.2)
	7 L	2	0.65	0.39	1.30
	17.5 L	2	0.60	0.30	1.20
	31.5 L	11	0.11	0.41	1.21
	57.4 L	2	0.53	0.13	1.06
	77.7 L	9	0.18	0.61	1.62
	105 L	7	0.15	0.12	1.04
46	Reference	4.33 (6.7)	0.57 (0.6)	0.30 (0.5)	1.37 (0.5)
	7 L	4	0.25	0.01	1.00
	17.5 L	0	Inf	0.00	Inf
	31.5 L	8	0.18	0.63	1.47
	57.4 L	2	0.50	0.00	1.00
	77.7 L	11	0.13	0.63	1.47
	105 L	7	0.42	1.40	2.93
74	Reference	4.00 (5.3)	0.31 (0.3)	0.11 (0.2)	1.06 (0.1)
	7 L	1	1.00	0.00	1.00
	17.5 L	2	0.51	0.04	1.01
	31.5 L	1	1.00	0.00	1.00
	57.4 L	3	0.35	0.10	1.04
	77.7 L	3	0.33	0.00	1.00
	105 L	3	0.33	0.00	1.00

Appendix Table B-28: Species diversity metrics within each treatment and study day from the Rotifer 1 primer eDNA zooplankton reads. Reference treatment represents the mean value (SD) (n = 3).

Study Day	Treatment	Richness	Evenness	Shannon's Diversity	Inverse Simpson's Diversity
20	Reference	8.67 (1.2)	0.26 (0.1)	1.05 (0.2)	2.24 (0.5)
	7 L	5	0.27	0.53	1.35
	17.5 L	8	0.47	1.48	3.77
	31.5 L	7	0.36	1.28	2.49
	57.4 L	2	0.99	0.69	1.98
	77.7 L	7	0.49	1.41	3.41
	105 L	8	0.15	0.46	1.22
46	Reference	10.0 (1.7)	0.44 (0.1)	1.67 (0.1)	4.31 (0.4)
	7 L	7	0.27	0.96	1.91
	17.5 L	1	1.00	0.00	1.00
	31.5 L	9	0.16	0.66	1.40
	57.4 L	9	0.38	1.54	3.40
	77.7 L	10	0.17	0.80	1.66
	105 L	7	0.49	1.47	3.42
74	Reference	10.33 (1.5)	0.31 (0.1)	1.36 (0.3)	3.24 (1.2)
	7 L	7	0.20	0.66	1.39
	17.5 L	9	0.36	1.49	3.24
	31.5 L	6	0.33	1.08	1.99
	57.4 L	8	0.46	1.51	3.69
	77.7 L	8	0.13	0.06	1.02
	105 L	11	0.17	1.02	1.83

Appendix Table B-29: The results of pairwise PERMANOVA testing the difference in zooplankton community composition between each treatment combination based on Bray-Curtis dissimilarity of the eDNA reads from the Rotifer 1 primer. Significant when p-value <= 0.05.

Primer	Comparison	R^2	F-statistic	p-value	Adjusted p-value	Significance
Rotifer 1	REF_vs_7 L	0.15	1.70	0.15	0.45	No
	REF vs 31.5 L	0.12	1.33	0.23	0.48	No
	REF vs 77.7 L	0.13	1.49	0.20	0.47	No
	REF vs 57.4 L	0.21	2.45	0.04	0.35	No
	REF vs 17.5 L	0.03	0.31	0.90	1.00	No
	REF vs 105 L	0.10	1.02	0.44	0.72	No
	7 L vs 31.5 L	0.42	2.85	0.10	0.35	No
	7 L vs 77.7 L	0.37	2.38	0.10	0.35	No
	7 L vs 57.4 L	0.60	4.43	0.10	0.35	No
	7 L vs 17.5 L	0.25	1.02	0.30	0.53	No
	7 L vs 105 L	0.37	1.73	0.10	0.35	No
	31.5 L vs 77.7 L	0.26	1.42	0.30	0.53	No
	31.5 L vs 57.4 L	0.46	2.52	0.20	0.47	No
	31.5 L vs 17.5 L	0.24	0.96	0.50	0.75	No
	31.5 L vs 105 L	0.12	0.43	0.90	1.00	No
	77.7 L vs 57.4 L	0.35	1.65	0.10	0.35	No
	77.7 L vs 17.5 L	0.20	0.77	0.80	0.99	No
	77.7 L vs 105 L	0.19	0.69	0.70	0.92	No
	57.4 L vs 17.5 L	0.33	0.98	0.67	0.92	No
	57.4 L vs 105 L	0.29	0.83	1.00	1.00	No
	17.5 L_vs_105 L	0.18	0.44	1.00	1.00	No

Appendix Table B-30: Species diversity metrics within each treatment and study day from the Rotifer 2 primer eDNA zooplankton reads. Reference treatment represents the mean value (SD) (n = 3).

Study Day	Treatment	Richness	Evenness	Shannon's Diversity	Inverse Simpson's Diversity
20	Reference	8.67 (1.2)	0.32 (0.1)	1.19 (0.1)	2.68 (0.5)
	7 L	10	0.38	1.56	3.82
	17.5 L	6	0.52	1.20	3.10
	31.5 L	7	0.25	0.94	1.72
	57.4 L	8	0.33	1.13	2.64
	77.7 L	7	0.34	1.03	2.40
	105 L	6	0.27	0.72	1.60
46	Reference	7.33 (0.6)	0.36 (0.2)	1.20 (0.3)	2.60 (1.2)
	7 L	10	0.14	0.68	1.40
	17.5 L	1	1.00	0.00	1.00
	31.5 L	7	0.53	1.50	3.69
	57.4 L	8	0.24	1.06	1.91
	77.7 L	7	0.23	0.79	1.62
	105 L	16	0.35	2.09	5.66
74	Reference	8.0 (2)	0.33 (0.03)	1.21 (0.3)	2.67 (0.9)
	7 L	9	0.22	1.01	1.94
	17.5 L	7	0.35	1.05	2.44
	31.5 L	11	0.30	1.40	3.32
	57.4 L	6	0.41	1.14	2.44
	77.7 L	7	0.46	1.38	3.24
	105 L	11	0.21	1.06	2.28

Appendix Table B-31: The correlations between morphological derived zooplankton data and eDNA metabarcoding derived zooplankton data determined using Spearman's rank correlation. All variables were log10(x+1) transformed prior to correlation. Statistically significant values are indicated in bold text.

Primer	Morphological Variable	eDNA variable	Correlation coefficient	p-value
Leray	Total zooplankton abundance	Total zooplankton reads	0.274	0.175
	Total copepod abundance	Total copepod reads	0.190	0.353
	Total cladoceran abundance	Total cladoceran reads	0.751	**9.65×10^{-6}**
	Total rotifer abundance	Total rotifer reads	0.360	0.0705
	Relative abundance of copepods	Relative reads of copepods	0.268	0.184
	Relative abundance of rotifers	Relative reads of rotifers	0.251	0.216
	Relative abundance of cladocerans	Relative reads of cladocerans	0.764	**5.58×10^{-6}**
Copepod	Total zooplankton abundance	Total zooplankton reads	0.218	0.282
	Total copepod abundance	Total copepod reads	0.0882	0.668
	Total cladoceran abundance	Total cladoceran reads	0.732	**2.1×10^{-5}**
	Total rotifer abundance	Total rotifer reads	0.403	**0.0414**
	Relative abundance of copepods	Relative reads of copepods	0.383	0.0546
	Relative abundance of rotifers	Relative reads of rotifers	0.308	0.125
	Relative abundance of cladocerans	Relative reads of cladocerans	0.718	**3.65×10^{-5}**
Daphnia	Total zooplankton abundance	Total zooplankton reads	-0.0525	0.817
	Total copepod abundance	Total copepod reads	-0.0729	0.747
	Total cladoceran abundance	Total cladoceran reads	0.764	**3.47×10^{-5}**
	Total rotifer abundance	Total rotifer reads	-0.0462	0.838
	Relative abundance of copepods	Relative reads of copepods	-0.0561	0.804
	Relative abundance of rotifers	Relative reads of rotifers	-0.0210	0.926
	Relative abundance of cladocerans	Relative reads of cladocerans	0.476	**0.025**
Rotifer 1	Total zooplankton abundance	Total zooplankton reads	0.409	0.054
	Total copepod abundance	Total copepod reads	-0.282	0.193
	Total cladoceran abundance	Total cladoceran reads	0.564	**0.0051**
	Total rotifer abundance	Total rotifer reads	0.194	0.376
	Relative abundance of copepods	Relative reads of copepods	0.208	0.341
	Relative abundance of rotifers	Relative reads of rotifers	0.0198	0.930

	Relative abundance of cladocerans	Relative reads of cladocerans	0.573	**0.0043**
Rotifer 2	Total zooplankton abundance	Total zooplankton reads	0.353	0.0774
	Total copepod abundance	Total copepod reads	0.0722	0.726
	Total cladoceran abundance	Total cladoceran reads	0.611	**0.0009**
	Total rotifer abundance	Total rotifer reads	0.552	**0.0035**
	Relative abundance of copepods	Relative reads of copepods	0.341	0.0889
	Relative abundance of rotifers	Relative reads of rotifers	0.373	0.0606
	Relative abundance of cladocerans	Relative reads of cladocerans	0.518	**0.0067**

Appendix Table B-32: The results of pairwise PERMANOVA testing the difference in zooplankton community composition between each treatment combination based on Bray-Curtis dissimilarity of the morphological zooplankton abundance data. Significant when p-value <= 0.05.

Primer	Comparison	R^2	F-statistic	p-value	Adjusted p-value	Significance
Morphological	REF_vs_12.6 L	0.06	1.31	0.26	0.43	No
	REF_vs_7 L	0.02	0.49	0.73	0.82	No
	REF_vs_31.5 L	0.05	1.17	0.27	0.44	No
	REF_vs_9.8 L	0.02	0.34	0.81	0.88	No
	REF_vs_77.7 L	0.12	2.96	0.04	0.33	No
	REF_vs_57.4 L	0.15	3.90	0.02	0.33	No
	REF_vs_42.7 L	0.13	3.14	0.04	0.33	No
	REF_vs_23.1 L	0.06	1.42	0.22	0.43	No
	REF_vs_17.5 L	0.01	0.24	0.85	0.89	No
	REF_vs_105 L	0.06	1.47	0.23	0.43	No
	12.6 L_vs_7 L	0.09	0.61	0.67	0.79	No
	12.6 L_vs_31.5 L	0.14	0.94	0.50	0.61	No
	12.6 L_vs_9.8 L	0.23	1.80	0.20	0.43	No
	12.6 L_vs_77.7 L	0.35	3.22	0.12	0.34	No
	12.6 L_vs_57.4 L	0.51	6.22	0.04	0.33	No
	12.6 L_vs_42.7 L	0.31	2.68	0.14	0.34	No
	12.6 L_vs_23.1 L	0.34	3.03	0.13	0.34	No
	12.6 L_vs_17.5 L	0.25	2.01	0.14	0.34	No
	12.6 L_vs_105 L	0.30	2.60	0.09	0.34	No
	7 L_vs_31.5 L	0.03	0.20	0.98	0.98	No
	7 L_vs_9.8 L	0.04	0.22	0.97	0.98	No
	7 L_vs_77.7 L	0.16	1.14	0.31	0.49	No
	7 L_vs_57.4 L	0.28	2.38	0.08	0.34	No
	7 L_vs_42.7 L	0.07	0.46	0.82	0.88	No
	7 L_vs_23.1 L	0.11	0.78	0.48	0.60	No
	7 L_vs_17.5 L	0.06	0.39	0.86	0.89	No
	7 L_vs_105 L	0.07	0.46	0.73	0.82	No
	31.5 L_vs_9.8 L	0.09	0.63	0.60	0.72	No
	31.5 L_vs_77.7 L	0.21	1.62	0.23	0.43	No
	31.5 L_vs_57.4 L	0.49	5.75	0.03	0.33	No
	31.5 L_vs_42.7 L	0.19	1.41	0.25	0.43	No
	31.5 L_vs_23.1 L	0.25	1.98	0.20	0.43	No
	31.5 L_vs_17.5 L	0.21	1.58	0.22	0.43	No
	31.5 L_vs_105 L	0.15	1.06	0.35	0.49	No
	9.8 L_vs_77.7 L	0.15	1.03	0.41	0.55	No
	9.8 L_vs_57.4 L	0.47	5.35	0.03	0.33	No
	9.8 L_vs_42.7 L	0.23	1.77	0.23	0.43	No
	9.8 L_vs_23.1 L	0.16	1.16	0.33	0.49	No
	9.8 L_vs_17.5 L	0.13	0.93	0.47	0.60	No
	9.8 L_vs_105 L	0.18	1.28	0.37	0.51	No

77.7 L_vs_57.4 L	0.42	4.29	0.06	0.34	No
77.7 L_vs_42.7 L	0.27	2.17	0.12	0.34	No
77.7 L_vs_23.1 L	0.13	0.91	0.48	0.60	No
77.7 L_vs_17.5 L	0.28	2.37	0.09	0.34	No
77.7 L_vs_105 L	0.22	1.65	0.18	0.43	No
57.4 L_vs_42.7 L	0.47	5.25	0.02	0.33	No
57.4 L_vs_23.1 L	0.23	1.80	0.24	0.43	No
57.4 L_vs_17.5 L	0.39	3.87	0.06	0.34	No
57.4 L_vs_105 L	0.32	2.87	0.07	0.34	No
42.7 L_vs_23.1 L	0.27	2.24	0.11	0.34	No
42.7 L_vs_17.5 L	0.25	2.01	0.13	0.34	No
42.7 L_vs_105 L	0.17	1.24	0.34	0.49	No
23.1 L_vs_17.5 L	0.24	1.88	0.13	0.34	No
23.1 L_vs_105 L	0.16	1.10	0.32	0.49	No
17.5 L_vs_105 L	0.25	2.01	0.06	0.34	No

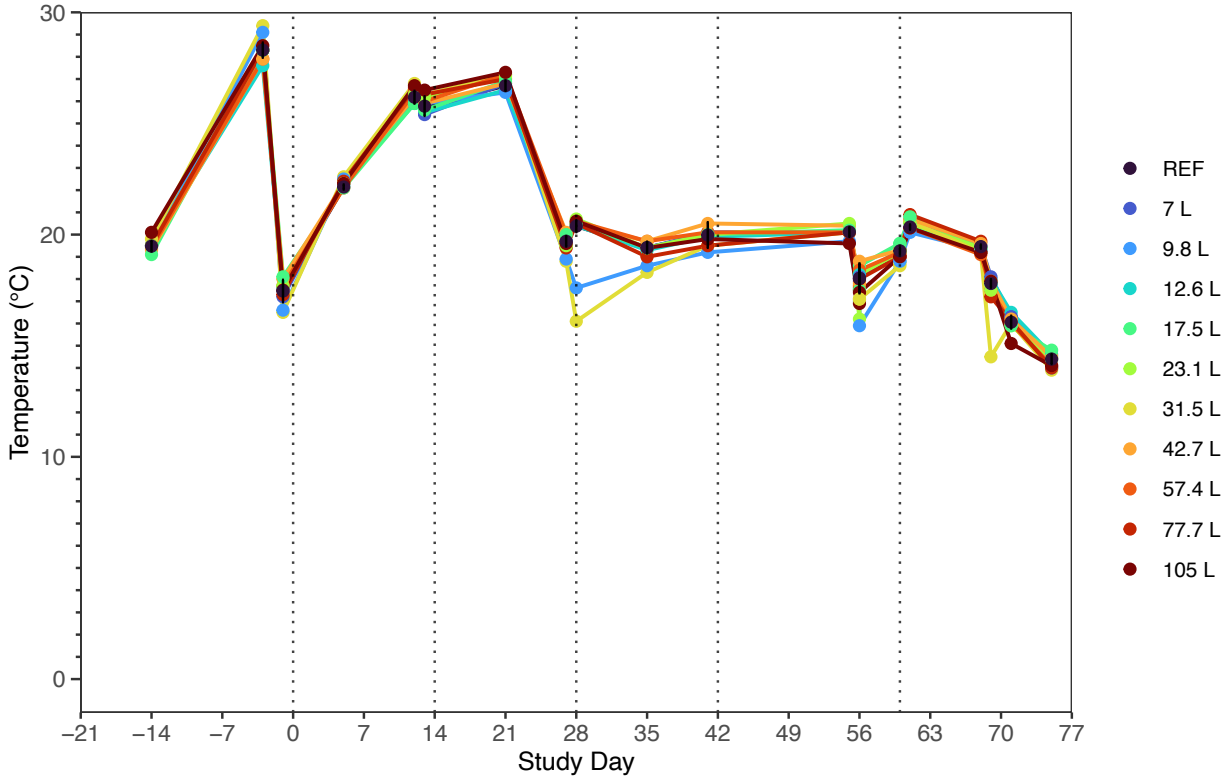

Appendix Figure B-1: Water temperature (°C) over the study duration within the RL commercial wetland mesocosms. The vertical dotted lines represent AWW addition days. REF displays the mean of the references (n = 5) with the error bars representing ± standard deviation.

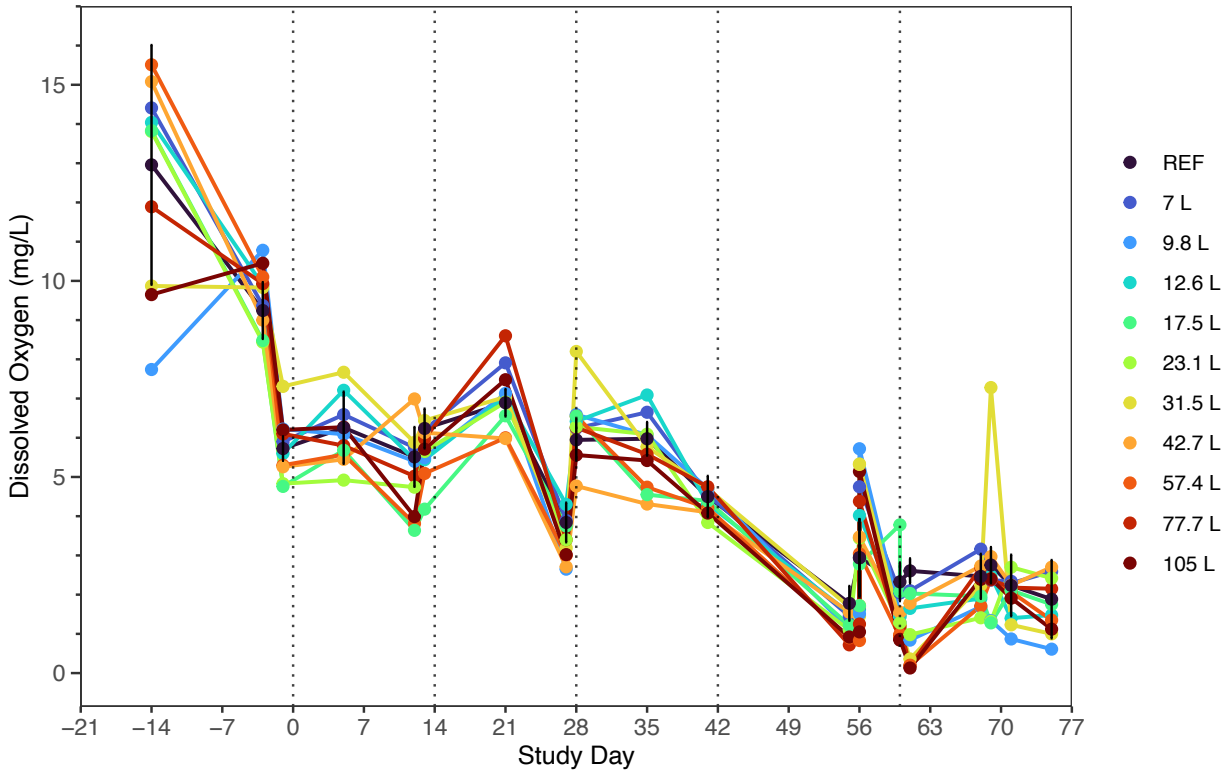

Appendix Figure B-2: Dissolved oxygen (mg/L) over the study duration within the RL commercial wild rice mesocosms. The vertical dotted lines represent AWW addition days. REF displays the mean of the references (n = 5) with the error bars representing ± standard deviation.

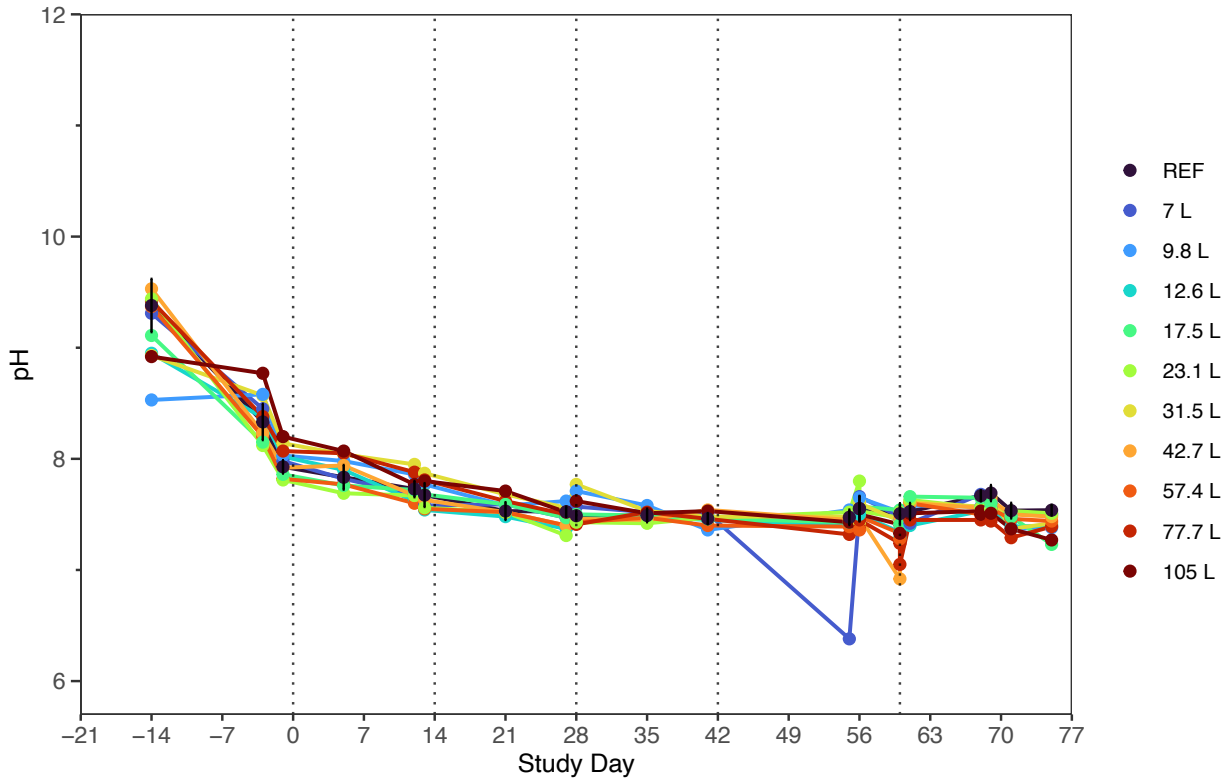

Appendix Figure B-3: pH over the study duration within the RL commercial wild rice mesocosms. The vertical dotted lines represent AWW addition days. REF displays the mean of the references (n = 5) with the error bars representing ± standard deviation.

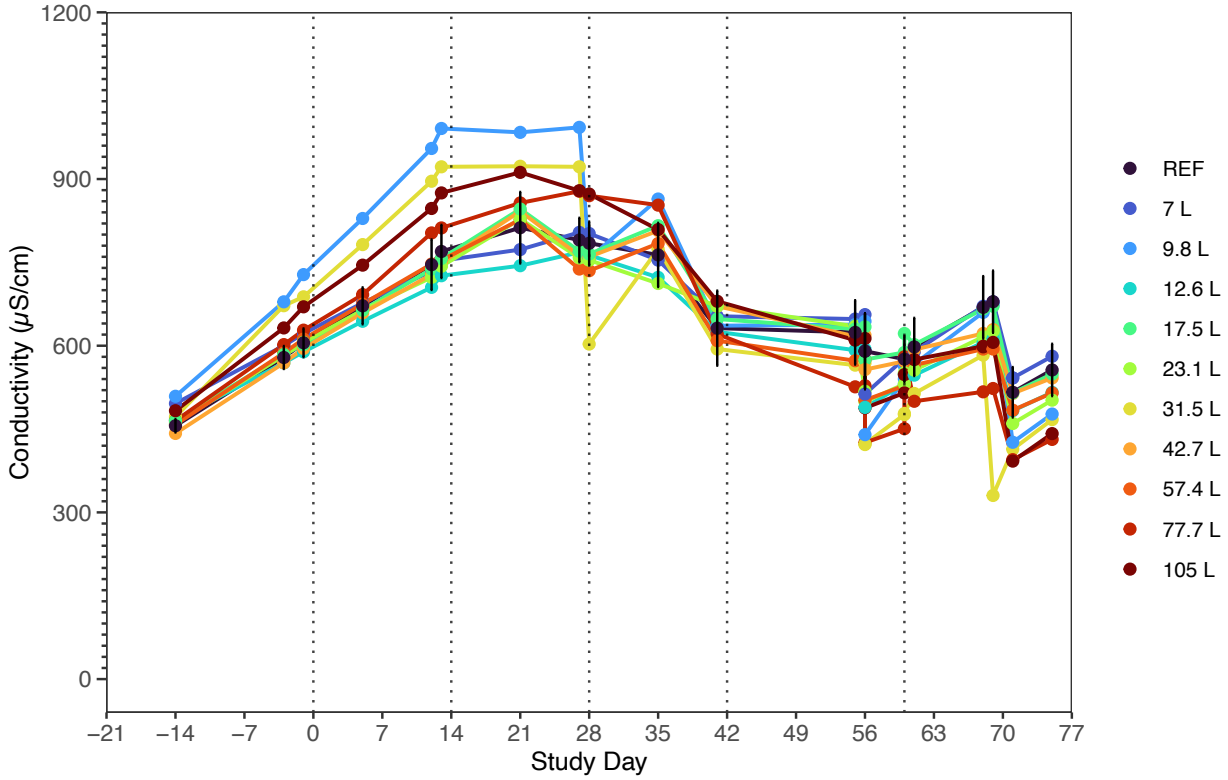

Appendix Figure B-4: Specific conductivity (µS/cm) over the study duration within the RL commercial wild rice mesocosms. The vertical dotted lines represent AWW addition days. REF displays the mean of the references (n = 5) with the error bars representing ± standard deviation.

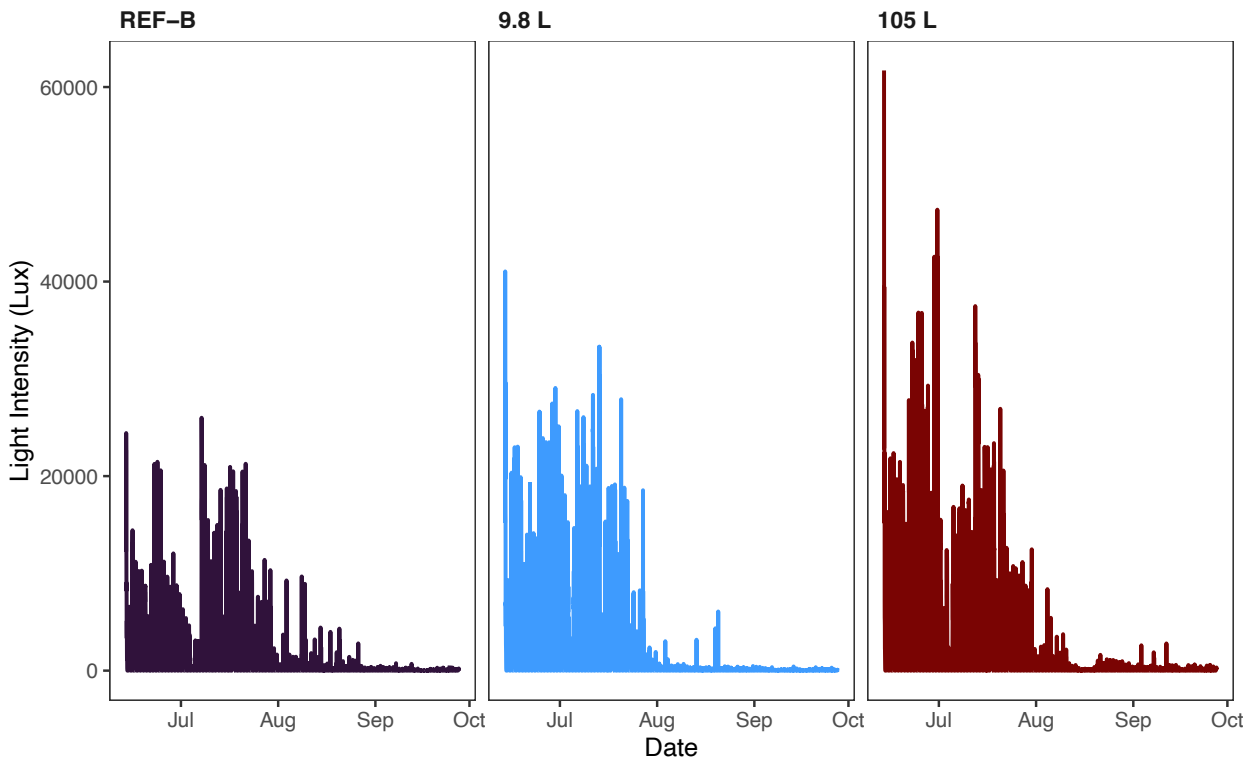

Appendix Figure B-5: Light intensity (lux) over the study duration within select RL mesocosms measured with HOBO loggers.

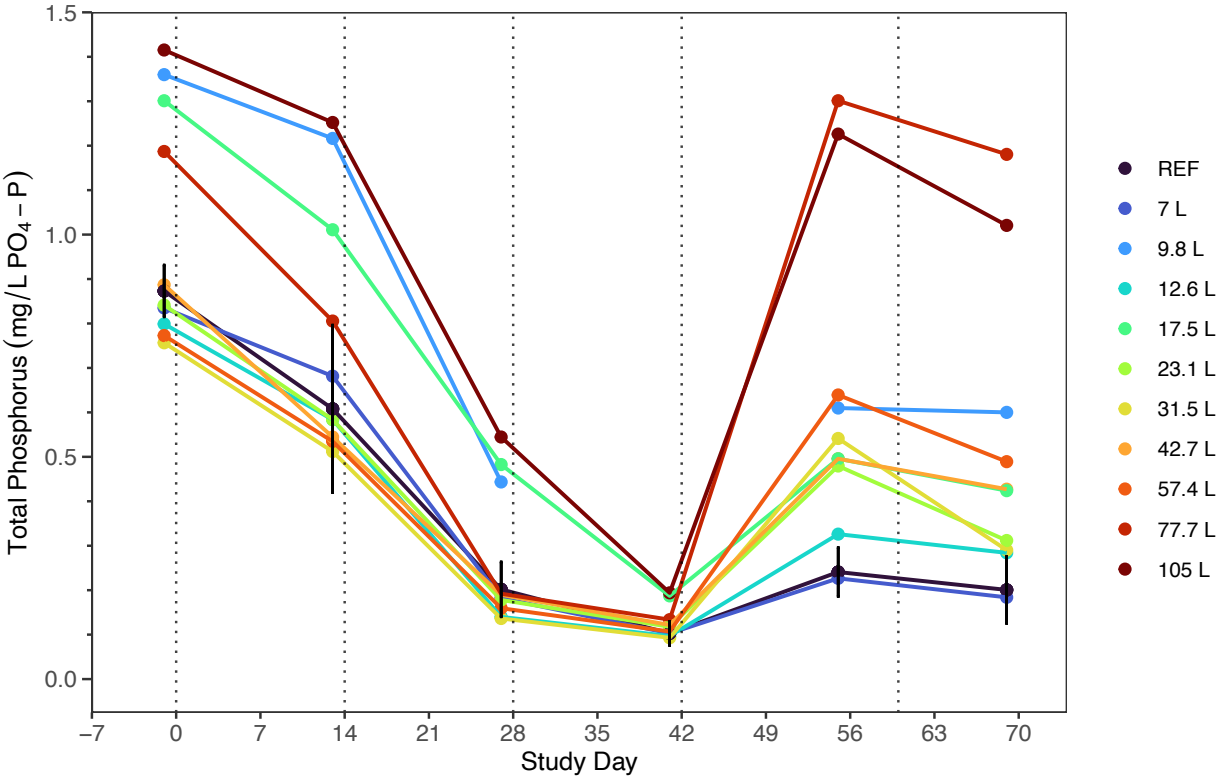

Appendix Figure B-6: Total phosphorus (mg/L PO_4-P) over the study duration within the RL commercial wild rice mesocosms. The vertical dotted lines represent AWW addition days. REF displays the mean of the references (n = 5) with the error bars representing ± standard deviation.

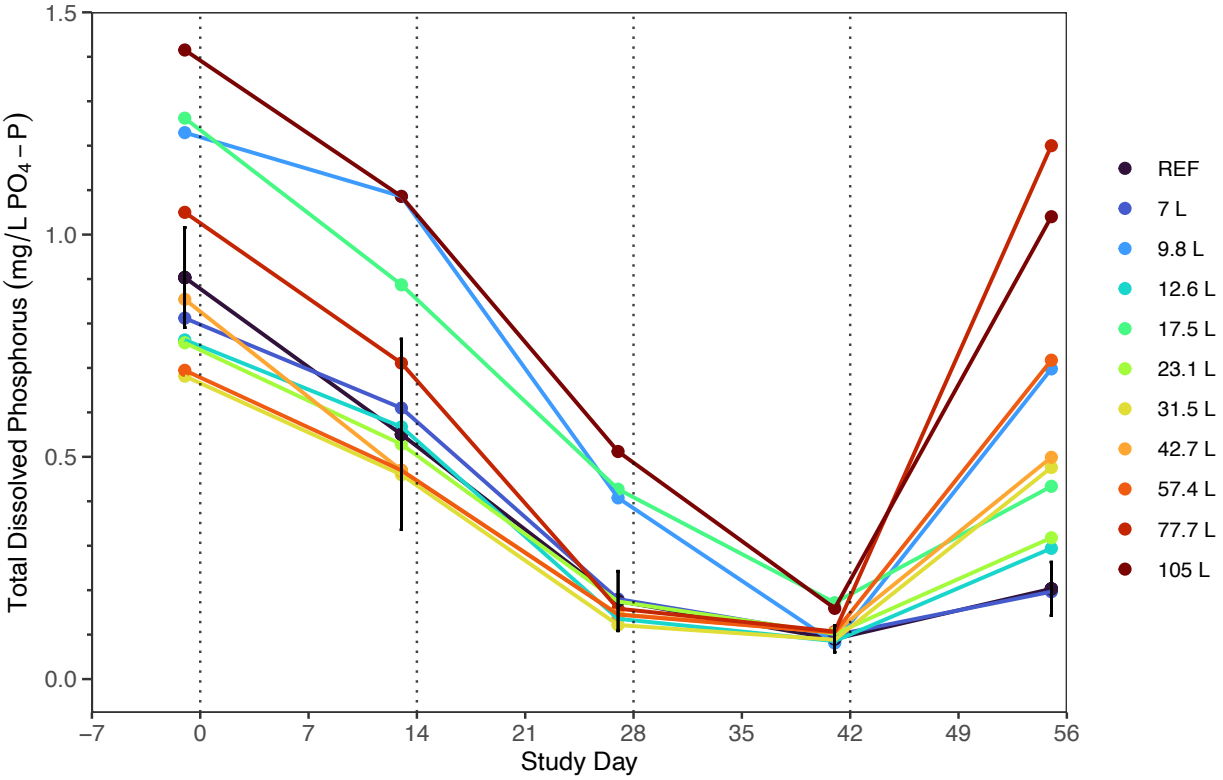

Appendix Figure B-7: Total dissolved phosphorus (mg/L PO_4-P) over the study duration within the RL commercial wild rice mesocosms. The vertical dotted lines represent AWW addition days. REF displays the mean of the references (n = 5) with the error bars representing ± standard deviation.

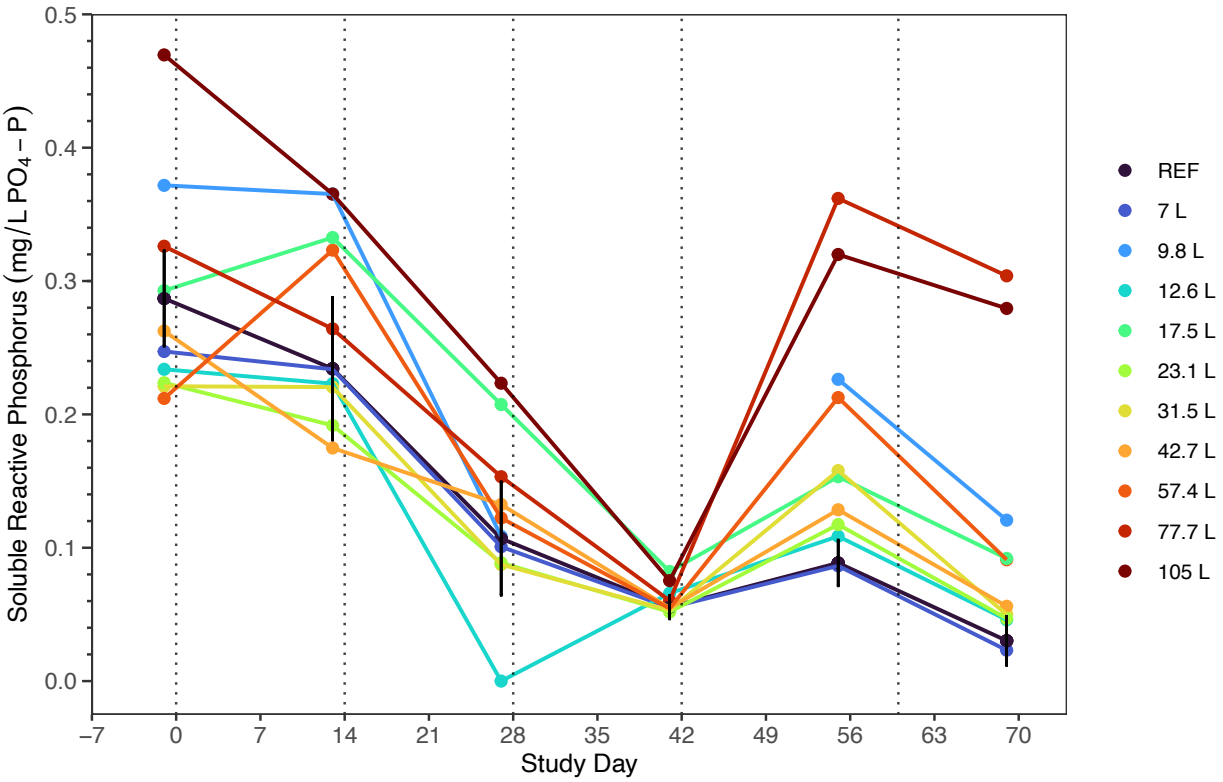

Appendix Figure B-8: Soluble reactive phosphorus (mg/L PO_4-P) over the study duration within the RL commercial wild rice mesocosms. The vertical dotted lines represent AWW addition days. REF displays the mean of the references (n = 5) with the error bars representing ± standard deviation.

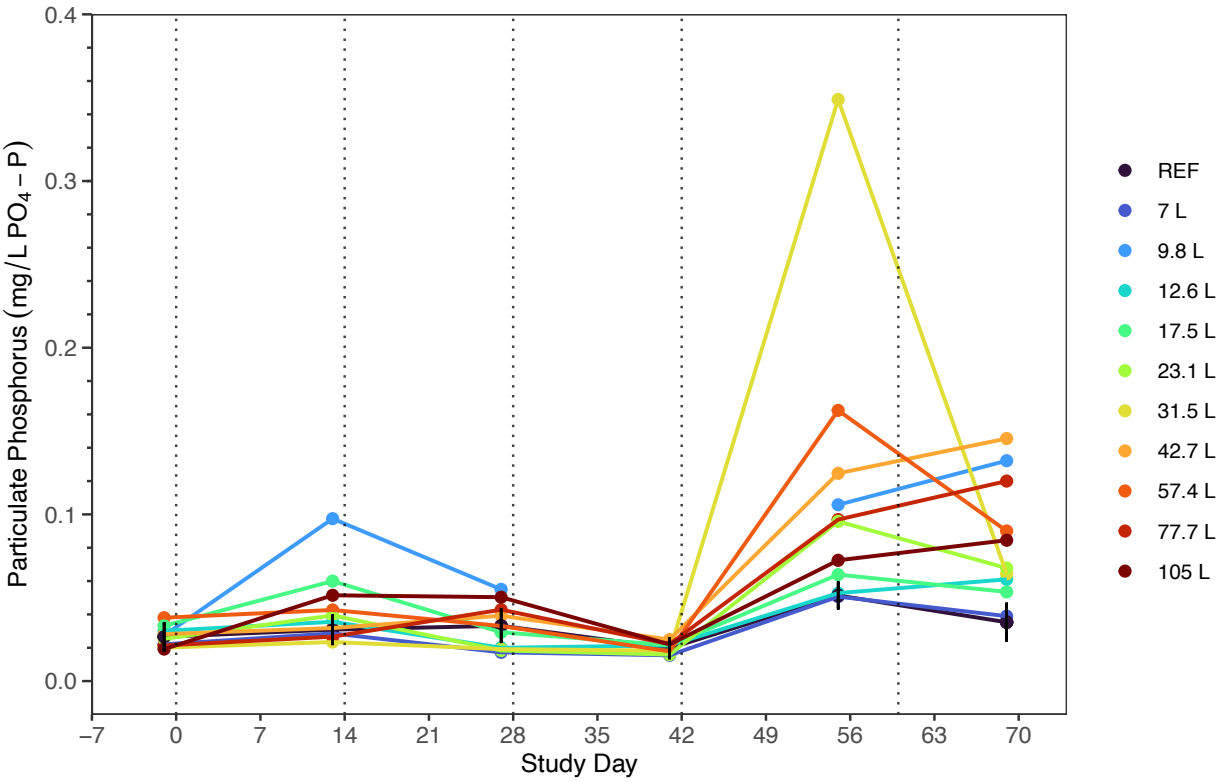

Appendix Figure B-9: Particulate phosphorus (mg/L PO_4-P) over the study duration within the RL commercial wild rice mesocosms. The vertical dotted lines represent AWW addition days. REF displays the mean of the references (n = 5) with the error bars representing ± standard deviation.

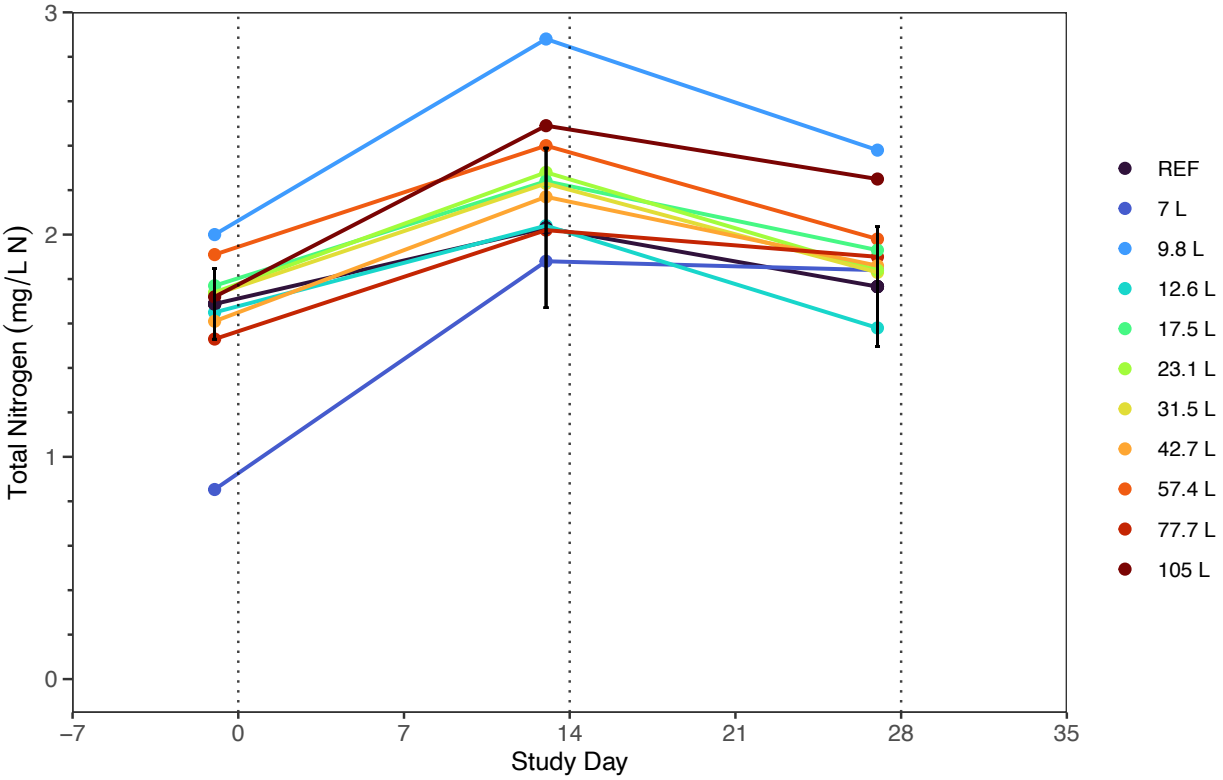

Appendix Figure B-10: Total nitrogen (mg/L N) over the study duration within the RL commercial wild rice mesocosms. The vertical dotted lines represent AWW addition days. REF displays the mean of the references (n = 5) with the error bars representing ± standard deviation.

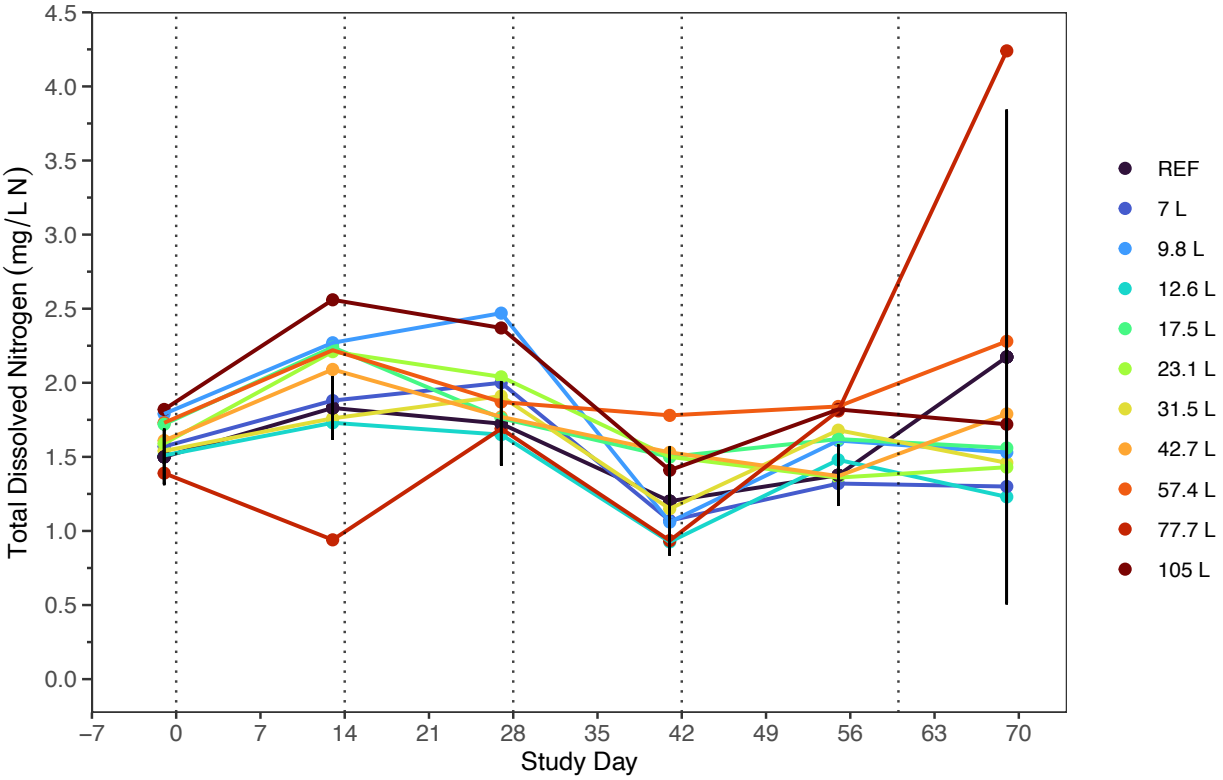

Appendix Figure B-11: Total dissolved nitrogen (mg/L N) over the study duration within the RL commercial wild rice mesocosms. The vertical dotted lines represent AWW addition days. REF displays the mean of the references (n = 5) with the error bars representing ± standard deviation.

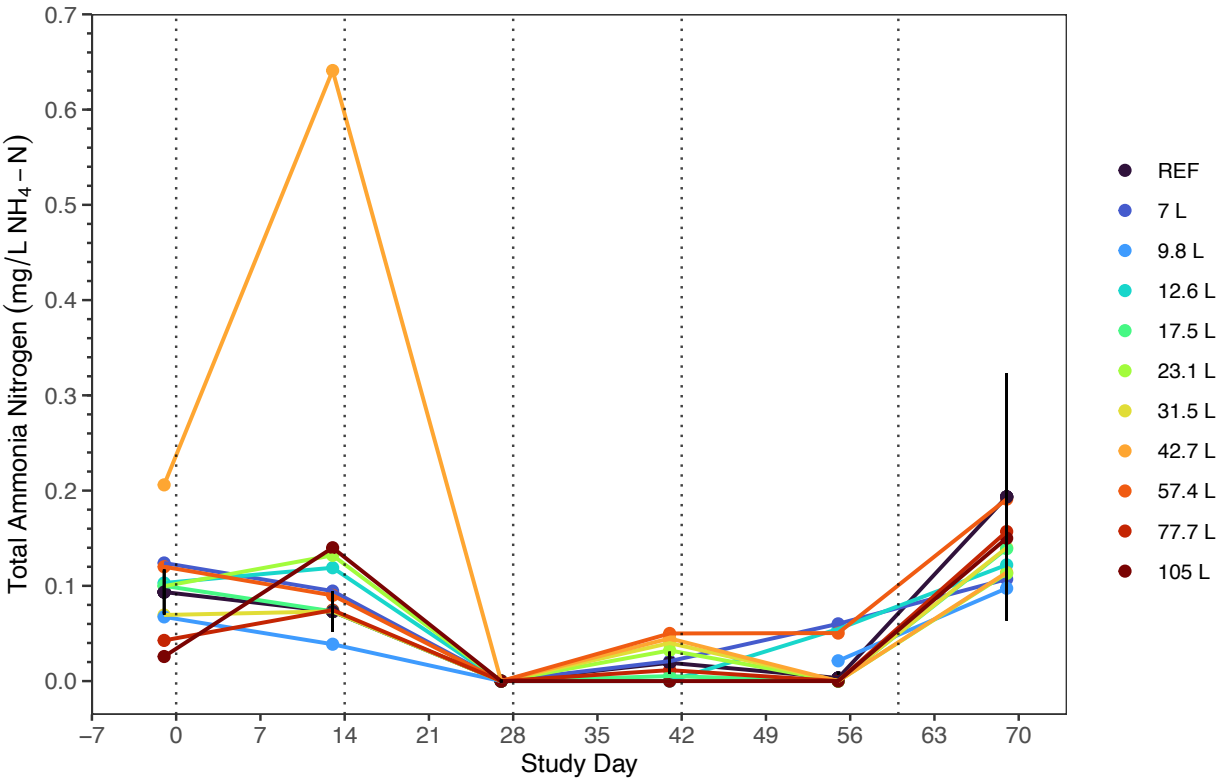

Appendix Figure B-12: Total ammonia nitrogen (mg/L NH_4-N) over the study duration within the RL commercial wild rice mesocosms. The vertical dotted lines represent AWW addition days. REF displays the mean of the references (n = 5) with the error bars representing ± standard deviation.

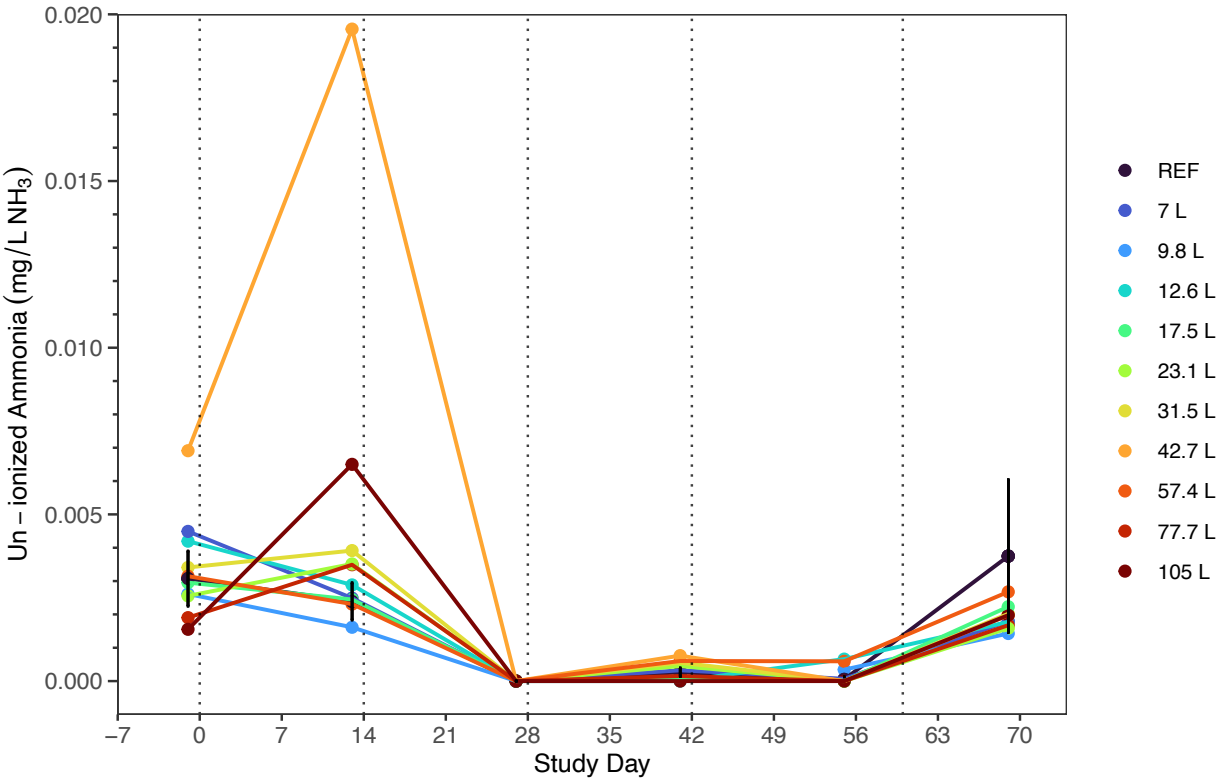

Appendix Figure B-13: Un-ionized ammonia (mg/L NH_3) over the study duration within the RL commercial wild rice mesocosms. The vertical dotted lines represent AWW addition days. These values were calculated from TAN, pH, and temperature, from the calculation in Armstrong et al. (2012) and Delos and Erickson (1999) (see methods for more detail). REF displays the mean of the references (n = 5) with the error bars representing ± standard deviation.

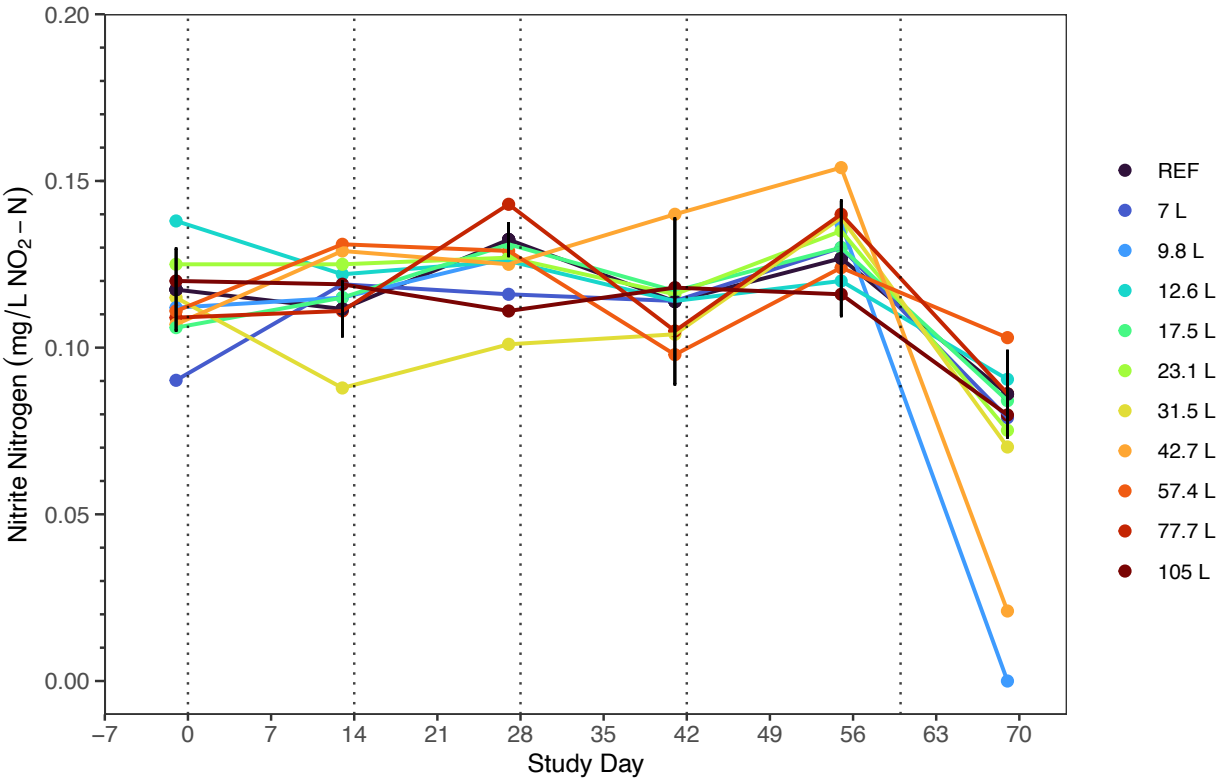

Appendix Figure B-14: Nitrite nitrogen (mg/L NO_2-N) over the study duration within the RL commercial wild rice mesocosms. The vertical dotted lines represent AWW addition days. REF displays the mean of the references (n = 5) with the error bars representing ± standard deviation.

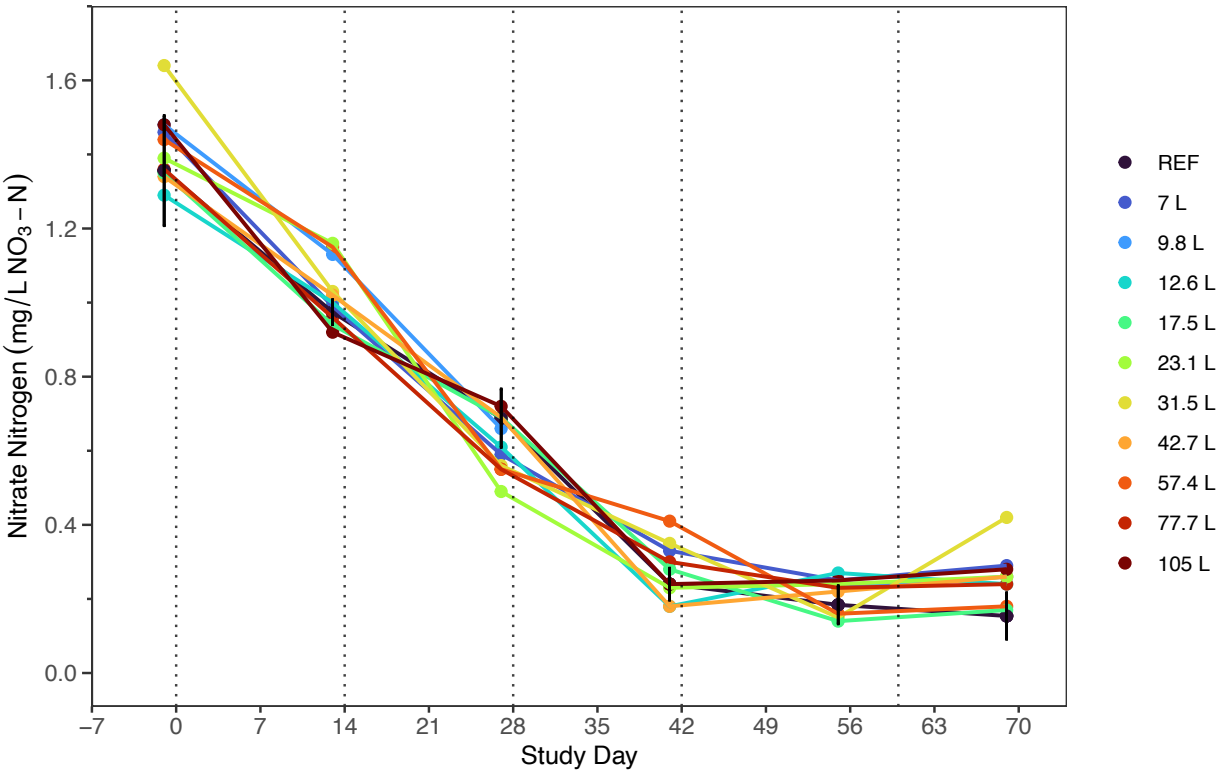

Appendix Figure B-15: Nitrate nitrogen (mg/L NO_3-N) over the study duration within the RL commercial wild rice mesocosms. The vertical dotted lines represent AWW addition days. REF displays the mean of the references (n = 5) with the error bars representing ± standard deviation.

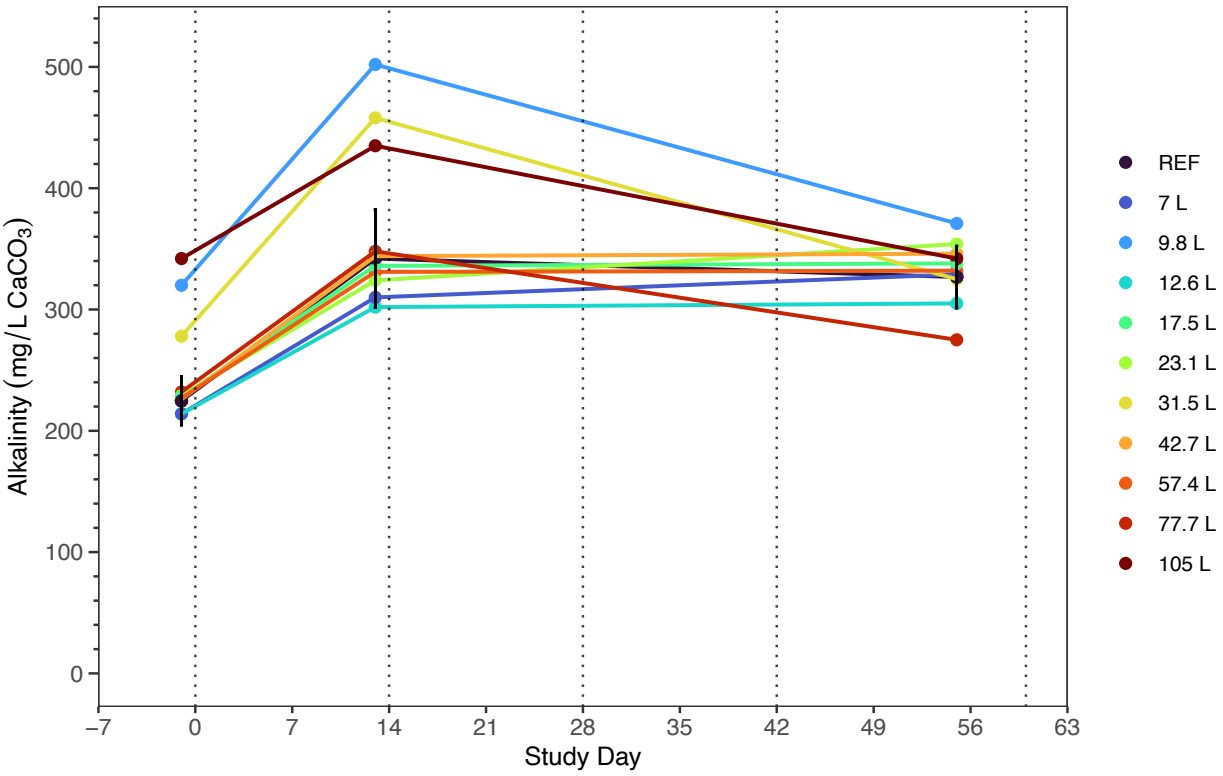

Appendix Figure B-16: Alkalinity (mg/L $CaCO_3$) over the study duration within the RL commercial wild rice mesocosms. The vertical dotted lines represent AWW addition days. REF displays the mean of the references (n = 5) with the error bars representing ± standard deviation.

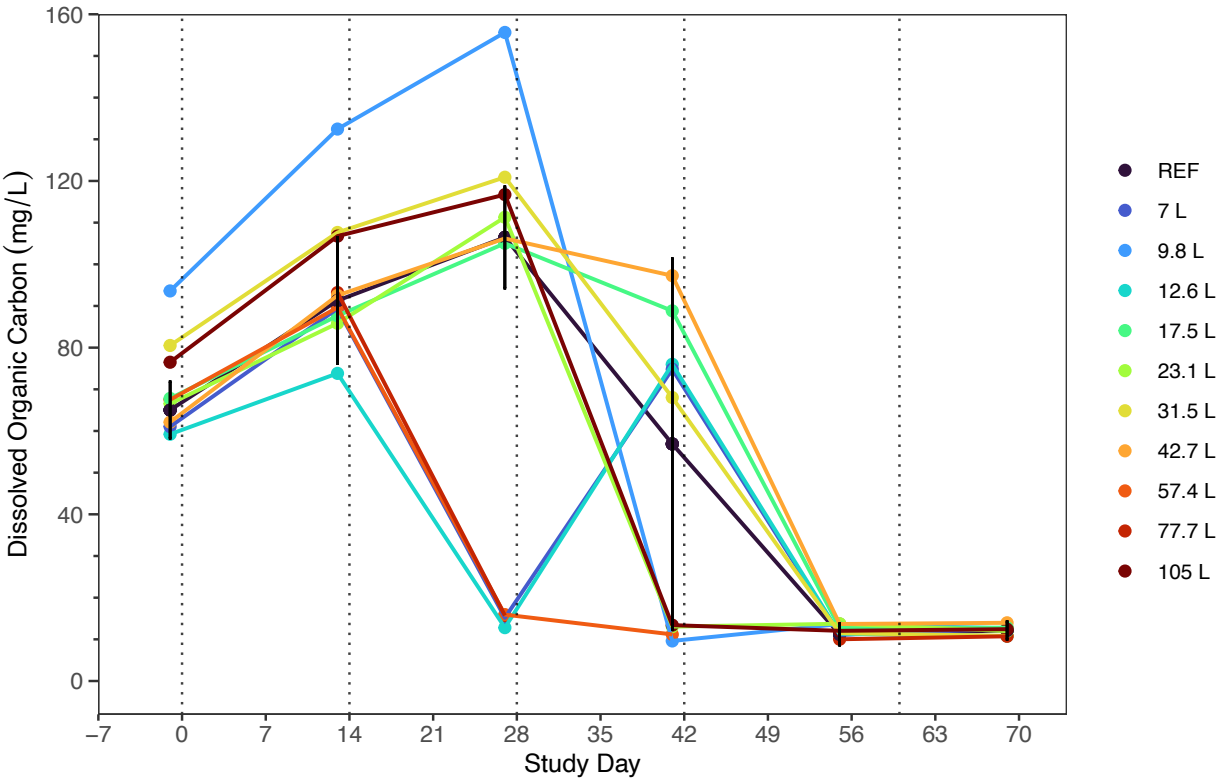

Appendix Figure B-17: Dissolved organic carbon (mg/L) over the study duration within the RL commercial wild rice mesocosms. The vertical dotted lines represent AWW addition days. REF displays the mean of the references (n = 5) with the error bars representing ± standard deviation.

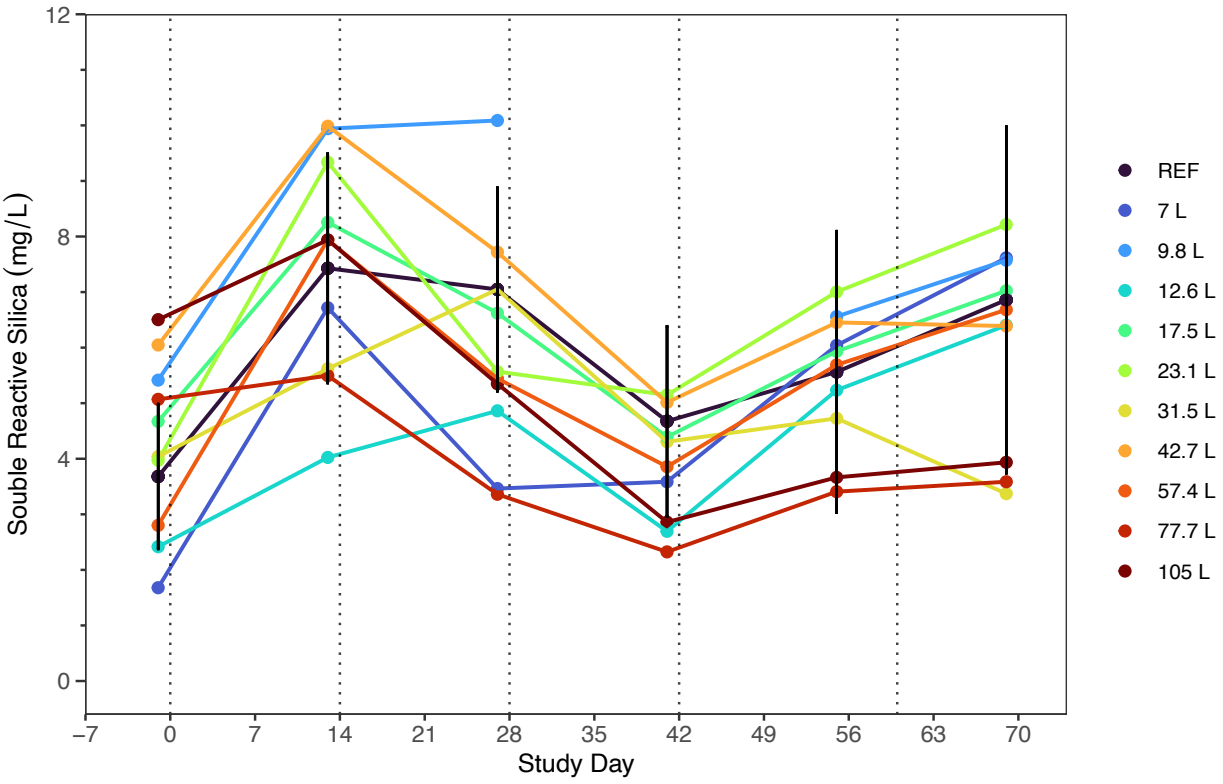

Appendix Figure B-18: Soluble reactive silica (mg/L) over the study duration within the RL commercial wild rice mesocosms. The vertical dotted lines represent AWW addition days. REF displays the mean of the references (n = 5) with the error bars representing ± standard deviation.

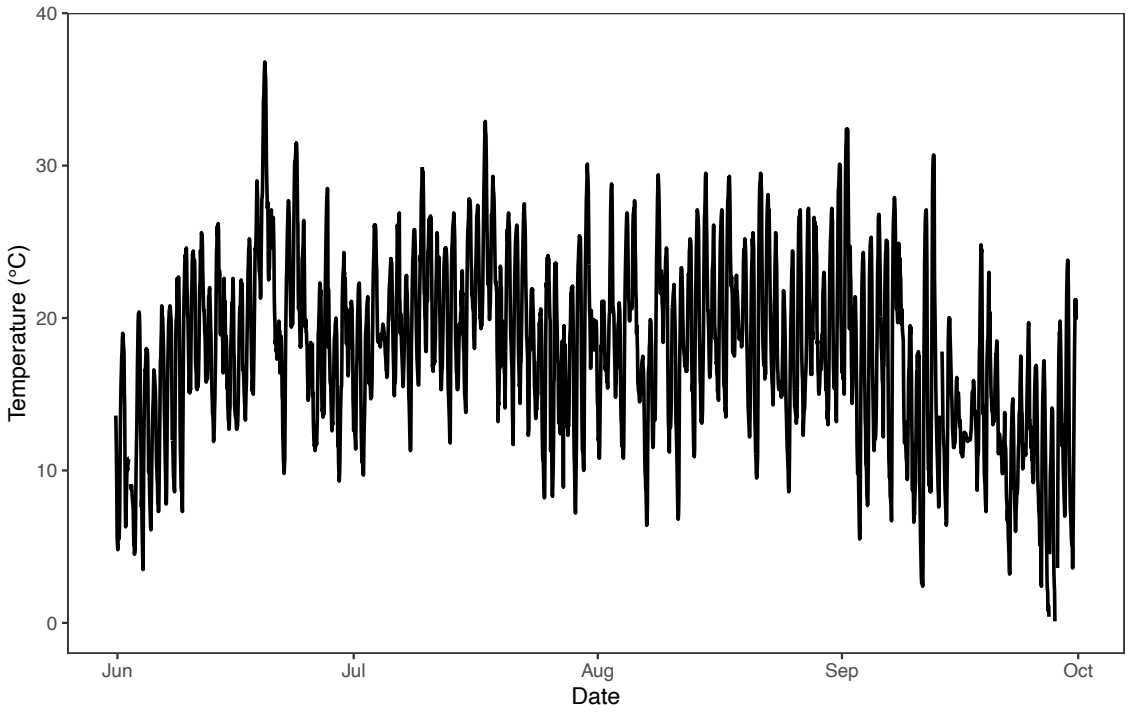

Appendix Figure B-19: Air temperature measured at the Environment Canada Carmen weather station from June to October.

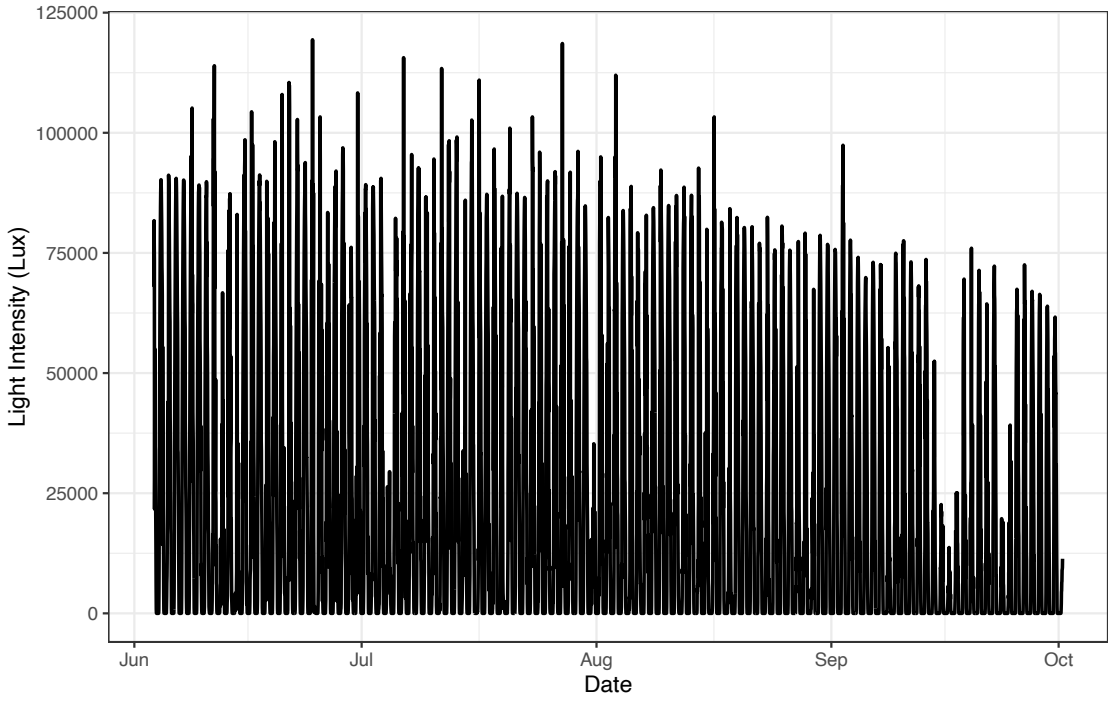

Appendix Figure B-20: Light intensity measured from June to October at the RL site.

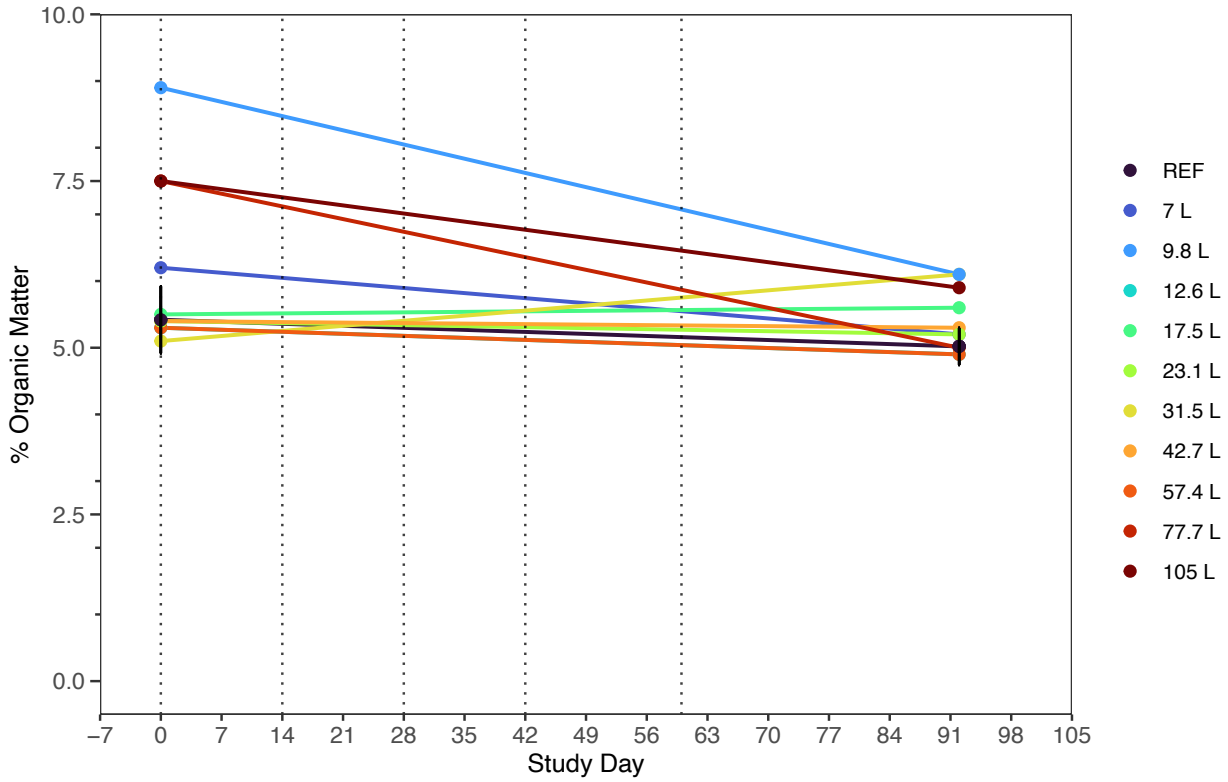

Appendix Figure B-21: Soil organic matter (%) over the study duration within the RL commercial wild rice mesocosms. The vertical dotted lines represent AWW addition days. REF displays the mean of the references (n = 5) with the error bars representing ± standard deviation.

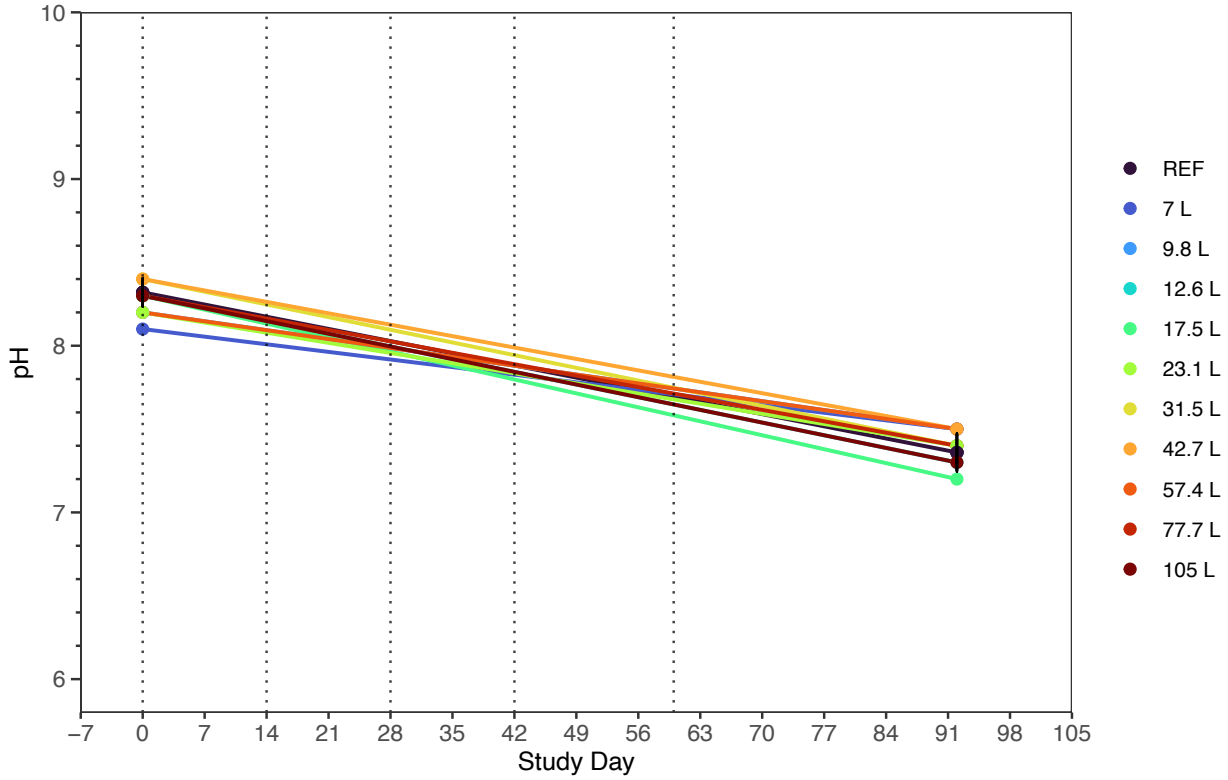

Appendix Figure B-22: Soil pH over the study duration within the RL commercial wild rice mesocosms. The vertical dotted lines represent AWW addition days. REF displays the mean of the references (n = 5) with the error bars representing ± standard deviation.

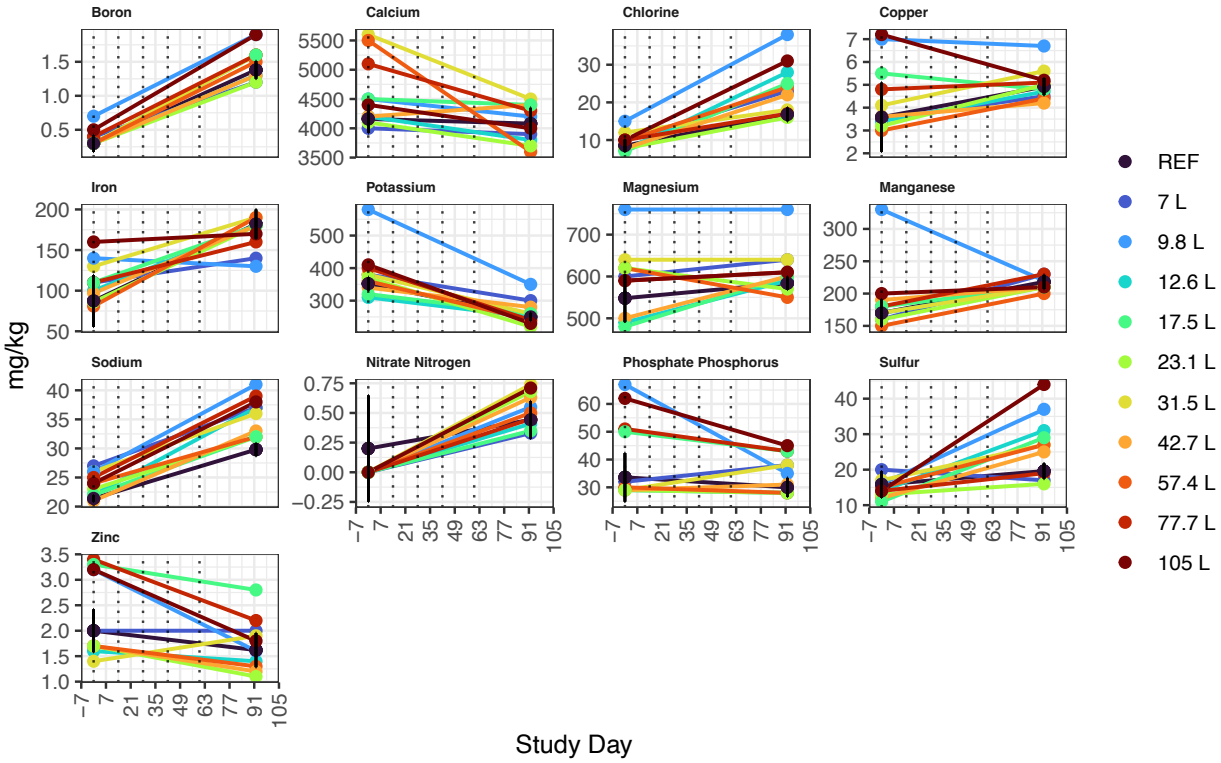

Appendix Figure B-23: Soil ions (mg/kg) over the study duration within the RL commercial wild rice mesocosms. The vertical dotted lines represent AWW addition days. REF displays the mean of the references (n = 5) with the error bars representing ± standard deviation.

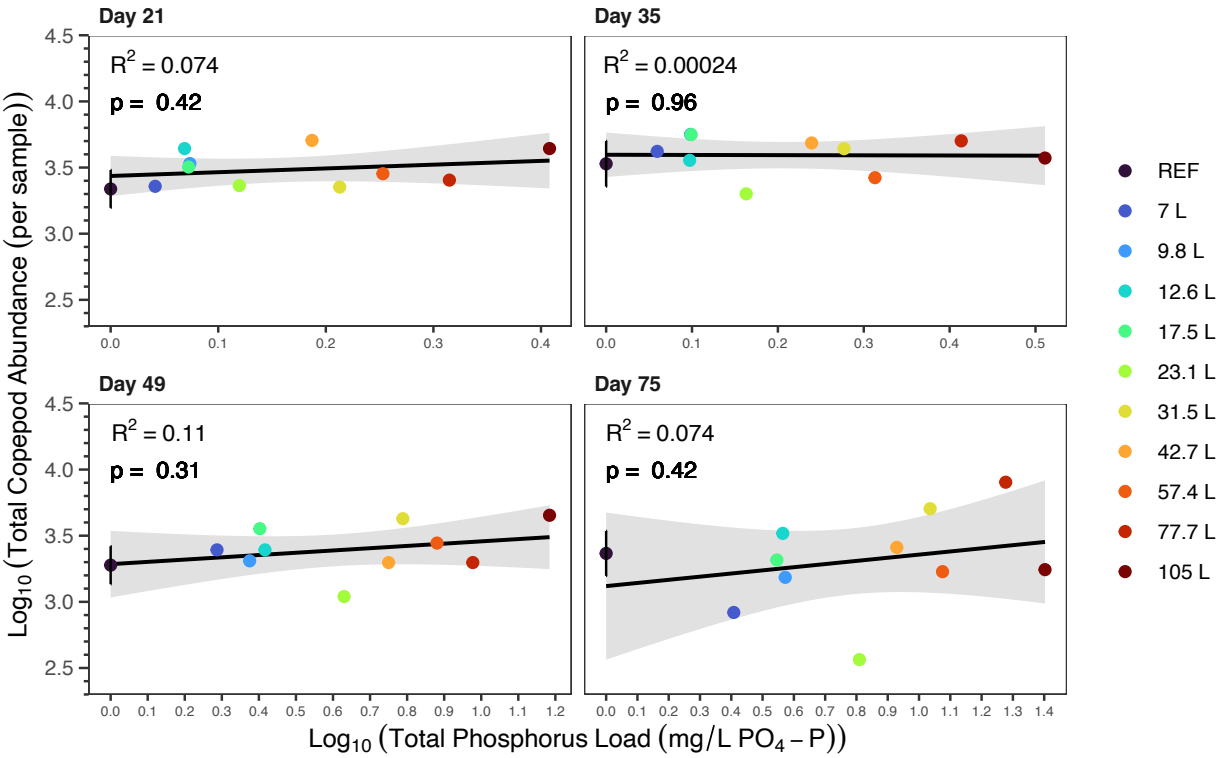

Appendix Figure B-24: Linear regression model results of the relationship between log10(x + 1) of cumulative AWW load concentration (TP used as the representative variable) and total copepod abundance. REF displays the mean of the references (n = 5) with the error bars representing ± standard deviation. Each plot displays the model results according to study day.

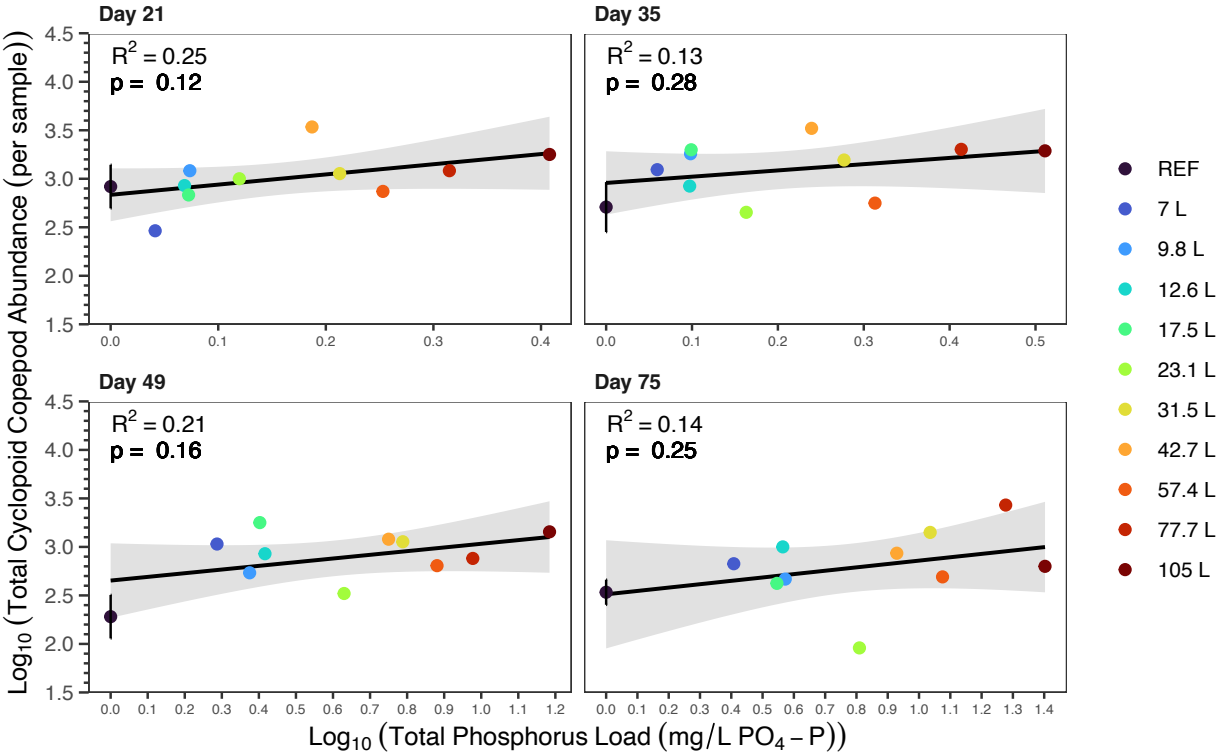

Appendix Figure B-25: Linear regression model results of the relationship between log10(x + 1) of cumulative AWW load concentration (TP used as the representative variable) and cyclopoid copepod abundance. REF displays the mean of the references (n = 5) with the error bars representing ± standard deviation. Each plot displays the model results according to study day.

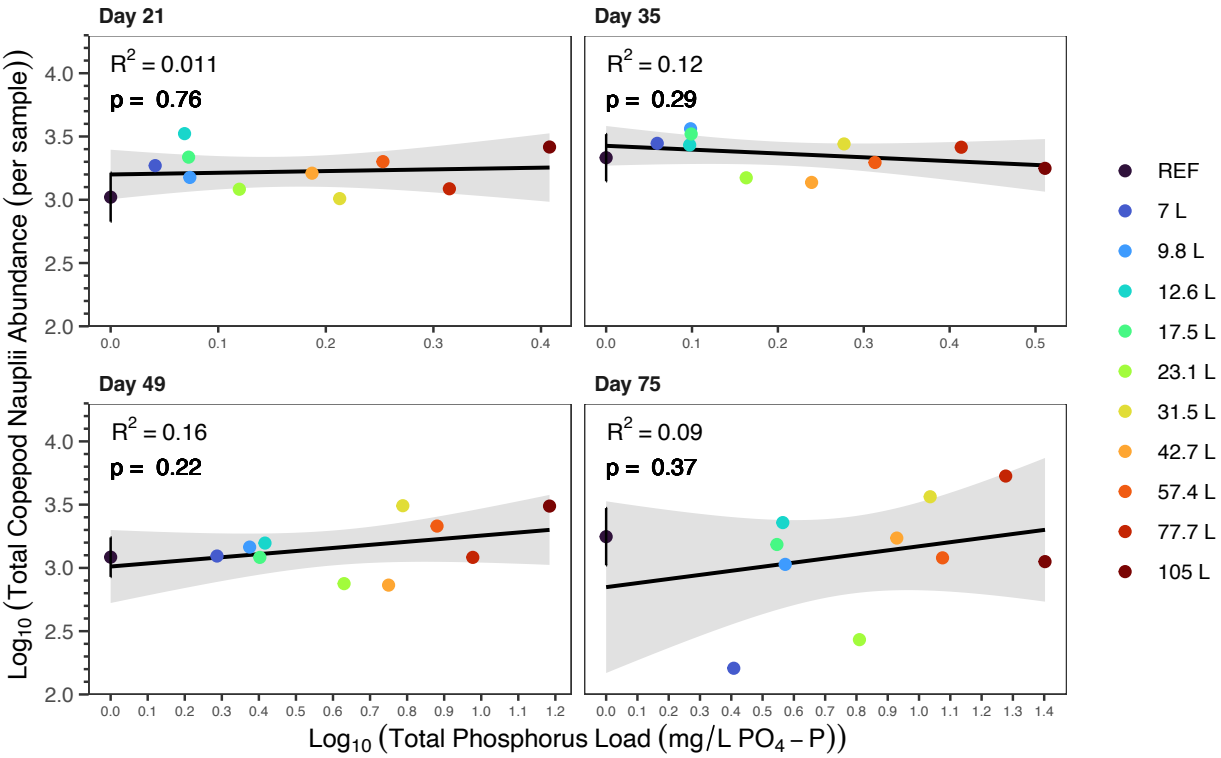

Appendix Figure B-26: Linear regression model results of the relationship between log10(x + 1) of cumulative AWW load concentration (TP used as the representative variable) and copepod nauplii abundance. REF displays the mean of the references (n = 5) with the error bars representing ± standard deviation. Each plot displays the model results according to study day.

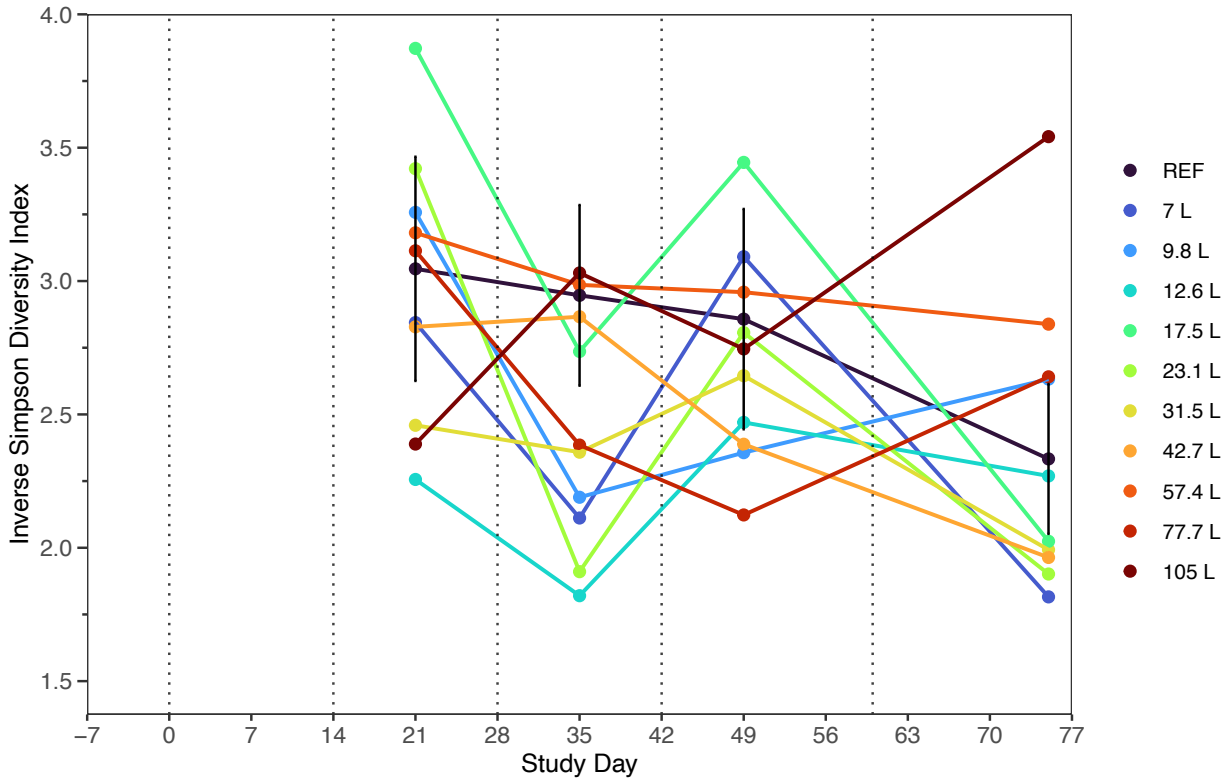

Appendix Figure B-27: Inverse Simpson Diversity over the study duration within the RL commercial wild rice mesocosms. The vertical dotted lines represent AWW addition days. REF displays the mean of the references (n = 5) with the error bars representing ± standard deviation.

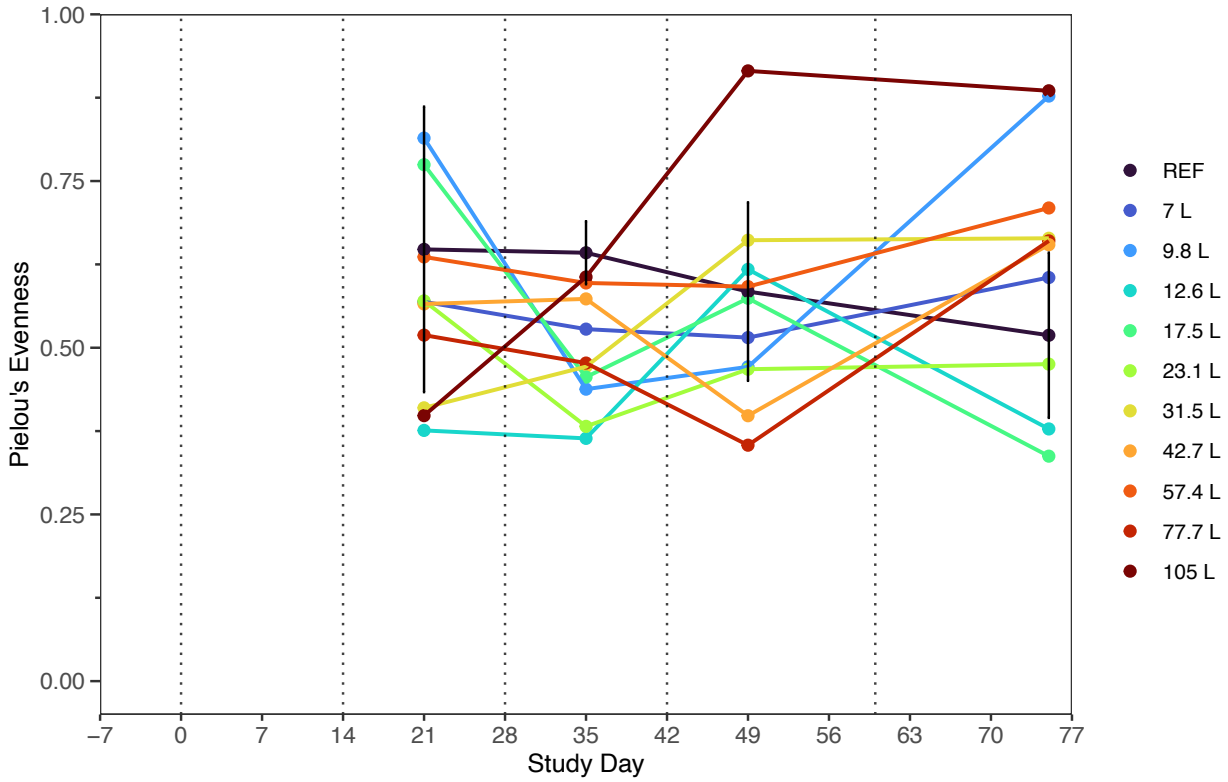

Appendix Figure B-28: Pielou's evenness over the study duration within the RL commercial wild rice mesocosms. The vertical dotted lines represent AWW addition days. REF displays the mean of the references (n = 5) with the error bars representing ± standard deviation.

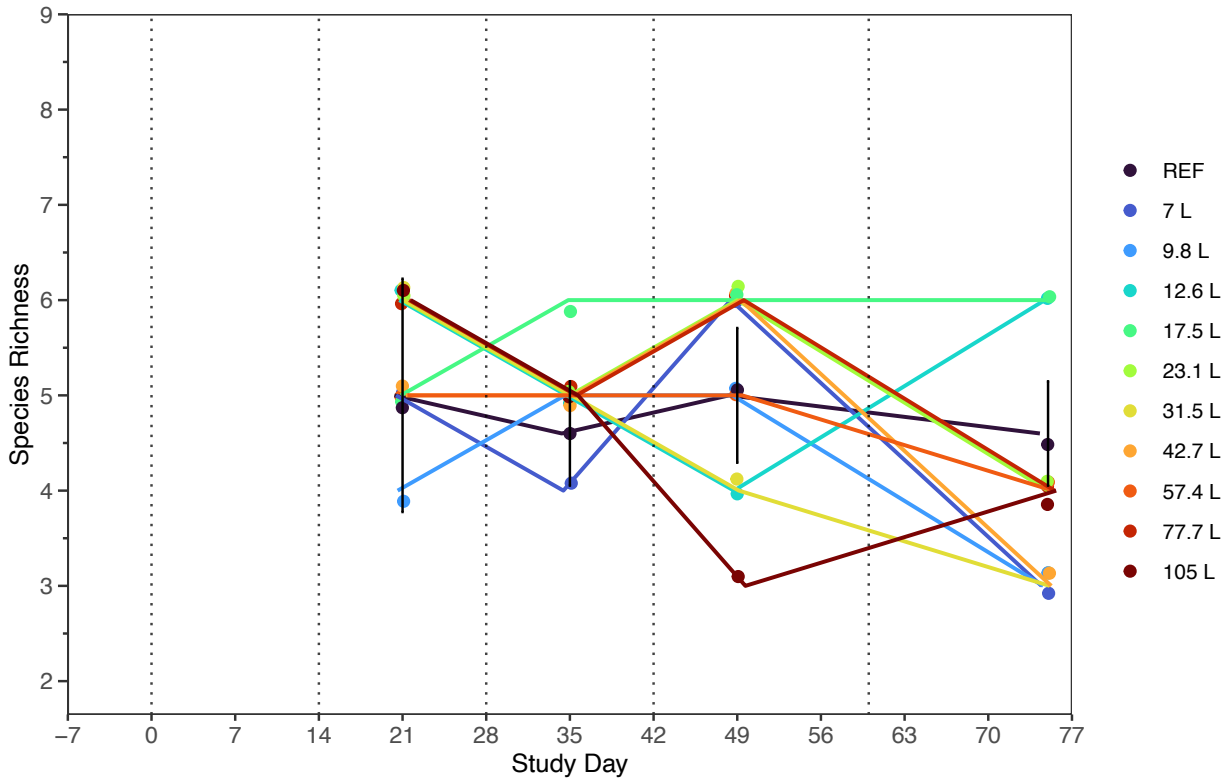

Appendix Figure B-29: Species richness over the study duration within the RL commercial wild rice mesocosms. The vertical dotted lines represent AWW addition days. REF displays the mean of the references (n = 5) with the error bars representing ± standard deviation.

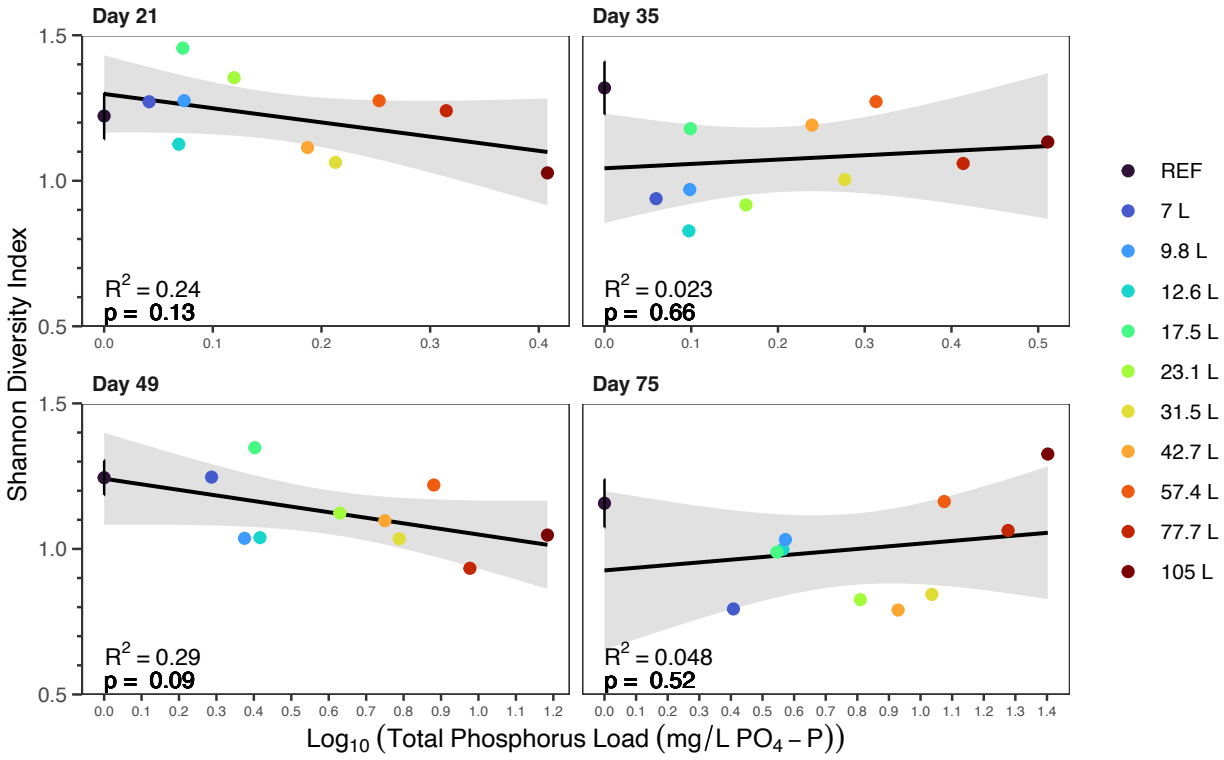

Appendix Figure B-30: Linear regression model results of the relationship between log10(x + 1) of cumulative AWW load concentration (TP used as the representative variable) and Shannon diversity. REF displays the mean of the references (n = 5) with the error bars representing ± standard deviation. Each plot displays the model results according to study day.

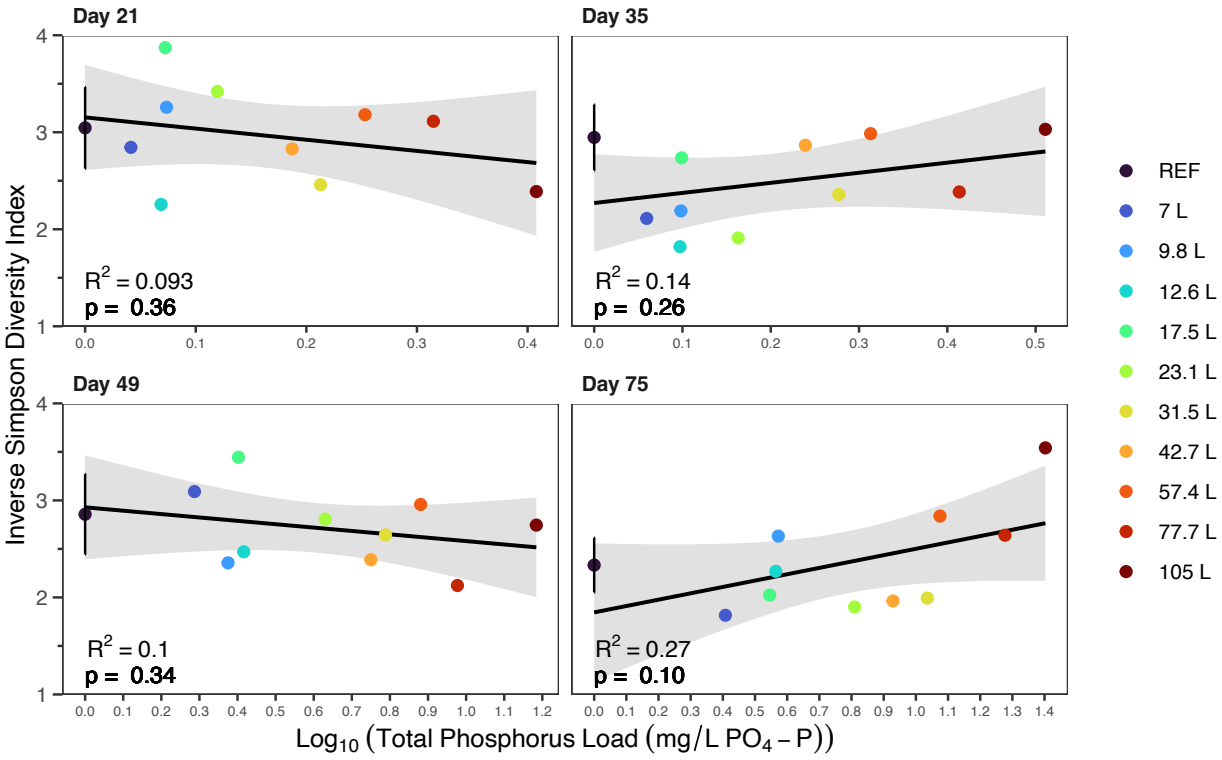

Appendix Figure B-31: Linear regression model results of the relationship between log10(x + 1) of cumulative AWW load concentration (TP used as the representative variable) and Inverse Simpson diversity. REF displays the mean of the references (n = 5) with the error bars representing ± standard deviation. Each plot displays the model results according to study day.

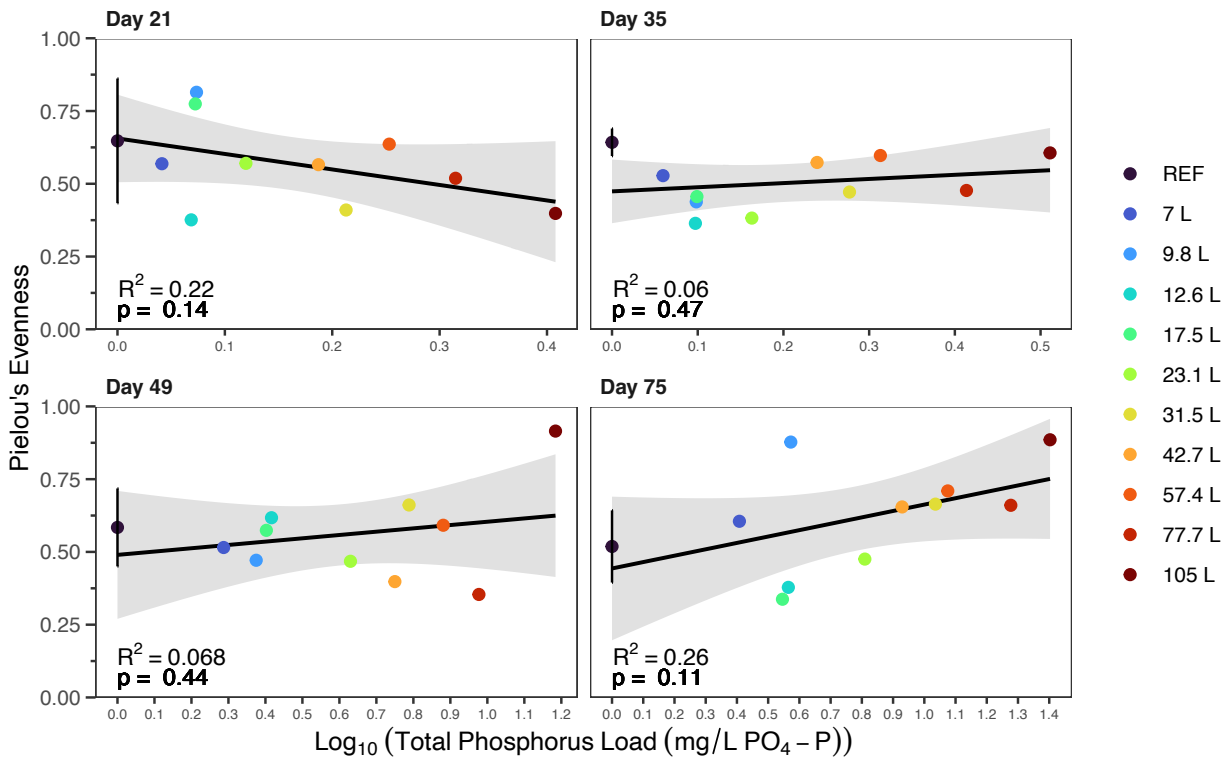

Appendix Figure B-32: Linear regression model results of the relationship between log10(x + 1) of cumulative AWW load concentration (TP used as the representative variable) and Pielous's evenness. REF displays the mean of the references (n = 5) with the error bars representing ± standard deviation. Each plot displays the model results on according to study day.

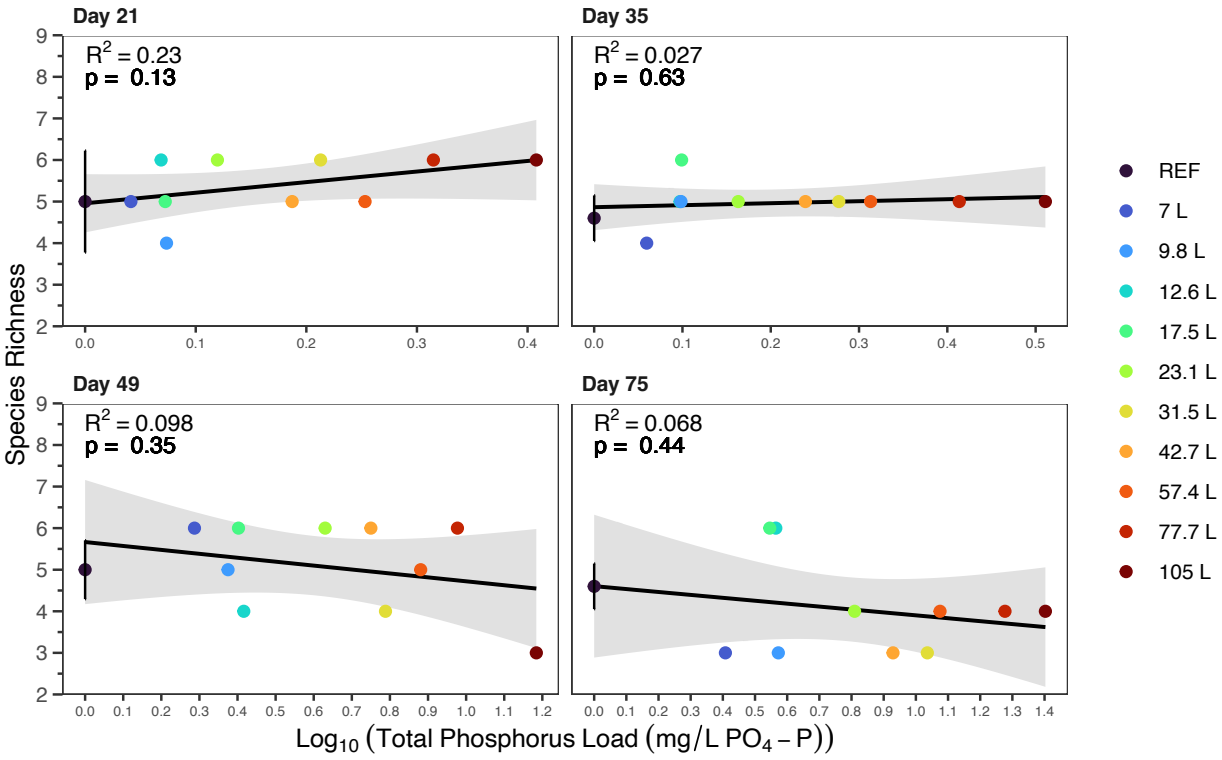

Appendix Figure B-33: Linear regression model results of the relationship between log10(x + 1) of cumulative AWW load concentration (TP used as the representative variable) and species richness. REF displays the mean of the references (n = 5) with the error bars representing ± standard deviation. Each plot displays the model results on according to study day.

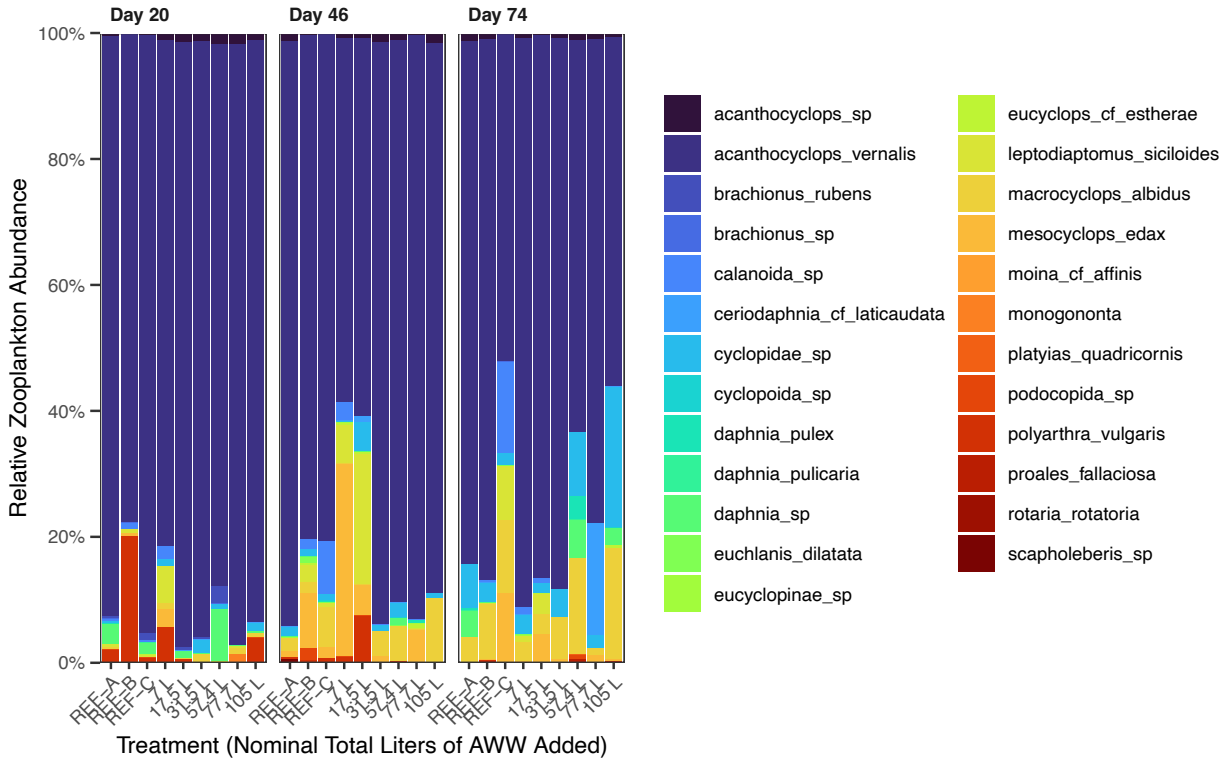

Appendix Figure B-34: The relative abundance (%) of each zooplankton taxa using the Leray primer.

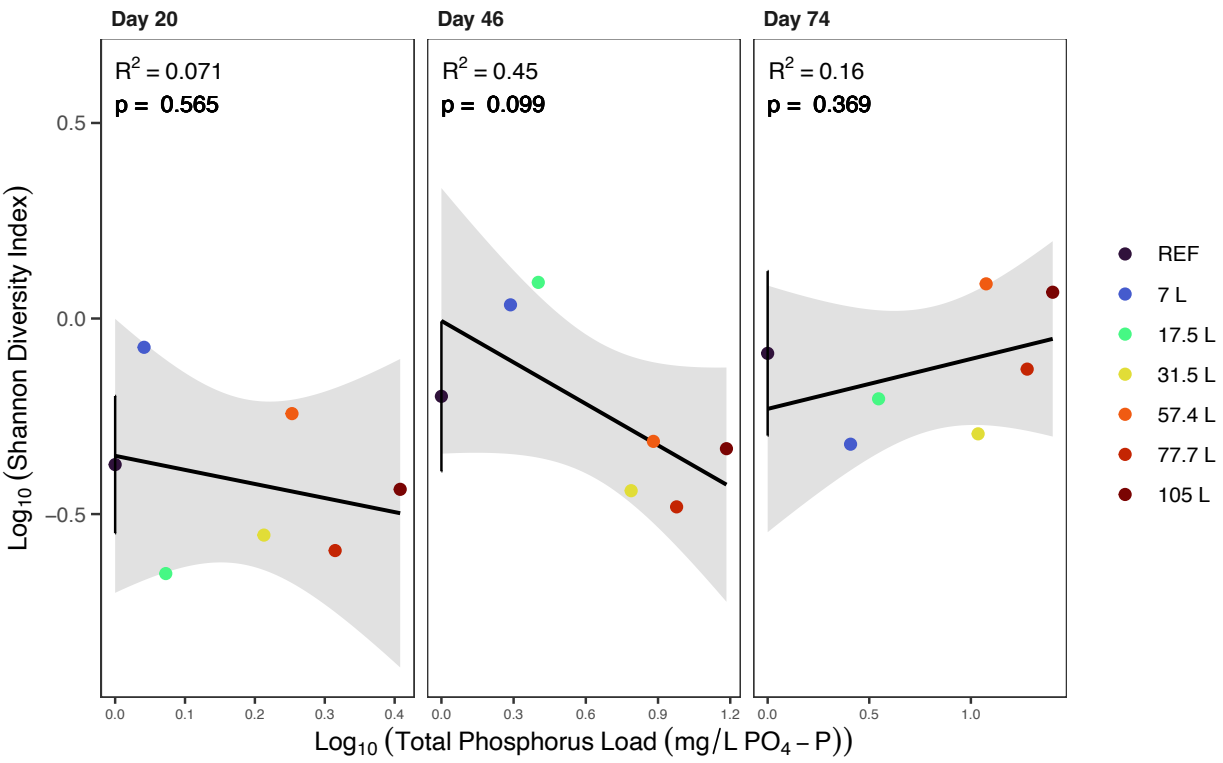

Appendix Figure B-35: Linear regression model results of the relationship between log10(x + 1) of cumulative AWW load concentration (TP used as the representative variable) and Shannon Diversity Index. REF displays the mean of the references (n = 3) with the error bars representing ± standard deviation. Each plot displays the model results according to study day. The diversity data was calculated from eDNA reads from the Leray primer.

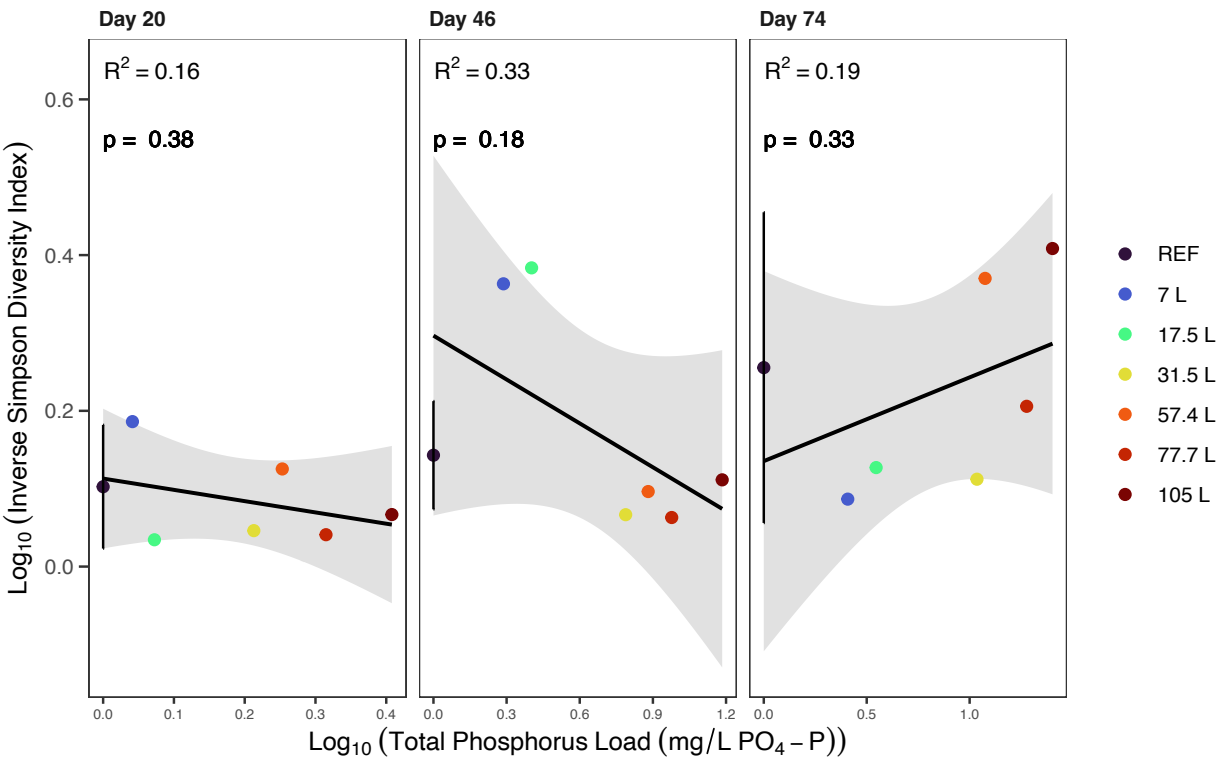

Appendix Figure B-36: Linear regression model results of the relationship between log10(x + 1) of cumulative AWW load concentration (TP used as the representative variable) and Inverse Simpson Diversity Index. REF displays the mean of the references (n = 3) with the error bars representing ± standard deviation. Each plot displays the model results according to study day. The diversity data was calculated from eDNA reads from the Leray primer.

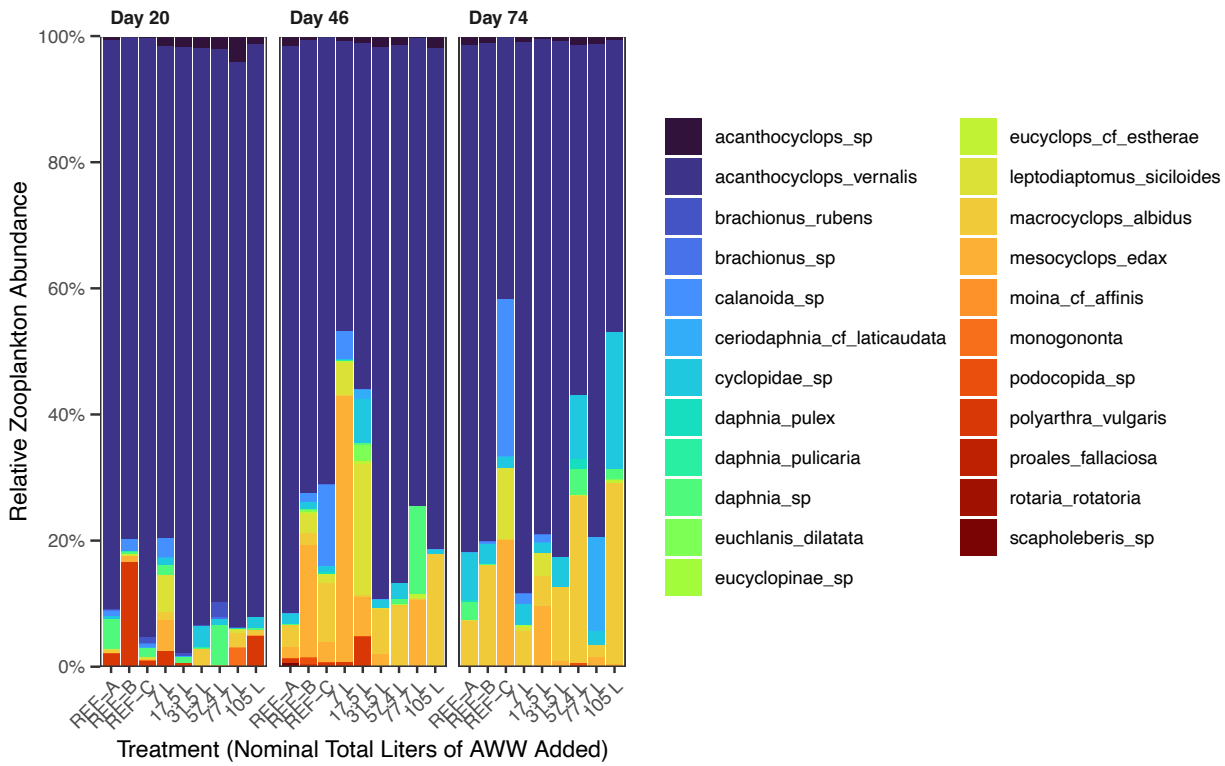

Appendix Figure B-37: The relative abundance (%) of each zooplankton taxa using the Copepod primer.

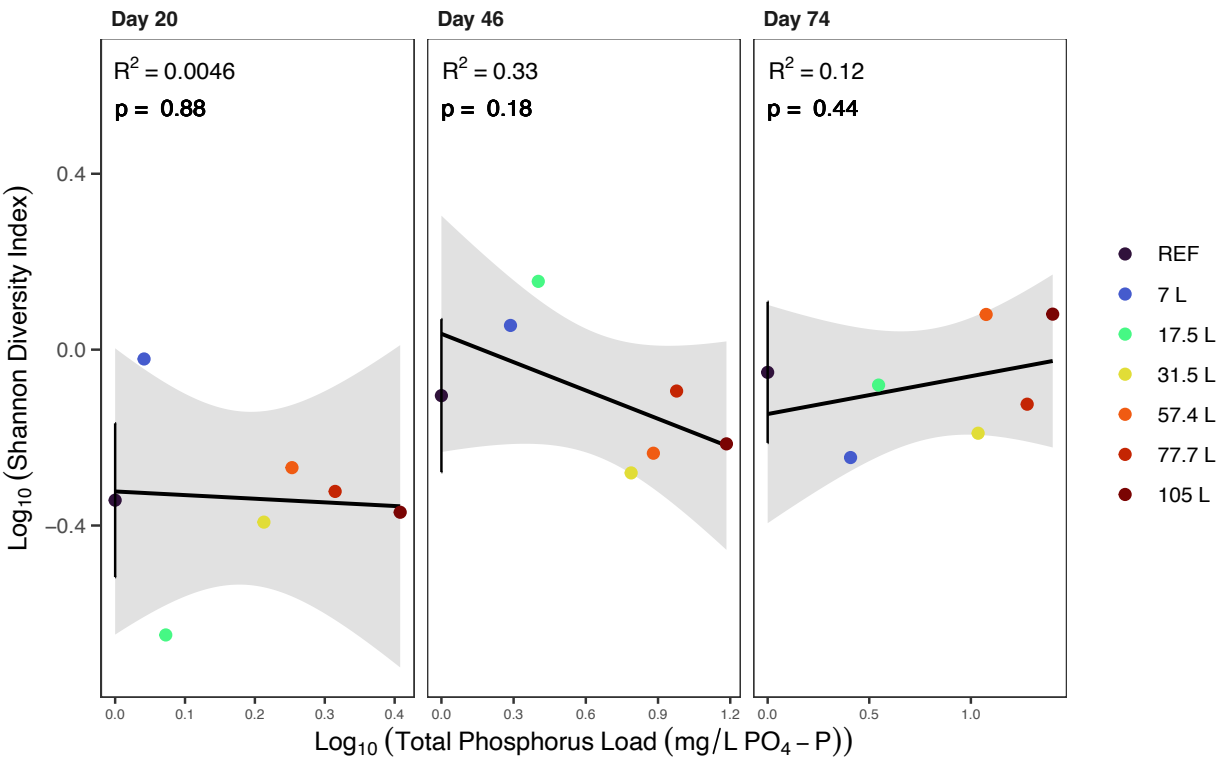

Appendix Figure B-38: Linear regression model results of the relationship between log10(x + 1) of cumulative AWW load concentration (TP used as the representative variable) and Shannon Diversity Index. REF displays the mean of the references (n = 3) with the error bars representing ± standard deviation. Each plot displays the model results according to study day. The diversity data was calculated from eDNA reads from the Copepod primer.

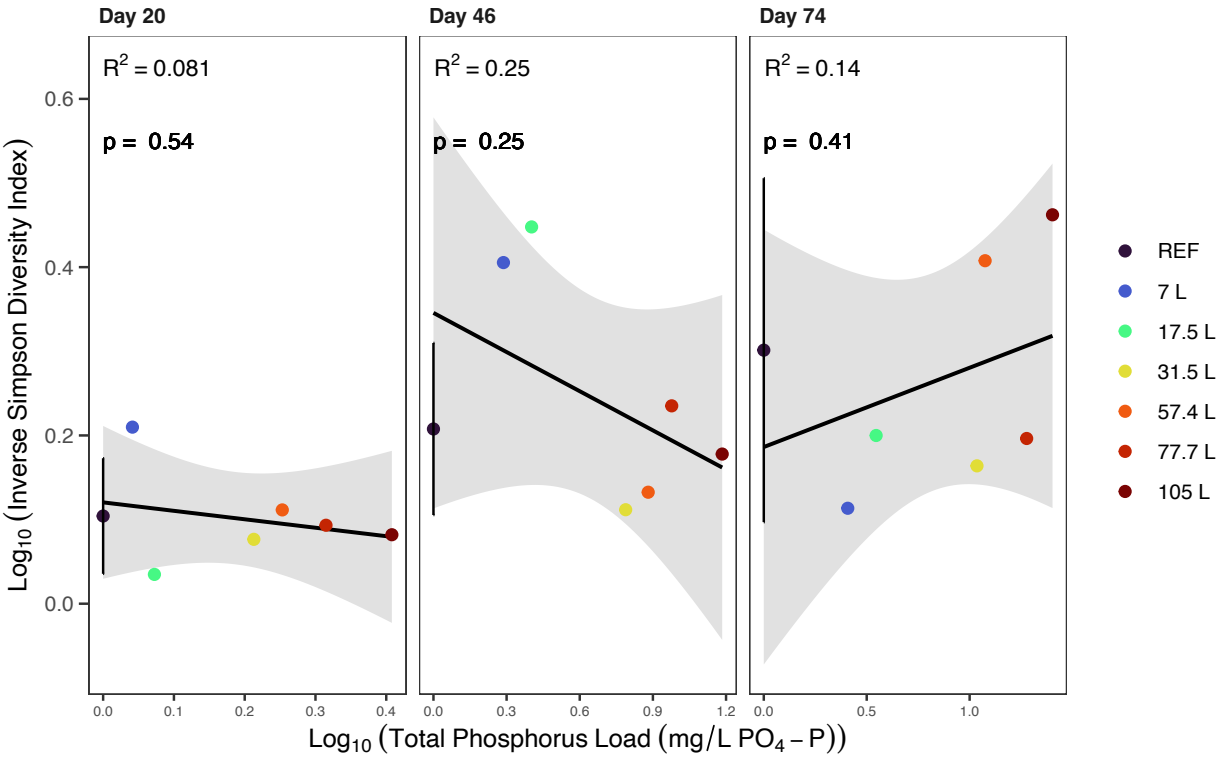

Appendix Figure B-39: Linear regression model results of the relationship between log10(x + 1) of cumulative AWW load concentration (TP used as the representative variable) and Inverse Simpson Diversity Index. REF displays the mean of the references (n = 3) with the error bars representing ± standard deviation. Each plot displays the model results according to study day. The diversity data was calculated from eDNA reads from the Copepod primer.

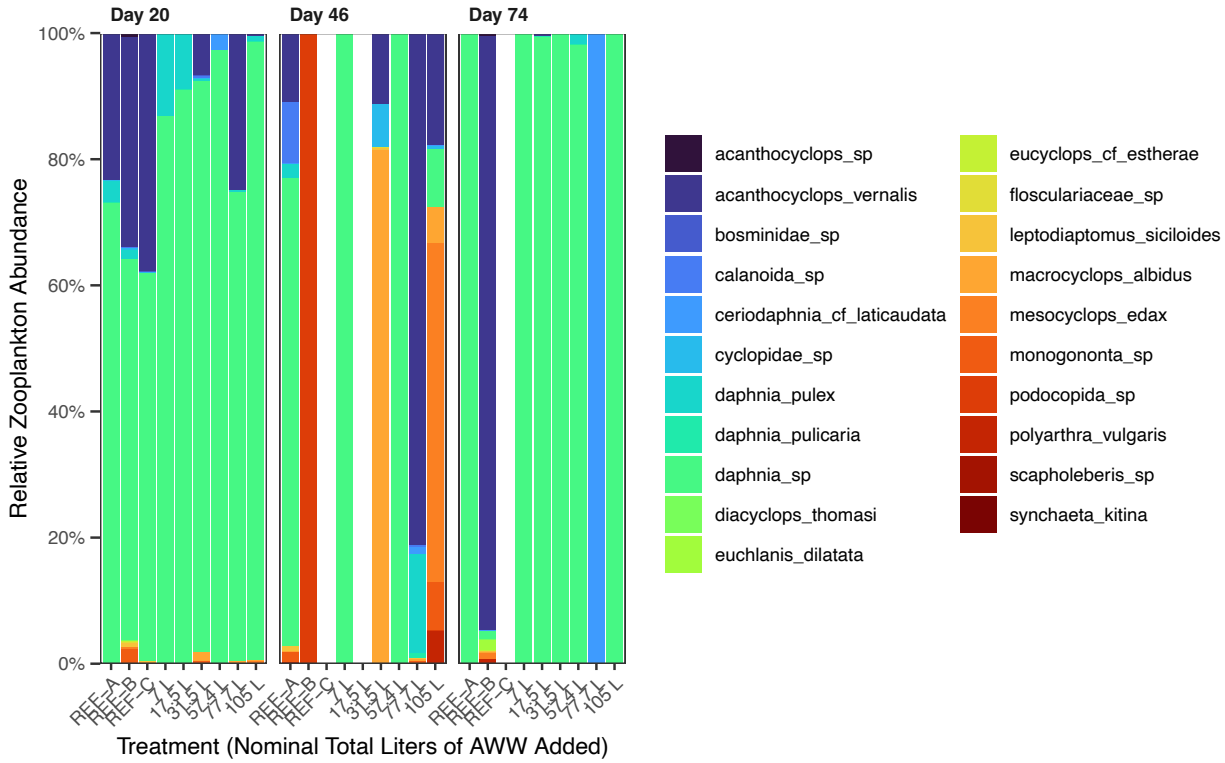

Appendix Figure B-40: The relative abundance (%) of each zooplankton taxa using the Daphnia primer.

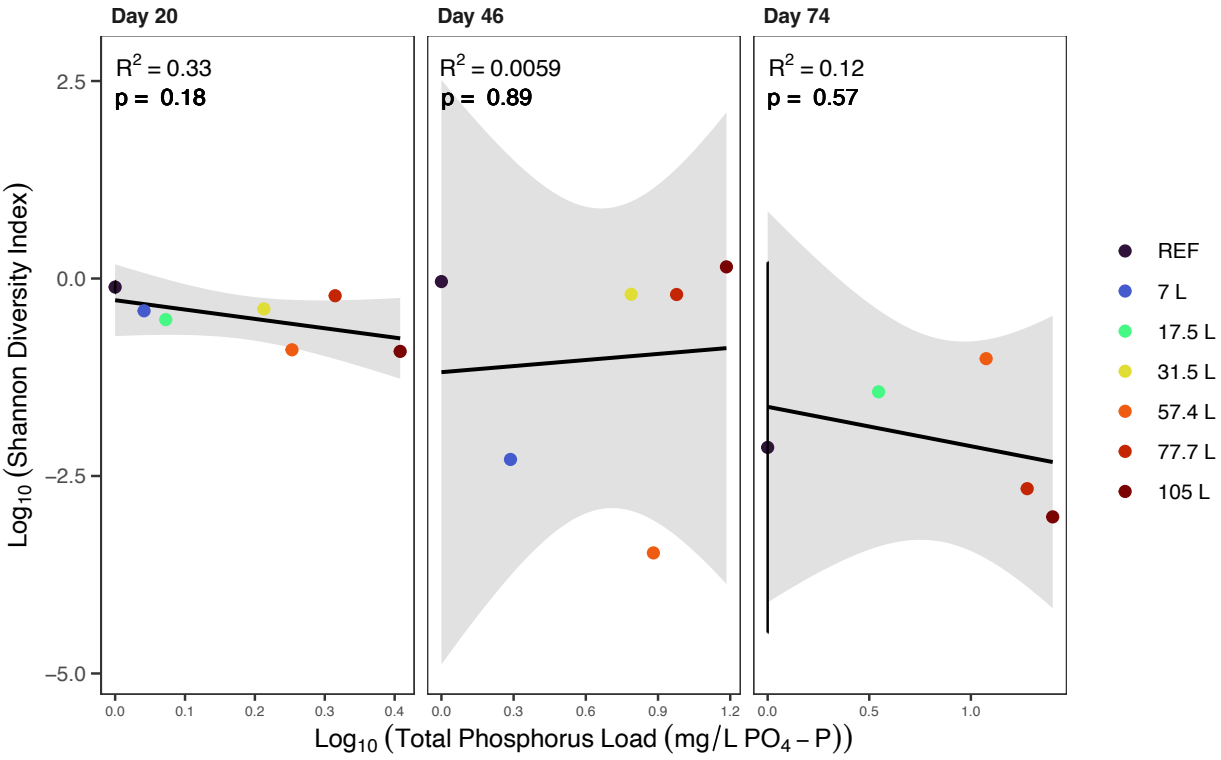

Appendix Figure B-41: Linear regression model results of the relationship between log10(x + 1) of cumulative AWW load concentration (TP used as the representative variable) and Shannon Diversity Index. REF displays the mean of the references (n = 3) with the error bars representing ± standard deviation. Each plot displays the model results according to study day. The diversity data was calculated from eDNA reads from the Daphnia primer.

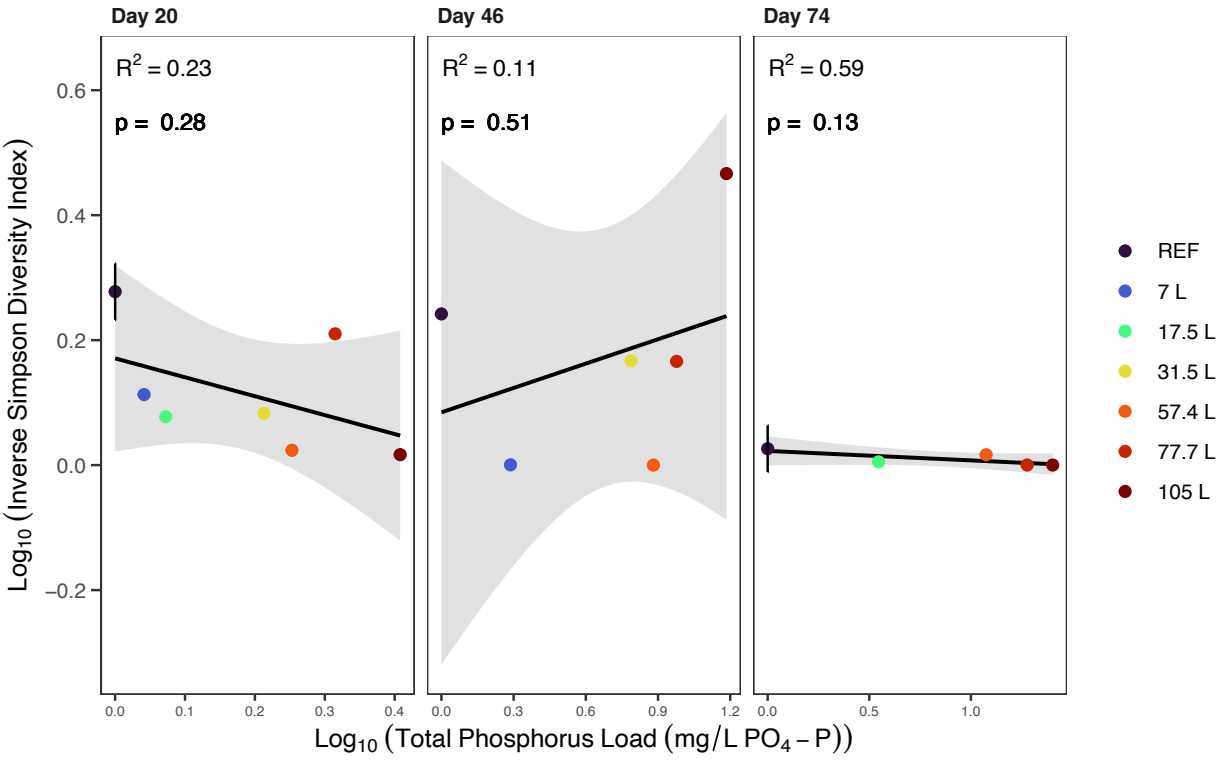

Appendix Figure B-42: Linear regression model results of the relationship between log10(x + 1) of cumulative AWW load concentration (TP used as the representative variable) and Inverse Simpson Diversity Index. REF displays the mean of the references (n = 3) with the error bars representing ± standard deviation. Each plot displays the model results according to study day. The diversity data was calculated from eDNA reads from the Daphnia primer.

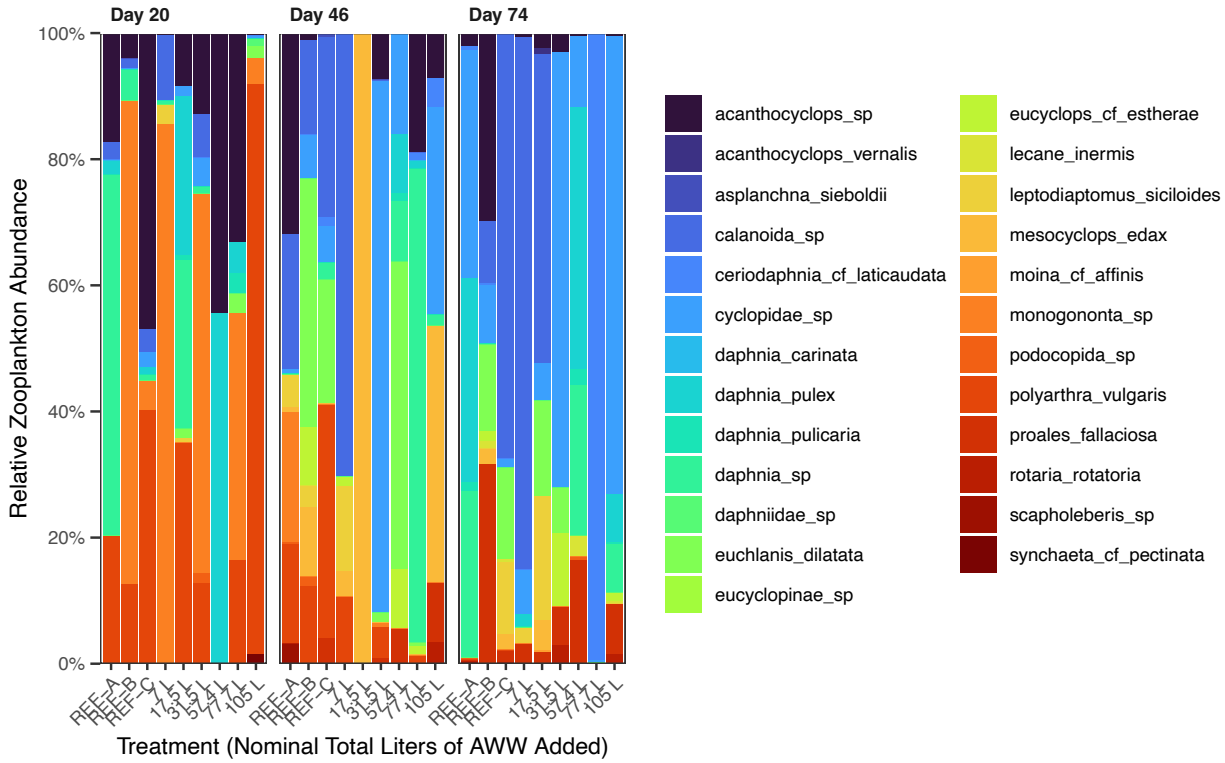

Appendix Figure B-43: The relative abundance (%) of each zooplankton taxa using the Rotifer 1 primer.

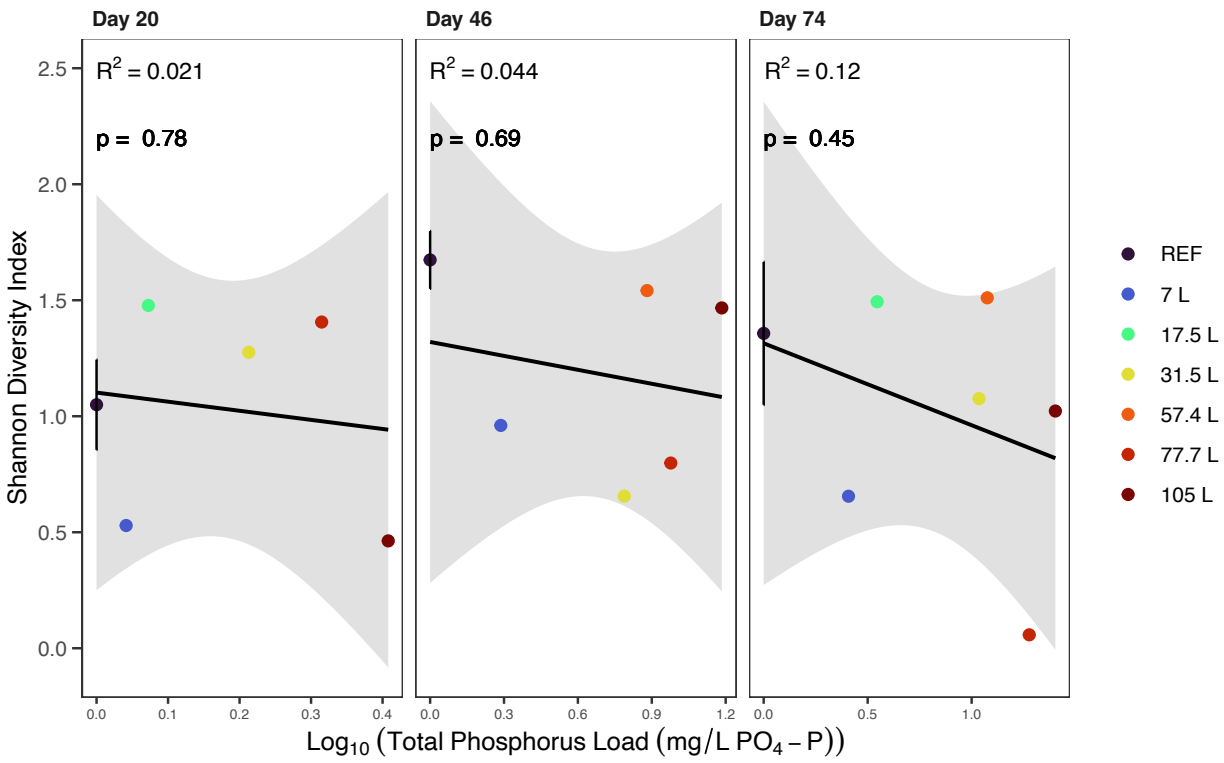

Appendix Figure B-44: Linear regression model results of the relationship between log10(x + 1) of cumulative AWW load concentration (TP used as the representative variable) and Shannon Diversity Index. REF displays the mean of the references (n = 3) with the error bars representing ± standard deviation. Each plot displays the model results according to study day. The diversity data was calculated from eDNA reads from the Rotifer 1 primer.

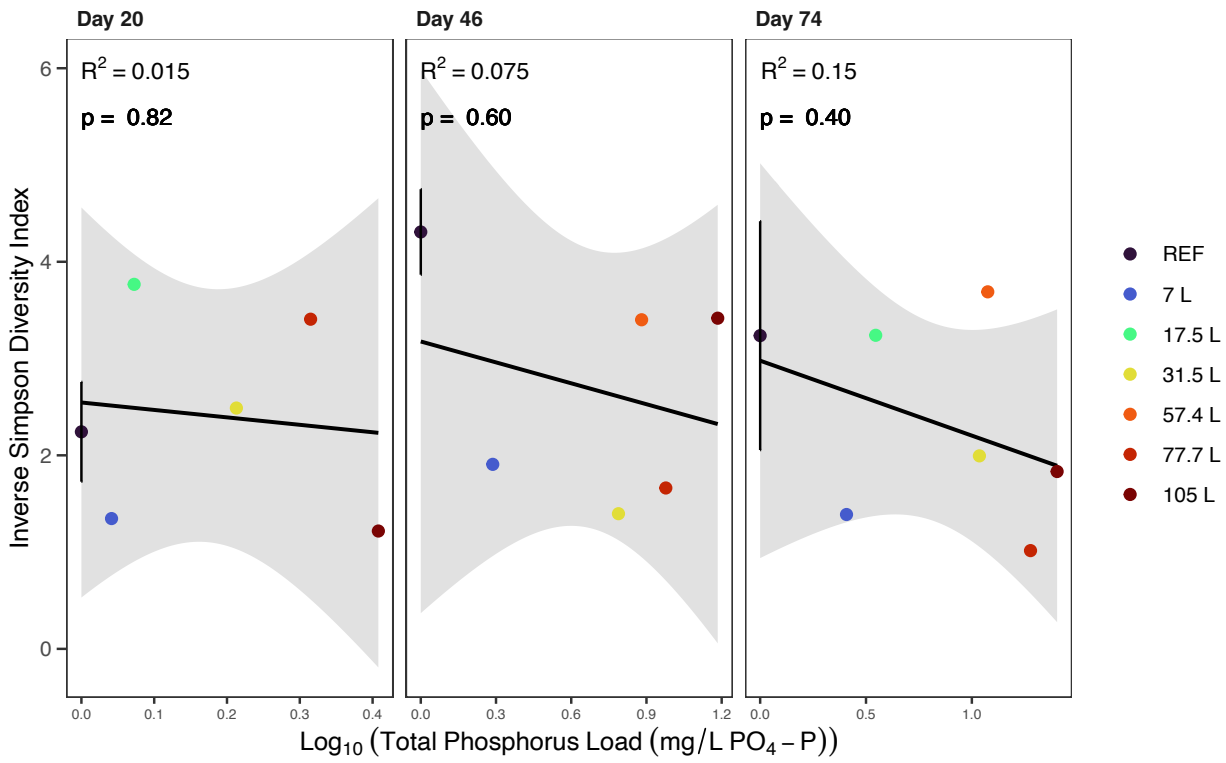

Appendix Figure B-45: Linear regression model results of the relationship between log10(x + 1) of cumulative AWW load concentration (TP used as the representative variable) and Inverse Simpson Diversity Index. REF displays the mean of the references (n = 3) with the error bars representing ± standard deviation. Each plot displays the model results according to study day. The diversity data was calculated from eDNA reads from the Rotifer 1 primer.

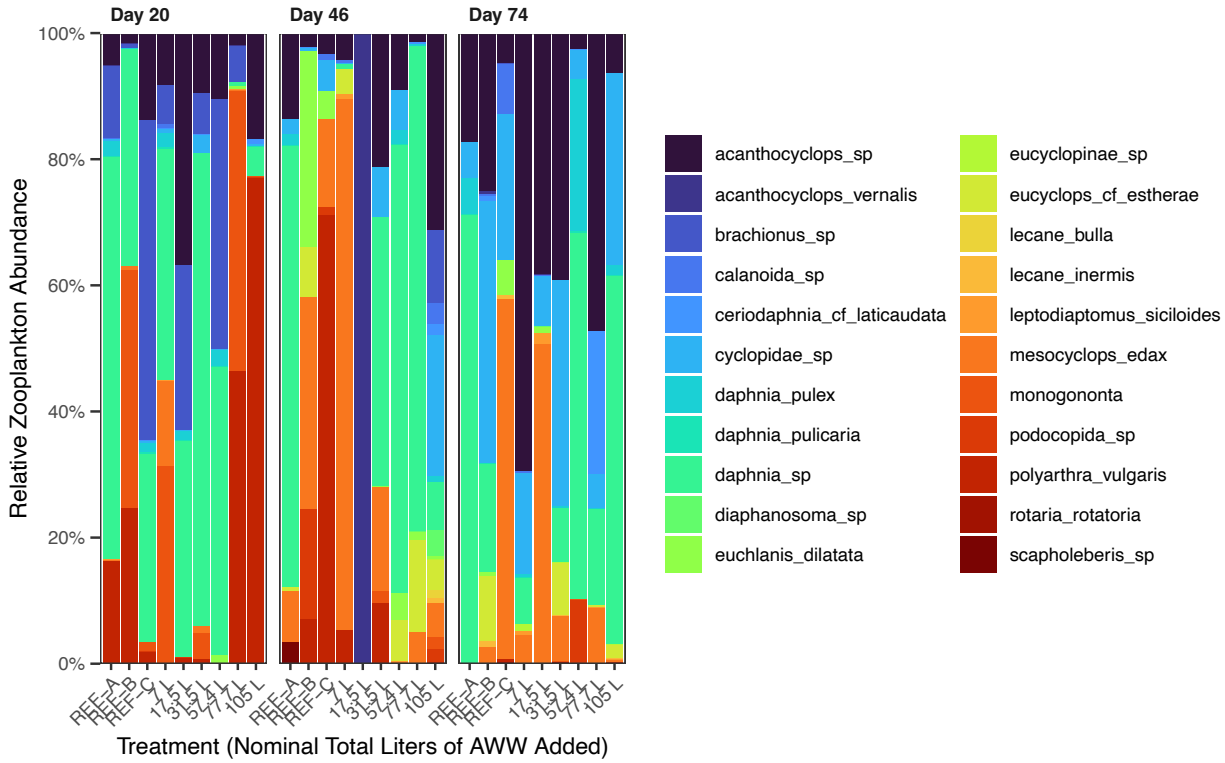

Appendix Figure B-46: The relative abundance (%) of each zooplankton taxa using the Rotifer 2 primer.

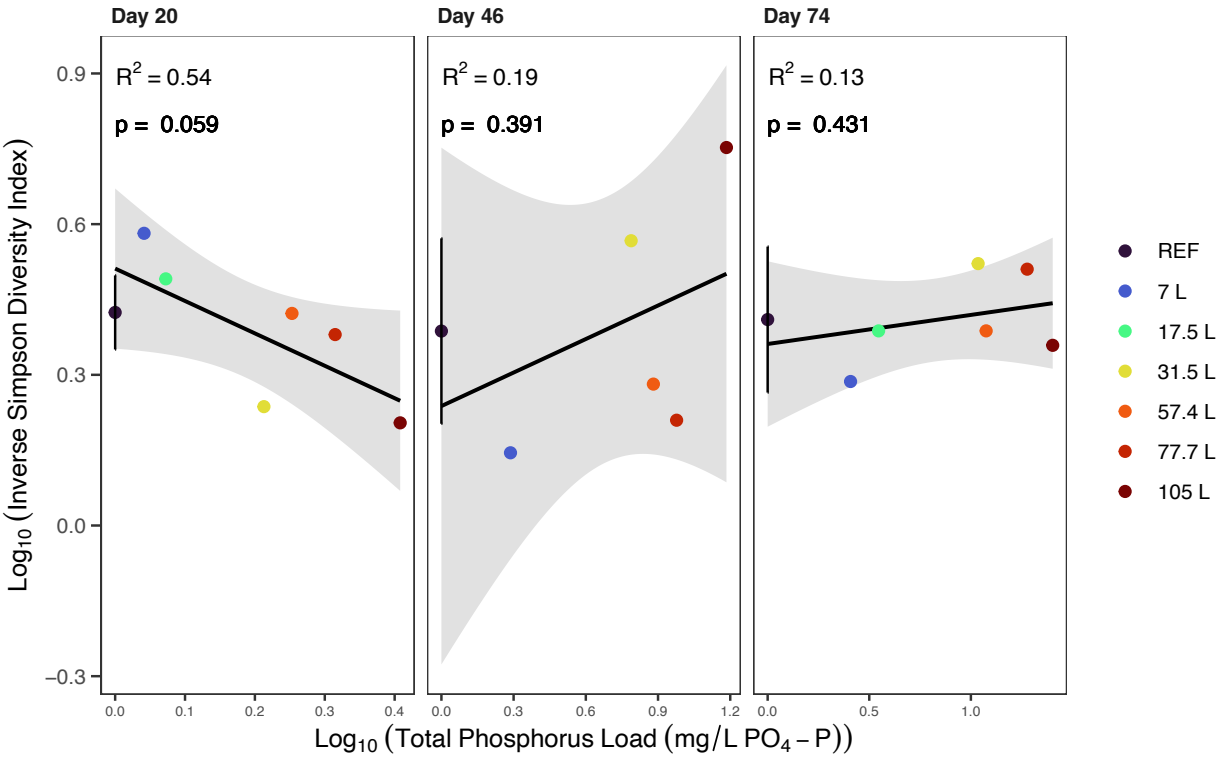

Appendix Figure B-47: Linear regression model results of the relationship between log10(x + 1) of cumulative AWW load concentration (TP used as the representative variable) and Inverse Simpson Diversity Index. REF displays the mean of the references (n = 3) with the error bars representing ± standard deviation. Each plot displays the model results according to study day. The diversity data was calculated from eDNA reads from the Rotifer 2 primer.

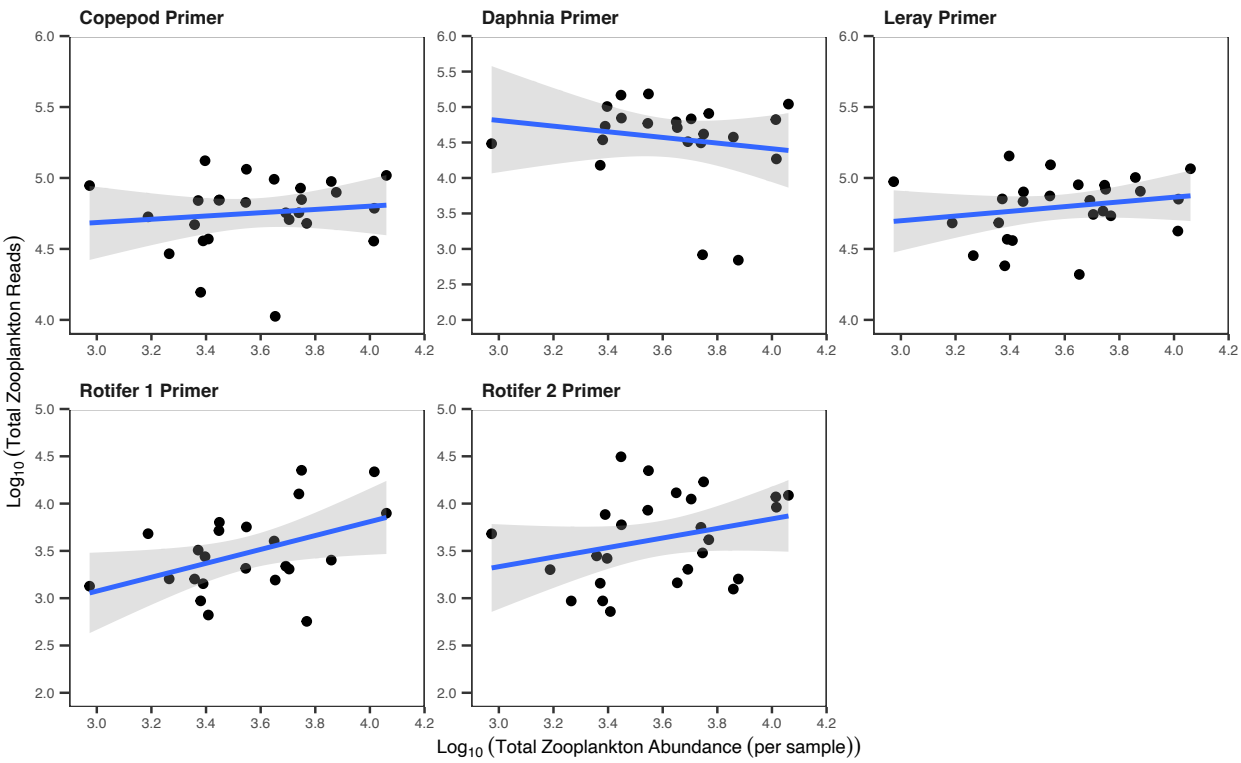

Appendix Figure B-48: Correlation between log10(x + 1) transformed total abundance derived from morphological methods and log10(x + 1) transformed total reads from eDNA metabarcoding methods. Each plot represents the results from a different primer while the morphological data remains the same for each plot.

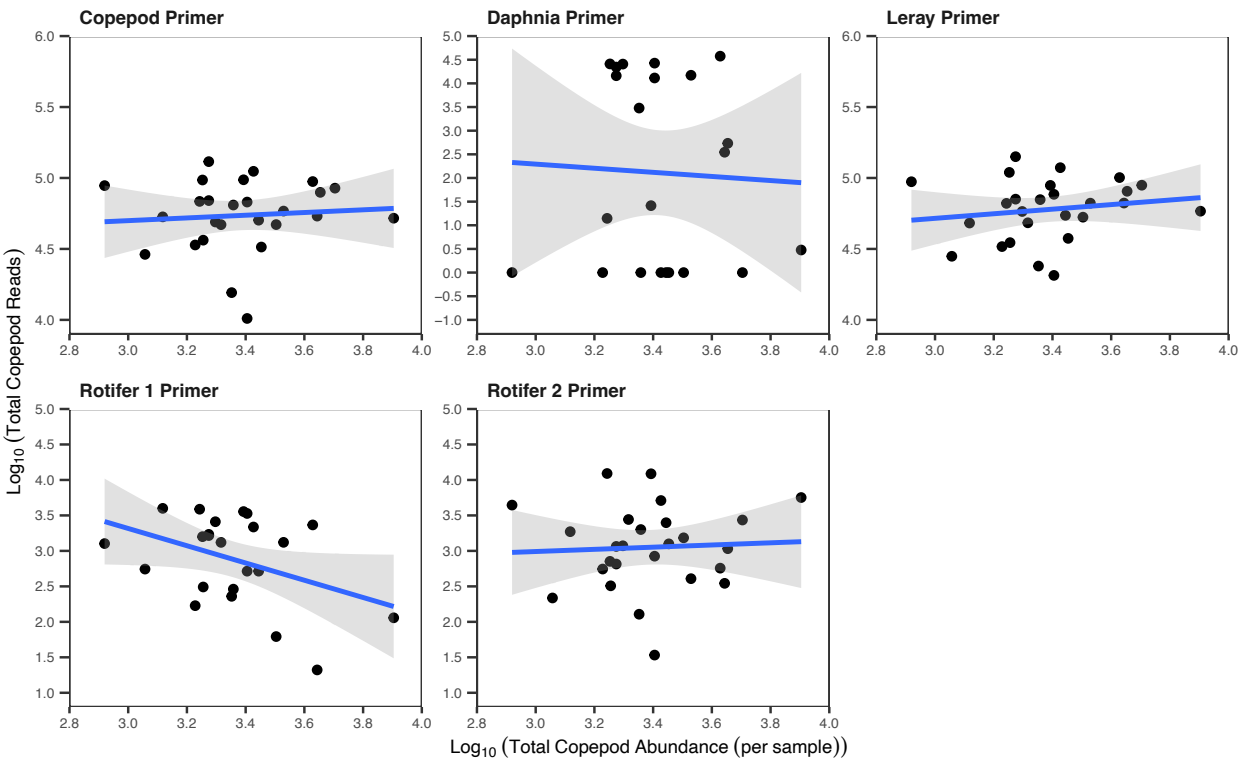

Appendix Figure B-49: Correlation between log10(x + 1) transformed copepod abundance derived from morphological methods and log10(x + 1) transformed copepod reads from eDNA metabarcoding methods. Each plot represents the results from a different primer while the morphological data remains the same for each plot.

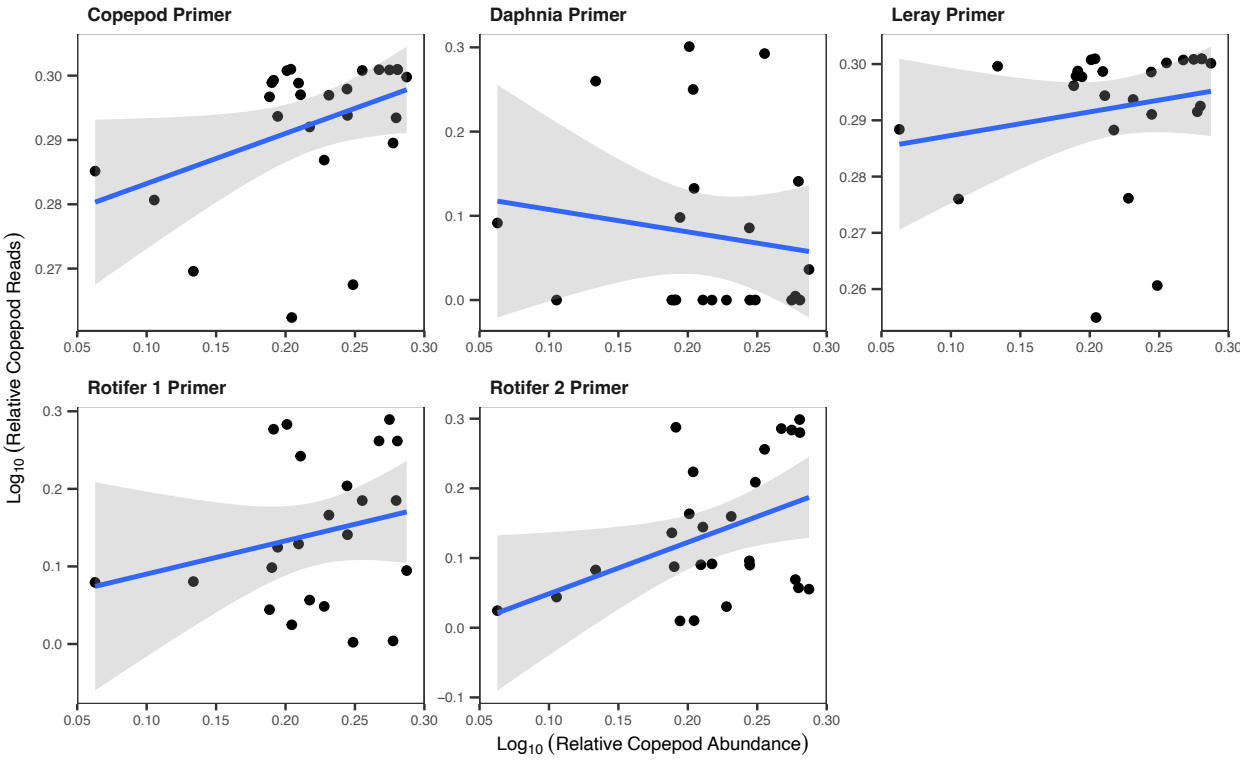

Appendix Figure B-50: Correlation between log10(x + 1) transformed relative copepod abundance derived from morphological methods and log10(x + 1) transformed relative copepod reads from eDNA metabarcoding methods. Each plot represents the results from a different primer while the morphological data remains the same for each plot.

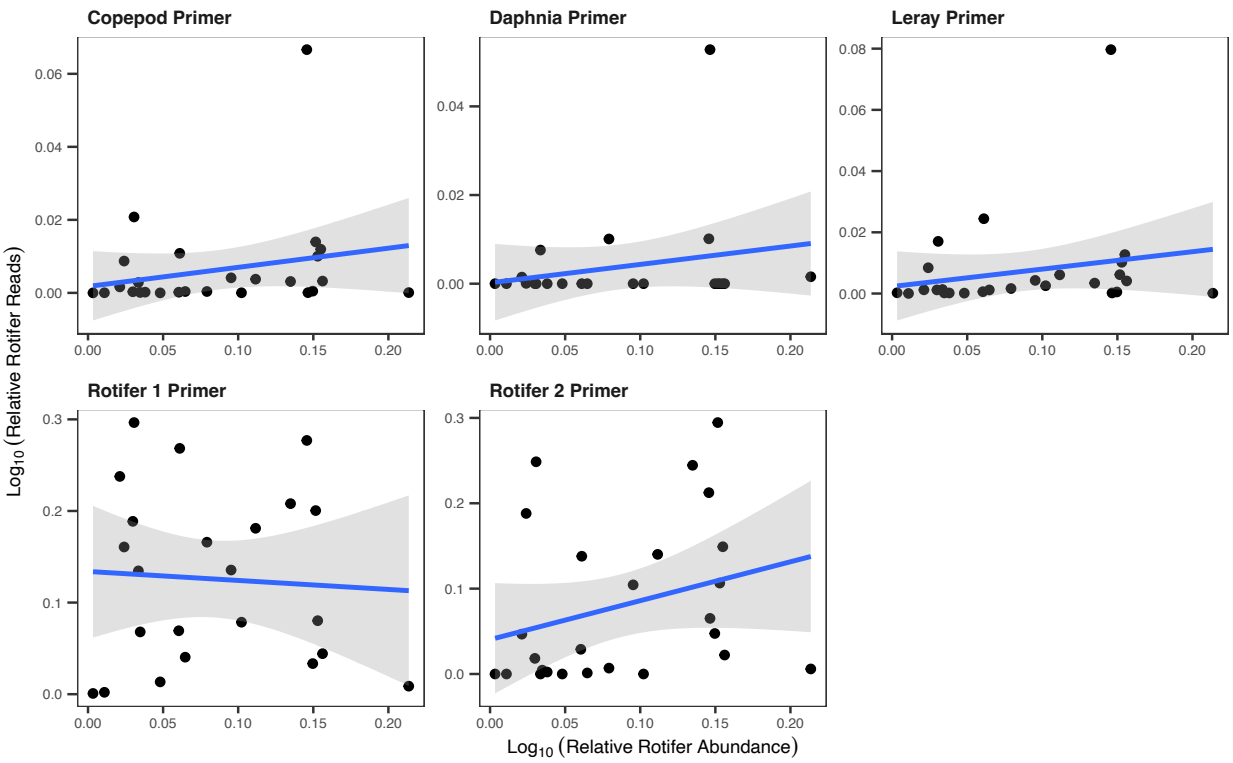

Appendix Figure B-51: Correlation between log10(x + 1) transformed relative rotifer abundance derived from morphological methods and log10(x + 1) transformed relative rotifer reads from eDNA metabarcoding methods. Each plot represents the results from a different primer while the morphological data remains the same for each plot.

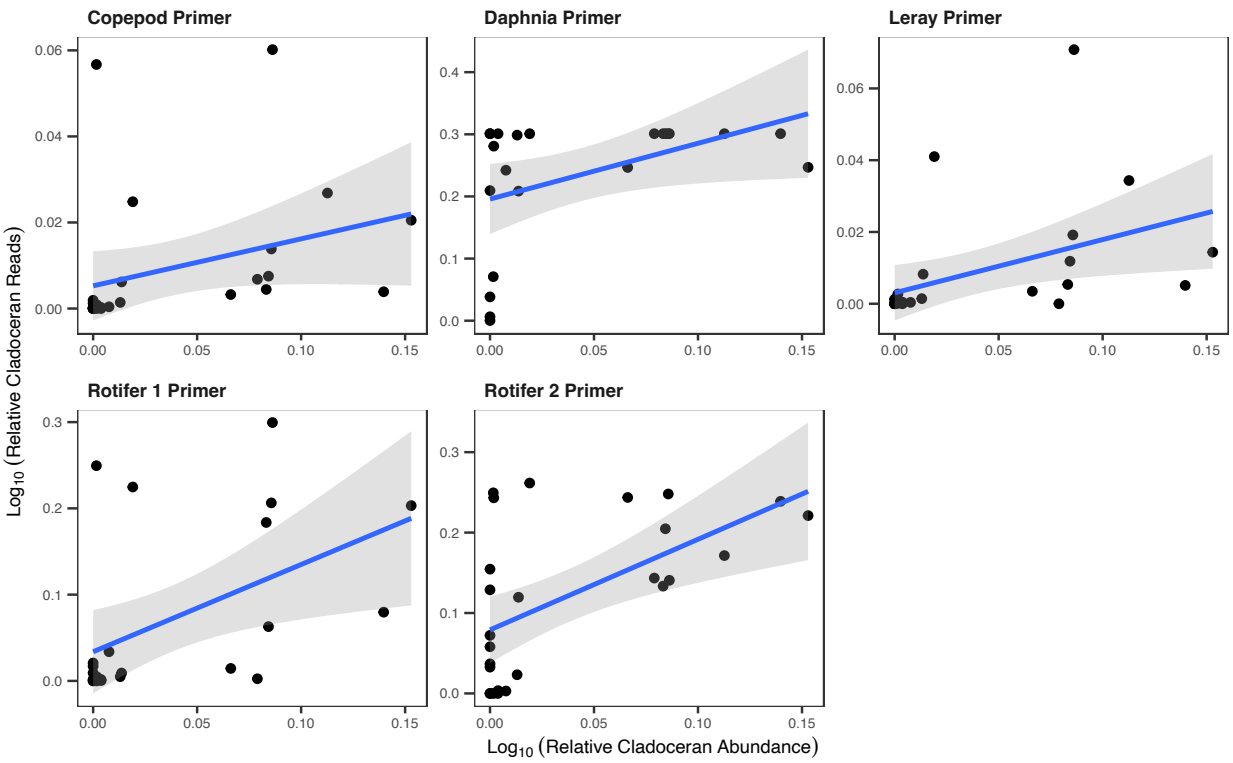

Appendix Figure B-52: Correlation between log10(x + 1) transformed relative cladoceran abundance derived from morphological methods and log10(x + 1) transformed relative cladoceran reads from eDNA metabarcoding methods. Each plot represents the results from a different primer while the morphological data remains the same for each plot.

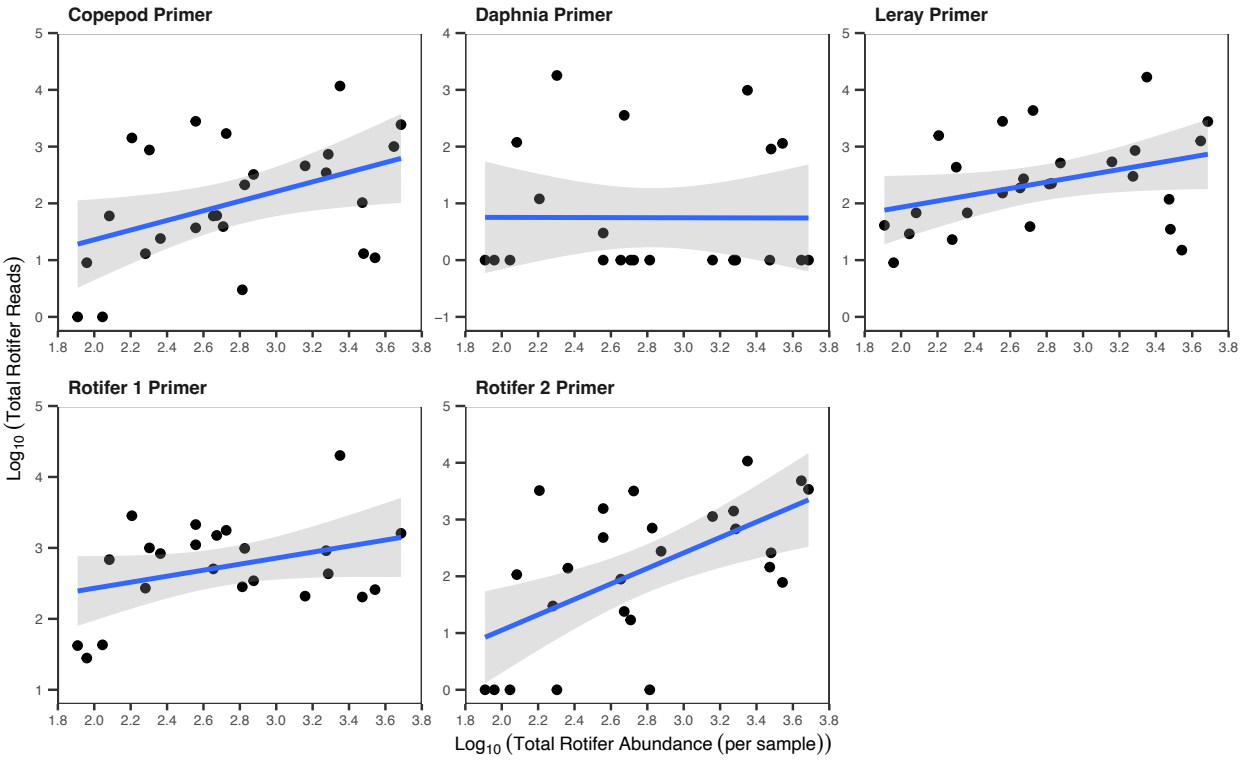

Appendix Figure B-53: Correlation between log10(x + 1) transformed rotifer abundance derived from morphological methods and log10(x + 1) transformed rotifer reads from eDNA metabarcoding methods. Each plot represents the results from a different primer while the morphological data remains the same for each plot.

Appendix C: UM-EW Supplemental Tables and Figures

Appendix Table C-1: The measured composition of the AWW prior to each addition at UM. Mean from collection source 1 used for TKN and density addition 1 and 5.

Addition #	TP (mg/L)	TAN (mg/L)	TKN (mg/L)	TK (mg/L)	TS (mg/L)	Dry Matter (%)	Moisture (%)	Density (g/mL)
1	48.8	285	296	NA	NA	NA	NA	0.998
2	40.0	184	195	4.99	128	0.16	99.8	0.998
3	42.4	203	250	4.79	95.9	0.181	99.8	0.998
4	31.1	200	562	5.45	104	0.12	99.9	0.999
5	41.8	290	296	NA	NA	NA	NA	0.998
6	46.7	208	256	18.4	26.0	0.122	99.9	0.999

Note: NA indicates where data was not obtained.

Appendix Table C-2: Cumulative nutrient concentration of TP (mg/L PO_4-P) within each treatment as a result of each AWW addition load. The cumulative concentration is a result of the sum of each mass of TP loaded, divided by the most recent volume.

Treatment	Addition #1	+Addition #2	+Addition #3	+Addition #4	+Addition #5	+Addition #6
Reference	0	0	0	0	0	0
15 L	0.1784	0.2558	0.2680	0.4483	0.4162	0.5645
23.4 L	0.1394	0.2725	0.3338	0.4554	0.4621	0.5601
36.6 L	0.2149	0.4047	0.5076	0.6792	0.7557	0.9026
57.6 L	0.4390	0.8932	1.1017	1.5410	1.5370	2.1789
90 L	0.6898	1.3771	1.7305	2.5167	2.5655	3.2556

Appendix Table C-3: Cumulative nutrient concentration of TKN (mg/L) within each treatment as a result of each AWW addition load. The cumulative concentration is a result of the sum of each mass of TKN loaded, divided by the most recent volume.

Treatment	Addition #1	+Addition #2	+Addition #3	+Addition #4	+Addition #5	+Addition #6
Reference	0	0	0	0	0	
15 L	1.0821	1.4946	1.5690	4.2760	3.7581	4.7235
23.4 L	0.8453	1.5077	1.8871	3.6586	3.6213	4.1447
36.6 L	1.3031	2.2391	2.8696	5.4570	5.9226	6.6793
57.6 L	2.6626	4.9418	6.2285	12.3805	12.0459	16.1240
90 L	4.1840	7.6192	9.7837	20.2198	20.1066	24.0920

Appendix Table C-4: Cumulative nutrient concentration of NH_4 (mg/L NH_4-N) within each treatment as a result of each AWW addition load. The cumulative concentration is a result of the sum of each mass of NH_4 loaded, divided by the most recent volume.

Treatment	Addition #1	+Addition #2	+Addition #3	+Addition #4	+Addition #5	+Addition #6
Reference	0	0	0	0	0	
15 L	1.0430	1.4355	1.4676	2.5839	2.4997	3.2266
23.4 L	0.8148	1.4402	1.7104	2.4476	2.6317	3.0604
36.6 L	1.2561	2.1388	2.6010	3.6508	4.3040	4.9319
57.6 L	2.5665	4.7205	5.6455	8.2827	8.7539	11.9057
90 L	4.0329	7.2780	8.8679	13.5272	14.6117	17.7890

Appendix Table C-5: Mean nutrient concentration within each treatment over the study duration (n = 6). Each concentration that contributed to the average is a result of the mass of the nutrient loaded divided by the known volume at the time of each addition.

Treatment	TP (mg/L PO_4-P)	NH_4 (mg/L NH_4-N)	TKN (mg/L)
Reference	0	0	0
15 L	0.0996	0.5688	0.8684
23.4 L	0.1094	0.5965	0.8170
36.6 L	0.1690	0.9234	1.2556
57.6 L	0.3689	2.0023	2.7541
90 L	0.5806	3.1691	4.3804

Appendix Table C-6: The cumulative and mean concentration of copper and zinc within each treatment as a result of each AWW loading (n =3).

Treatment	Cumulative Cu (mg/L)	Mean Cu (mg/L)	Cumulative Zn (mg/L)	Mean Zn (mg/L)
Reference	0	0	0	0
15 L	0.0057	0.0010	0.0447	0.0079
23.4 L	0.0057	0.0011	0.0441	0.0085
36.6 L	0.0091	0.0017	0.0711	0.0133
57.6 L	0.0220	0.0037	0.1717	0.0290
90 L	0.0329	0.0059	0.2566	0.0458

Appendix Table C-7: Mean (±SD) concentration of environmental variables after the first AWW treatment to the end of the study duration, within each treatment.

Treatment	TP (mg/L PO_4-P) (n = 5)	TDP (mg/L PO_4-P) (n = 5)	SRP (mg/L PO_4-P) (n = 6)	Part-P (mg/L PO_4-P) (n = 7)	TN (mg/L N) (n = 2)	TDN (mg/L N) (n = 6)	TAN (mg/L NH_4-N) (n = 6)	NH_3 (mg/L NH_3) (n = 6)	NO_2 (mg/L NO_2-N) (n = 6)	NO_3 (mg/L NO_3-N) (n = 6)	Chl-*a* (µg/L) (n = 7)
Reference	0.089 (0.108)	0.068 (0.095)	0.042 (0.042)	0.017 (0.011)	1.38 (0.29)	1.42 (0.46)	0.037 (0.068)	0.002 (0.004)	0.099 (0.025)	0.563 (0.367)	5.67 (4.43)
15L	0.055 (0.024)	0.044 (0.021)	0.031 (0.019)	0.025 (0.017)	1.18 (0.77)	1.58 (0.25)	0.035 (0.065)	0.002 (0.003)	0.112 (0.015)	0.595 (0.348)	5.15 (7.33)
23.4L	0.024 (0.017)	0.018 (0.008)	0.026 (0.018)	0.017 (0.004)	1.18 (0.13)	1.29 (0.25)	0.036 (0.088)	0.002 (0.004)	0.099 (0.023)	0.562 (0.375)	3.40 (1.35)
36.6L	0.290 (0.064)	0.258 (0.062)	0.106 (0.055)	0.029 (0.006)	1.72 (0.13)	1.85 (0.22)	0.046 (0.087)	0.040 (0.080)	0.095 (0.034)	0.595 (0.384)	1.90 (0.76)
57.6L	0.323 (0.074)	0.306 (0.074)	0.102 (0.063)	0.020 (0.011)	1.82 (0.06)	2.20 (0.49)	0.049 (0.108)	0.004 (0.009)	0.103 (0.016)	0.577 (0.439)	2.79 (1.63)
90L	0.122 (0.026)	0.092 (0.022)	0.056 (0.035)	0.040 (0.029)	1.58 (0.14)	1.79 (0.29)	0.039 (0.079)	0.001 (0.001)	0.097 (0.032)	0.598 (0.364)	9.34 (9.76)

Appendix Table C-8: Mean (±SD) concentration of environmental variables after the first AWW treatment to the end of the study duration.

Treatment	**Alkalinity (mg/L $CaCO_3$)** (n = 3)	**DOC (mg/L)** (n = 6)	**SRSi (mg/L)** (n = 6)
Reference	242.5 (49.8)	39.9 (25.1)	0.21 (0.12)
15L	228.0 (54.8)	41.6 (29.7)	0.26 (0.22)
23.4L	193.7 (57.5)	37.6 (18.9)	0.28 (0.33)
36.6L	294.3 (140.9)	40.5 (25.0)	2.29 (1.17)
57.6L	274.3 (79.1)	36.4 (26.3)	0.42 (0.37)
90L	269.7 (73.5)	42.1 (28.5)	0.42 (0.28)

Appendix Table C-9: Monthly average (+/- SD) meteorological variables and total precipitation from May to September 2022. Light intensity was measured on site via loggers and all other data was retrieved from Environment Canada weather station in Winnipeg, MB.

Month	Mean Air Temperature (°C)	Mean Relative Humidity (%)	Total Precipitation (mm)	Mean Wind Speed (km/h)	Mean Light Intensity (lux)
June	18.4 (5.6)	58.4 (19.2)	86.3	6.6 (3.1)	26660 (31516)
July	21.3 (4.0)	65.5 (16.1)	136.2	5.8 (3.2)	24792 (30217)
August	20.6 (3.9)	68.1 (15.1)	137.9	5.7 (3.2)	22660 (28340)
September	15.3 (5.2)	65.9 (17.9)	41	5.6 (3.3)	16422 (23452)

Appendix Table C-10: Linear regression model results of the relationship between log10(x + 1) of cumulative AWW load concentration (TP used as the dependant variable) and each zooplankton metric. The zooplankton metrics were log10 transformed when required to meet model assumptions. Significant when p-value <= 0.05.

Zooplankton metric	Transformation	Study Day	Intercept	Slope	R^2	p-value	Significant
Total zooplankton abundance	Log10	8	3.28	-1.93	0.17	0.423	No
	Log10	22	3.24	-0.41	0.057	0.649	No
	Log10	36	3.12	0.53	0.12	0.510	No
	Log10	50	3.02	1.44	0.47	0.134	No
	Log10	64	3.44	0.058	0.004	0.902	No
	Log10	91	2.92	0.69	0.61	0.065	No
Copepod abundance	Log10	8	2.67	-0.75	0.016	0.81	No
	Log10	22	2.88	-0.34	0.039	0.71	No
	Log10	36	2.75	0.75	0.23	0.34	No
	Log10	50	2.75	1.00	0.31	0.25	No
	Log10	64	3.14	-0.36	0.051	0.67	No
	Log10	91	2.56	0.36	0.13	0.49	No
Cyclopoid copepod abundance	Log10	8	2.19	-1.43	0.029	0.746	No
	Log10	22	2.55	-0.56	0.1	0.538	No
	Log10	36	2.41	0.36	0.11	0.530	No
	Log10	50	2.19	1.54	0.65	0.053	No
	Log10	64	2.79	-0.60	0.13	0.486	No
	Log10	91	1.99	0.77	0.16	0.431	No
Copepod Nauplii abundance	Log10	8	2.38	0.04	$5.6x10^{-5}$	0.99	No
	Log10	22	2.57	-0.09	0.0021	0.93	No
	Log10	36	2.45	1.05	0.27	0.29	No
	Log10	50	2.58	0.65	0.1	0.54	No
	Log10	64	2.88	-0.20	0.016	0.81	No
	Log10	91	2.36	0.16	0.033	0.73	No
Cladoceran abundance	Log10	8	2.64	-1.75	0.19	0.39	No
	Log10	22	2.59	-0.52	0.039	0.71	No
	Log10	36	2.15	0.10	0.00048	0.97	No
	Log10	50	2.02	2.51	0.4	0.17	No
	Log10	64	2.80	-0.18	0.006	0.88	No
	Log10	91	2.09	1.17	0.32	0.24	No
Rotifer abundance	Log10	8	2.90	-3.13	0.31	0.25	No
	Log10	22	2.45	-0.08	0.0008	0.96	No
	Log10	36	2.56	0.47	0.11	0.52	No
	Log10	50	2.08	1.77	0.34	0.23	No
	Log10	64	2.66	0.20	0.011	0.85	No
	Log10	91	2.35	0.84	0.52	0.11	No
Inverse Simpson	NA	8	4.15	4.10	0.14	0.46	No
	NA	22	3.98	2.03	0.18	0.40	No
	NA	36	3.99	-1.35	0.085	0.58	No

	NA	50	4.54	-2.00	0.21	0.36	No
	NA	64	4.93	-3.59	0.37	0.20	No
	NA	91	3.86	-0.41	0.0065	0.88	No
Pielou's	NA	8	0.42	0.92	0.35	0.219	No
Evenness	NA	22	0.50	0.14	0.057	0.648	No
	NA	36	0.60	-0.31	0.2	0.376	No
	NA	50	0.67	-0.53	0.43	0.157	No
	NA	64	0.63	-0.50	0.71	0.035	Yes
	NA	91	0.71	-0.38	0.28	0.281	No
Species	NA	8	9.75	-7.49	0.46	0.14	No
Richness	NA	22	8.06	1.64	0.047	0.68	No
	NA	36	6.69	1.19	0.081	0.58	No
	NA	50	6.89	3.76	0.25	0.31	No
	NA	64	7.94	-0.08	0.0003	0.98	No
	NA	91	5.44	2.99	0.25	0.31	No

Appendix Table C-11: Dominant zooplankton taxa, the proportion of the total sample abundance that the dominant taxa makes up, and species diversity metrics within each treatment on study day 0, prior to the first AWW addition. Reference treatment represents the mean value (SD) (n = 2).

Treatment	Dominant Taxa	Proportion of Abundance	Richness	Evenness	Shannon's Diversity	Inverse Simpson's Diversity
Reference	Rotifer	0.36	9 (1.41)	0.48 (0.13)	1.66 (0.01)	4.24 (0.50)
15 L	Ceriodaphnia	0.34	9	0.48	1.74	4.35
23.4 L	Rotifer	0.38	10	0.35	1.54	3.46
36.6 L	Chydroid	0.34	8	0.59	1.75	4.73
57.6 L	Rotifer	0.43	8	0.50	1.69	3.98
90 L	Rotifer	0.39	7	0.58	1.62	4.05

Appendix Table C-12: Dominant zooplankton taxa, the proportion of the total sample abundance that the dominant taxa makes up, and species diversity metrics within each treatment on study day 8. Reference treatment represents the mean value (SD) (n = 2).

Treatment	Dominant Taxa	Proportion of Abundance	Richness	Evenness	Shannon's Diversity	Inverse Simpson's Diversity
Reference	Rotifer	0.46	9 (0)	0.45 (0.17)	1.65 (0.26)	4.06 (1.49)
15 L	Rotifer and Nauplii	0.21 each	9	0.65	1.88	5.84
23.4 L	Rotifer	0.49	10	0.33	1.51	3.25
36.6 L	Rotifer	0.40	10	0.45	1.83	4.53
57.6 L	Copepod Nauplii	0.33	8	0.58	1.70	4.63
90 L	Copepod Nauplii	0.31	8	0.63	1.81	5.03

Appendix Table C-13: Dominant zooplankton taxa, the proportion of the total sample abundance that the dominant taxa makes up, and species diversity metrics within each treatment on study day 22. Reference treatment represents the mean value (SD) (n = 2).

Treatment	Dominant Taxa	Proportion of Abundance	Richness	Evenness	Shannon's Diversity	Inverse Simpson's Diversity
Reference	Cyclopoid Copepod	0.29	7 (0)	0.57 (0.02)	1.59 (0.01)	3.97 (0.13)
15 L	Cyclopoid copepod	0.35	8	0.54	1.67	4.28
23.4 L	Copepod Nauplii	0.26	10	0.49	1.77	4.95
36.6 L	Ceriodaphnia	0.48	8	0.45	1.65	3.56
57.6 L	Copepod Nauplii	0.35	9	0.44	1.59	3.94
90 L	Copepod Nauplii	0.26	8	0.66	1.79	5.25

Appendix Table C-14: Dominant zooplankton taxa, the proportion of the total sample abundance that the dominant taxa makes up, and species diversity metrics within each treatment on study day 36. Reference treatment represents the mean value (SD) (n = 2).

Treatment	Dominant Taxa	Proportion of Abundance	Richness	Evenness	Shannon's Diversity	Inverse Simpson's Diversity
Reference	Rotier	0.49	6.5 (2.12)	0.49 (0.08)	1.37 (0.26)	3.12 (0.53)
15 L	Rotifer	0.30	7	0.70	1.70	4.90
23.4 L	Rotifer	0.32	6	0.62	1.42	3.71
36.6 L	Ceriodaphnia	0.35	8	0.47	1.58	3.78
57.6 L	Copepod Nauplii	0.34	7	0.58	1.56	4.07
90 L	Rotifer	0.50	7	0.40	1.24	2.80

Appendix Table C-15: Dominant zooplankton taxa, the proportion of the total sample abundance that the dominant taxa makes up, and species diversity metrics within each treatment on study day day 50. Reference treatment represents the mean value (SD) (n = 2).

Treatment	Dominant Taxa	Proportion of Abundance	Richness	Evenness	Shannon's Diversity	Inverse Simpson's Diversity
Reference	Rotifer	0.35	6 (0)	0.61 (0.01)	1.43 (0.02)	3.63 (0.08)
15 L	Copepod Nauplii	0.24	9	0.61	1.79	5.47
23.4 L	Ostracod and cyclopoid	0.26	6	0.78	1.64	4.70
36.6 L	Copepod Nauplii	0.43	9	0.41	1.62	3.73
57.6 L	Ceriodaphnia	0.49	9	0.37	1.55	3.35
90 L	Rotifer	0.47	8	0.42	1.46	3.37

Appendix Table C-16: Dominant zooplankton taxa, the proportion of the total sample abundance that the dominant taxa makes up, and species diversity metrics within each treatment on study day 64. Reference treatment represents the mean value (SD) (n = 2).

Treatment	Dominant Taxa	Proportion of Abundance	Richness	Evenness	Shannon's Diversity	Inverse Simpson's Diversity
Reference	Rotifer (1) and Copepod Nauplii (1)	0.34 each	6.5 (0.7)	0.57 (0.02)	1.45 (0.09)	3.71 (0.27)
15 L	Cyclopoid	0.28	8	0.55	1.65	4.39
23.4 L	Rotifer	0.27	9	0.60	1.84	5.40
36.6 L	Ceriodaphnia	0.32	9	0.51	1.70	4.58
57.6 L	Copepod Nauplii	0.40	8	0.51	1.67	4.11
90 L	Rotifer	0.70	7	0.28	1.01	1.93

Appendix Table C-17: Dominant zooplankton taxa, the proportion of the total sample abundance that the dominant taxa makes up, and species diversity metrics within each treatment on study day 91. Reference treatment represents the mean value (SD) (n = 2).

Treatment	Dominant Taxa	Proportion of Abundance	Richness	Evenness	Shannon's Diversity	Inverse Simpson's Diversity
Reference	Rotifer	0.43	4 (0)	0.77 (0.02)	1.21 (0.03)	3.07 (0.10)
15 L	Cyclopoid	0.28	7	0.75	1.76	5.22
23.4 L	Rotifer	0.57	6	0.41	1.16	2.45
36.6 L	Copepod Nauplii	0.33	8	0.62	1.76	4.92
57.6 L	Rotifer	0.33	6	0.67	1.51	4.02
90 L	Rotifer	0.50	7	0.39	1.22	2.76

Appendix Table C-18: Linear regression model results of the relationship between log10(x + 1) of zooplankton abundance and each fish metric. The fish in the sampling jars was treated as a binomial, with 0 being no fish in jar, and 1 being fish found in jar. Significant when p-value <= 0.05.

Fish Metric	Study Day	Intercept	Slope	R^2	p-value	Significant
Number of fish retrieved	91	3.01	0.02	0.071	0.61	No
Binomial larval fish in jar	22	3.20	-0.12	0.037	0.68	No
	36	3.28	-0.23	0.22	0.28	No
	50	3.36	-0.13	0.024	0.74	No
	64	3.46	-0.14	0.067	0.56	No
	91	3.24	-0.37	0.86	0.0027	Yes

Appendix Table C-19: Species scores (b_k) as generated from principal response curve analysis of the zooplankton taxa included in the analysis.

Zooplankton taxa	**b_k**
Daphnia sp.	-0.046
Chydorus sp.	0.313
Scapholeberis sp.	0.320
Copepoda nauplii	0.407
Diaphanosoma sp.	1.750
Ostracoda	0.261
Cyclopoida	0.329
Rotifera	-0.062
Calanoida	0.916
Ceriodaphnia sp.	2.121
Macrothrix sp.	-0.213
Simocephalus sp.	-0.209
Bosmina sp.	-0.073
Polyphemus sp.	-0.008

Appendix Table C-20: Eigenvalues, explained variance, environmental variable canonical coefficients, and species scores, associated with the first and second RDA axis.

	RDA Axis 1	**RDA Axis 2**
Eigenvalue	0.03669	0.004973
Variance explained	0.30951	0.041944
Dissolved oxygen	0.50217	0.01314
Total dissolved nitrogen	0.31445	0.04271
Soluble reactive phosphorus	0.56193	-0.29643
Nitrite	-0.06022	0.37155
Chlorophyll *a*	-0.39645	-0.36768
Dissolved organic carbon	-0.02797	0.13929
Un-ionized ammonia	0.51840	-0.15729
Daphnia sp.	-0.0200938	0.015397
Chydorus sp.	-0.0636727	-0.00960
Ceriodaphnia sp.	0.5228931	-0.019832
Ostracoda	-0.0620118	0.121394
Calanoida	0.1158325	0.060415
Macrothrix sp.	-0.0430592	-0.041466
Diaphanosoma sp.	0.2636911	-0.146053
Copepoda nauplii	0.1158689	0.081999
Cyclopoida	-0.1149828	0.111054
Rotifera	-0.4313860	-0.123115
Scapholeberis sp.	0.0139753	-0.002926
Simocephalus sp.	-0.0504523	0.048822
Bosmina sp.	-0.0020442	0.008662
Polyphemus sp.	-0.0008659	-0.005649

Appendix Table C-21: The number of adult fathead minnow (*Pimephales promelas*) fish retrieved from the mesocosms by the final fish sampling date on September 17, 2024. A total of 12 fish were originally introduced to the mesocosms.

Treatment	Fish abundance
Reference-A	4
Reference-B	7
15 L	1
23.4 L	5
36.6 L	5
57.6 L	7
90 L	9

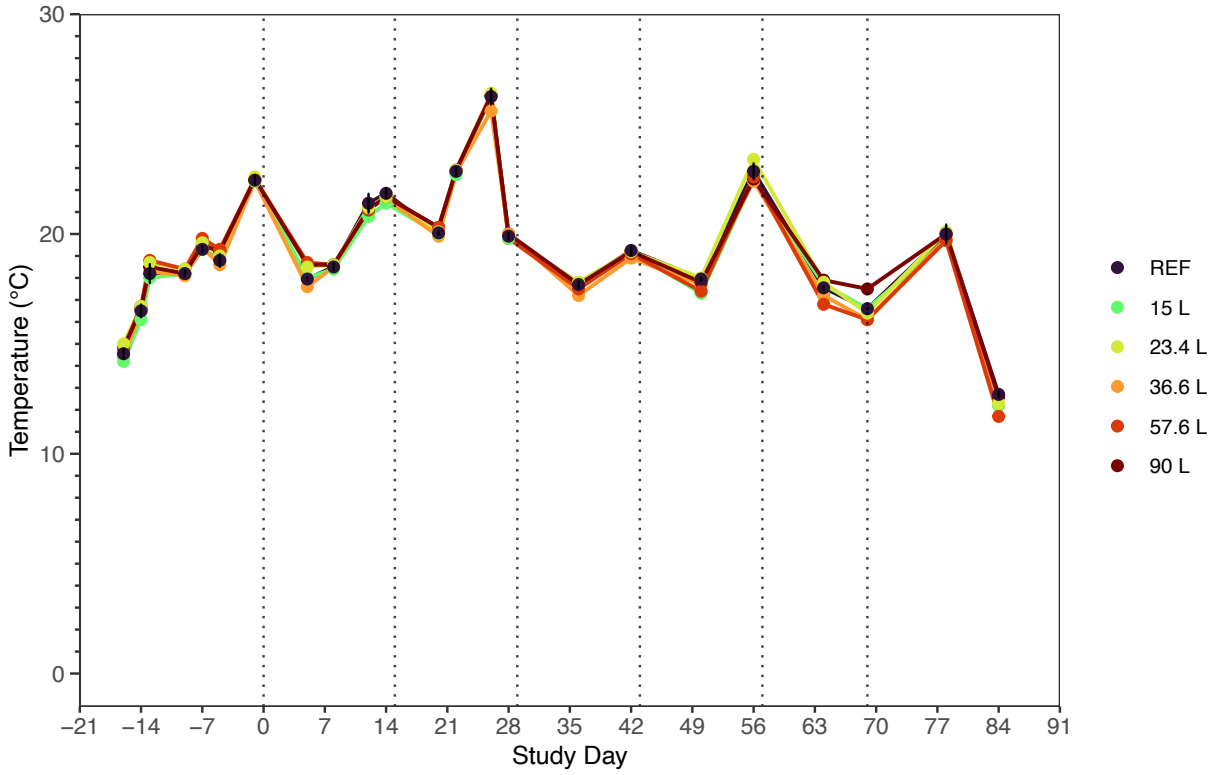

Appendix Figure C-1: Water temperature (°C) over the study duration within the established wetland mesocosms. The vertical dotted lines represent AWW addition days. REF displays the mean of the references (n = 2) with the error bars representing ± standard deviation.

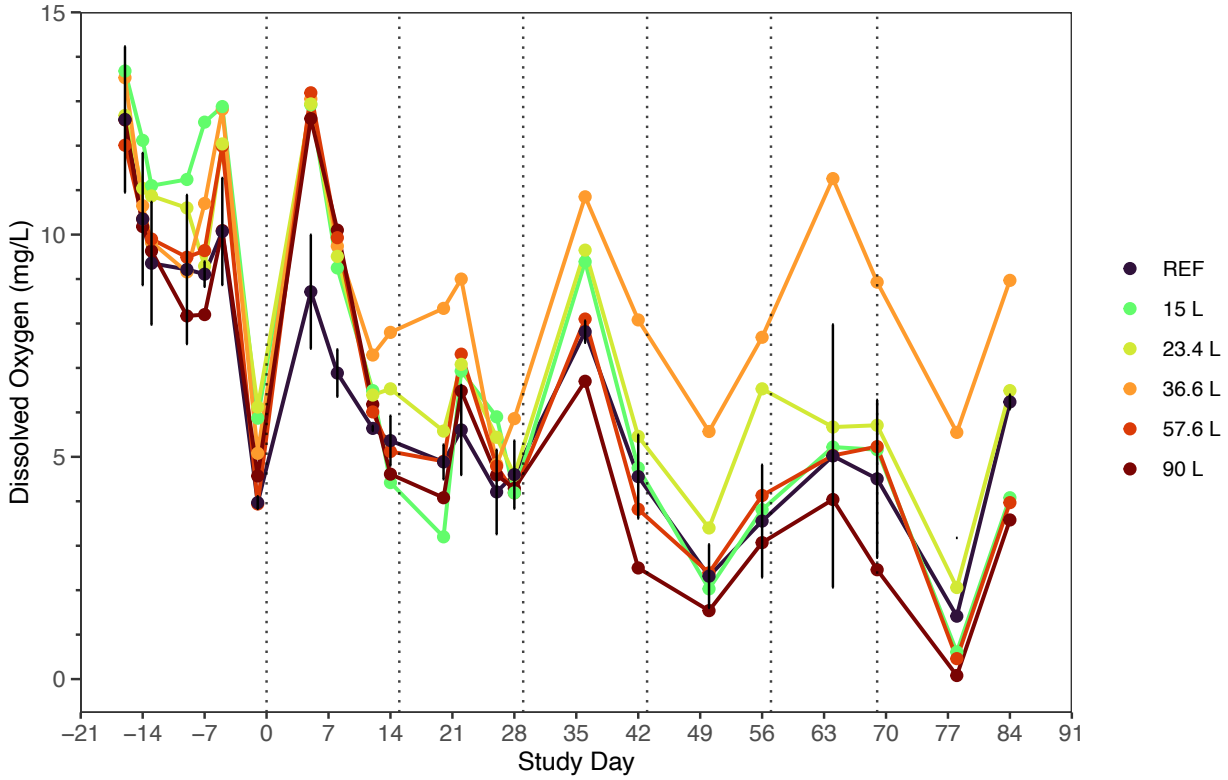

Appendix Figure C-2: Dissolved oxygen (mg/L) over the study duration within the established wetland mesocosms. The vertical dotted lines represent AWW addition days. REF displays the mean of the references (n = 2) with the error bars representing ± standard deviation.

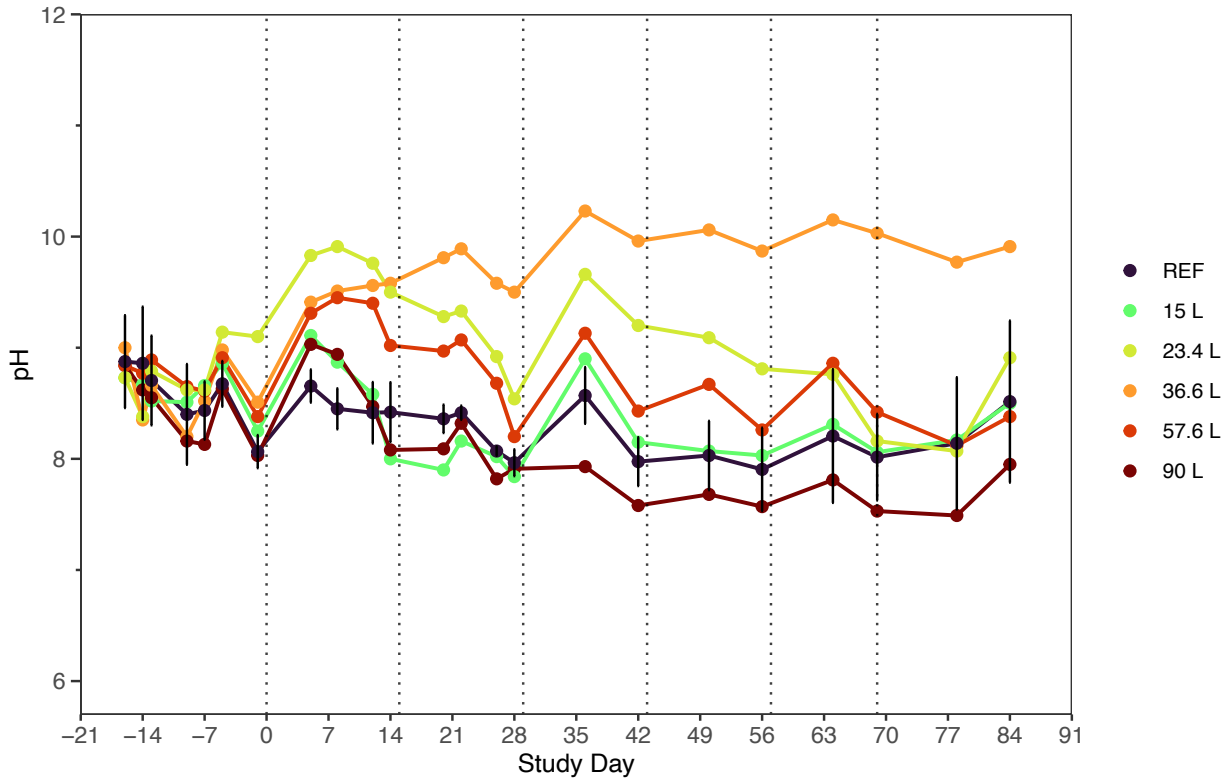

Appendix Figure C-3: pH over the study duration within the established wetland mesocosms. The vertical dotted lines represent AWW addition days. REF displays the mean of the references (n = 2) with the error bars representing ± standard deviation.

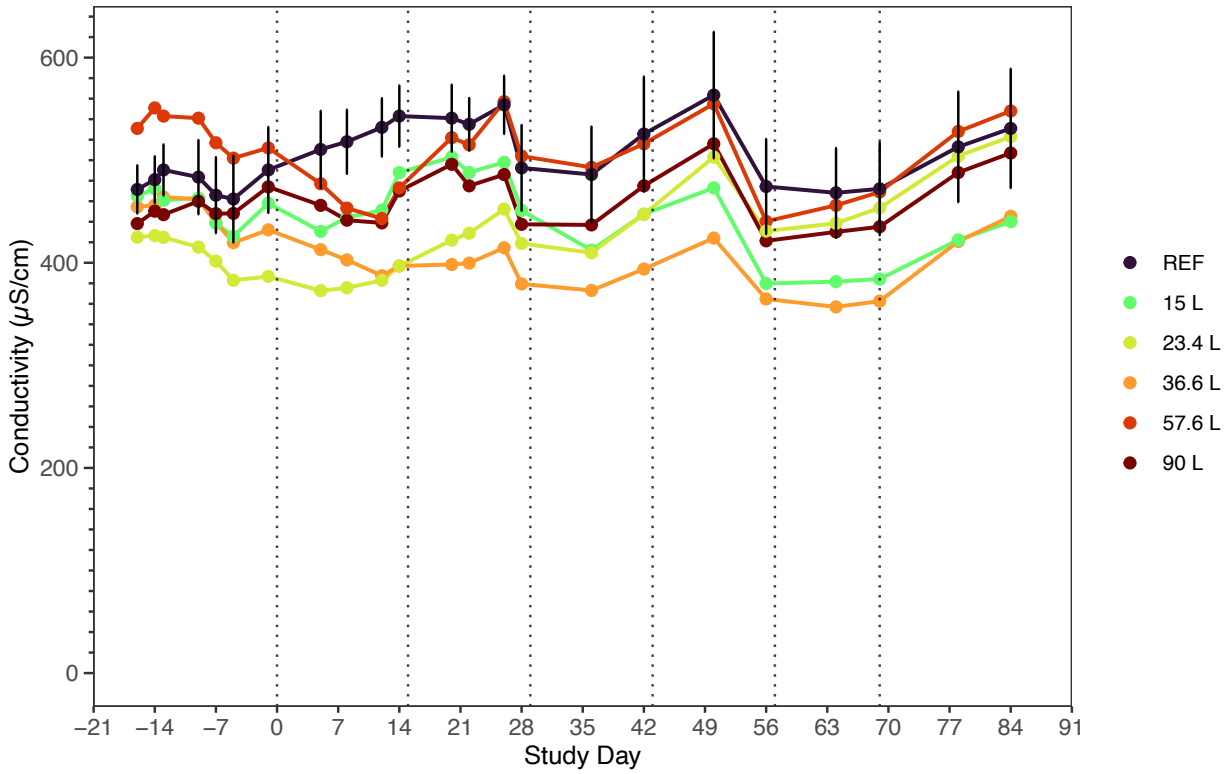

Appendix Figure C-4: Conductivity (µS/cm) over the study duration within the established wetland mesocosms. The vertical dotted lines represent AWW addition days. REF displays the mean of the references (n = 2) with the error bars representing ± standard deviation.

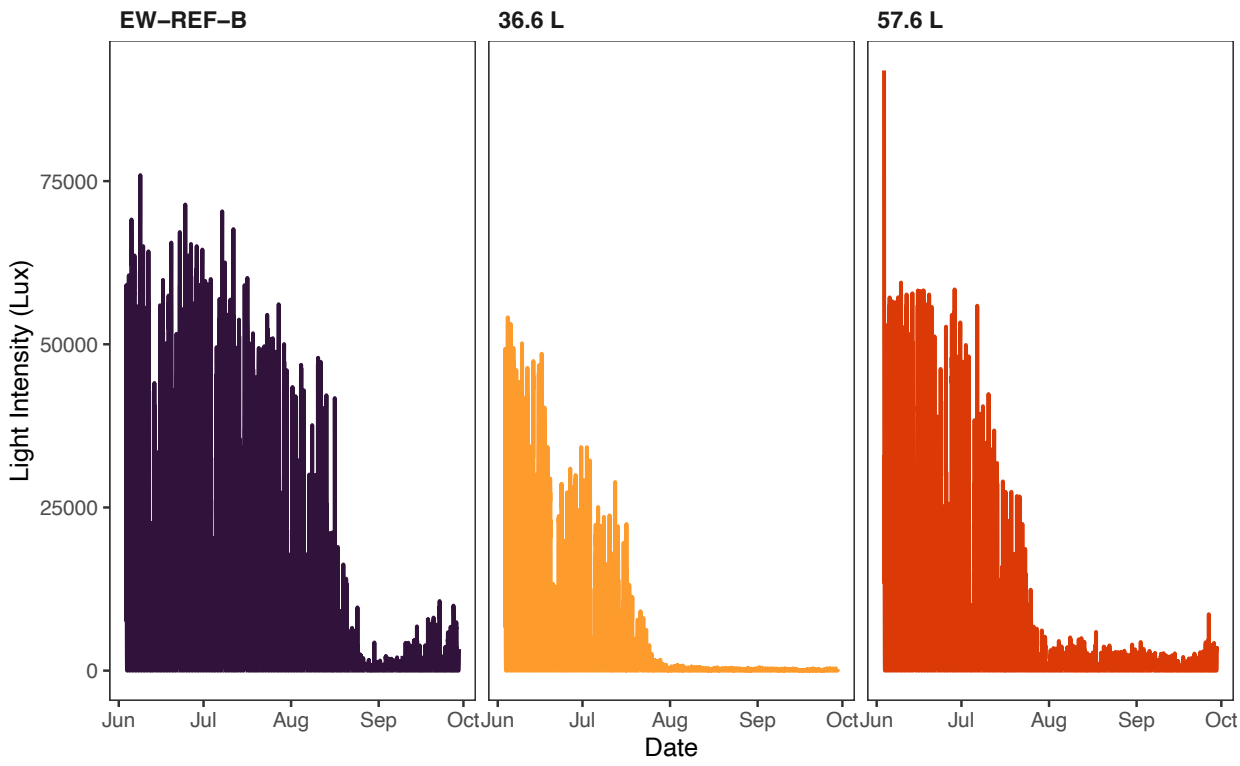

Appendix Figure C-5: Light intensity in the three of the treatments of the UM established wetland site.

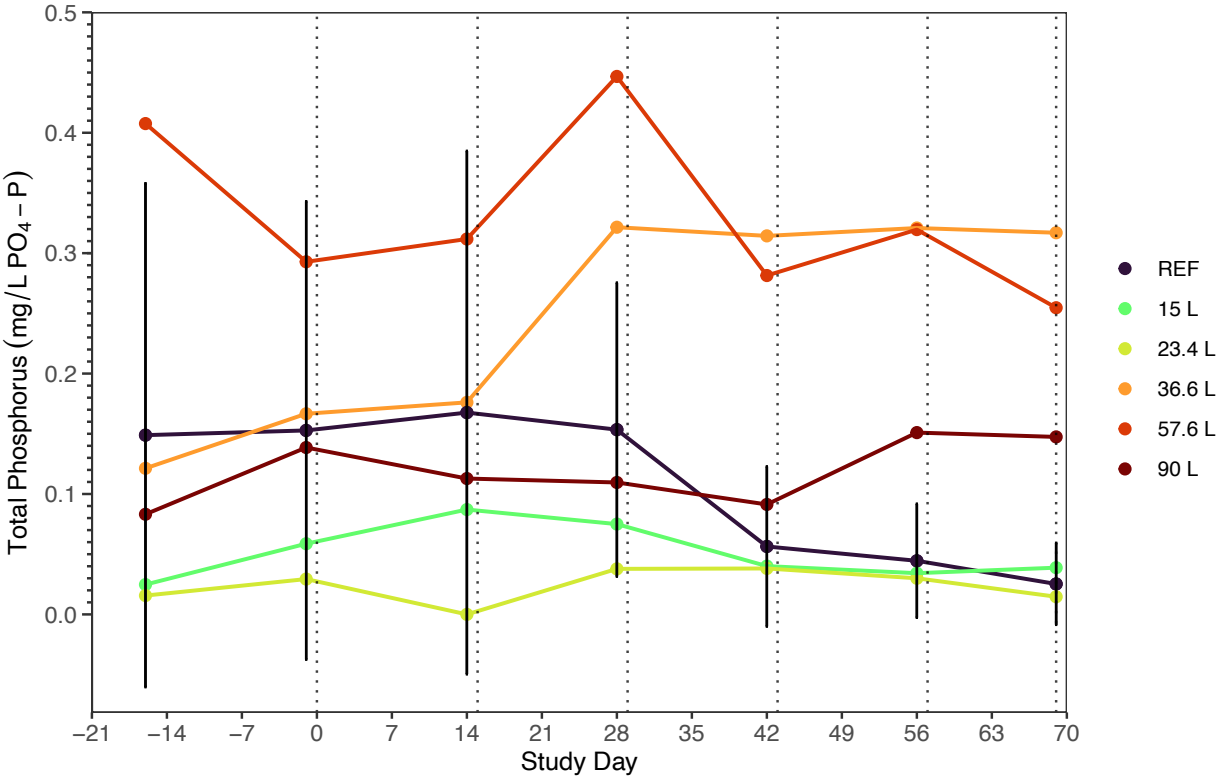

Appendix Figure C-6: Total phosphorus (mg/L PO_4-P) over the study duration within the established wetland mesocosms. The vertical dotted lines represent AWW addition days. REF displays the mean of the references (n = 2) with the error bars representing ± standard deviation.

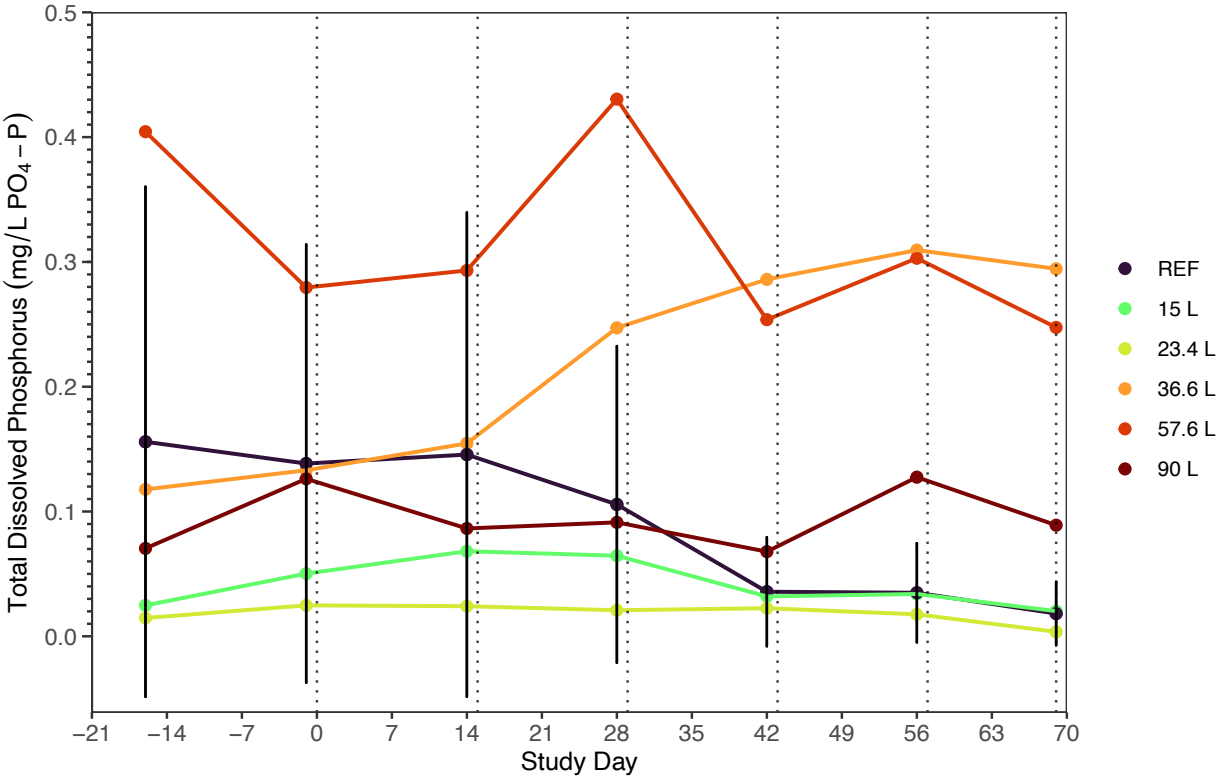

Appendix Figure C-7: Total dissolved phosphorus (mg/L PO_4-P) over the study duration within the established wetland mesocosms. The vertical dotted lines represent AWW addition days. REF displays the mean of the references (n = 2) with the error bars representing ± standard deviation.

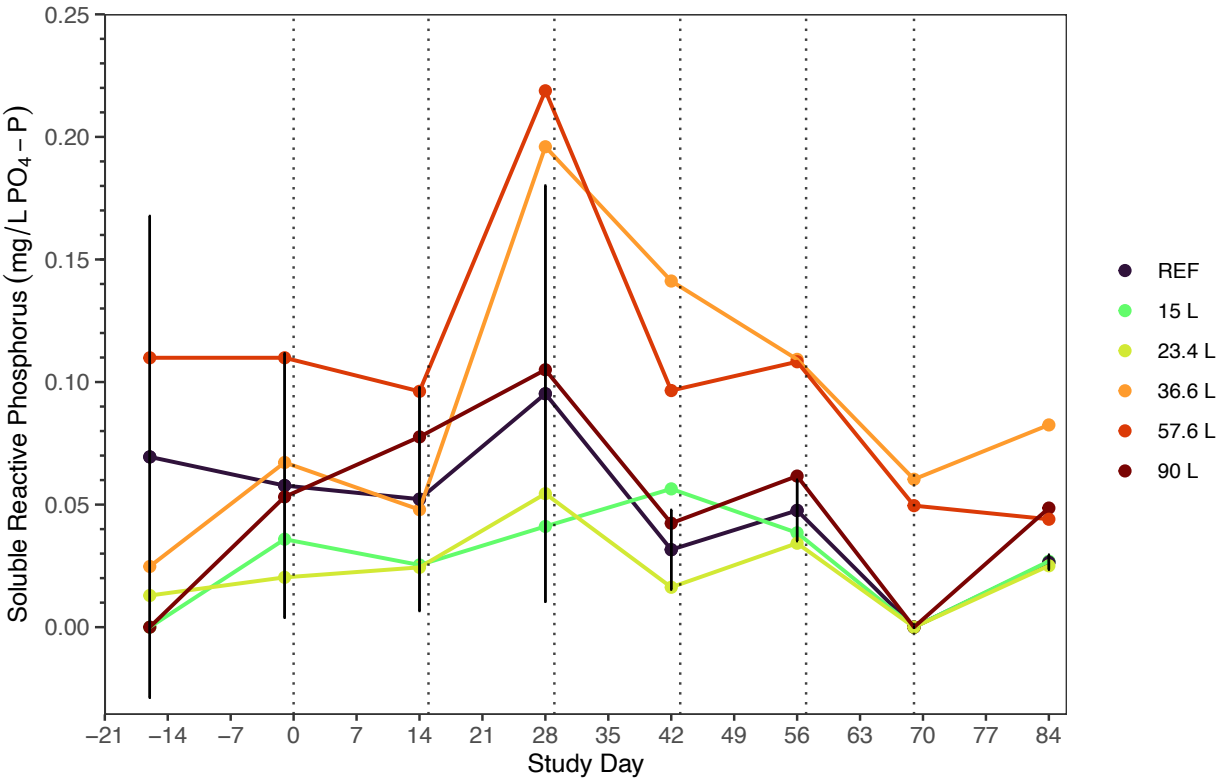

Appendix Figure C-8: Soluble reactive phosphorus (mg/L PO_4-P) over the study duration within the established wetland mesocosms. The vertical dotted lines represent AWW addition days. REF displays the mean of the references (n = 2) with the error bars representing ± standard deviation.

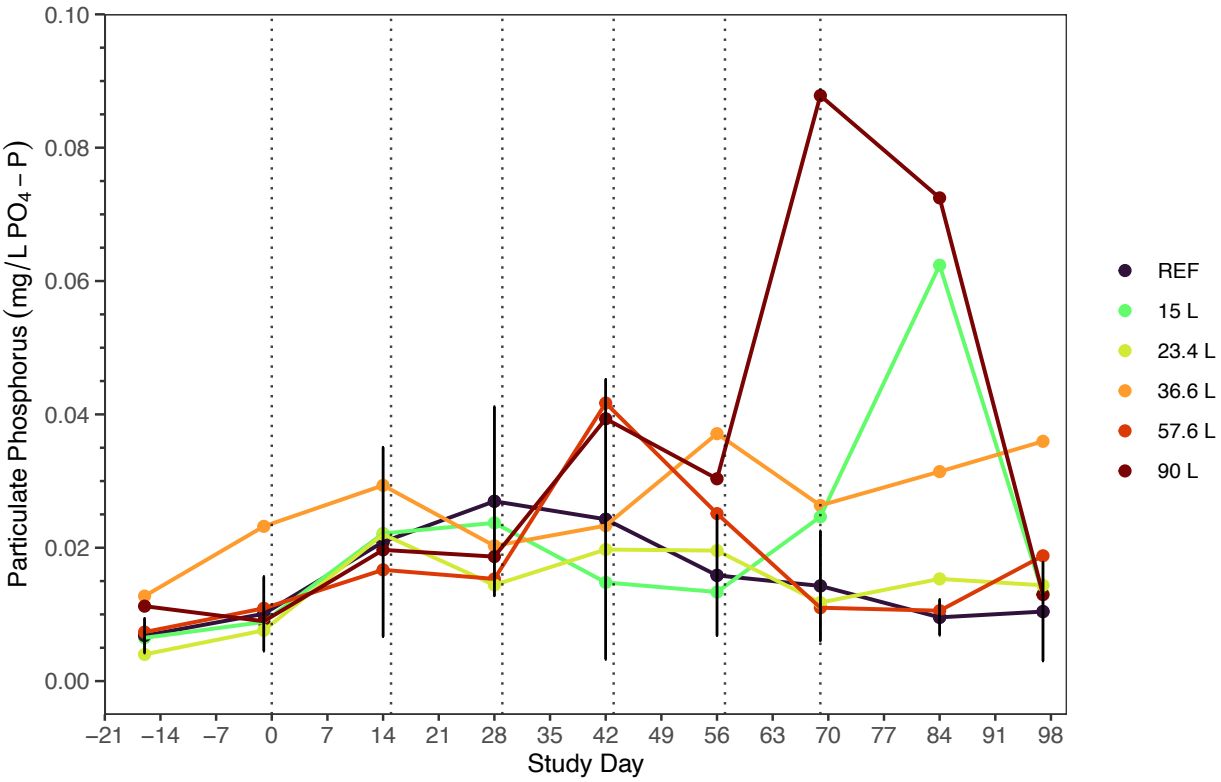

Appendix Figure C-9: Particulate phosphorus (µg/L PO_4-P) over the study duration within the established wetland mesocosms. The vertical dotted lines represent AWW addition days. REF displays the mean of the references (n = 2) with the error bars representing ± standard deviation.

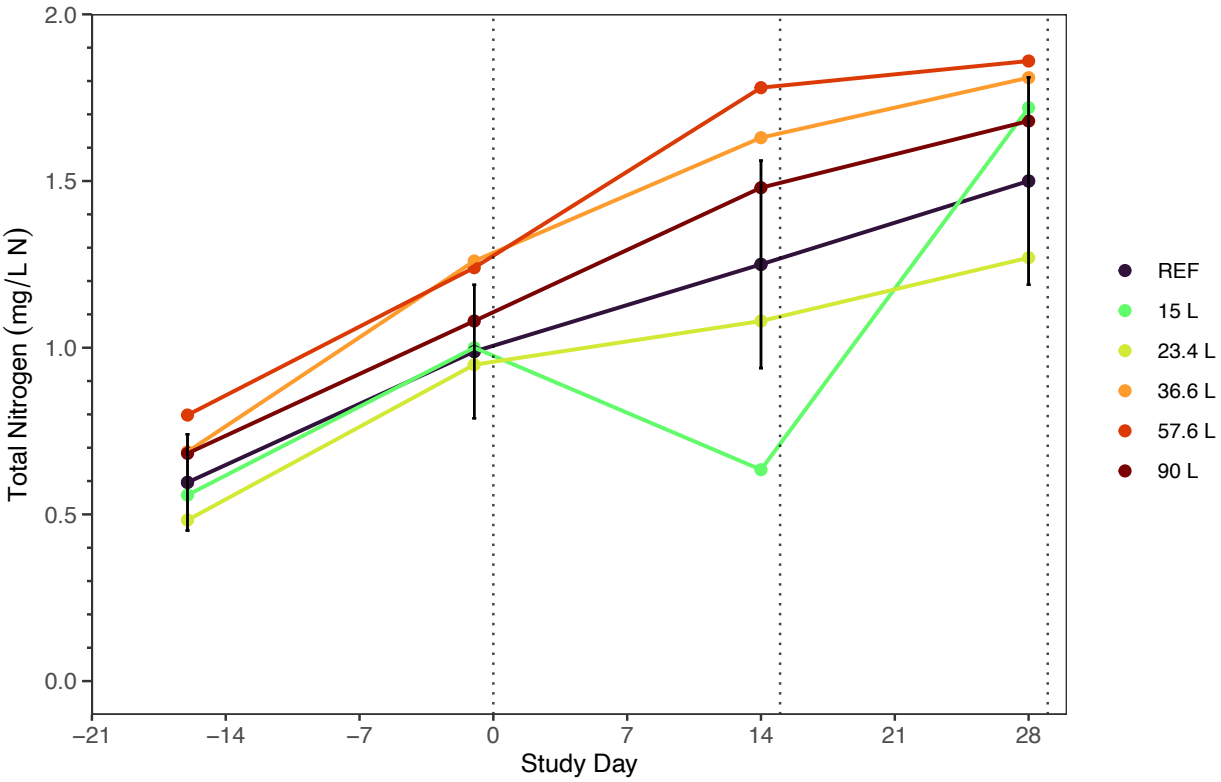

Appendix Figure C-10: Total nitrogen (mg/L N) over the study duration within the established wetland mesocosms. The vertical dotted lines represent AWW addition days. REF displays the mean of the references (n = 2) with the error bars representing ± standard deviation.

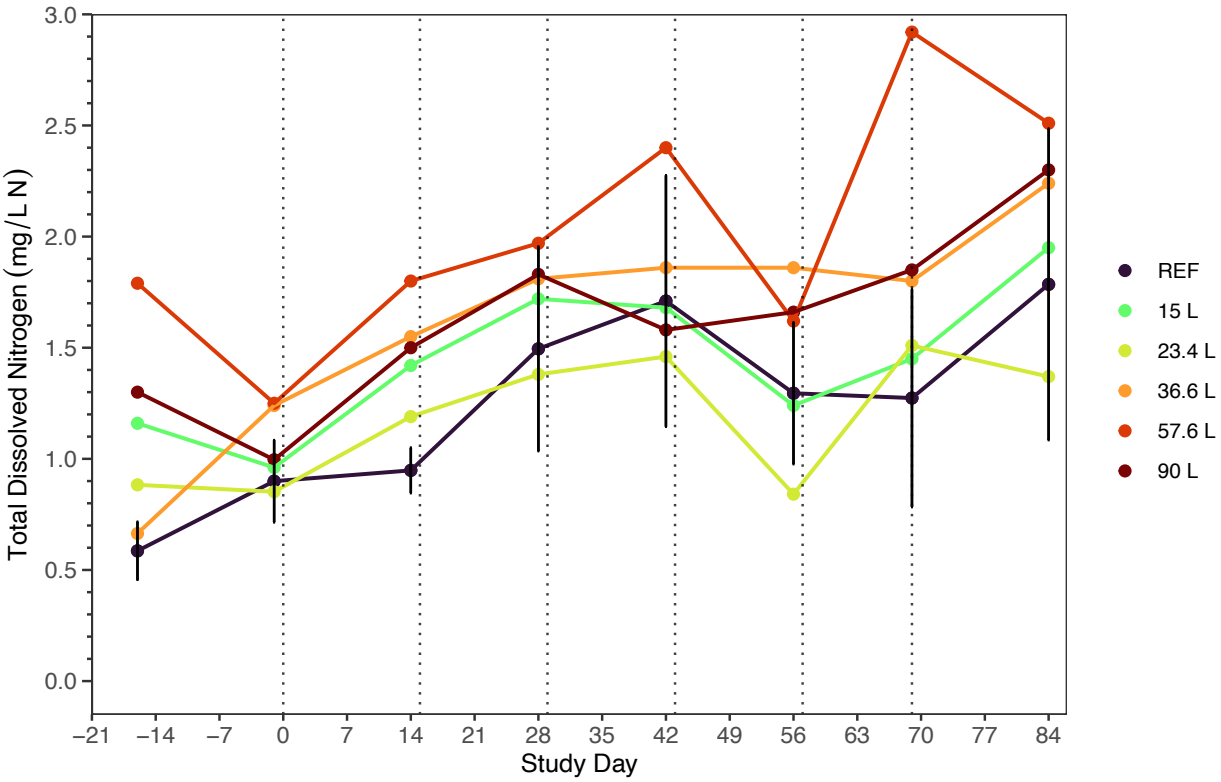

Appendix Figure C-11: Total dissolved nitrogen (mg/L N) over the study duration within the established wetland mesocosms. The vertical dotted lines represent AWW addition days. REF displays the mean of the references (n = 2) with the error bars representing ± standard deviation.

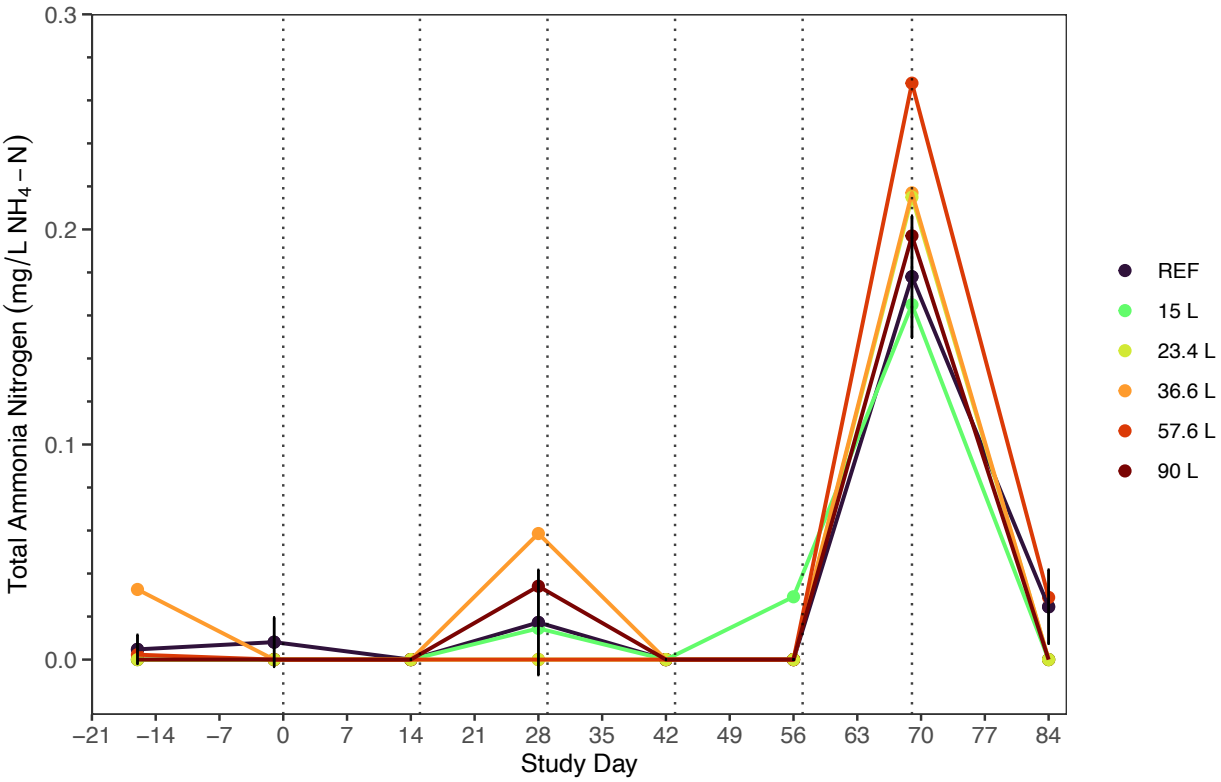

Appendix Figure C-12: Total ammonia nitrogen (mg/L NH_4-N) over the study duration within the established wetland mesocosms. The vertical dotted lines represent AWW addition days. REF displays the mean of the references (n = 2) with the error bars representing ± standard deviation.

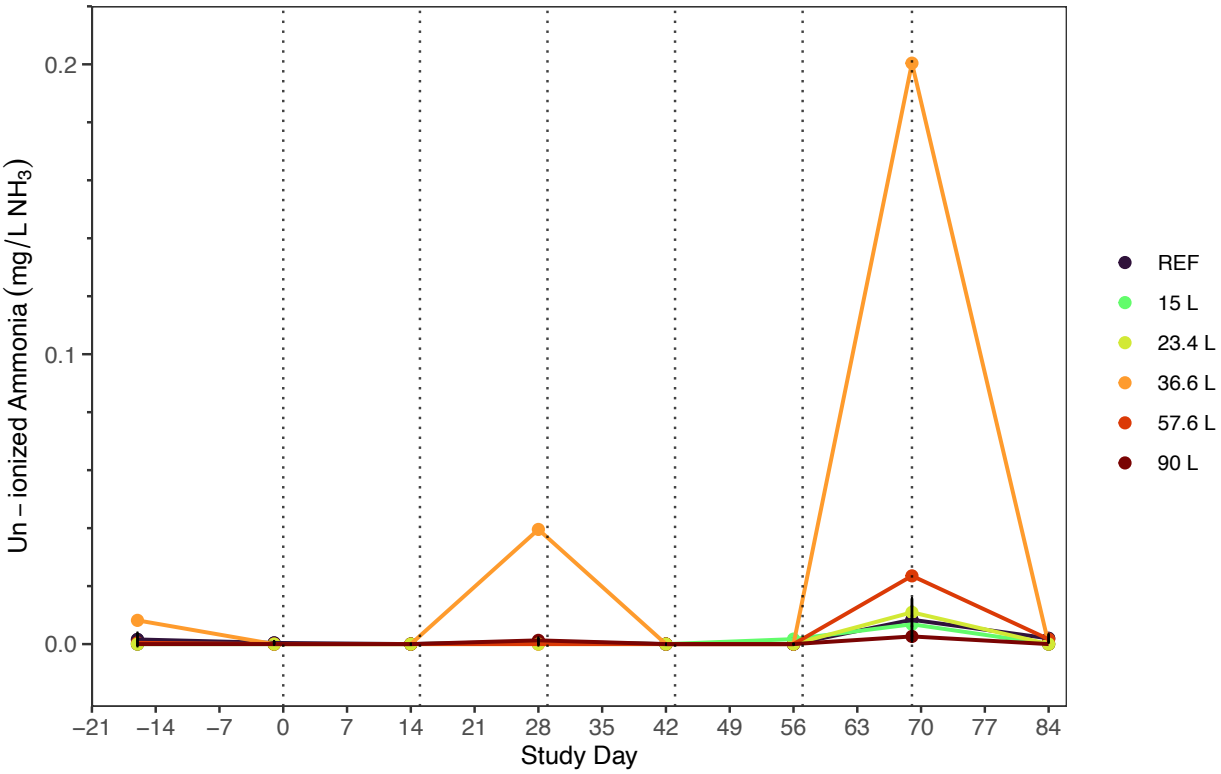

Appendix Figure C-13: Un-ionized ammonia (mg/L NH_3) over the study duration within the established wetland mesocosms. The vertical dotted lines represent AWW addition days. These values were calculated from TAN, pH, and temperature, from the calculation in Armstrong et al. (2012) and Delos and Erickson (1999) (see methods for more detail). REF displays the mean of the references (n = 2) with the error bars representing ± standard deviation.

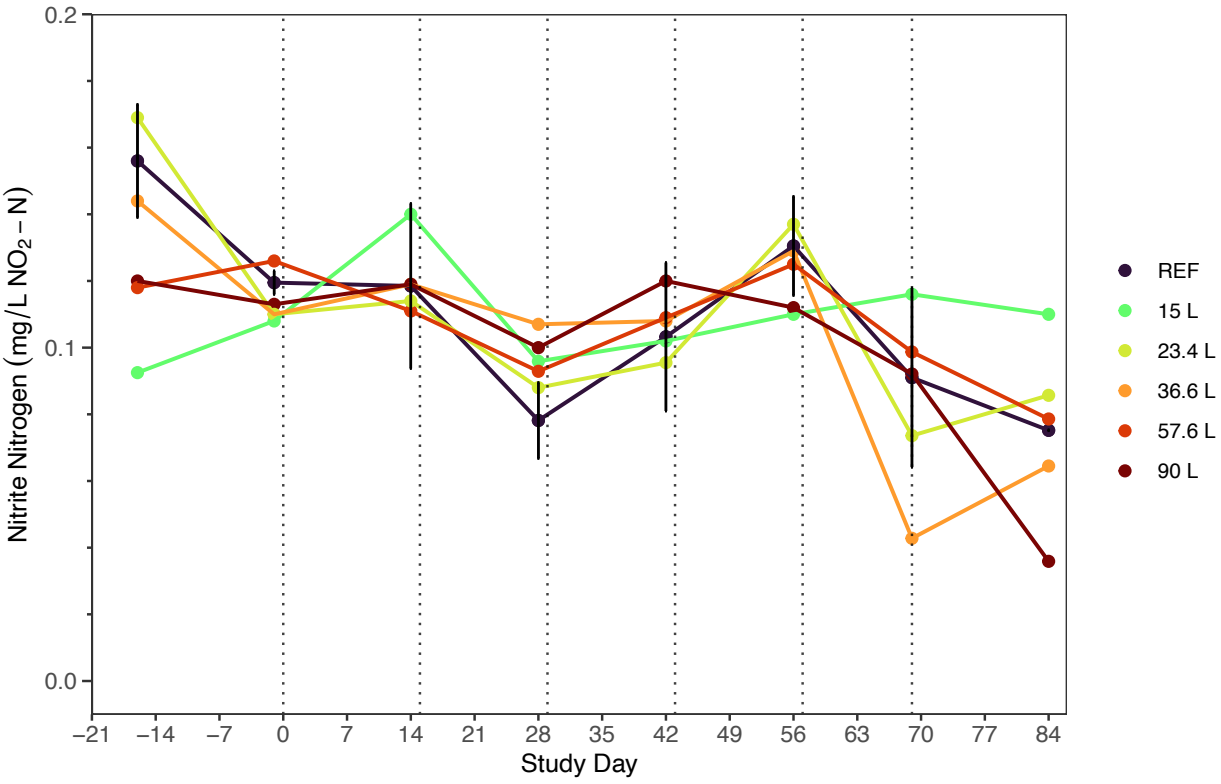

Appendix Figure C-14: Nitrite nitrogen (mg/L NO_2-N) over the study duration within the established wetland mesocosms. The vertical dotted lines represent AWW addition days. REF displays the mean of the references (n = 2) with the error bars representing ± standard deviation.

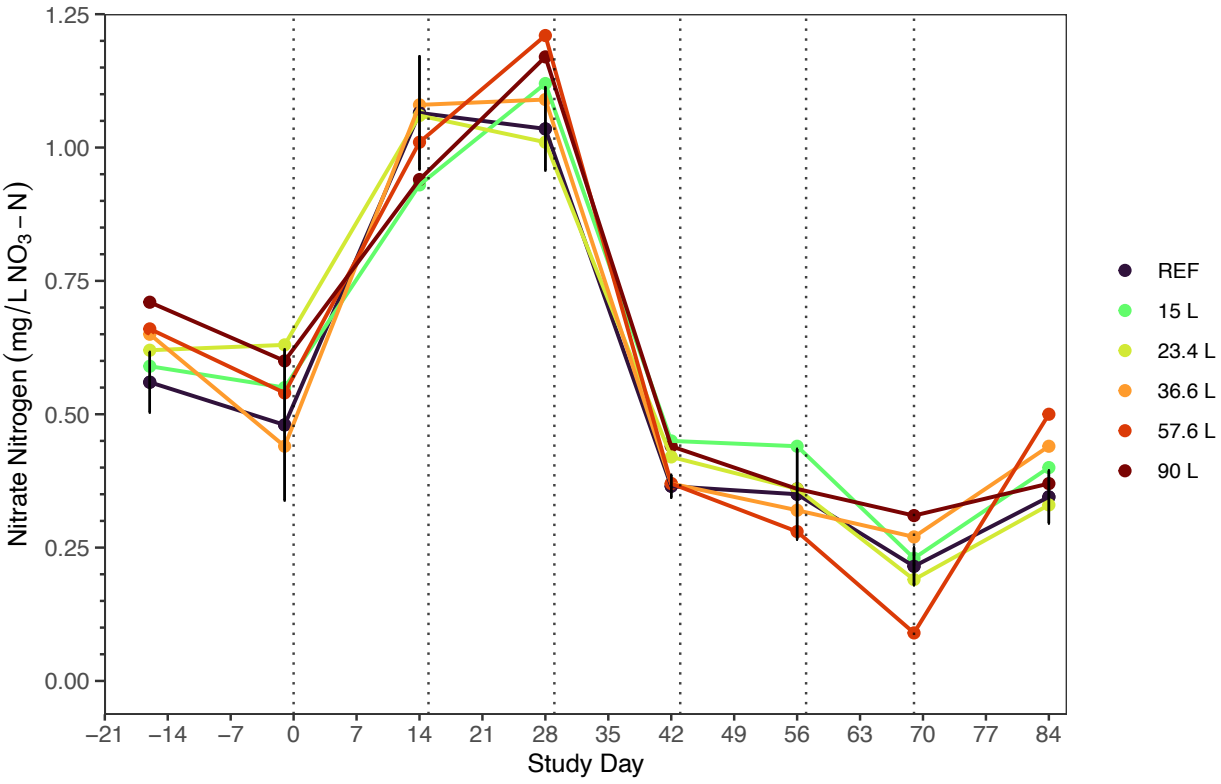

Appendix Figure C-15: Nitrate nitrogen (mg/L NO_3-N) over the study duration within the established wetland mesocosms. The vertical dotted lines represent AWW addition days. REF displays the mean of the references (n = 2) with the error bars representing ± standard deviation.

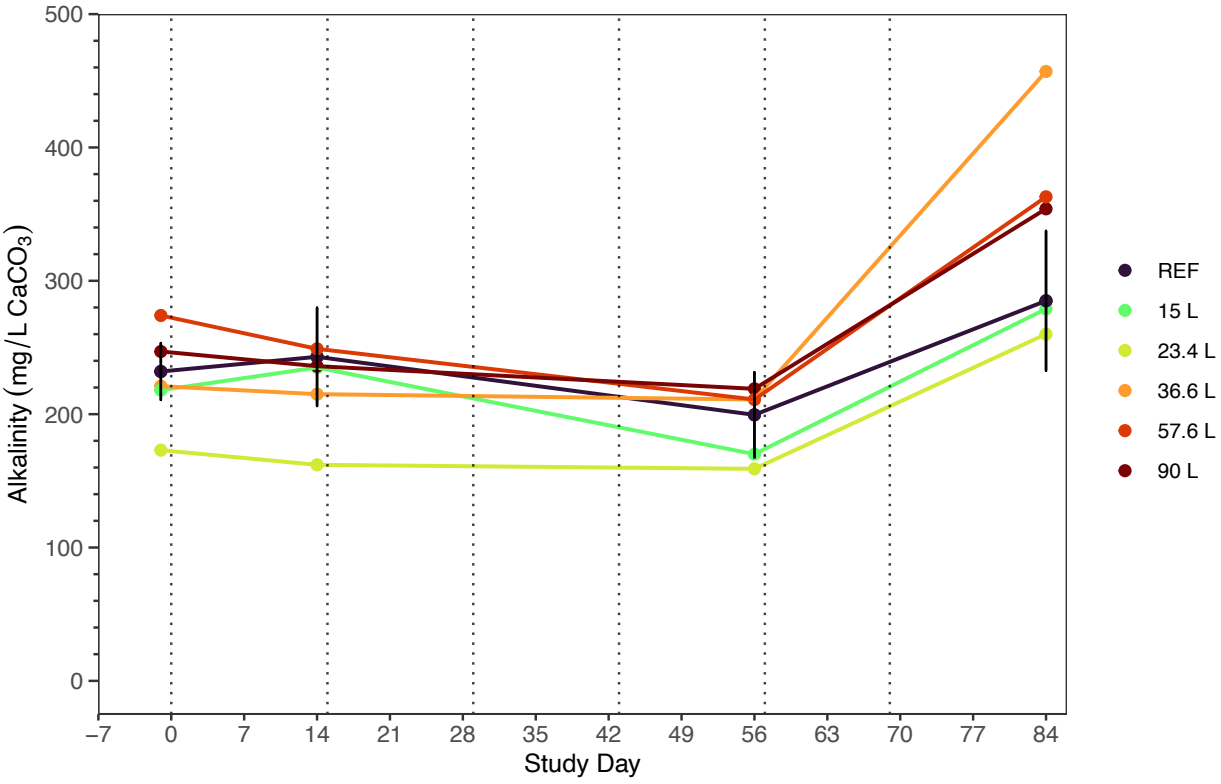

Appendix Figure C-16: Alkalinity (mg/L $CaCO_3$) over the study duration within the established wetland mesocosms. The vertical dotted lines represent AWW addition days. REF displays the mean of the references (n = 2) with the error bars representing ± standard deviation.

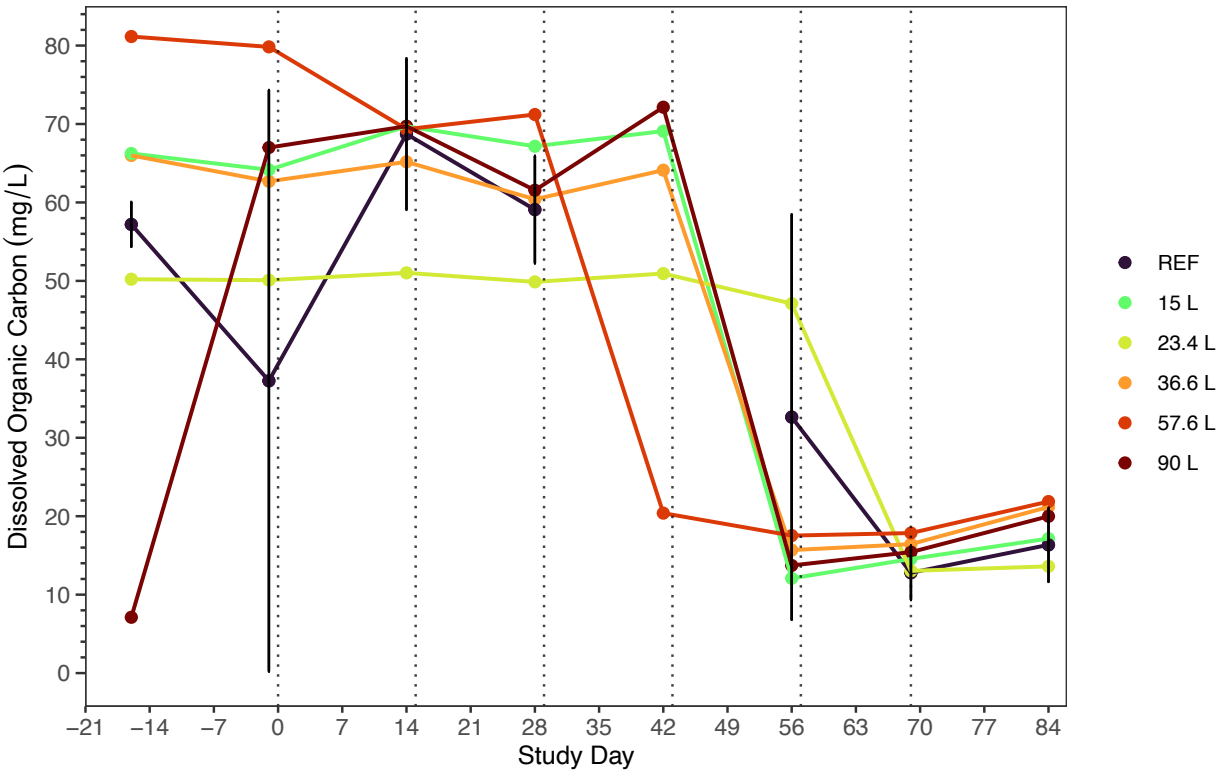

Appendix Figure C-17: Dissolved organic carbon (mg/L) over the study duration within the established wetland mesocosms. The vertical dotted lines represent AWW addition days. REF displays the mean of the references (n = 2) with the error bars representing ± standard deviation.

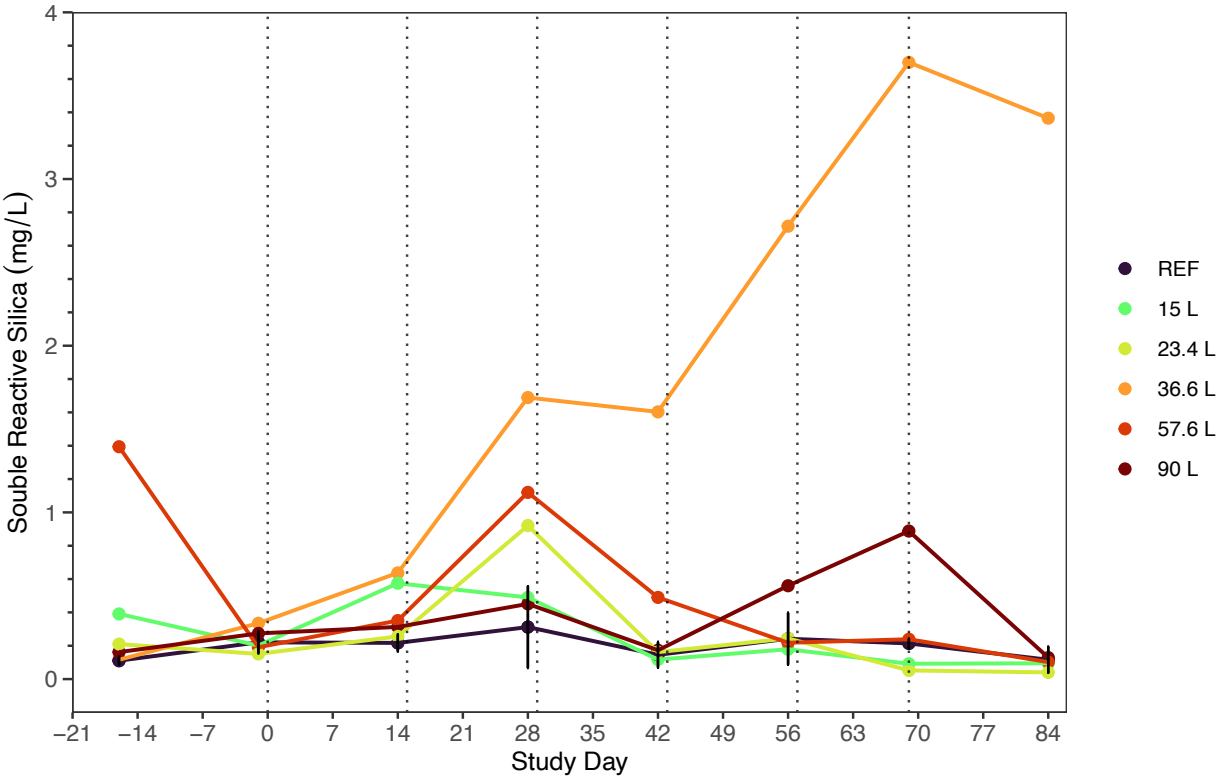

Appendix Figure C-18: Soluble reactive silica (mg/L) over the study duration within the established wetland mesocosms. The vertical dotted lines represent AWW addition days. REF displays the mean of the references (n = 2) with the error bars representing ± standard deviation.

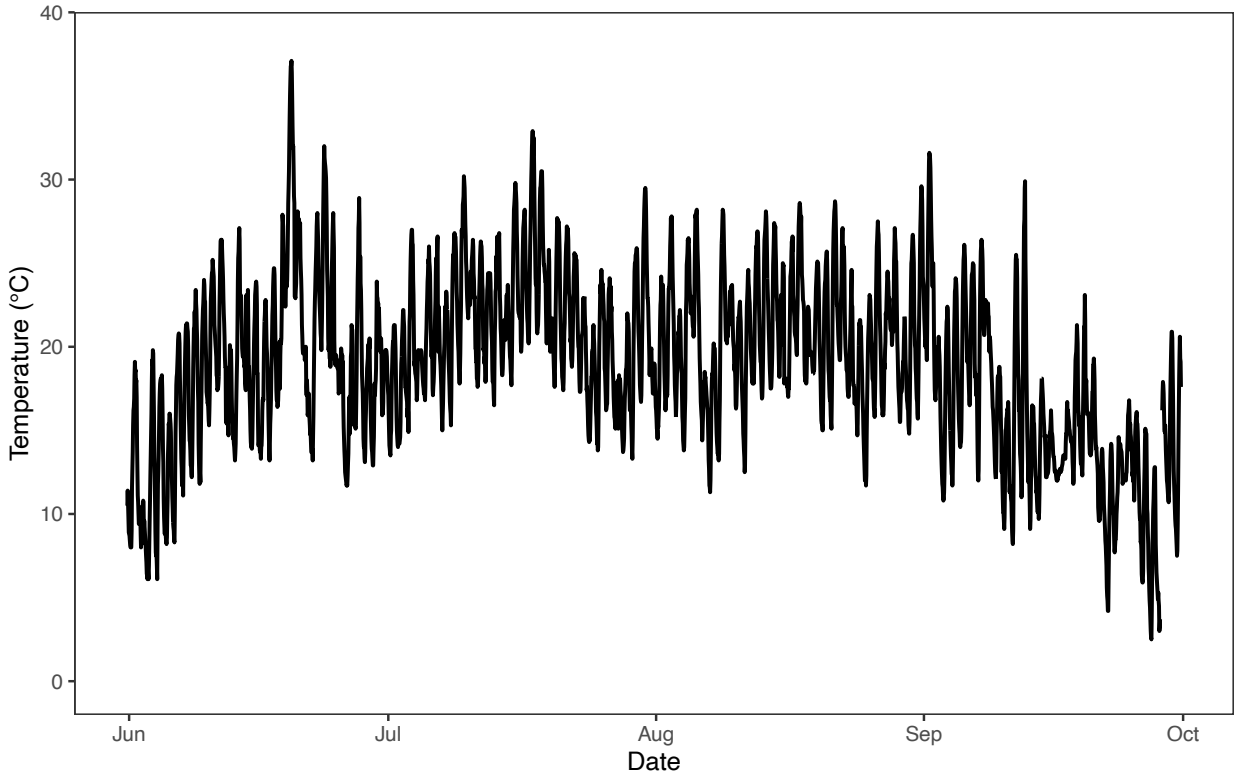

Appendix Figure C-19: Air temperature measured at the Environment Canada Winnipeg weather station from June to October.

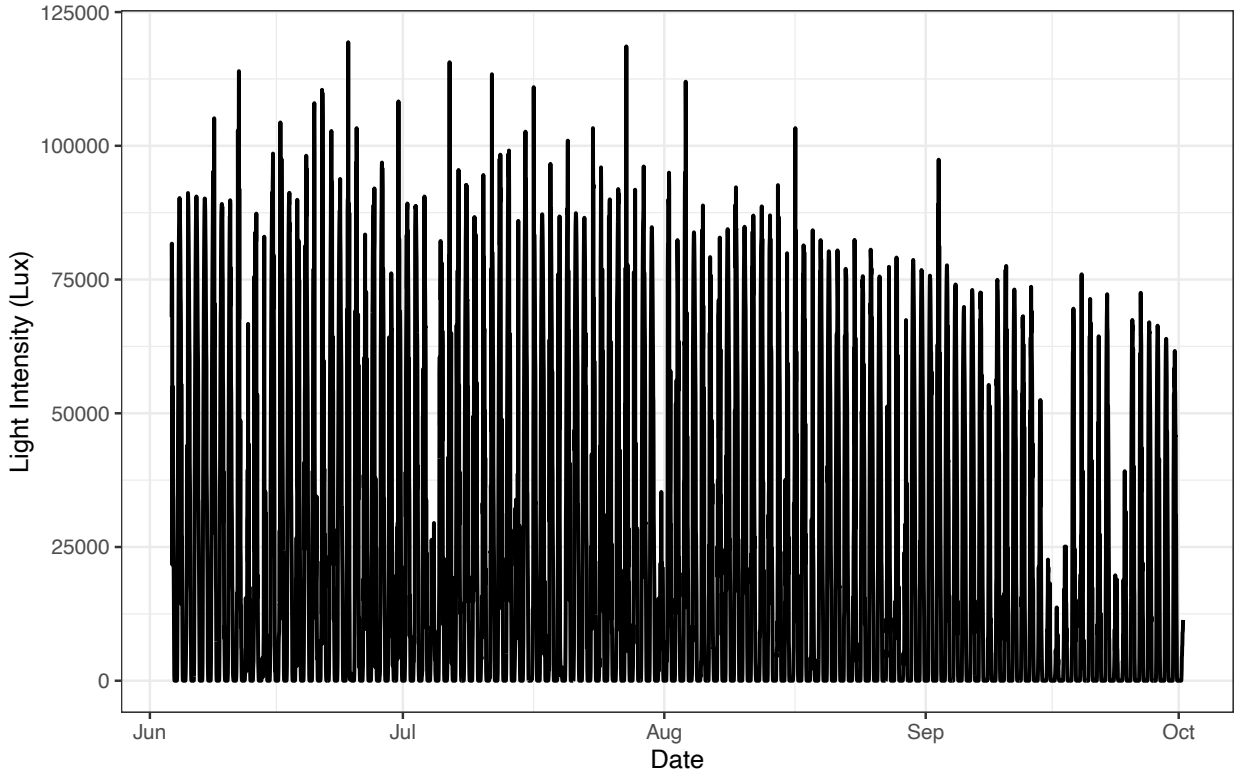

Appendix Figure C-20: Light intensity measured from June to October at the RL site.

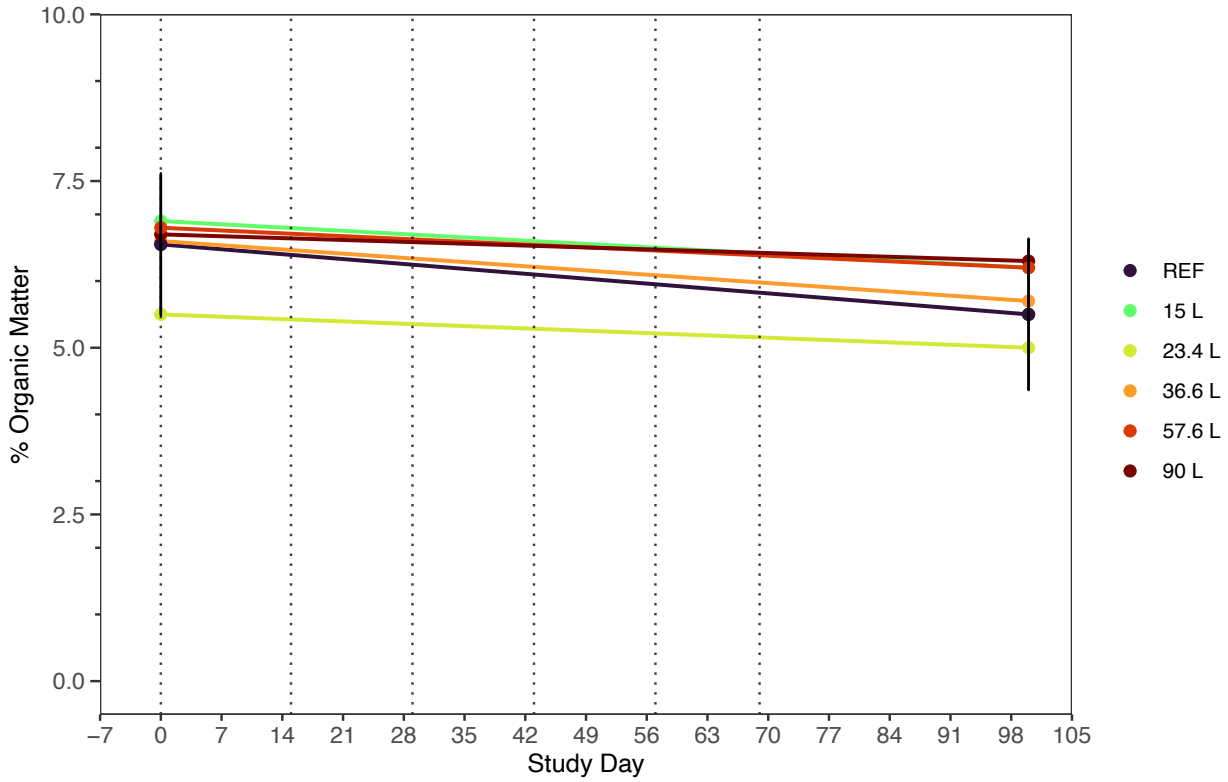

Appendix Figure C-21: Soil organic matter (%) over the study duration within the UM established wetland mesocosms. The vertical dotted lines represent AWW addition days. REF displays the mean of the references (n = 2) with the error bars representing ± standard deviation.

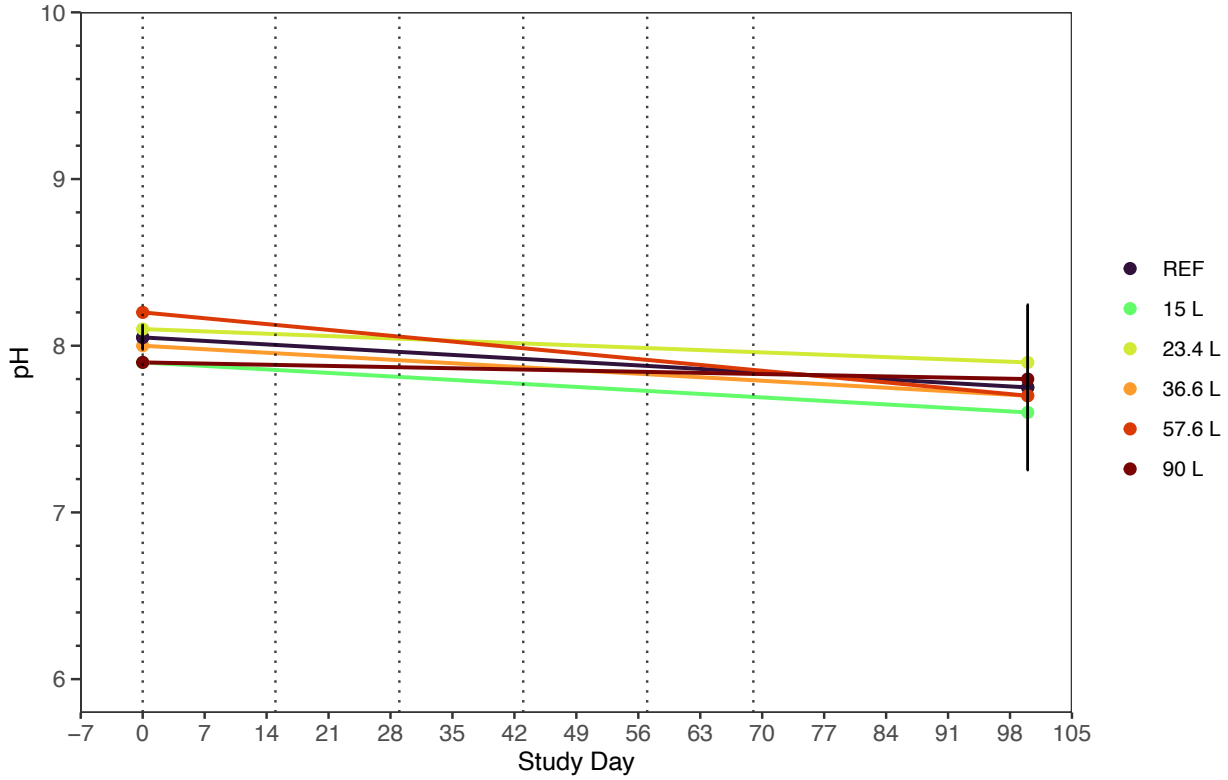

Appendix Figure C-22: Soil pH over the study duration within the UM established wetland mesocosms. The vertical dotted lines represent AWW addition days. REF displays the mean of the references (n = 2) with the error bars representing ± standard deviation.

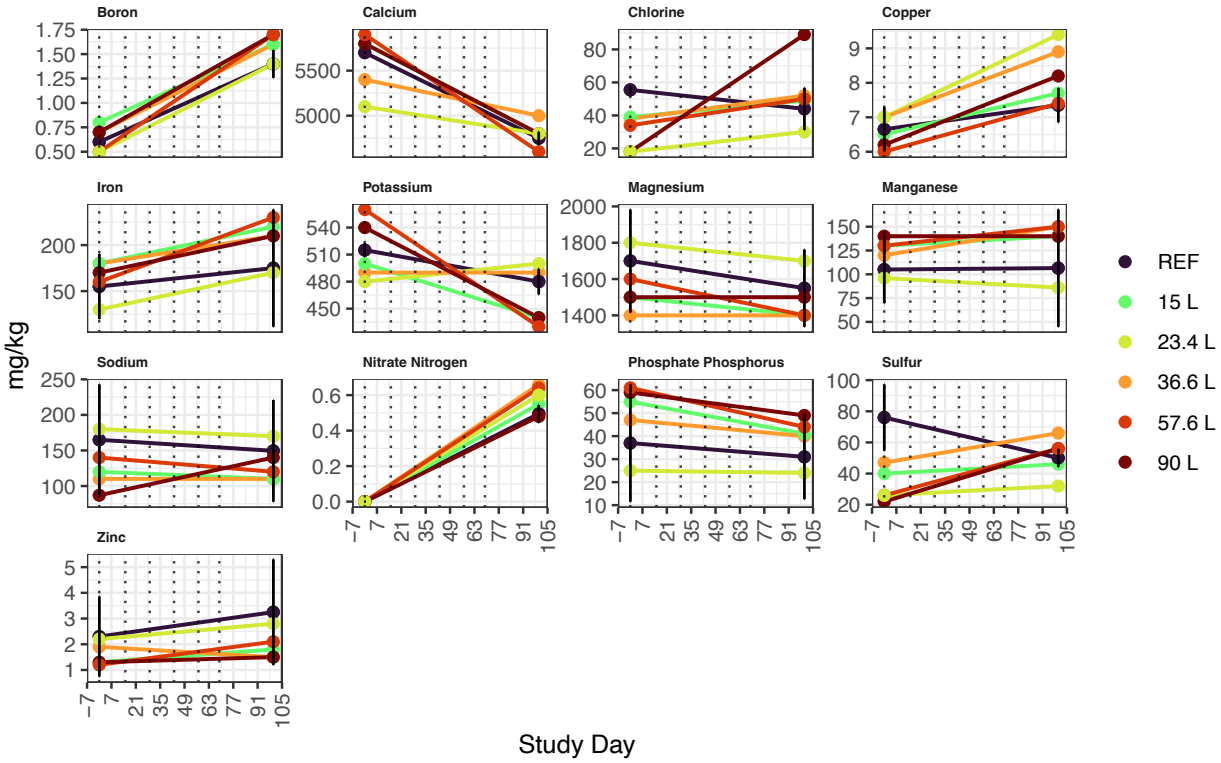

Appendix Figure C-23: Soil ions (mg/kg) over the study duration within the RL commercial wild rice mesocosms. The vertical dotted lines represent AWW addition days. REF displays the mean of the references (n = 2) with the error bars representing ± standard deviation.

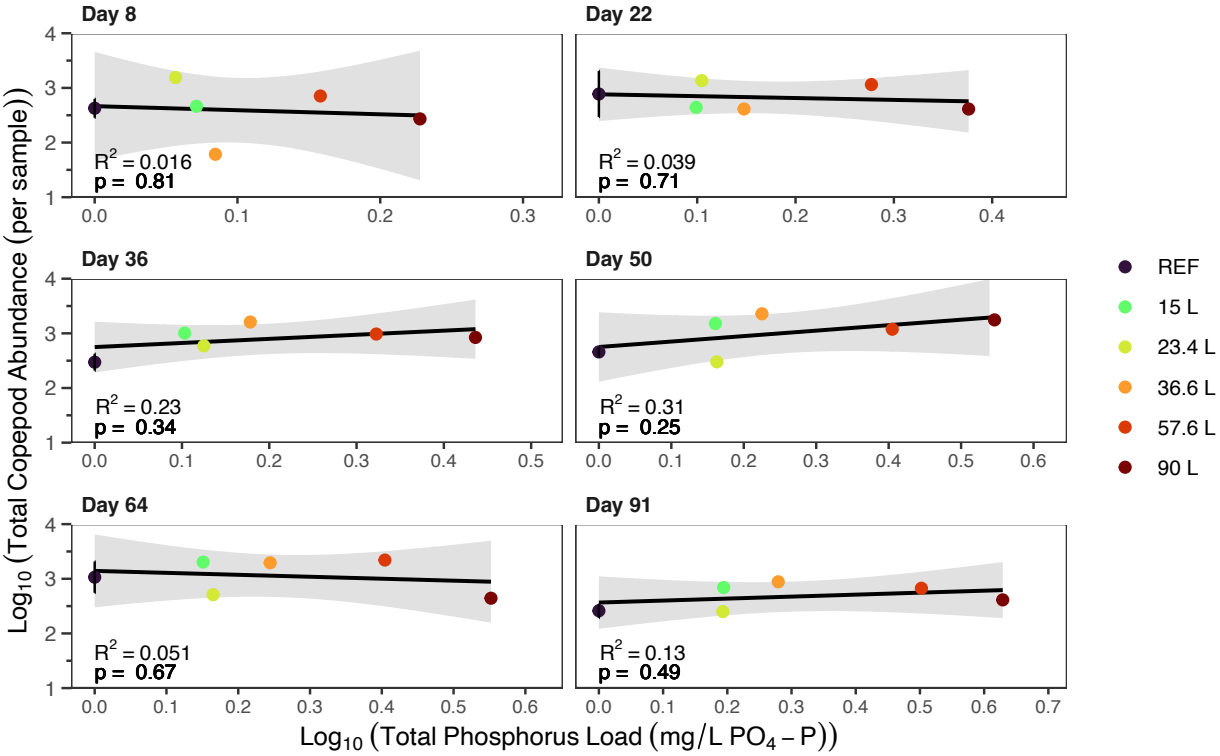

Appendix Figure C-24: Linear regression model results of the relationship between log10(x + 1) of cumulative AWW load concentration (TP used as the representative variable) and total copepod abundance. REF displays the mean of the references (n = 2) with the error bars representing ± standard deviation. Each plot displays the model results according to study day.

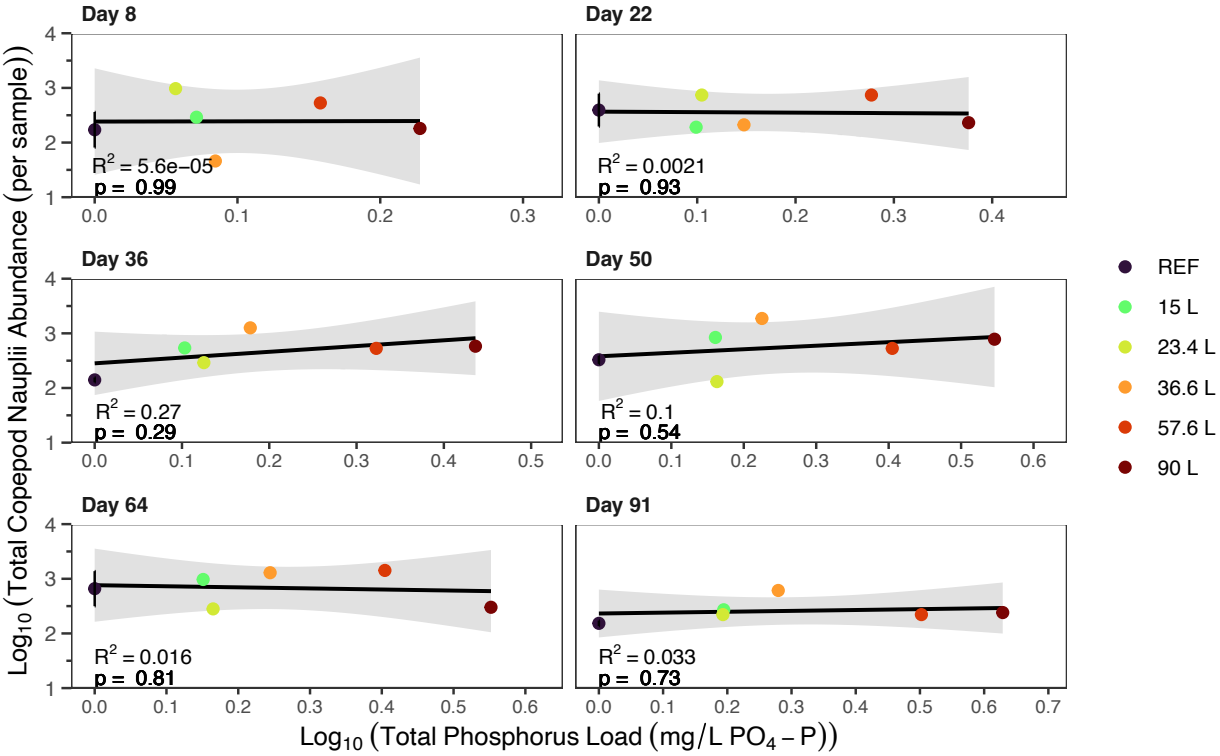

Appendix Figure C-25: Linear regression model results of the relationship between log10(x + 1) of cumulative AWW load concentration (TP used as the representative variable) and total copepod nauplii abundance. REF displays the mean of the references (n = 2) with the error bars representing ± standard deviation. Each plot displays the model results according to study day.

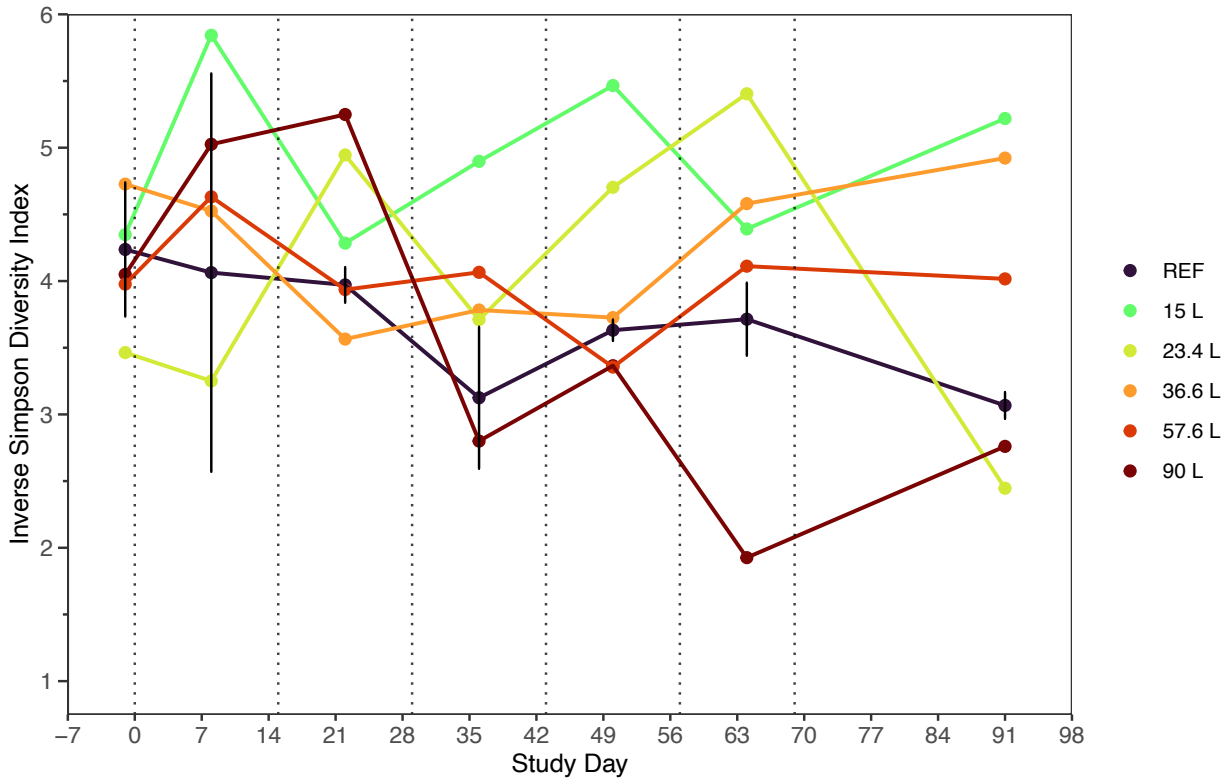

Appendix Figure C-26: Inverse Simpson Diversity over the study duration within the established wetland mesocosms. The vertical dotted lines represent AWW addition days. REF displays the mean of the references (n = 2) with the error bars representing ± standard deviation.

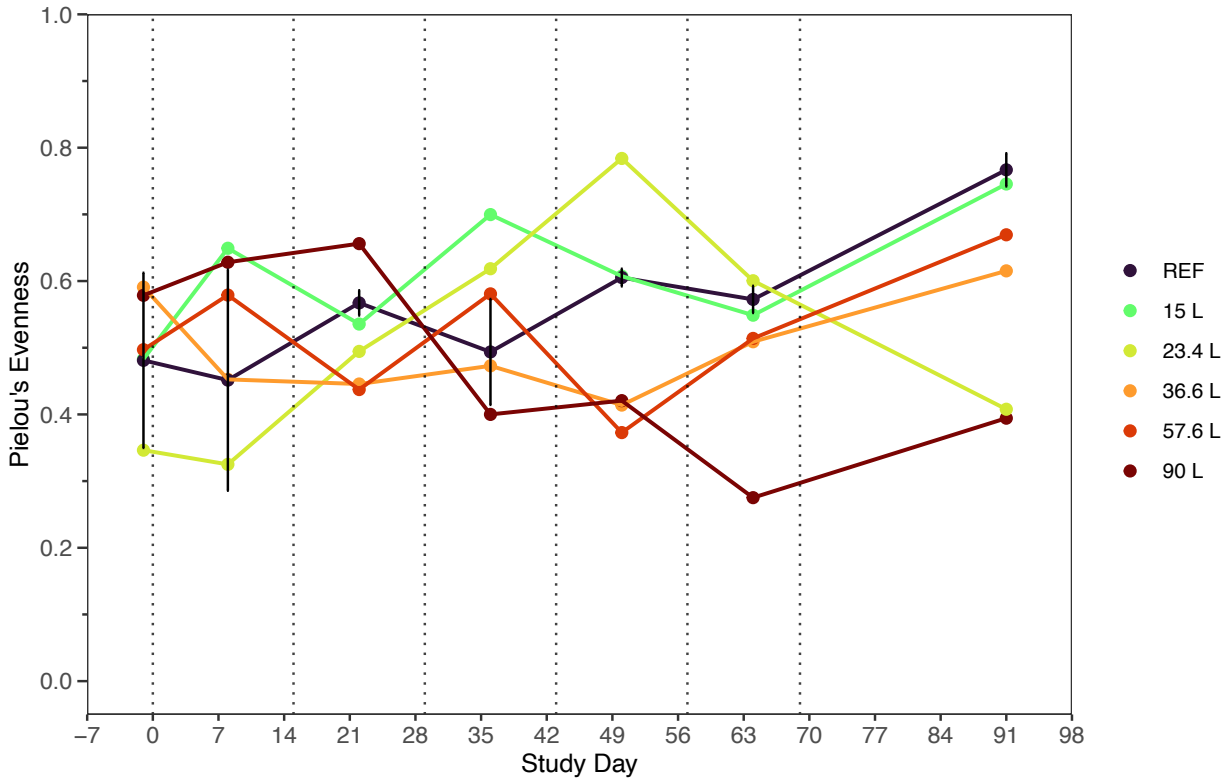

Appendix Figure C-27: Pielou's evenness over the study duration within the established wetland mesocosms. The vertical dotted lines represent AWW addition days. REF displays the mean of the references (n = 2) with the error bars representing ± standard deviation.

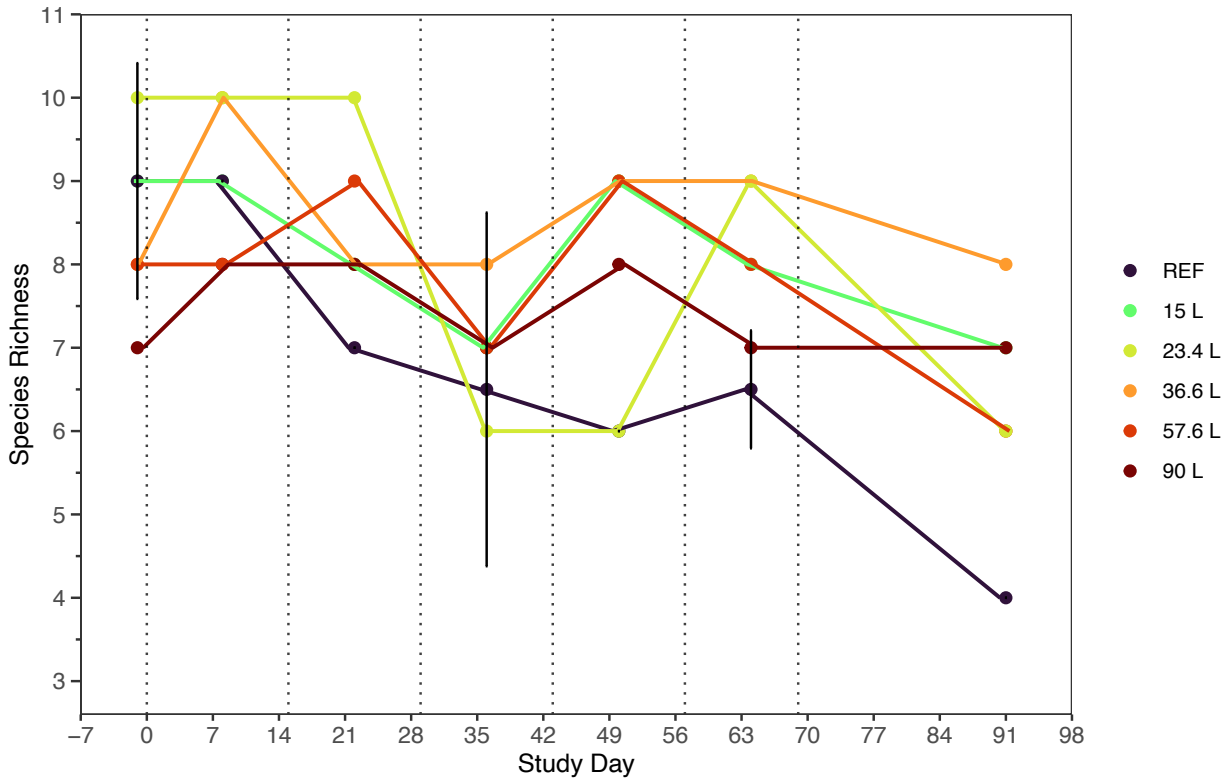

Appendix Figure C-28: Species richness over the study duration within the established wetland mesocosms. The vertical dotted lines represent AWW addition days. REF displays the mean of the references (n = 2) with the error bars representing ± standard deviation.

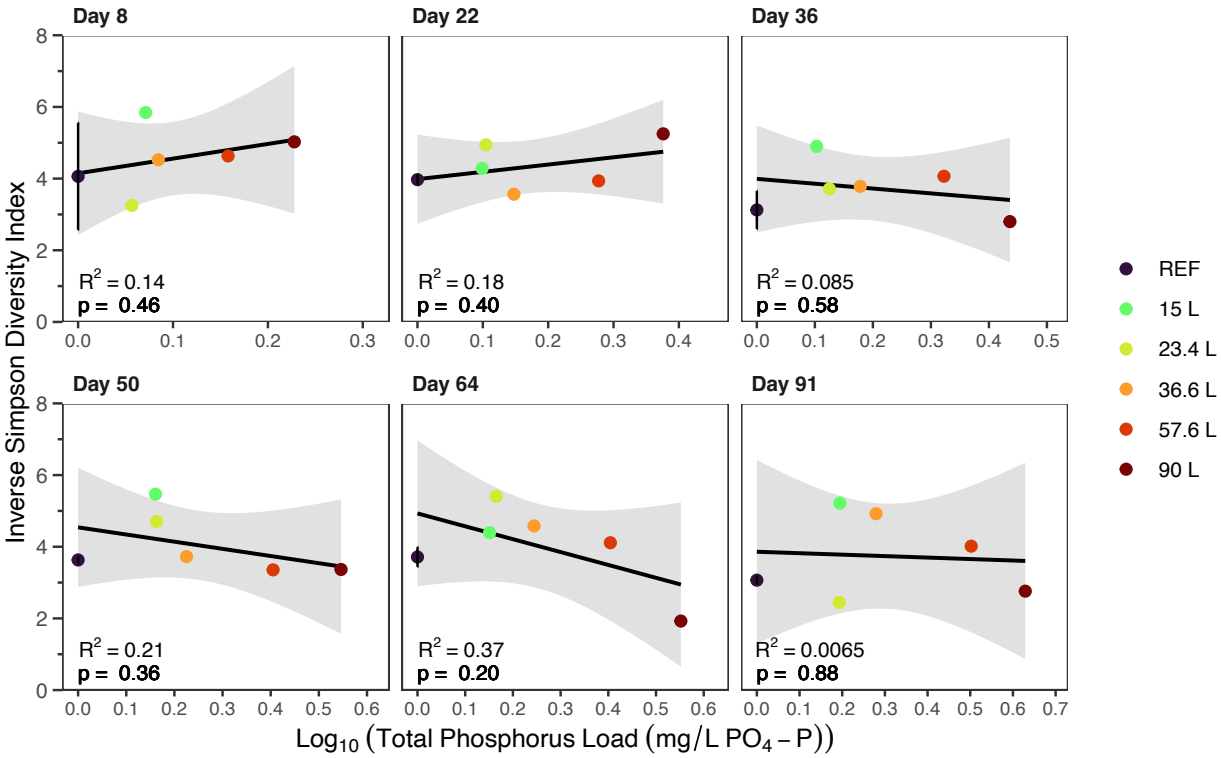

Appendix Figure C-29: Linear regression model results of the relationship between log10(x + 1) of cumulative AWW load concentration (TP used as the representative variable) and Inverse Simpson Diversity. REF displays the mean of the references (n = 2) with the error bars representing ± standard deviation. Each plot displays the model results according to study day.

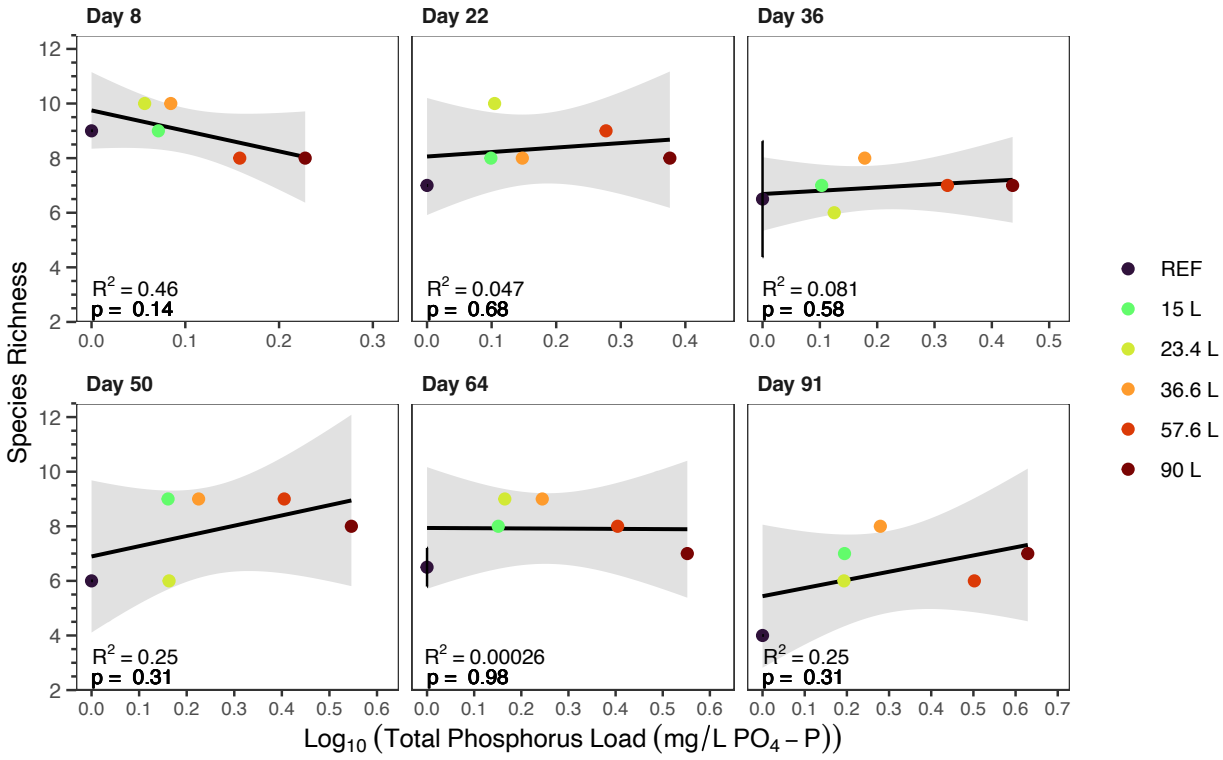

Appendix Figure C-30: Linear regression model results of the relationship between log10(x + 1) of cumulative AWW load concentration (TP used as the representative variable) and Species Richness. REF displays the mean of the references (n = 2) with the error bars representing ± standard deviation. Each plot displays the model results according to study day.

Appendix D UM-WR Supplemental Tables and Figures

Appendix Table D-1: Cumulative nutrient concentration of TP (mg/L PO_4-P) within each treatment as a result of each AWW addition load. The cumulative concentration is a result of the sum of each mass of TP loaded, divided by the most recent volume.

Treatment	Addition #1	+Addition #2	+Addition #3	+Addition #4	+Addition #5	+Addition #6
Reference	0	0	0	0	0	0
6 L	0.0414	0.0791	0.0972	0.1313	0.1452	0.1715
9.6 L	0.0675	0.1269	0.1628	0.2139	0.2329	0.2751
15 L	0.1031	0.1969	0.2528	0.3372	0.3524	0.4388
23.4 L	0.1697	0.3250	0.4141	0.5546	0.6162	0.7358
36.6 L	0.2462	0.4621	0.5499	0.7483	0.8449	1.0124
57.6 L	0.4032	0.7710	0.9068	1.2215	1.4507	1.7582
90 L	0.6525	1.2498	1.5687	2.0985	2.0681	2.7517

Appendix Table D-2: Cumulative nutrient concentration of TKN (mg/L) within each treatment as a result of each AWW addition load. The cumulative concentration is a result of the sum of each mass of TKN loaded, divided by the most recent volume.

Treatment	Addition #1	+Addition #2	+Addition #3	+Addition #4	+Addition #5	+Addition #6
Reference	0	0	0	0	0	0
6 L	0.2510	0.4375	0.5496	1.0547	1.1380	1.2693
9.6 L	0.4093	0.7021	0.9202	1.7185	1.8251	2.0357
15 L	0.6251	1.0893	1.4291	2.7095	2.7619	3.2470
23.4 L	1.0290	1.7980	2.3410	4.4560	4.8293	5.4447
36.6 L	1.4930	2.5570	3.1091	6.0117	6.6217	7.4917
57.6 L	2.4457	4.2657	5.1269	9.8136	11.3697	13.0111
90 L	3.9576	6.9153	8.8685	16.8597	16.2082	20.3636

Appendix Table D-3: Cumulative nutrient concentration of NH_4 (mg/L NH_4-N) within each treatment as a result of each AWW addition load. The cumulative concentration is a result of the sum of each mass of NH_4 loaded, divided by the most recent volume.

Treatment	Addition #1	+Addition #2	+Addition #3	+Addition #4	+Addition #5	+Addition #6
Reference	0	0	0	0	0	0
6 L	0.2419	0.4179	0.4981	0.7056	0.8270	0.9372
9.6 L	0.3946	0.6706	0.8341	1.1497	1.3263	1.5031
15 L	0.6026	1.0405	1.2953	1.8127	2.0071	2.3975
23.4 L	0.9918	1.7174	2.1219	2.9811	3.5095	4.0203
36.6 L	1.4391	2.4424	2.8181	4.0219	4.8121	5.5317
57.6 L	2.3574	4.0747	4.6471	6.5654	8.2625	9.6072
90 L	3.8146	6.6056	8.0385	11.2793	11.7787	15.0360

Appendix Table D-4: Mean nutrient concentration as a result of AWW loading within each treatment over the study duration (n = 6). Each concentration that contributed to the average is a result of the mass of the nutrient loaded divided by the known volume at the time of each addition.

Treatment	TP (mg/L PO_4-P)	TAN (mg/L NH_4-N)	TKN (mg/L)
Reference	0	0	0
6 L	0.0325	0.1778	0.2419
9.6 L	0.0529	0.2887	0.3932
15 L	0.0820	0.4471	0.6114
23.4 L	0.1366	0.7460	1.0168
36.6 L	0.1895	1.0352	1.4019
57.6 L	0.3171	1.7308	2.3341
90 L	0.5101	2.7735	3.7970

Appendix Table D-5: The cumulative and mean concentration of copper and zinc within each treatment as a result of each AWW loading (n = 3).

Treatment	Cumulative Cu (mg/L)	Mean Cu (mg/L)	Cumulative Zn (mg/L)	Mean Zn (mg/L)
Reference	0	0	0	0
6 L	0.0017	0.0003	0.0135	0.0025
9.6 L	0.0028	0.0005	0.0217	0.0041
15 L	0.0037	0.0007	0.0346	0.0064
23.4 L	0.0074	0.0014	0.0580	0.0107
36.6 L	0.0102	0.0019	0.0798	0.0148
57.6 L	0.0177	0.0032	0.1386	0.0248
90 L	0.0278	0.0051	0.2169	0.0398

Appendix Table D-6: Mean (±SD) concentration of environmental variables after the first AWW treatment to the end of the study duration, within each treatment.

	TP (mg/L PO_4-P) (n = 5)	**TDP (mg/L PO_4-P)** (n = 5)	**SRP (mg/L PO_4-P)** (n = 6)	**Part-P (mg/L PO_4-P)** (n = 7)	**TN (mg/L N)** (n = 2)	**TDN (mg/L N)** (n = 6)	**TAN (mg/L NH_4-N)** (n = 6)	**NH_3 (mg/L NH_3)** (n = 6)	**NO_2 (mg/L NO_2-N)** (n = 6)	**NO_3 (mg/L NO_3-N)** (n = 6)	**Chl-*a* (µg/L)** (n = 7)
Reference	0.042 (0.034)	0.025 (0.020)	0.031 (0.029)	0.040 (0.029)	1.25 (0.28)	1.16 (0.19)	0.038 (0.071)	0.028 (0.056)	0.106 (0.022)	0.576 (0.403)	2.44 (2.04)
6L	0.124 (0.043)	0.062 (0.028)	0.025 (0.021)	0.020 (0.011)	1.54 (0.13)	1.22 (0.10)	0.053 (0.095)	0.044 (0.080)	0.101 (0.031)	0.615 (0.380)	8.43 (4.73)
9.6L	0.064 (0.019)	0.022 (0.012)	0.033 (0.029)	0.040 (0.029)	0.96 (0.18)	1.03 (0.17)	0.045 (0.080)	0.029 (0.066)	0.103 (0.015)	0.542 (0.375)	6.75 (3.61)
15L	0.025 (0.010)	0.017 (0.007)	0.034 (0.027)	0.017 (0.011)	1.17 (0.01)	1.19 (0.20)	0.043 (0.094)	0.039 (0.087)	0.086 (0.060)	0.642 (0.328)	2.55 (2.13)
23.4L	0.153 (0.056)	0.053 (0.010)	0.029 (0.024)	0.025 (0.017)	1.62 (0.18)	1.22 (0.19)	0.044 (0.087)	0.035 (0.070)	0.111 (0.017)	0.582 (0.395)	8.16 (5.59)
36.6L	0.055 (0.031)	0.036 (0.021)	0.023 (0.027)	0.017 (0.004)	1.24 (0.14)	1.38 (0.34)	0.048 (0.078)	0.031 (0.063)	0.101 (0.020)	0.508 (0.452)	3.46 (3.79)
57.6L	0.211 (0.051)	0.125 (0.032)	0.063 (0.025)	0.029 (0.006)	1.83 (0.38)	1.46 (0.32)	0.045 (0.104)	0.043 (0.100)	0.110 (0.026)	0.572 (0.391)	17.03 (11.97)
90L	0.067 (0.018)	0.053 (0.012)	0.034 (0.023)	0.040 (0.029)	1.12 (0.16)	1.34 (0.43)	0.054 (0.103)	0.060 (0.116)	0.090 (0.031)	0.545 (0.375)	1.60 (1.04)

Appendix Table D-7: Mean (±SD) concentration of environmental variables after the first AWW treatment to the end of the study duration.

Treatment	**Alkalinity (mg/L $CaCO_3$)** (n = 3)	**DOC (mg/L)** (n = 6)	**SRSi (mg/L)** (n = 6)
Reference	269.7 (73.5)	23.7 (13.0)	1.00 (1.07)
6L	274.3 (79.1)	22.3 (12.9)	3.00 (1.00)
9.6L	269.7 (73.5)	24.8 (10.9)	0.61 (0.34)
15L	242.5 (49.8)	22.8 (12.3)	0.14 (0.07)
23.4L	228.0 (54.8)	25.6 (14.5)	3.22 (0.59)
36.6L	193.7 (57.5)	31.4 (9.4)	0.38 (0.53)
57.6L	294.3 (140.9)	31.0 (12.7)	3.24 (0.82)
90L	269.7 (73.5)	23.8 (11.8)	0.54 (0.30)

Appendix Table D-8: Linear regression model results of the relationship between log10(x + 1) of cumulative AWW load concentration (TP used as the dependant variable) and each zooplankton metric. The zooplankton metrics were log10 transformed when required to meet model assumptions. Significant when p-value <= 0.05.

Zooplankton metric	Transformation	Study Day	Intercept	Slope	R^2	p-value	Significant
Total zooplankton abundance	Log10	8	3.61	1.13	0.21	0.25	No
	Log10	22	3.36	0.41	0.017	0.76	No
	Log10	36	3.03	0.39	0.032	0.67	No
	Log10	50	3.22	0.08	0.0011	0.94	No
	Log10	64	3.19	0.33	0.025	0.71	No
	Log10	91	2.84	1.11	0.24	0.21	No
Copepod abundance	Log10	8	3.22	1.27	0.15	0.34	No
	Log10	22	2.99	0.73	0.061	0.55	No
	Log10	36	2.90	-0.014	$5x10^{-5}$	0.99	No
	Log10	50	3.05	-0.19	0.0068	0.85	No
	Log10	64	2.82	0.78	0.14	0.36	No
	Log10	91	2.68	1.06	0.22	0.25	No
Cyclopoid copepod abundance	Log10	8	1.99	3.09	0.48	0.057	No
	Log10	22	2.40	0.42	0.088	0.476	No
	Log10	36	2.18	0.51	0.12	0.410	No
	Log10	50	2.32	-0.19	0.025	0.711	No
	Log10	64	2.26	0.81	0.19	0.277	No
	Log10	91	2.04	0.30	0.043	0.624	No
Calanoid copepod abundance	Log10	8	2.11	0.19	0.0022	0.91	No
	Log10	22	2.28	-1.53	0.27	0.19	No
	Log10	36	0.88	-1.57	0.067	0.53	No
	Log10	50	1.51	-1.23	0.26	0.19	No
	Log10	64	1.01	-1.90	0.18	0.30	No
	Log10	91	NA	NA	NA	NA	NA
Copepod Nauplii abundance	Log10	8	3.11	1.46	0.16	0.33	No
	Log10	22	2.68	0.97	0.052	0.59	No
	Log10	36	2.73	-0.006	$5.6x10^{-6}$	1.00	No
	Log10	50	2.90	-0.26	0.0069	0.85	No
	Log10	64	2.64	0.83	0.14	0.36	No
	Log10	91	2.56	1.20	0.24	0.22	No
Cladoceran abundance	Log10	8	2.71	1.35	0.04	0.63	No
	Log10	22	2.55	0.38	0.0048	0.87	No
	Log10	36	1.45	0.92	0.019	0.74	No
	Log10	50	1.79	1.15	0.082	0.49	No
	Log10	64	1.93	0.52	0.031	0.68	No
	Log10	91	1.54	0.62	0.017	0.76	No
Rotifer abundance	Log10	8	2.71	1.97	0.065	0.541	No
	Log10	22	2.31	1.35	0.048	0.602	No
	Log10	36	1.90	2.37	0.54	0.038	Yes

	Log10	50	2.37	0.82	0.059	0.562	No
	Log10	64	2.91	-0.98	0.12	0.393	No
	Log10	91	1.95	1.22	0.19	0.278	No
Inverse	NA	8	3.32	2.17	0.023	0.72	No
Simpson	NA	22	4.30	-1.99	0.088	0.48	No
Diversity	NA	36	2.86	1.02	0.042	0.63	No
Index	NA	50	2.79	1.44	0.086	0.48	No
	NA	64	2.85	0.03	0.0008	0.95	No
	NA	91	2.70	-0.82	0.059	0.56	No
Pielou's	NA	8	0.40	0.006	$1.8x10^{-5}$	0.99	No
Evenness	NA	22	0.50	-0.09	0.0076	0.84	No
	NA	36	0.50	0.07	0.0038	0.88	No
	NA	50	0.40	0.03	0.0032	0.89	No
	NA	64	0.40	-0.02	0.0015	0.93	No
	NA	91	0.48	0.01	0.0001	0.98	No
Species	NA	8	8.50	4.27	0.14	0.36	No
Richness	NA	22	8.35	-0.12	0.0002	0.98	No
	NA	36	6.05	2.37	0.022	0.73	No
	NA	50	7.07	3.55	0.12	0.40	No
	NA	64	7.45	0.03	$1.3x10^{-5}$	0.99	No
	NA	91	5.50	0.52	0.005	0.87	No

Appendix Table D-9: Dominant zooplankton taxa, the proportion of the total sample abundance that the dominant taxa makes up, and species diversity metrics within each treatment on study day 0, prior to the first AWW addition. Reference treatment represents the mean value (SD) (n = 3).

Treatment	Dominant Taxa	Proportion of Abundance	Richness	Evenness	Shannon's Diversity	Inverse Simpson's Diversity
Reference	Ceriodaphnia	0.34	8.67 (0.58)	0.54 (0.11)	1.74 (0.25)	4.68 (1.23)
6 L	Ostracod	0.32	9	0.53	1.79	4.80
9.6 L	Ceriodaphnia	0.48	10	0.37	1.74	3.71
15 L	Ceriodaphnia	0.50	11	0.29	1.60	3.24
23.4 L	Ceriodaphnia	0.36	10	0.50	1.88	4.98
36.6 L	Daphnia	0.82	9	0.16	0.79	1.47
57.6 L	Copepod Nauplii	0.67	9	0.24	1.22	2.13
90 L	Chydorid	0.33	9	0.46	1.67	4.14

Appendix Table D-10: Dominant zooplankton taxa, the proportion of the total sample abundance that the dominant taxa makes up, and species diversity metrics within each treatment on study day 8. Reference treatment represents the mean value (SD) (n = 3).

Treatment	Dominant Taxa	Proportion of Abundance	Richness	Evenness	Shannon's Diversity	Inverse Simpson's Diversity
Reference	Copepod Nauplii	0.52	8.67 (1.53)	0.46 (0.23)	1.52 (0.41)	3.82 (1.68)
6 L	Rotifer	0.52	7	0.39	1.25	2.72
9.6 L	Ostracod	0.31	9	0.55	1.81	4.98
15 L	Copepod Nauplii	0.63	9	0.26	1.29	2.35
23.4 L	Rotifer	0.47	9	0.31	1.30	2.80
36.6 L	Copepod Nauplii	0.41	10	0.43	1.77	4.29
57.6 L	Rotifer	0.53	9	0.27	1.08	2.39
90 L	Copepod Nauplii	0.31	9	0.51	1.73	4.57

Appendix Table D-11: Dominant zooplankton taxa, the proportion of the total sample abundance that the dominant taxa makes up, and species diversity metrics within each treatment on study day 22. Reference treatment represents the mean value (SD) (n = 3).

Treatment	Dominant Taxa	Proportion of Abundance	Richness	Evenness	Shannon's Diversity	Inverse Simpson's Diversity
Reference	Copepod Nauplii	0.55	8.67 (0.58)	0.41 (0.16)	1.50 (0.45)	3.61 (1.56)
6 L	Rotifer	0.48	8	0.43	1.53	3.42
9.6 L	Diaphanosoma sp.	0.25	9	0.64	1.89	5.74
15 L	Copepod Nauplii	0.38	9	0.51	1.80	4.60
23.4 L	Copepod Nauplii	0.35	8	0.49	1.58	3.95
36.6 L	Rotifer	0.49	8	0.43	1.58	3.46
57.6 L	Cyclopoid copepod	0.36	6	0.68	1.56	4.10
90 L	Copepod Nauplii	0.49	10	0.34	1.57	3.41

Appendix Table D-12: Dominant zooplankton taxa, the proportion of the total sample abundance that the dominant taxa makes up, and species diversity metrics within each treatment on study day 36. Reference treatment represents the mean value (SD) (n = 3).

Treatment	Dominant Taxa	Proportion of Abundance	Richness	Evenness	Shannon's Diversity	Inverse Simpson's Diversity
Reference	Copepod Nauplii	0.63	8.33 (0.58)	0.38 (0.23)	1.33 (0.44)	3.09 (1.77)
6 L	Copepod Nauplii	0.35	7	0.57	1.54	4.00
9.6 L	Copepod Nauplii	0.66	7	0.29	1.03	2.06
15 L	Copepod Nauplii	0.50	6	0.49	1.30	2.93
23.4 L	Copepod Nauplii	0.61	3	0.74	0.94	2.23
36.6 L	Rotifer	0.37	5	0.67	1.33	3.34
57.6 L	Rotifer	0.50	5	0.56	1.15	2.78
90 L	Copepod Nauplii	0.45	10	0.37	1.67	3.72

Appendix Table D-13: Dominant zooplankton taxa, the proportion of the total sample abundance that the dominant taxa makes up, and species diversity metrics within each treatment on study day 50. Reference treatment represents the mean value (SD) (n = 3).

Treatment	Dominant Taxa	Proportion of Abundance	Richness	Evenness	Shannon's Diversity	Inverse Simpson's Diversity
Reference	Copepod Nauplii	0.49	9 (1)	0.29 (0.04)	1.28 (0.07)	2.61 (0.09)
6 L	Copepod Nauplii	0.53	7	0.39	1.31	2.75
9.6 L	Copepod Nauplii	0.30	8	0.57	1.69	4.54
15 L	Copepod Nauplii	0.59	6	0.39	1.08	2.33
23.4 L	Copepod Nauplii	0.44	7	0.41	1.27	2.85
36.6 L	Copepod Nauplii	0.60	8	0.29	1.13	2.31
57.6 L	Rotifer	0.44	6	0.52	1.31	3.14
90 L	Copepod Nauplii	0.43	11	0.36	1.70	3.99

Appendix Table D-14: Dominant zooplankton taxa, the proportion of the total sample abundance that the dominant taxa makes up, and species diversity metrics within each treatment on study day 64. Reference treatment represents the mean value (SD) (n = 3).

Treatment	Dominant Taxa	Proportion of Abundance	Richness	Evenness	Shannon's Diversity	Inverse Simpson's Diversity
Reference	Copepod Nauplii	0.42	8.67 (0.58)	0.31 (0.01)	1.32 (0.06)	2.71 (0.30)
6 L	Rotifer	0.52	5	0.56	1.21	2.79
9.6 L	Rotifer	0.52	8	0.38	1.46	3.02
15 L	Rotifer	0.40	7	0.44	1.27	3.10
23.4 L	Copepod Nauplii	0.54	9	0.31	1.36	2.81
36.6 L	Rotifer	0.56	8	0.32	1.15	2.54
57.6 L	Copepod Nauplii	0.46	6	0.52	1.30	3.10
90 L	Copepod Nauplii	0.56	8	0.35	1.42	2.78

Appendix Table D-15: Dominant zooplankton taxa, the proportion of the total sample abundance that the dominant taxa makes up, and species diversity metrics within each treatment on study day 91. Reference treatment represents the mean value (SD) (n = 3).

Treatment	Dominant Taxa	Proportion of Abundance	Richness	Evenness	Shannon's Diversity	Inverse Simpson's Diversity
Reference	Copepod Nauplii	0.60	6 (1)	0.37 (0.03)	1.07 (0.22)	2.25 (0.46)
6 L	Copepod Nauplii	0.63	6	0.34	0.92	2.05
9.6 L	Copepod Nauplii	0.53	6	0.49	1.36	2.97
15 L	Copepod Nauplii	0.57	5	0.51	1.17	2.54
23.4 L	Copepod Nauplii	0.37	5	0.79	1.47	3.93
36.6 L	Copepod Nauplii	0.52	6	0.38	0.97	2.27
57.6 L	Copepod Nauplii	0.62	3	0.71	0.88	2.12
90 L	Copepod Nauplii	0.71	8	0.24	1.12	1.91

Appendix Table D-16: Linear regression model results of the relationship between log10(x + 1) of zooplankton abundance and each fish metric. The number of larval fish in jar was log10 transformed. Significant when p-value <= 0.05.

Fish Metric	Study Day	Intercept	Slope	R^2	p-value	Significant
Number of fish retrieved	91	3.23	-0.029	0.034	0.66	No
Number of larval fish in jar	22	3.64	-0.34	0.40	0.09	No
	36	3.25	-0.26	0.35	0.12	No
	50	3.37	-0.22	0.14	0.37	No
	64	3.22	0.05	0.009	0.82	No
	91	3.17	-0.10	0.025	0.71	No

Appendix Table D-17: Species scores (b_k) as generated from principal response curve analysis of the zooplankton taxa included in the analysis.

Zooplankton taxa	**b_k**
Daphnia sp.	0.287
Chydorus sp.	-1.351
Scapholeberis sp.	-0.072
Copepoda nauplii	-0.697
Diaphanosoma sp.	-1.713
Ostracoda	-0.584
Cyclopoida	-0.584
Rotifera	-0.391
Calanoida	-0.216
Ceriodaphnia sp.	-1.983
Macrothrix sp.	-1.073
Simocephalus sp.	-0.642
Polyphemus sp.	-0.052

Appendix Table D-18: Eigenvalues, explained variance, environmental variable canonical coefficients, and species scores, associated with the first and second RDA axis.

	RDA Axis 1	**RDA Axis 2**
Eigenvalue	0.02295	0.009442
Variance explained	0.15544	0.063934
Dissolved oxygen	-0.39260	-0.21020
pH	-0.49350	-0.27533
Total dissolved nitrogen	0.09511	0.43181
Total ammoniacal nitrogen	0.03040	0.49005
Soluble reactive phosphorus	0.05541	0.14213
Nitrite	0.12819	0.03854
Particulate phosphorus	0.67719	-0.06500
Chlorophyll *a*	0.50634	-0.26085
Dissolved organic carbon	0.09479	-0.02782
Daphnia sp.	0.0914841	0.054678
Chydorus sp.	-0.1773431	-0.101792
Ceriodaphnia sp.	-0.3338013	-0.062295
Ostracoda	0.0148052	0.036840
Calanoida	0.1036200	-0.168451
Macrothrix sp.	-0.1663812	-0.093844
Diaphanosoma sp.	-0.2399133	-0.015615
Copepoda nauplii	-0.1253844	0.284111
Cyclopoida	0.1275669	-0.096790
Rotifera	0.2678859	0.007638
Scapholeberis sp.	0.0009037	-0.007145
Simocephalus sp.	-0.0659448	0.005582

Appendix Table D-19: The number of adult fathead minnow (*Pimephales promelas*) fish retrieved from the mesocosms by the final fish sampling date on September 17, 2024. A total of 12 fish were originally introduced to the mesocosms.

Treatment	Fish abundance
Reference	2
Reference	6
Reference	5
6 L	2
9.6 L	10
15 L	6
23.4 L	5
36.6 L	6
57.6 L	3
90 L	1

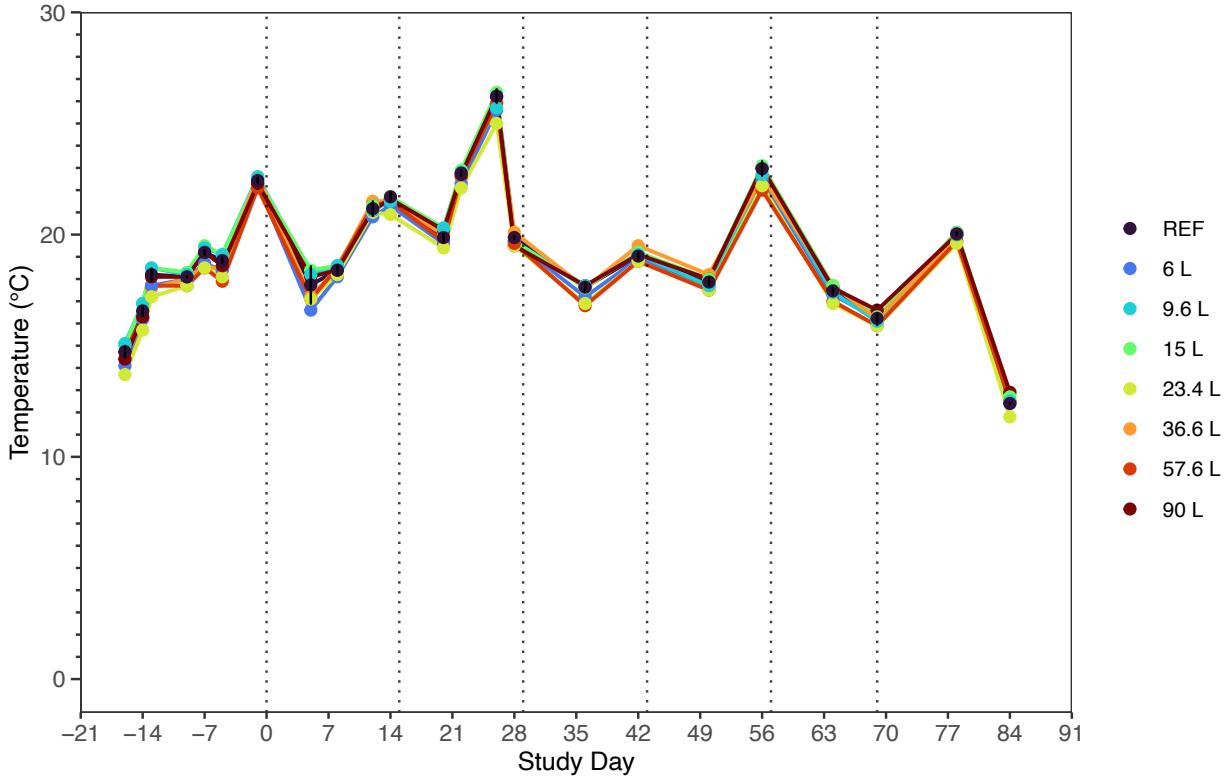

Appendix Figure D-1: Water temperature (°C) over the study duration within the UM wild rice wetland mesocosms. The vertical dotted lines represent AWW addition days. REF displays the mean of the references (n = 3) with the error bars representing ± standard deviation.

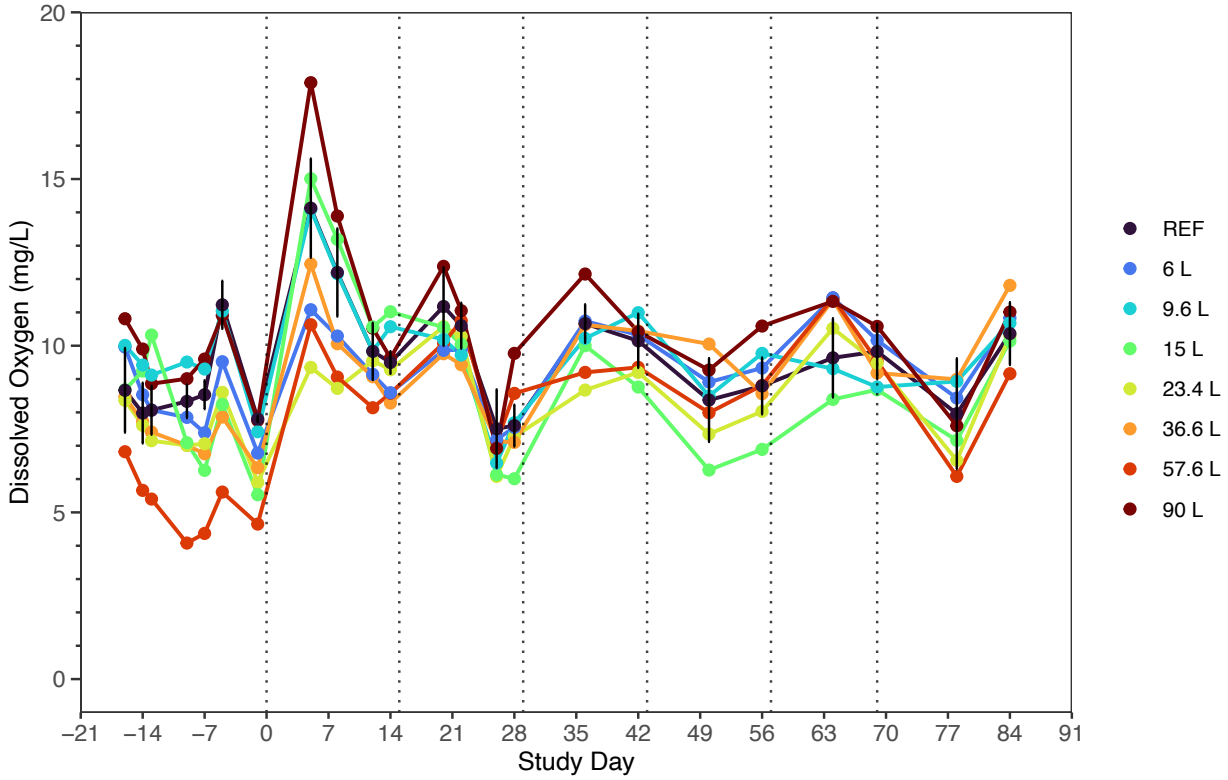

Appendix Figure D-2: Dissolved oxygen (mg/L) over the study duration within the UM wild rice wetland mesocosms. The vertical dotted lines represent AWW addition days. REF displays the mean of the references (n = 3) with the error bars representing ± standard deviation.

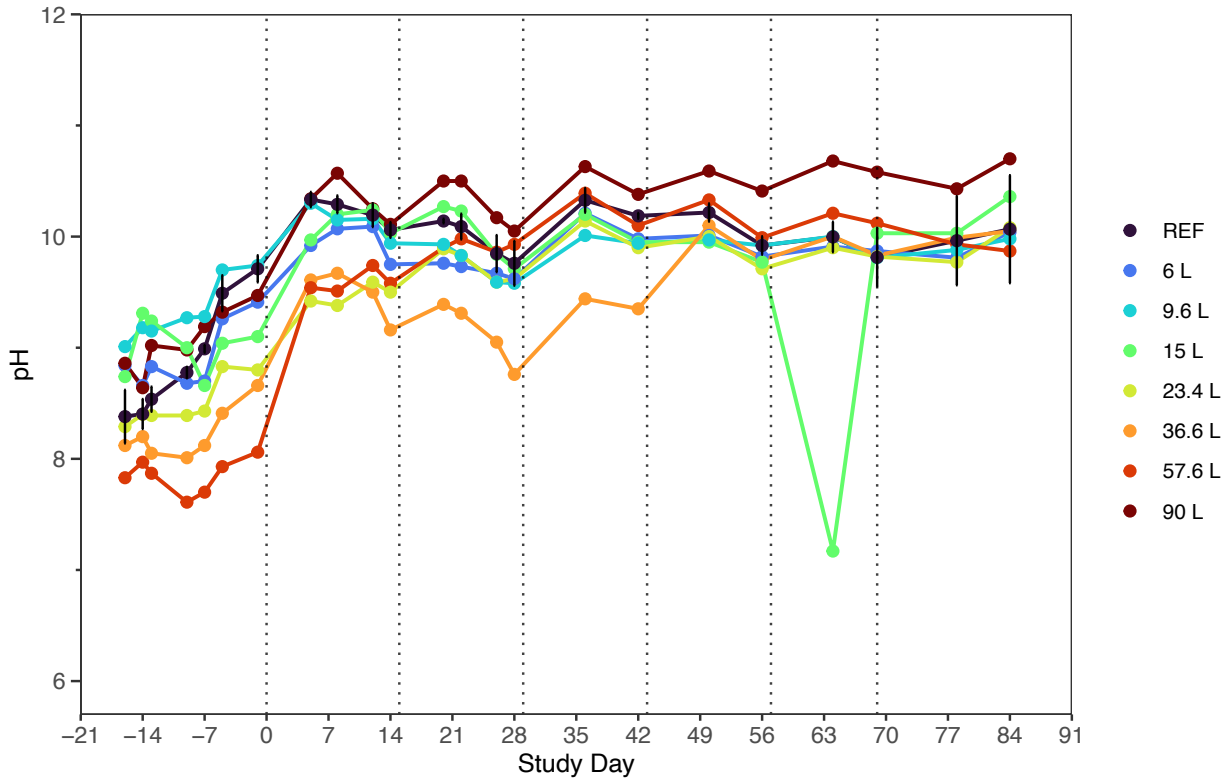

Appendix Figure D-3: pH over the study duration within the UM wild rice wetland mesocosms. The vertical dotted lines represent AWW addition days. REF displays the mean of the references (n = 3) with the error bars representing ± standard deviation.

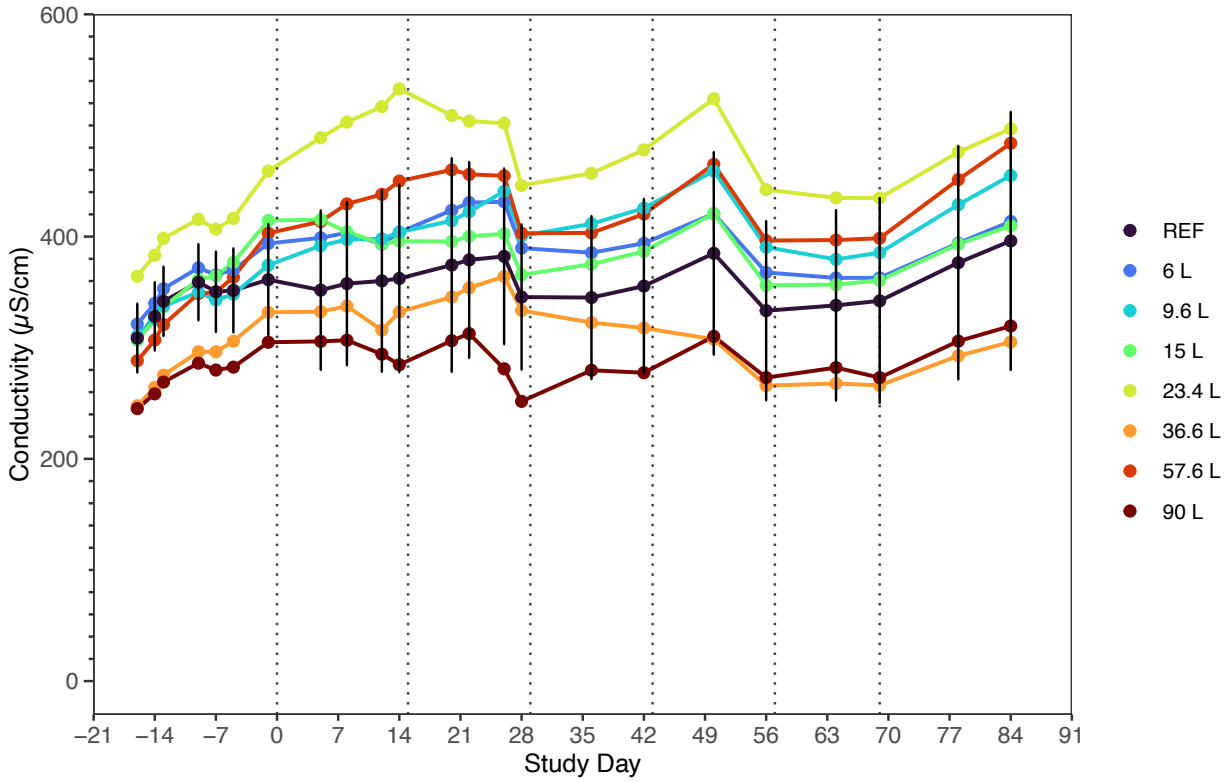

Appendix Figure D-4: Conductivity (µS/cm) over the study duration within the UM wild rice wetland mesocosms. The vertical dotted lines represent AWW addition days. REF displays the mean of the references (n = 3) with the error bars representing ± standard deviation.

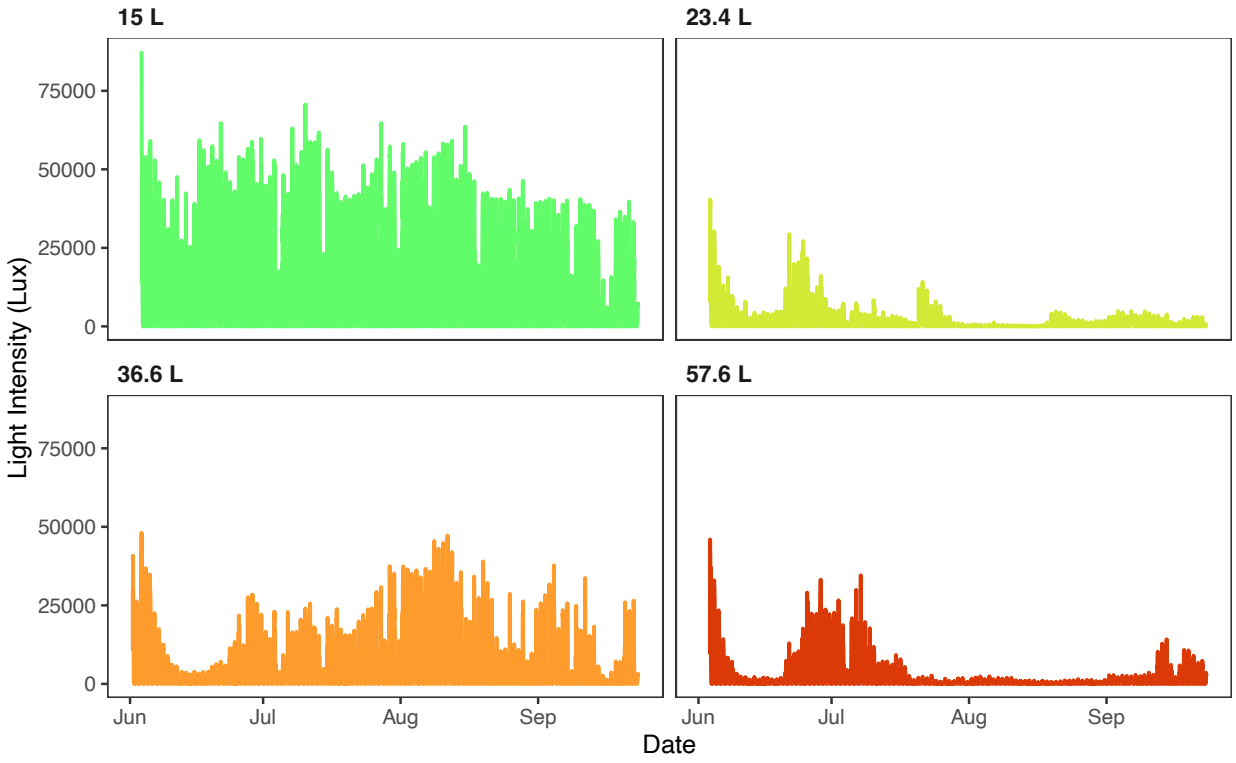

Appendix Figure D-5: Light intensity in the four of the treatments of the UM wild rice site.

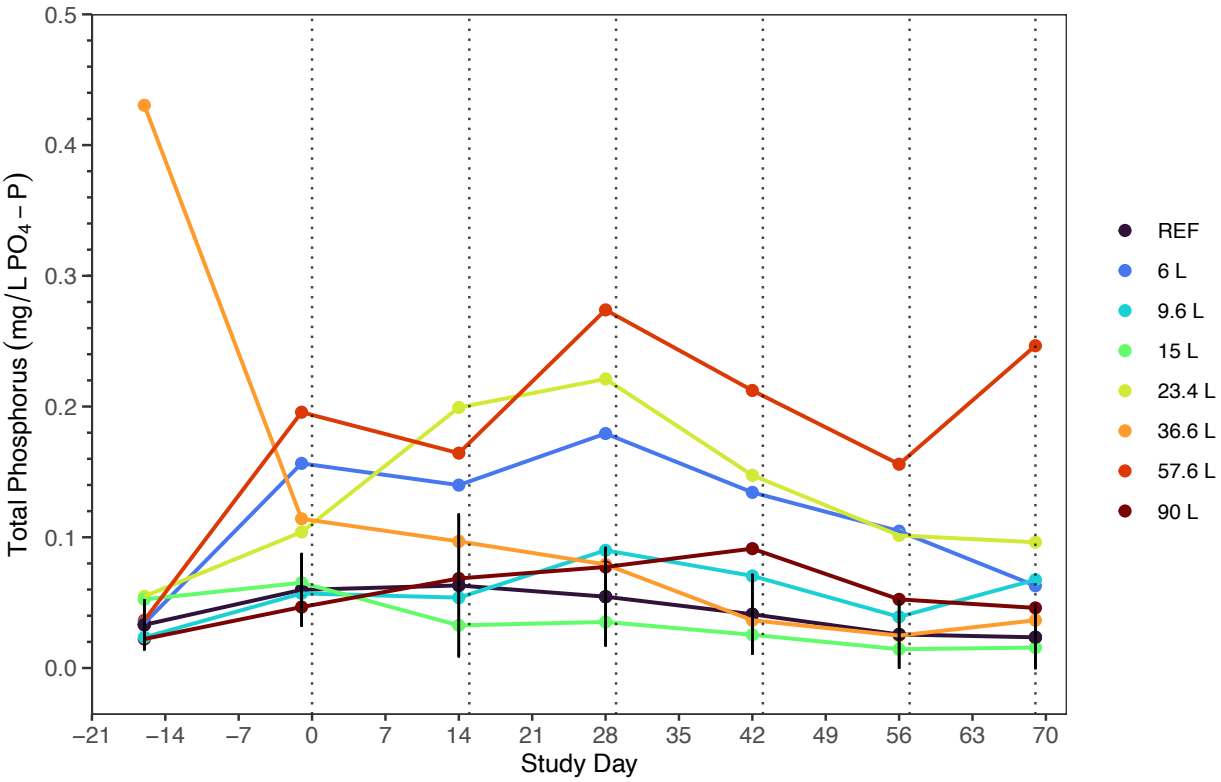

Appendix Figure D-6: Total phosphorus (mg/L PO_4-P) over the study duration within the UM wild rice mesocosms. The vertical dotted lines represent AWW addition days. REF displays the mean of the references (n = 3) with the error bars representing ± standard deviation.

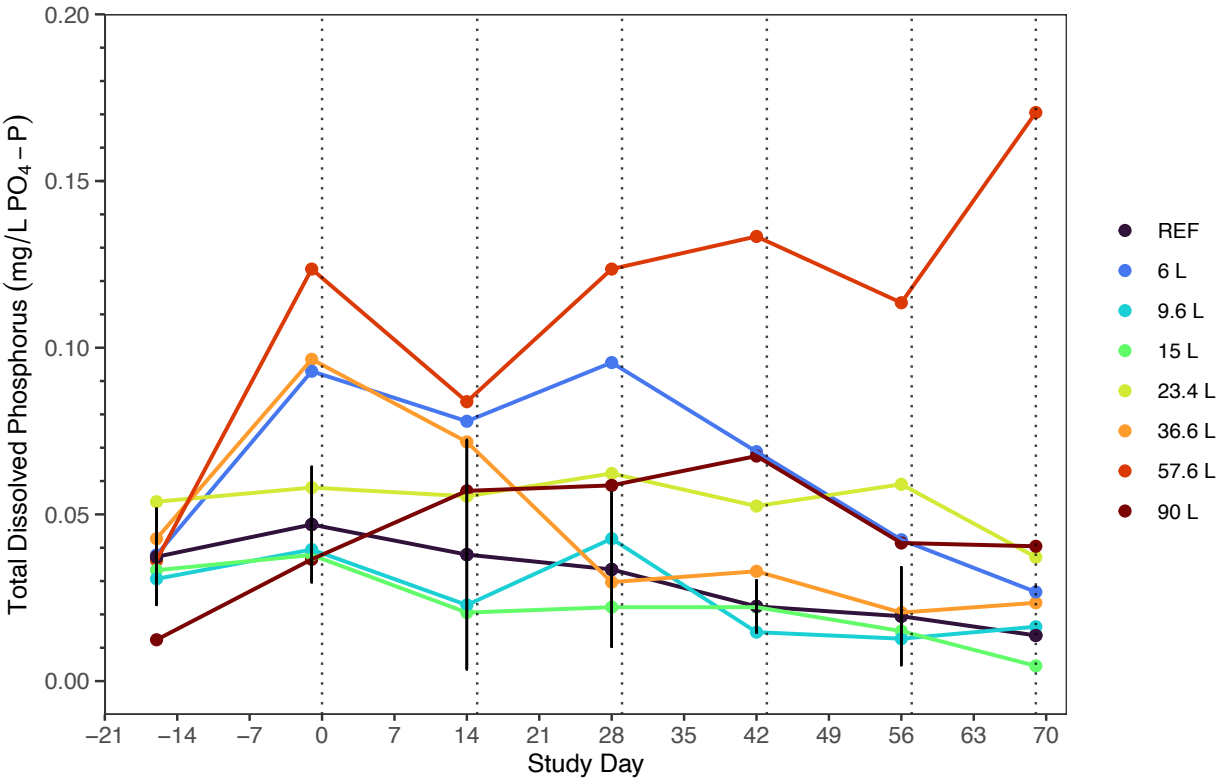

Appendix Figure D-7: Total dissolved phosphorus (mg/L PO_4-P) over the study duration within the UM wild rice mesocosms. The vertical dotted lines represent AWW addition days. REF displays the mean of the references (n = 3) with the error bars representing ± standard deviation.

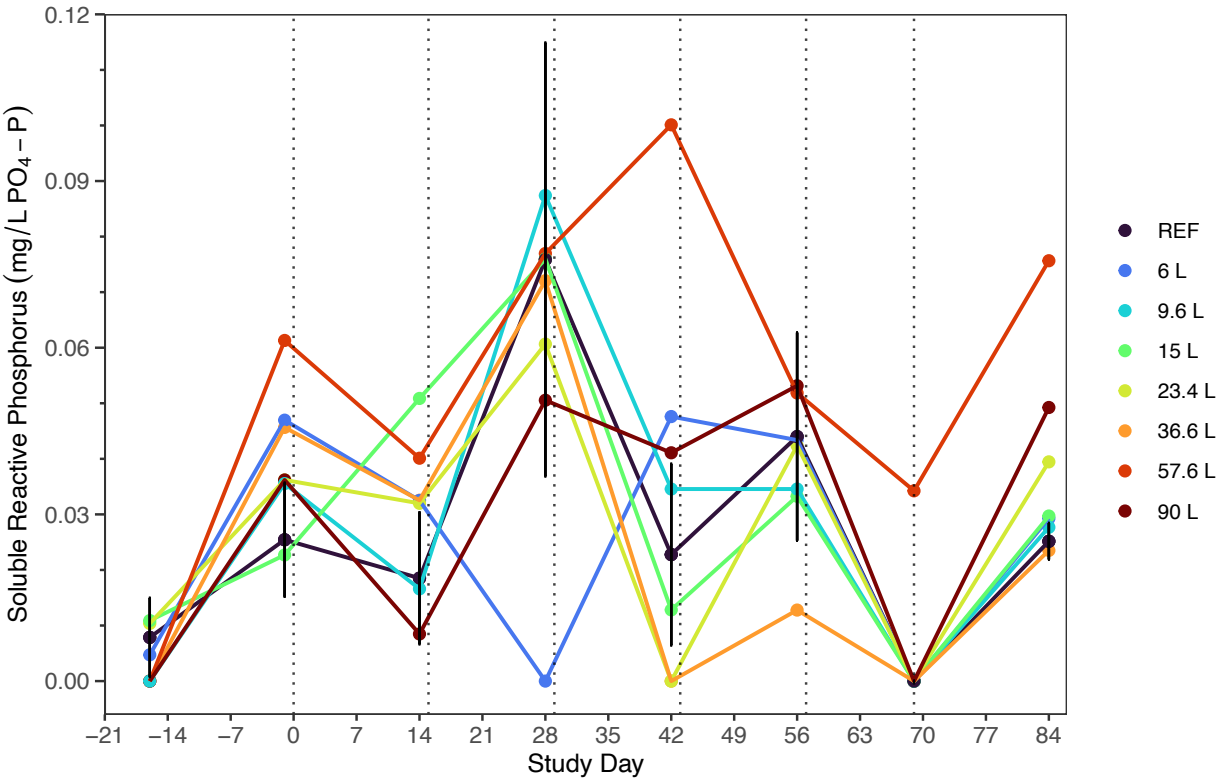

Appendix Figure D-8: Soluble reactive phosphorus (mg/L PO_4-P) over the study duration within the UM wild rice mesocosms. The vertical dotted lines represent AWW addition days. REF displays the mean of the references (n = 3) with the error bars representing ± standard deviation.

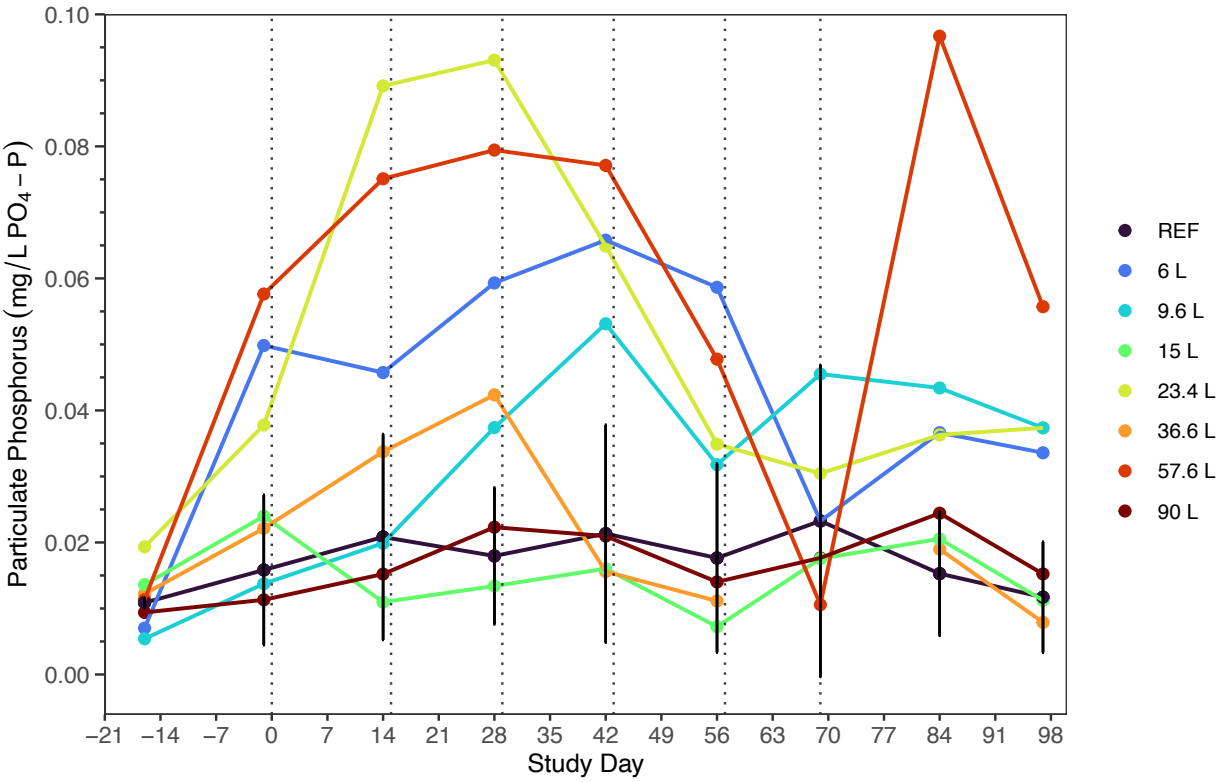

Appendix Figure D-9: Particulate phosphorus (µg/L PO_4-P) over the study duration within the UM wild rice mesocosms. The vertical dotted lines represent AWW addition days. REF displays the mean of the references (n = 3) with the error bars representing ± standard deviation.

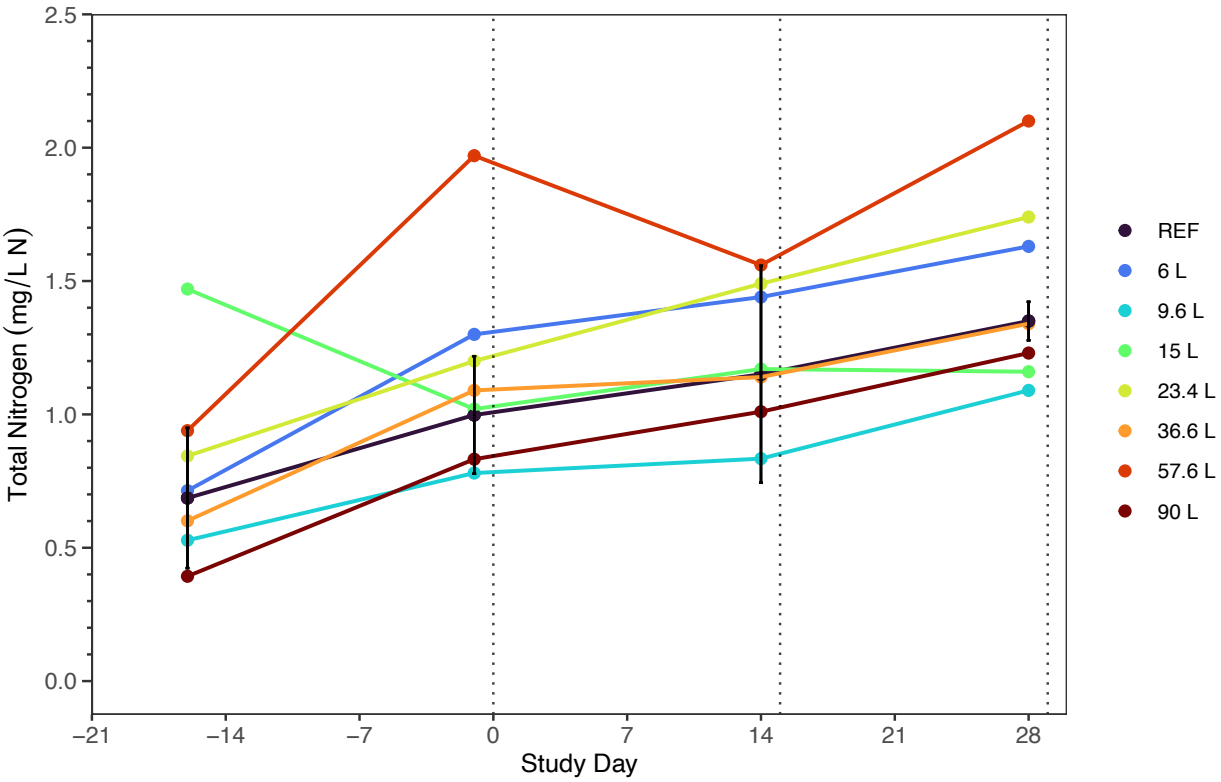

Appendix Figure D-10: Total nitrogen (mg/L N) over the study duration within the UM wild rice mesocosms. The vertical dotted lines represent AWW addition days. REF displays the mean of the references (n = 3) with the error bars representing ± standard deviation.

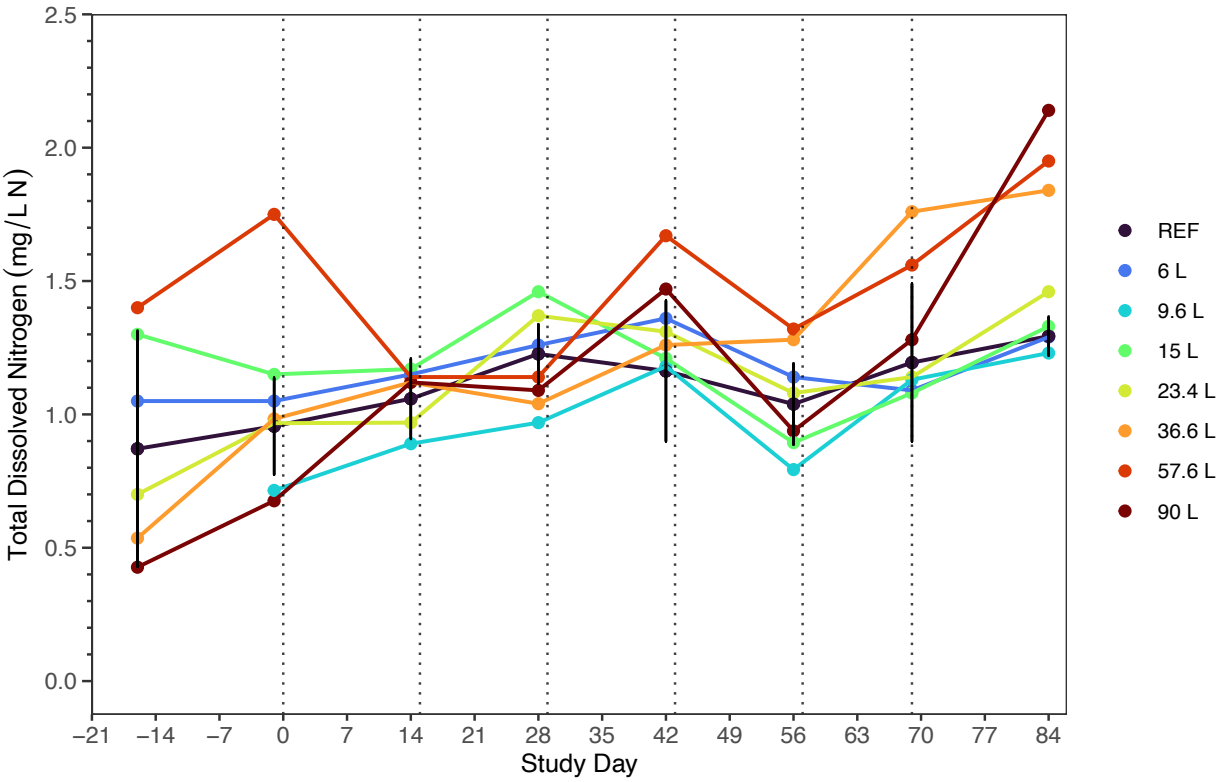

Appendix Figure D-11: Total dissolved nitrogen (mg/L N) over the study duration within the UM wild rice mesocosms. The vertical dotted lines represent AWW addition days. REF displays the mean of the references (n = 3) with the error bars representing ± standard deviation.

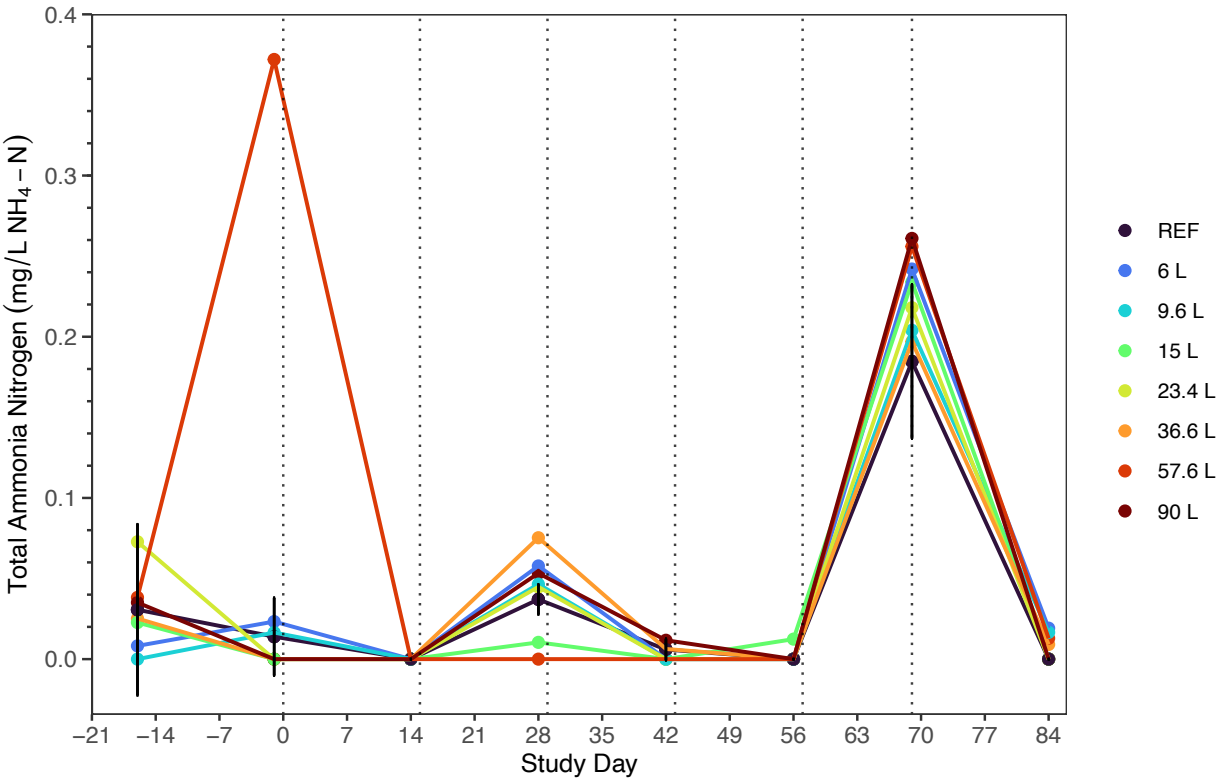

Appendix Figure D-12: Total ammonia nitrogen (mg/L NH_4-N) over the study duration within the UM wild rice mesocosms. The vertical dotted lines represent AWW addition days. REF displays the mean of the references (n = 3) with the error bars representing ± standard deviation.

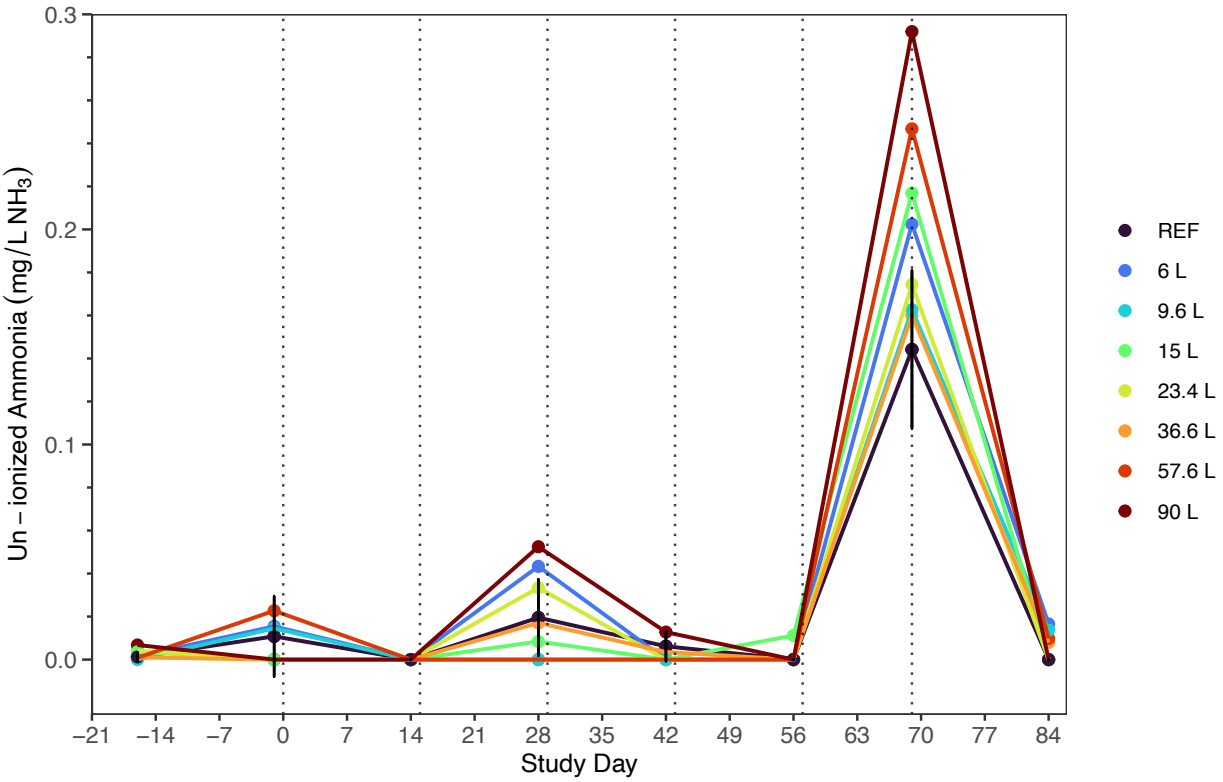

Appendix Figure D-13: Un-ionized ammonia (mg/L NH_3) over the study duration within the UM wild rice mesocosms. The vertical dotted lines represent AWW addition days. These values were calculated from TAN, pH, and temperature, from the calculation in Armstrong et al. (2012) and Delos and Erickson (1999) (see methods for more detail). REF displays the mean of the references (n = 3) with the error bars representing ± standard deviation.

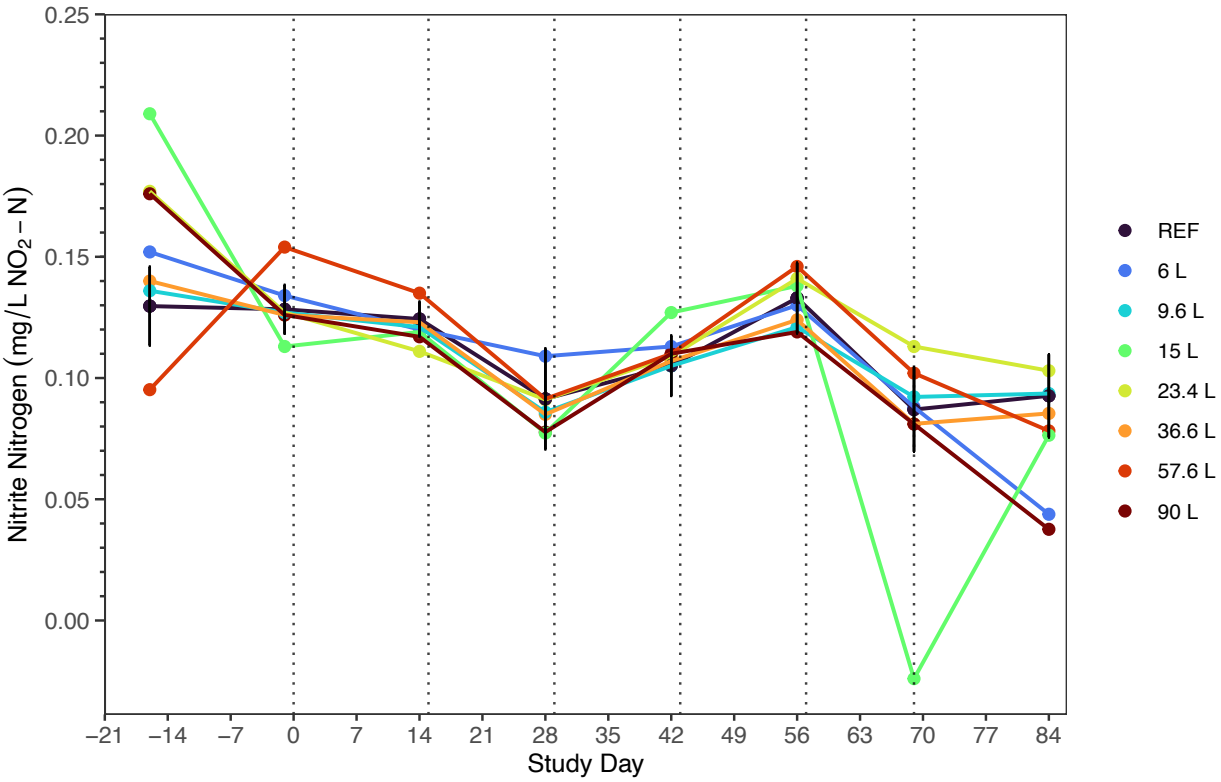

Appendix Figure D-14: Nitrite nitrogen (mg/L NO_2-N) over the study duration within the UM wild rice mesocosms. The vertical dotted lines represent AWW addition days. REF displays the mean of the references (n = 3) with the error bars representing ± standard deviation.

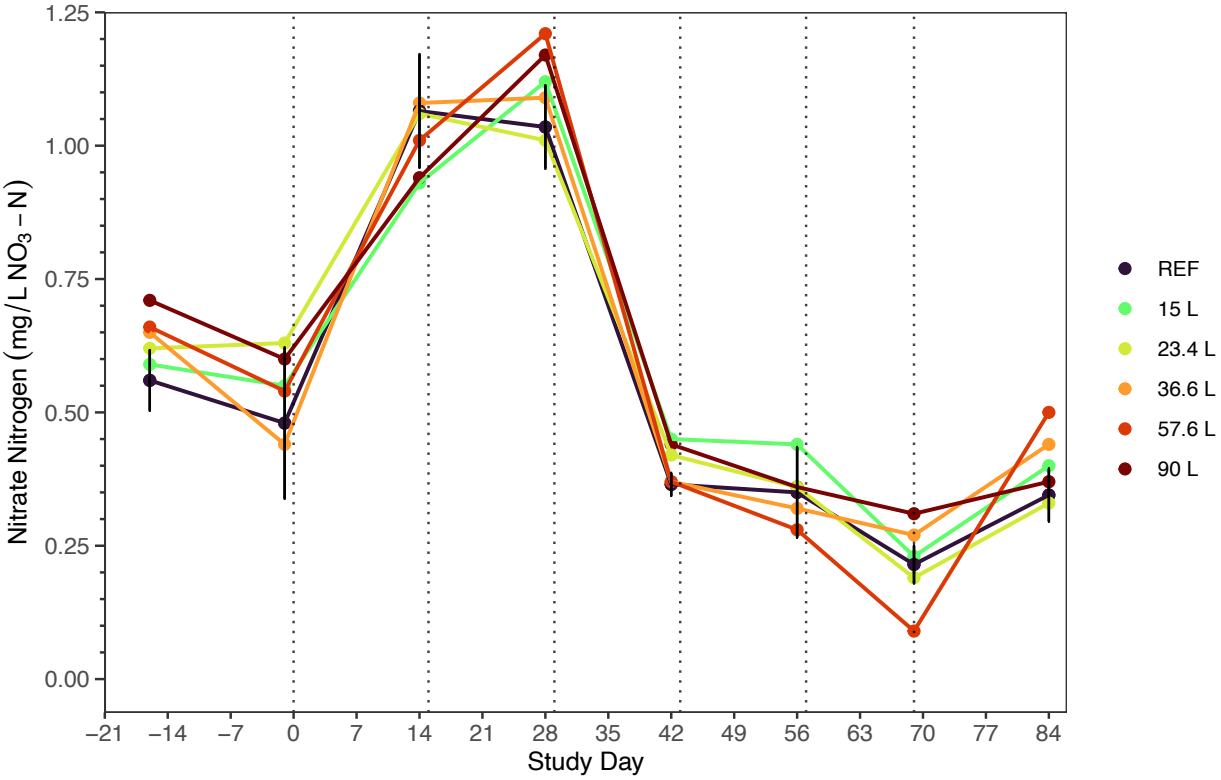

Appendix Figure D-15: Nitrate nitrogen (mg/L NO_3-N) over the study duration within the UM wild rice mesocosms. The vertical dotted lines represent AWW addition days. REF displays the mean of the references (n = 3) with the error bars representing ± standard deviation.

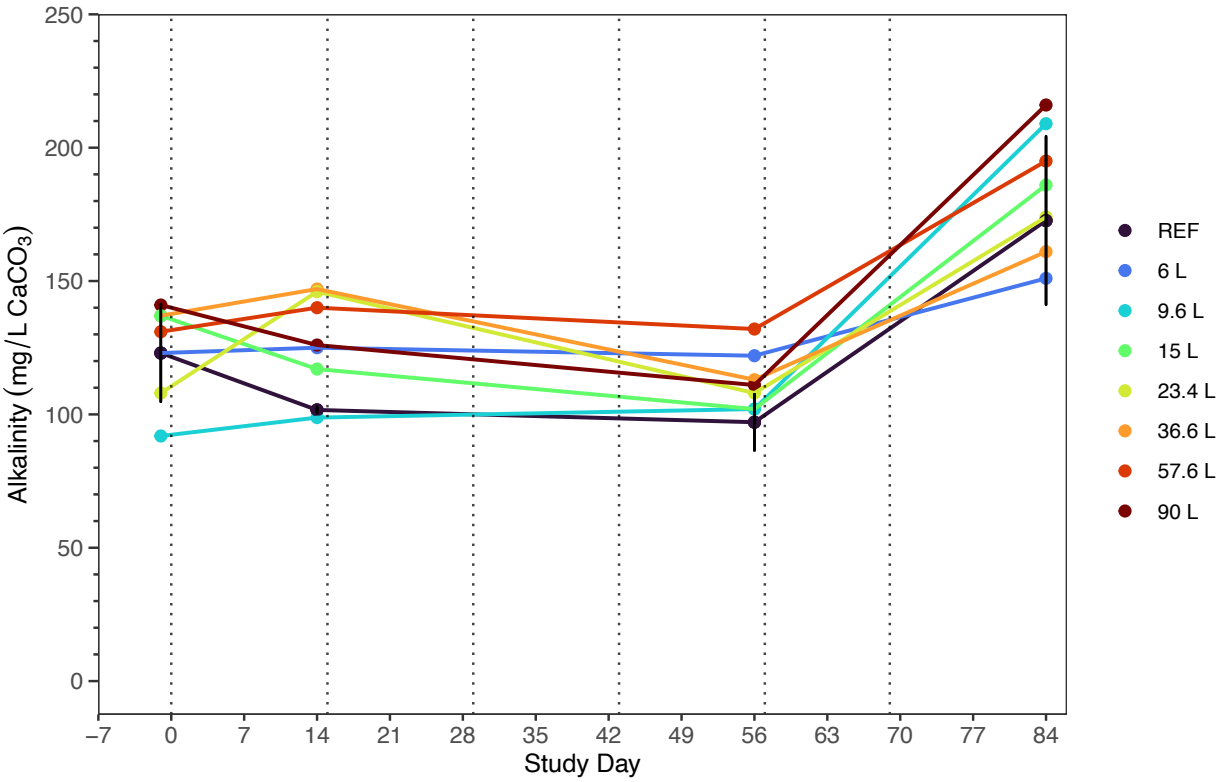

Appendix Figure D-16: Alkalinity (mg/L $CaCO_3$) over the study duration within the UM wild rice mesocosms. The vertical dotted lines represent AWW addition days. REF displays the mean of the references (n = 3) with the error bars representing ± standard deviation.

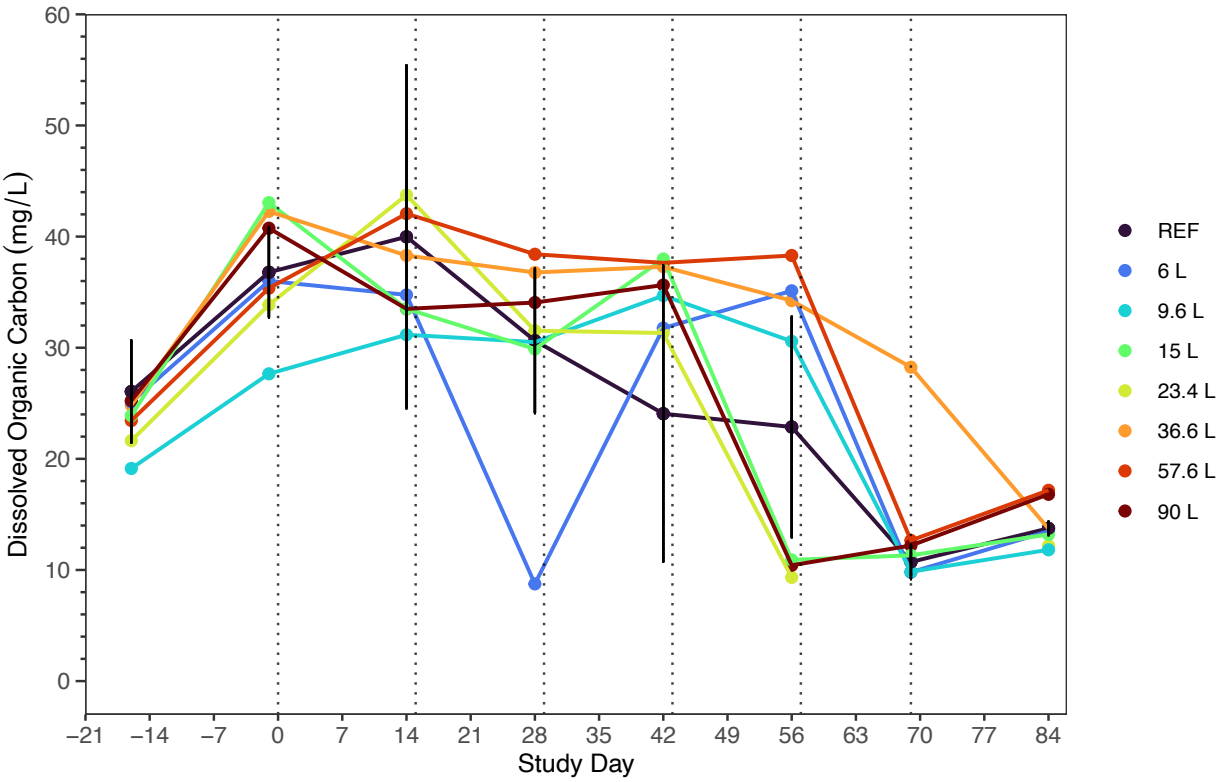

Appendix Figure D-17: Dissolved organic carbon (mg/L) over the study duration within the UM wild rice mesocosms. The vertical dotted lines represent AWW addition days. REF displays the mean of the references (n = 3) with the error bars representing ± standard deviation.

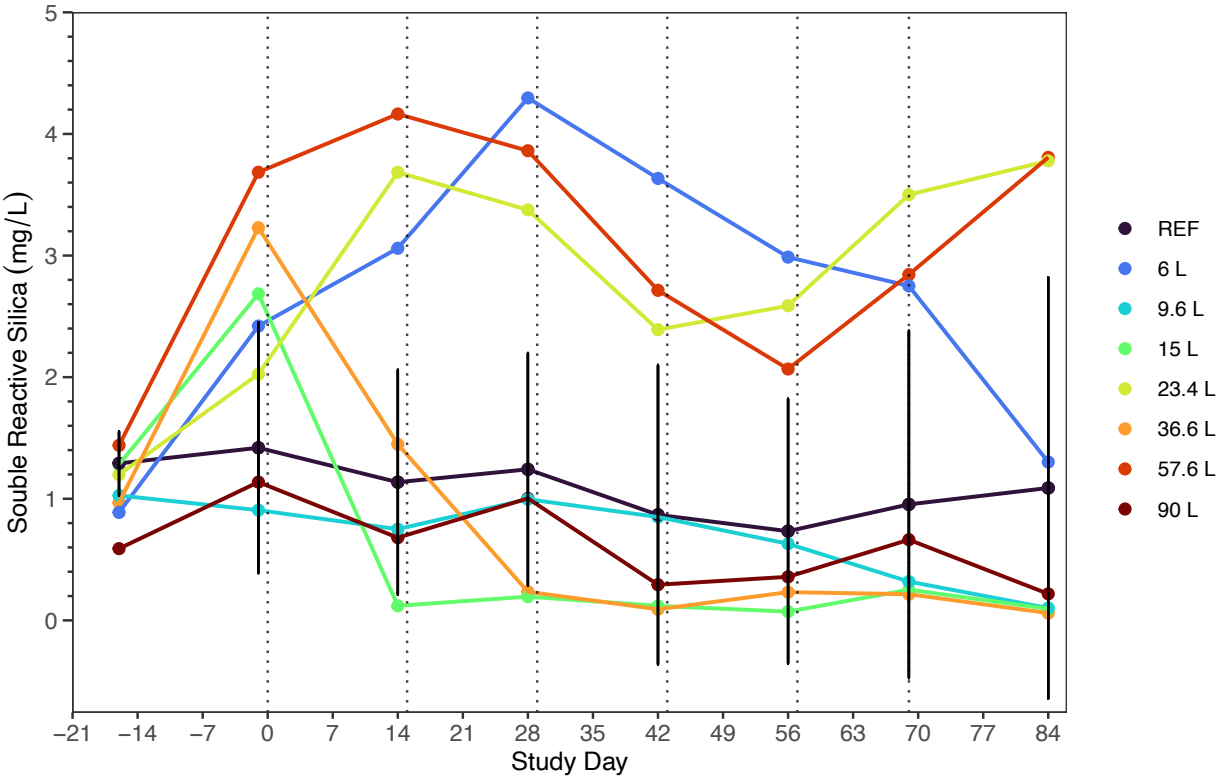

Appendix Figure D-18: Soluble reactive silica (mg/L) over the study duration within the UM wild rice mesocosms. The vertical dotted lines represent AWW addition days. REF displays the mean of the references (n = 3) with the error bars representing ± standard deviation.

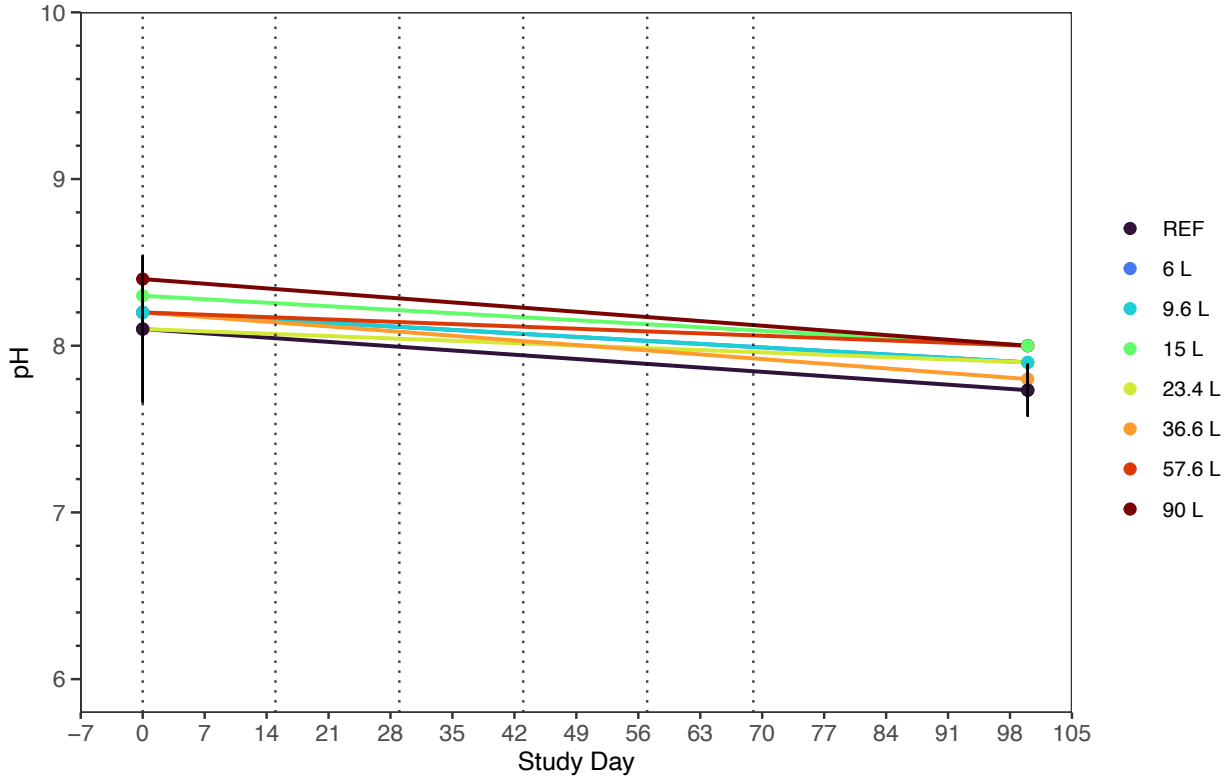

Appendix Figure D-19: Soil pH over the study duration within the UM wild rice mesocosms. The vertical dotted lines represent AWW addition days. REF displays the mean of the references (n = 3) with the error bars representing ± standard deviation.

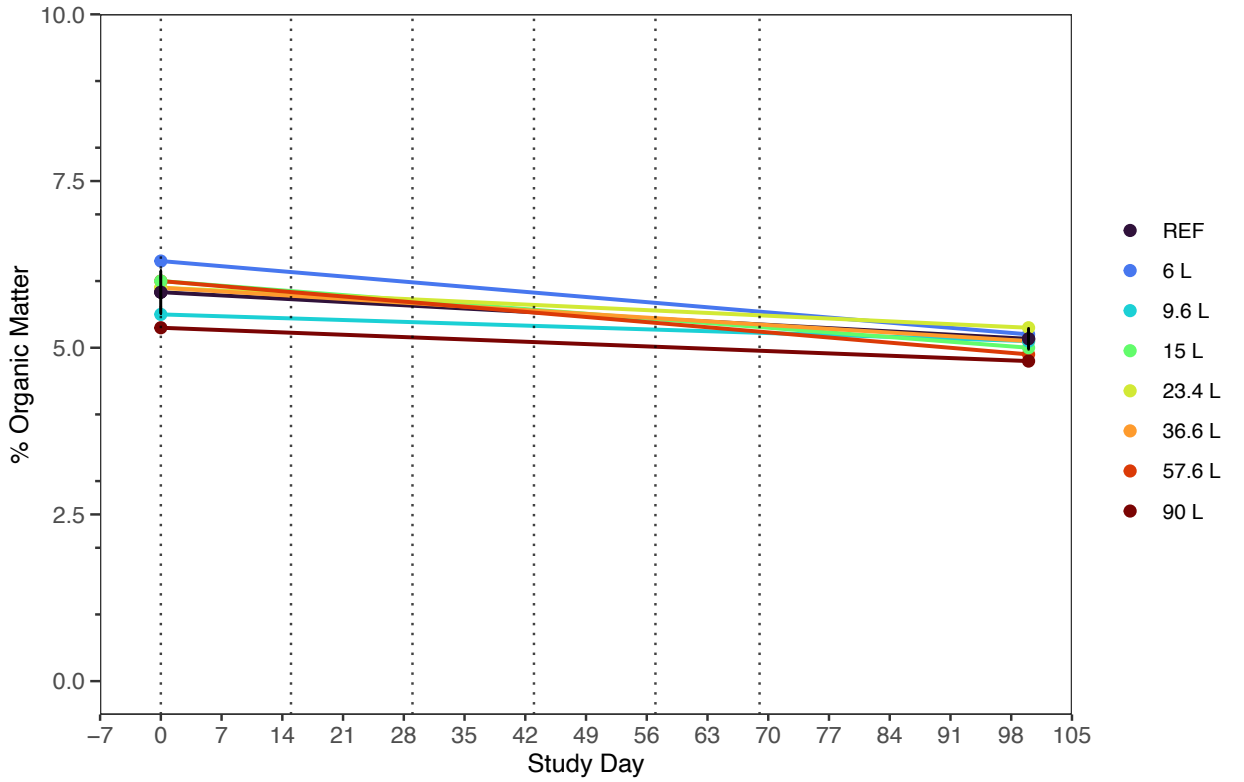

Appendix Figure D-20: Soil organic matter (%) over the study duration within the UM wild rice mesocosms. The vertical dotted lines represent AWW addition days. REF displays the mean of the references (n = 3) with the error bars representing ± standard deviation.

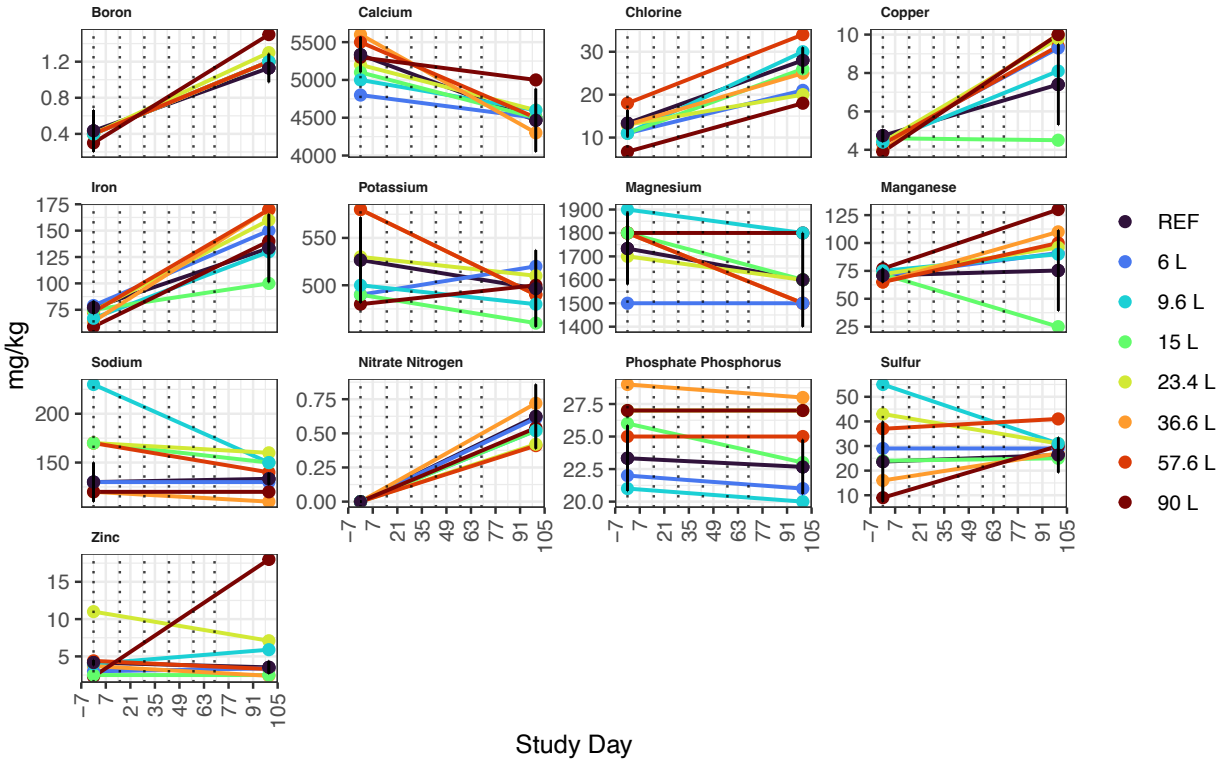

Appendix Figure D-21: Soil ions (mg/kg) over the study duration within the UM wild rice mesocosms. The vertical dotted lines represent AWW addition days. REF displays the mean of the references (n = 3) with the error bars representing ± standard deviation.

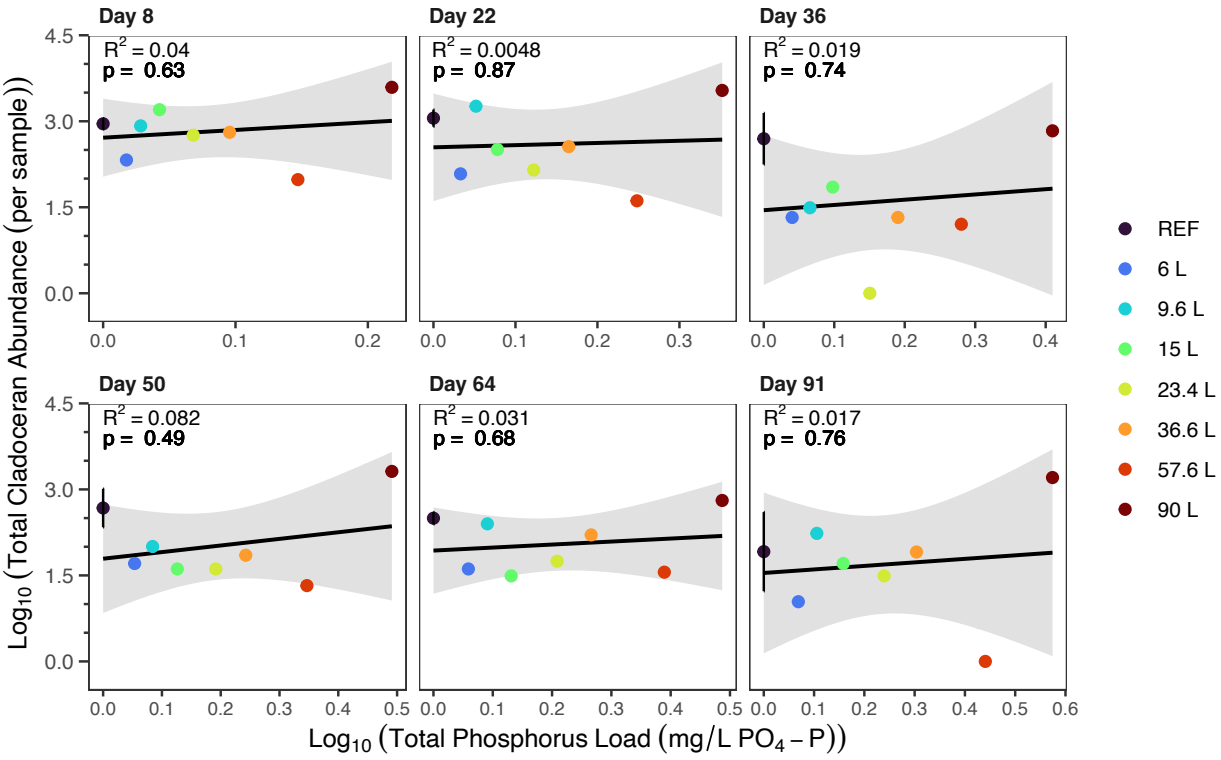

Appendix Figure D-22: Linear regression model results of the relationship between log10(x + 1) of cumulative AWW load concentration (TP used as the representative variable) and total cladoceran abundance. REF displays the mean of the references (n = 3) with the error bars representing ± standard deviation. Each plot displays the model results according to study day.

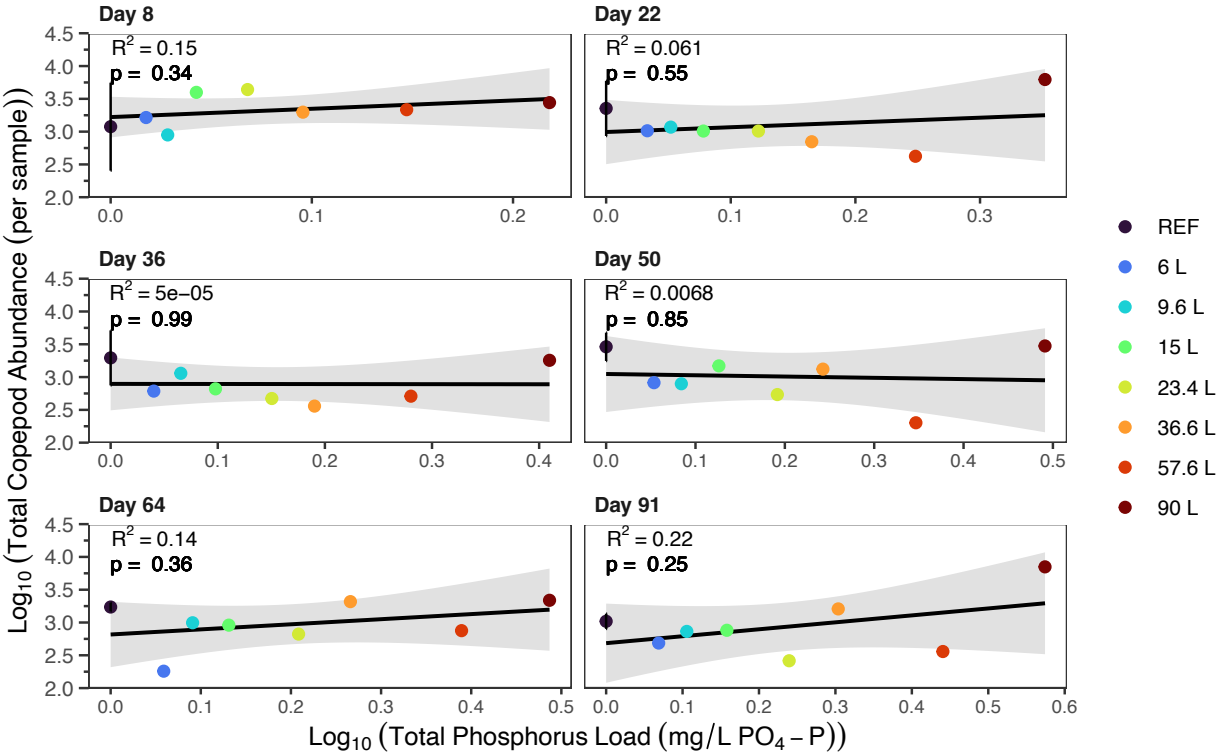

Appendix Figure D-23: Linear regression model results of the relationship between log10(x + 1) of cumulative AWW load concentration (TP used as the representative variable) and total copepod abundance. REF displays the mean of the references (n = 3) with the error bars representing ± standard deviation. Each plot displays the model results according to study day.

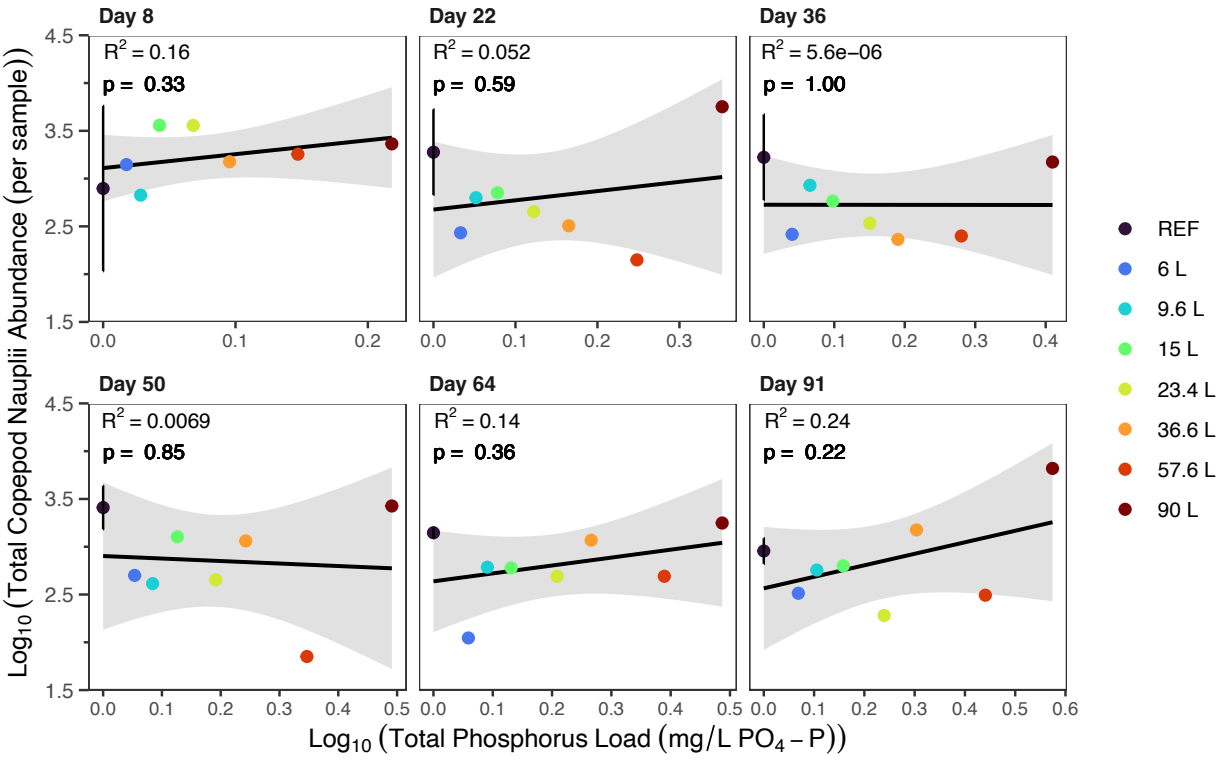

Appendix Figure D-24: Linear regression model results of the relationship between log10(x + 1) of cumulative AWW load concentration (TP used as the representative variable) and total copepod nauplii abundance. REF displays the mean of the references (n = 3) with the error bars representing ± standard deviation. Each plot displays the model results according to study day.

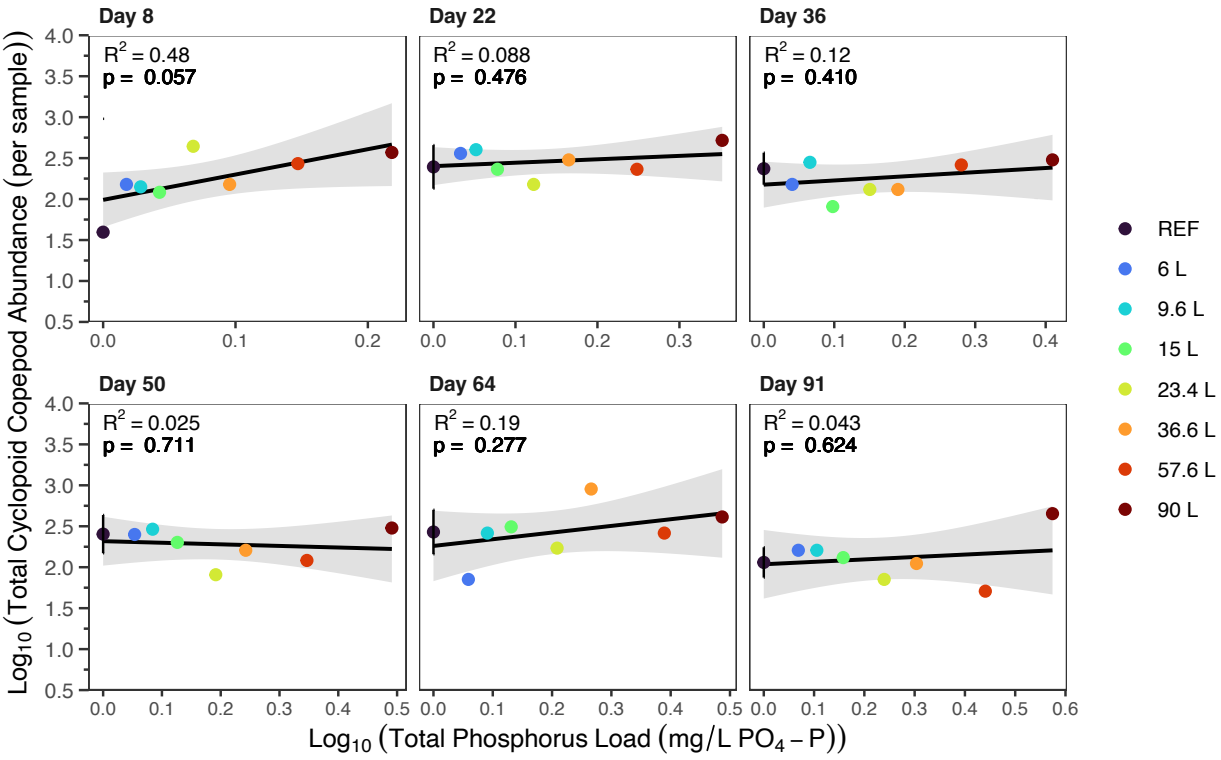

Appendix Figure D-25: Linear regression model results of the relationship between log10(x + 1) of cumulative AWW load concentration (TP used as the representative variable) and total cyclopoid copepod abundance. REF displays the mean of the references (n = 3) with the error bars representing ± standard deviation. Each plot displays the model results according to study day.

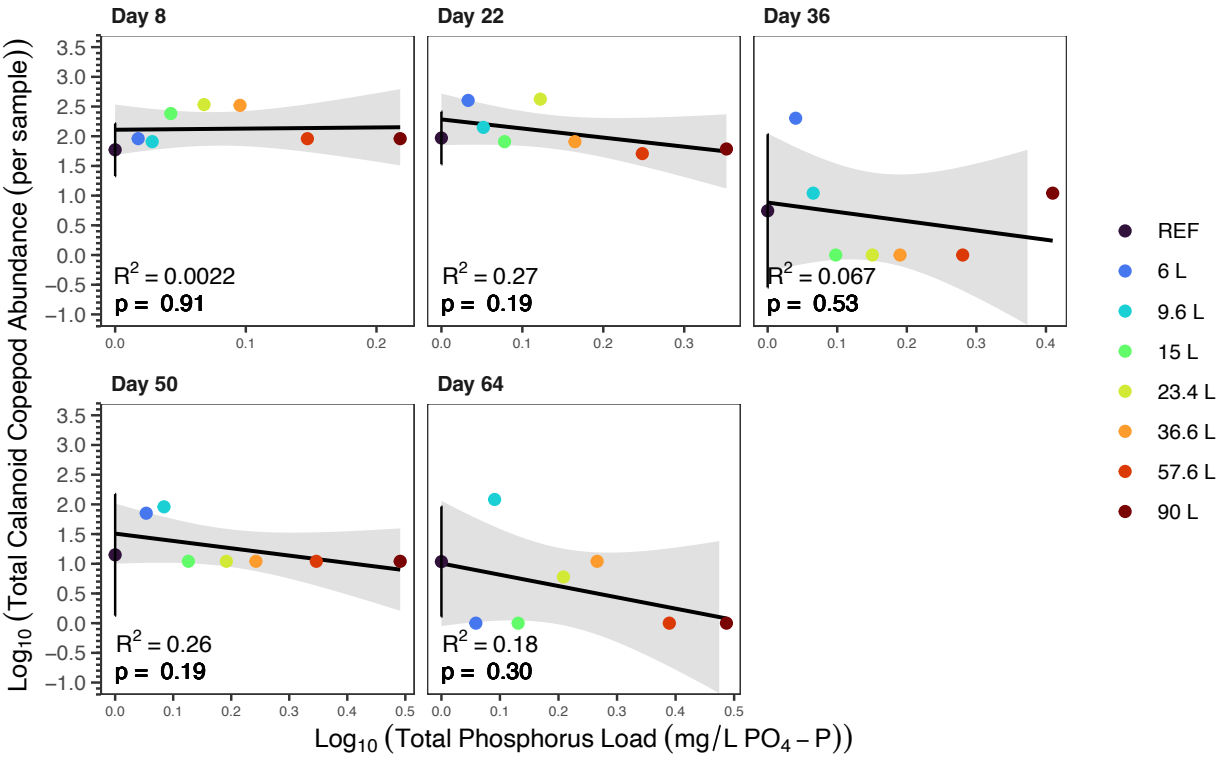

Appendix Figure D-26: Linear regression model results of the relationship between log10(x + 1) of cumulative AWW load concentration (TP used as the representative variable) and total calanoid copepod abundance. REF displays the mean of the references (n = 3) with the error bars representing ± standard deviation. Each plot displays the model results according to study day.

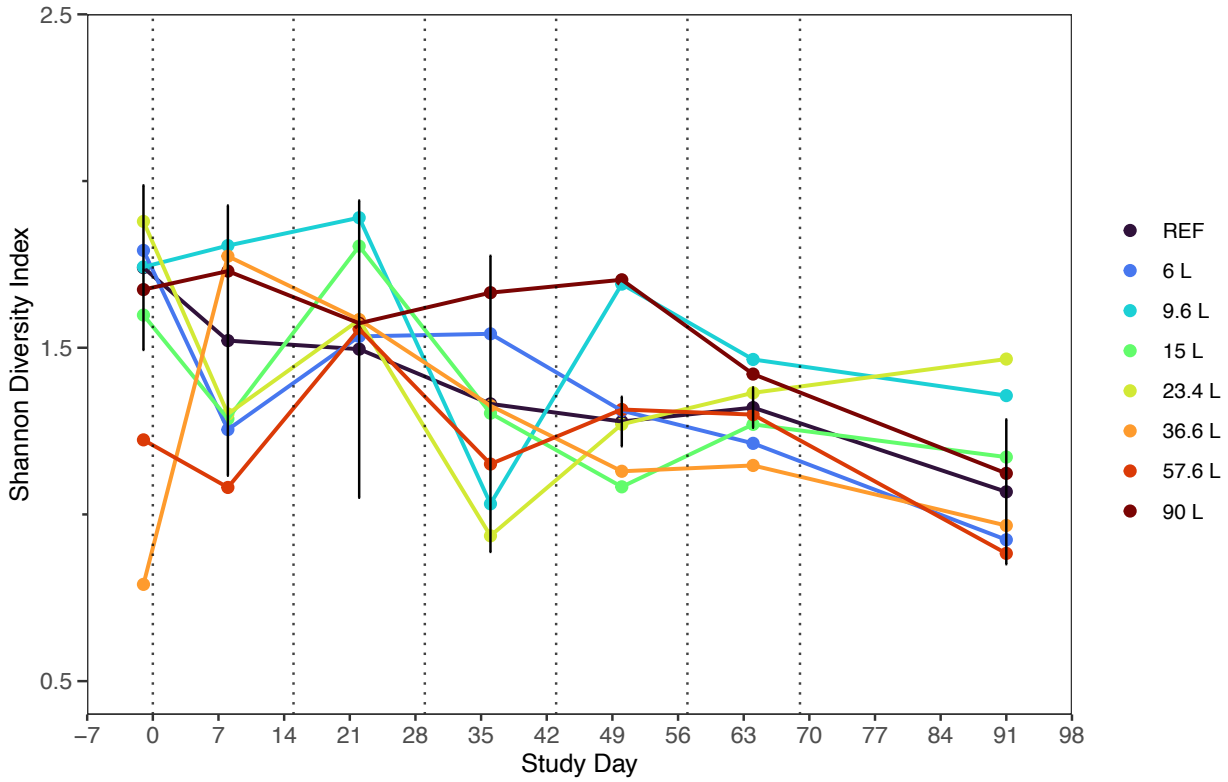

Appendix Figure D-27: Shannon Diversity Index over the study duration within the UM wild rice mesocosms. The vertical dotted lines represent AWW addition days. REF displays the mean of the references (n = 3) with the error bars representing ± standard deviation.

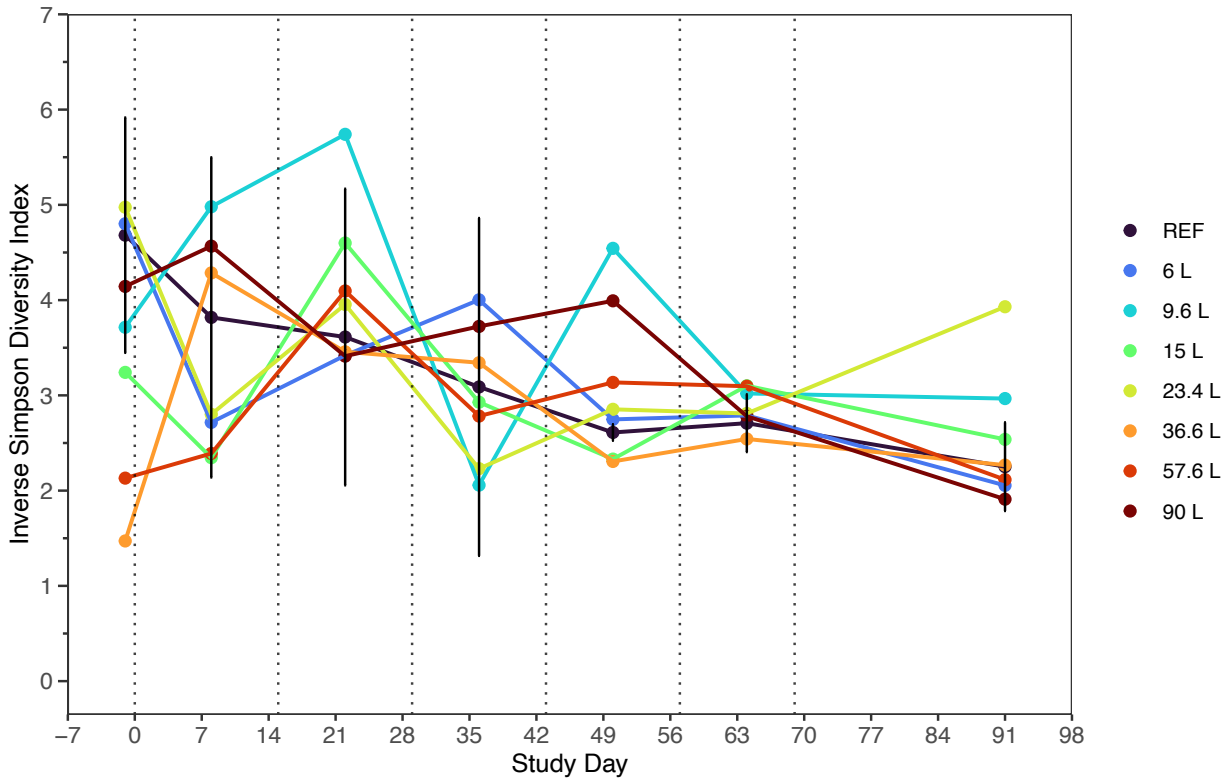

Appendix Figure D-28: Inverse Simpson Diversity Index over the study duration within the UM wild rice mesocosms. The vertical dotted lines represent AWW addition days. REF displays the mean of the references (n = 3) with the error bars representing ± standard deviation.

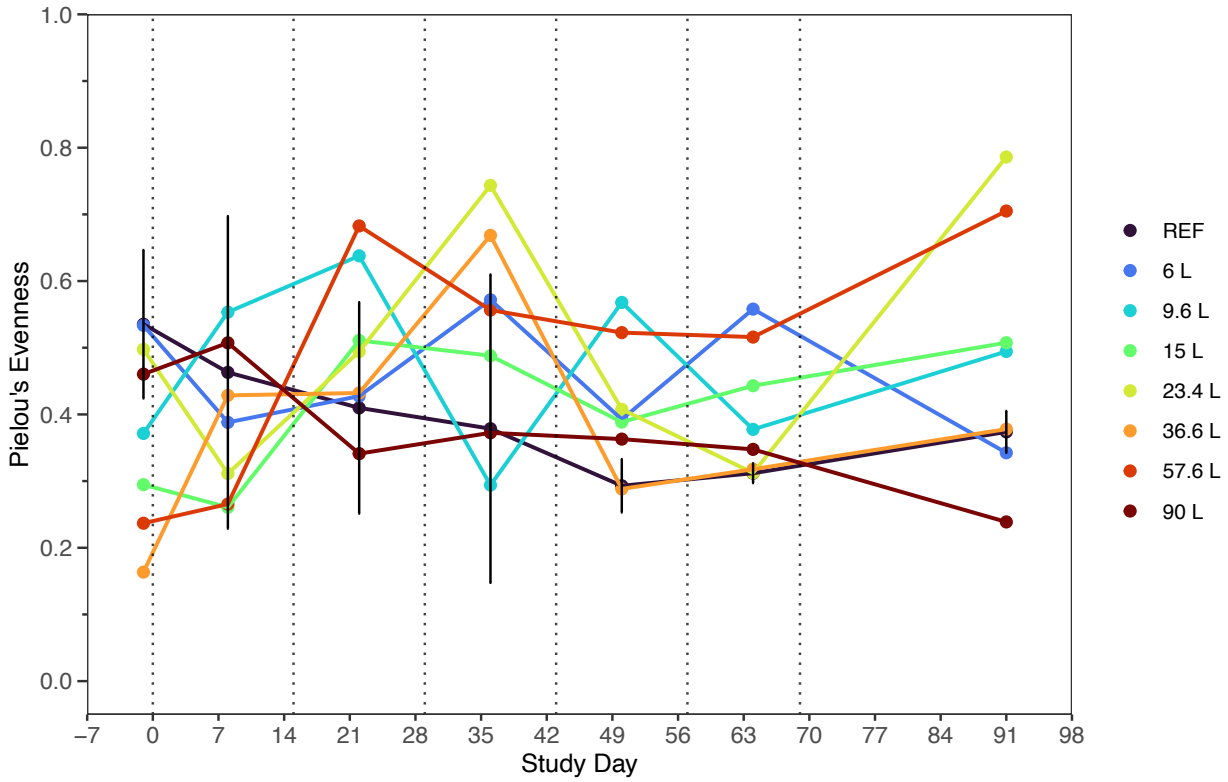

Appendix Figure D-29: Pielou's evenness over the study duration within the UM wild rice mesocosms. The vertical dotted lines represent AWW addition days. REF displays the mean of the references (n = 3) with the error bars representing ± standard deviation.

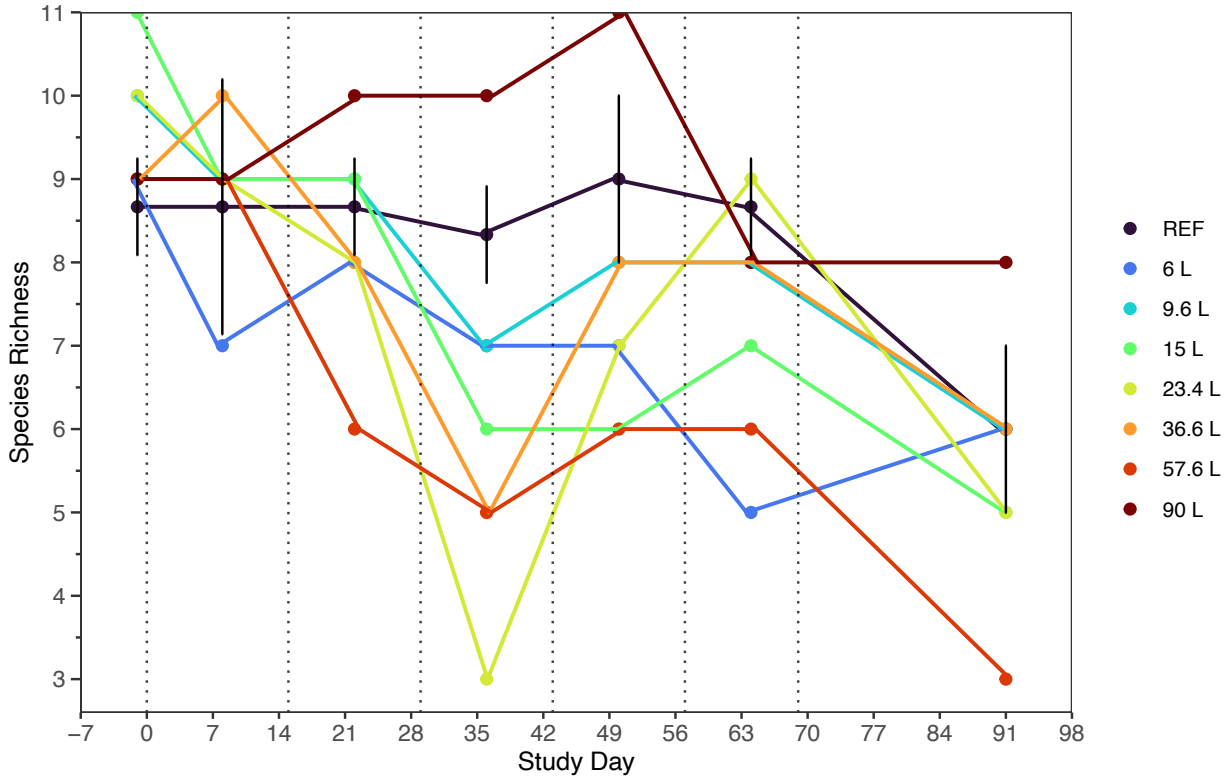

Appendix Figure D-30: Species richness over the study duration within the UM wild rice mesocosms. The vertical dotted lines represent AWW addition days. REF displays the mean of the references (n = 3) with the error bars representing ± standard deviation.

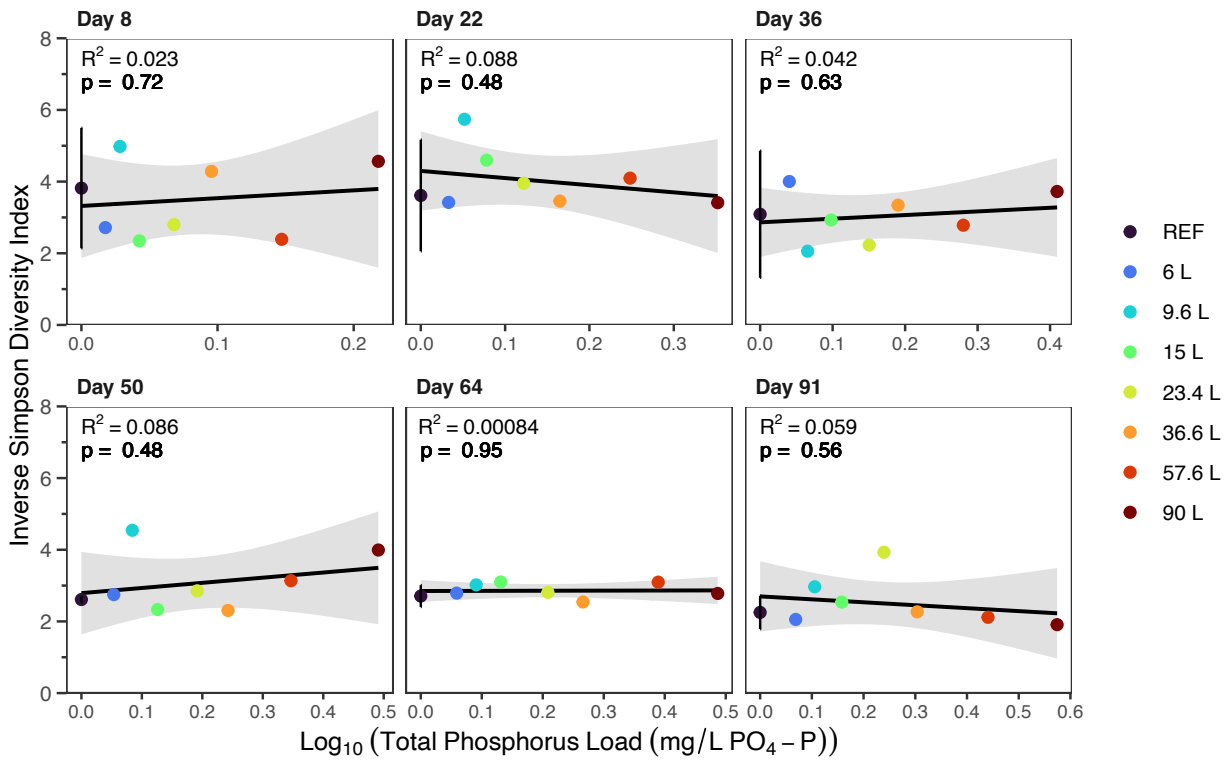

Appendix Figure D-31: Linear regression model results of the relationship between log10(x + 1) of cumulative AWW load concentration (TP used as the representative variable) and Inverse Simpson Diversity. REF displays the mean of the references (n = 3) with the error bars representing ± standard deviation. Each plot displays the model results according to study day.

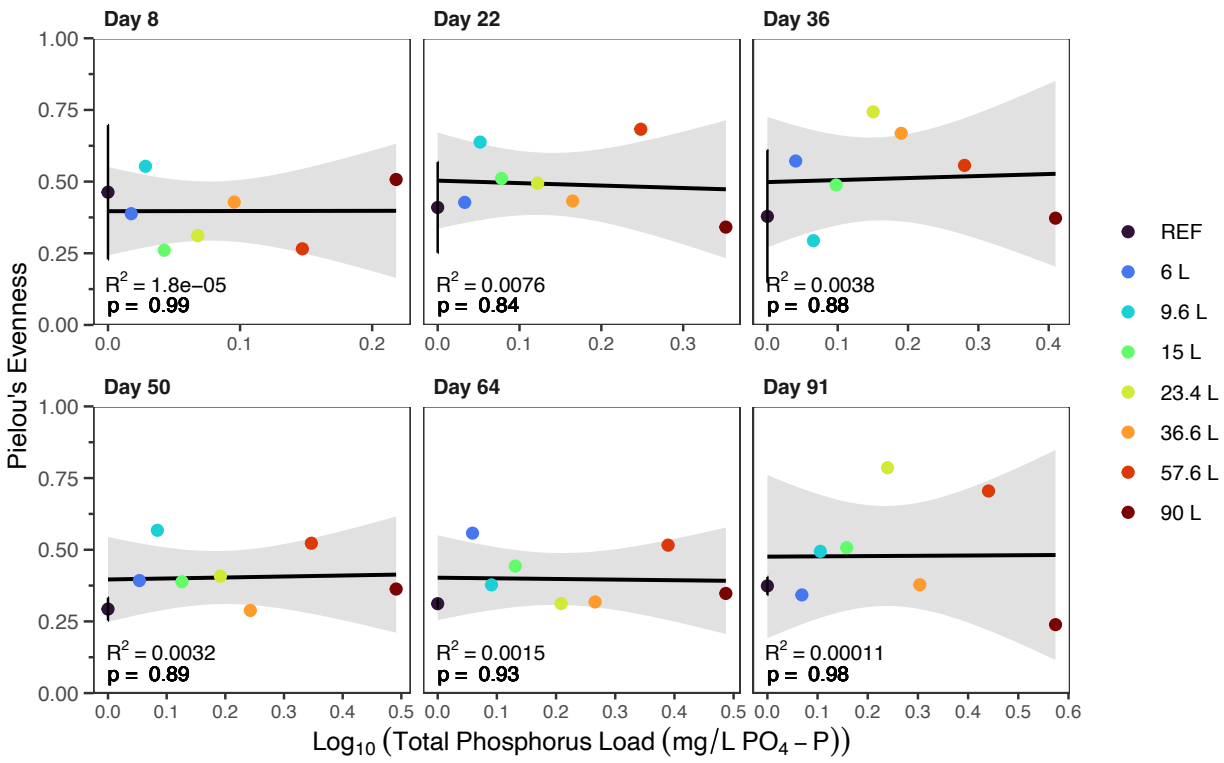

Appendix Figure D-32: Linear regression model results of the relationship between log10(x + 1) of cumulative AWW load concentration (TP used as the representative variable) and Pielou's Evenness. REF displays the mean of the references (n = 3) with the error bars representing ± standard deviation. Each plot displays the model results according to study day.

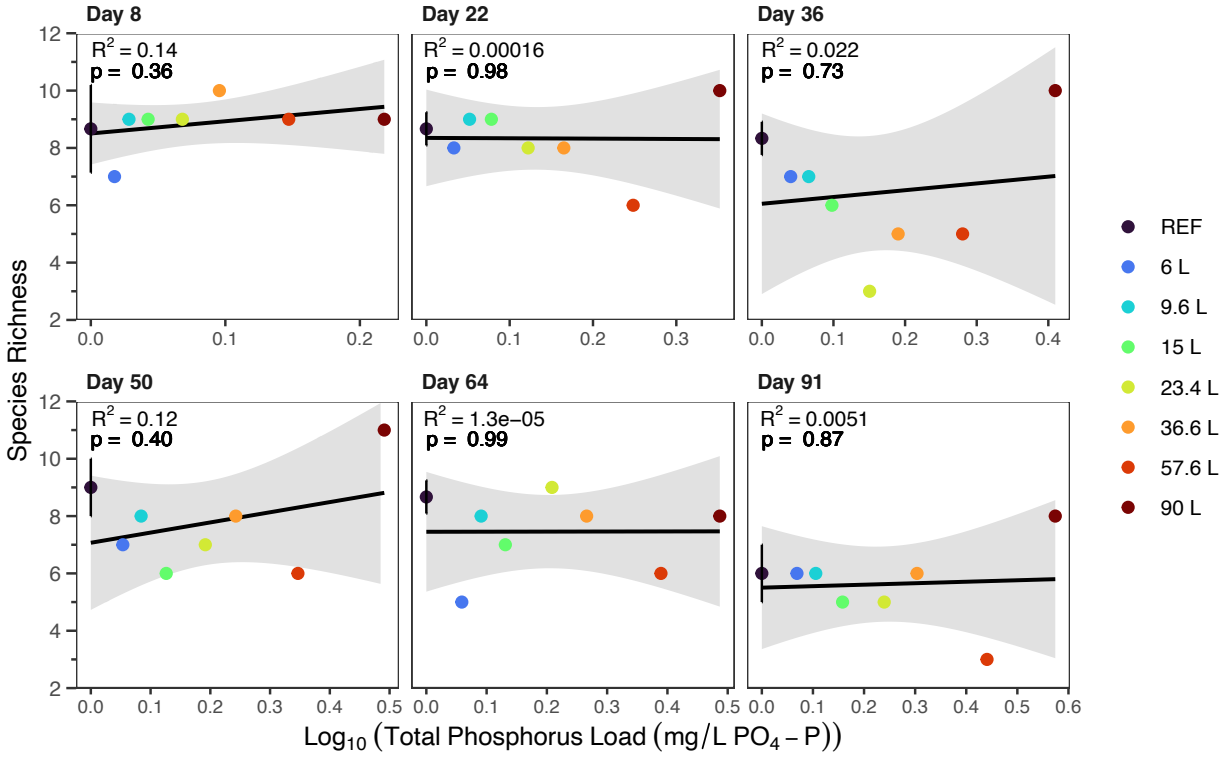

Appendix Figure D-33: Linear regression model results of the relationship between log10(x + 1) of cumulative AWW load concentration (TP used as the representative variable) and Species Richness. REF displays the mean of the references (n = 3) with the error bars representing ± standard deviation. Each plot displays the model results according to study day.